Many-body interference in the Fano map of a symmetric triple quantum dot

Milena Grifoni

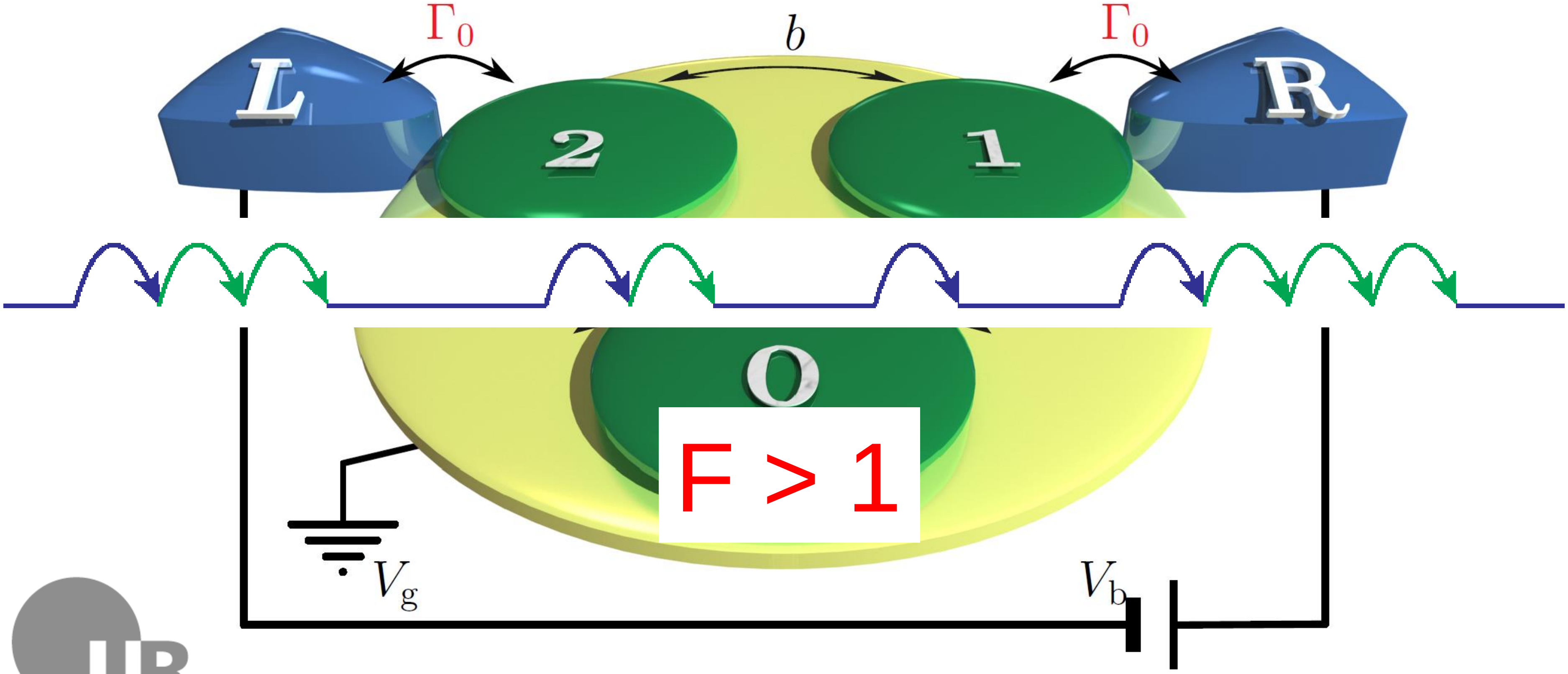

$F > 1$

Dresden, 19.4.2017

About lateral TQD devices see …

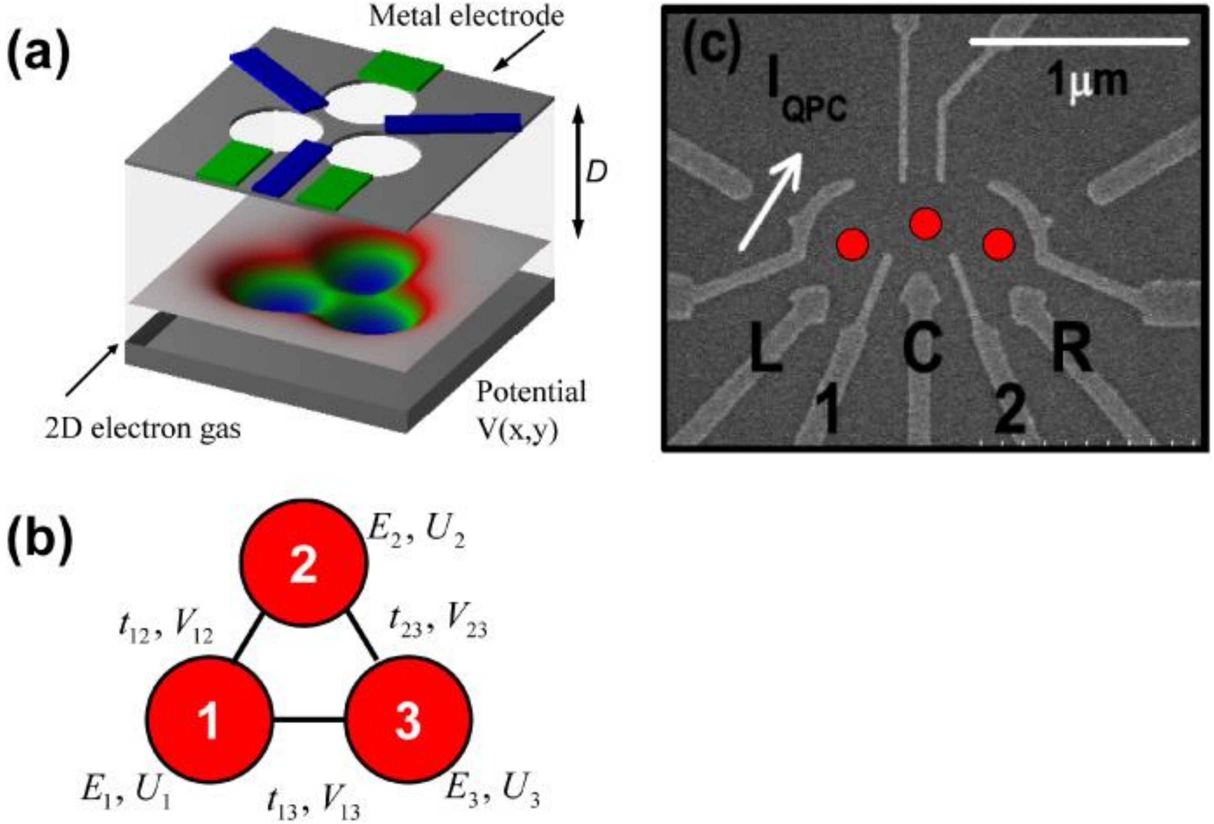

Hsieh et al., *Rep. Prog. Phys.* ***75***, 114501 (2012)

A frustrated trio

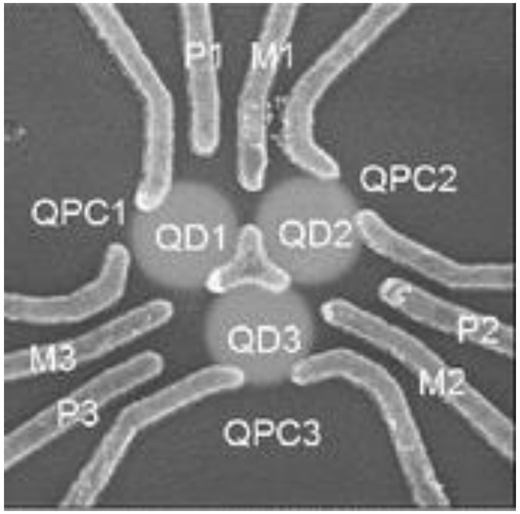

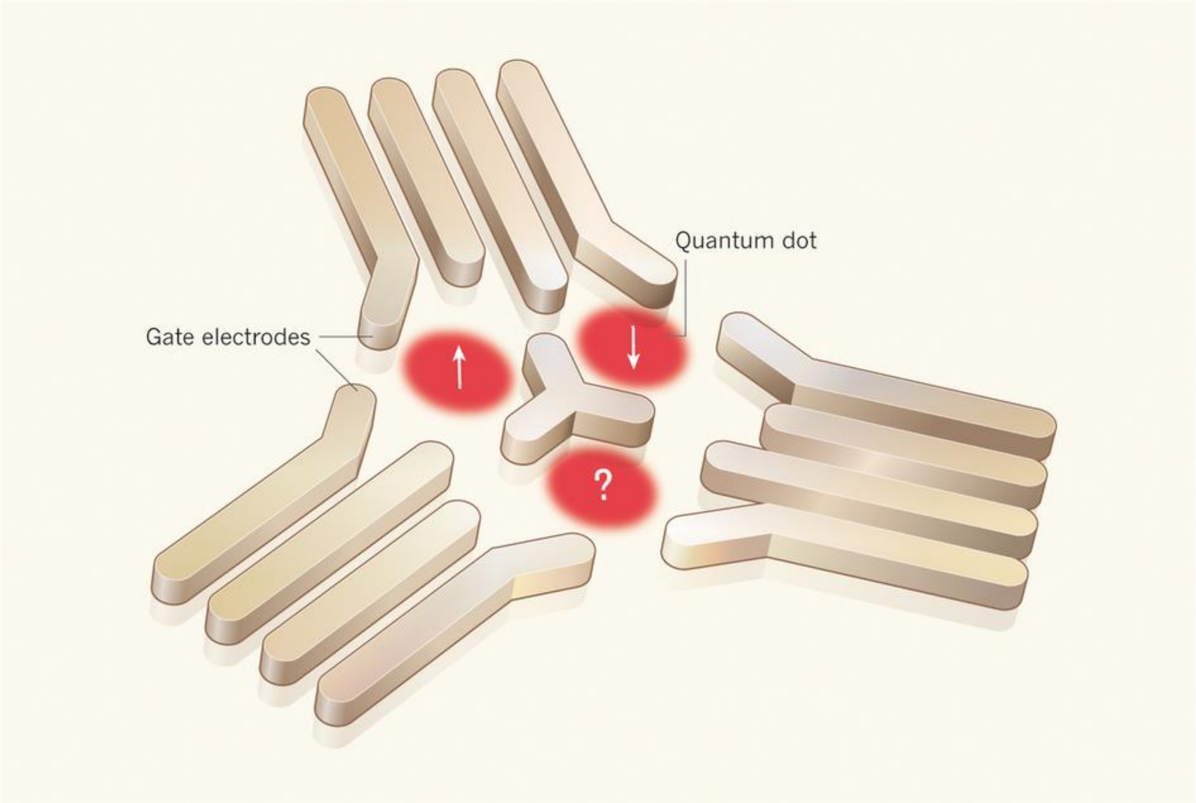

Seo et al, *Phys. Rev. Lett*. **110**, 046804 (2013)
Andergassen, *Nature* **495**, 321 (2013)

Coherent population trapping in quantum dots

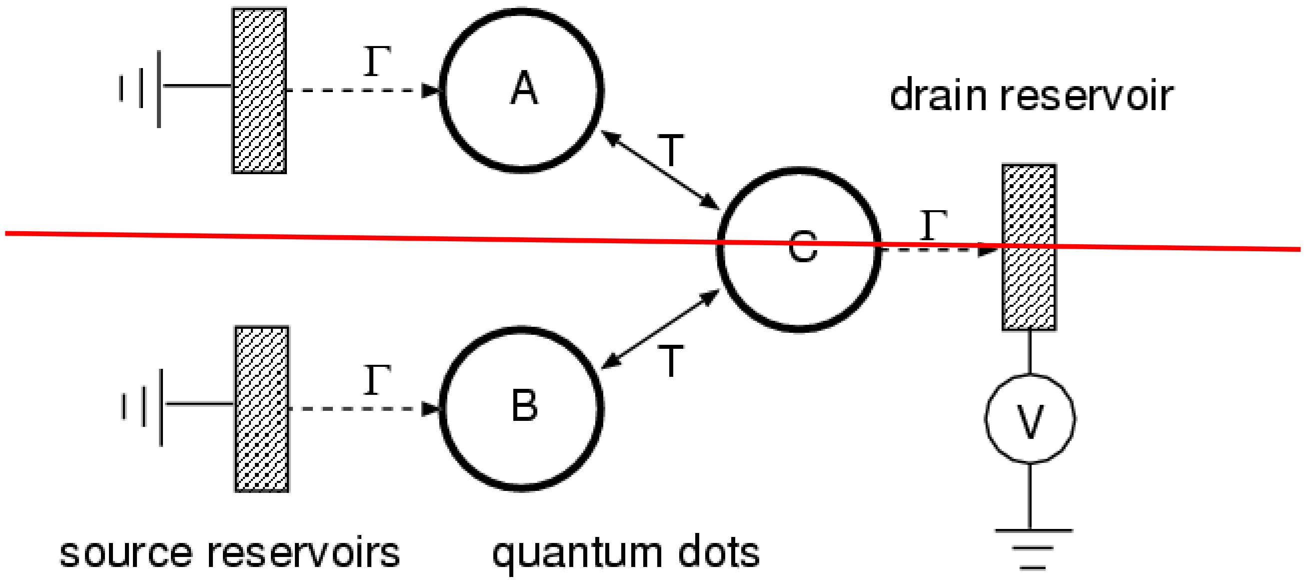

- Finite Coulomb interaction, N=0 & N=1
- Finite bias → unidirectional motion

Michaelis, Emary and Beenakker, EPL **75**, 677 (2006)

Coherent population trapping in quantum dots

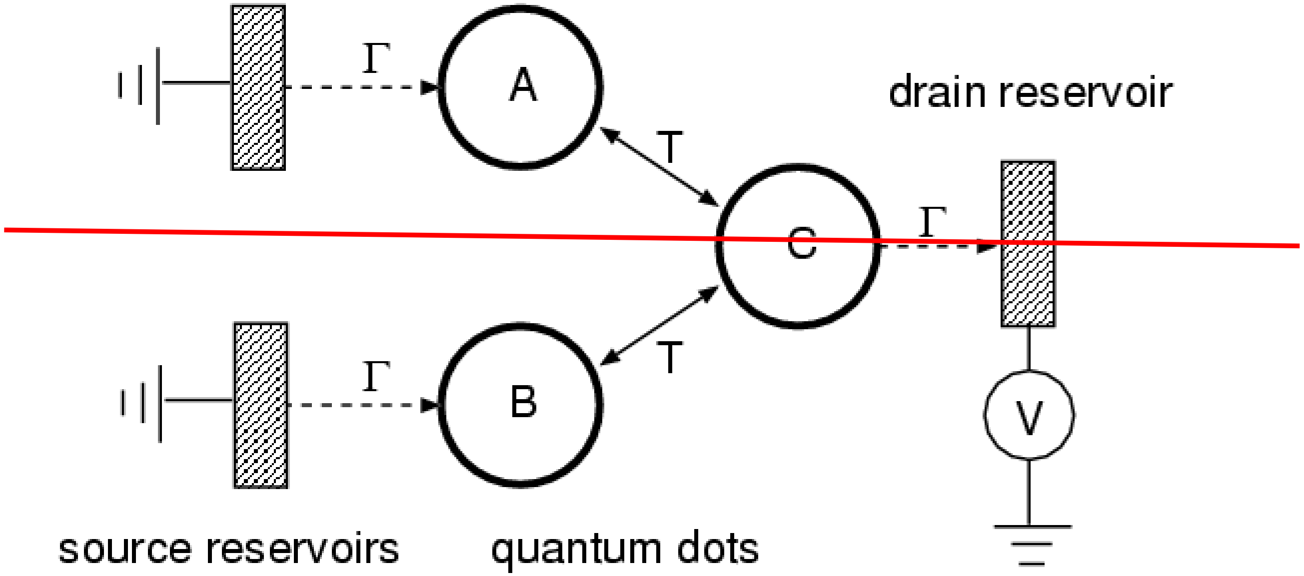

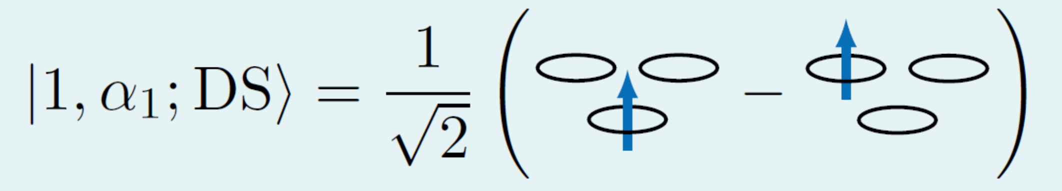

$$|1,\alpha_1;\mathrm{DS}\rangle = \frac{1}{\sqrt{2}}\left(\quad - \quad \right)$$

Michaelis, Emary and Beenakker, EPL **75**, 677 (2006)

Symmetric triple quantum dot

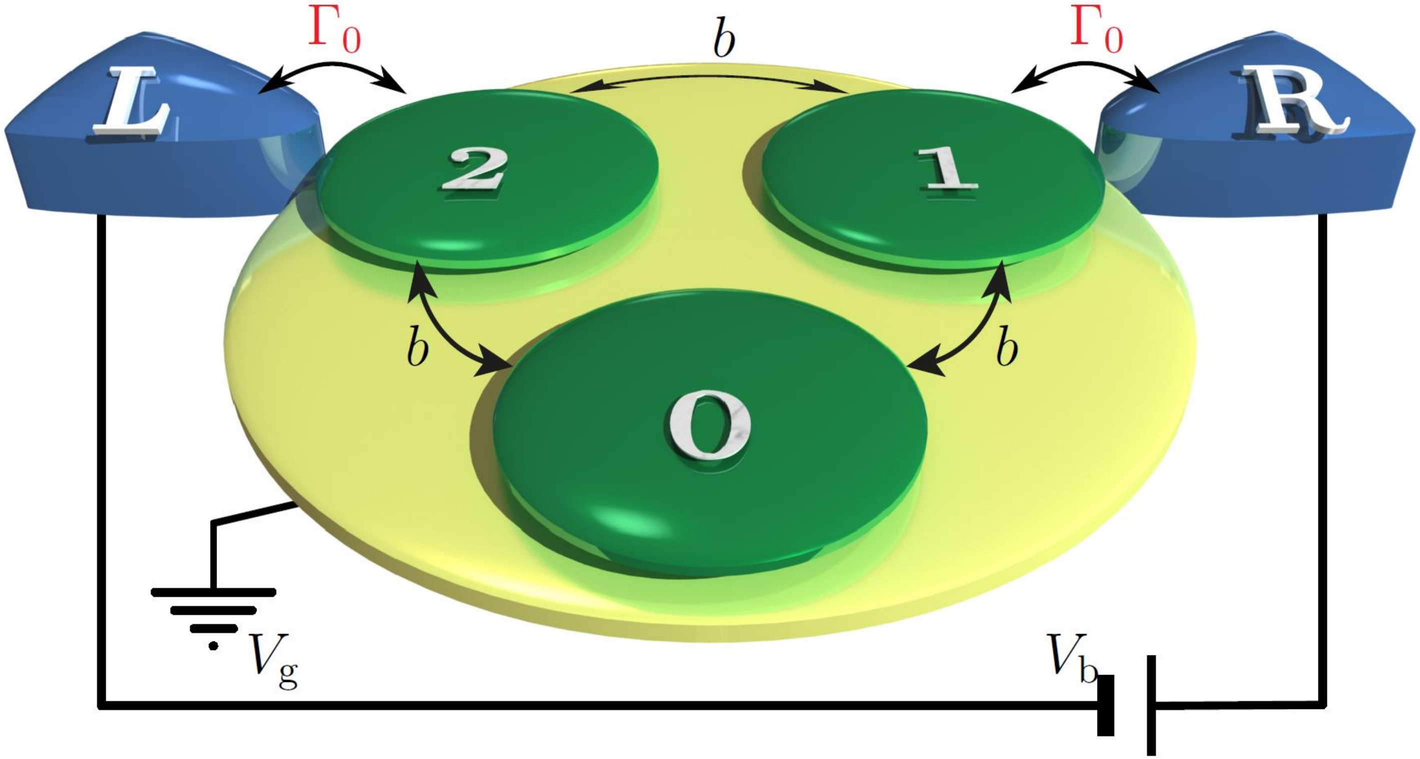

$$\hat{H} = \boxed{\hat{H}_{\mathsf{TQD}}} + \boxed{\hat{H}_{\mathsf{res}}} + \boxed{\hat{H}_{\mathsf{tun}}}$$

TQD Hamiltonian

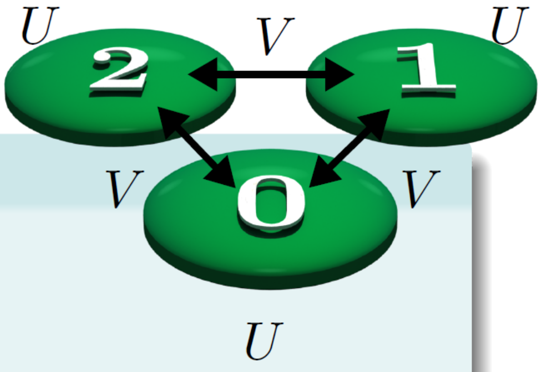

Extended Hubbard model

$$\hat{H}_{\mathsf{TQD}} = \xi \sum_{i\sigma} n_{i\sigma} + b \sum_{i\neq j,\sigma} d^{\dagger}_{j\sigma} d_{i\sigma}$$
$$+ U \sum_{i} \left(n_{i\uparrow} - \frac{1}{2}\right)\left(n_{i\downarrow} - \frac{1}{2}\right)$$
$$+ V \sum_{i<j} (n_i - 1)(n_j - 1)$$

TQD Hamiltonian

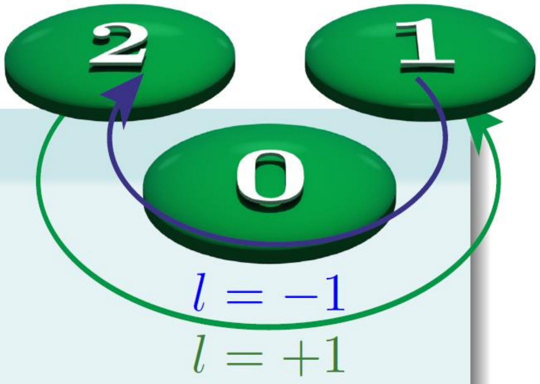

Extended Hubbard model

$$\hat{H}_{\mathsf{TQD}} = \xi \sum_{i\sigma} n_{i\sigma} + b \sum_{i\neq j,\sigma} d^{\dagger}_{j\sigma} d_{i\sigma} + U \sum_{i} \left(n_{i\uparrow} - \frac{1}{2}\right)\left(n_{i\downarrow} - \frac{1}{2}\right) + V \sum_{i<j} \left(n_i - 1\right)\left(n_j - 1\right)$$

- single particle part is diagonal in angular momentum basis

$$|l\rangle = \frac{1}{\sqrt{3}} \sum_{j=0}^{2} e^{-i\frac{2\pi}{3} lj} |j\rangle, \quad l = 0, \pm 1$$

TQD Hamiltonian

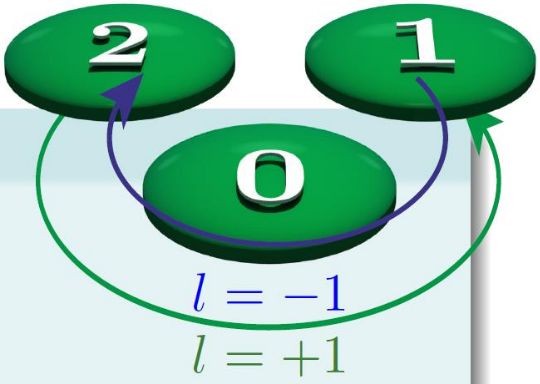

Extended Hubbard model

$$\hat{H}_{\mathsf{TQD}} = \xi \sum_{i\sigma} n_{i\sigma} + b \sum_{i\neq j,\sigma} d^\dagger_{j\sigma} d_{i\sigma} + U \sum_{i} \left(n_{i\uparrow} - \frac{1}{2}\right)\left(n_{i\downarrow} - \frac{1}{2}\right) + V \sum_{i<j} (n_i - 1)(n_j - 1)$$

- single particle part is diagonal in angular momentum basis
- many-body states are fully characterized by

$$|n_{0\uparrow}, n_{1\uparrow}, n_{-1\uparrow}; n_{0\downarrow}, n_{1\downarrow}, n_{-1\downarrow}\rangle$$

TQD Spectrum

N	Eigenenergy	S	S_z	L_z	Eigenstate in the basis $\{\lvert n_{0\uparrow}, n_{1\uparrow}, n_{-1\uparrow}; n_{0\downarrow}, n_{1\downarrow}, n_{-1\downarrow}\rangle\}$
0	$E_0 = 0$	0	0	0	$\lvert 000, 000\rangle$
1	$E_{1_0} = \xi - \frac{U}{2} - 2V + 2b$	$\frac{1}{2}$	$-\frac{1}{2}$	0	$\lvert 000, 100\rangle$
			$\frac{1}{2}$		$\lvert 100, 000\rangle$
	$E_{1_1} = \xi - \frac{U}{2} - 2V - b$	$\frac{1}{2}$	$-\frac{1}{2}$	-1	$\lvert 000, 001\rangle$
				1	$\lvert 000, 010\rangle$
			$\frac{1}{2}$	-1	$\lvert 001, 000\rangle$
				1	$\lvert 010, 000\rangle$
2	$E_{2_0} = 2\xi - U - 3V + b + \frac{U-V}{2} - s_{-2}$	0	0	0	$\cos(\phi_{-2})\lvert 100, 100\rangle - \sin(\phi_{-2})\frac{1}{\sqrt{2}}\left(\lvert 010, 001\rangle + \lvert 001, 010\rangle\right)$
	$E_{2_1} = 2\xi - U - 3V + b$	1	-1	-1	$\lvert 000, 101\rangle$
				1	$\lvert 000, 110\rangle$
			0	-1	$\frac{1}{\sqrt{2}}\left(\lvert 100, 001\rangle - \lvert 001, 100\rangle\right)$
				1	$\frac{1}{\sqrt{2}}\left(\lvert 100, 010\rangle - \lvert 010, 100\rangle\right)$
			1	-1	$\lvert 101, 000\rangle$
				1	$\lvert 110, 000\rangle$
	$E_{2_2} = 2\xi - U - 3V - \frac{b}{2} + \frac{U-V}{2} - s_1$	0	0	-1	$\cos(\phi_1)\lvert 010, 010\rangle - \sin(\phi_1)\frac{1}{\sqrt{2}}\left(\lvert 100, 001\rangle + \lvert 001, 100\rangle\right)$
				1	$\cos(\phi_1)\lvert 001, 001\rangle - \sin(\phi_1)\frac{1}{\sqrt{2}}\left(\lvert 100, 010\rangle + \lvert 010, 100\rangle\right)$
	$E_{2_3} = 2\xi - U - 3V - 2b$	1	-1	0	$\lvert 000, 011\rangle$
			0		$\frac{1}{\sqrt{2}}\left(\lvert 010, 001\rangle - \lvert 001, 010\rangle\right)$
			1		$\lvert 011, 000\rangle$
	$E_{2_4} = 2\xi - U - 3V - \frac{b}{2} + \frac{U-V}{2} + s_1$	0	0	-1	$\sin(\phi_1)\lvert 010, 010\rangle + \cos(\phi_1)\frac{1}{\sqrt{2}}\left(\lvert 100, 001\rangle + \lvert 001, 100\rangle\right)$
				1	$\sin(\phi_1)\lvert 001, 001\rangle + \cos(\phi_1)\frac{1}{\sqrt{2}}\left(\lvert 100, 010\rangle + \lvert 010, 100\rangle\right)$
	$E_{2_5} = 2\xi + b - U - 3V + \frac{U-V}{2} + s_{-2}$	0	0	0	$\sin(\phi_{-2})\lvert 100, 100\rangle + \cos(\phi_{-2})\frac{1}{\sqrt{2}}\left(\lvert 010, 001\rangle + \lvert 001, 010\rangle\right)$
	$E_{3_0} = 3\xi - \frac{3}{2}U - 3V + \frac{2}{3}\left(U - V\right)\left[1 - \lambda_0/(2\lvert a\rvert)\right]$	$\frac{1}{2}$	$-\frac{1}{2}$	-1	$v_{0,1}\lvert 100, 101\rangle - v_{0,0}\lvert 010, 110\rangle - v_{0,-1}\lvert 001, 011\rangle$
				1	$v_{0,1}\lvert 100, 110\rangle + v_{0,0}\lvert 001, 101\rangle - v_{0,-1}\lvert 010, 011\rangle$
			$\frac{1}{2}$	-1	$v_{0,1}\lvert 101, 100\rangle - v_{0,0}\lvert 110, 010\rangle - v_{0,-1}\lvert 011, 001\rangle$
				1	$v_{0,1}\lvert 110, 100\rangle - v_{0,0}\lvert 101, 001\rangle + v_{0,-1}\lvert 011, 010\rangle$
	$E_{3_1} = 3\xi - \frac{3}{2}U - 3V$	$\frac{3}{2}$	$-\frac{3}{2}$	0	$\lvert 000, 111\rangle$
			$-\frac{1}{2}$		$\frac{1}{\sqrt{3}}\left(\lvert 001, 110\rangle - \lvert 010, 101\rangle + \lvert 100, 011\rangle\right)$
			$\frac{1}{2}$		$\frac{1}{\sqrt{3}}\left(\lvert 011, 100\rangle - \lvert 101, 010\rangle + \lvert 110, 001\rangle\right)$

TQD Spectrum

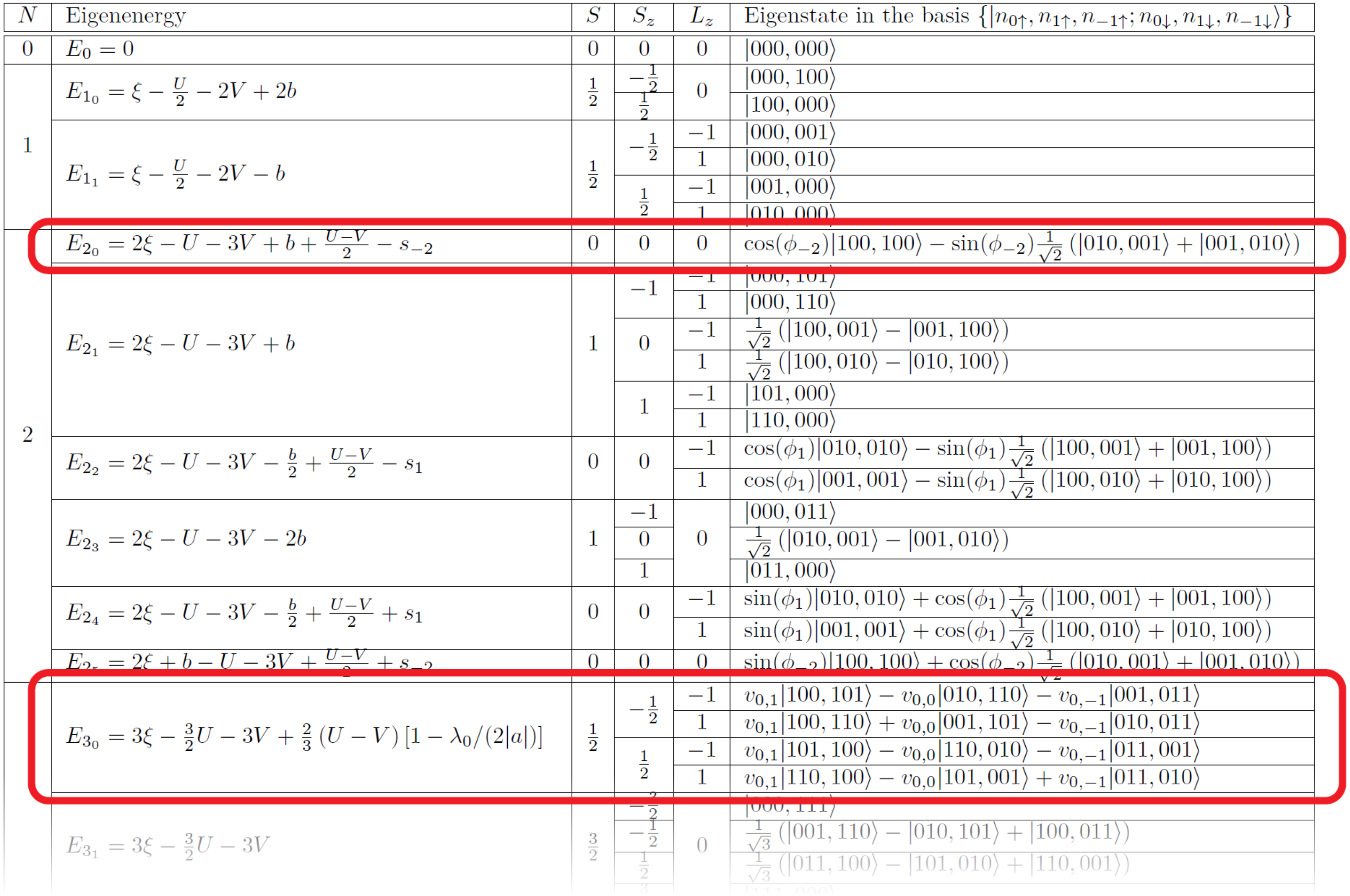

N	Eigenenergy	S	S_z	L_z	Eigenstate in the basis $\{\lvert n_{0\uparrow}, n_{1\uparrow}, n_{-1\uparrow}; n_{0\downarrow}, n_{1\downarrow}, n_{-1\downarrow}\rangle\}$
0	$E_0 = 0$	0	0	0	$\lvert 000,000\rangle$
1	$E_{1_0} = \xi - \frac{U}{2} - 2V + 2b$	$\frac{1}{2}$	$-\frac{1}{2}$	0	$\lvert 000,100\rangle$
			$\frac{1}{2}$		$\lvert 100,000\rangle$
	$E_{1_1} = \xi - \frac{U}{2} - 2V - b$	$\frac{1}{2}$	$-\frac{1}{2}$	-1	$\lvert 000,001\rangle$
				1	$\lvert 000,010\rangle$
			$\frac{1}{2}$	-1	$\lvert 001,000\rangle$
				1	$\lvert 010,000\rangle$
2	$E_{2_0} = 2\xi - U - 3V + b + \frac{U-V}{2} - s_{-2}$	0	0	0	$\cos(\phi_{-2})\lvert 100,100\rangle - \sin(\phi_{-2})\frac{1}{\sqrt{2}}(\lvert 010,001\rangle + \lvert 001,010\rangle)$
	$E_{2_1} = 2\xi - U - 3V + b$	1	-1	-1	$\lvert 000,101\rangle$
				1	$\lvert 000,110\rangle$
			0	-1	$\frac{1}{\sqrt{2}}(\lvert 100,001\rangle - \lvert 001,100\rangle)$
				1	$\frac{1}{\sqrt{2}}(\lvert 100,010\rangle - \lvert 010,100\rangle)$
			1	-1	$\lvert 101,000\rangle$
				1	$\lvert 110,000\rangle$
	$E_{2_2} = 2\xi - U - 3V - \frac{b}{2} + \frac{U-V}{2} - s_1$	0	0	-1	$\cos(\phi_1)\lvert 010,010\rangle - \sin(\phi_1)\frac{1}{\sqrt{2}}(\lvert 100,001\rangle + \lvert 001,100\rangle)$
				1	$\cos(\phi_1)\lvert 001,001\rangle - \sin(\phi_1)\frac{1}{\sqrt{2}}(\lvert 100,010\rangle + \lvert 010,100\rangle)$
	$E_{2_3} = 2\xi - U - 3V - 2b$	1	-1	0	$\lvert 000,011\rangle$
			0		$\frac{1}{\sqrt{2}}(\lvert 010,001\rangle - \lvert 001,010\rangle)$
			1		$\lvert 011,000\rangle$
	$E_{2_4} = 2\xi - U - 3V - \frac{b}{2} + \frac{U-V}{2} + s_1$	0	0	-1	$\sin(\phi_1)\lvert 010,010\rangle + \cos(\phi_1)\frac{1}{\sqrt{2}}(\lvert 100,001\rangle + \lvert 001,100\rangle)$
				1	$\sin(\phi_1)\lvert 001,001\rangle + \cos(\phi_1)\frac{1}{\sqrt{2}}(\lvert 100,010\rangle + \lvert 010,100\rangle)$
	$E_{2_5} = 2\xi + b - U - 3V + \frac{U-V}{2} + s_{-2}$	0	0	0	$\sin(\phi_{-2})\lvert 100,100\rangle + \cos(\phi_{-2})\frac{1}{\sqrt{2}}(\lvert 010,001\rangle + \lvert 001,010\rangle)$
3	$E_{3_0} = 3\xi - \frac{3}{2}U - 3V + \frac{2}{3}(U-V)[1 - \lambda_0/(2\lvert a\rvert)]$	$\frac{1}{2}$	$-\frac{1}{2}$	-1	$v_{0,1}\lvert 100,101\rangle - v_{0,0}\lvert 010,110\rangle - v_{0,-1}\lvert 001,011\rangle$
				1	$v_{0,1}\lvert 100,110\rangle + v_{0,0}\lvert 001,101\rangle - v_{0,-1}\lvert 010,011\rangle$
			$\frac{1}{2}$	-1	$v_{0,1}\lvert 101,100\rangle - v_{0,0}\lvert 110,010\rangle - v_{0,-1}\lvert 011,001\rangle$
				1	$v_{0,1}\lvert 110,100\rangle - v_{0,0}\lvert 101,001\rangle + v_{0,-1}\lvert 011,010\rangle$
	$E_{3_1} = 3\xi - \frac{3}{2}U - 3V$	$\frac{3}{2}$	$-\frac{3}{2}$	0	$\lvert 000,111\rangle$
			$-\frac{1}{2}$		$\frac{1}{\sqrt{3}}(\lvert 001,110\rangle - \lvert 010,101\rangle + \lvert 100,011\rangle)$
			$\frac{1}{2}$		$\frac{1}{\sqrt{3}}(\lvert 011,100\rangle - \lvert 101,010\rangle + \lvert 110,001\rangle)$
			$\frac{3}{2}$		$\lvert 111,000\rangle$

Symmetry protected orbital degeneracies → potential existence of dark states

Dark states (DS)

A DS is a **linear combination** of orbitally degenerate states
with non vanishing tunnelling amplitude at the L lead

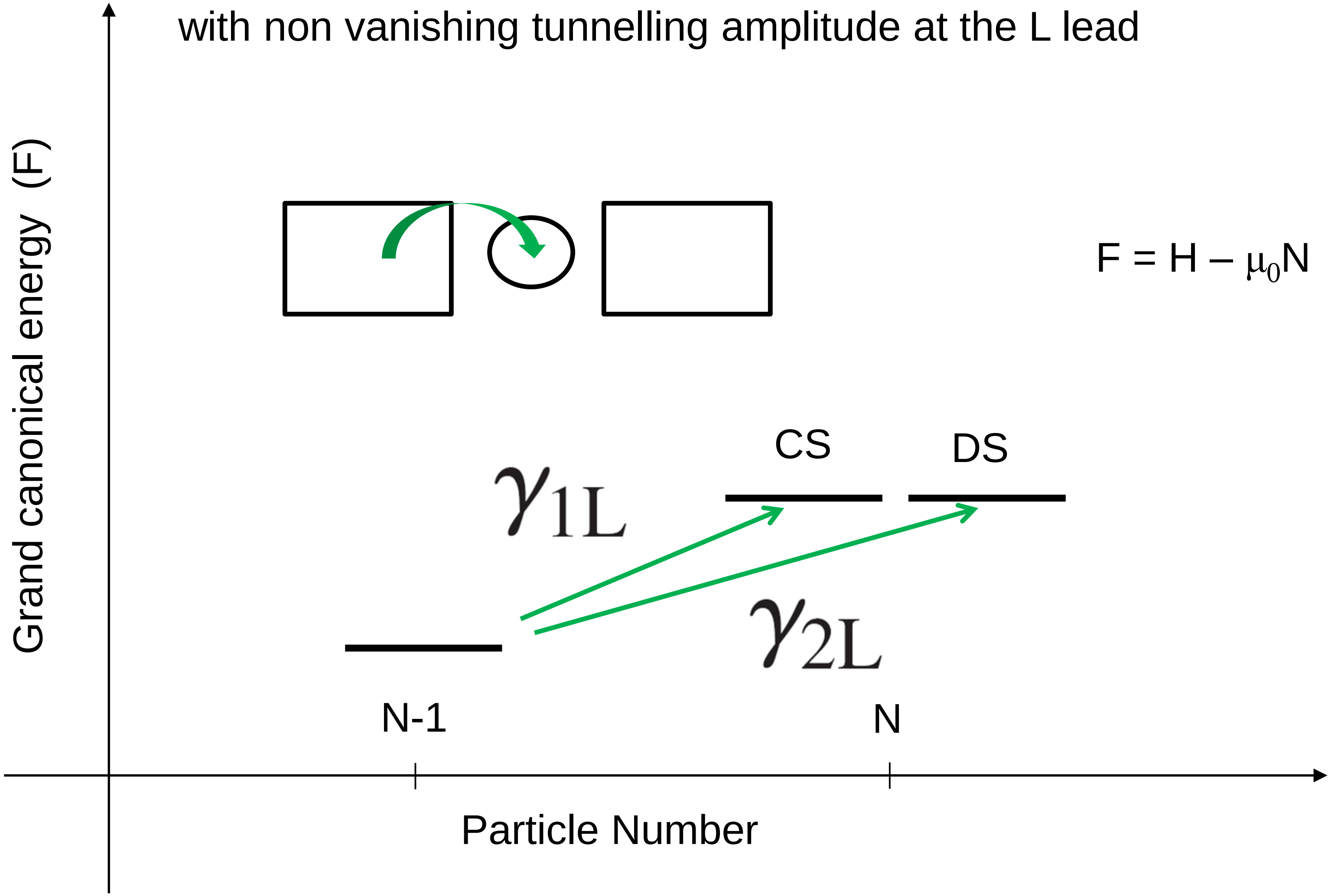

$$F = H - \mu_0 N$$

Dark states (DS)

… but with vanishing amplitude at the R lead

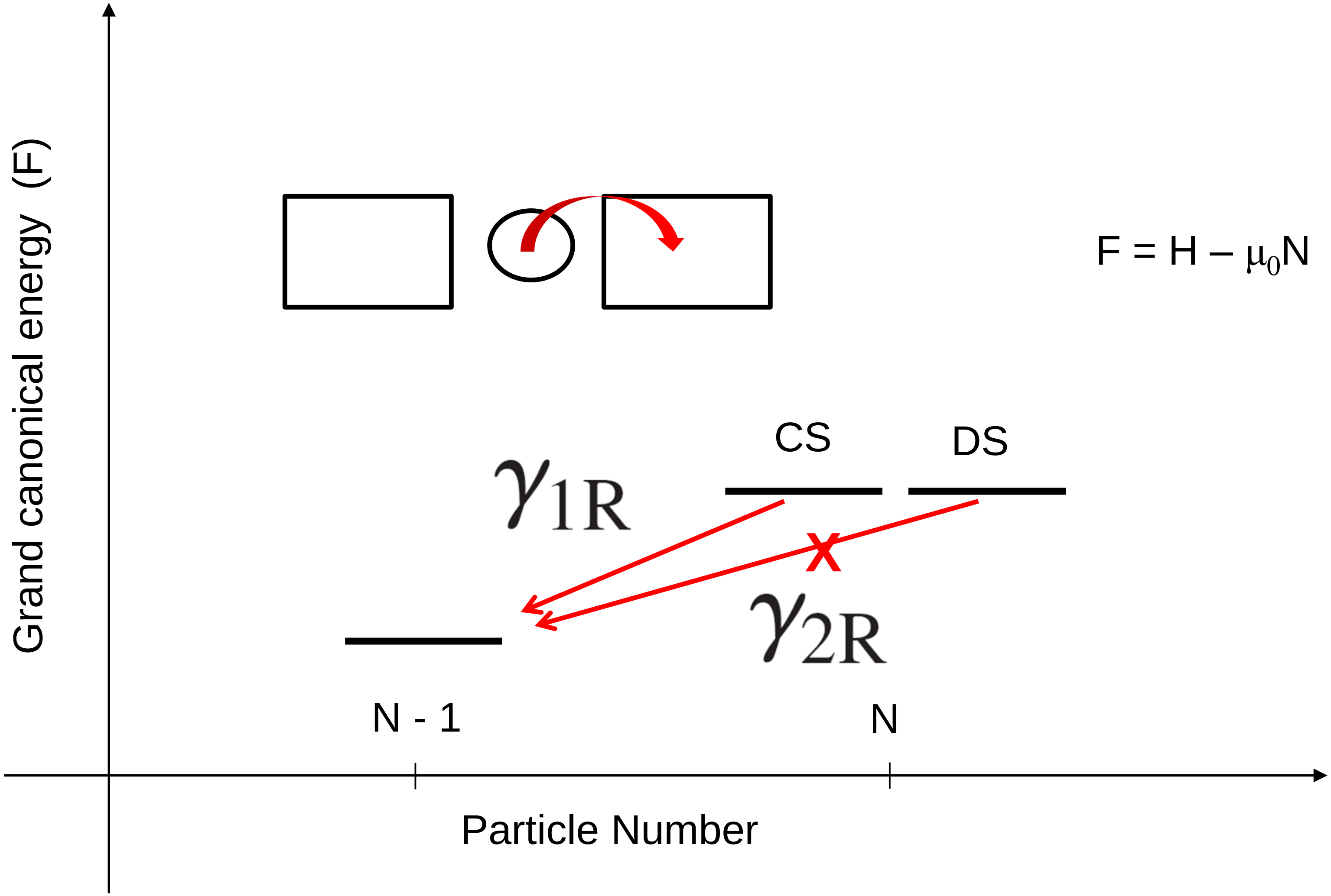

$F = H - \mu_0 N$

Dark states in aTQD

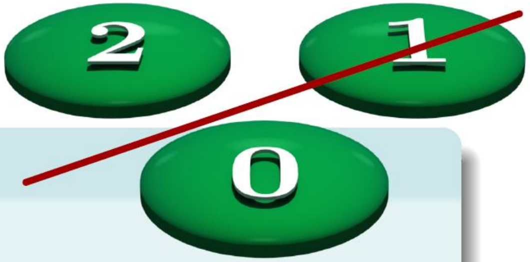

Dark states

$$|N,\alpha_i;\mathrm{DS}\rangle = \frac{1}{\sqrt{2}}\left[e^{i\frac{2\pi}{3}}|N,\alpha_i,L_z=1\rangle - e^{-i\frac{2\pi}{3}}|N,\alpha_i,L_z=-1\rangle\right]$$

fulfills [3]

$$\langle N-1,\alpha_i;L_z=0|d_{1\sigma}|N,\alpha_j;\mathrm{DS}\rangle = 0$$

[3] Kostryrko and Bulka, PRB **79**, 075310 (2009)

Dark states in a TQD

The generic DS in a triple quantum dot

$$|N,\alpha_i;DS\rangle = \frac{1}{\sqrt{2}}\left[e^{i\frac{2\pi}{3}}|N,\alpha_i,1\rangle - e^{-i\frac{2\pi}{3}}|N,\alpha_i,-1\rangle\right]$$

Proof:

$$\begin{aligned}\gamma_R =& \langle N-1;0|d_{1\sigma}|N;DS\rangle = \\ & \langle N-1;0|\sum_l e^{-il2\pi/3} d_{l\sigma}\left[e^{i2\pi/3}|N;1\rangle - e^{-i2\pi/3}|N;-1\rangle\right] \\ & = \langle N-1;0|d_{l=1\sigma}|N;1\rangle - \langle N-1;0|d_{l=-1\sigma}|N;-1\rangle \\ & = 0,\end{aligned}$$

$$\gamma_L = \langle N-1;0|d_{2\sigma}|N;DS\rangle \neq 0$$

Dark states in a TQD

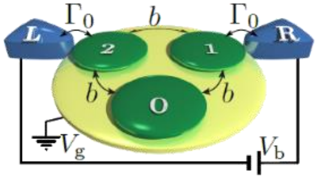

DS in the position basis

one-particle first excited state with $S_z = 1/2$ [4]

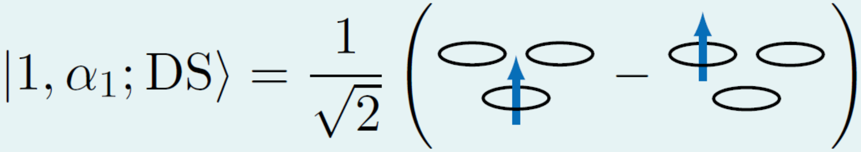

two-particle first excited state with $S_z = 0$

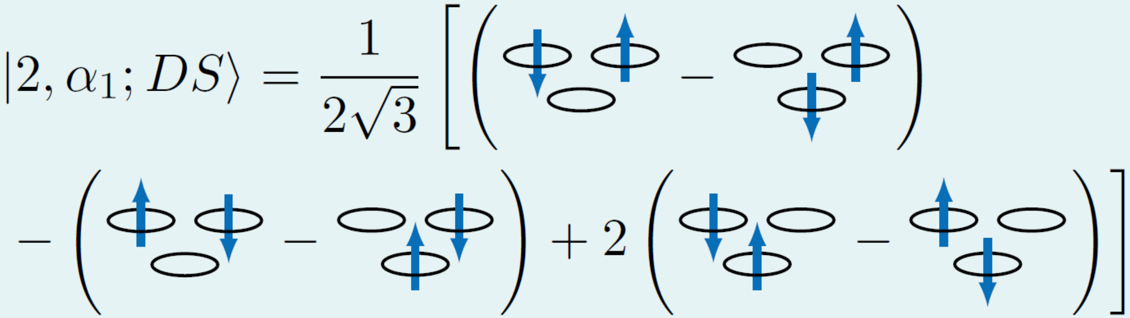

The **right coupled** dot CAN be occupied. The DS is antisymmetric with respect to

$$\sigma_{v1} : |1\tau\rangle \rightarrow |1\tau\rangle, \quad |0\tau\rangle \leftrightarrow |2\tau\rangle$$

[4] Michaelis, Emary and Beenakker, EPL **75**, 677 (2006)

Dark states in a TQD

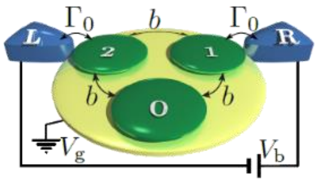

DS in the position basis

three-particle ground state with $S_z = 1/2$

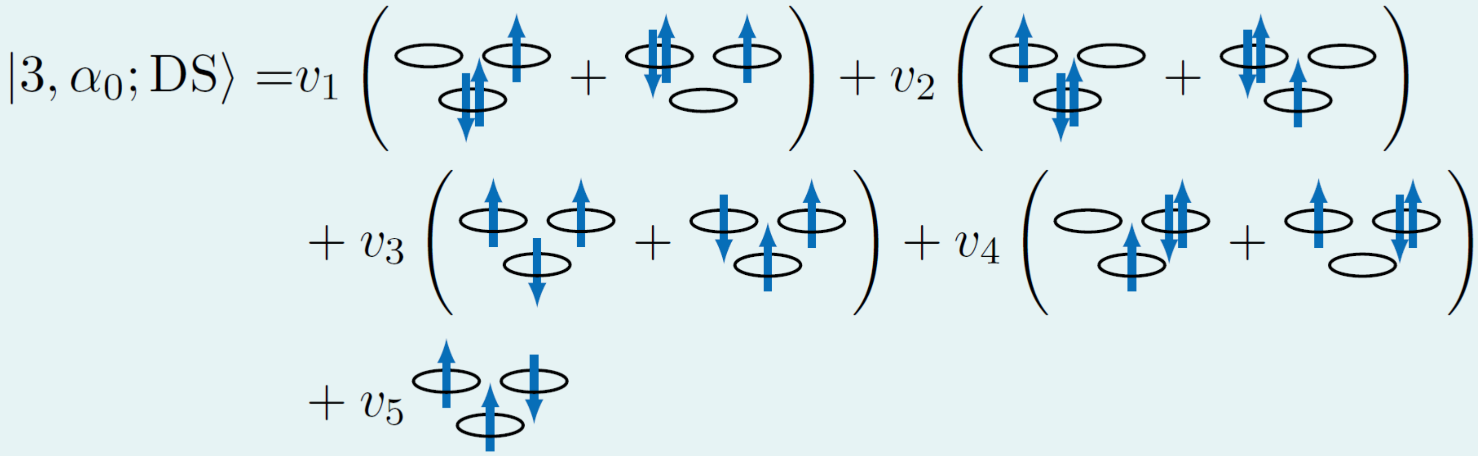

Transport

Generalized reduced density matrix

$$\rho_\chi = \mathrm{tr}_{\mathsf{res}}\left\{e^{i\chi N}\rho^{\mathrm{tot}}\right\} = \rho + \sum_{k=1}^{\infty}\frac{(i\chi)^k}{k!}\mathcal{F}_k$$

Generalized master equation

$$\dot{\rho}_\chi = \mathcal{L}\rho_\chi + \left(e^{i\chi} - 1\right)\mathcal{J}^{+}\rho_\chi + \left(e^{-i\chi} - 1\right)\mathcal{J}^{-}\rho_\chi$$

Liouvillian

$$\mathcal{L}\rho = -\frac{i}{\hbar}\left[\boxed{\hat{H}_{\mathsf{TQD}}} + \boxed{\hat{H}_{\mathsf{LS}}}, \rho\right] + \boxed{\mathcal{L}_{\mathsf{tun}}}\rho$$

- orbital degeneracies require inclusion of coherences

Transport

Stationary solution[2]

$$\mathcal{L}\rho^{\infty} = 0$$

$$\mathcal{L}\mathcal{F}_{1\perp}^{\infty} = \left(-eI - \mathcal{J}^{+} + \mathcal{J}^{-}\right)\rho^{\infty}$$

with $\mathcal{F}_{1\perp} = (1 - \rho^{\infty}\mathrm{tr}_{\mathsf{TQD}})\mathcal{F}_1$

Current, noise and Fano factor

$$I = -e\partial_t \langle N \rangle = -e\mathrm{tr}_{\mathsf{TQD}}\left\{\left(\mathcal{J}^{+} - \mathcal{J}^{-}\right)\rho^{\infty}\right\}$$

$$S = e^2\partial_t\left(\langle N^2\rangle - \langle N\rangle^2\right)$$

$$= e^2\mathrm{tr}_{\mathsf{TQD}}\left\{2\left(\mathcal{J}^{+} - \mathcal{J}^{-}\right)\mathcal{F}_{1\perp}^{\infty} + \left(\mathcal{J}^{+} + \mathcal{J}^{-}\right)\rho^{\infty}\right\}$$

$$F = \frac{S}{e|I|}$$

---

[2] Kaiser and Kohler, *Ann. Phys*. **716**, 702 (2007)

Transport statistics

Fano factor

$F < 1$	$F = \frac{S}{e\lvert I\rvert}$	$F > 1$
	1	
Anti-bunching	Independent tunnelling events	Bunching
Sub-poissonian noise	Poissonian noise	Super-poissonian noise

Current stability diagram

$U = 5|b|$, $V = 2|b|$, $k_BT = 0.002|b|$, $k_BT = 20\Gamma$ and $b < 0$

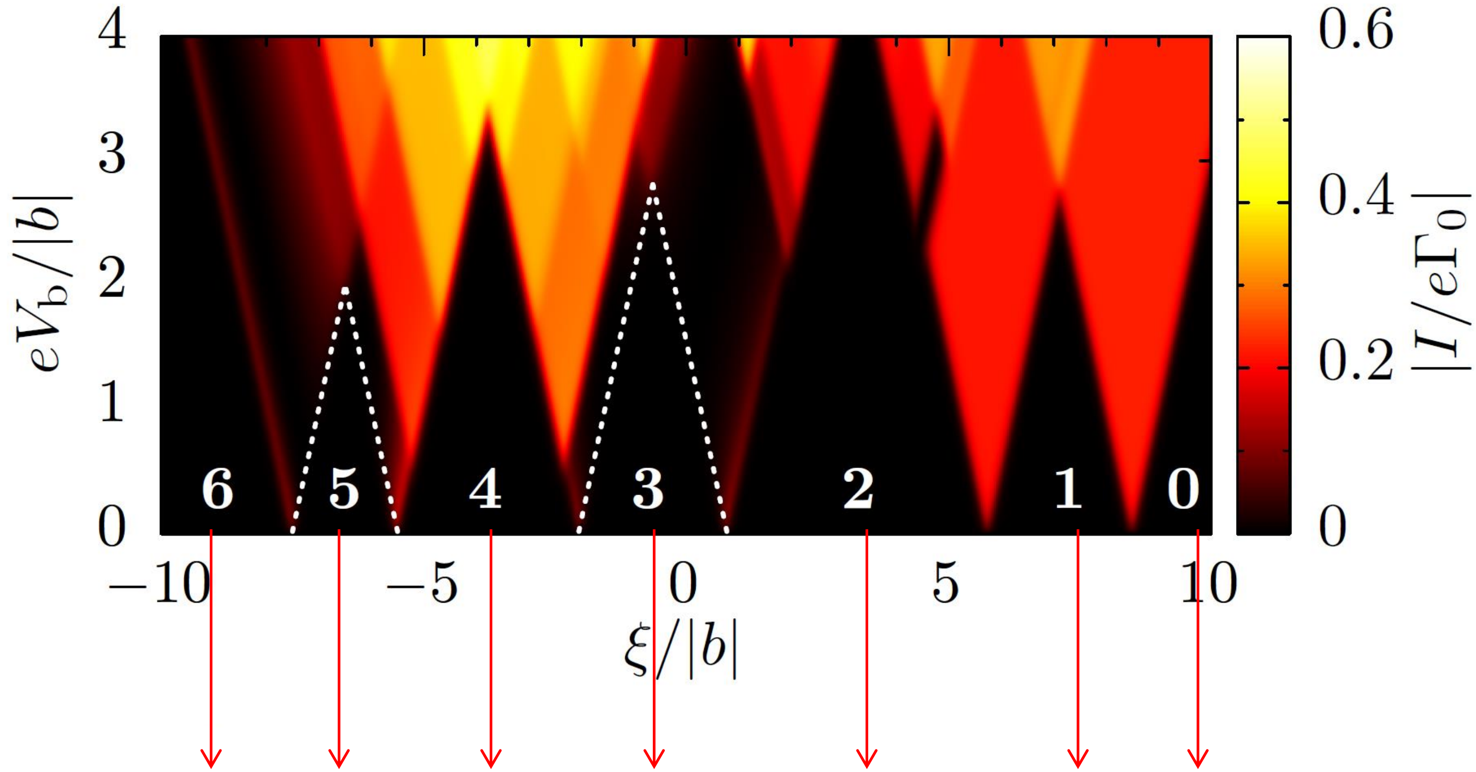

1x1 2x2 1x3 2x2 1x1 1x2 1x1

Orbital degeneracy
Spin degeneracy

Donarini, Begemann and Grifoni, *Nano Lett.* **9**, 2897 (2009)

Fano stability diagram

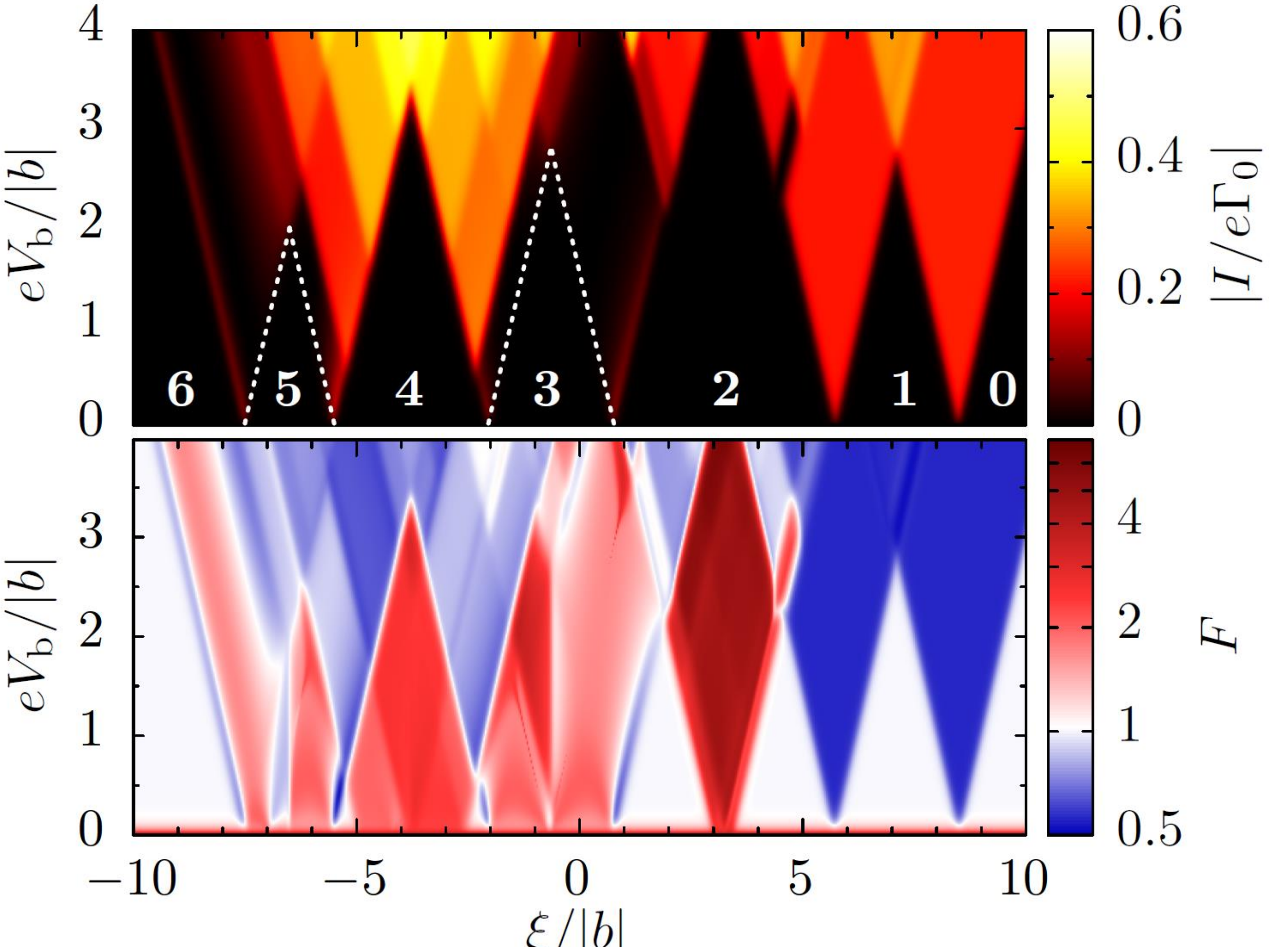

Niklas, Trottmann, Donarini and Grifoni, PRB **95**, 115133 (2017)

Fano without principal parts

Principal parts (H_{LS}) blur everything → solve without

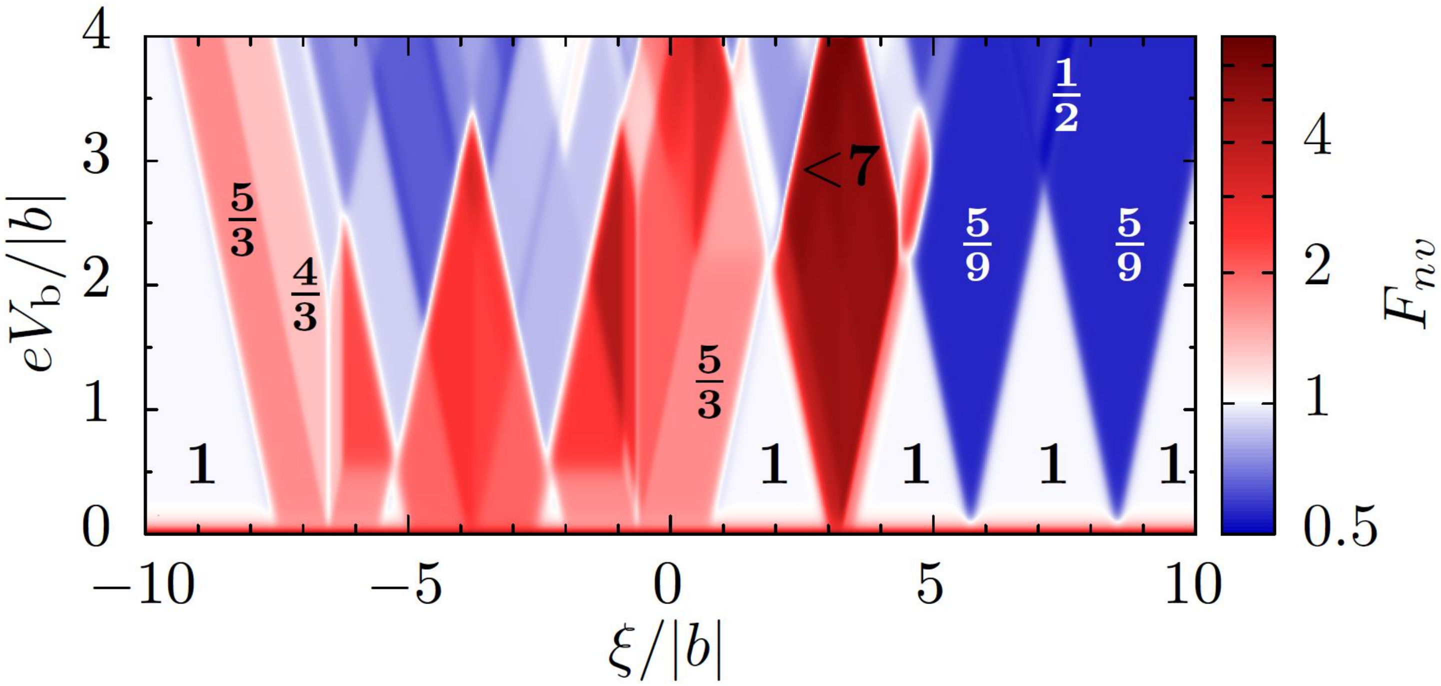

- clear polygons
- super-Poissonian noise ($F > 1$) indicates blocking

Niklas, Trottmann, Donarini and Grifoni, PRB **95**, 115133 (2017)

Fano without principal parts

Principal parts (H_{LS}) blur everything → solve without

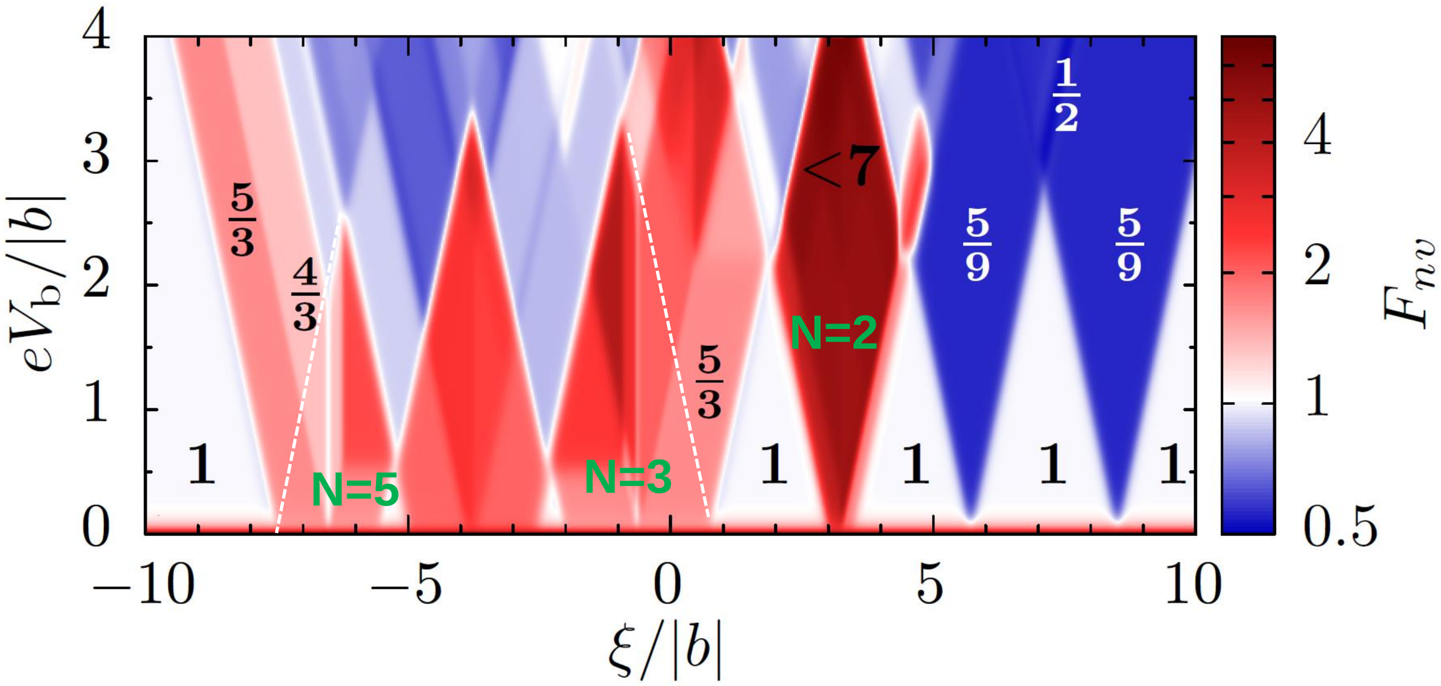

- clear polygons
- super-Poissonian noise ($F > 1$) indicates blocking

Niklas, Trottmann, Donarini and Grifoni, PRB **95**, 115133 (2017)

Blockade mechanisms

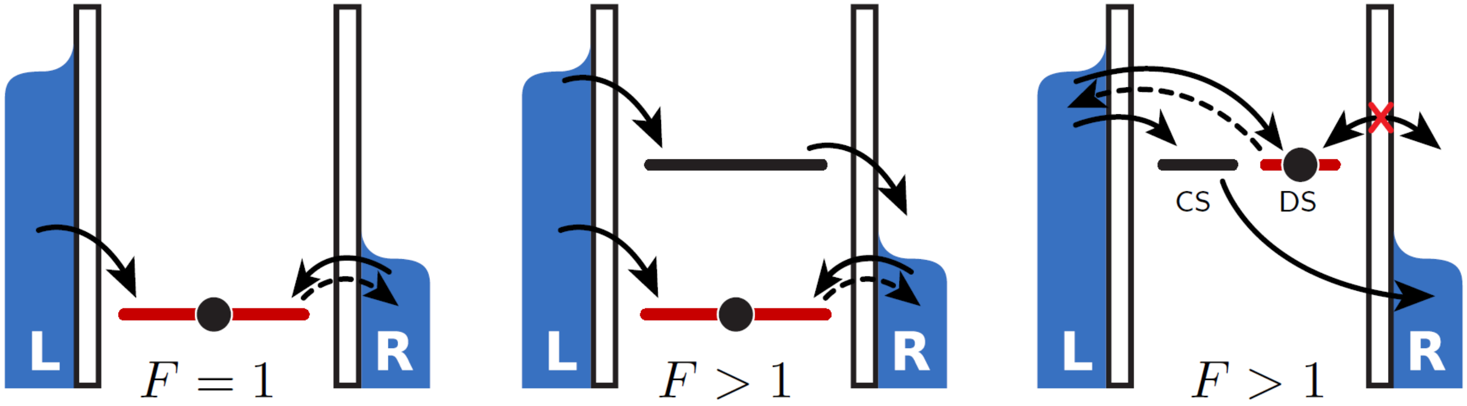

Coulomb blockade Channel blockade[5,6] Interference blockade

In both cases a **two effective channels model** provides the Fano factor

$$F_{nv} = 1 + \frac{2\Gamma_L^f}{\Gamma_L^s + \Gamma_R^s}, \qquad \mu_L > \mu_R$$

[5] Belzig, PRB **71**, 161301 (R) (2005), [6] Groth et al. PRB **74**, 125315 (2006)

Niklas, Trottmann, Donarini and Grifoni, PRB **95**, 115133 (2017)

Interference at the 2_0 <--> 3_0 resonance

$\Gamma_\alpha = \Gamma \mathcal{R}_\alpha$ and the rate matrices in

angular momentum basis

$$\mathcal{R}_L = \begin{pmatrix} 1 & e^{i\frac{2\pi}{3}} \\ e^{-i\frac{2\pi}{3}} & 1 \end{pmatrix}$$

$$\mathcal{R}_R = \begin{pmatrix} 1 & e^{-i\frac{2\pi}{3}} \\ e^{i\frac{2\pi}{3}} & 1 \end{pmatrix}$$

dark state basis

$$\mathcal{R}_L = \begin{pmatrix} \frac{3}{2} & -i\frac{\sqrt{3}}{2} \\ i\frac{\sqrt{3}}{2} & \frac{1}{2} \end{pmatrix}$$

$$\mathcal{R}_R = \begin{pmatrix} 0 & 0 \\ 0 & 2 \end{pmatrix}$$

$$F_{nv} = 1 + \frac{2\Gamma_L^f}{\Gamma_L^s + \Gamma_R^s}$$

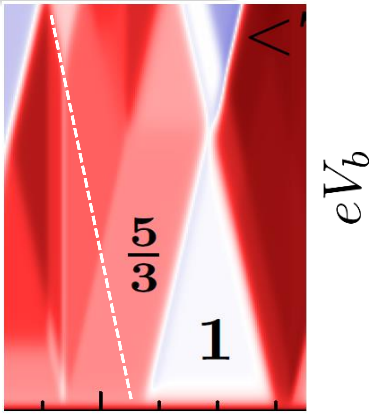

Interference at the 2_0 <--> 3_0 resonance

$\Gamma_\alpha = \Gamma \mathcal{R}_\alpha$ and the rate matrices in

angular momentum basis

$$\mathcal{R}_L = \begin{pmatrix} 1 & e^{i\frac{2\pi}{3}} \\ e^{-i\frac{2\pi}{3}} & 1 \end{pmatrix}$$

$$\mathcal{R}_R = \begin{pmatrix} 1 & e^{-i\frac{2\pi}{3}} \\ e^{i\frac{2\pi}{3}} & 1 \end{pmatrix}$$

dark state basis

$$\mathcal{R}_L = \begin{pmatrix} \frac{3}{2} & -i\frac{\sqrt{3}}{2} \\ i\frac{\sqrt{3}}{2} & \frac{1}{2} \end{pmatrix}$$

$$\mathcal{R}_R = \begin{pmatrix} 0 & 0 \\ 0 & 2 \end{pmatrix}$$

$$F_{nv} = 1 + \frac{2\Gamma_L^f}{\Gamma_L^s + \Gamma_R^s} = 1 + \frac{2\frac{1}{2}}{\frac{3}{2} + 0} = \frac{5}{3}$$

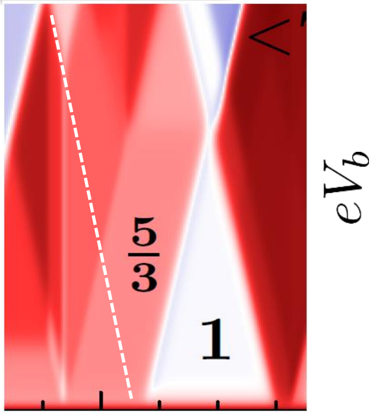

Lamb shift at the 5_0 <--> 6_0 resonance

$$H_{\mathrm{LS}} = \hbar \sum_\alpha \omega_\alpha \mathcal{R}_\alpha$$

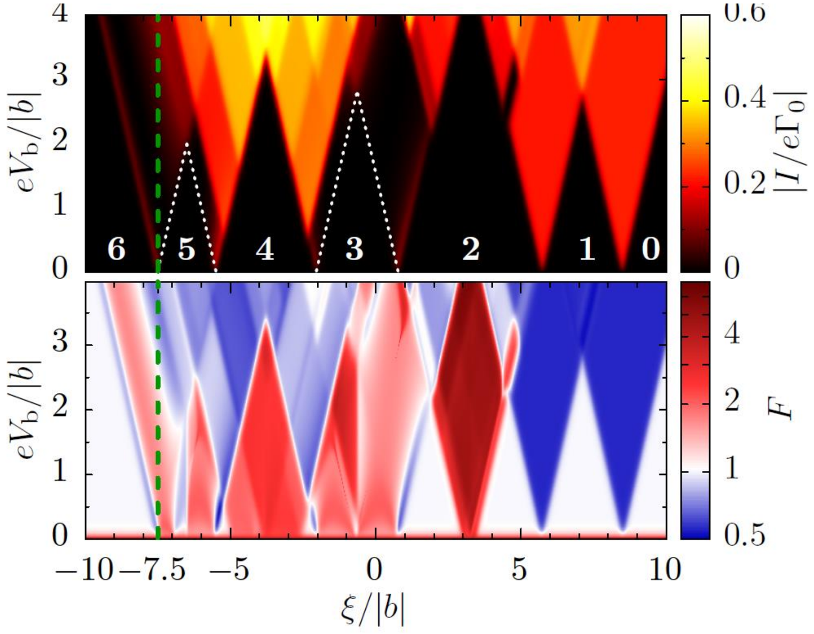

master equation

$$0 = -\frac{i}{\hbar}\left[H_{\mathrm{LS}}, \rho_5\right] + 2\Gamma \mathcal{R}_R \rho_6 - \frac{\Gamma}{2}\left\{\mathcal{R}_L, \rho_5\right\},$$

$$0 = \Gamma \mathrm{Tr}_{\mathrm{TQD}}\left(\mathcal{R}_L \rho_5\right) - 4\Gamma \rho_6$$

Lamb shift at the 5_0 <--> 6_0 resonance

$$\rho^{\infty}=\frac{1}{D}\begin{array}{cc}\left(\begin{array}{c}D-3\omega_R^2\\ 2\omega_R^2\\ \omega_R^2\\ -\sqrt{3}\omega_R(\Gamma-i2(\omega_L-\omega_R))\\ -\sqrt{3}\omega_R(\Gamma+i2(\omega_L-\omega_R))\end{array}\right) & \begin{array}{c}\rho^{dd}\\ \rho^{cc}\\ \rho^{6}\\ \rho^{dc}\\ \rho^{cd}\end{array}\end{array}$$

with $D = 2\Gamma^2 + 8\omega_L^2 - 12\omega_L\omega_R + 9\omega_R^2.$

$$I = -e4\Gamma\omega_R^2/3D$$

$$F = \frac{16\omega_R^2\left(2\Gamma^2+53\omega_L^2\right)-176\omega_L\omega_R\left(\Gamma^2+4\omega_L^2\right)}{3D^2} + \frac{20\left(\Gamma^2+4\omega_L^2\right)^2-576\omega_L\omega_R^3+195\omega_R^4}{3D^2}$$

Lamb shift → precession dynamics

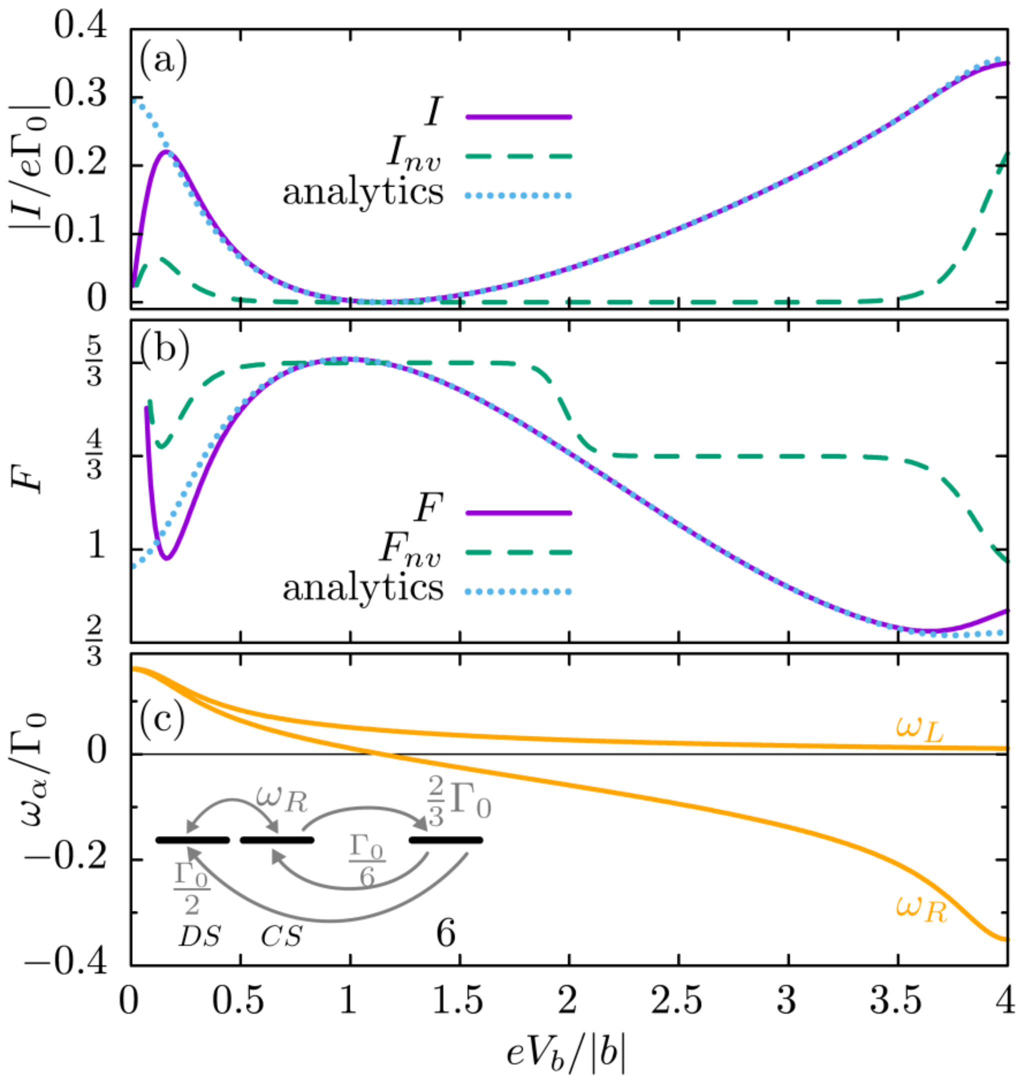

Robustness

We tested the robustness of the interference effects on the $5_0 \leftrightarrow 6$ transition against the perturbation

$$H_\Delta = \frac{1}{2}\begin{pmatrix} 0 & \Delta E \\ \Delta E & 0 \end{pmatrix}$$

and kept $\Delta E \ll k_B T$ to neglect modification of the tunnelling Liouvillean

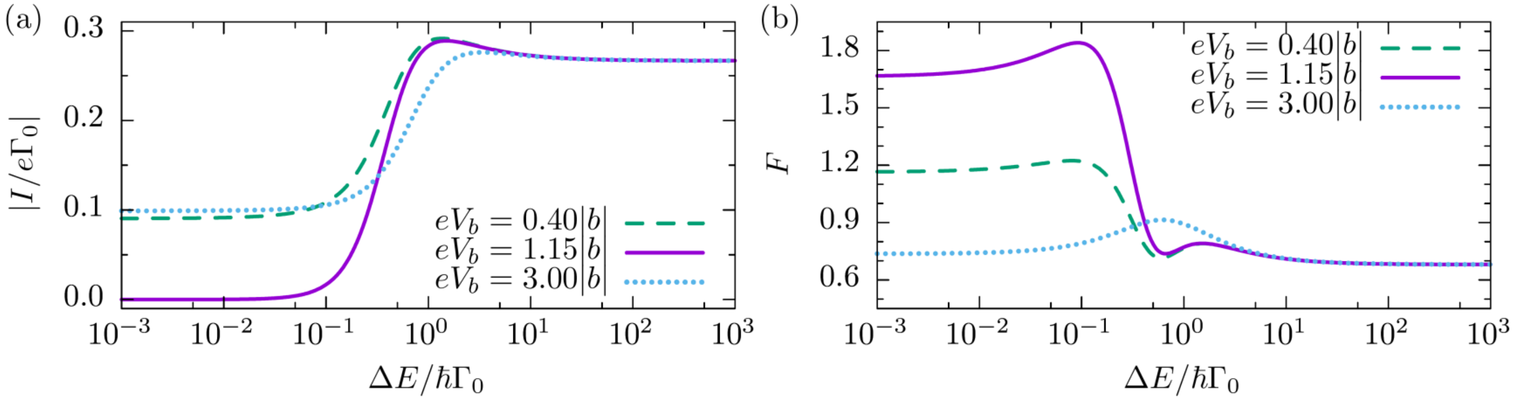

Conclusions

interference

Interference occurs when energetically equivalent paths involving degenerate states contribute to the dynamics

dark states

$$|2, \alpha_1; DS\rangle = \frac{1}{\sqrt{6}}$$

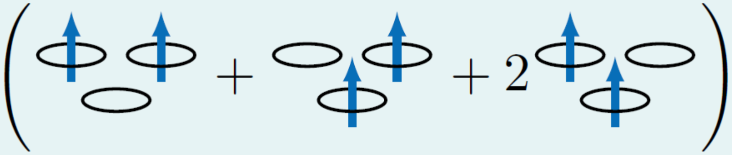

fingerprints of interference

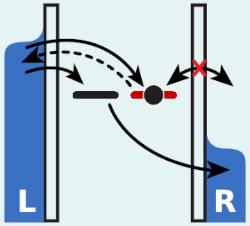

super-Poissonian Fano factors (e.g. $F = 5/3$) which indicate a characteristic bunching dynamics

and thanks to

Michael Nicklas

Andreas Trottmann

Andrea Donarini

SFB 689

GRK 1570

Lamb shift Hamiltonian

Hamiltonian

$$H_{\mathrm{LS}} = \hbar \sum_{\alpha} \omega_{\alpha} \mathcal{R}_{\alpha}$$

precession frequencies

The precession frequencies for the block $\rho^{N}(E^{*})$ with spin S is independent of S_z $(\omega_{\alpha,S_z} = \omega_{\alpha})$

$$\omega_{\alpha} = \frac{\Gamma_{0\alpha}}{2\pi} \sum_{\tau,E} \langle N, \alpha^{*}, L_z | d_{0\tau} \mathcal{P}_{N+1,E} d^{\dagger}_{0\tau} | N, \alpha^{*}, -L_z \rangle p_{\alpha}\left(E - E^{*}\right)$$
$$+ \langle N, \alpha^{*}, L_z | d^{\dagger}_{0\tau} \mathcal{P}_{N-1,E} d_{0\tau} | N, \alpha^{*}, -L_z \rangle p_{\alpha}\left(E^{*} - E\right)$$

- $\mathcal{P}_{NE} = \sum_{S_z, L_z} |N, E; S, S_z, L_z\rangle\langle N, E; S, S_z, L_z|$
- $p_{\alpha}\left(\Delta E\right) = -\operatorname{Re}\psi\left(\frac{1}{2} + i\frac{\Delta E - \mu_{\alpha}}{2\pi k_{\mathrm{B}} T}\right)$

Spectrum of the TQD

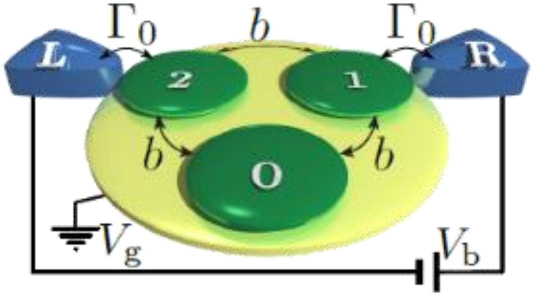

The single particle component of H_{TQD} is diagonalized by the angular momentum states

$$|l\rangle = \frac{1}{\sqrt{3}} \sum_{j=0}^{2} e^{-i\frac{2\pi}{3}lj} |j\rangle, \quad l = 0, \pm 1$$

The many-body states can be written in the basis

$$|n_{0\uparrow}, n_{1\uparrow}, n_{-1\uparrow}; n_{0\downarrow}, n_{1\downarrow}, n_{-1\downarrow}\rangle$$

H_{TQD} commutes with the operators

$$\left.\begin{aligned}
N &= \textstyle\sum_{l\sigma} n_{l\sigma} \\
S^2 &= \textstyle\sum_{i\,l\sigma\sigma'} (d^\dagger_{l\sigma} s^i_{\sigma\sigma'} d_{l\sigma'})^2 \\
S_z &= \frac{\hbar}{2} \sum_{l\sigma} \sigma n_{l\sigma} \\
L_z &= \hbar \sum_{l\sigma} l n_{l\sigma} |_{\mathrm{mod}\ 3}
\end{aligned}\right\}$$

By exploiting these symmetries we diagonalize analytically H_{TQD} and obtain the eigenstates

$$|N, E; S, S_z, L_z\rangle$$

Symmetry protected degeneracies are associated to the group of the Hamiltonian

$$\mathrm{C}_{3v} \otimes \mathrm{SU}(2)$$

Generalized Landauer formula for time-dependent potentials and zero–bias dc current

Shmuel Gurvitz

Weizmann Institute of Science, Rehovot 7610001, Israel

based on: “Single-electron approach to electron transport”
S.G. Physica Scripta, **T165**, 014013 (2015);
S.G., A. Aharony and O. Entin-Wohlman, Phys. Rev. **B94**, 075437 (2016);
S.G., to be submitted.

Generalized Landauer formula for time-dependent potentials and zero–bias dc current

Shmuel Gurvitz

Weizmann Institute of Science, Rehovot 7610001, Israel

based on: “Single-electron approach to electron transport”
S.G. Physica Scripta, **T165**, 014013 (2015);
S.G., A. Aharony and O. Entin-Wohlman, Phys. Rev. **B94**, 075437 (2016);
S.G., to be submitted.
Earlier works:
I. Bar-Joseph and S.G., Phys. Rev. **B44**, 3332 (1991),
S.G., Phys. Rev, **B44**, 11924 (1991),
F. Li, Xin-Qi Li, Wei-Min Zhang, and S.G., Europhysics Letters, **88**, 37001 (2009).

Zero-bias current

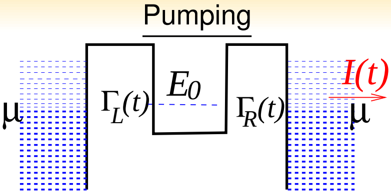

$\Gamma_{L,R}(t) = \Gamma[1 \pm \xi \sin(\omega t)]^2$

Adiabatic limit: $\omega \to 0$

$$I(t) = -\frac{2\mu\,\Gamma\,\xi\,\omega}{\pi(4\mu^2 + \Gamma^2)} + O\left[\left(\frac{\omega}{\Gamma}\right)^3 (\Gamma t)\right]$$

Zero-bias current

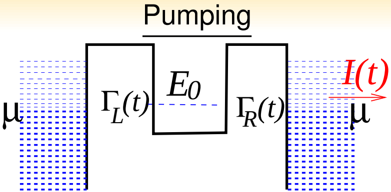

$$\Gamma_{L,R}(t) = \Gamma[1 \pm \xi \sin(\omega t)]^2$$

Adiabatic limit: $\omega \to 0$

$$I(t) = -\frac{2\mu\,\Gamma\,\xi\,\omega}{\pi(4\mu^2 + \Gamma^2)} + O\left[\left(\frac{\omega}{\Gamma}\right)^3 (\Gamma t)\right]$$

Exact time-dependent current $I(t)$ (solid lines) and the adiabatic limit (dashed lines) for $\xi = 0.2$, $\mu = 0.25\,\Gamma$ and two values of oscillation frequency: $\omega = 0.02\,\Gamma$ (blue) and $\omega = 0.05\Gamma$ (red) (S.G. Physica Scripta, **T165**, 014013 (2015)).

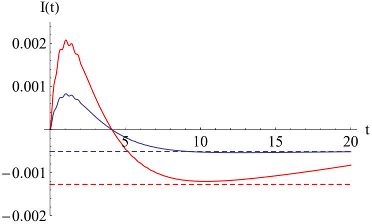

Zero-bias current

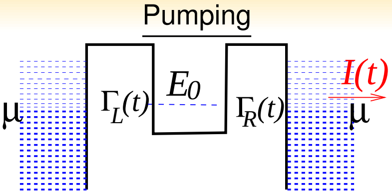

$$\Gamma_{L,R}(t) = \Gamma[1 \pm \xi \sin(\omega t)]^2$$

Adiabatic limit: $\omega \to 0$

$$I(t) = -\frac{2\mu\,\Gamma\,\xi\,\omega}{\pi(4\mu^2 + \Gamma^2)} + O\left[\left(\frac{\omega}{\Gamma}\right)^3 (\Gamma t)\right]$$

Exact time-dependent current $I(t)$ (solid lines) and the adiabatic limit (dashed lines) for $\xi = 0.2$, $\mu = 0.25\,\Gamma$ and two values of oscillation frequency: $\omega = 0.02\,\Gamma$ (blue) and $\omega = 0.05\Gamma$ (red) (S.G. Physica Scripta, **T165**, 014013 (2015)).

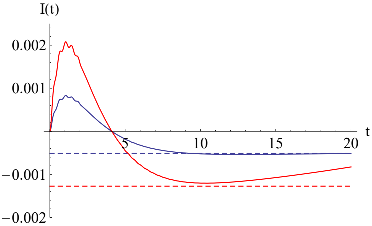

Is it possible to find steady-state zero-bias current for time-dependent Hamiltonian?

Resonant tunneling under the noise

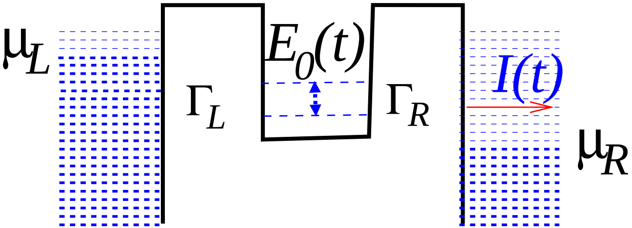

The level $E_0(t)$ randomly fluctuates: $E_0(t) = \bar{E}_0 + \frac{U}{2}\xi(t)$, where $\xi(t) = \pm 1$. The current $I(t)$, averaged over the noise, reaches its steady-state, $\langle I(t \to \infty)\rangle = \bar{I}$. However, $\bar{I} \to 0$ for $\mu_L - \mu_R \to 0$. No zero-bias current.

Double-dot under the noise

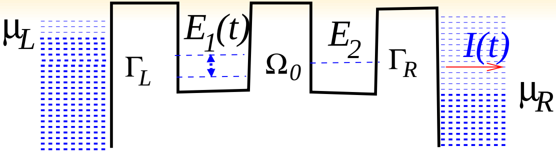

In contrast with the previous case, the steady-state current, averaged over the noise, $\bar{I} = \langle I(t \to \infty) \rangle$, survives at zero bias,

$\boxed{\bar{I} \neq 0 \text{ when } \mu_L - \mu_R \to 0}$

Double-dot under the noise

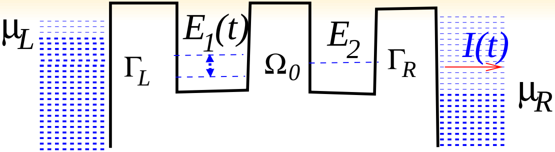

In contrast with the previous case, the steady-state current, averaged over the noise, $\bar{I} = \langle I(t \to \infty) \rangle$, survives at zero bias,

$\boxed{\bar{I} \neq 0 \text{ when } \mu_L - \mu_R \to 0}$

It happens when the transport takes place via a linear superposition of different isolate states of the system, which is destroyed by the noise (decoherence).

Double-dot under the noise

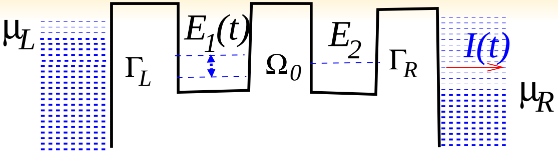

In contrast with the previous case, the steady-state current, averaged over the noise, $\bar{I} = \langle I(t \to \infty) \rangle$, survives at zero bias,

$\boxed{\bar{I} \neq 0 \text{ when } \mu_L - \mu_R \to 0}$

It happens when the transport takes place via a linear superposition of different isolate states of the system, which is destroyed by the noise (decoherence).This in its turn, generate violation of the time-reversal symmetry: $\bar{T}_{L\to R} \neq \bar{T}_{R\to L}$ where $\bar{T}_{L\to R}$ and $\bar{T}_{R\to L}$ are the transmission probabilities from left-to-right and right-to-left leads, averaged over the noise. As a result, the zero bias current would appear.

Particular realization of the noise-source

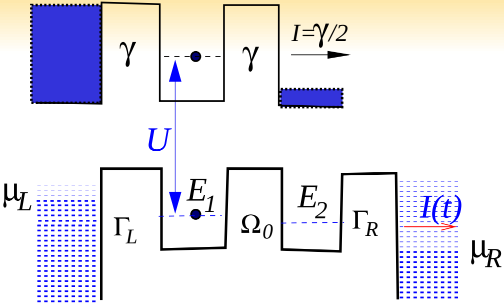

Here γ is the tunneling rate for electrons entering the upper dot and leaving it. Electron in the upper dot interacts (capacitively) with electron, occupying the left site of the double-dot. As a result, the energy energy in the left site fluctuates randomly between E_1 and $E_1 + U$.

Particular realization of the noise-source

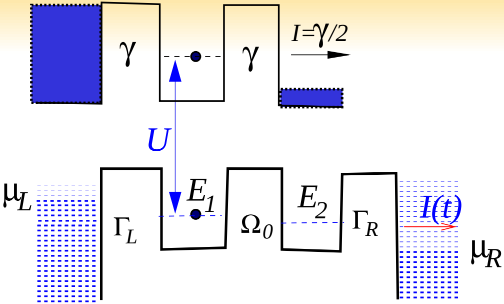

Here γ is the tunneling rate for electrons entering the upper dot and leaving it. Electron in the upper dot interacts (capacitively) with electron, occupying the left site of the double-dot. As a result, the energy energy in the left site fluctuates randomly between E_1 and $E_1 + U$.

The set-up may resemble the Coulomb drag. However, direction of the zero-bias current is determined by the double-dot parameters only, and not related to the noise source.

Another examples

Two dots on the Aharonov-Bohm ring

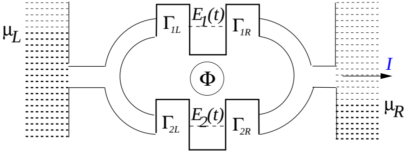

Zero bias current appears due to decoherence, destroying the linear superposition of two dots states.

Another examples

Two dots on the Aharonov-Bohm ring

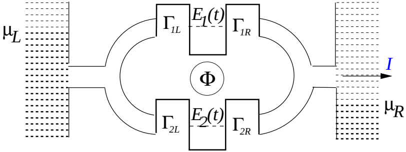

Zero bias current appears due to decoherence, destroying the linear superposition of two dots states.

One dots on the Aharonov-Bohm ring

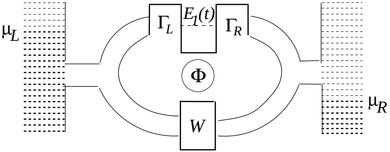

No zero bias current, since there is no states in linear superposition inside the system.

Landauer formula (steady-state)

$$I = \frac{1}{2\pi}\int_{-\infty}^{\infty} T(E)\Big[f_L(\mu_L, E) - f_R(\mu_R, E)\Big]dE$$

where $f_{L,R}(\mu_{L,R}, E)$ are the Fermi functions and $T(E)$ is the transmission probability. For the resonant tunneling:

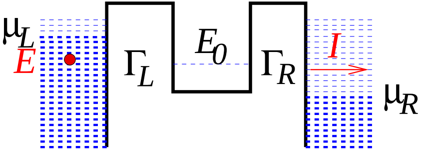

$$T(E) = \frac{\Gamma_L \Gamma_R}{(E - E_0)^2 + \frac{\Gamma^2}{4}}$$

Landauer formula (steady-state)

$$I = \frac{1}{2\pi} \int_{-\infty}^{\infty} T(E)\Big[f_L(\mu_L, E) - f_R(\mu_R, E)\Big] dE$$

where $f_{L,R}(\mu_{L,R}, E)$ are the Fermi functions and $T(E)$ is the transmission probability. For the resonant tunneling:

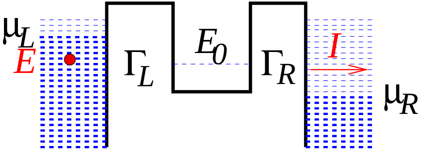

$$T(E) = \frac{\Gamma_L \Gamma_R}{(E - E_0)^2 + \frac{\Gamma^2}{4}}$$

Problem with the Pauli exclusion principle:

On first sight the Landauer (scattering) approach does not prevent simultaneous occupation of the level E_0 by two or more electrons.

Single-Electron Approach

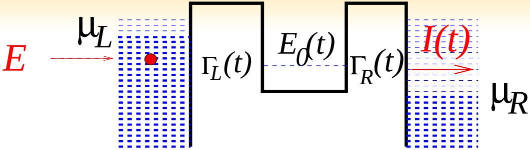

Modified Landauer formula for time-dependent potentials

$$I(t) = \frac{1}{2\pi} \int_{-\infty}^{\infty} \left[T_{L\to R}(E,t) f_L(\mu_L, E) - T_{R\to L}(E,t) f_R(\mu_R, E) \right] dE$$

$T_{L\to R}(E,t)$ and $T_{R\to L}(E,t)$ are the transmission probabilities of a single electron from the left-to-right and right-to-left leads, respectively, at time t, where E is the electron *initial* energy (at $t = 0$) in the left or the right lead.

Comparison with Landauer formula for zero temperature

Modified Landauer formula for time-dependent potentials

$$I(t) = \int_{-\infty}^{\mu_L} T_{L\to R}(E,t)\frac{dE}{2\pi} - \int_{-\infty}^{\mu_R} T_{R\to L}(E,t)\frac{dE}{2\pi}$$

Landauer formula for time-independent potentials (steady state)

$$I = \int_{\mu_R}^{\mu_L} T(E)\frac{dE}{2\pi}$$

If for the steady-state the time-reversal symmetry holds, $T_{L\to R}(E, t\to\infty) = T_{R\to L}(E, t\to\infty) = T(E)$, the both expressions coincide.

Modified Landauer formula, averaged over the noise

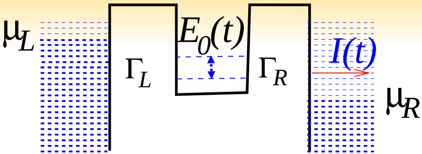

$E_0(t) = \bar{E}_0 + \frac{U}{2}\xi(t)$, where
$\xi(t) = \pm 1$.
The noise correlator:
$\langle \xi(t_1)\xi(t_2)\rangle = \exp(-\gamma|t_1 - t_2|)$

$$\langle I(t)\rangle = \frac{1}{2\pi}\int_{-\infty}^{\infty}\Big[\langle T_{L\to R}(E,t)\rangle f_L(\mu_L, E) - \langle T_{R\to L}(E,t)\rangle f_R(\mu_R, E)\Big]dE$$

Modified Landauer formula, averaged over the noise

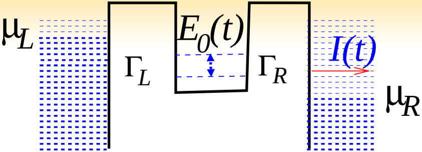

$E_0(t) = \bar{E}_0 + \frac{U}{2}\xi(t)$, where
$\xi(t) = \pm 1$.
The noise correlator:
$\langle \xi(t_1)\xi(t_2) \rangle = \exp(-\gamma |t_1 - t_2|)$

$$\langle I(t) \rangle = \frac{1}{2\pi} \int\limits_{-\infty}^{\infty} \Big[\langle T_{L \to R}(E,t) \rangle f_L(\mu_L, E) - \langle T_{R \to L}(E,t) \rangle f_R(\mu_R, E) \Big] dE$$

In the steady-state limit: $\bar{I} = \langle I(t \to \infty) \rangle, \quad \bar{T}(E) = \langle T(E, t \to \infty) \rangle$

$$\bar{I} = \frac{1}{2\pi} \int\limits_{-\infty}^{\infty} \Big[\bar{T}_{L \to R}(E) f_L(\mu_L, E) - \bar{T}_{R \to L}(E) f_R(\mu_R, E) \Big] dE$$

Noise does not violate the time-reversal symmetry:
$\bar{T}_{L \to R}(E) = \bar{T}_{R \to L}(E)$. As a result: $\bar{I} = 0$ for zero bias, $\mu_L = \mu_R$.

Double-dot under the noise (steady-state current)

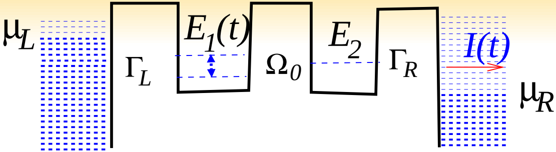

$$\bar{I} = \frac{1}{2\pi}\int_{-\infty}^{\infty}\left[\bar{T}_{L\to R}(E) f_L(\mu_L, E) - \bar{T}_{R\to L}(E) f_R(\mu_R, E)\right] dE$$

Noise *violates* the time-reversal symmetry: $\boxed{\bar{T}_{L\to R}(E) \neq \bar{T}_{R\to L}(E)}$
As a result, zero bias current appears:

$$\bar{I}_{zb} = \frac{1}{2\pi}\int_{-\infty}^{\infty}\left[\bar{T}_{L\to R}(E) - \bar{T}_{R\to L}(E)\right] f(\mu, E)\, dE$$

where $\mu_L = \mu_R = \mu$ and $f_L(\mu_L, E) = f_R(\mu_R, E) = f(\mu, E)$.

Double-dot under the noise (steady-state current)

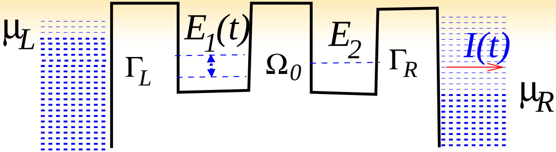

$$\bar{I} = \frac{1}{2\pi}\int_{-\infty}^{\infty}\left[\bar{T}_{L\to R}(E)f_L(\mu_L, E) - \bar{T}_{R\to L}(E)f_R(\mu_R, E)\right]dE$$

Noise *violates* the time-reversal symmetry: $\boxed{\bar{T}_{L\to R}(E) \neq \bar{T}_{R\to L}(E)}$
As a result, zero bias current appears:

$$\bar{I}_{zb} = \frac{1}{2\pi}\int_{-\infty}^{\infty}\left[\bar{T}_{L\to R}(E) - \bar{T}_{R\to L}(E)\right]f(\mu, E)dE$$

where $\mu_L = \mu_R = \mu$ and $f_L(\mu_L, E) = f_R(\mu_R, E) = f(\mu, E)$.
Why it is different from the current through a single dot?

Comparison with a single dot.

$$\bar{I}_{zb} = \frac{1}{2\pi}\int\limits_{-\infty}^{\infty}\left[\bar{T}_{L\to R}(E) - \bar{T}_{R\to L}(E)\right] f(\mu, E)dE$$

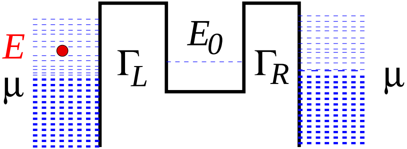

$\bar{T}_{L\to R}(E) = q_0^{(L)}(E)\Gamma_R$
$\bar{T}_{R\to L}(E) = q_0^{(R)}(E)\Gamma_L$ where $q_0^{(L,R)}(E)$ are occupation of the dot for electrons, coming from left and right leads.

Without the noise

$$q_0^{(L)}(E) = \frac{\Gamma_L}{(E-E_0)^2 + \frac{\Gamma^2}{4}}, \quad q_0^{(R)}(E) = \frac{\Gamma_R}{(E-E_0)^2 + \frac{\Gamma^2}{4}}$$

Comparison with a single dot.

$$\bar{I}_{zb} = \frac{1}{2\pi}\int_{-\infty}^{\infty}\left[\bar{T}_{L\to R}(E) - \bar{T}_{R\to L}(E)\right] f(\mu, E)\,dE$$

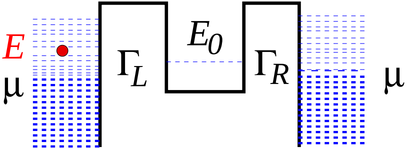

$\bar{T}_{L\to R}(E) = q_0^{(L)}(E)\Gamma_R$
$\bar{T}_{R\to L}(E) = q_0^{(R)}(E)\Gamma_L$ where $q_0^{(L,R)}(E)$ are occupation of the dot for electrons, coming from left and right leads.

Without the noise

$$q_0^{(L)}(E) = \frac{\Gamma_L}{(E-E_0)^2 + \frac{\Gamma^2}{4}}, \quad q_0^{(R)}(E) = \frac{\Gamma_R}{(E-E_0)^2 + \frac{\Gamma^2}{4}}$$

For *asymmetric* dot ($\Gamma_L \neq \Gamma_R$), occupations probabilities ($q_0^{(L,R)}$) are different. However, transmission probabilities remain symmetric under the time-reversal, $\bar{T}_{L\to R}(E) = \bar{T}_{R\to L}(E) = \bar{T}(E)$. This also holds in the presence of noise, since the noise only fluctuates the energy E_0, whereas $\Gamma_{L,R}$ are energy independent (wide-band limit).

Double-dot under the noise

$$\bar{I}_{zb} = \frac{1}{2\pi}\int\limits_{-\infty}^{\infty}\Big[\bar{T}_{L\to R}(E) - \bar{T}_{R\to L}(E)\Big] f(\mu,E)\,dE$$

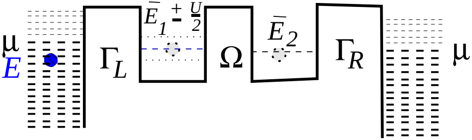

Electron inside the system, is in the linear superposition of the two-dot states.

The off-diagonal density-matrix element (coherency) $q_{12}^{(L,R)}(E)$ determines the electron current through the system.

$T_{L\to R} = 2\Gamma_L\Omega\,\mathrm{Im}[q_{12}^{(L)}]$, $\quad T_{R\to L} = -2\Gamma_R\Omega\,\mathrm{Im}[q_{12}^{(R)}]$. Without noise, $\Gamma_L\,\mathrm{Im}[q_{12}^{(L)}] + \Gamma_R\,\mathrm{Im}[q_{12}^{(R)}] = 0$, so that: $T_{L\to R} = T_{R\to L}$.

Double-dot under the noise

$$\bar{I}_{zb} = \frac{1}{2\pi}\int_{-\infty}^{\infty}\Big[\bar{T}_{L\to R}(E) - \bar{T}_{R\to L}(E)\Big]f(\mu, E)dE$$

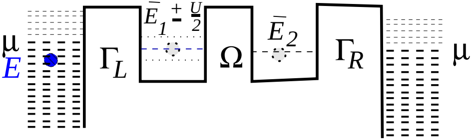

Electron inside the system, is in the linear superposition of the two-dot states.

The off-diagonal density-matrix element (coherency) $q_{12}^{(L,R)}(E)$ determines the electron current through the system.

$T_{L\to R} = 2\Gamma_L\Omega\,\mathrm{Im}[q_{12}^{(L)}]$, $T_{R\to L} = -2\Gamma_R\Omega\,\mathrm{Im}[q_{12}^{(R)}]$. Without noise, $\Gamma_L\,\mathrm{Im}[q_{12}^{(L)}] + \Gamma_R\,\mathrm{Im}[q_{12}^{(R)}] = 0$, so that: $T_{L\to R} = T_{R\to L}$.

The noise produces decoherence, which destroys coherency during infinite time. However, the noise acts finite time, when the first dot is occupied. Therefore decoherence is not complete. Since the occupation $q_1^{(L)} \neq q_1^{(R)}$, decoherence is different for electron coming from left or right lead. Hence, $\bar{T}_{L\to R} \neq \bar{T}_{R\to L}$.

Double-dot under the noise

$$\bar{I}_{zb} = \frac{1}{2\pi}\int\limits_{-\infty}^{\infty}\Big[\bar{T}_{L\to R}(E) - \bar{T}_{R\to L}(E)\Big] f(\mu, E)dE$$

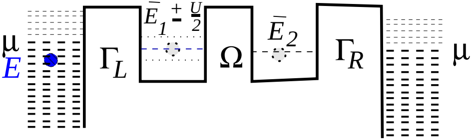

Electron inside the system, is in the linear superposition of the two-dot states.

The off-diagonal density-matrix element (coherency) $q_{12}^{(L,R)}(E)$ determines the electron current through the system.
$T_{L\to R} = 2\Gamma_L\Omega\,\mathrm{Im}[q_{12}^{(L)}]$, $T_{R\to L} = -2\Gamma_R\Omega\,\mathrm{Im}[q_{12}^{(R)}]$. Without noise, $\Gamma_L\,\mathrm{Im}[q_{12}^{(L)}] + \Gamma_R\,\mathrm{Im}[q_{12}^{(R)}] = 0$, so that: $T_{L\to R} = T_{R\to L}$.
The noise produces decoherence, which destroys coherency during infinite time. However, the noise acts finite time, when the first dot is occupied. Therefore decoherence is not complete. Since the occupation $q_1^{(L)} \neq q_1^{(R)}$, decoherence is different for electron coming from left or right lead. Hence, $\bar{T}_{L\to R} \neq \bar{T}_{R\to L}$. The time-reversal symmetry is broken!

Time-reversal symmetry (no noise)

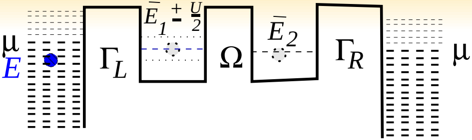

$E_0(t) = \bar{E}_0 + \frac{U}{2}\xi(t)$, where $\xi(t) = \pm 1$.

The noise correlator:

$\langle \xi(t_1)\xi(t_2) \rangle = \exp(-\gamma|t_1 - t_2|)$

Time-reversal symmetry (no noise)

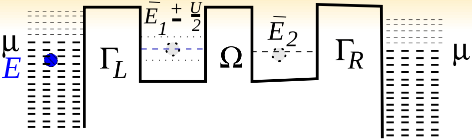

$E_0(t) = \bar{E}_0 + \frac{U}{2}\xi(t)$, where
$\xi(t) = \pm 1$.
The noise correlator:
$\langle \xi(t_1)\xi(t_2)\rangle = \exp(-\gamma|t_1 - t_2|)$

No-noise $\underline{\gamma = 0}$; $\mu = -1, \Gamma_L = \Gamma_R = 1, U = 1, E_{1,2} = \pm 1/2$

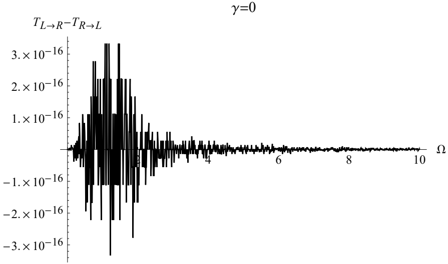

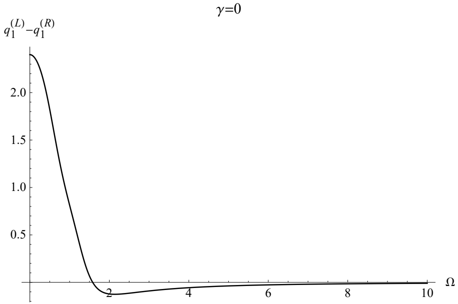

Time-reversal symmetry violation due to noise

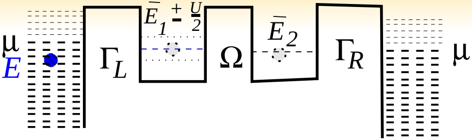

$E_0(t) = \bar{E}_0 + \frac{U}{2}\xi(t)$, where $\xi(t) = \pm 1$.

The noise correlator:

$\langle \xi(t_1)\xi(t_2) \rangle = \exp(-\gamma|t_1 - t_2|)$

Time-reversal symmetry violation due to noise

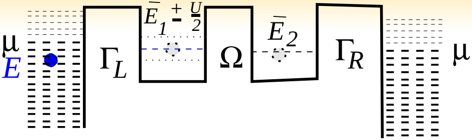

$E_0(t) = \bar{E}_0 + \frac{U}{2}\xi(t)$, where

$\xi(t) = \pm 1$.

The noise correlator:

$\langle \xi(t_1)\xi(t_2) \rangle = \exp(-\gamma|t_1 - t_2|)$

With noise $\underline{\gamma = 1}$; $\mu = -1, \Gamma_L = \Gamma_R = 1, U = 1, E_{1,2} = \pm 1/2$

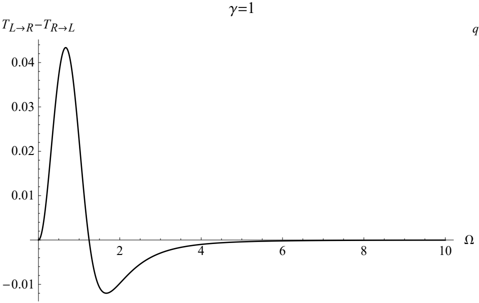

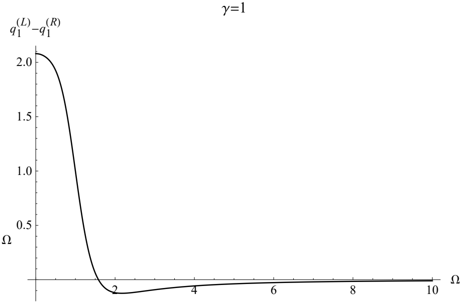

Derivation of the single-particle approach

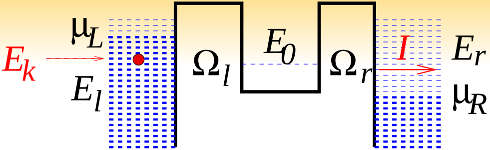

Derivation of the single-particle approach

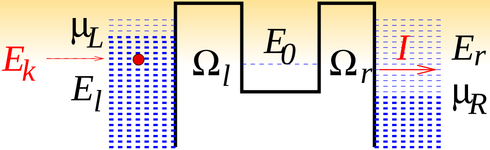

The (time-dependent) Hamiltonian:

$$H(t) = \sum_l E_l \hat{c}_l^\dagger \hat{c}_l + \sum_r E_r \hat{c}_r^\dagger \hat{c}_r + E_0(t)\hat{c}_0^\dagger \hat{c}_0 + \Big(\sum_l \Omega_l(t)\hat{c}_l^\dagger \hat{c}_0$$

$$+ \sum_r \Omega_r(t)\hat{c}_r^\dagger \hat{c}_0 + H.c.\Big)$$

The initial state: $|\Psi(0)\rangle = \prod_k \hat{c}_k^\dagger |0\rangle$, where $k \in \{E_l \le \mu_L, E_r \le \mu_R\}$.

Derivation of the single-particle approach

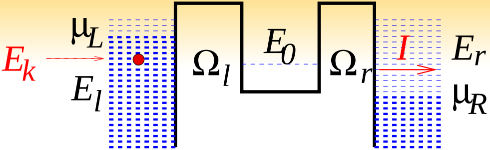

The (time-dependent) Hamiltonian:

$$H(t) = \sum_l E_l \hat{c}_l^\dagger \hat{c}_l + \sum_r E_r \hat{c}_r^\dagger \hat{c}_r + E_0(t) \hat{c}_0^\dagger \hat{c}_0 + \Big(\sum_l \Omega_l(t) \hat{c}_l^\dagger \hat{c}_0 + \sum_r \Omega_r(t) \hat{c}_r^\dagger \hat{c}_0 + H.c. \Big)$$

The initial state: $|\Psi(0)\rangle = \prod_k \hat{c}_k^\dagger |0\rangle$, where $k \in \{E_l \le \mu_L, E_r \le \mu_R\}$.

The Anzatz: $|\Psi(t)\rangle = \prod_k \hat{\Phi}^{(k)}(t)|0\rangle$

where $\boxed{\hat{\Phi}^{(k)}(t) = \sum_l b_l^{(k)}(t)\, \hat{c}_l^\dagger + b_0^{(k)}(t)\, \hat{c}_0^\dagger + \sum_r b_r^{(k)}(t)\, \hat{c}_r^\dagger}$

Substituting $|\Psi(t)\rangle$ in the Schrödinger equation $i\partial_t |\Psi(t)\rangle = H(t)|\Psi(t)\rangle$, we find a set of couples equations for the amplitudes $b_j^{(k)}(t)$.

Derivation of the single-particle approach

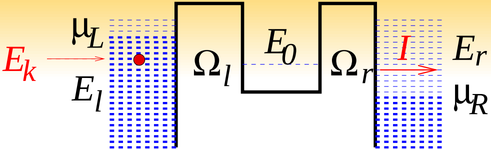

The initial state: $|\Psi(0)\rangle = \prod_k \hat{c}_k^\dagger|0\rangle$, where $k \in \{E_l \le \mu_L\,, E_r \le \mu_R\}$.

The Anzatz: $|\Psi(t)\rangle = \prod_k \hat{\Phi}^{(k)}(t)|0\rangle$

where $\boxed{\hat{\Phi}^{(k)}(t) = \sum_l b_l^{(k)}(t)\,\hat{c}_l^\dagger + b_0^{(k)}(t)\,\hat{c}_0^\dagger + \sum_r b_r^{(k)}(t)\,\hat{c}_r^\dagger}$

Substituting $|\Psi(t)\rangle$ into $i\partial_t|\Psi(t)\rangle = H(t)|\Psi(t)\rangle$, we find

$$i\dot{b}_l^{(k)}(t) = E_l\, b_l^{(k)}(t) + \Omega_l(t)\, b_0^{(k)}(t)$$

$$i\dot{b}_0^{(k)}(t) = E_0(t)\, b_0^{(k)}(t) + \sum_l \Omega_l(t)\, b_l^{(k)}(t) + \sum_r \Omega_r(t)\, b_r^{(k)}(t)$$

$$i\dot{b}_r^{(k)}(t) = E_r\, b_r^{(k)}(t) + \Omega_r(t)\, b_0^{(k)}(t)$$

The states with different k are decoupled!

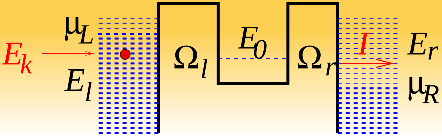

$$\boxed{|\Psi(t)\rangle = \prod_k \Big[\sum_l b_l^{(k)}(t)\, \hat{c}_l^\dagger + b_0^{(k)}(t)\, \hat{c}_0^\dagger + \sum_r b_r^{(k)}(t)\, \hat{c}_r^\dagger \Big] |0\rangle}$$

$$i\dot{b}_l^{(k)}(t) = E_l\, b_l^{(k)}(t) + \Omega_l(t)\, b_0^{(k)}(t)$$

$$i\dot{b}_0^{(k)}(t) = E_0(t)\, b_0^{(k)}(t) + \sum_l \Omega_l(t)\, b_l^{(k)}(t) + \sum_r \Omega_r(t)\, b_r^{(k)}(t)$$

$$i\dot{b}_r^{(k)}(t) = E_r\, b_r^{(k)}(t) + \Omega_r(t)\, b_0^{(k)}(t)$$

The average charge in the right (left) reservoir: $Q_{R(L)}(t)$, and inside the quantum dot, $Q_0(t)$ are given by

$$Q_{R(L)}(t) = \langle \Psi(t)| \sum_{r(l)} \hat{c}_{r(l)}^\dagger \hat{c}_{r(l)} |\Psi(t)\rangle = \sum_k \sum_{r(l)} |b_{r(l)}^{(k)}(t)|^2$$

$$Q_0(t) = \langle \Psi(t)| \hat{c}_0^\dagger \hat{c}_0 |\Psi(t)\rangle = \sum_k |b_0^{(k)}(t)|^2$$

Sum over (l, r) takes place over all reservoir states.

Solution of the single-electron equations

$$i\dot{b}_l^{(k)}(t) = E_l\, b_l^{(k)}(t) + \Omega_L(t)\, b_0^{(k)}(t)$$

$$i\dot{b}_0^{(k)}(t) = E_0(t)\, b_0^{(k)}(t) + \sum_l \Omega_L(t)\, b_l^{(k)}(t) + \sum_r \Omega_R(t)\, b_r^{(k)}(t)$$

$$i\dot{b}_r^{(k)}(t) = E_r\, b_r^{(k)}(t) + \Omega_R(t)\, b_0^{(k)}(t)$$

From the first equation

$$b_l^{(k)}(t) = e^{-iE_l t}\Big[\delta_{kl} - \int_0^t i\,\Omega_l(t')b_0^{(k)}(t')e^{iE_l t'}\,dt'\Big]$$

and the same from the third equation with $l \longleftrightarrow r$. Substituting to the second equation we obtain in continuous limit $\sum_l \to \int \varrho_L\, dE_l$,

$$\dot{b}_0^{(k)}(t) = \Big(-iE_0(t) - \frac{\Gamma(t)}{2}\Big)b_0^{(k)}(t) - i\,\Omega_k(t)e^{-iE_k t}$$

where the total width $\Gamma(t) = 2\pi[\Omega_L^2(t)\varrho_L + \Omega_R^2(t)\varrho_R]$ is time-dependent.

Final expressions

$$b_0^{(k)}(t) = -i\,e^{-i\mathcal{E}_0(t)t}\int_0^t \Omega_k(t')e^{i[\mathcal{E}_0(t')-E_k]t'}dt'$$

where

$$\mathcal{E}_0(t) = \frac{1}{t}\int_0^t \left[E_0(t') - i\frac{\Gamma(t')}{2}\right]dt'$$

and

$$b_l^{(k)}(t) = e^{-iE_l t}\left[\delta_{kl} - \int_0^t i\,\Omega_l(t')b_0^{(k)}(t')e^{iE_l t'}dt'\right]$$

and the same from the third equation with $l \longleftrightarrow r$. The average charge on the dot and the currents

$$Q_0(t) = \sum_k |b_0^{(k)}(t)|^2, \;\; Q_{R(L)}(t) = \sum_k\sum_{r(l)} |b_{r(l)}^{(k)}(t)|^2 = \Gamma_{R(L)}(t)Q_0(t)$$

Fluctuating energy level (hopping amplitudes)

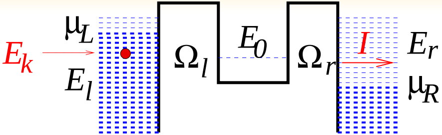

$$\boxed{E_0(t) = \bar{E}_0 + \xi(t)U/2}$$

where $\xi(t) = \pm 1$ is a random variable, which follows a Markov process: it jumps randomly from 1 to -1 (and vice versa) at the same rate $\gamma/2$ (telegraph noise). We need to average the amplitude $b_0^{(k)}(t) = \widetilde{b}_0^{(k)}(t)e^{-iE_k t}|$ over the noise. It is better to do in the equation of motion

$$\frac{d}{dt}\widetilde{b}_0^{(k)}(t) = i\left[E_k - \bar{E}_0 - \xi(t)U/2 + i\Gamma/2\right]\widetilde{b}_0^{(k)}(t) - i\Omega_k$$

Average over the noise

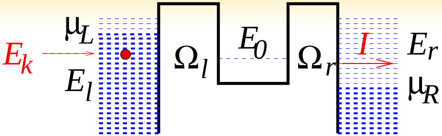

$\boxed{E_0(t) = \bar{E}_0 + \xi(t)U/2}$ where $\xi(t) = \pm 1$.

$$\frac{d}{dt}\langle\widetilde{b}_0^{(k)}(t)\rangle = i[E_k + i\Gamma/2]\langle\widetilde{b}_0^{(k)}(t)\rangle - iU\langle\xi(t)\widetilde{b}_0^{(k)}(t)\rangle/2 - i\Omega_k$$

Multiply the equation of motion by $\xi(t)$ and taking into account that $\xi^2(t) = 1$, we obtain

$$\langle\xi(t)\frac{d}{dt}\widetilde{b}_0^{(k)}(t)\rangle = i[E_k + i\Gamma/2]\langle\xi(t)\widetilde{b}_0^{(k)}(t)\rangle - iU\langle\widetilde{b}_0^{(k)}(t)\rangle/2$$

How to evaluate $\langle\xi(t)\frac{d}{dt}\widetilde{b}_0^{(k)}(t)\rangle$?

Shapiro and Loginov formula, Physica **91 A**, 563 (1978)

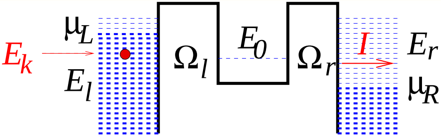

$\boxed{E_0(t) = \bar{E}_0 + \xi(t)U/2}$ where $\xi(t) = \pm 1$.

In the case of an exponential noise-correlator, $\langle \xi(t_1)\xi(t_1+\tau)\rangle = e^{-\gamma\tau}$ one can derive the following "differential formula"

$$\langle \xi(t)\frac{d}{dt}\widetilde{b}_0^{(k)}(t)\rangle = \frac{d}{dt}\langle \xi(t)\widetilde{b}_0^{(k)}(t)\rangle + \gamma\langle \xi(t)\widetilde{b}_0^{(k)}(t)\rangle$$

Using this formula we find the system of closed linear equations for the averaged amplitude $\langle \widetilde{b}_0^{(k)}(t)\rangle$.

Final results

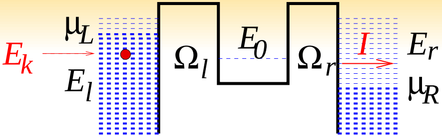

$\boxed{E_0(t) = \bar{E}_0 + \xi(t)U/2}$ with $\langle \xi(t_1)\xi(t_1+\tau)\rangle = e^{-\gamma\tau}$

$$\frac{d}{dt}\langle \widetilde{b}_0^{(k)}(t)\rangle = i[E_k + i\Gamma/2]\langle \widetilde{b}_0^{(k)}(t)\rangle - iU\langle \xi(t)\widetilde{b}_0^{(k)}(t)\rangle/2 - i\Omega_k$$

$$\frac{d}{dt}\langle \xi(t)\widetilde{b}_0^{(k)}(t)\rangle = i[E_k + i(\Gamma/2+\gamma)]\langle \xi(t)\widetilde{b}_0^{(k)}(t)\rangle - iU\langle \widetilde{b}_0^{(k)}(t)\rangle/2$$

However, we need to evaluate $\langle |\widetilde{b}_0^{(k)}(t)|^2\rangle$. We derive the following differential equation for this quantity

$$\frac{d}{dt}|\widetilde{b}_0^{(k)}(t)|^2 = -\Gamma|\widetilde{b}_0^{(k)}(t)|^2 - 2\Omega_k \mathrm{Im}\Big[\widetilde{b}_0^{(k)}(t)\Big]$$

$$\frac{d}{dt}\langle \widetilde{b}_0^{(k)}(t)\rangle = i[E_k + i\Gamma/2]\langle \widetilde{b}_0^{(k)}(t)\rangle - iU\langle \xi(t)\widetilde{b}_0^{(k)}(t)\rangle/2 - i\Omega_k$$

$$\frac{d}{dt}\langle \xi(t)\widetilde{b}_0^{(k)}(t)\rangle = i[E_k + i(\Gamma/2+\gamma)]\langle \xi(t)\widetilde{b}_0^{(k)}(t)\rangle - iU\langle \widetilde{b}_0^{(k)}(t)\rangle/2$$

However, we need to evaluate $\langle|\widetilde{b}_0^{(k)}(t)|^2\rangle$. We derive the following differential equation for this quantity

$$\frac{d}{dt}|\widetilde{b}_0^{(k)}(t)|^2 = -\Gamma|\widetilde{b}_0^{(k)}(t)|^2 - 2\Omega_k \mathrm{Im}\Big[\widetilde{b}_0^{(k)}(t)\Big]$$

In the steady-state limit, $\frac{d}{dt}|\widetilde{b}_0^{(k)}(t\to\infty)|^2 \to 0$, this relation is similar to the “Optical Theorem” of scattering theory.
For transient regime

$$\langle|\widetilde{b}_0^{(k)}(t)|^2\rangle = -2\Omega_k \int_0^t e^{\Gamma(t'-t)}\mathrm{Im}\Big[\langle\widetilde{b}_0^{(k)}(t')\rangle\Big]dt'$$

Summary.

- Generalized Landauer formula for time-dependent potentials is used for randomly fluctuating energy levels.

Summary.

- Generalized Landauer formula for time-dependent potentials is used for randomly fluctuating energy levels.
- For multi-dot systems, noise generates decoherence, depending on occupation of the dot, which is under the noise. If the occupation is different for electrons, coming from left or right leads, decoherence results in time-reversal symmetry breaking. This leads to zero bias current.

Graph-theoretical Evaluation of the Inelastic Propensity Rules for Molecules with Destructive Quantum Interference

Rudolf Sýkora and Tomáš Novotný

Department of Condensed Matter Physics
Faculty of Mathematics and Physics
Charles University in Prague

- Paper accepted in J. Chem. Phys.
- Code available at
  http://qi.karlov.mff.cuni.cz:1345
- Poster No. 7

Dresden, 18th of April 2017

Introduction I

- electronic transport through molecules may often be coherent → **room for quantum interference**, for instance if several transport paths exist
  Review: C. J. Lambert, Chem. Soc. Rev. **44**, 875, (2015)

- for certain setups (leads attachments, voltage bias) a molecule can display **complete destructive quantum interference** (**DQI**), i.e., ideally, no elastic current flows through the terminals, in practice strongly suppressed (**orange dashed lines in our graphs**), cf., e.g., C. M. Guedon et al., Nat Nano **7**, 305 (2012)

- we want a means of DQI prediction in systems describable by **Hückel**'s tight-binding approach; often, so-called **conjugated molecules** (having delocalized e^-s moving through π-bonds) follow such a theory

Introduction II

- we further want to estimate if and where the **DQI is lifted** when **inelastic effects** brought about by **molecular vibrations** are taken into account→ **propensity rules**

- the process should be **automated**, with molecule data lookup → a **computer program** (no error-prone manual application of 'graphical rules')

(though it was misunderstanding of the rules in the first place)

Breakdown of Interference Rules in Azulene, a Nonalternant Hydrocarbon

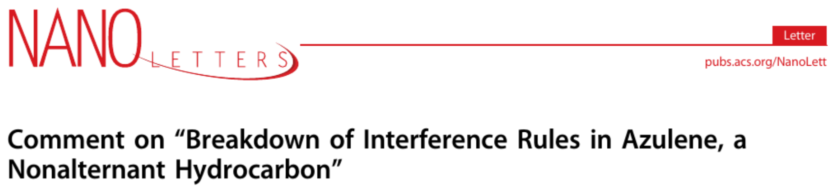

Comment on "Breakdown of Interference Rules in Azulene, a Nonalternant Hydrocarbon"

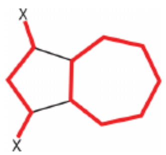

Reply to "Comment on 'Breakdown of Interference Rules in Azulene, a Nonalternant Hydrocarbon'"

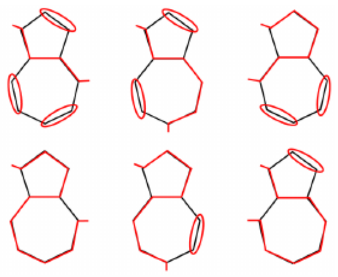

Introduction III

So we now have:

http://qi.karlov.mff.cuni.cz:1345
(at this moment running at :80 and
at kfes-120.karlov. ..., too)

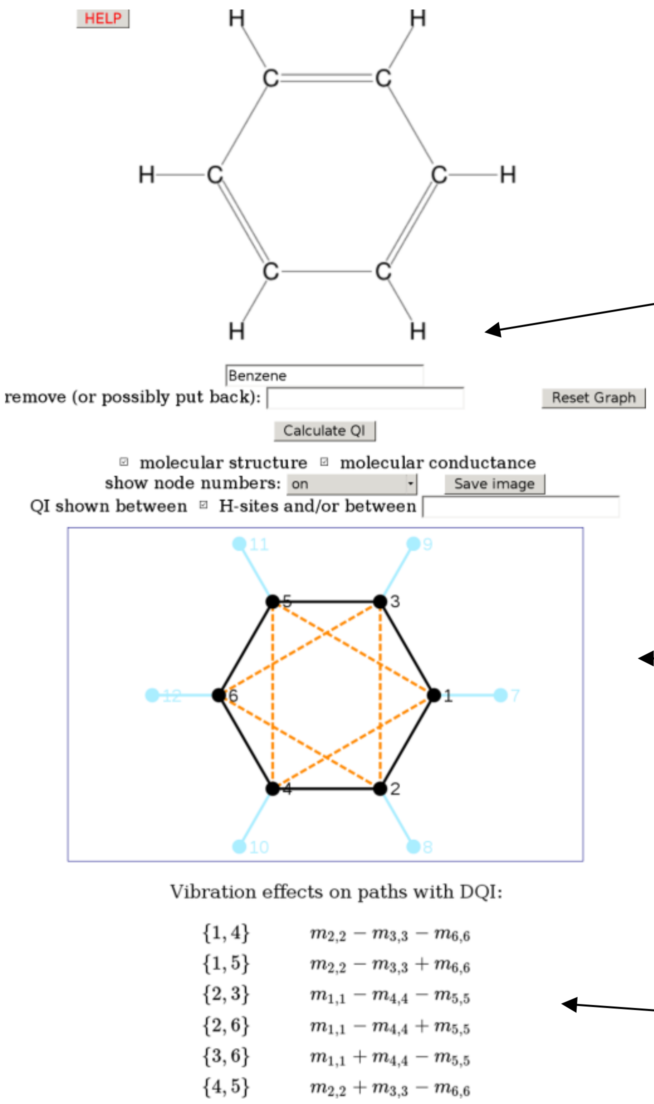

Benzene

remove (or possibly put back):

☑ molecular structure ☑ molecular conductance

show node numbers: on

QI shown between ☑ H-sites and/or between

Vibration effects on paths with DQI:

$\{1,4\}$	$m_{2,2} - m_{3,3} - m_{6,6}$
$\{1,5\}$	$m_{2,2} - m_{3,3} + m_{6,6}$
$\{2,3\}$	$m_{1,1} - m_{4,4} - m_{5,5}$
$\{2,6\}$	$m_{1,1} - m_{4,4} + m_{5,5}$
$\{3,6\}$	$m_{1,1} + m_{4,4} - m_{5,5}$
$\{4,5\}$	$m_{2,2} + m_{3,3} - m_{6,6}$

molecule look-up from a database
(access through Wolfram Mathematica)

(possibly interactive) selection of
relevant subgraph
(black: considered, light-blue: ignored)

+

calculation of paths with **DQI** (orange)

effects of **vibrations**

… details follow

Theory I – elastic part

Hückel: molecular-structure adjacency graph of π-conjugated subsystem

$$T_{\mathrm{el}}(\varepsilon) = \mathrm{Tr}\left[\Gamma_L G(\varepsilon)\Gamma_R G^\dagger(\varepsilon)\right]$$

$$H^{\text{Hückel}}_{\text{benzene}} \propto \begin{pmatrix} 0 & 1 & 1 & 0 & 0 & 0 \\ 1 & 0 & 0 & 1 & 0 & 0 \\ 1 & 0 & 0 & 0 & 1 & 0 \\ 0 & 1 & 0 & 0 & 0 & 1 \\ 0 & 0 & 1 & 0 & 0 & 1 \\ 0 & 0 & 0 & 1 & 1 & 0 \end{pmatrix}$$

$$G(\varepsilon) \equiv \left(\varepsilon - H_{\mathrm{mol}} + i\frac{\Gamma_L + \Gamma_R}{2}\right)^{-1}$$

$$dI/dV = 2e^2/h \times T_{\mathrm{el}}(\varepsilon_F)$$

$$\varepsilon_F = 0$$

$$\Gamma_L = \gamma_L |L\rangle\langle L|, \quad \Gamma_R = \gamma_R |R\rangle\langle R|$$

$$T_{\mathrm{el}}(\varepsilon_F) = \gamma_L \gamma_R |\langle L|G(\varepsilon_F)|R\rangle|^2$$

Theory II – inelastic part

Electron – vibration coupling:

$$H_{e-v} \propto \sum_{\lambda,i,j} m_{i,j}^{\lambda} c_i^{\dagger} c_j (a_{\lambda} + a_{\lambda}^{\dagger}) + H.c.$$

λ indexes vibration modes, $c_i^{\dagger}$ creates e$^-$ at site *i*, $a_{\lambda}^{\dagger}$ excites vibrational mode λ

Lowest-order-expansion: M. Paulsson et al., Phys. Rev. B **72**, 201101 (2005); J. K. Viljas et al., Phys. Rev. B **72**, 245415 (2005); L. de la Vega et al., Phys. Rev. B **73**, 075428 (2006)

- $\boldsymbol{m_{i,j}}$ is the coupling matrix **assumed nonzero** only if *i*,*j* are the **nearest neighbours in the π-conjugated system** and on the diagonal *i* = *j*

Theory III – inelastic (cont'd)

Change in transmission due to vibration (LOE) - 2 parts:

$$\Delta_\lambda^{\text{Sym}} = \text{Tr}\Big[G^\dagger \Gamma_L G \{ M_\lambda G \Gamma_R G^\dagger M_\lambda + \\ + \frac{i}{2}(\Gamma_R G^\dagger M_\lambda A M_\lambda - \text{h.c.}) \}\Big]$$

$$A \equiv i(G - G^\dagger)$$

$$\Delta_\lambda^{\text{Asym}} = \text{Tr}\Big[G^\dagger \Gamma_L G \{ \Gamma_R G^\dagger M_\lambda G (\Gamma_R - \Gamma_L) G^\dagger M_\lambda + \text{h.c.} \}\Big]$$

Considerable simplification takes place when DQI occurs:

DQI ↔ $\langle L | G(\varepsilon_F) | R \rangle = 0$

we are left only with

$$\Delta_\lambda^{\text{Sym}} = \gamma_L \gamma_R \left| \langle L | G M_\lambda G | R \rangle \right|^2 \approx \gamma_L \gamma_R \left| \langle L | G_{M_\lambda} | R \rangle \right|^2$$

$$G_{M_\lambda} \qquad H_{\text{mol}} \rightarrow H_{\text{mol}} + M_\lambda$$

Justification, Range of Validity

- LOE valid for energy (nearly) independent GF's around Fermi energy; but good enough for realistic parameters

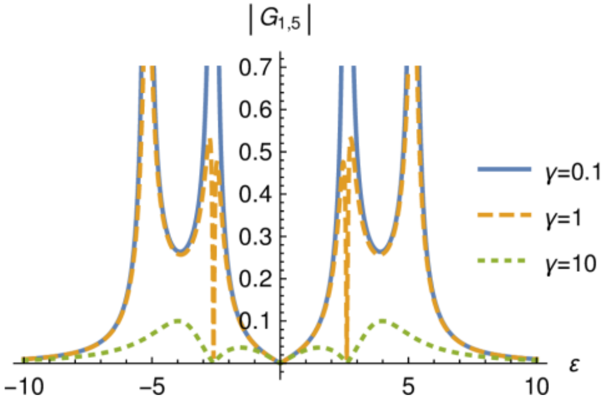

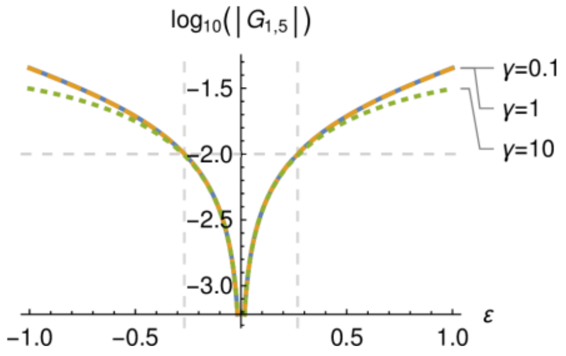

- Some vibrational modes invisible in our approach (as they couple to the σ-system); only π-active **subset of IETS**

- Hückel model described by the adjacency matrix of the conjugated part, i.e., constant nearest neighbor hopping elements – implicitly requires **planarity** (compare biphenyl)

3-methylene-1,4-pentadiyne

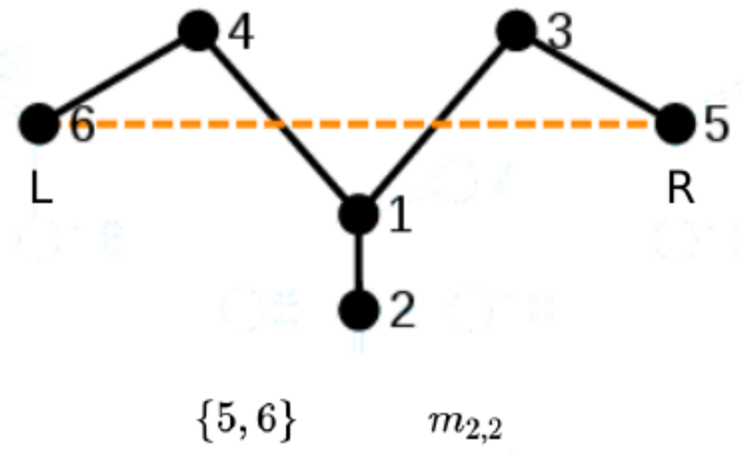

J. Lykkebo et al., ACS Nano **7**, 9183 (2013)

- **toy molecule** (real, nonetheless), contacted at atoms 6 (L), 5 (R)
- possesses **DQI** between **5, 6**
  (also between other sites, here, exceptionally, not shown for clarity)
- we may understand this particular DQI by considering paths 6-4-1-3-5 *vs.* 6-4-1-2-1-3-5; the extra 1-2-1 piece changes phase by π exactly (at zero energy that we concentrate on); Fano resonance
- DQI lifted by vibrations active at site 2 – **which path interferometer**

Time for hands-on experience (hopefully…)

Biphenyl

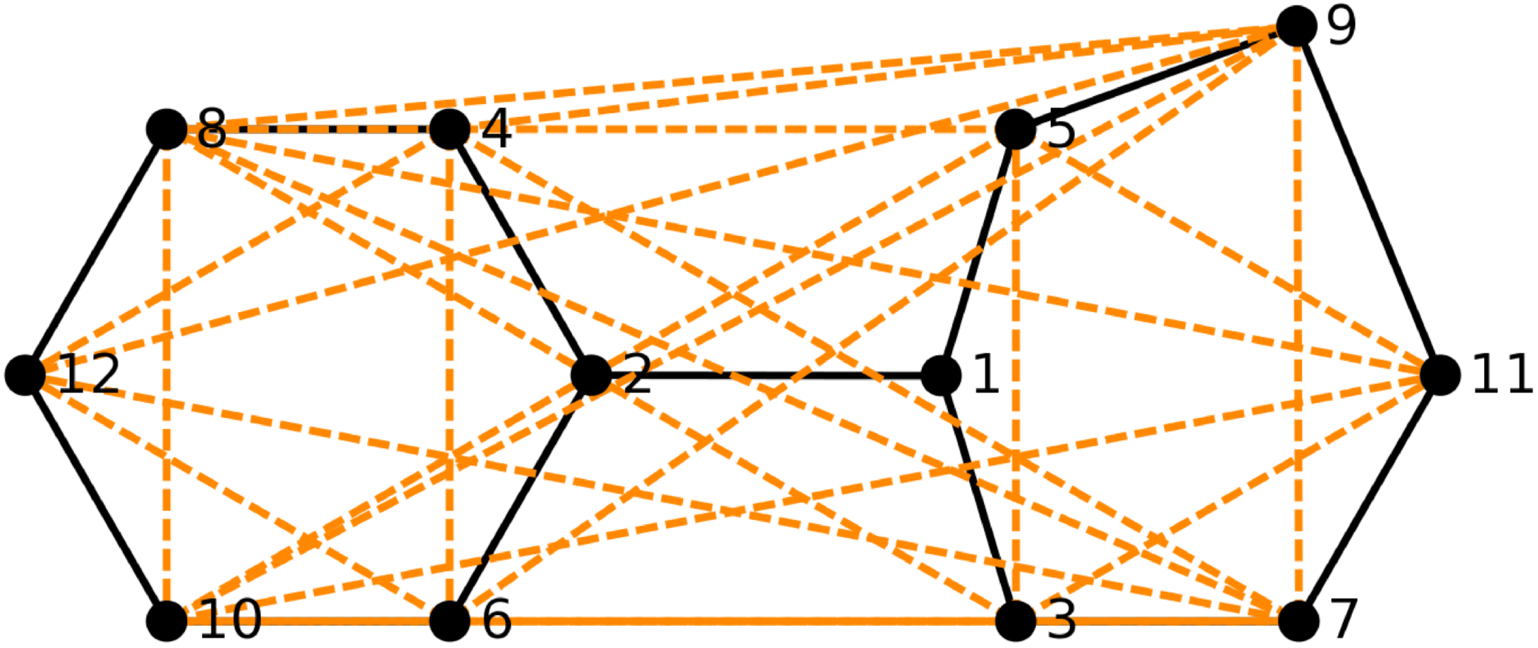

$\{3,5\}$	$4m_{1,1}+m_{4,4}+m_{6,6}-4m_{7,7}-4m_{9,9}+m_{12,12}$
$\{3,8\}$	$2\,(-m_{4,4}+m_{6,6}+m_{12,12})$
$\{3,10\}$	$2\,(m_{4,4}-m_{6,6}+m_{12,12})$
$\{3,11\}$	$4m_{1,1}+m_{4,4}+m_{6,6}-4m_{7,7}+4m_{9,9}+m_{12,12}$
$\{7,8\}$	0
$\{7,9\}$	$4\,(m_{3,3}+m_{5,5}-m_{11,11})$
$\{7,10\}$	0
$\{7,12\}$	$2\,(m_{3,3}-m_{5,5}-m_{11,11})$

- DQI between {7,8} is ‘vibration resistent’

- although reported here for easier orientation, {7,10} and {3,10} are actually symmetry-equivalent to {7,8} and {3,8}, respectively

Azulene

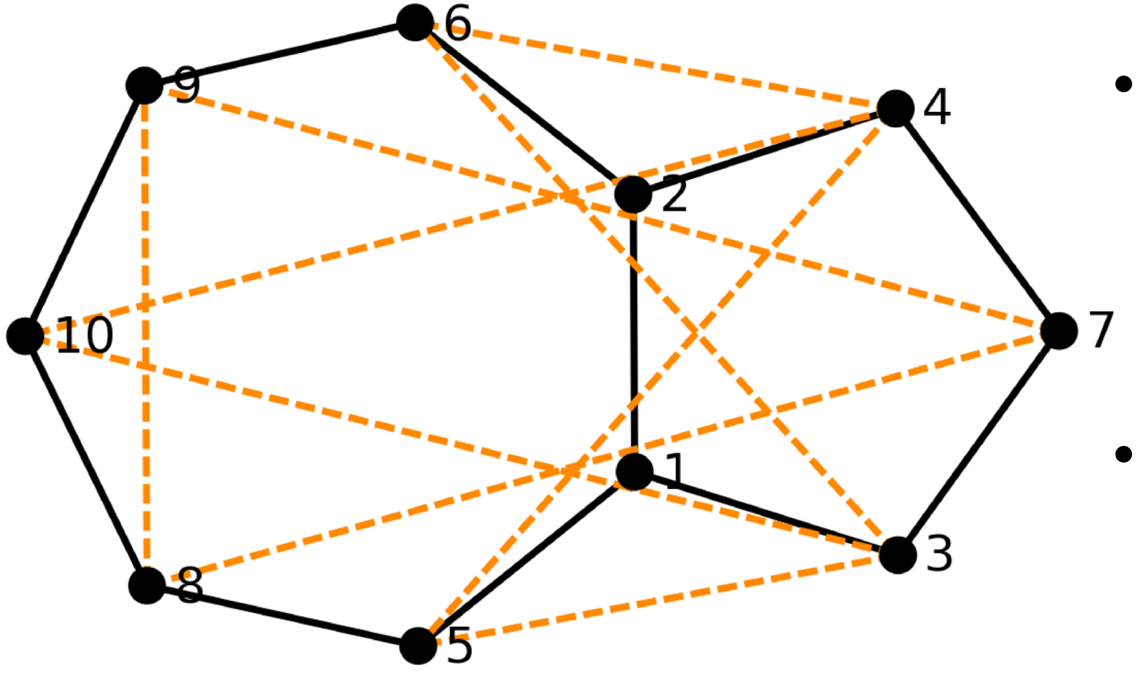

- **non-alternant** hydrocarbon
- **off-diagonal el.-vib. elem's** are present (due to being non-alternant?; Gemma)
- (this molecule was much discussed in the literature in connection with applicability of various graphical rules for DQI prediction)

$\{3,5\}$	$m_{1,1}+m_{1,2}-m_{1,5}-m_{2,1}-m_{2,2}+m_{2,6}+m_{3,1}-m_{3,7}-m_{4,2}+m_{4,7}-m_{7,7}+m_{8,5}-m_{8,8}-m_{8,10}-m_{9,6}-m_{9,9}+m_{9,10}$
$\{3,6\}$	$m_{1,1}+m_{1,2}-m_{1,5}-m_{2,1}-m_{2,2}+m_{2,6}+m_{3,1}-m_{3,7}-m_{4,2}+m_{4,7}-m_{7,7}+m_{8,5}+m_{8,8}-m_{8,10}-m_{9,6}+m_{9,9}+m_{9,10}$
$\{3,10\}$	$m_{1,1}+m_{1,2}-m_{1,5}-m_{2,1}-m_{2,2}+m_{2,6}+m_{3,1}-m_{3,7}-m_{4,2}+m_{4,7}-m_{7,7}+m_{8,5}+m_{8,8}-m_{8,10}-m_{9,6}-m_{9,9}+m_{9,10}$
$\{7,8\}$	$m_{3,3}-m_{4,4}+m_{5,5}-m_{6,6}-m_{10,10}$
$\{8,9\}$	$m_{3,3}+m_{4,4}+m_{5,5}+m_{6,6}-m_{10,10}$

Two Interesting Points

- where the **‘graphical rules’ really fail** (in spite of being applied correctly)

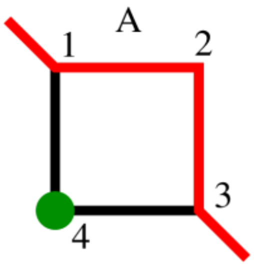

Yet no DQI!

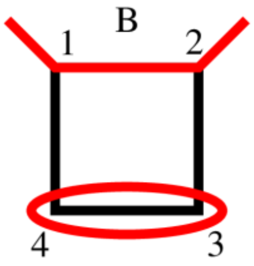

Yet with DQI!

$$G_{LR} = \lim_{\eta \to 0^+} \frac{(-1)^{L+R} \det_{LR}(H_{\text{mol}} + i\eta)}{\det(H_{\text{mol}} + \Sigma_L + \Sigma_R + i\eta)}$$

- the **rules consider the numerator only,** while here the denominator is important: “0 / 0”
- this is relevant for physically existing systems, too → use of **pseudoinverse** in our code

- Fano resonance in the square with arbitrary asymmetry, $a \neq 1$ ($\xi = (a\text{-}1)/2$)

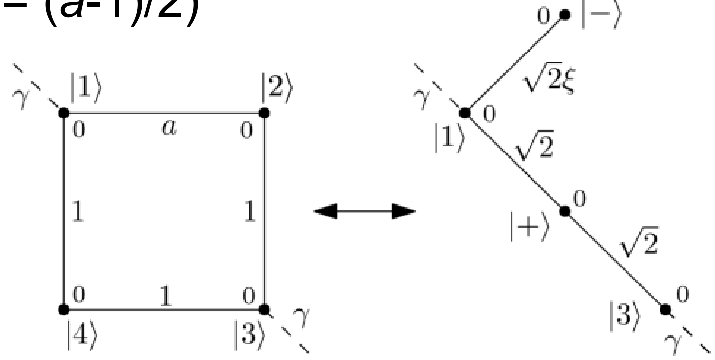

$|+\rangle \equiv 1/\sqrt{2}(|2\rangle + |4\rangle)$

$|-\rangle \equiv 1/\sqrt{2}(|2\rangle - |4\rangle)$

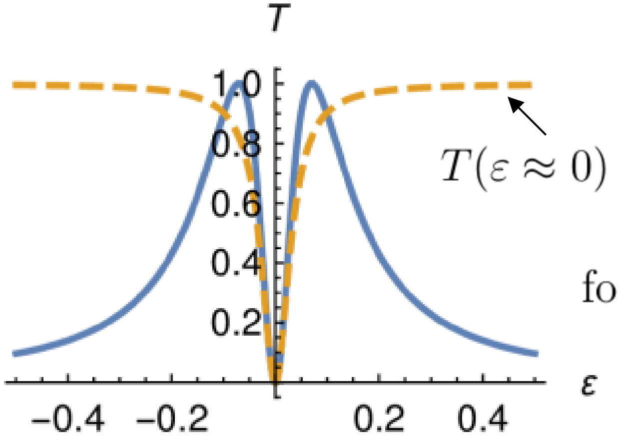

$$T(\varepsilon \approx 0) = \frac{1}{1 + \left(\frac{2\xi^2}{\varepsilon\gamma}\right)^2}$$

for $\xi/\gamma \ll 1$

Conclusions

- ✓ automated code for **evaluation** of **DQI configurations** of wide class of conjugated molecules

- ✓ Combinations of el.-vib. matrix elements **contributing to IETS** calculated
  - ➢ analysis in terms of **propensity rules** (effects of symmetries etc.)

- ◆ Still desperately missing **Hückel-like prescription** for el.-vib. matrix
(only ab-initio now - shaky, nonintuitive)

Thank you for your attention!

MPIPKS Dresden April 2017

The many ways for a current to interact with ionic motion

Stefano Sanvito
School of Physics and CRANN, Trinity College Dublin, IRELAND

Trinity College The University of Dublin
UCC University College Cork, Ireland Coláiste na hOllscoile Corcaigh
sfi science foundation ireland fondúireacht eolaíochta éireann

The question

Mesoscopic

Molecules

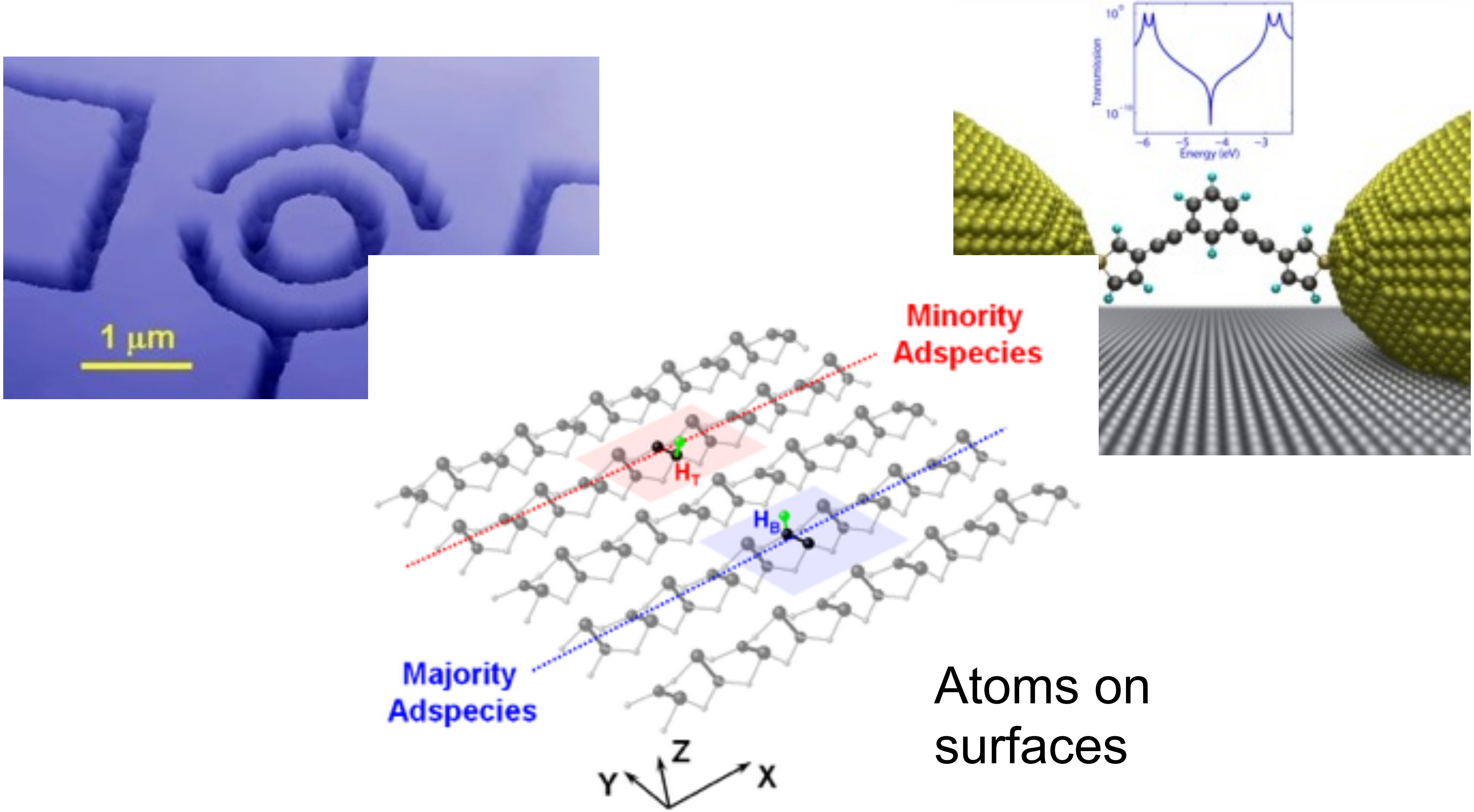

Atoms on surfaces

Outline

CRANN

Quantitative quantum transport: Smeagol

Quick overview (very quick!! … with some new stuff)

Interference on a surface

Atomic-scale quantum devices on Si (100)

Moving atoms

Phonons in an electric field/current

Quantitative quantum transport
The *Smeagol* project

Alex Reily Rocha, Ivan Rungger, Chaitanya Das Pemmaraju, Maria Stamenova ….

The basic concept

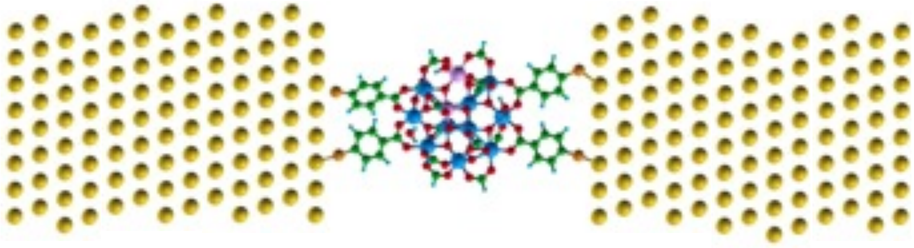

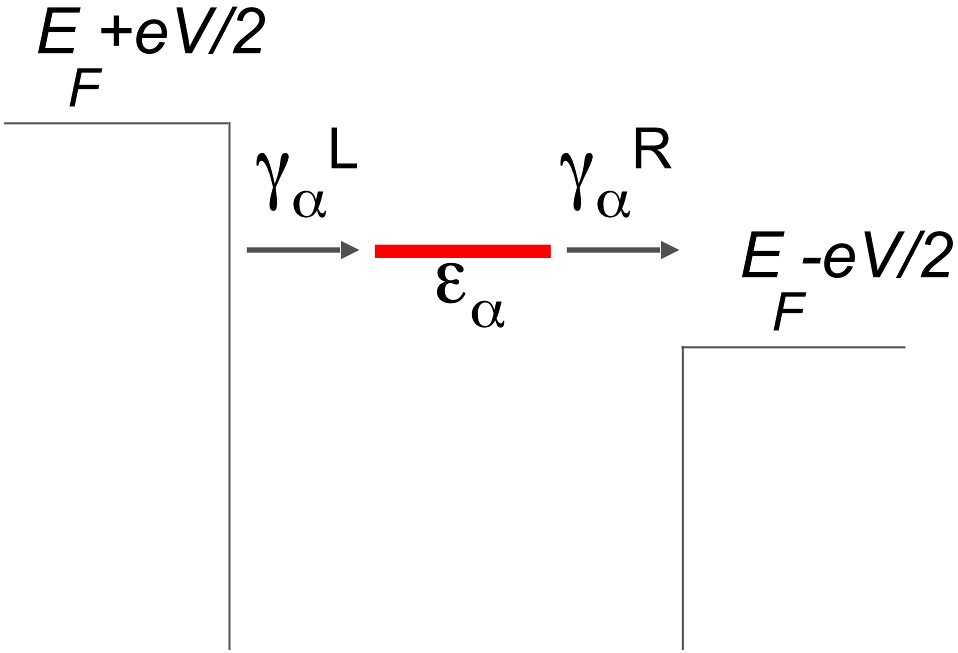

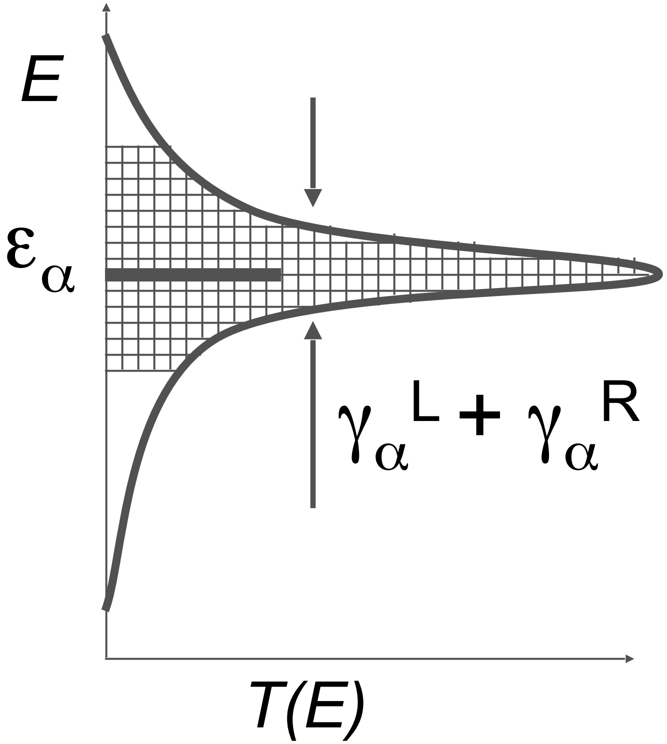

$$I^\sigma \approx \frac{e}{h}\int_{E_F-eV/2}^{E_F+eV/2} T^\sigma(E;V)\,dE$$

Smeagol

NEGF + DFT (*Siesta …. AIMS & CP2K*)

$$H_L[\rho_L] + \quad H_M[\rho] + \Sigma_{in}[E,\rho,\delta] \quad + H_R[\rho_R]$$

$$\Sigma_L(E) \qquad \qquad \Sigma_R(E)$$

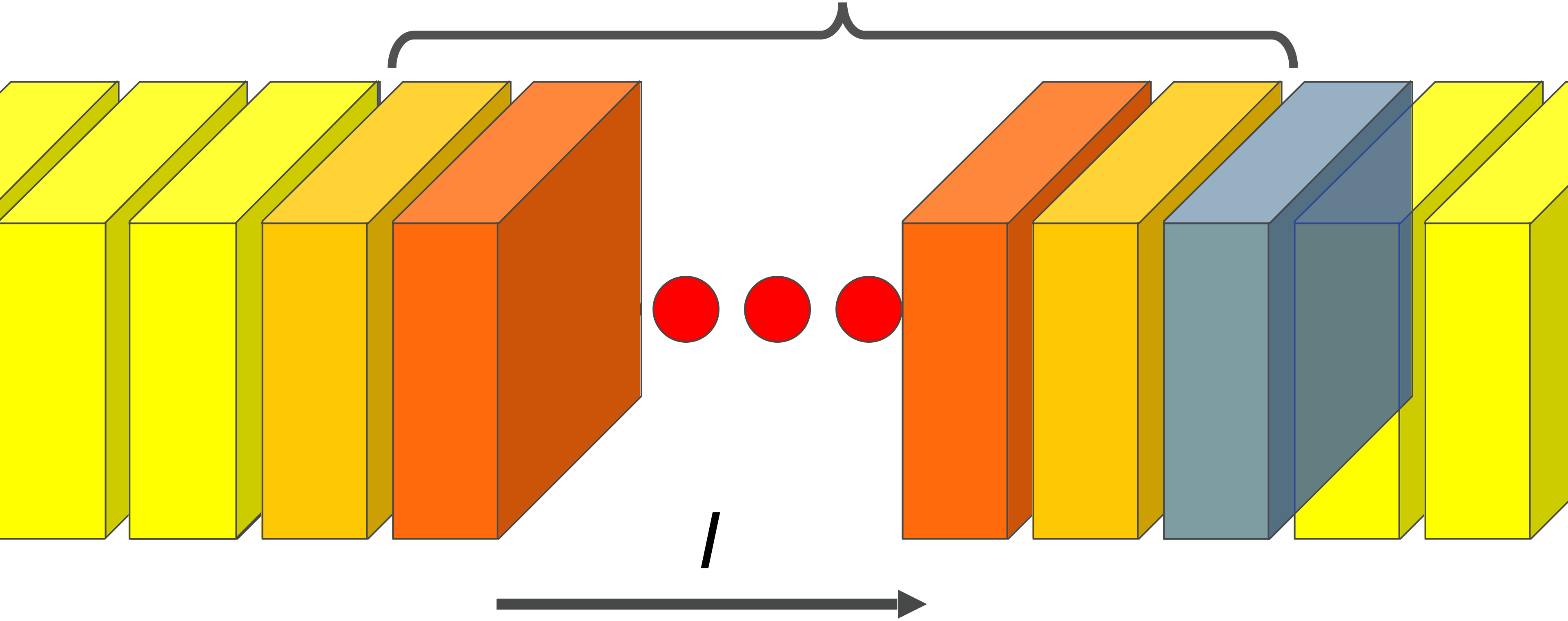

Smeagol

http://www.smeagol.tcd.ie/

Phys. Rev. B **73**, 085414 (2006); Nature Materials **4**, 335 (2005); Phys. Rev. B **78**, 035407 (2008)

One question, many systems

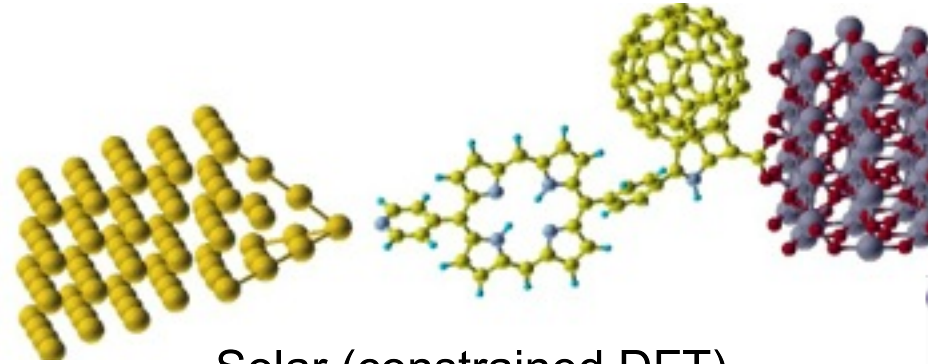

Solar (constrained DFT)

Spintronics devices (design)

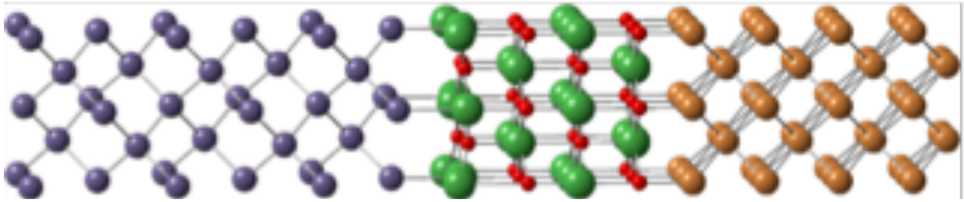

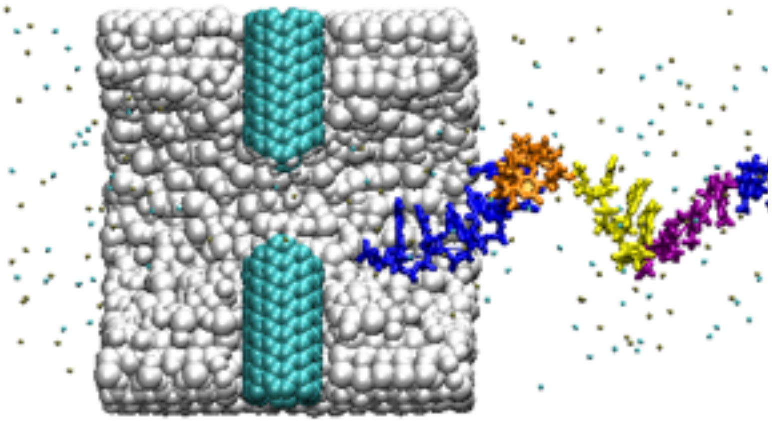

Sensors (statistics)

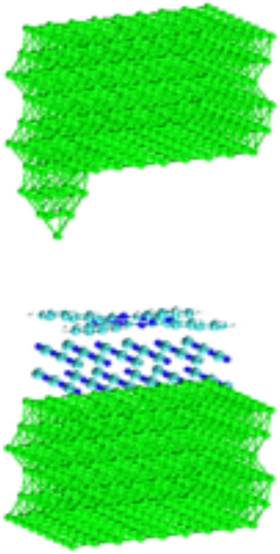

STM (accuracy)

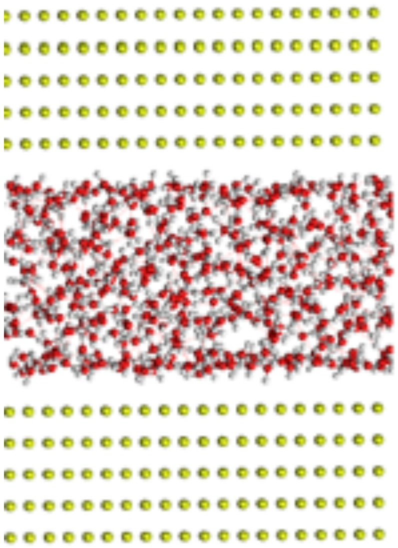

Liquids (MD+statistics)

What to ask to the electronic structure theory ?

Molecules	**Solids**
Ionization potential (*I*) and electron affinity (EA) at the right place	Correct band-alignment (and transport gap)
Accurate for fractional occupation	Interface states well described
Scalable to large number of electrons	Scalable to large number of electrons

Smeagol: what is new

Constrained DFT

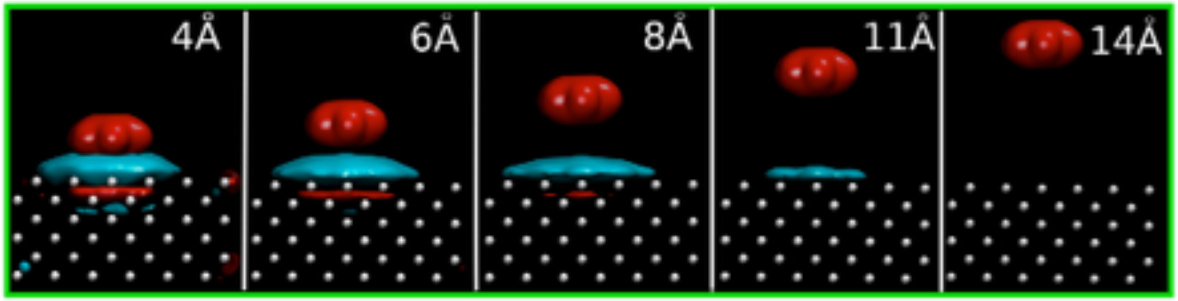

$$V(d) = \frac{-q^2}{4(d - d_0)}$$

A.M. Souza *et al.*, PRB **88**, 165112 (2013); S. Roychoudhury *et al.*, PRB **93**, 045130 (2016)

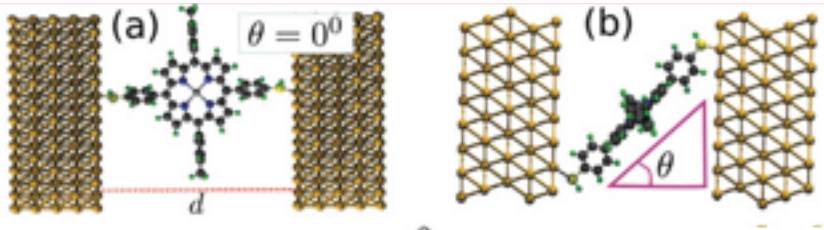

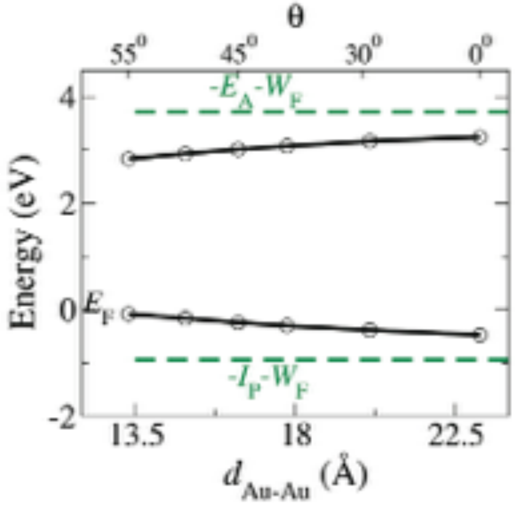

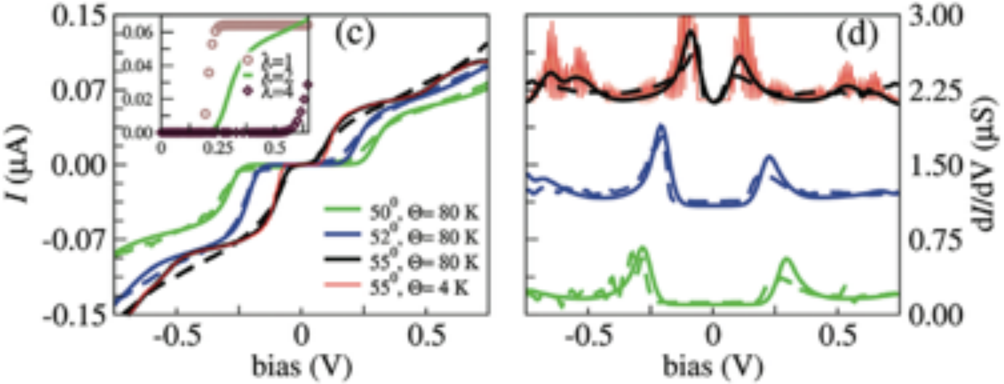

A.M. Souza *et al.*, Nanoscale **7**, 19231 (2015)

What to ask to the electronic structure theory ?

Molecules	**Solids**
• Ionization potential (*I*) and electron affinity (EA) at the right place	• Correct band-alignment (and transport gap)
• Accurate for fractional occupation	• Interface states well described
• Scalable to large number of electrons	• Scalable to large number of electrons

Recursive NEGF for order-*N*

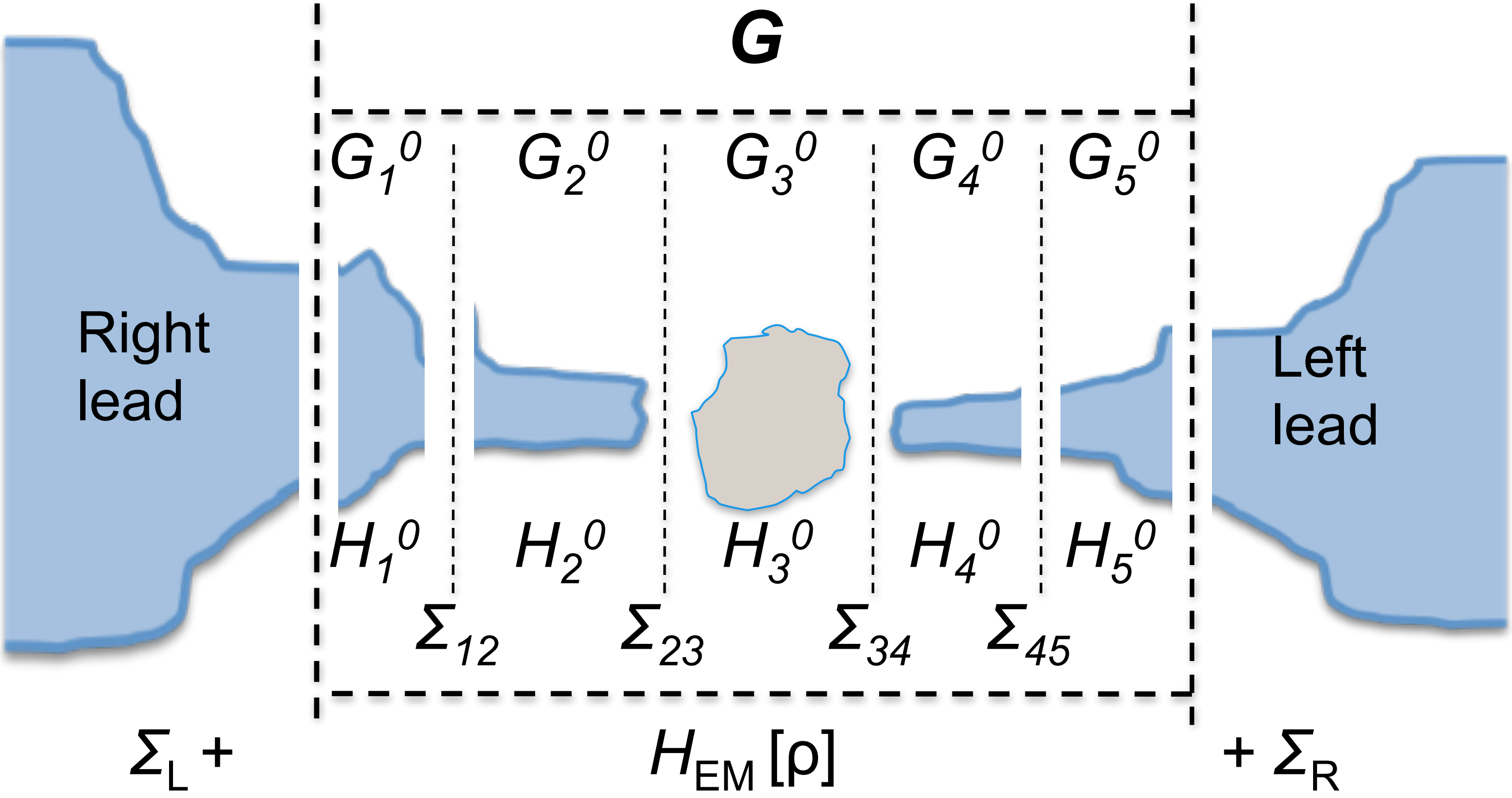

Smeagol: what is new

STT and multi-scale

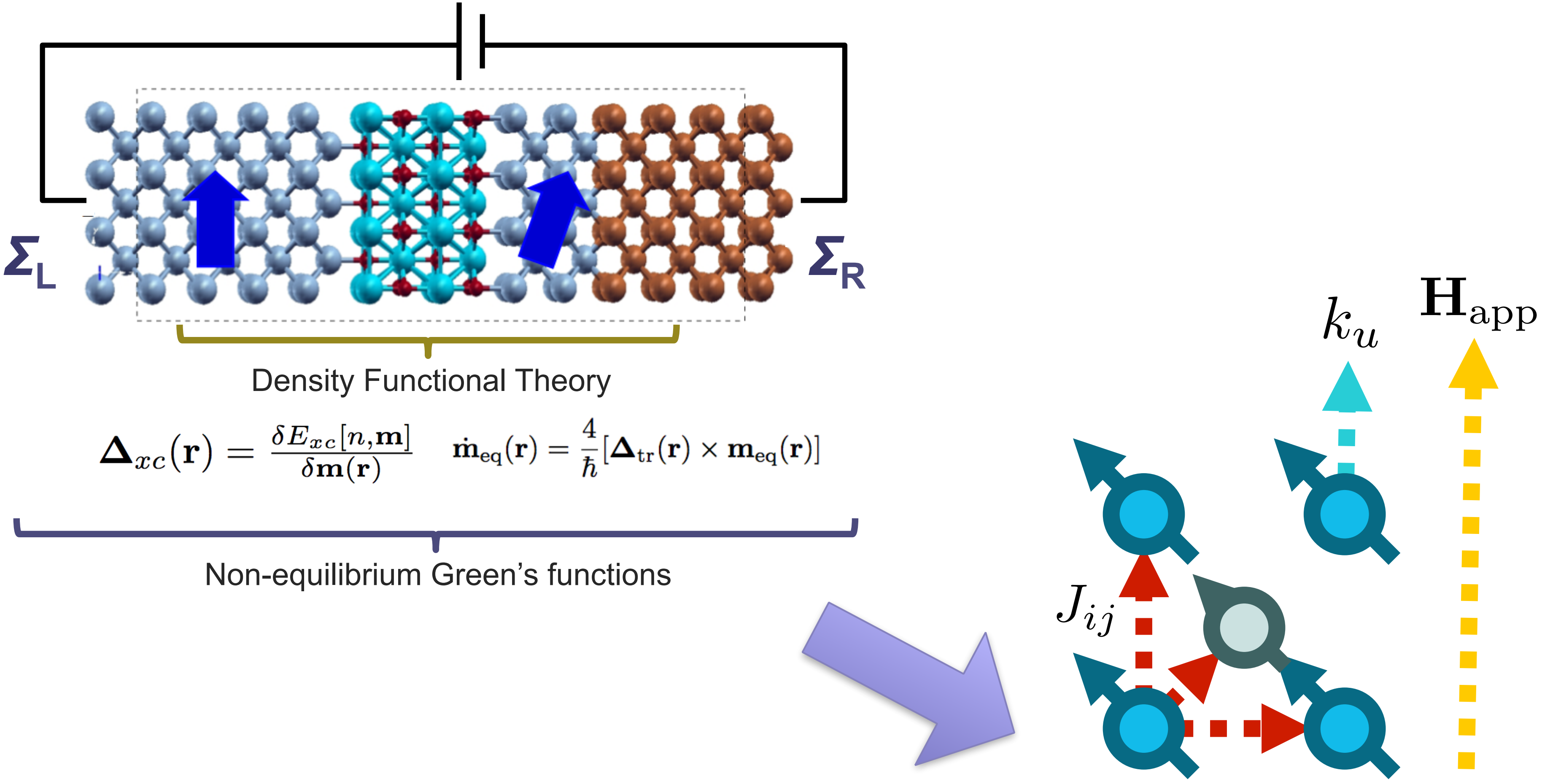

$$\mathbf{\Delta}_{xc}(\mathbf{r}) = \frac{\delta E_{xc}[n,\mathbf{m}]}{\delta \mathbf{m}(\mathbf{r})} \qquad \dot{\mathbf{m}}_{\mathrm{eq}}(\mathbf{r}) = \frac{4}{\hbar}[\mathbf{\Delta}_{\mathrm{tr}}(\mathbf{r}) \times \mathbf{m}_{\mathrm{eq}}(\mathbf{r})]$$

atomistic micromagnetics

Interference on a surface

Single H on Si (100)

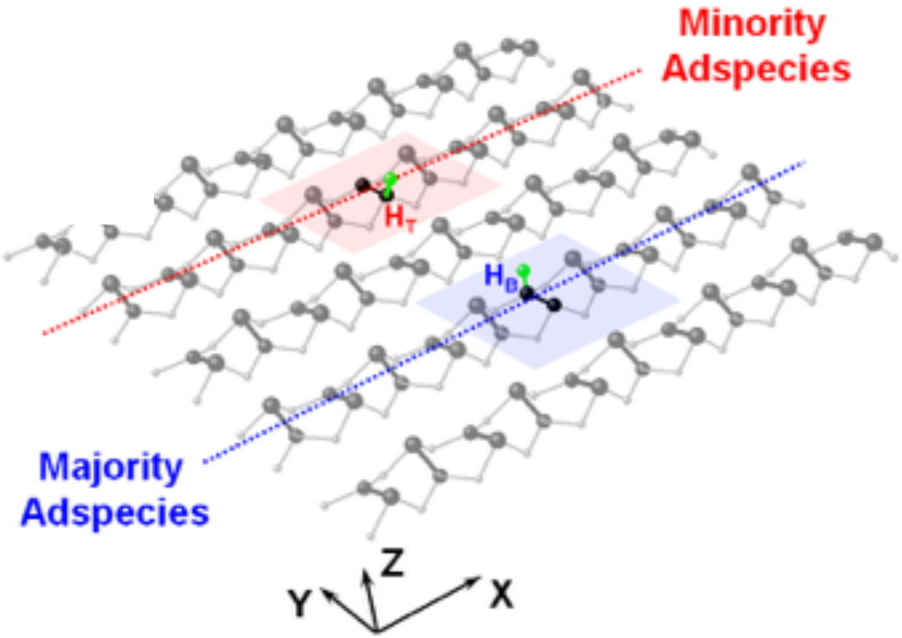

B. Naydenov, et al., PRB **84**, 195321 (2011)

H on Si (100)

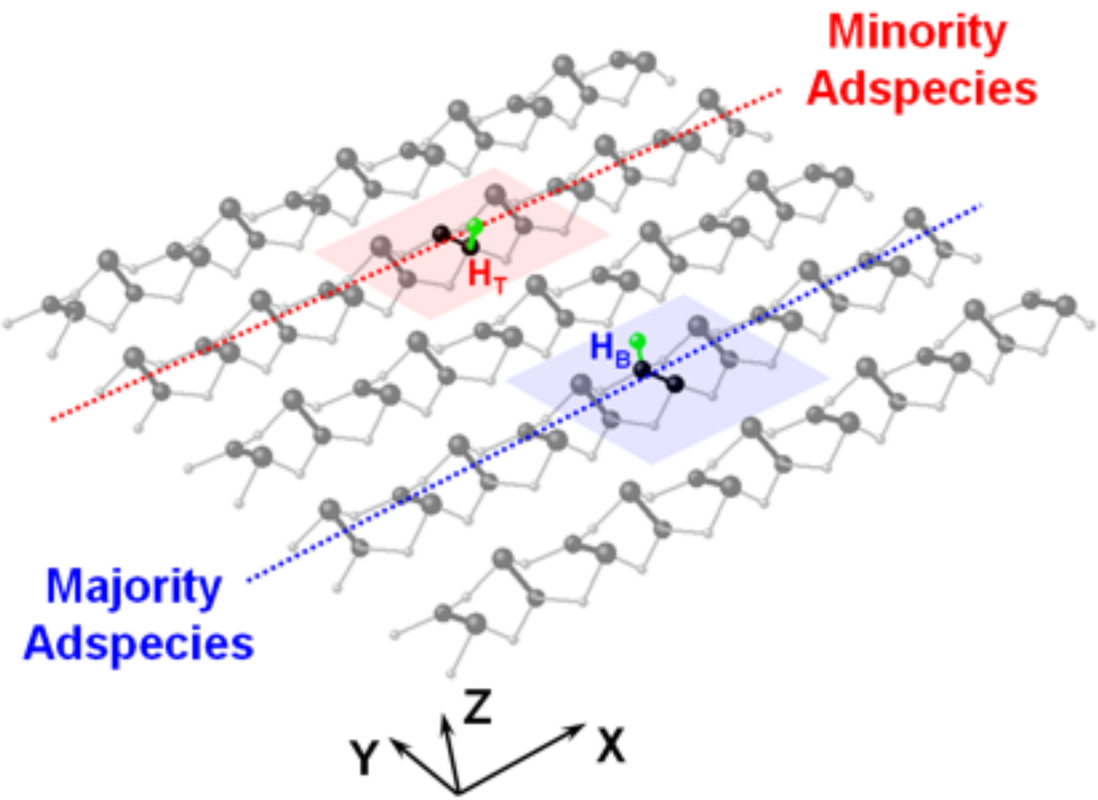

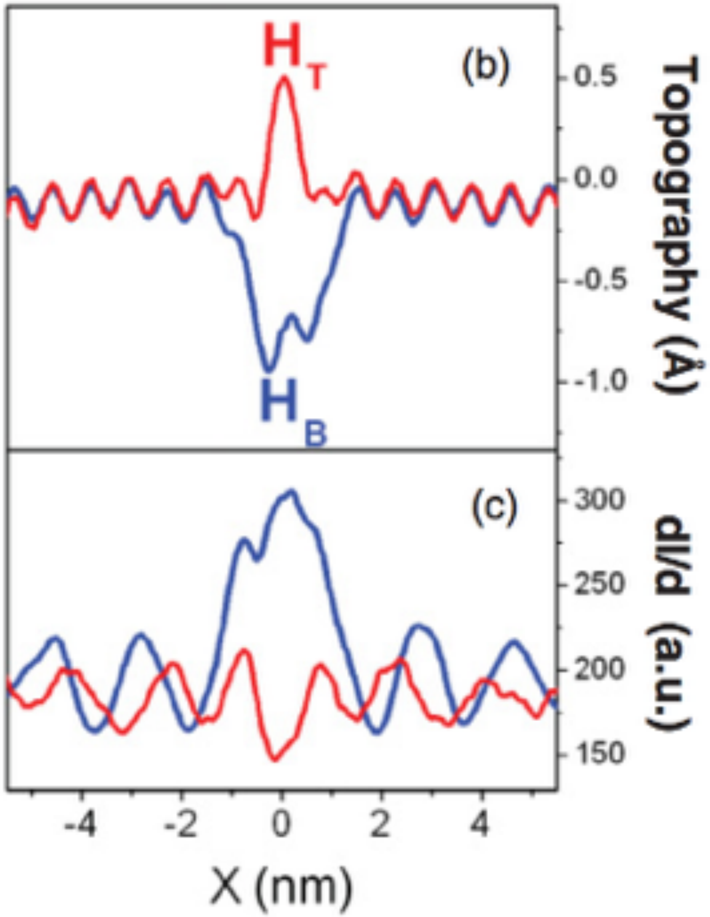

B. Naydenov, et al., PRB **84**, 195321 (2011)

H on Si (100)

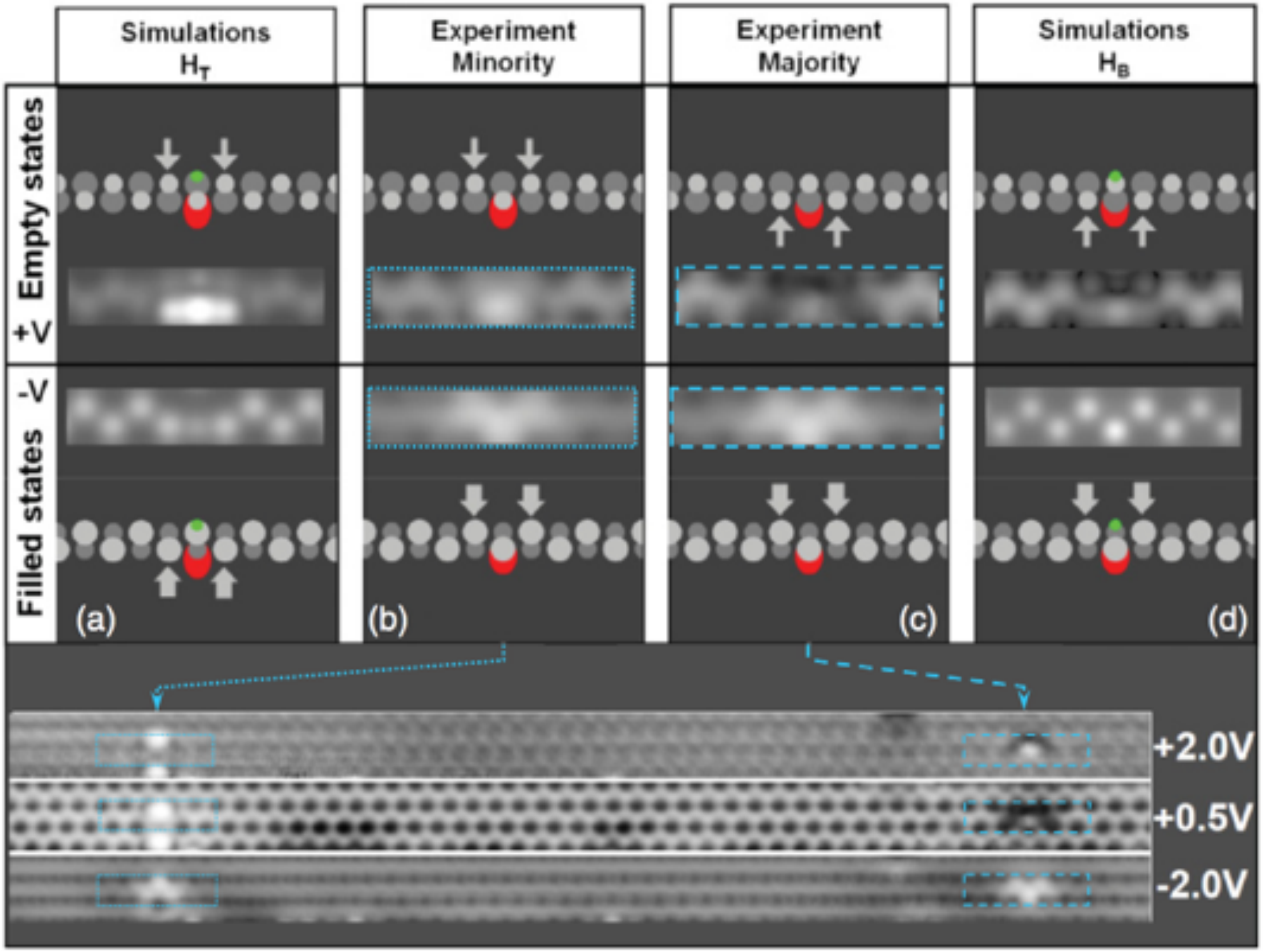

B. Naydenov, et al., PRB **84**, 195321 (2011)

H on Si (100)

GW Band

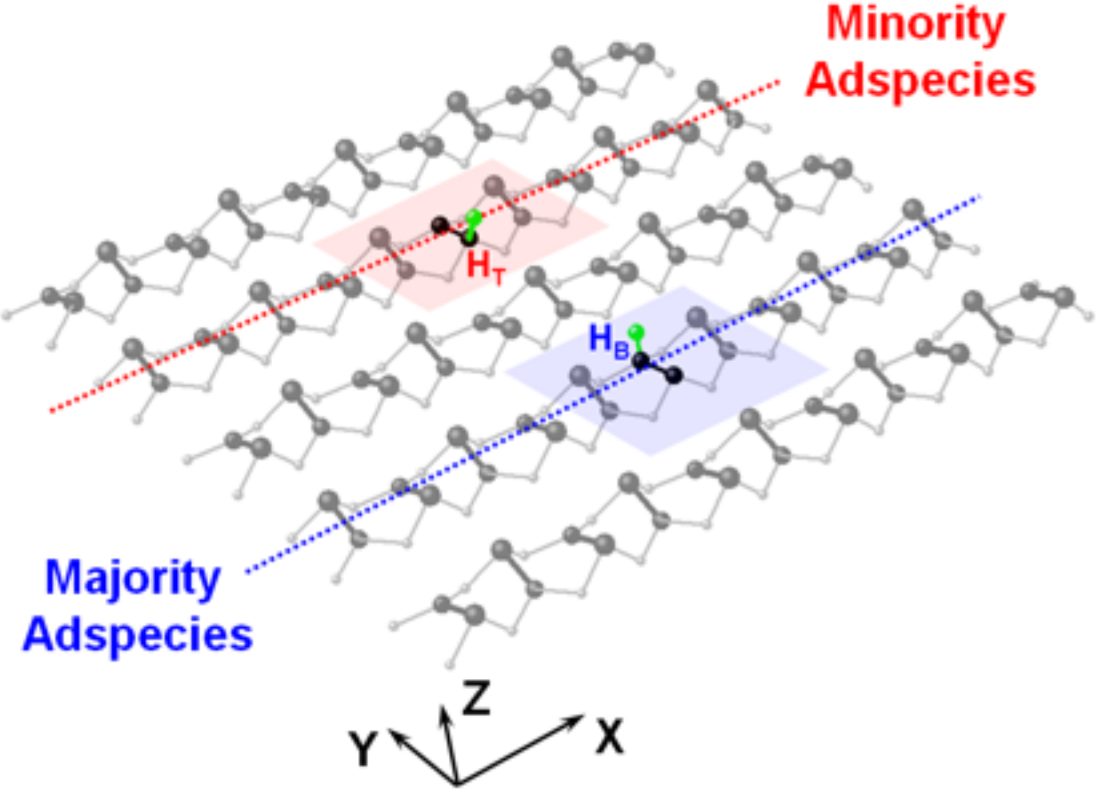

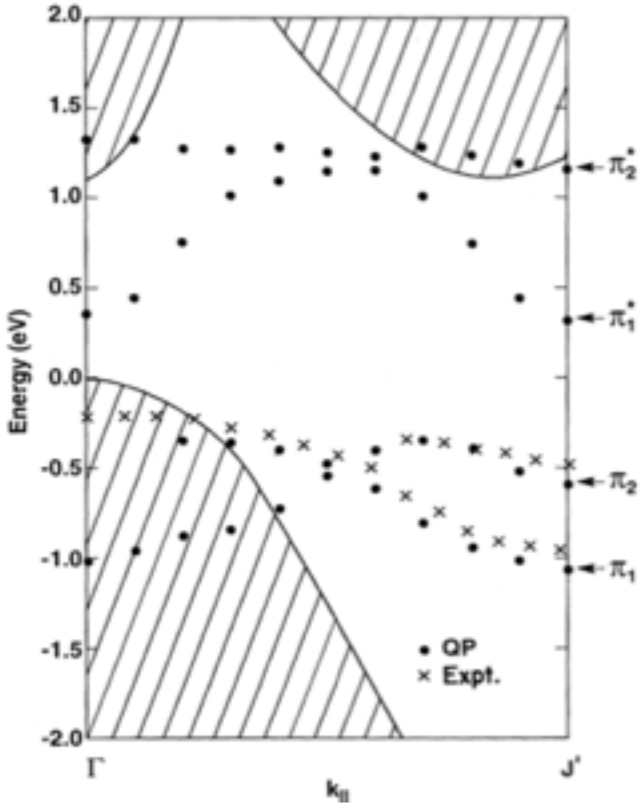

J.E. Northrup, PRB **47**, 10032 (1993)

H on Si (100): single centre

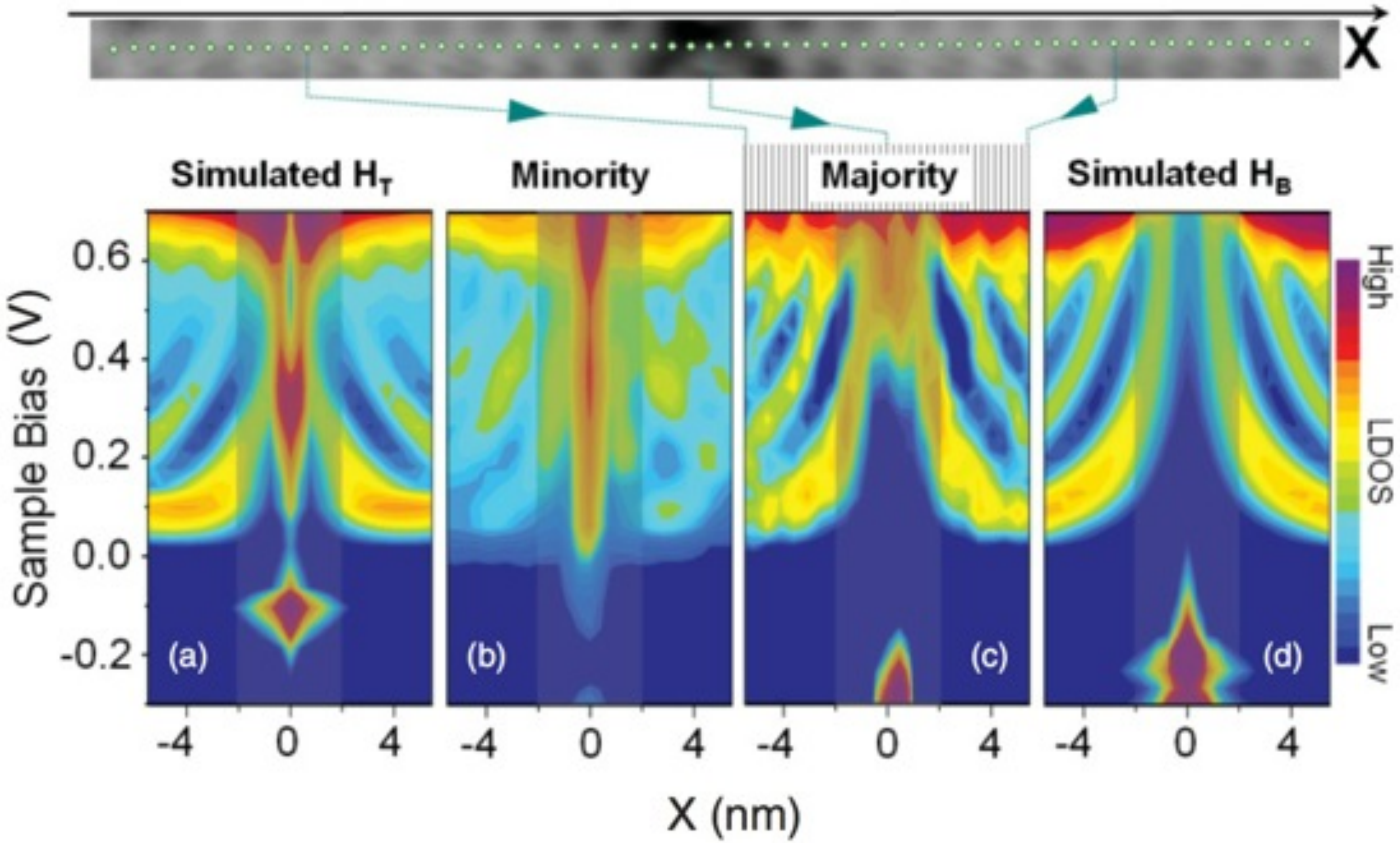

STM dI/dV

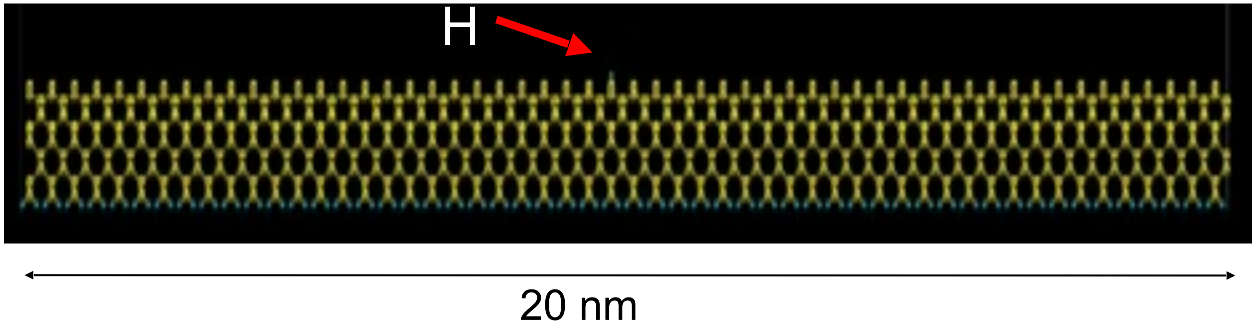

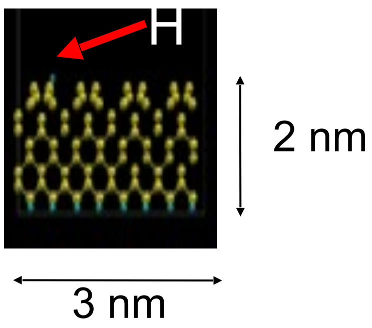

H on Si (100): single centre

Scattering analysis

$$LDOS \propto |\psi(x)|^2 \propto 1 + 2\cos(2kx + \Theta)$$

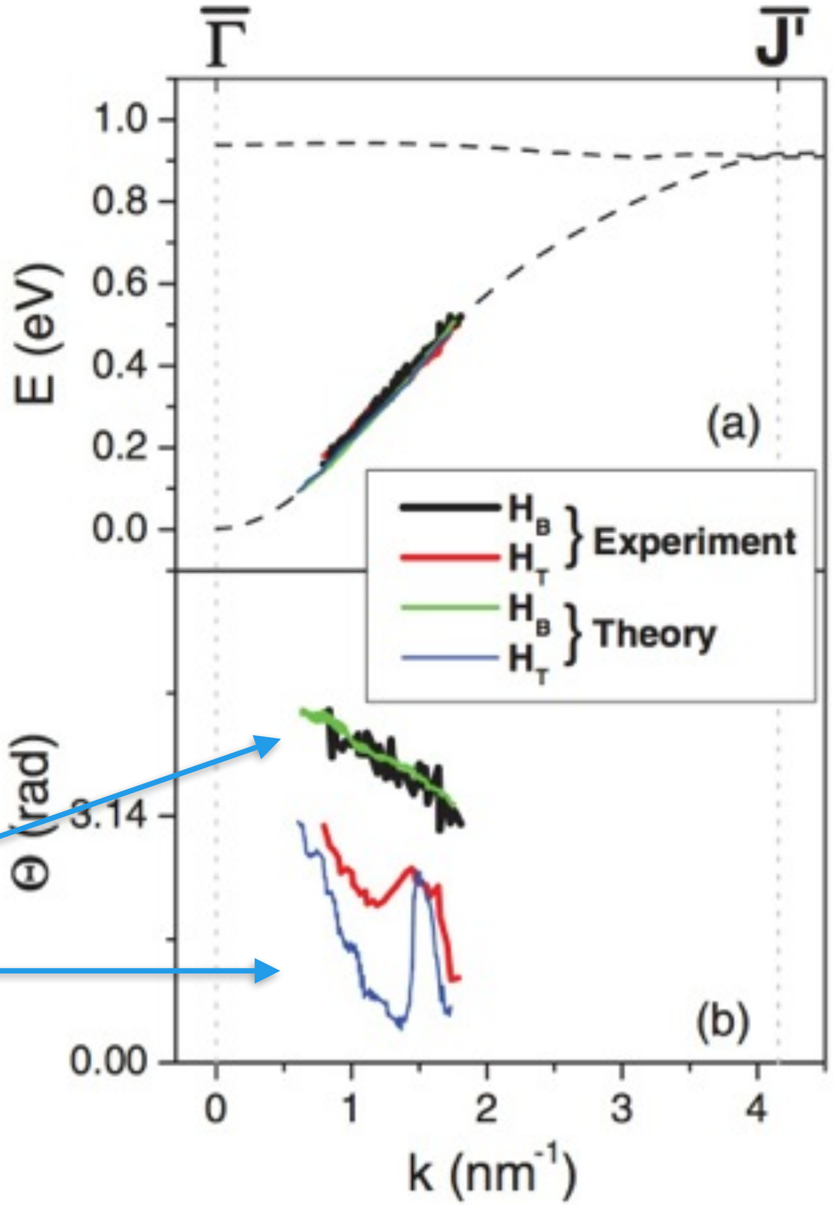

These are measured away from the scattering site!

Quantum interference device

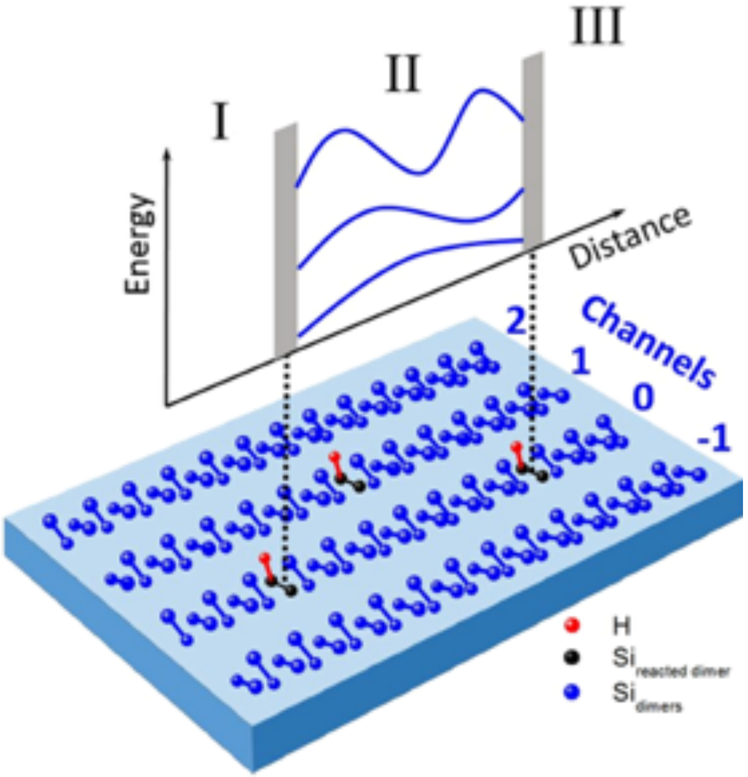

B. Naydenov, et al., Nano Lett. **15**, 2881 (2015)

QID on Si (100)

Quantum well

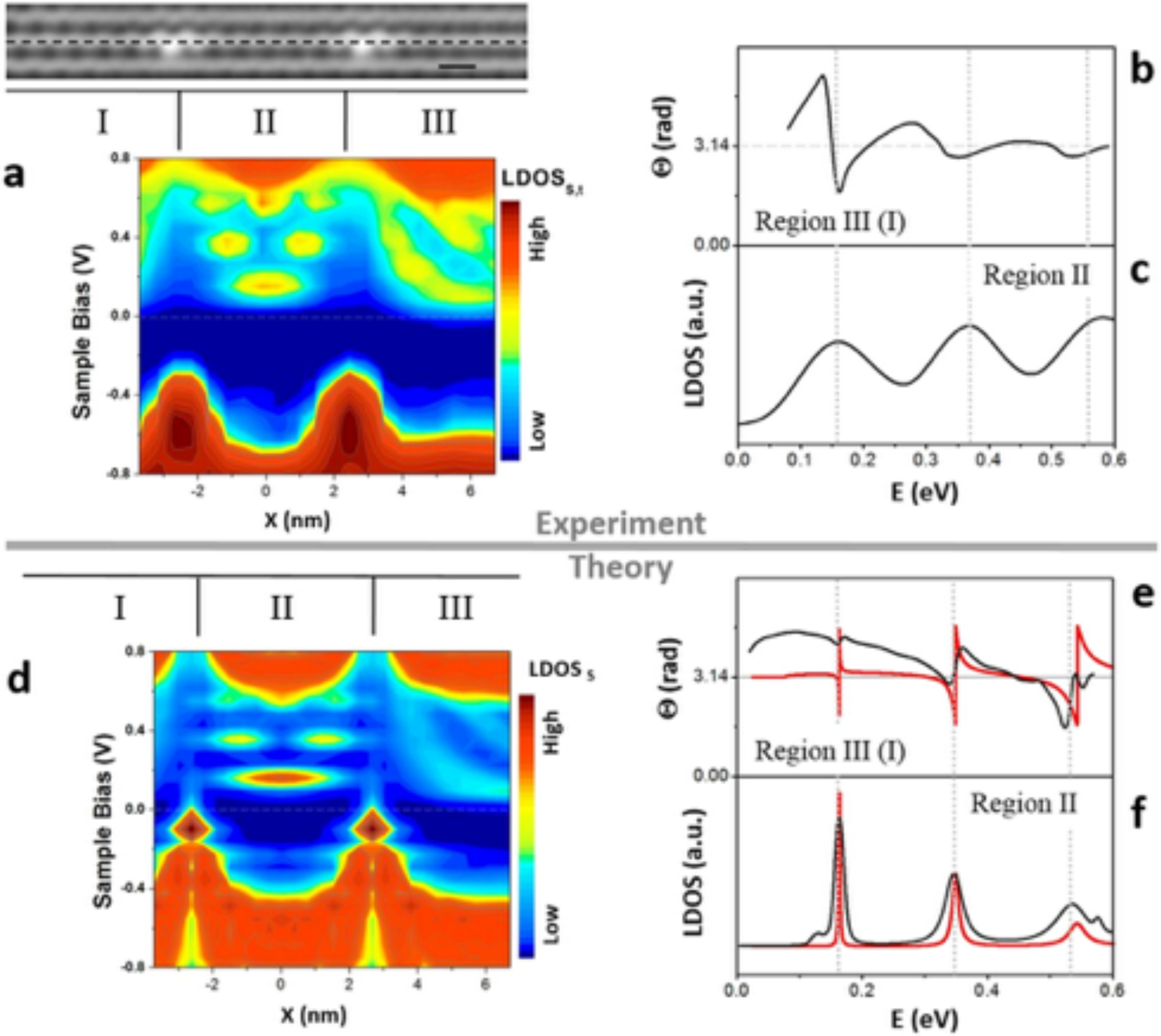

QID on Si (100)

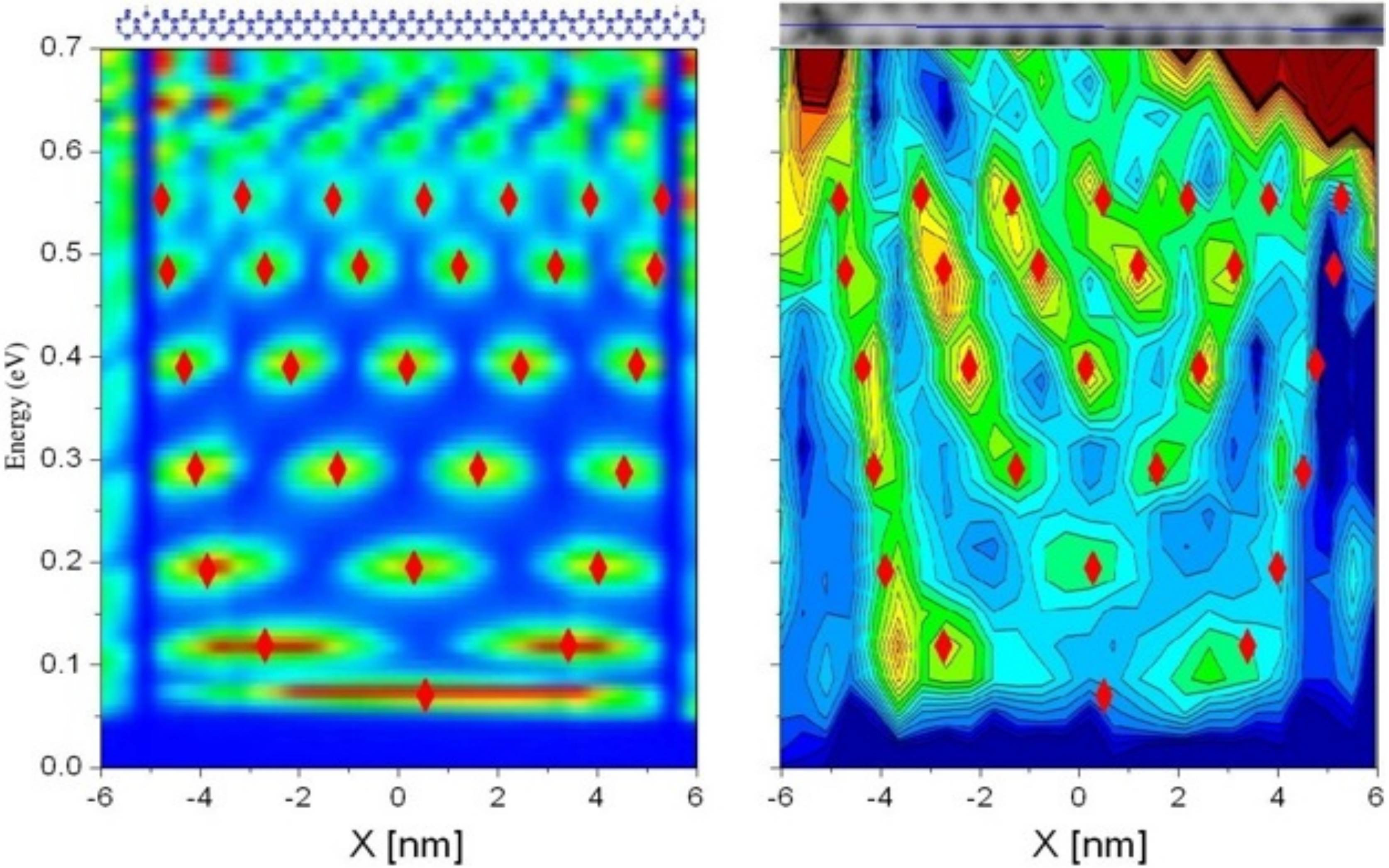

Theory

Experiment

QID on Si (100)

Gating

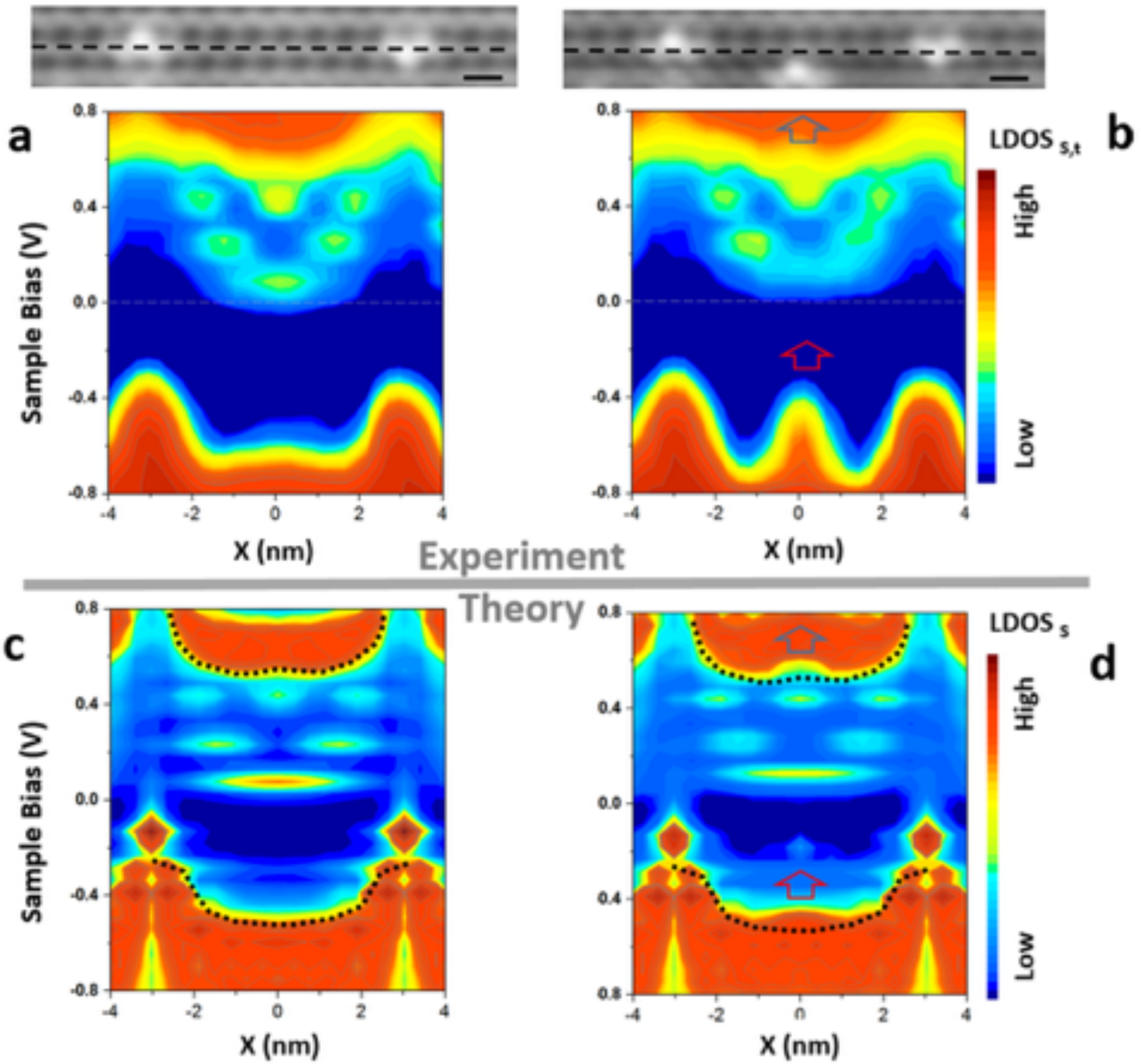

QID on Si (100)

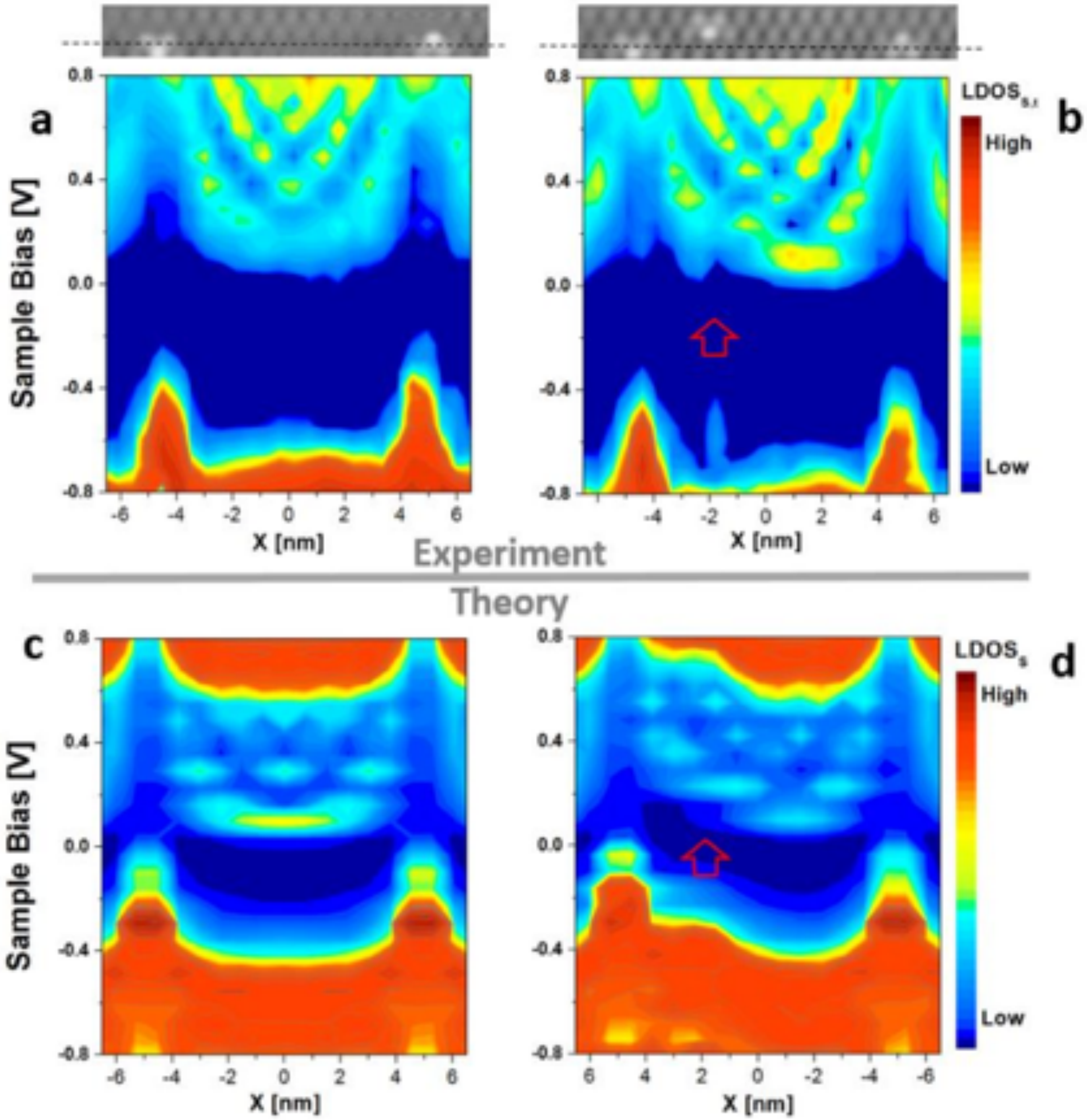
a
b
c
d
Sample Bias [V]
X [nm]
LDOS
High
Low
Experiment
Theory
0.8
0.4
0.0
-0.4
-0.8
-6
-4
-2
0
2
4
6

QID on Si (100)

Gating

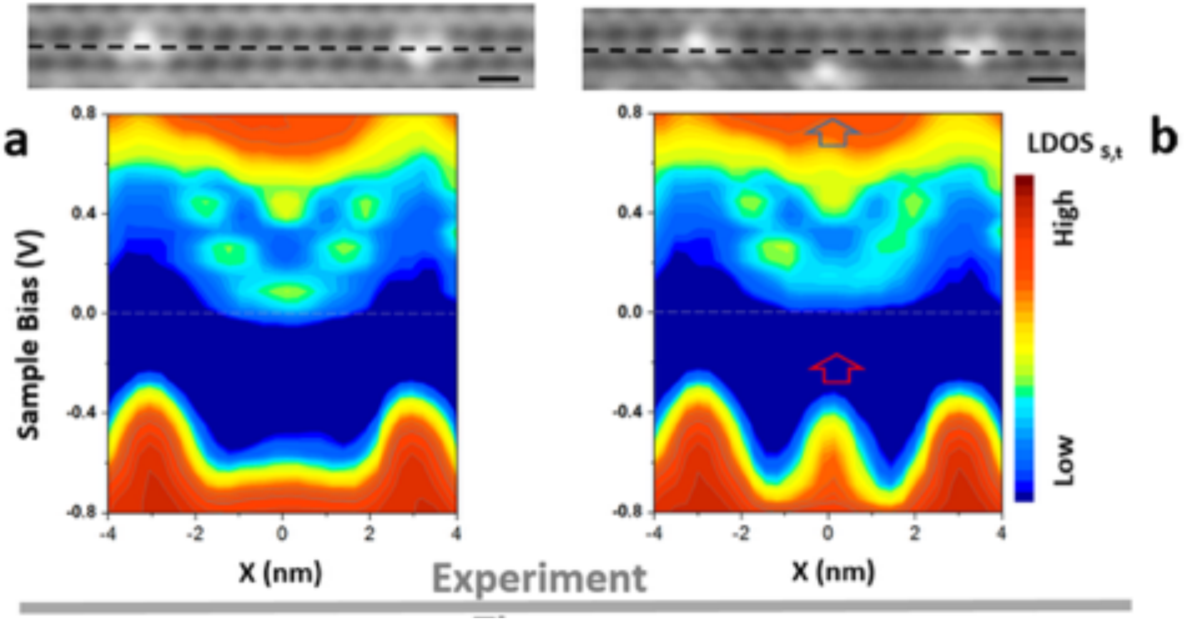

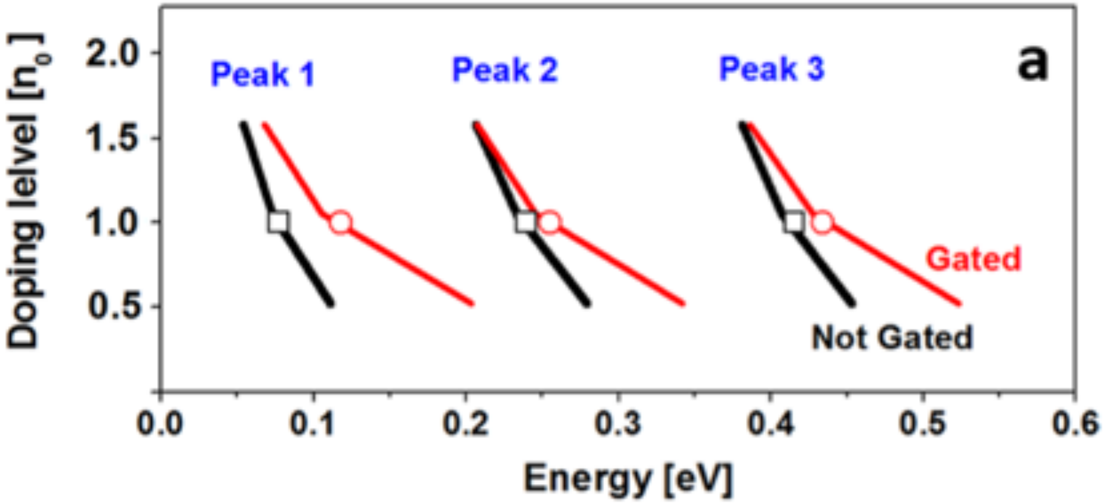

$n_0 = 6.5x10^{19}$

QID on Si (100)

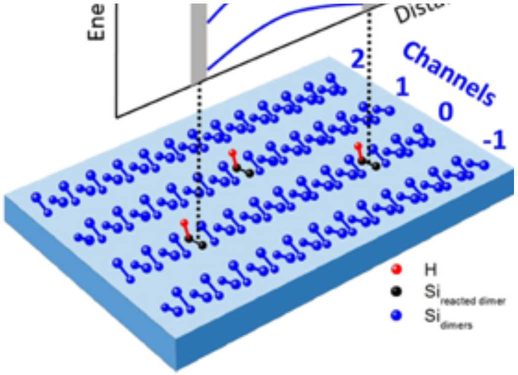

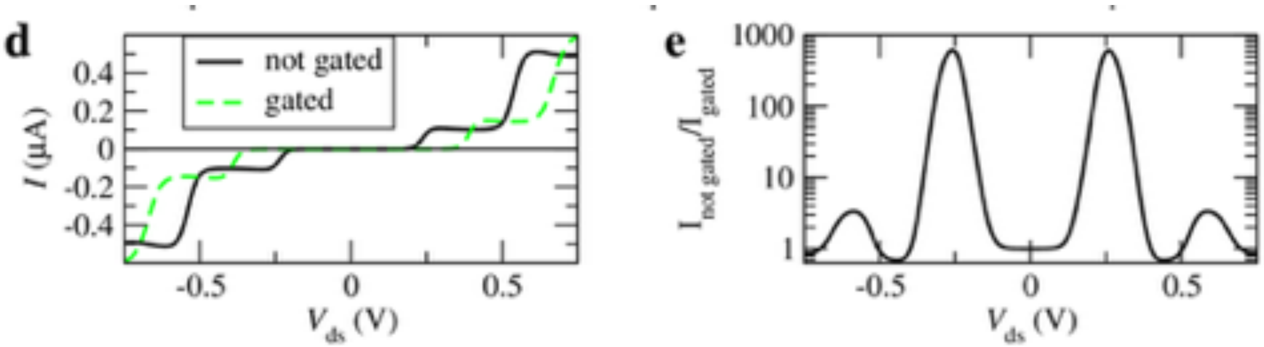

0.49 eV

0.49 eV

0.08 eV

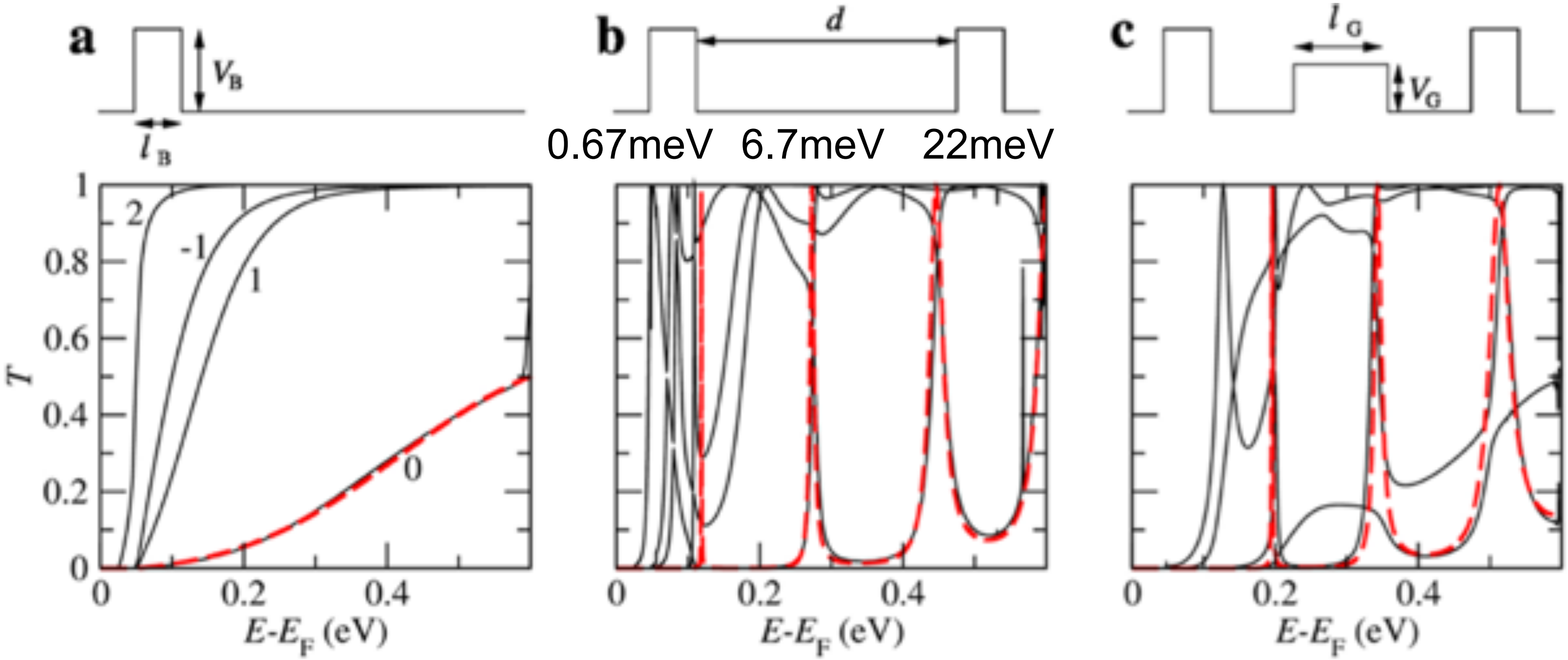

0.67meV 6.7meV 22meV

QID on Si (100)

- 1D devices on top of “peculiar” surfaces are possible

- Gating demonstrated

- Now need to put contact down (moving to Ge - more stable)!

Ivan Rungger, Rouxing Zhang, Shimin Hou

Moving Atoms: Forces

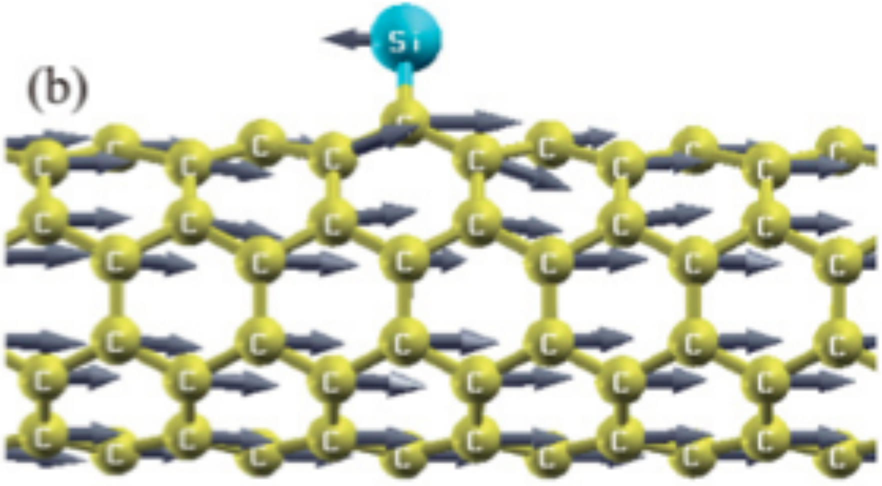

R. Zhang, I. Rungger, S. Sanvito and S. Hou, PRB **84**, 085445 (2011)

Forces

$$\boxed{\vec{F}_I = \frac{\partial}{\partial t}\langle\Psi(t)| - i\hbar \frac{\partial}{\partial \vec{R}_I}|\Psi(t)\rangle}$$

$$\vec{F}_I = -\frac{\partial \langle\psi|\,\hat{H}\,|\psi\rangle}{\partial \vec{R}_I}$$

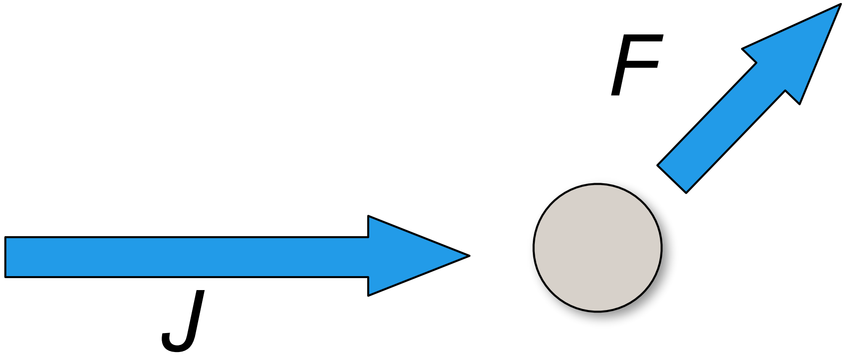

$$= \left[-\langle\Psi|\frac{\partial \hat{H}(\vec{R}_I)}{\partial \vec{R}_I}|\Psi\rangle\right]$$

Hellmann-Feynman

$$+\left[-\left\langle\frac{\partial\Psi}{\partial\vec{R}_I}\right|\hat{H}(\vec{R}_I)|\Psi\rangle - \langle\Psi|\hat{H}(\vec{R}_I)\left|\frac{\partial\Psi}{\partial\vec{R}_I}\right\rangle\right]$$

Pulay

Forces

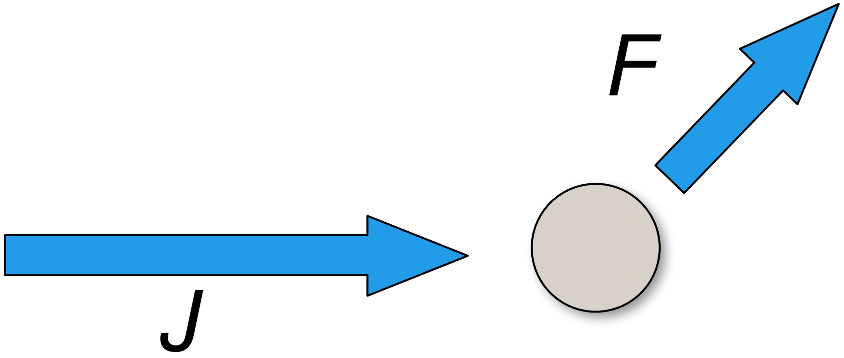

Wind force defined by subtraction

$$\boxed{F = F_{Field} + F_{\mathrm{Wind}}}$$

$$\vec{F}_{\mathrm{Field}}(V) = \vec{F}[\rho_{\mu\upsilon}(0); H_{\mu\upsilon}(0) + \Delta H_{\mu\upsilon}(V)]$$

$$\vec{F}_{\mathrm{Wind}}(V) = \vec{F}[\rho_{\mu\upsilon}(V); H_{\mu\upsilon}(V)] - \vec{F}_{\mathrm{Field}}(V)$$

Forces

Tests

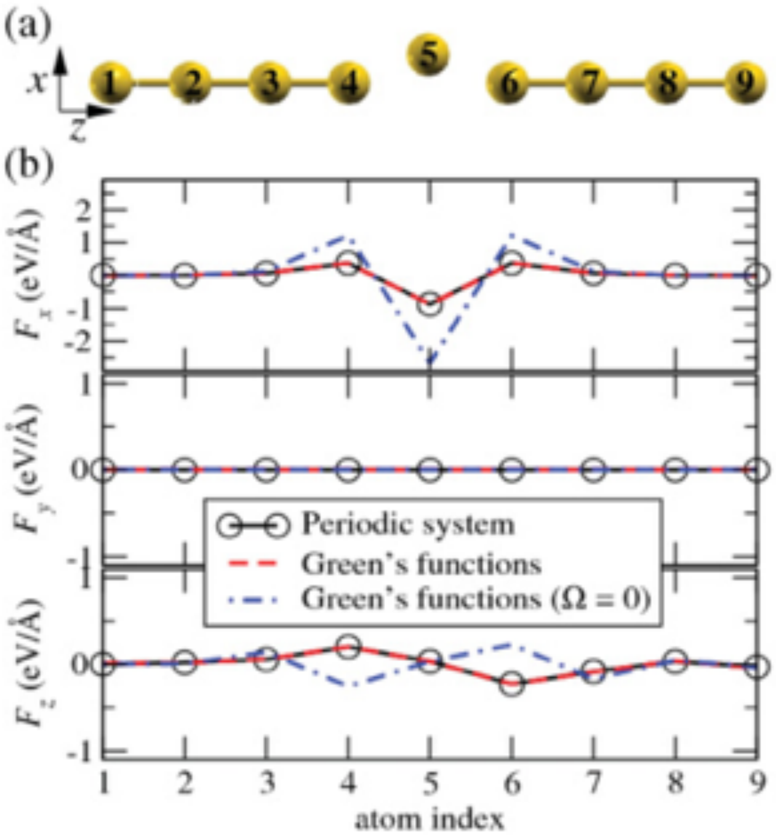

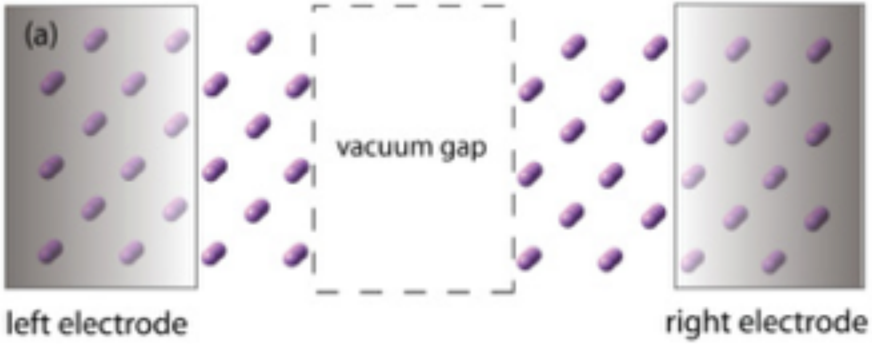

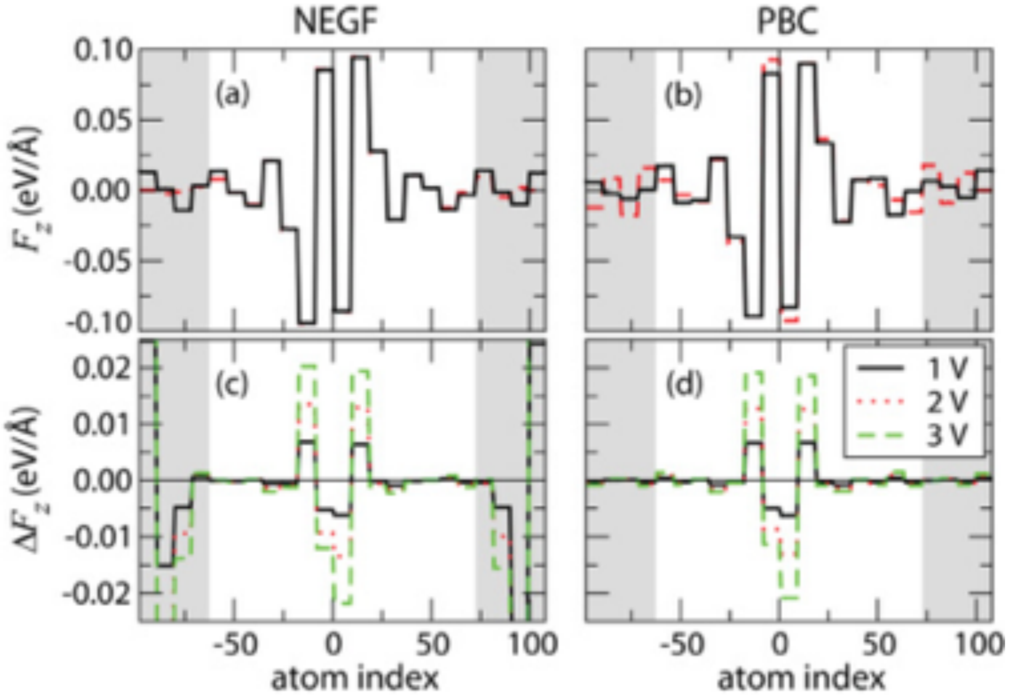

Electromigration: Si @ CNT

Stable position: bridge site

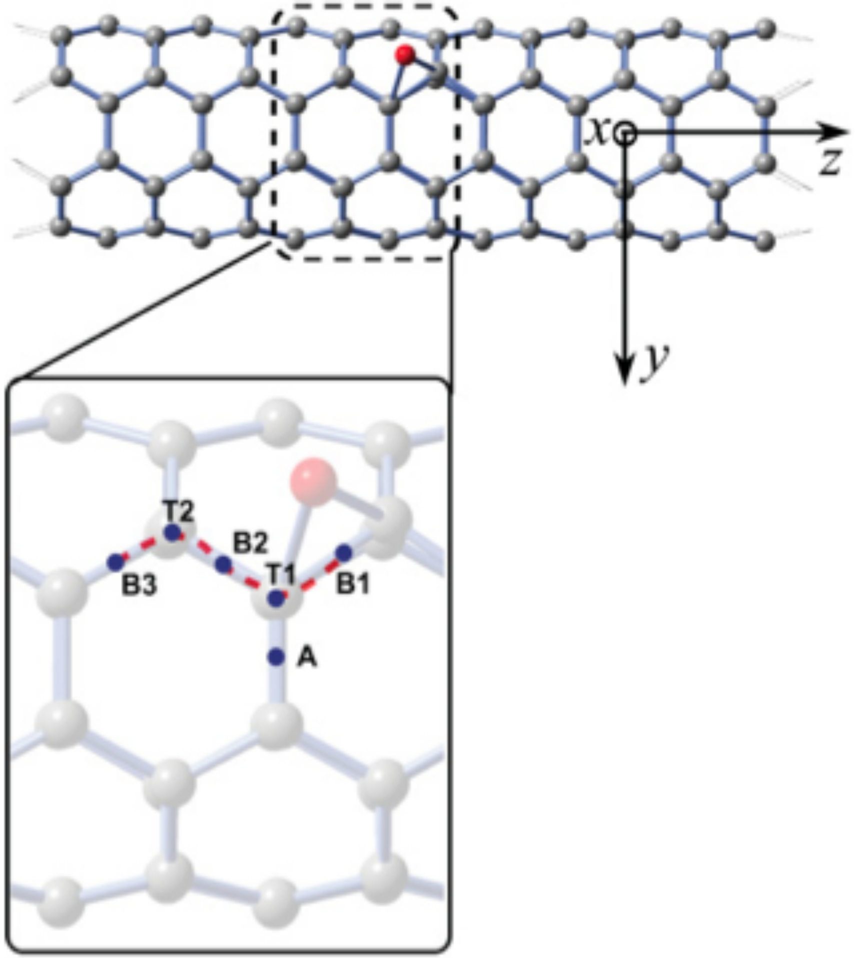

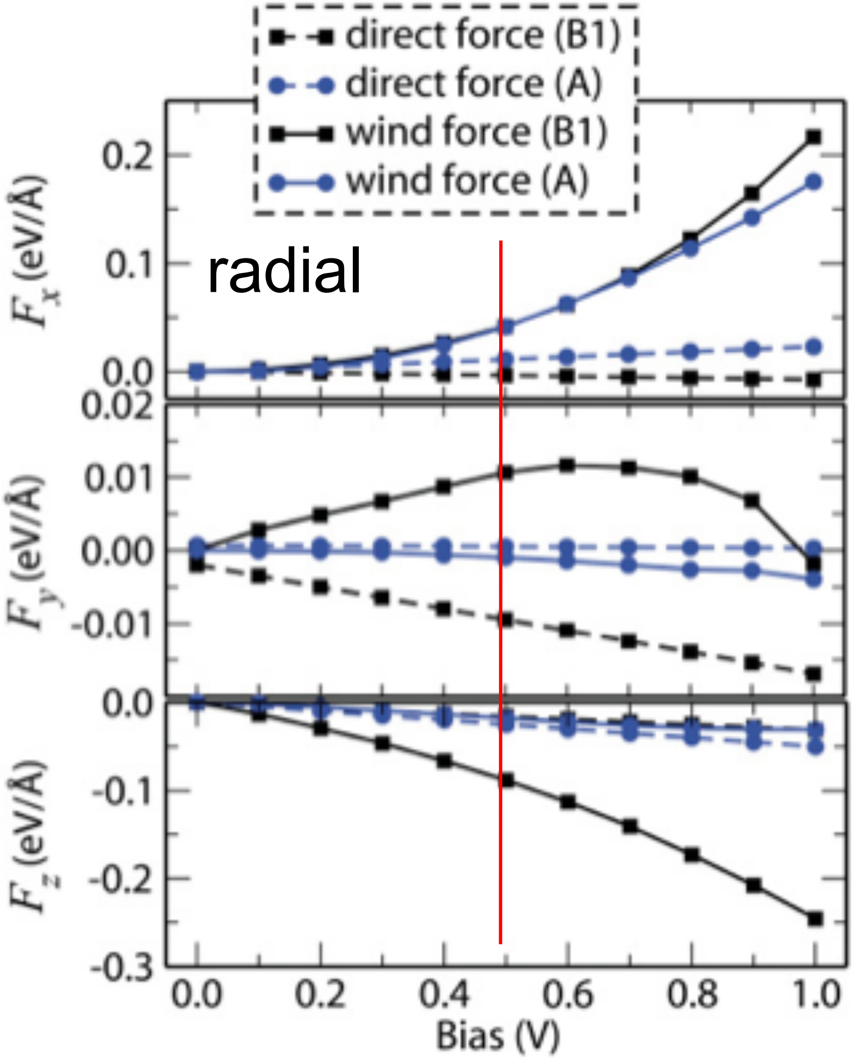

radial

I_C~60 μA

Electromigration

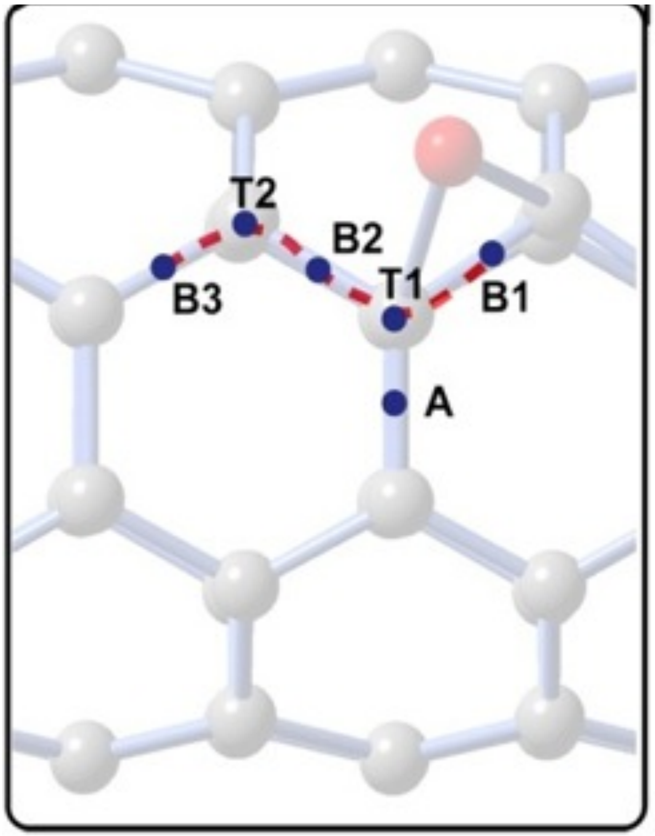

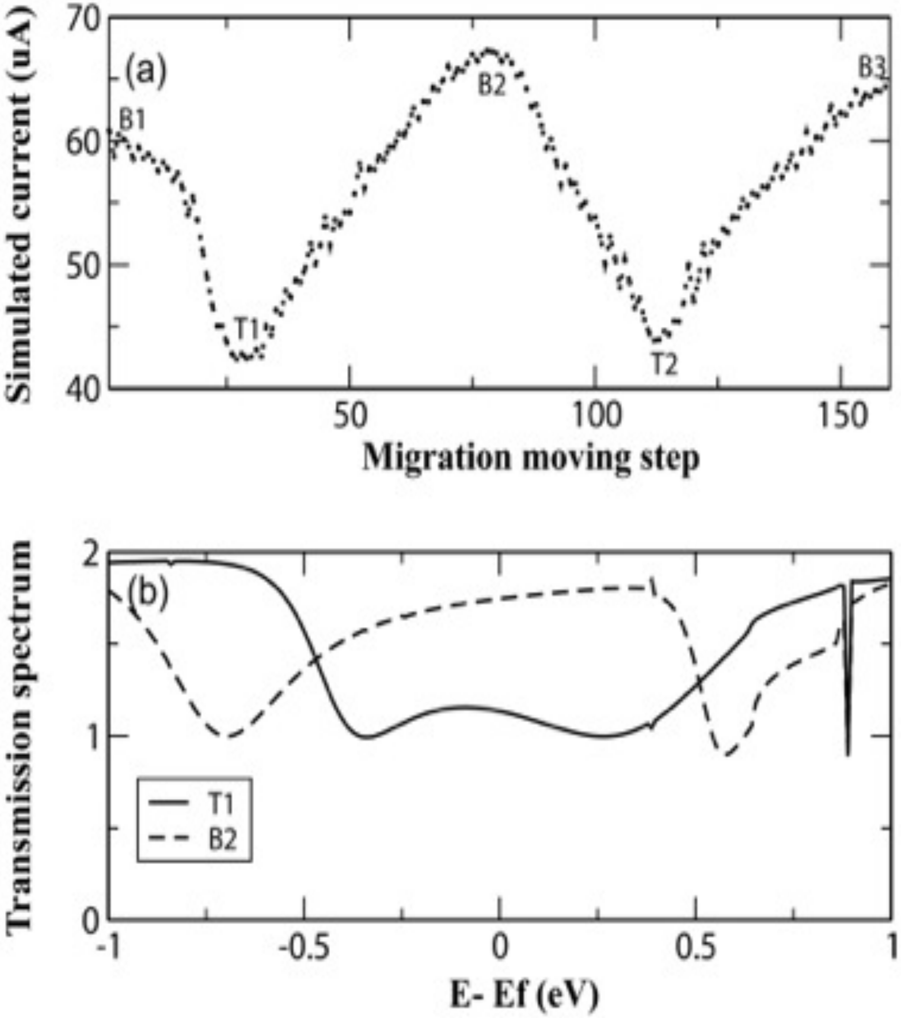

Meilin Bai, Shimin Hou, Ivan Rungger, Clotilde Cucinotta

Moving Atoms: Phonons

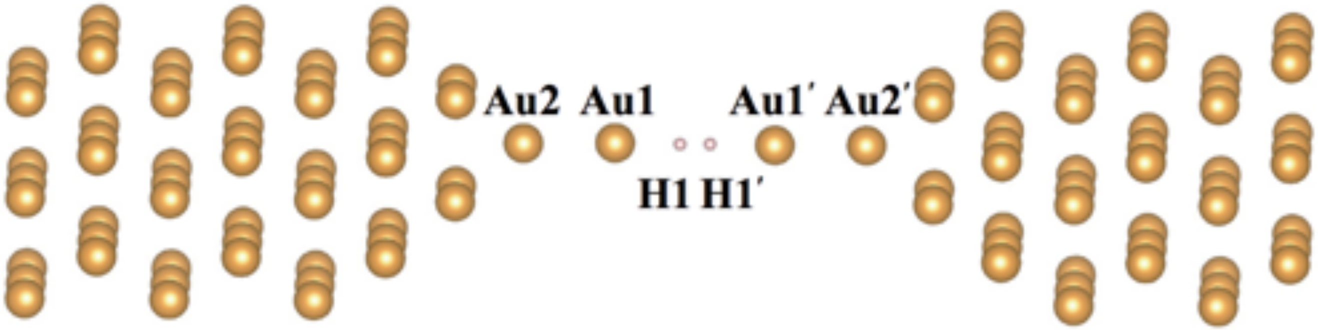

R. Zhang, I. Rungger, S. Sanvito and S. Hou, PRB 9**4**, 035411 (2016)

Phonons

In equilibrium

$$C_{\alpha i\beta j}=\left(\frac{\partial^2 V}{\partial q_{\alpha i}\partial q_{\beta j}}\right)_0=\left(\frac{\partial^2 E}{\partial q_{\alpha i}\partial q_{\beta j}}\right)_0$$

Under bias

$$C_{\alpha i\beta j}=-\left(\frac{\partial F_{\alpha i}}{\partial q_{\beta j}}\right)_0=-\left(\frac{\partial F_{\beta j}}{\partial q_{\alpha i}}\right)_0=C_{\beta j\alpha i}$$

By finite difference: displacement 0.02A

Phonons

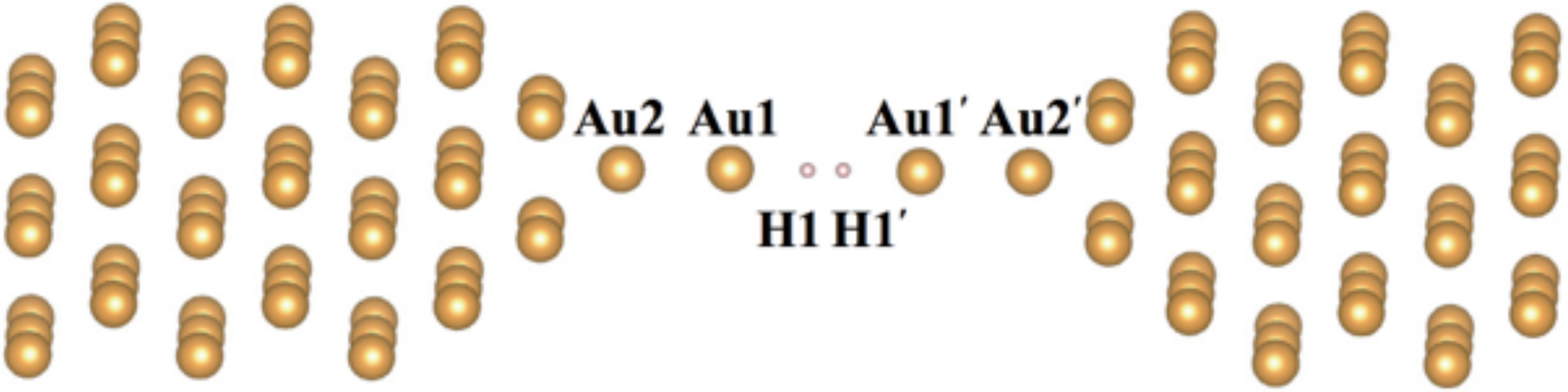
Au2 Au1
Au1′ Au2′
H1 H1′

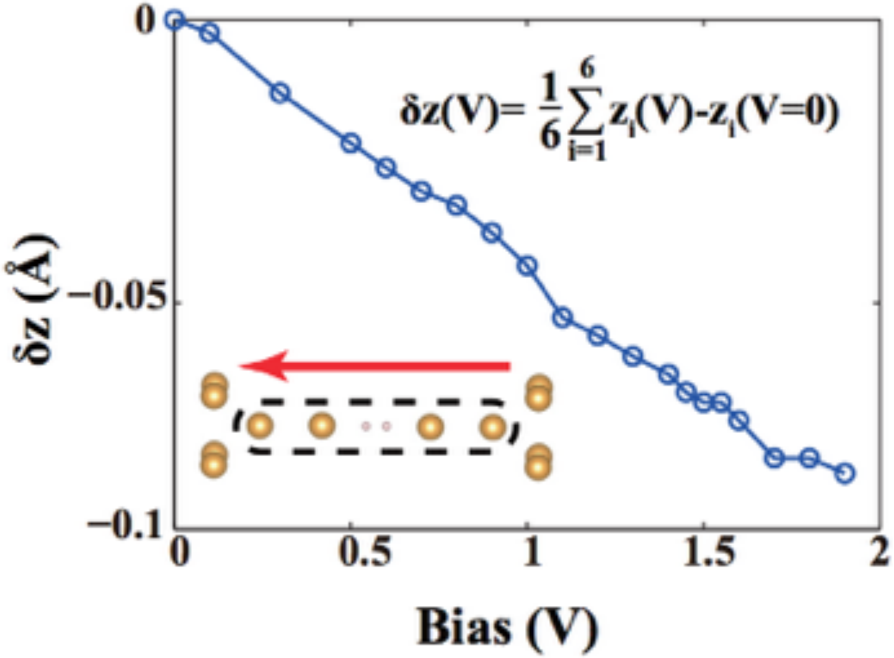
0
−0.05
−0.1
δz (Å)
$\delta z(V)=\frac{1}{6}\sum_{i=1}^{6} z_i(V)-z_i(V=0)$
0
0.5
1
1.5
2
Bias (V)

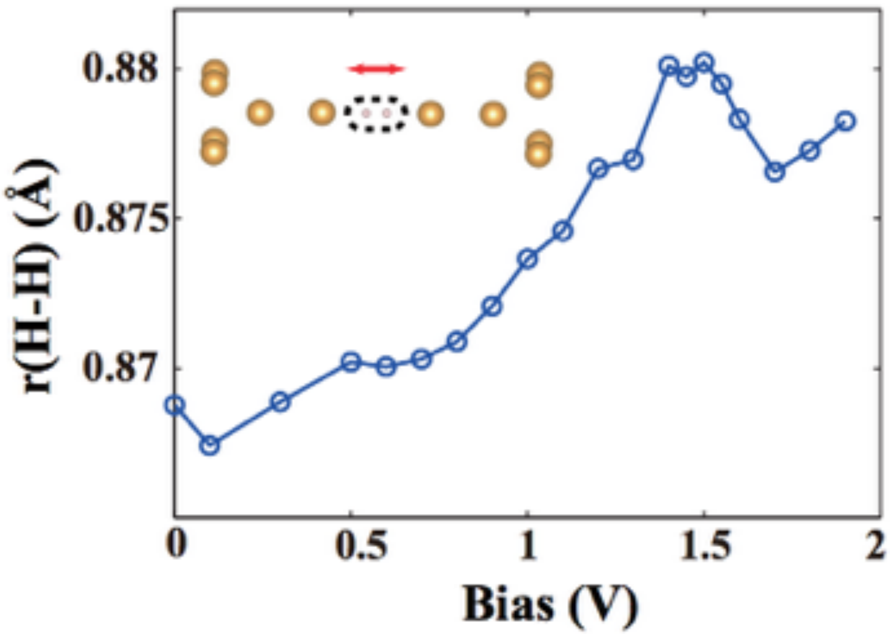
0.88
0.875
0.87
r(H-H) (Å)
0
0.5
1
1.5
2
Bias (V)

Phonons

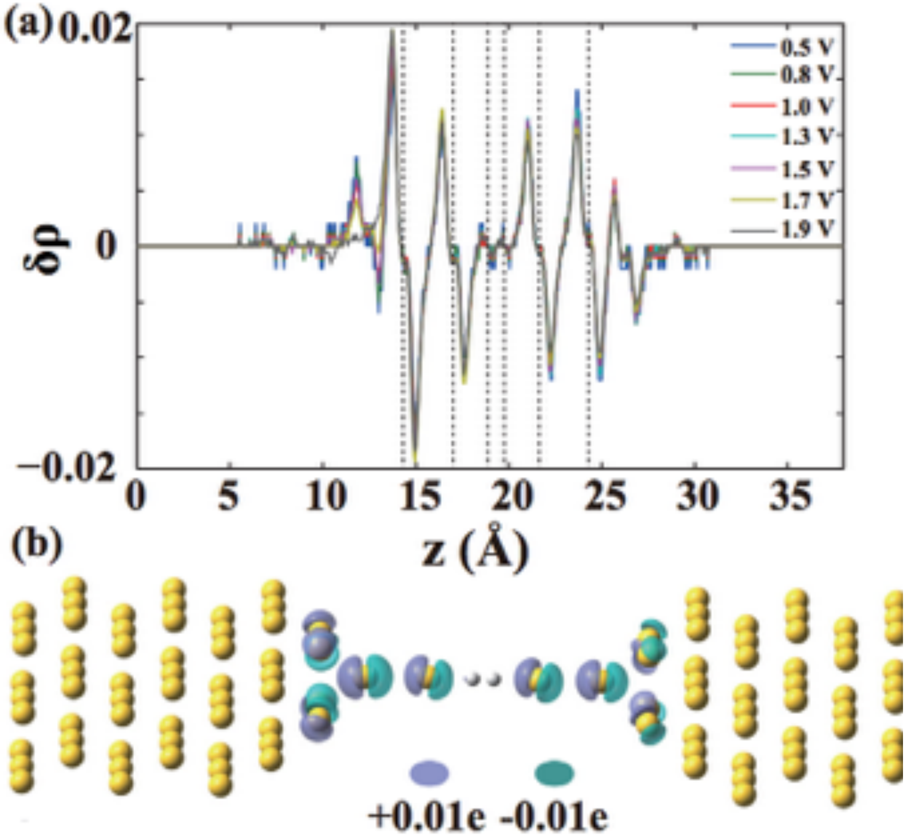

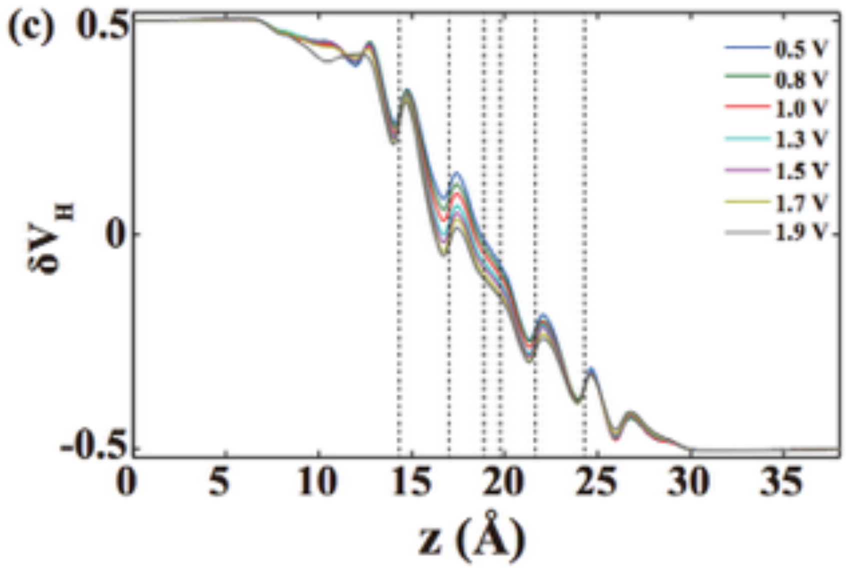

Formation of a dipole under bias

Charge density difference *D*(1V)-*D*(0V)

Phonons

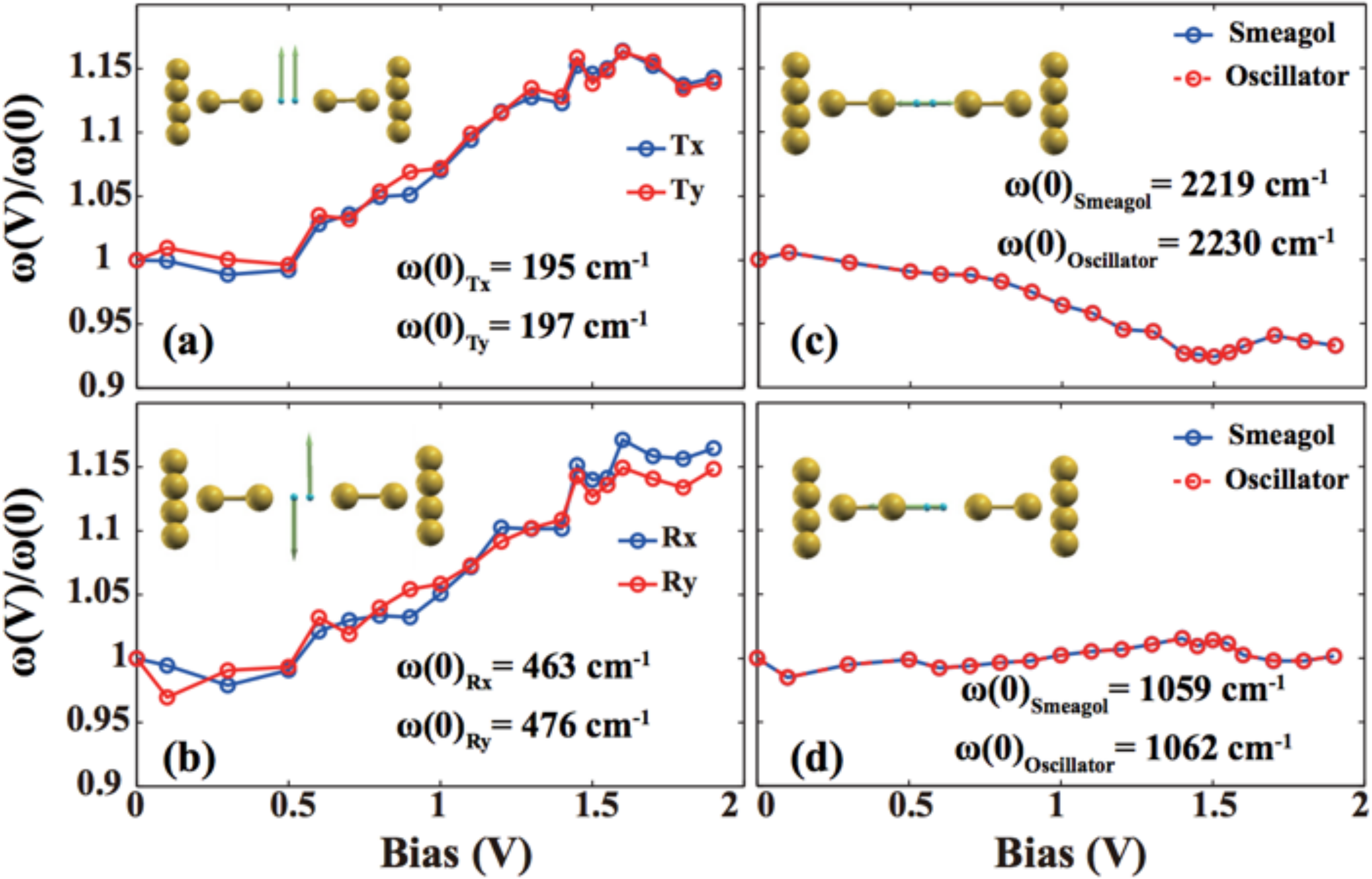
ω(V)/ω(0)
1.15
1.1
1.05
1
0.95
0.9
Tx
Ty
ω(0)_Tx = 195 cm-1
ω(0)_Ty = 197 cm-1
(a)
Smeagol
Oscillator
ω(0)_Smeagol = 2219 cm-1
ω(0)_Oscillator = 2230 cm-1
(c)
Rx
Ry
ω(0)_Rx = 463 cm-1
ω(0)_Ry = 476 cm-1
(b)
ω(0)_Smeagol = 1059 cm-1
ω(0)_Oscillator = 1062 cm-1
(d)
0
0.5
1
1.5
2
Bias (V)

Phonons

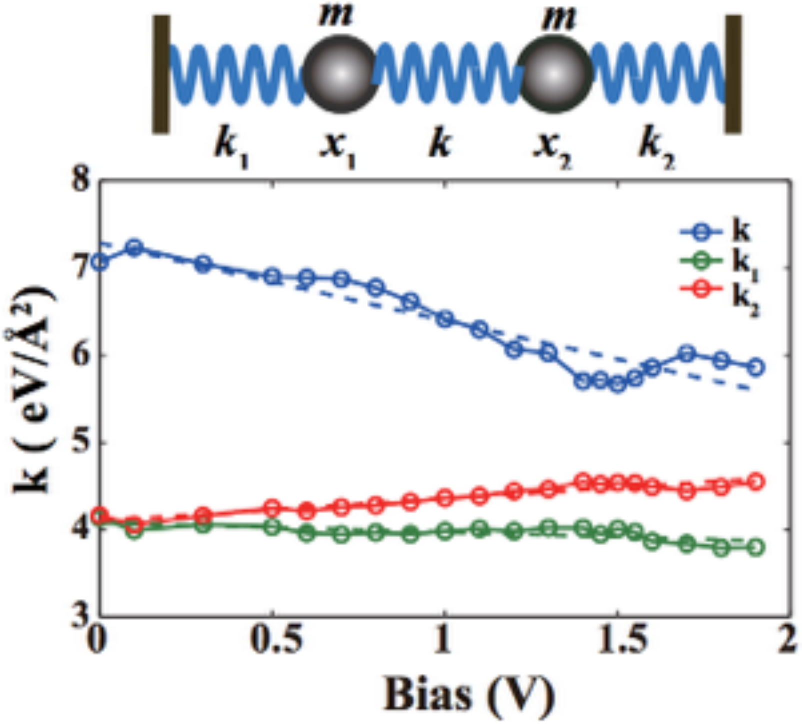

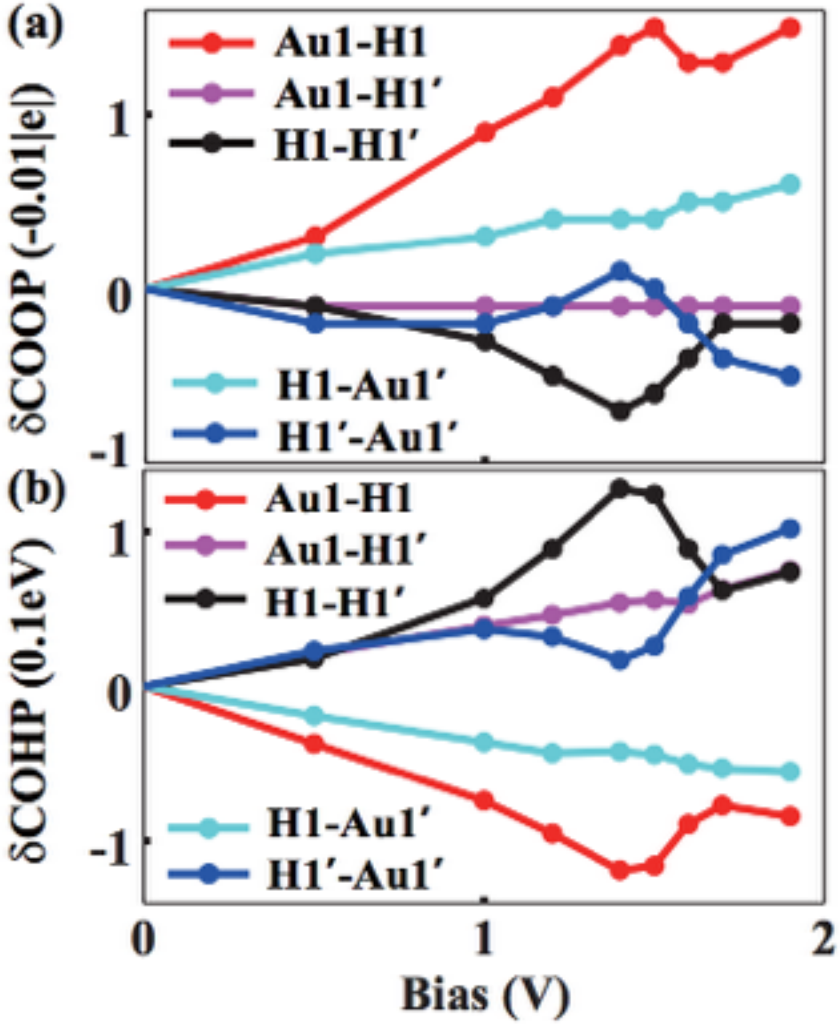

crystal orbital overlap population

crystal orbital Hamiltonian population

Phonons

Electrostatic energy between H_2 and Au increases

$$E_{\mathrm{int}} = \sum_{i<j} \frac{Q_i Q_j}{4\pi \varepsilon_0 r_{ij}}$$

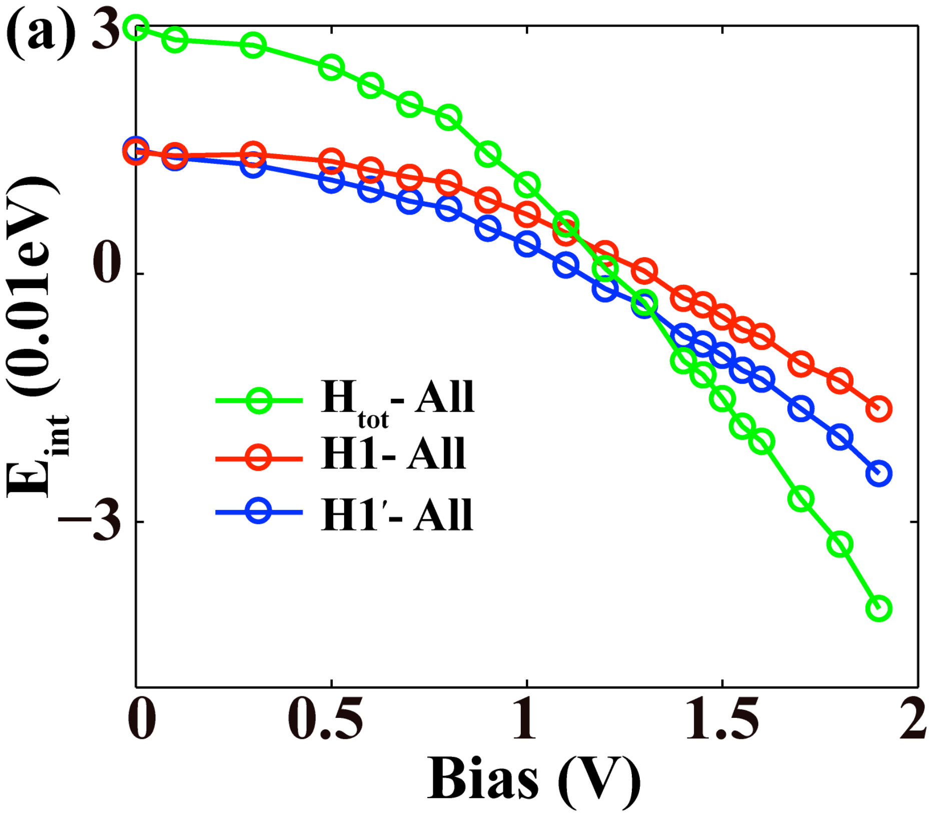

Phonons

- Calculations of phonon softening/hardening under bias demonstrated
- Interpretation in terms of bond strength change and electrostatic contribution
- How can we measure that?

COMPUTATIONAL SPINTRONICS
SANVITO RESEARCH GROUP
TRINITY COLLEGE, DUBLIN

CRANN

TCD Team:

Amaury Souza, Awadhesh Narayan, Ivan Rungger, Clotilde Cucinotta

Beijing Team:

Shimin Hou, Meilin Bai, Rouxin Zhang

CRANN
sfi science foundation ireland
SEVENTH FRAMEWORK PROGRAMME
KAUST King Abdullah University of Science and Technology
TCHPC
ICHEC Irish Centre for High-End Computing

CSIC
CONSEJO SUPERIOR DE INVESTIGACIONES CIENTÍFICAS
INSTITUTO DE CIENCIA DE MATERIALES
DE MADRID (ICMM)

ICMM

Long range transport and quantum interferences in quantum dots arrays

G. Platero
Instituto de Ciencia de Materiales de Madrid, CSIC, Spain

Dresden, MPI april 2017

Universidad Carlos III de Madrid

Rafael Sánchez

Fernando Gallego

Gloria Platero

ICMM

CSIC

CONSEJO SUPERIOR DE INVESTIGACIONES CIENTÍFICAS

INSTITUTO DE CIENCIA DE MATERIALES
DE MADRID (ICMM)

VOLUME 78, NUMBER 16 PHYSICAL REVIEW LETTERS 21 APRIL 1997

Quantum State Transfer and Entanglement Distribution among Distant Nodes in a Quantum Network

J. I. Cirac,[1,2] P. Zoller,[1,2] H. J. Kimble,[1,3] and H. Mabuchi[1,3]

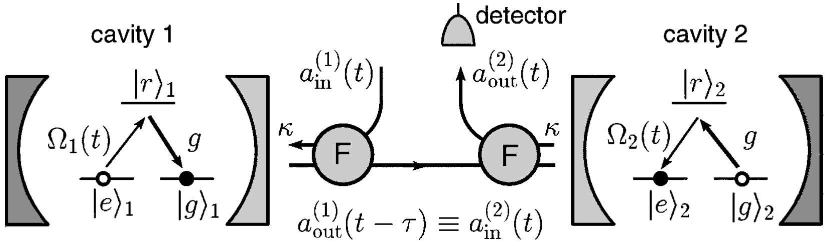

VOLUME 93, NUMBER 12 PHYSICAL REVIEW LETTERS week ending 17 SEPTEMBER 2004

Mesoscopic One-Way Channels for Quantum State Transfer via the Quantum Hall Effect

T. M. Stace,[1,2,*] C. H. W. Barnes,[1] and G. J. Milburn[3]

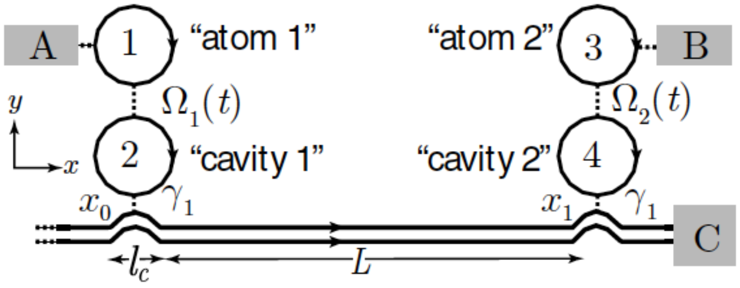

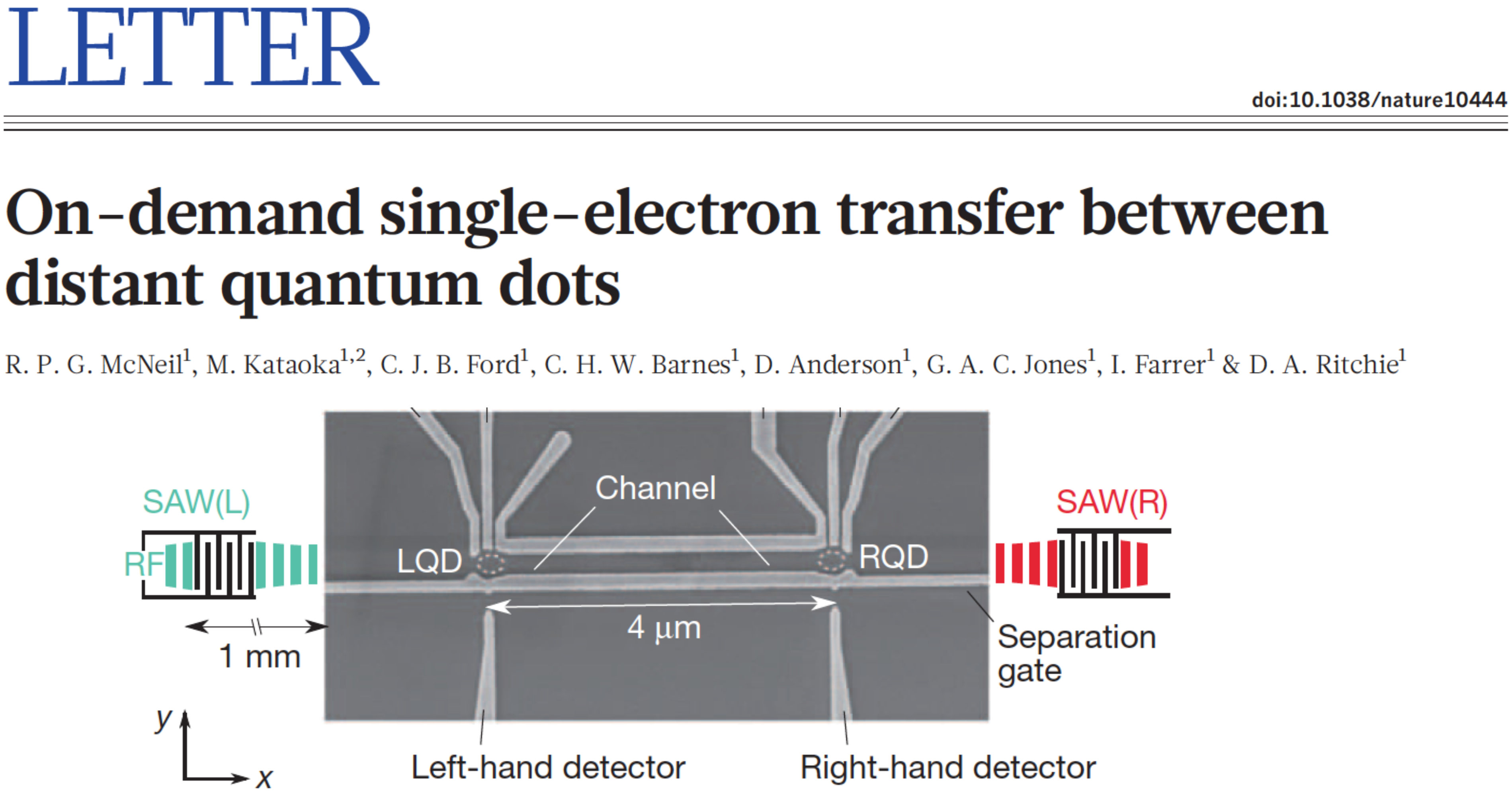

LETTER

doi:10.1038/nature10444

On-demand single-electron transfer between distant quantum dots

R. P. G. McNeil[1], M. Kataoka[1,2], C. J. B. Ford[1], C. H. W. Barnes[1], D. Anderson[1], G. A. C. Jones[1], I. Farrer[1] & D. A. Ritchie[1]

M. Benito et al., PRB, 94, 115404 (2016)

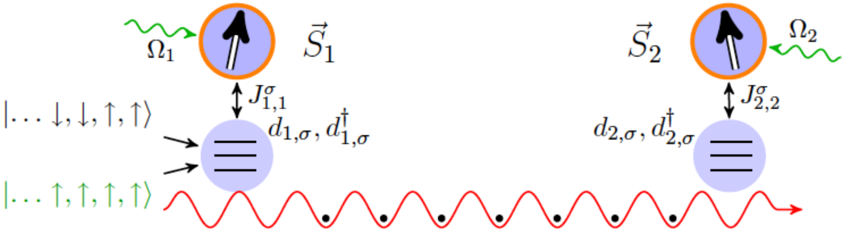

“Coherent transfer by adiabatic passage” (CTAP)

Electron transfer
from dot 1 to dot 3
without occupying dot 2

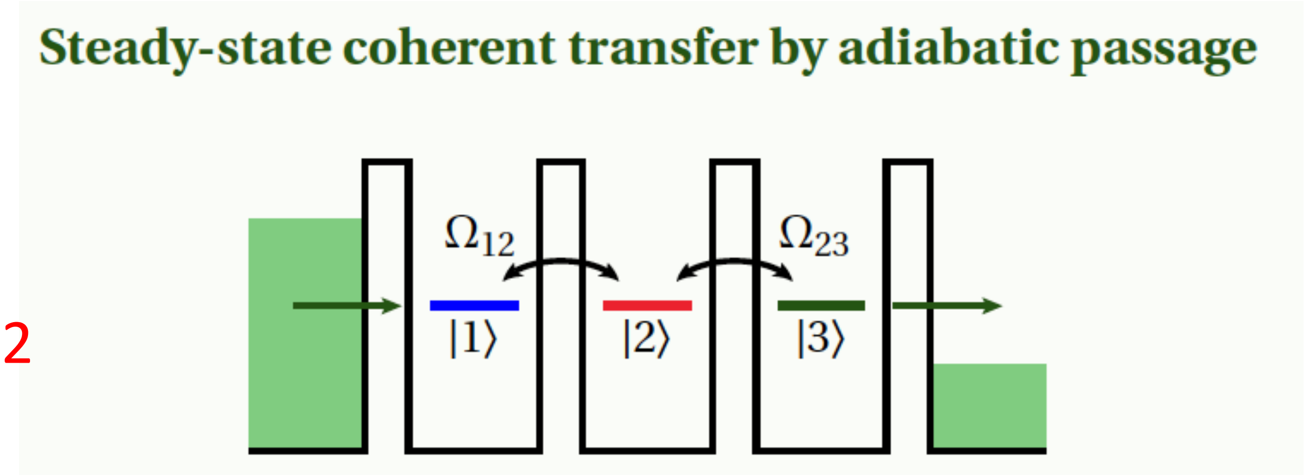

Greentree et al., PRB 2004

$$H = \begin{pmatrix} 0 & \Omega_{12} & 0 \\ \Omega_{12} & 0 & \Omega_{23} \\ 0 & \Omega_{23} & 0 \end{pmatrix};$$

$$\varepsilon = 0$$

$$|\varphi\rangle = \cos\theta|1\rangle - \sin\theta|3\rangle$$

$$\theta = \arctan(\Omega_{12} / \Omega_{23})$$

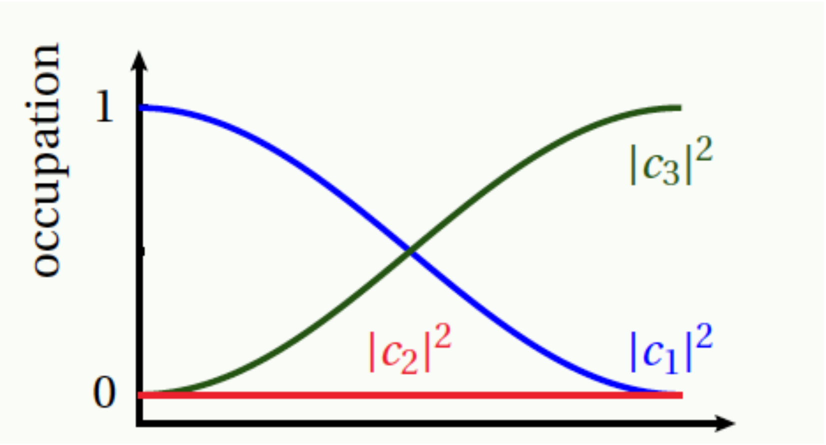

Ratio of the tunneling rates Ω_{12}, Ω_{23}

Jan Huneke, Gloria Platero, and Sigmund Kohler, Phys. Rev. Lett. 110, 036802 (2013)

Quantum electron transfer between distant sites in triple quantum dots

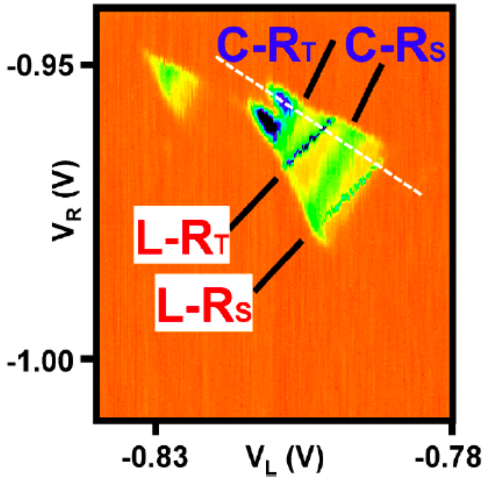

L-R lines:

$$|\Psi\rangle = \alpha|1,1,2\rangle + \beta|2,1,1\rangle$$

M. Busl et al.,
Nature Nanotech, 8, 262 (2013).

Long range transfer by quantum superpositions

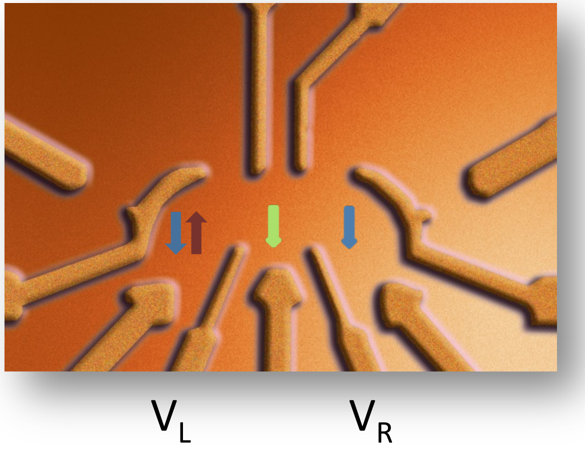

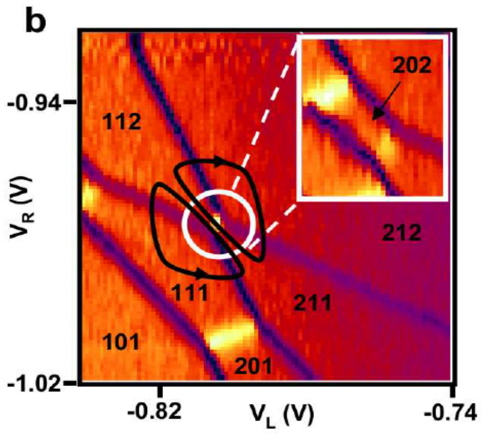

Quantum electron transfer between distant sites in triple quantum dots

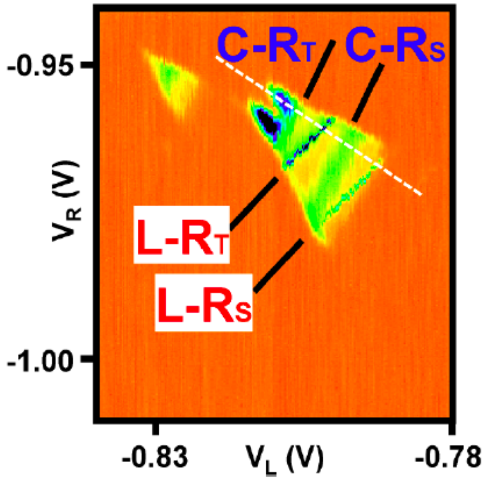

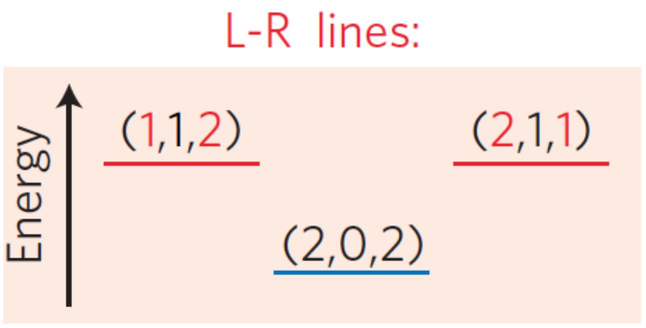
L-R lines:

$$|\Psi\rangle = \alpha|1,1,2\rangle + \beta|2,1,1\rangle$$

M. Busl et al.,
Nature Nanotech, 8, 262 (2013).

Long range transfer by quantum superpositions

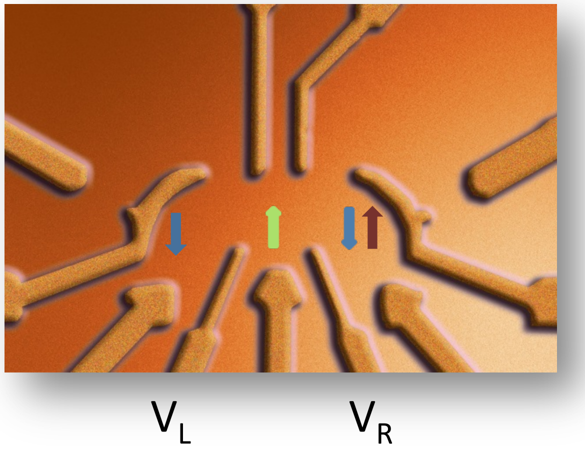

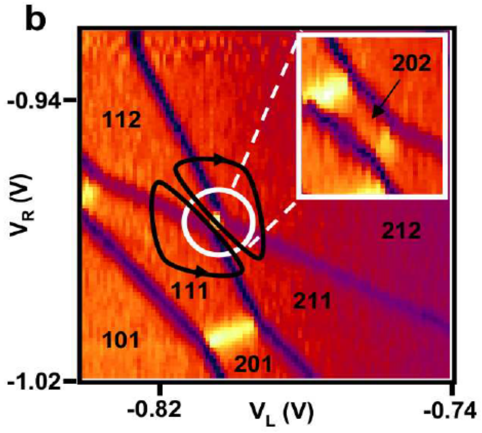

L-R resonance of (2,0,1) and (1,0,2) ,
intermediate (1,1,1) far in energy

R. Sánchez et al., PRL, 112, 176803 (2014)

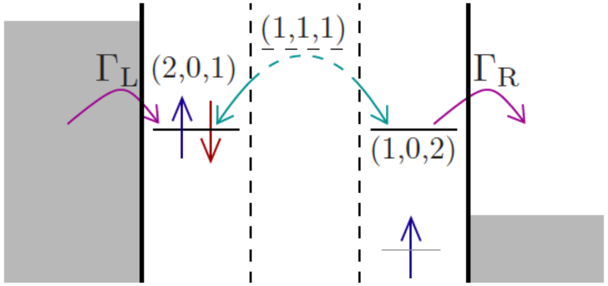

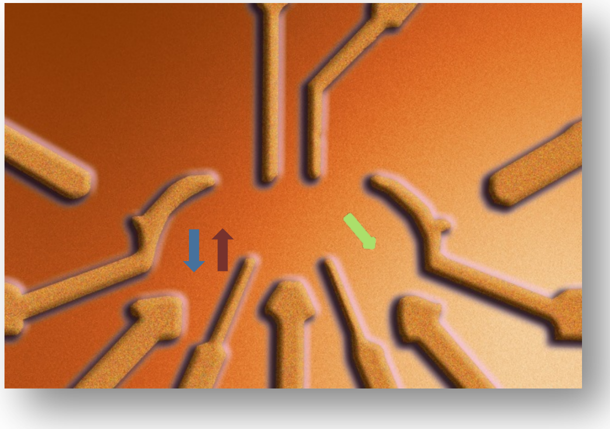

$$\Delta E \gg \tau \qquad |LR_-\rangle = \frac{1}{\sqrt{2}}\left(|\uparrow\downarrow,0,\psi\rangle - |\psi,0,\uparrow\downarrow\rangle\right)$$

As an electron tunnels from one extreme to the other an arbitrary spin state ψ is transferred in the opposite direction:

$$|\psi\rangle_{l=L,R} = c_\uparrow|\uparrow\rangle_l + c_\downarrow|\downarrow\rangle_l$$

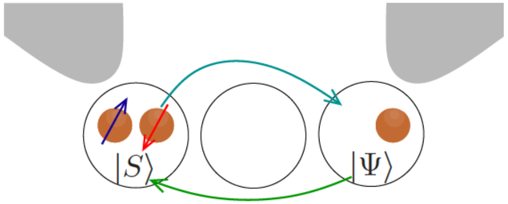

R. Sánchez et al., PRL, 112, 176803 (2014)

L-R resonance of (2,0,1) and (1,0,2) ,
intermediate (1,1,1) far in energy

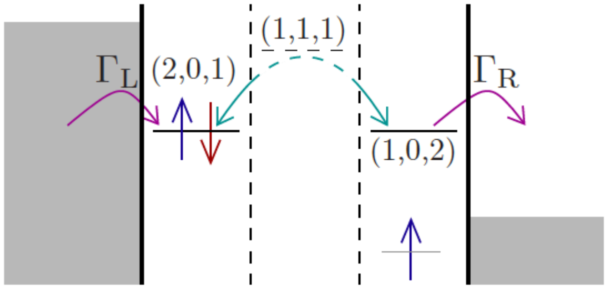

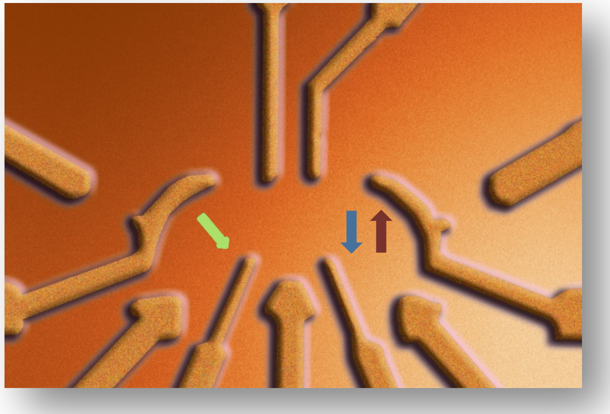

$\Delta E \gg \tau$ $\qquad |LR_-\rangle = \frac{1}{\sqrt{2}}\left(|\uparrow\downarrow,0,\psi\rangle - |\psi,0,\uparrow\downarrow\rangle\right)$

As an electron tunnels from one extreme to the other an arbitrary spin state ψ is transferred in the opposite direction:

$$|\psi\rangle_{l=L,R} = c_\uparrow|\uparrow\rangle_l + c_\downarrow|\downarrow\rangle_l$$

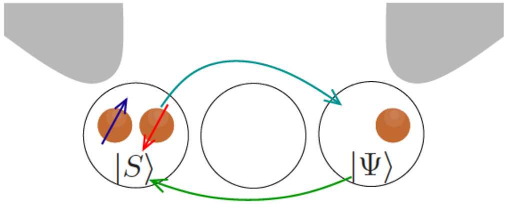

Long range interaction

In the chemical bond: Resonance Hybrid States

L. Pauling 1931

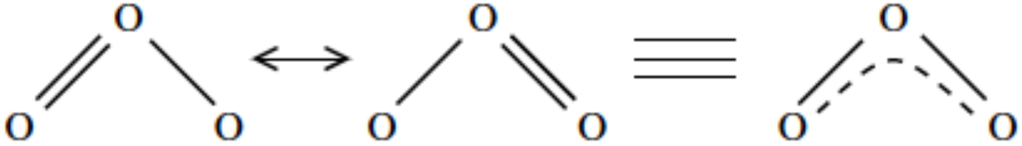

In TQDs, Amaha et al.,
PRB, RC, 2012

Long range interaction

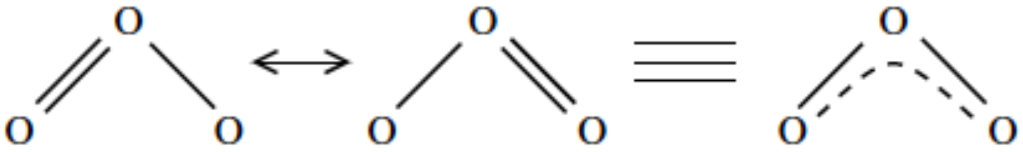

Delocalized charge in TQDs:

$$\Phi = \frac{1}{\sqrt{2}}\left(\left(1,0,0\right)-\left(0,1,0\right)\right)$$

Dark State

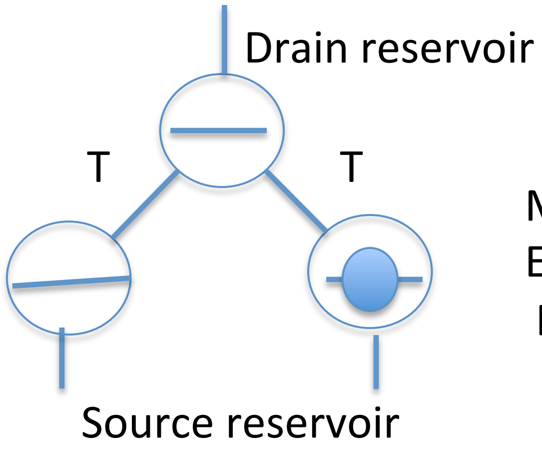

Michaelis ,
Emary and Beenakker
EPL 06

All-electronic coherent population trapping in quantum dots

Long range interaction

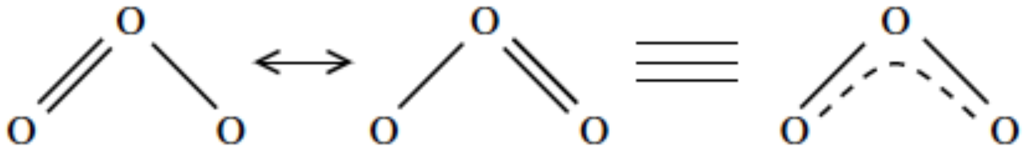

Delocalized charge in TQDs:

$$\Phi = \frac{1}{\sqrt{2}}\big((1,0,0)-(0,1,0)\big)$$

Dark State

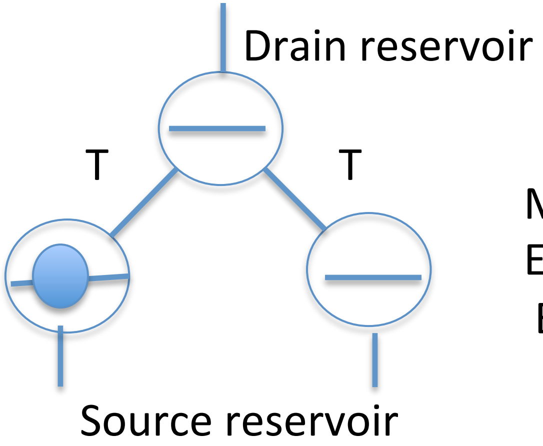

Michaelis ,
Emary and Beenakker
EPL 06

All-electronic coherent population trapping in quantum dots

Long range interaction

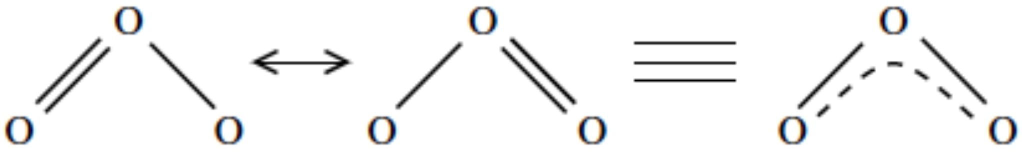

Delocalized charge in TQDs:

$$\Phi = \frac{1}{\sqrt{2}}\big(\left(1,0,0\right)-\left(0,1,0\right)\big)$$

Dark State

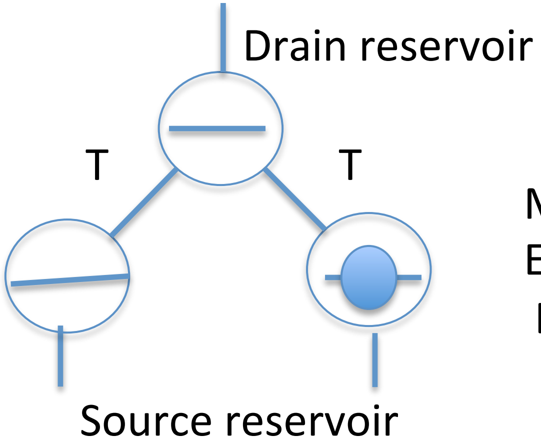

Michaelis ,
Emary and Beenakker
EPL 06

All-electronic coherent population trapping in quantum dots

Long range interaction

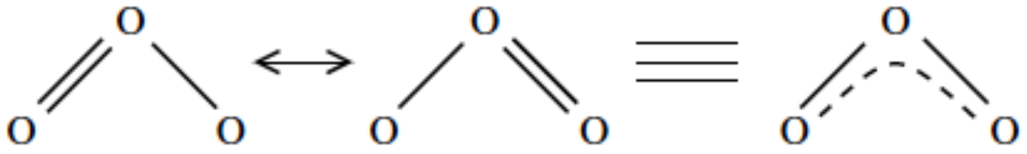

Delocalized charge in TQDs:

$$\Phi = \frac{1}{\sqrt{2}}\big((1,0,0)-(0,1,0)\big)$$

Dark State

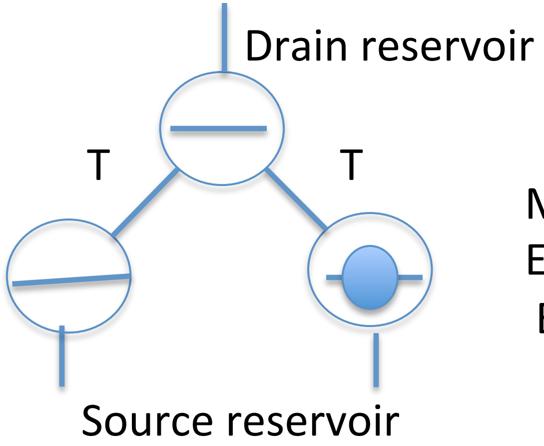

Michaelis ,
Emary and Beenakker
EPL 06

All-electronic coherent population trapping in quantum dots

⇩

Coherent Trapping of Atomic Populations in optics

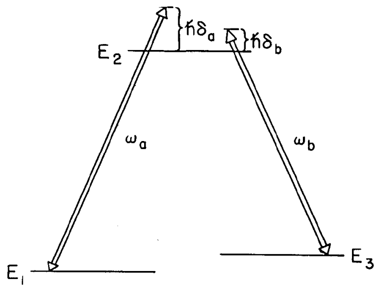

Coherent resonant electromagnetic field

⇕

Coherent resonant tunneling

Quantum interferences in long range tunneling

Minimal system affected by charge and spin correlations: 2 electrons

Left-right resonance: (1,1,0)↔(0,1,1)

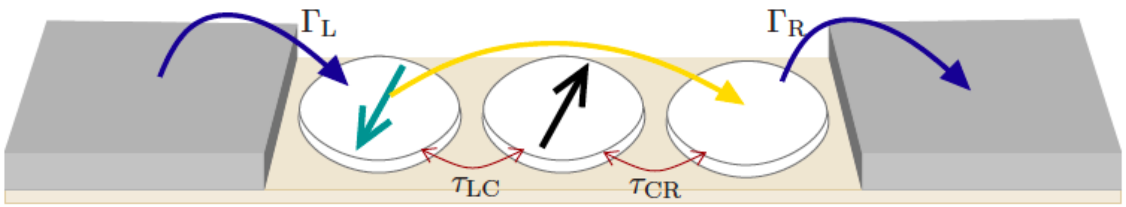

(1,1,0) → (0,2,0) → (0,1,1)

(1,1,0) → (1,0,1) → (0,1,1) Transport state

$$\hat{H}_{\mathrm{TQD}} = \sum_{i\sigma} \varepsilon_i \hat{c}^{\dagger}_{i\sigma}\hat{c}_{i\sigma} + \sum_{i} U_i \hat{n}_{i\uparrow}\hat{n}_{i\downarrow} + \frac{1}{2}\sum_{i\neq j} U_{ij}\hat{n}_i\hat{n}_j$$

$$- \sum_{i\neq j,\sigma} \tau_{ij}\hat{c}^{\dagger}_{i\sigma}\hat{c}_{j\sigma} + \mathrm{H.c.}$$

$$\dot{\hat{\rho}} = -i\hbar^{-1}[\hat{H}_{\mathrm{TQD}},\hat{\rho}] + \mathcal{L}_{\Gamma}\hat{\rho} \qquad I = q\Gamma_{\mathrm{R}}\sum_{\sigma\sigma'}\langle 0,\sigma,\sigma'|\hat{\rho}|0,\sigma,\sigma'\rangle$$

Minimal system affected by charge and spin correlations: 2 electrons

Left-right resonance: (1,1,0)↔(0,1,1)

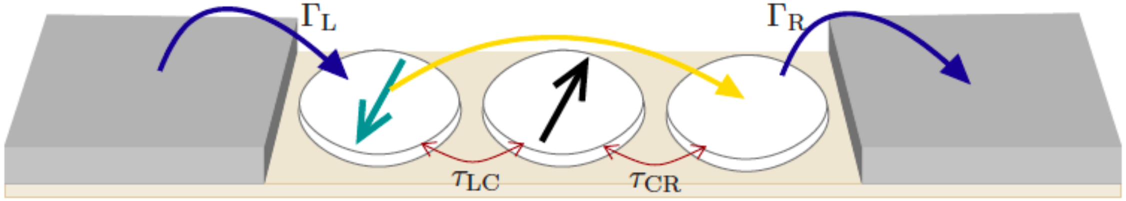

1D interferometer with branches defined by two different virtual intermediate states

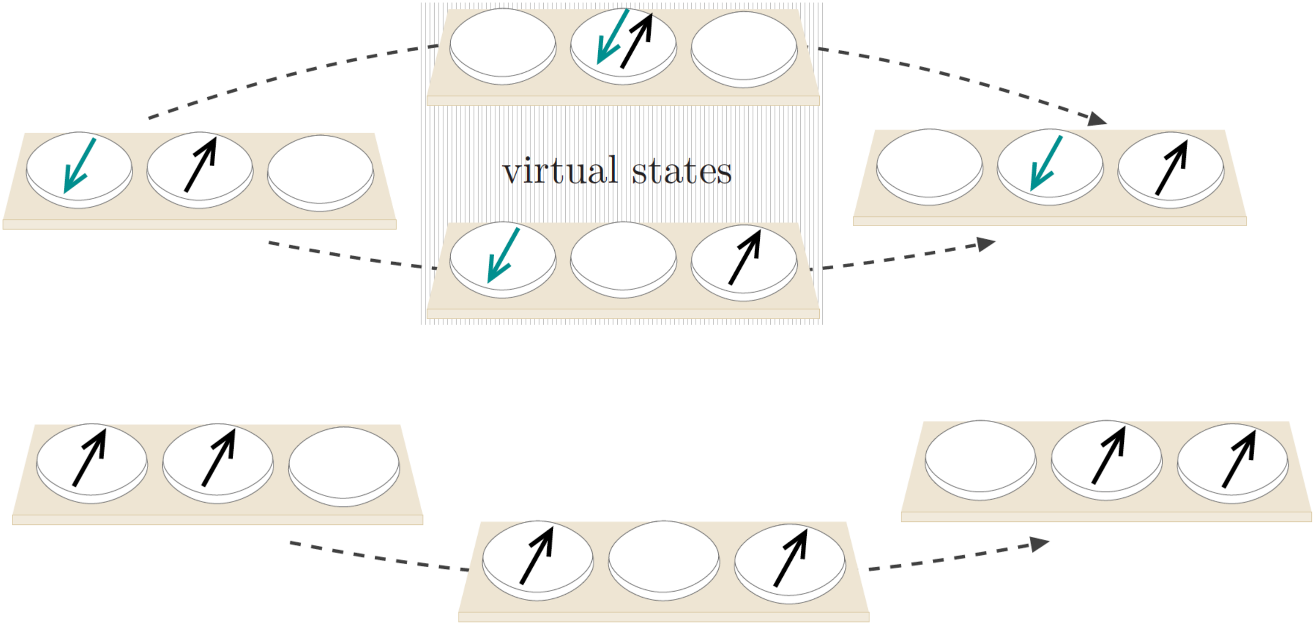

Singlet States

Triplet States

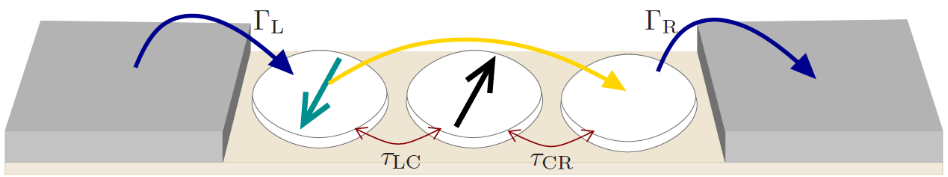

By means of a perturbative expansion and tracing out (020) and (101) an effective Hamiltonian in the singlet −triplet basis (110) and (011) is obtained

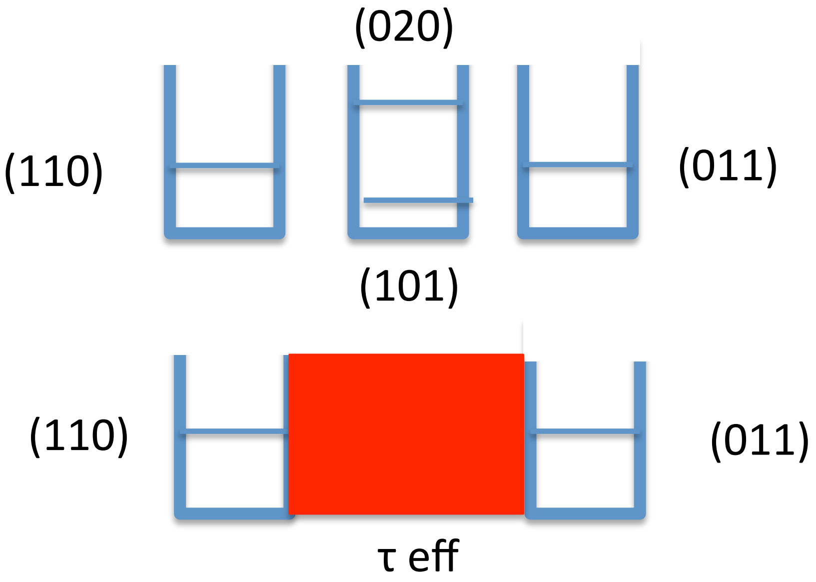
(020)

(110)

(011)

(101)

(110)

(011)

τ eff

$$\tau_{ij} << |\delta_{101}|,|\delta_{020}|$$

$$\delta_{101} = E_{110} - E_{101}$$

$$\delta_{020} = E_{110} - E_{020}$$

$$H_{eff} = \sum_{\Lambda,q} E_{\Lambda_q} |\Lambda_q\rangle\langle\Lambda_q| + \tau^S_{eff} |S_{LC}\rangle\langle S_{CR}| + \tau^T_{eff} |T^\alpha_{LC}\rangle\langle T^\alpha_{CR}| + H.C.$$

$$\alpha = 0, \pm$$

$$\boxed{\tau^S_{eff} = \tau_{LC}\tau_{CR}\left(\frac{1}{\delta_{101}} + \frac{2}{\delta_{020}}\right)}$$

$$\boxed{\tau^T_{eff} = \frac{\tau_{LC}\tau_{CR}}{\delta_{101}}}$$

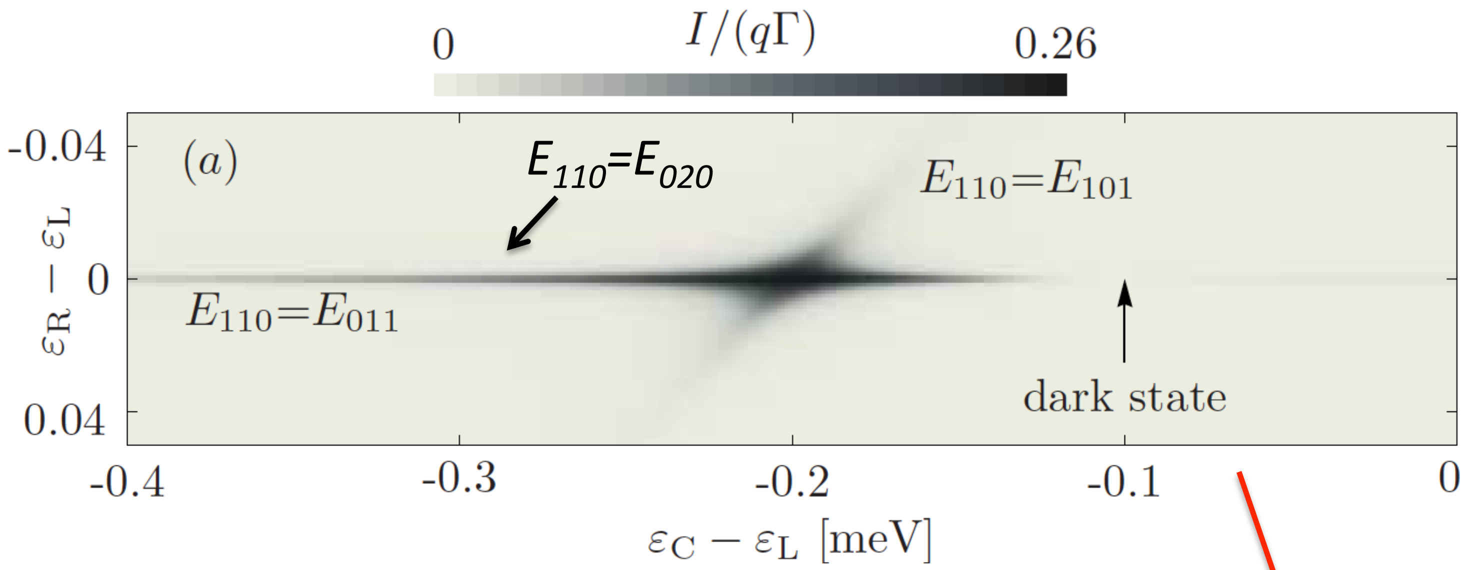

1-Resonant left-right transfer line

Lorentzian shape:

E_C-E_L=-0.4

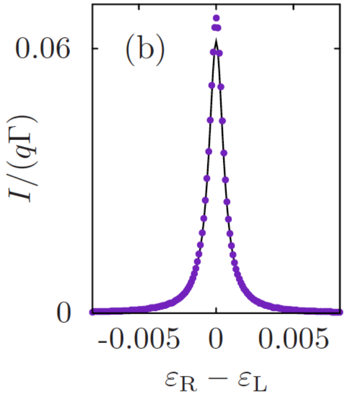

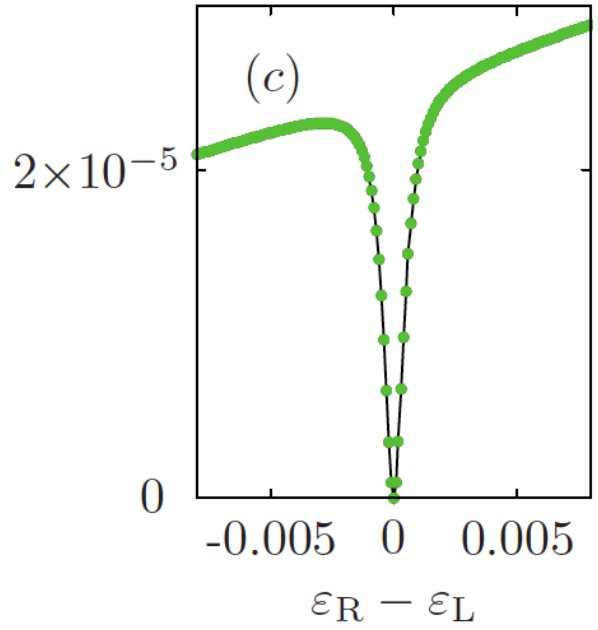

2-Dark state due to destructive interference

$$\delta_{1,0,1} = -\delta_{020}/2 \longrightarrow \tau_{eff}^{S} = \tau_{LC}\tau_{CR}\left(\delta_{101}^{-1} + 2\delta_{020}^{-1}\right) = 0$$

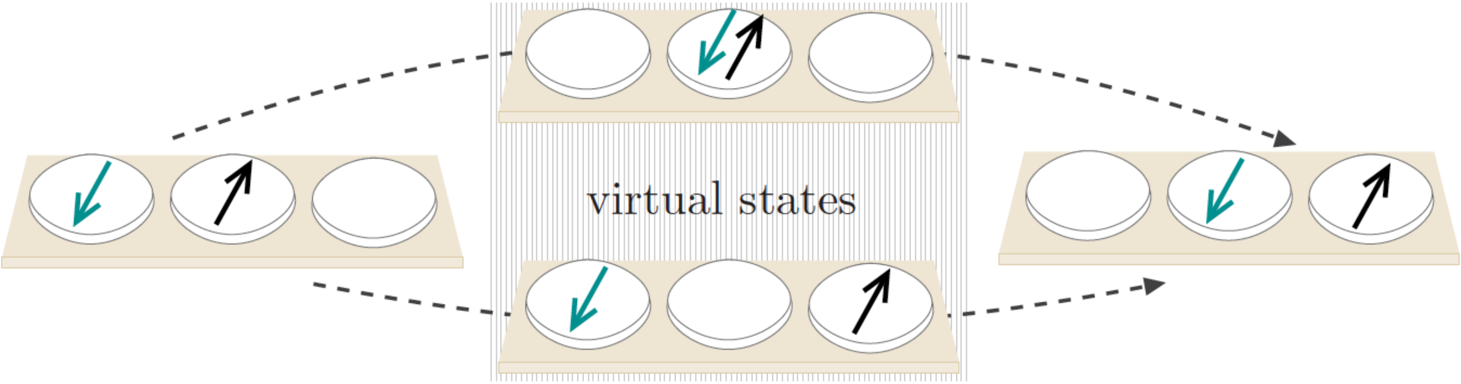

The two singlet long range paths interfer destructively

$$\tau_{LC} = \tau_{CR} \qquad \Delta = \delta_{1,0,1} = -\delta_{020}/2$$

$$\tau^{S}_{eff} = 0 \rightarrow \left|DS\right\rangle = \frac{1}{N}\left(\Delta\left|1,1,0\right\rangle - \tau\left|0,2,0\right\rangle + \frac{1}{\sqrt{2}}\tau\left|1,0,1\right\rangle\right)$$

$$N = \sqrt{\Delta^2 + \frac{3}{2}\tau^2}$$

No contribution of $\left|0,1,1\right\rangle$ which carries current to the right

The Dark State blocks the current

DECOHERENCE:

↓

L-R resonance peak is reduced

Life-time enhanced resonance at E_{110}=E_{020}

Dark State washed out

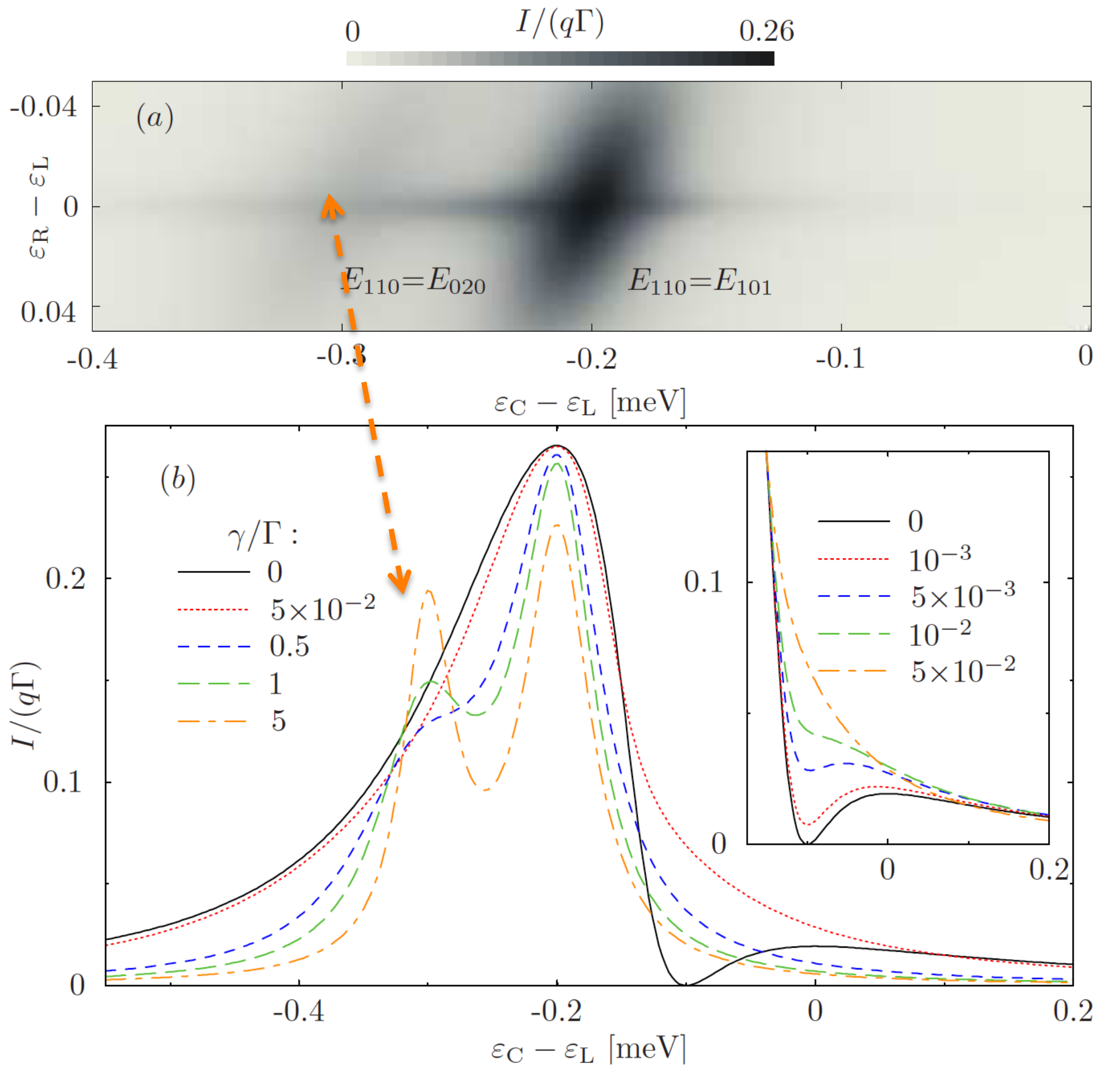

$$T_1^{-1} = 5 * 10^{-3}\gamma$$

$$T_2^{-1} = \gamma$$

R. Sánchez, F. Gallego-Marcos, and G. Platero, Phys. Rev. B 89, 161402(R) (2014).

Driving with periodic AC electric fields

Photoassisted Tunneling (PAT) in quantum dots

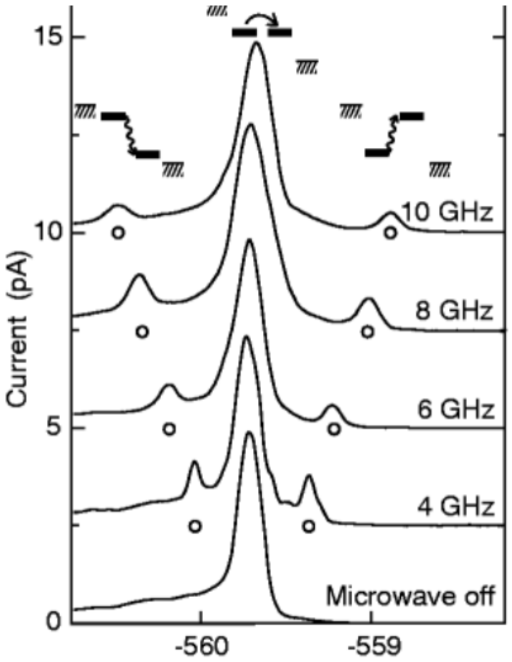

Coherent destruction of tunnel, P. Hänggi, PRL, 1991

↓

Bonds renormalization

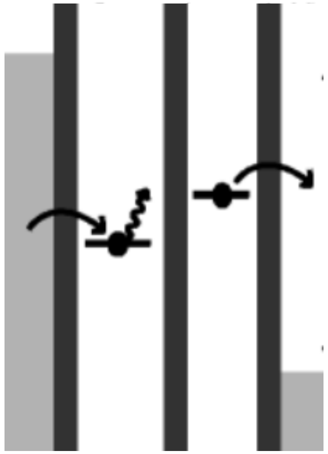

T. H. Oosterkamp et al., Nature 395, 873-876, 1998

Floquet-Bloch Theory and Topology in Periodically Driven Lattices,
A. Gómez-León and G. P. , PRL, 2013.

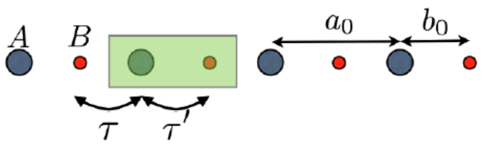

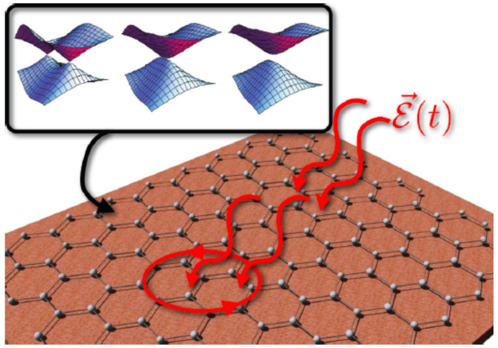

P. Delplace et al.,
PRB, 88,245 (2013)

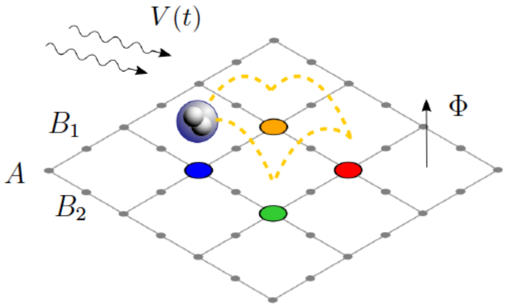

M. Bello et al., PRB 2017

Dimer chain: AC driven transport to characterize the topology

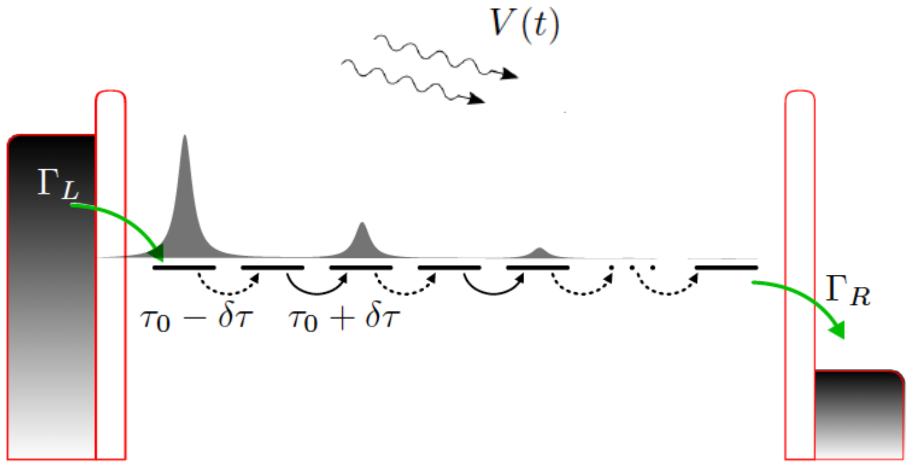

M. Niklas et al., Nanotechnology, 2017

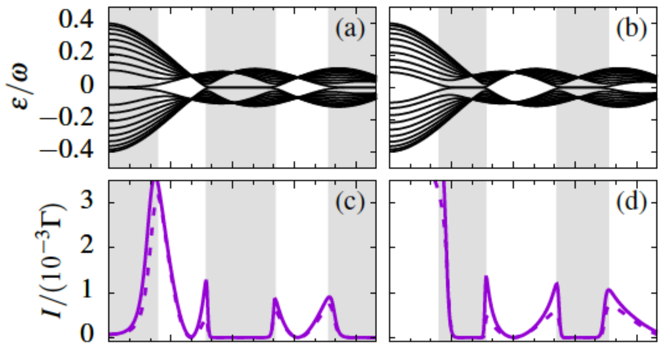

A/w

A

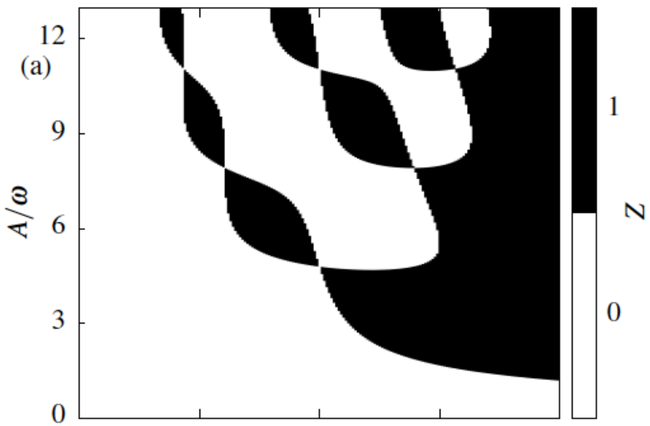

b_0/a_0

Zak phase

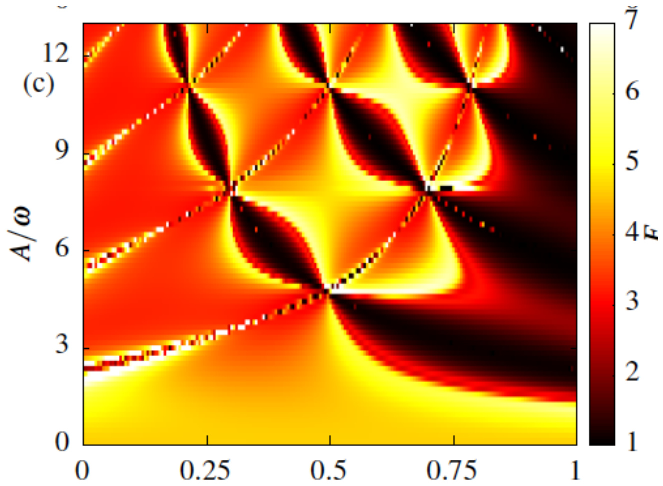

b_0/a_0

Shot noise

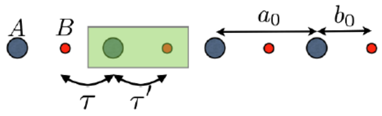

Long range photo-assisted transport

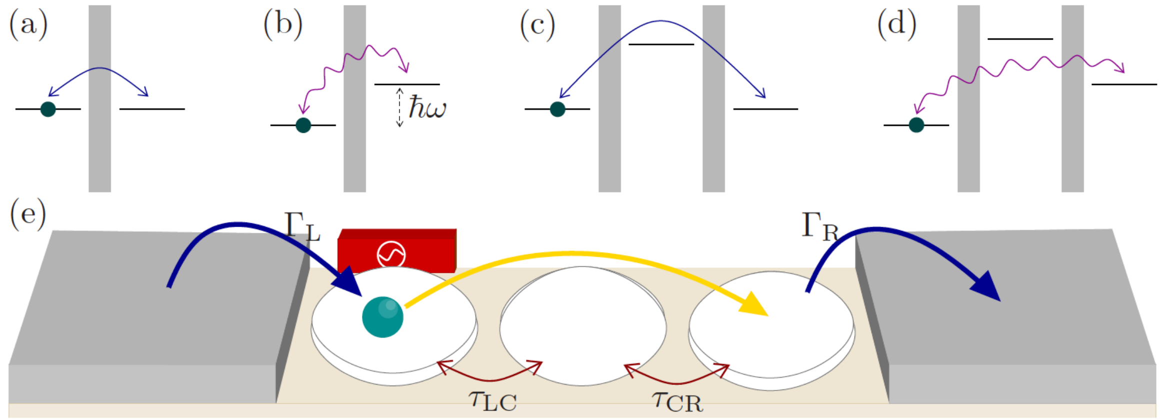

$$\hat{H}_{\mathrm{ac}}(t) = \frac{V_{\mathrm{ac}}}{2}\cos(\omega t)\hat{n}_L$$

$$\hat{\hat{H}}_\tau(t) = \sum_{\nu=-\infty}^{\infty} J_\nu\left(\frac{V_{AC}}{2\hbar\omega}\right) e^{i\nu\omega t}\sum_\sigma \tau_{LC}\hat{c}^\dagger_{L\sigma}\hat{c}_{C\sigma} + \sum_\sigma\left(\tau_{CR}\hat{c}^\dagger_{C\sigma}\hat{c}_{R\sigma} + \text{h.c.}\right)$$

$$\dot{\rho}(t) = -\frac{i}{\hbar}\left[\hat{H}_\epsilon + \hat{\hat{H}}_\tau(t), \rho(t)\right] + \mathcal{L}_\Gamma\rho(t)$$

$$I = e\Gamma_{\mathrm{R}}\bar{\rho}_{RR}$$

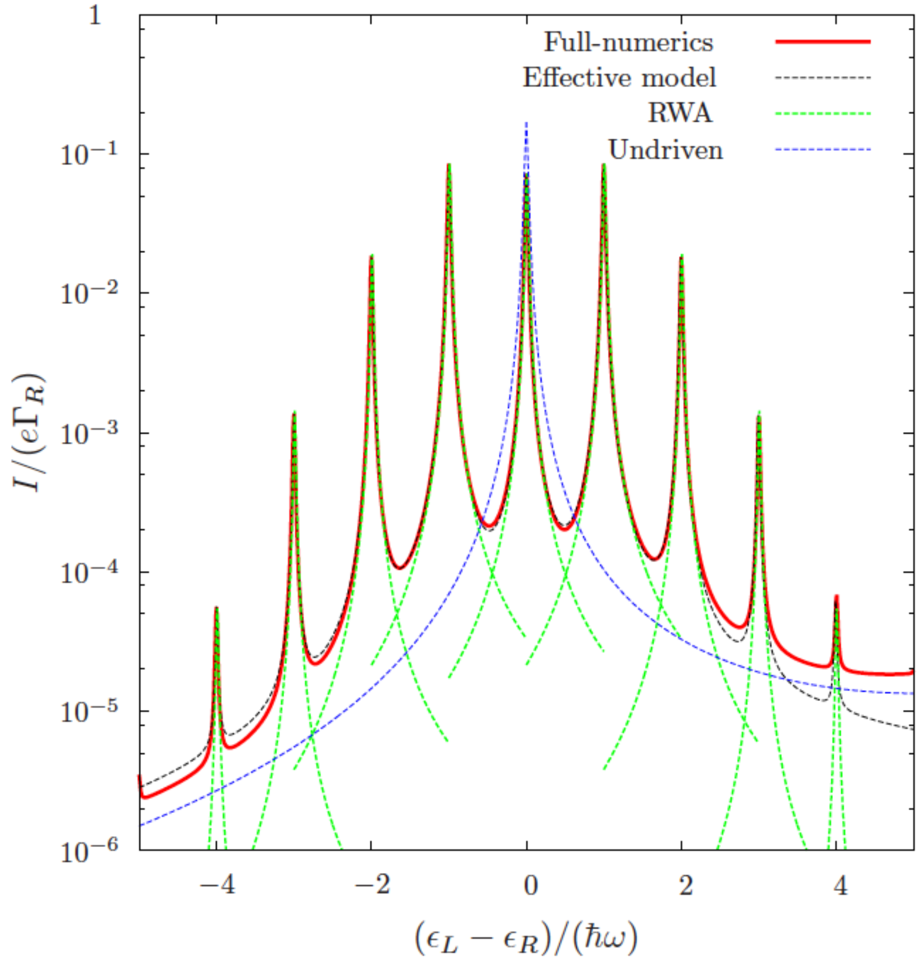

$E_C >> E_R, E_L$ Effective hamiltonian

$$H_{\text{eff}} = \begin{bmatrix} \tilde{\epsilon}_L & -\tau_{\text{eff}}(t) \\ -\tau_{\text{eff}}(t) & \tilde{\epsilon}_R \end{bmatrix}$$

$$\tau_{\text{eff}}(t) = \sum_{\nu} J_\nu(\alpha) \frac{\tau_{LC}\tau_{CR}}{\epsilon_L - \epsilon_C + \nu\hbar\omega} e^{i\nu\omega t}$$

Rotating Wave Approx

$$\hat{H}_{\text{RWA}} = \begin{pmatrix} \tilde{\epsilon}_L & J_n\left(\frac{V_{\text{ac}}}{2\hbar\omega}\right) \frac{\tau_{LC}\tau_{CR}}{\epsilon_L - \epsilon_C + \nu\hbar\omega} \\ J_n\left(\frac{V_{\text{ac}}}{2\hbar\omega}\right) \frac{\tau_{LC}\tau_{CR}}{\epsilon_L - \epsilon_C + \nu\hbar\omega} & \tilde{\epsilon}_R - n\hbar\omega \end{pmatrix}$$

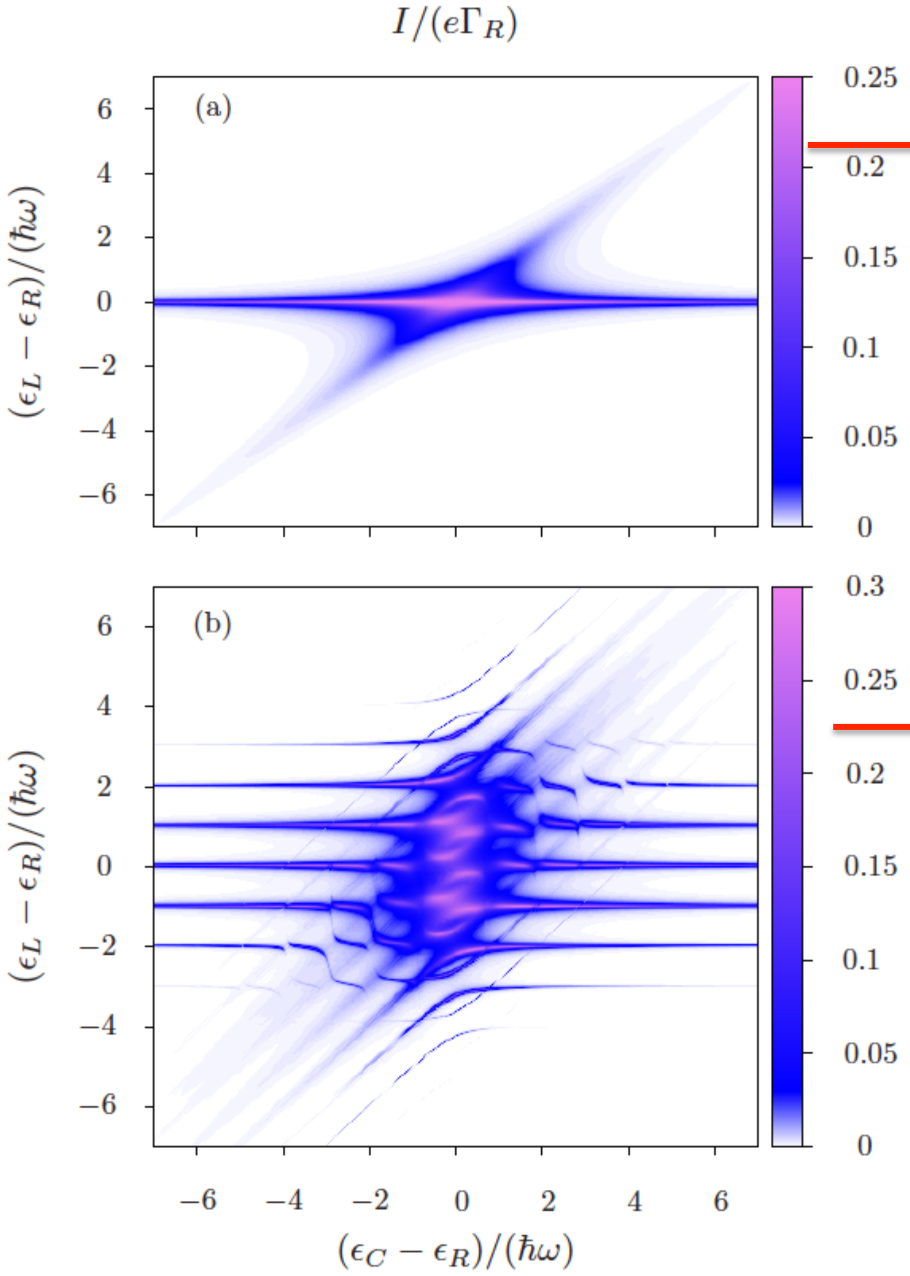

$$\tau_{LC} = \tau_{CR} = \tau = 10\Gamma$$

Undriven: Long range tunnel between left and right quantum dots

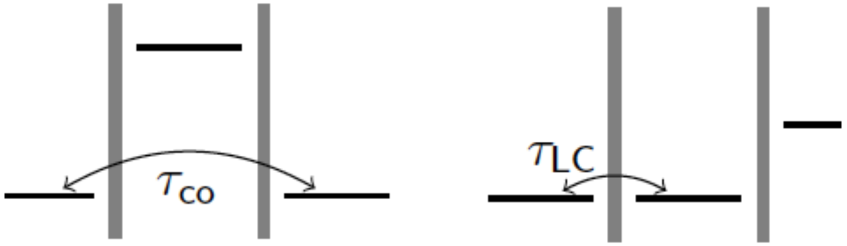

$$|\pm\rangle = \frac{1}{\sqrt{2}}\left[|L\rangle \pm |R\rangle\right]$$

AC: Tunnel renormalized by the ac

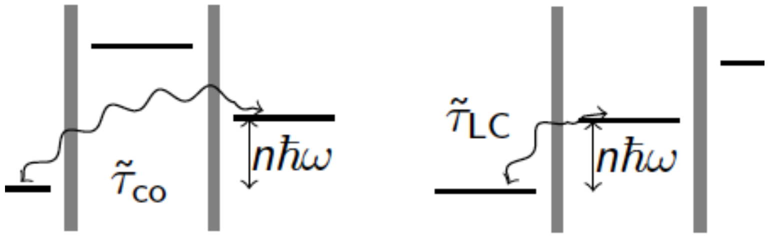

Anticrossings due to the hybridization of the center and right dot states:

$$J_\nu(\alpha)\tau_{LC} < \tau_{CR}$$

ICPS 2014, JAP, 2015

Multiphoton Landau Zener Stückelberg Tunneling involving virtual transitions

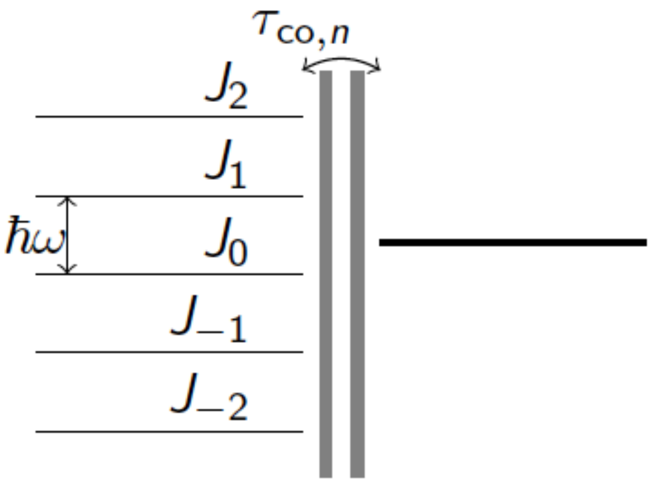

$$\tau_{co,n} = J_n\left(\frac{V_{ac}}{2\hbar\omega}\right)\frac{\tau_{LC}\tau_{CR}}{\epsilon_C - n\hbar\omega}$$

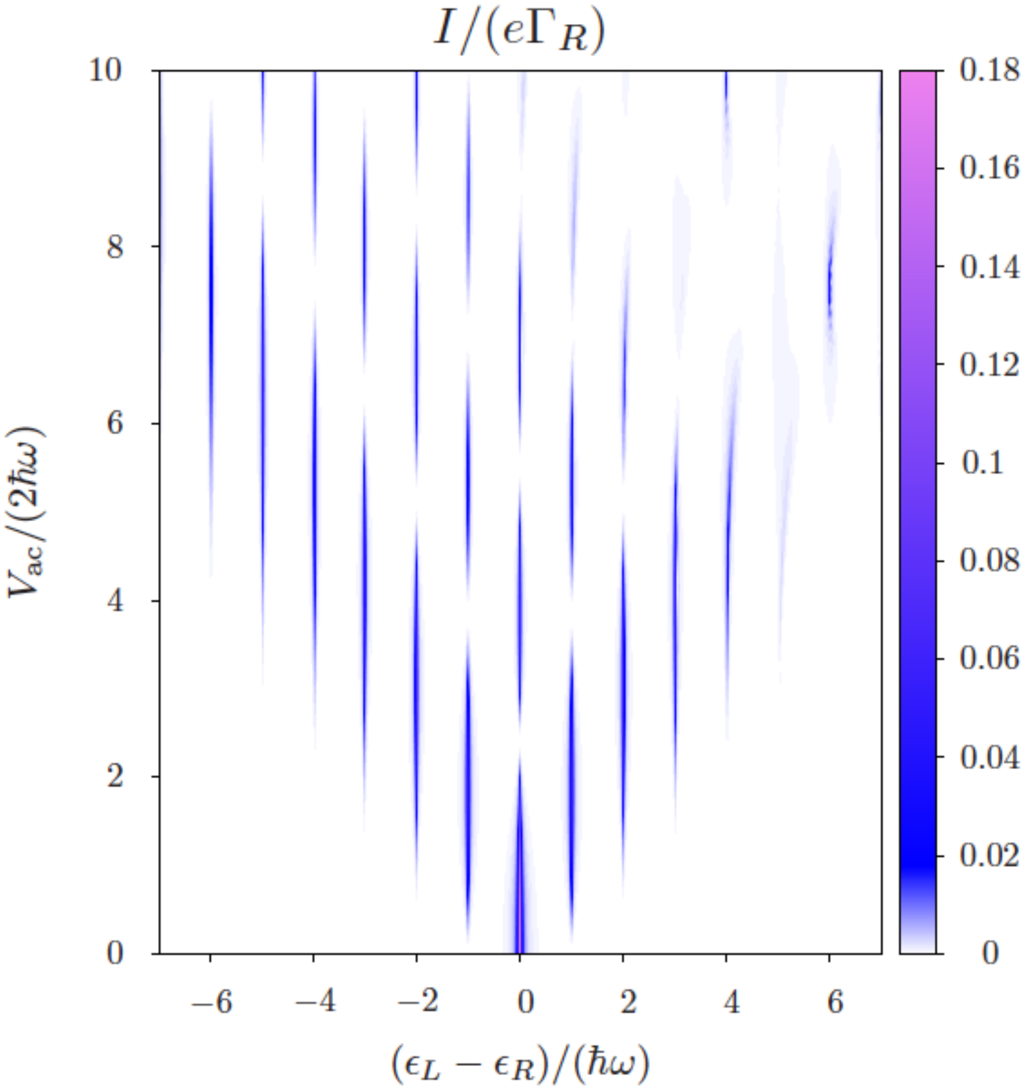

Multiphoton Landau Zener Stückelberg Tunneling involving virtual transitions

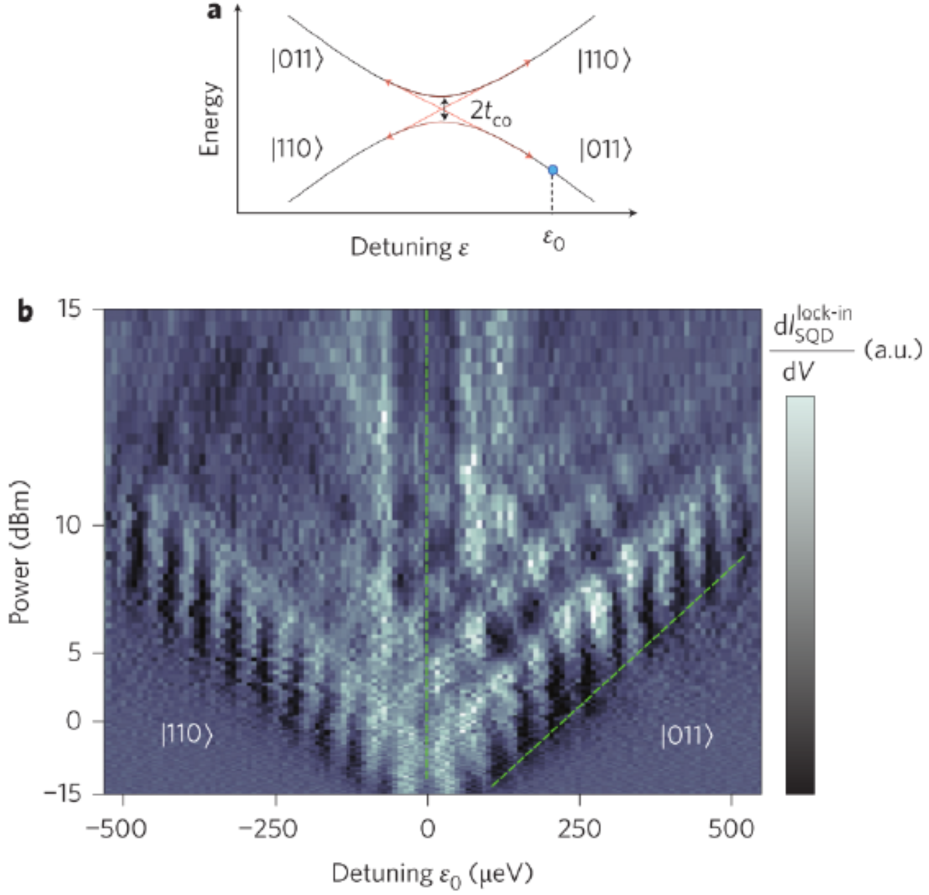

F.R. Braakman, et al. Nature nanotechnology **8** 432-7 (2013)

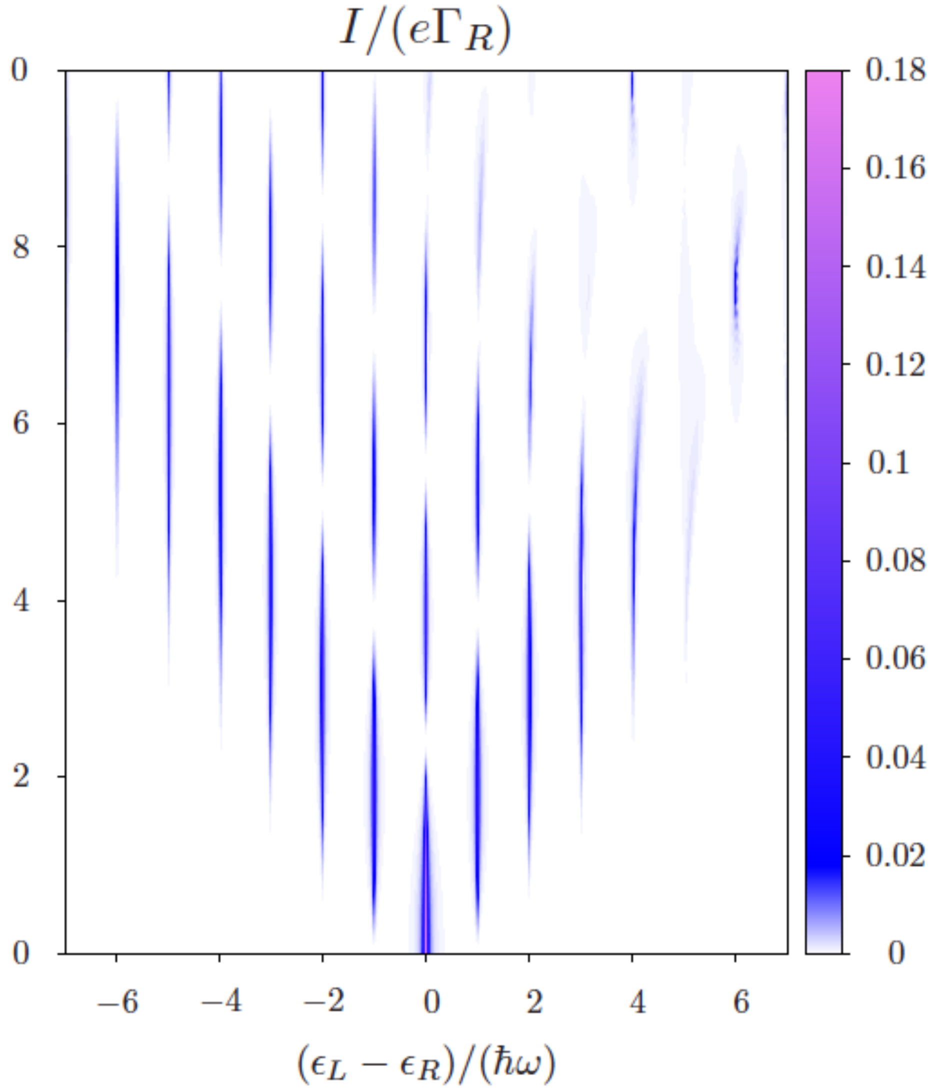

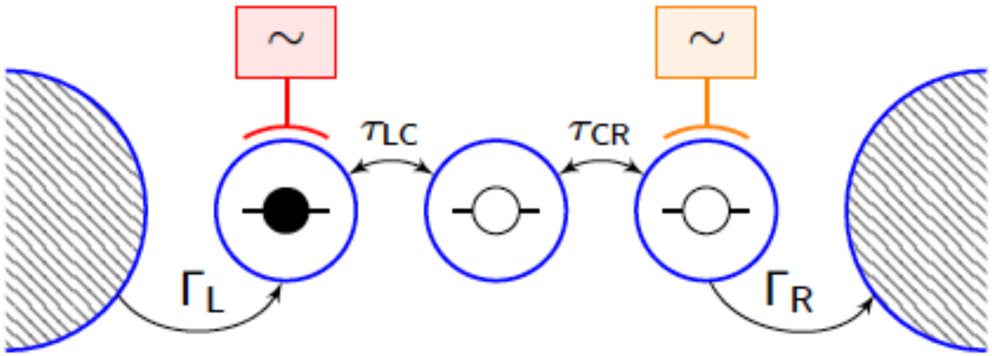

$$\hat{H}_{\rm ac}(t) = \frac{V_{\rm ac}}{2}\cos(\omega t)\hat{c}_L^{\dagger}\hat{c}_L + \frac{V_{\rm ac}}{2}\cos(\omega t + \phi)\hat{c}_R^{\dagger}\hat{c}_R$$

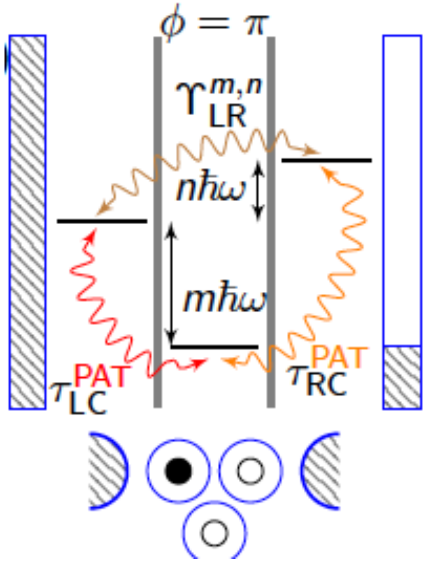

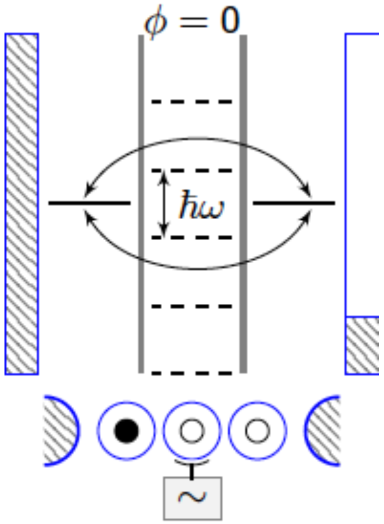

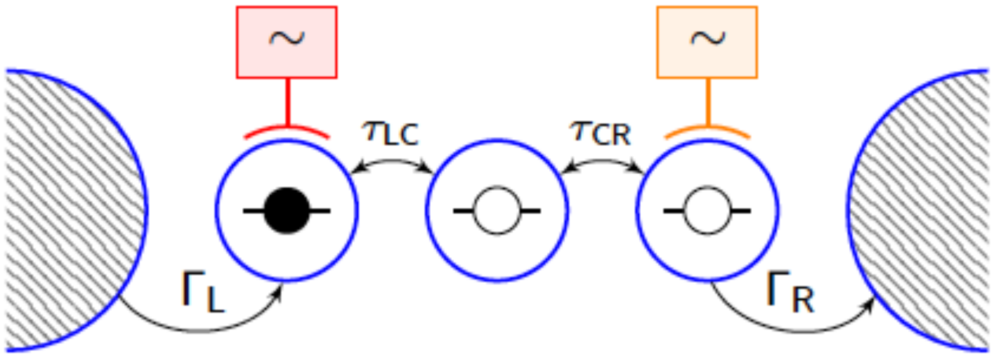

$$\hat{H}'_\tau = \sum_\nu t^\nu_{LC}\mathrm{e}^{i\nu\omega t}\hat{c}^\dagger_C\hat{c}_L + t^\nu_{CR}\mathrm{e}^{-i\nu\omega t}\hat{c}^\dagger_R\hat{c}_C + h.c.$$

$$t^\nu_{LC} = \tau_{LC}J_\nu(V_{\mathrm{ac}}/\hbar\omega) \quad t^\nu_{CR} = \tau_{CR}J_\nu(V_{\mathrm{ac}}/\hbar\omega)e^{-i\nu\phi}$$

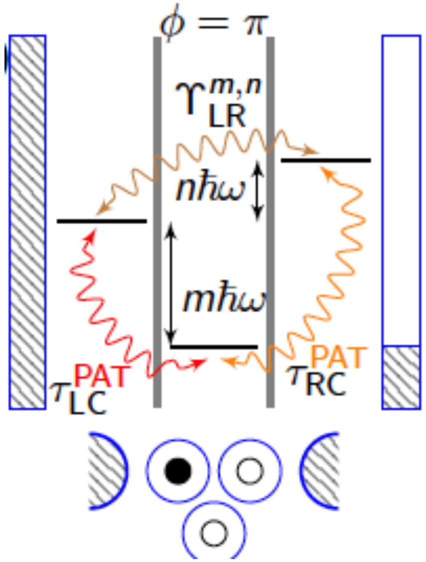

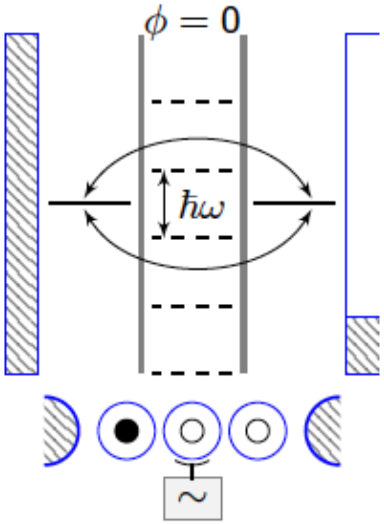

t_{12}

t_{23}

$$\hat{H}_{\mathrm{RWA}} = \begin{bmatrix} \tilde{\epsilon}_{\mathrm{L},n} + \Lambda^{m,n}_{\mathrm{LL}} & t^{-m}_{\mathrm{LC}} & \Upsilon^{m,n^*}_{\mathrm{LR}}(\phi) \\ t^{-m}_{\mathrm{CL}} & \tilde{\epsilon}_{\mathrm{C},m+n} + \Lambda^{m,n}_{\mathrm{CC}} & t^{-m-n}_{\mathrm{CR}}(\phi) \\ \Upsilon^{m,n}_{\mathrm{LR}}(\phi) & t^{-m-n}_{\mathrm{RC}}(\phi) & \tilde{\epsilon}_{\mathrm{R},0} + \Lambda^{m,n}_{\mathrm{RR}} \end{bmatrix}$$

Effective hopping between left and right QDs: t_{13}

$$\Upsilon^{m,n}_{\mathrm{LR}}(\phi) = \tau_{\mathrm{LC}}\tau_{\mathrm{CR}} \sum_{\nu=-\infty}^{\infty} J_\nu \left[\frac{(J_{\nu+n} - J_{m+2n})e^{i\nu\phi}}{2(\nu - m - n)\hbar\omega} + \frac{(J_{\nu-n}e^{i\nu\phi} - J_{m-n}e^{im\phi})e^{-in\phi}}{2(\nu - m)\hbar\omega} \right]$$

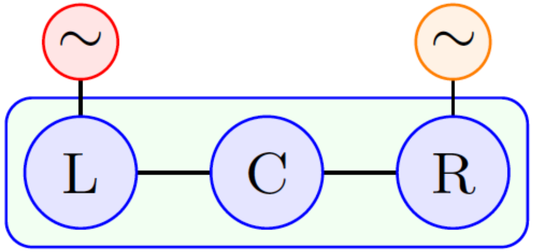

$$\underset{\phi = \pi}{\approx}$$

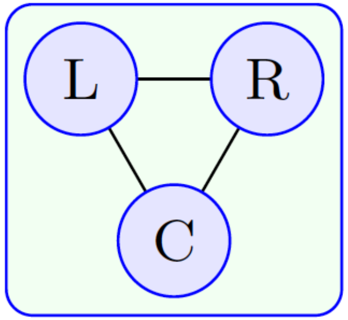

$$\hat{H}_{\mathrm{RWA}} = \begin{bmatrix} \tilde{\epsilon}_{\mathrm{L},n} + \Lambda^{m,n}_{\mathrm{LL}} & t^{-m}_{\mathrm{LC}} & \Upsilon^{m,n^*}_{\mathrm{LR}}(\phi) \\ t^{-m}_{\mathrm{CL}} & \tilde{\epsilon}_{\mathrm{C},m+n} + \Lambda^{m,n}_{\mathrm{CC}} & t^{-m-n}_{\mathrm{CR}}(\phi) \\ \Upsilon^{m,n}_{\mathrm{LR}}(\phi) & t^{-m-n}_{\mathrm{RC}}(\phi) & \tilde{\epsilon}_{\mathrm{R},0} + \Lambda^{m,n}_{\mathrm{RR}} \end{bmatrix}$$

→ t_{12}

→ t_{23}

↓ Effective hopping between left and right QDs: t_{13}

$$\mathcal{H} = \begin{pmatrix} \Delta & t_{12} & t_{13} \\ t_{12} & -\Delta & t_{23} \\ t_{13} & t_{23} & \epsilon \end{pmatrix}$$

Dark State Condition

$$\Delta = \Delta_0 \equiv \frac{t_{12}}{2 t_{13} t_{23}} (t_{13}^2 - t_{23}^2)$$

$$|\Psi_{\mathrm{dark}}\rangle = \frac{1}{\sqrt{t_{13}^2 + t_{23}^2}} (t_{23}|1\rangle - t_{13}|2\rangle)$$

C. Emary, PRB 2007

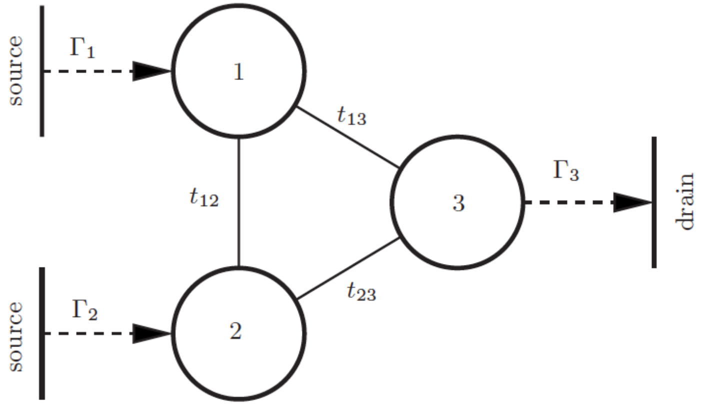

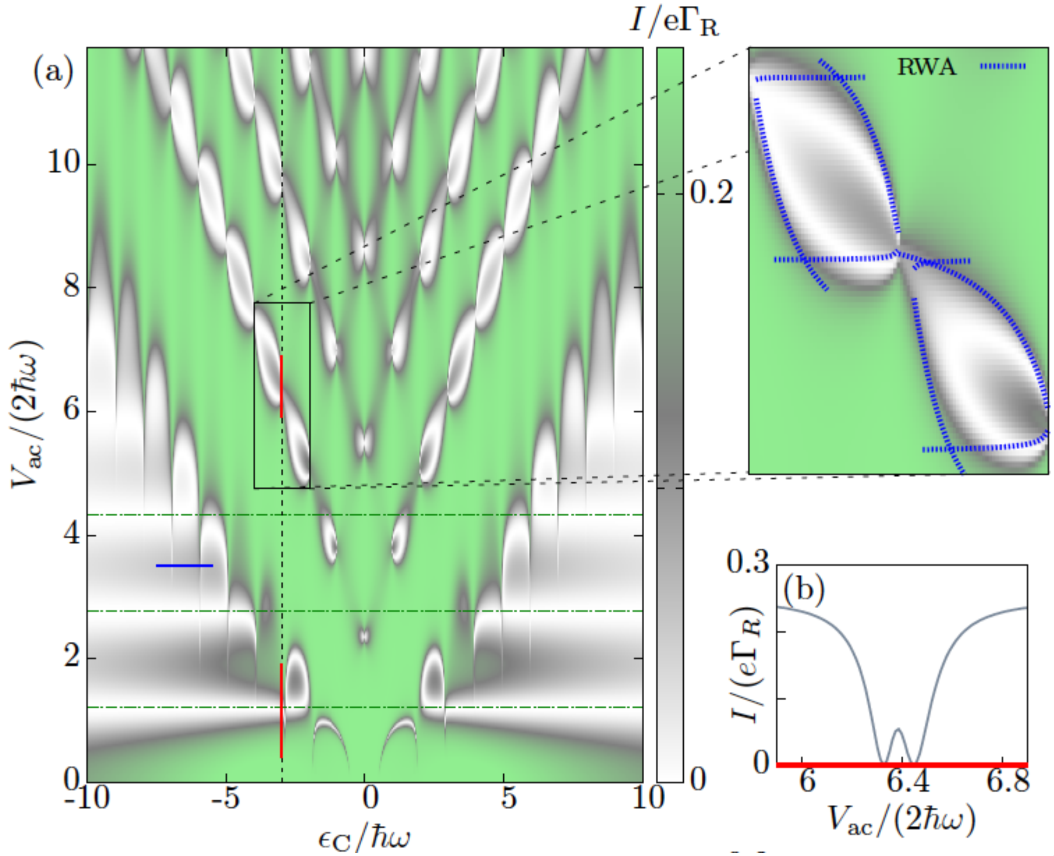

$$\phi = \pi$$

Blue lines: Dark state condition

Destructive interferences between real and virtual paths

$$|\Psi_\mathrm{DS}\rangle = N\left[t_\mathrm{CR}^{-m}(\phi)\,|L\rangle - \Upsilon_\mathrm{LR}^{m,0}(\phi)\,|C\rangle\right]$$

$$\varepsilon_L = \varepsilon_R$$

$$\alpha = V_\mathrm{ac}/(2|\varepsilon_\mathrm{C}|)$$ for $$\alpha < 1$$

$$t_{LC}^{\nu} = \tau_{LC} J_\nu\left(V_{ac}/2\hbar\omega\right)$$

$$t_{CR}^{\nu}(\phi) = \tau_{CR} J_\nu\left(V_{ac}/2\hbar\omega\right) e^{-i\nu\phi}$$

<<1

Dashed green lines: cotunnel suppression:

Long Range CDT , $J_N=0$

$$\hat{H}_\mathrm{RWA}^{m,n}(\pi) \approx (\tilde{\epsilon}_{\mathrm{L},n} - \tilde{\epsilon}_{\mathrm{R},0})\boldsymbol{\sigma}_z - J_n\left(\frac{V_\mathrm{ac}}{\hbar\omega}\right)\frac{\tau_\mathrm{LC}\tau_\mathrm{CR}}{m\hbar\omega}\boldsymbol{\sigma}_x$$

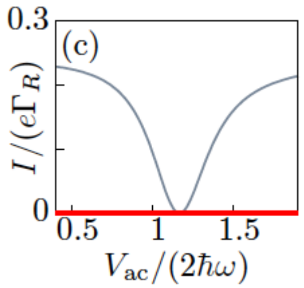

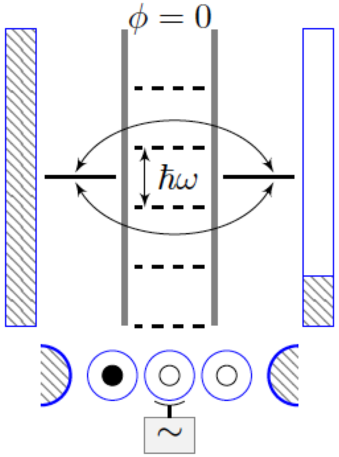

$E_R = E_L = 0$, $E_C = \Delta + m\hbar\omega$

$$\hat{H}^0_{\mathrm{RWA}} \approx \Delta\sigma_z + \tau_{LC}\tau_{CR} \sum_\nu \Omega_{\nu,m}(\Delta)\,\sigma_x$$

with the sideband-dependent couplings

$$\Omega_{\nu,m}(\Delta) = J_\nu^2/[(\nu - m)\hbar\omega - \Delta]$$

For

$$\sum_{\nu=-\infty}^{m} \Omega_{\nu,m}(\Delta) = -\sum_{\nu=m+1}^{\infty} \Omega_{\nu,m}(\Delta)$$

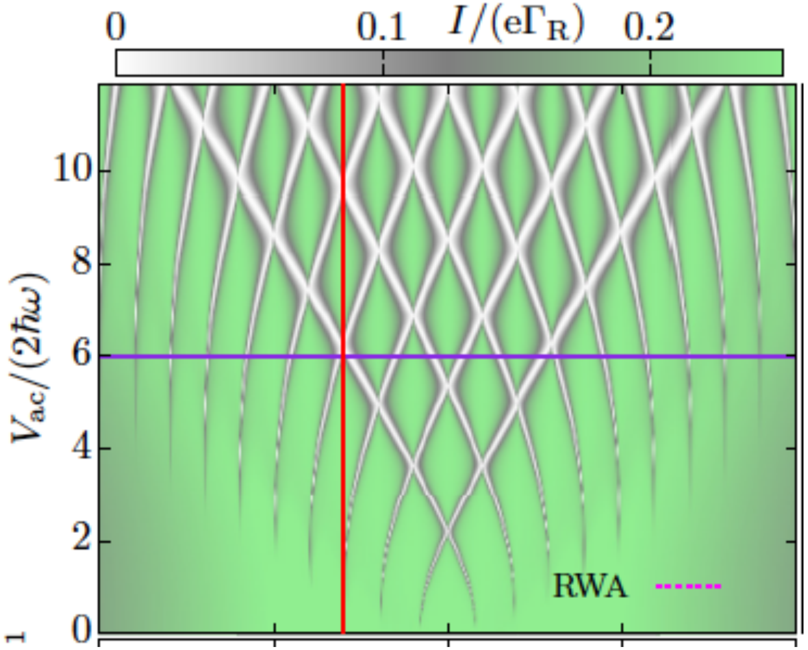

The system behaves as an ac driven interferometer of multiple virtual transitions.
Sidebands with positive (ν>m) and negative (ν<m) detuning destructively interfer.

F. Gallego-Marcos et al., PRB, 2016

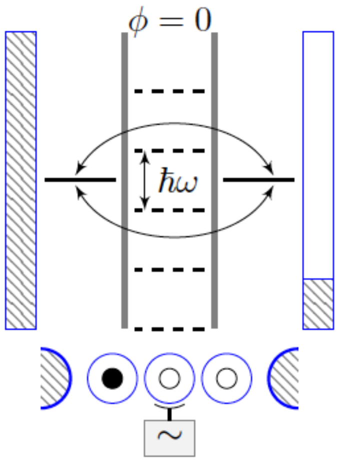

$E_R=E_L=0$, $E_C=\Delta+m\hbar\omega$

$$\hat{H}^0_{\mathrm{RWA}} \approx \Delta\boldsymbol{\sigma}_z + \tau_{LC}\tau_{CR}\sum_\nu \Omega_{\nu,m}(\Delta)\,\boldsymbol{\sigma}_x$$

with the sideband-dependent couplings

$$\Omega_{\nu,m}(\Delta) = J_\nu^2/[(\nu-m)\hbar\omega-\Delta]$$

For

$$\sum_{\nu=-\infty}^{m}\Omega_{\nu,m}(\Delta) = -\sum_{\nu=m+1}^{\infty}\Omega_{\nu,m}(\Delta)$$

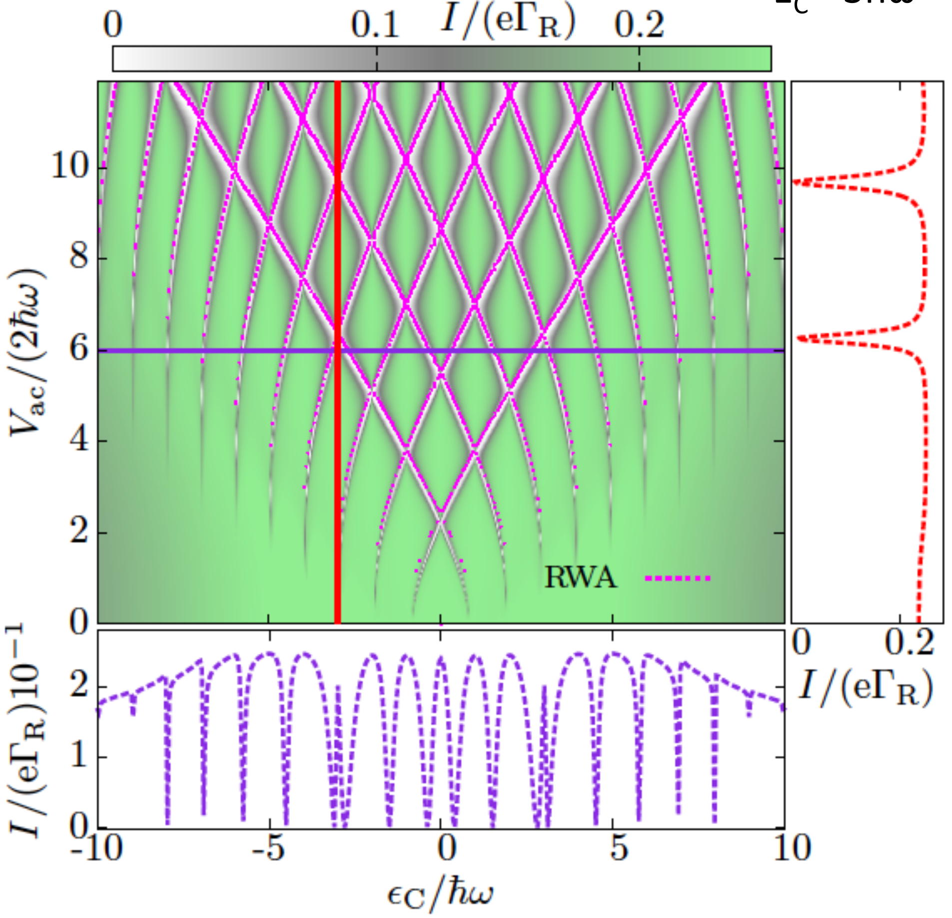

Current at $E_C=-3\hbar\omega$

$J_3=0$

$J_3=0$

The system behaves as an ac driven interferometer of multiple virtual transitions.
Sidebands with positive (ν>m) and negative (ν<m) detuning destructively interfer.

F. Gallego-Marcos et al., PRB, 2016

Long range energy and heat transfer: direct energy and heat transfer between outer dots

F. Gallego-Marcos et al., PRB 2017

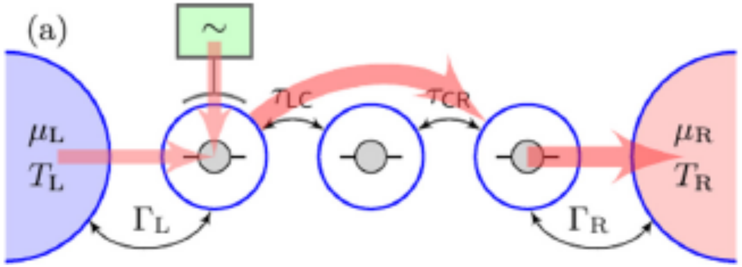

Conclusions

Long range transport in triple quantum dots:

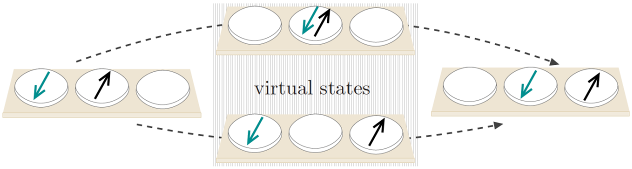

Electrons are transferred directly between edge dots with only virtual participation of the center dots: Different long range (virtual) transitions interfere Destructively.

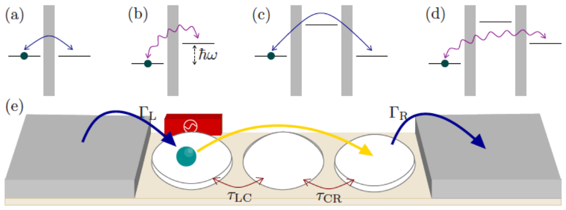

Long range photoassisted transport:
Photoassisted virtual transitions:

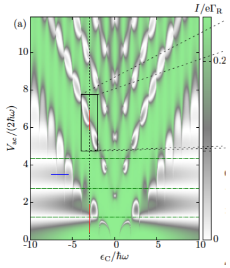

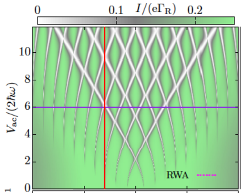

Destructive interferences between direct and virtual PAT transitions.
Coherent destruction of cotunneling.
Phase dependent transport.

Quantum interference in large area molecular junctions

Philippe Lafarge

C. Salhani, C. Bessis, R. Bonnet, M. L. Della Rocca, C. Barraud, P. Martin
J.-C. Lacroix

Matériaux et Phénomènes Quantiques (MPQ) and ITODYS
Université Paris Diderot, CNRS, Paris, France

Quantum interference in mesoscopic systems

Aharonov-Bohm effect in a metal ring

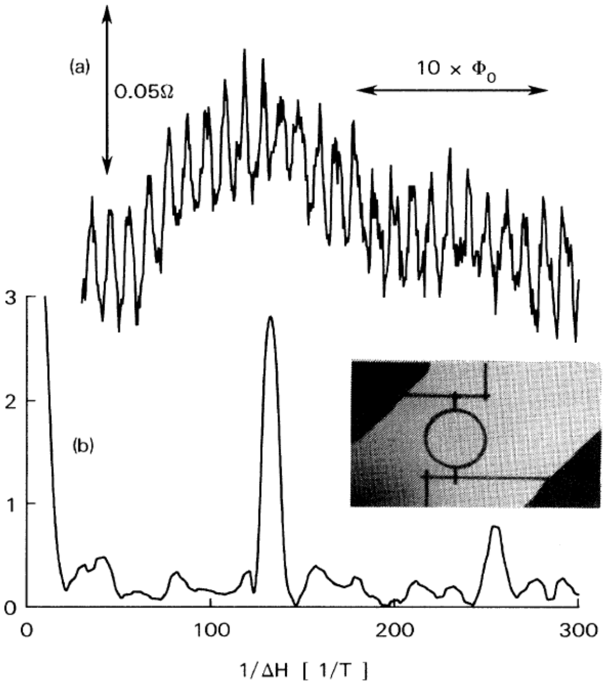

R. A. Webb *et al*., Phys. Rev. Lett. **54**, 2696 (1985)

phase coherent transport

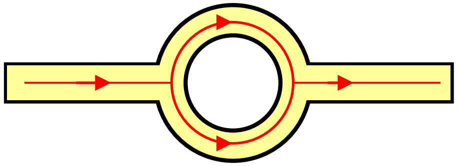

$$|\psi\rangle = c_1|\varphi_1\rangle + c_2|\varphi_2\rangle$$

$$P = |A_1 + A_2|^2$$

quantum interference

phase shift controlled by magnetic flux

$$\Delta\varphi = \pi\, \Phi/\Phi_0$$

Quantum interference in molecules

Essence of QI: simultaneous coupling between two molecular orbital levels and a Fermi sea of conduction electrons

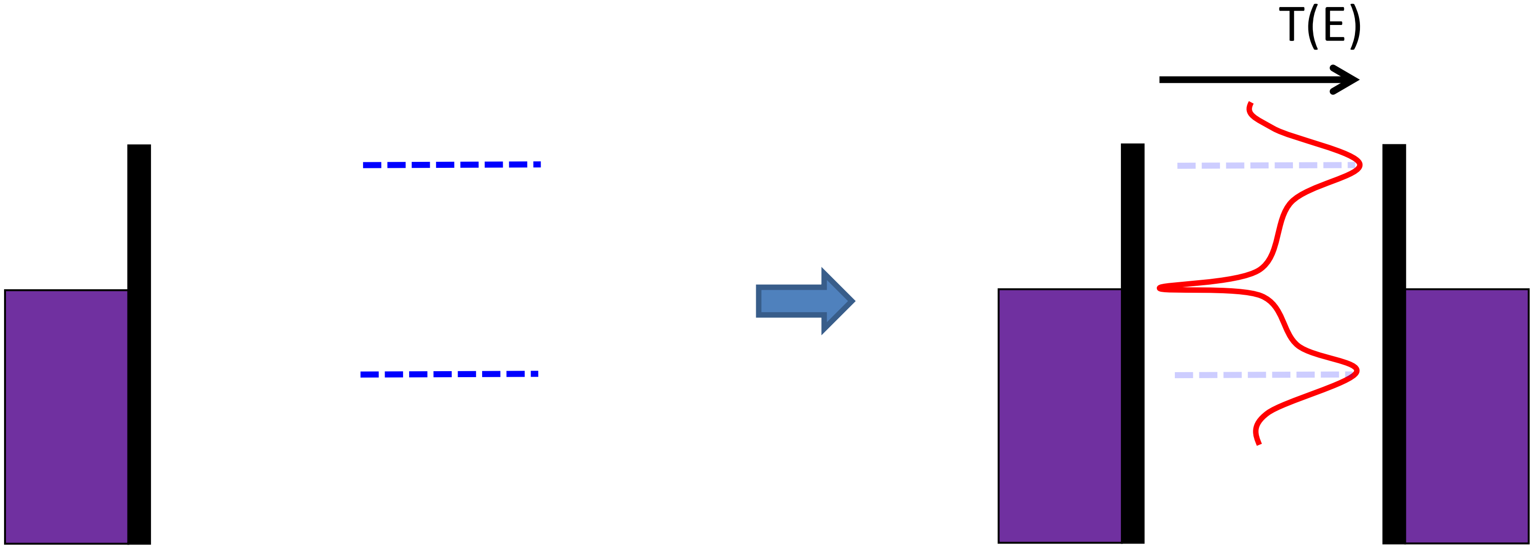

Quantum interference in molecules

Essence of QI: simultaneous coupling between two molecular orbital levels and a Fermi sea of conduction electrons

Kondo effect in quantum dots

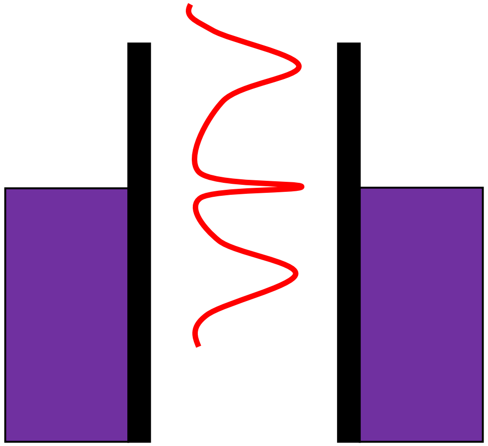

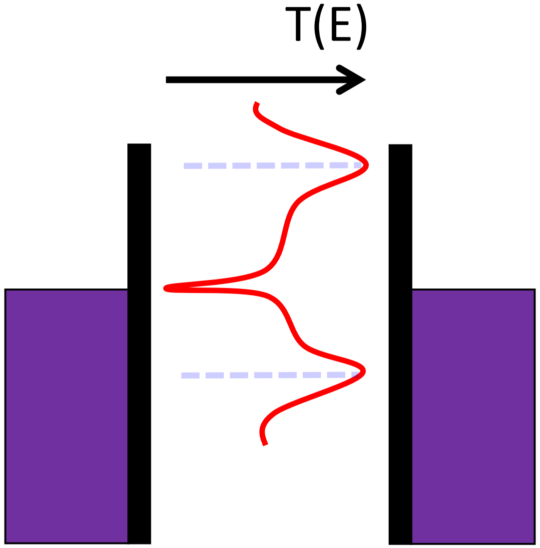

Kondo effect: dynamical screening of an unpaired spin by conduction electrons. Coupling between an interacting discrete level and a Fermi sea of conduction electrons

Molecules coupled to conduction electrons

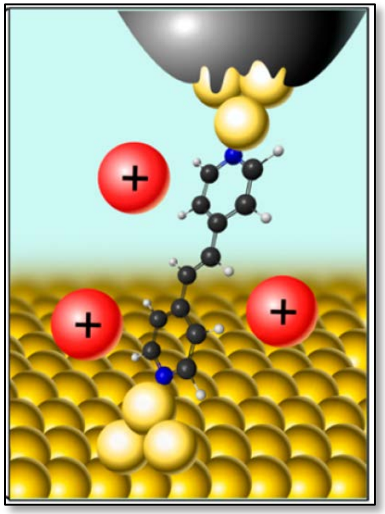

Capozzi et al., Nano Lett. 14, 1400 (2014)

STM-BJ, Columbia, Arizona state

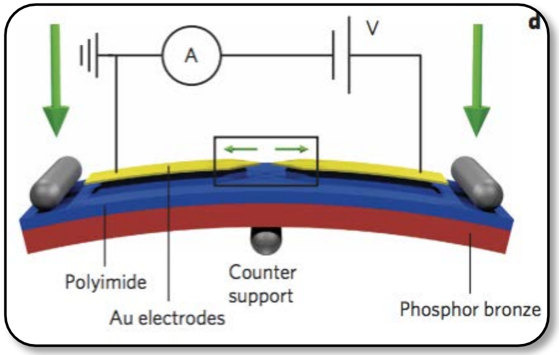

Perrin et al., Nature Nanotech. 9, 830 (2014)

MCBJ + SAMs
Delft, Leiden,
Konstanz, Erlangen

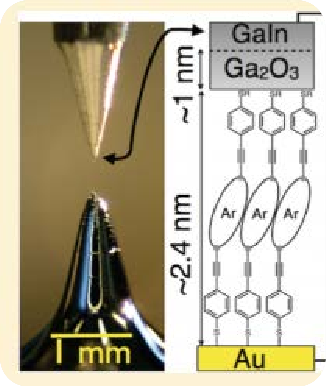

Fracasso et al., JACS 133, 9556 (2011)

C-AFM or EGaIn on SAMs
Harvard, Groningen, Leiden, Lille

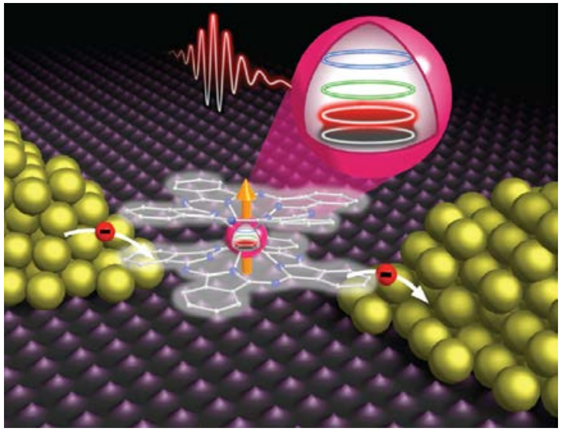

Thiele et al., Science 344, 1135 (2014)

Electromigration + SMM
Grenoble

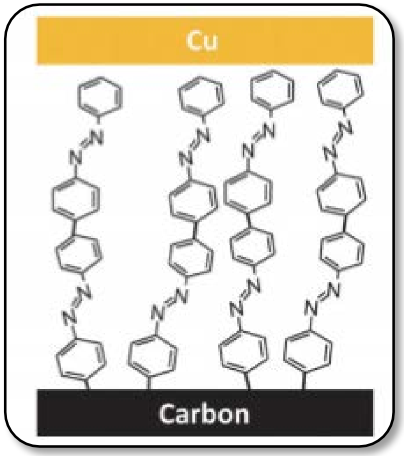

Planar junctions + grafting
Edmonton, Paris

Experimental observation of quantum interference

Meta and para substituted benzene molecules, MCBJ

C. R. Arroyo *et al.*, Angew. Chem. Int. Ed. **52**, 3152 (2013)

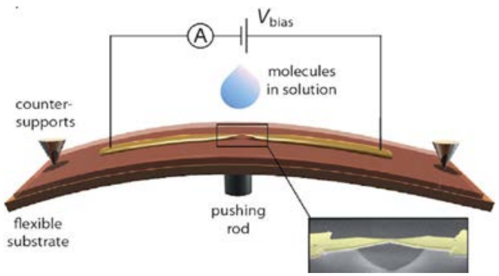

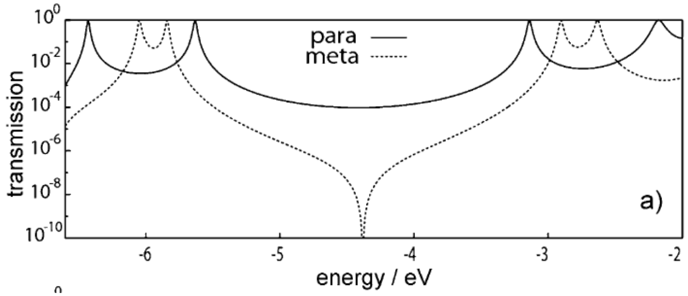

two-dimensional histograms of conductance

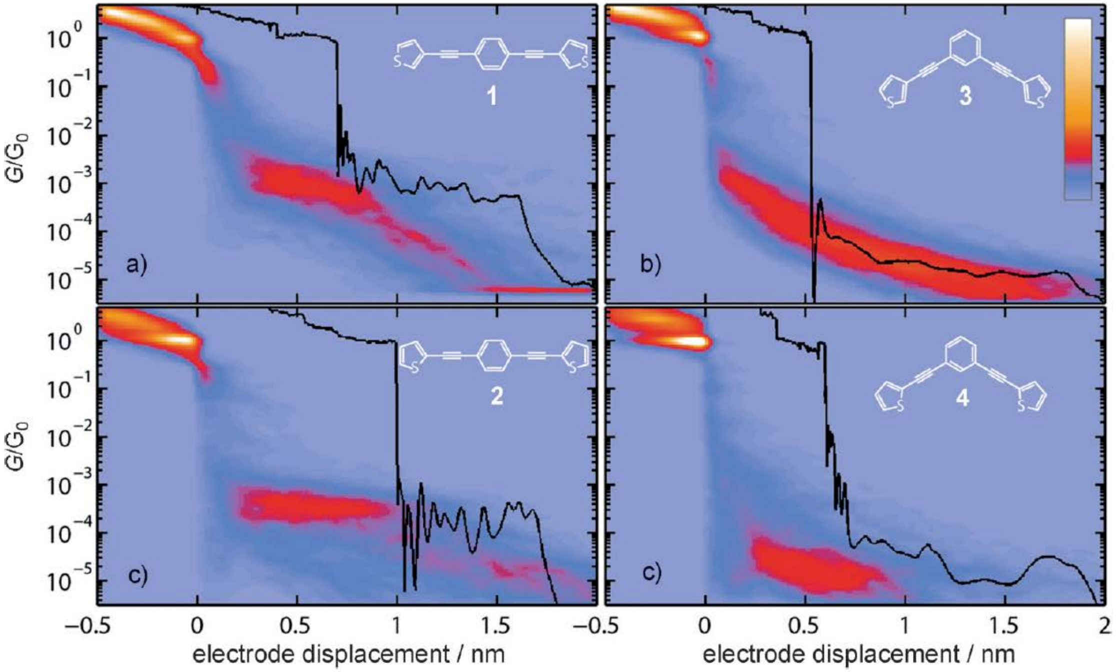

T = 300 K
V_{bias} = 0.1 V

Experimental observation of quantum interference

molecular junctions based on SAMs, statistical analysis

Evidence of QI: dip and negative curvature of the conductance

C-AFM junctions

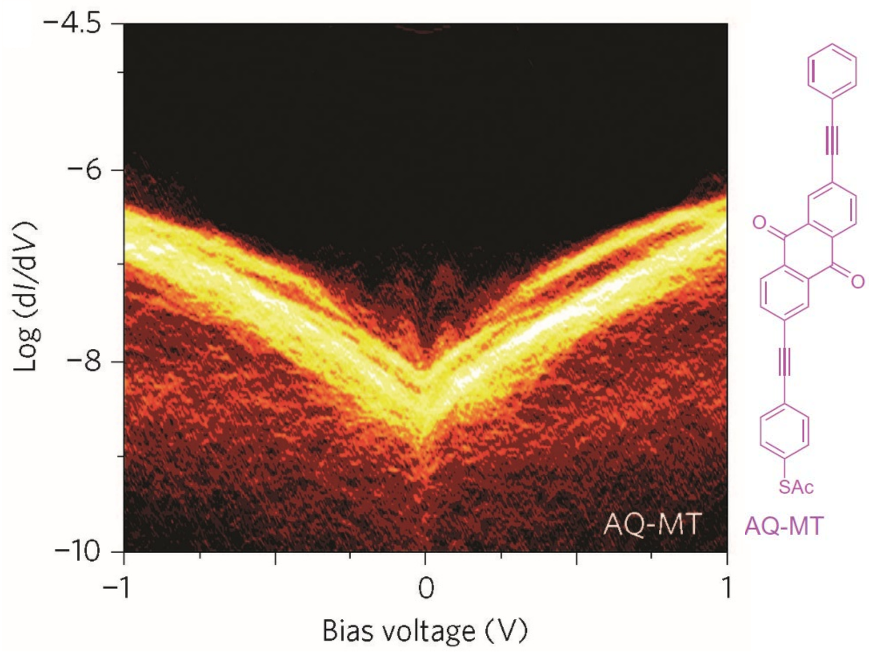

Guedon *et al.*, Nat. Nanotech. **7**, 305 (2012)

EGaIn junctions

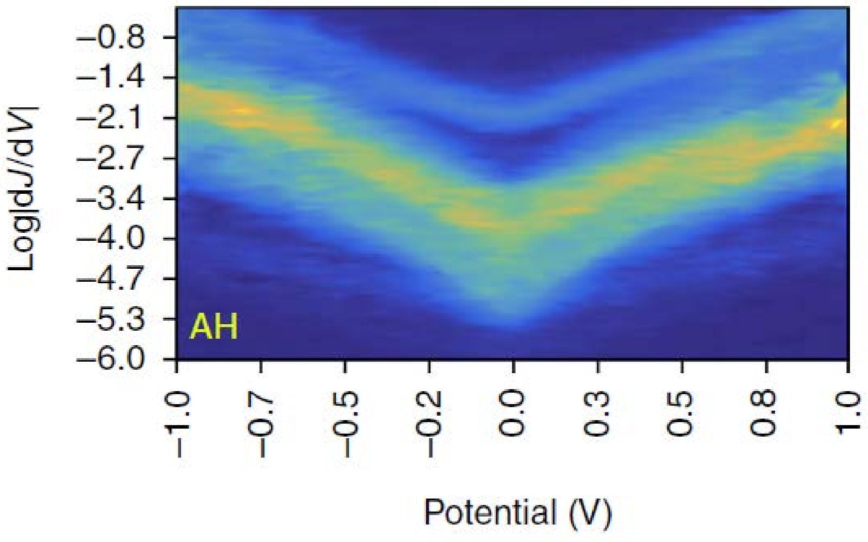

Carlotti *et al.*, Nat. Comm. **7**, 13904 (2016)

Electrochemichal grafting

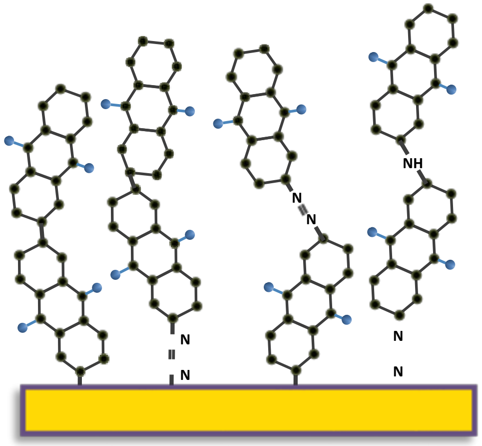

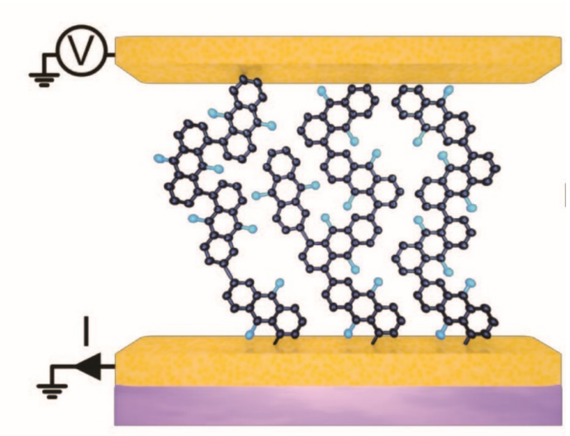

Au/AQ/TiAu junctions
Area: from 5x5µm^2 to
75x75µm^2

Growth of an organic film by electroreduction of diazonium salt

AQ precursor

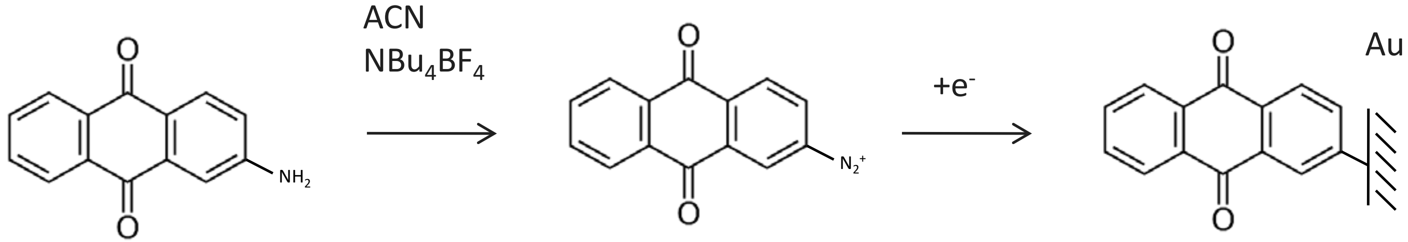

9,10-dioxo-1-anthracenediazonium (AQD)

P. Martin, J.-C. Lacroix ITODYS lab, Paris Diderot University

Fave C. et al., JACS **129**, 1890 (2007)
Fave C. et al., JPC C **112**, 18638 (2008)
A. Bousquet et al., Langmuir **28**, 1267 (2012)

formation of robust, disordered
multilayers with covalent bonds
5 to 10 nm thick

Fabrication process

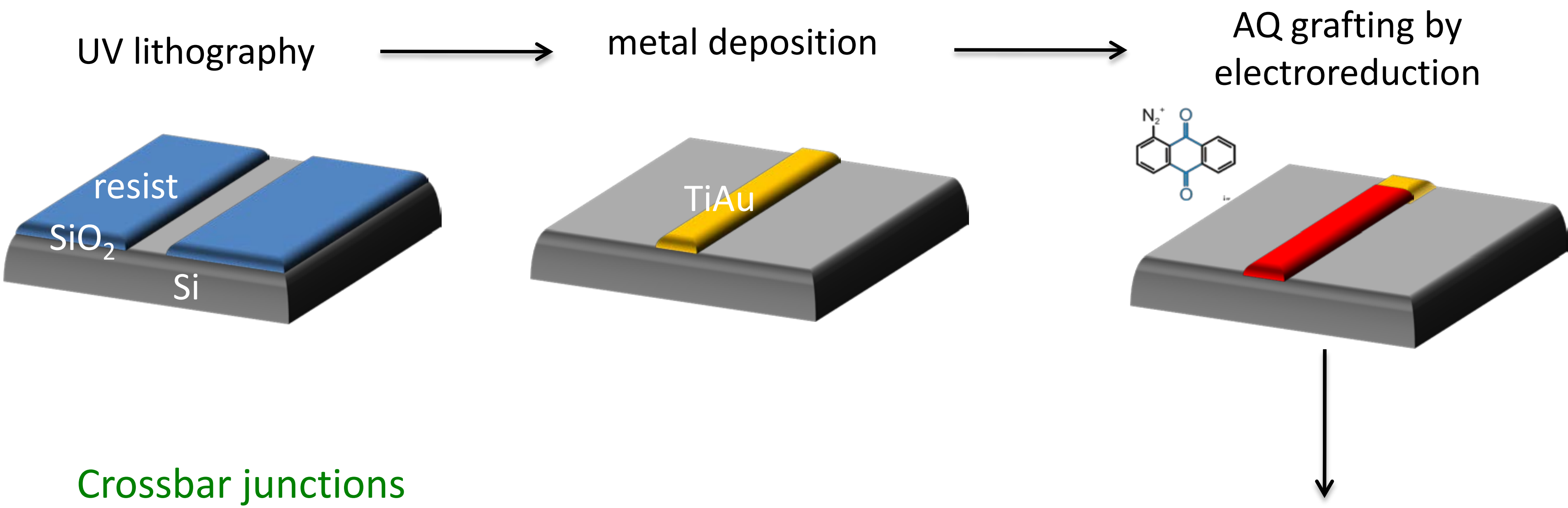

UV lithography → metal deposition → AQ grafting by electroreduction

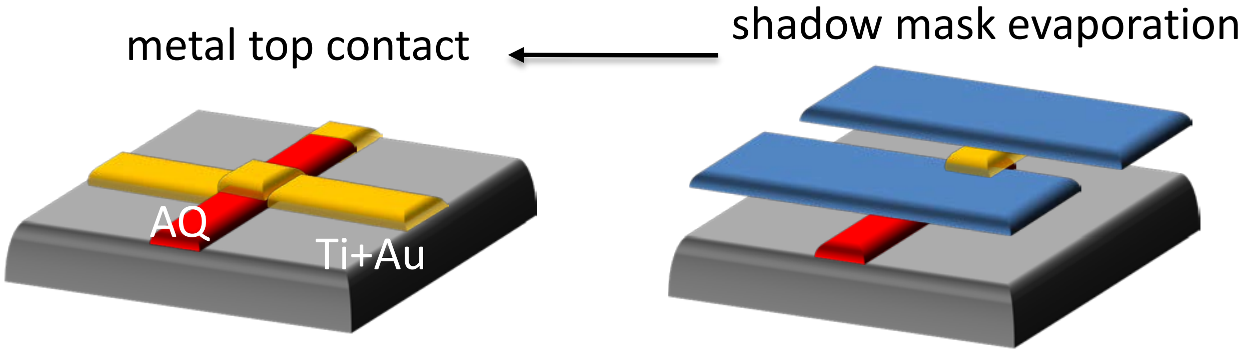

shadow mask evaporation → metal top contact

Crossbar junctions

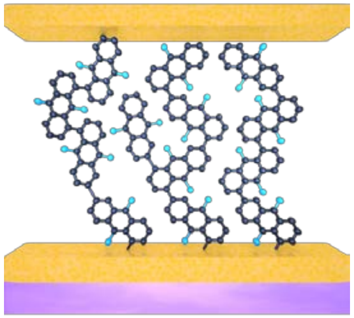

5x5μm^2 < junction area < 75x75 μm^2

A. J. Bergren *et al.*, J. Phys. Chem **114**, 15806 (2010)
P. Martin *et al.*, JACS **134**, 154 (2012)

Molecular layer caracterization

typical cyclic voltammograms

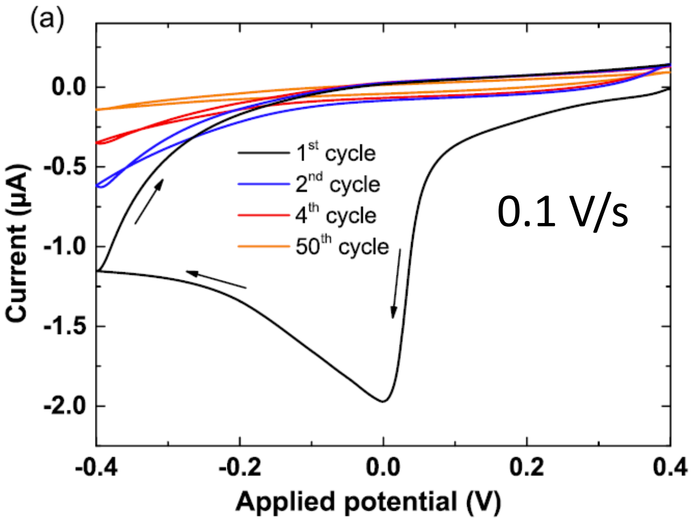

0.1 V/s

thickness depends on number of grafting cycles

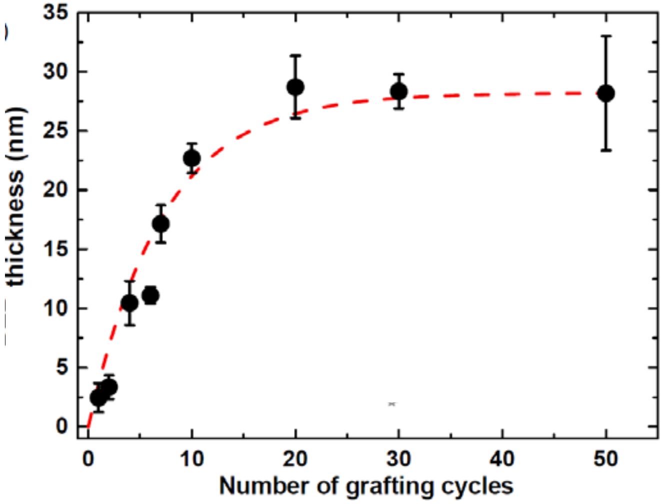

thickness and roughness measured by AFM

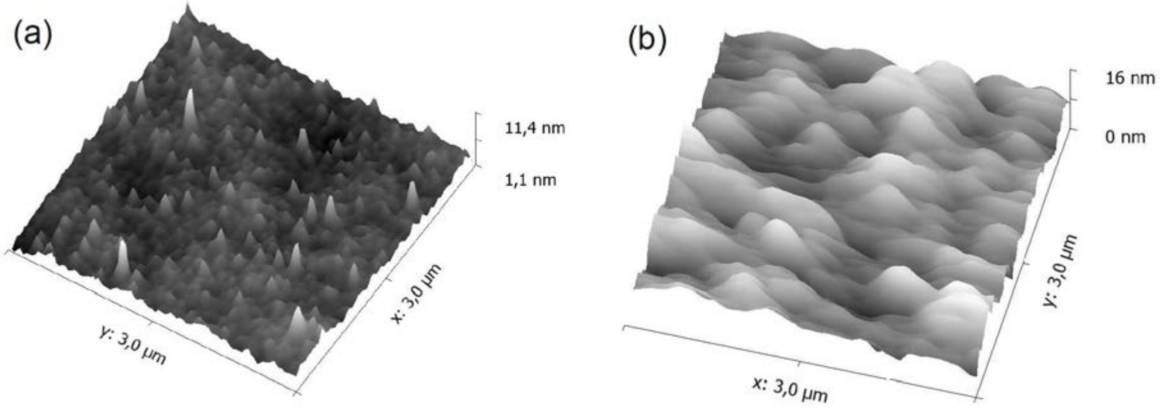

T. Fluteau *et al.*, J. Appl. Phys. **116**, 114509 (2014)

Transport characteristics of AQ based junctions

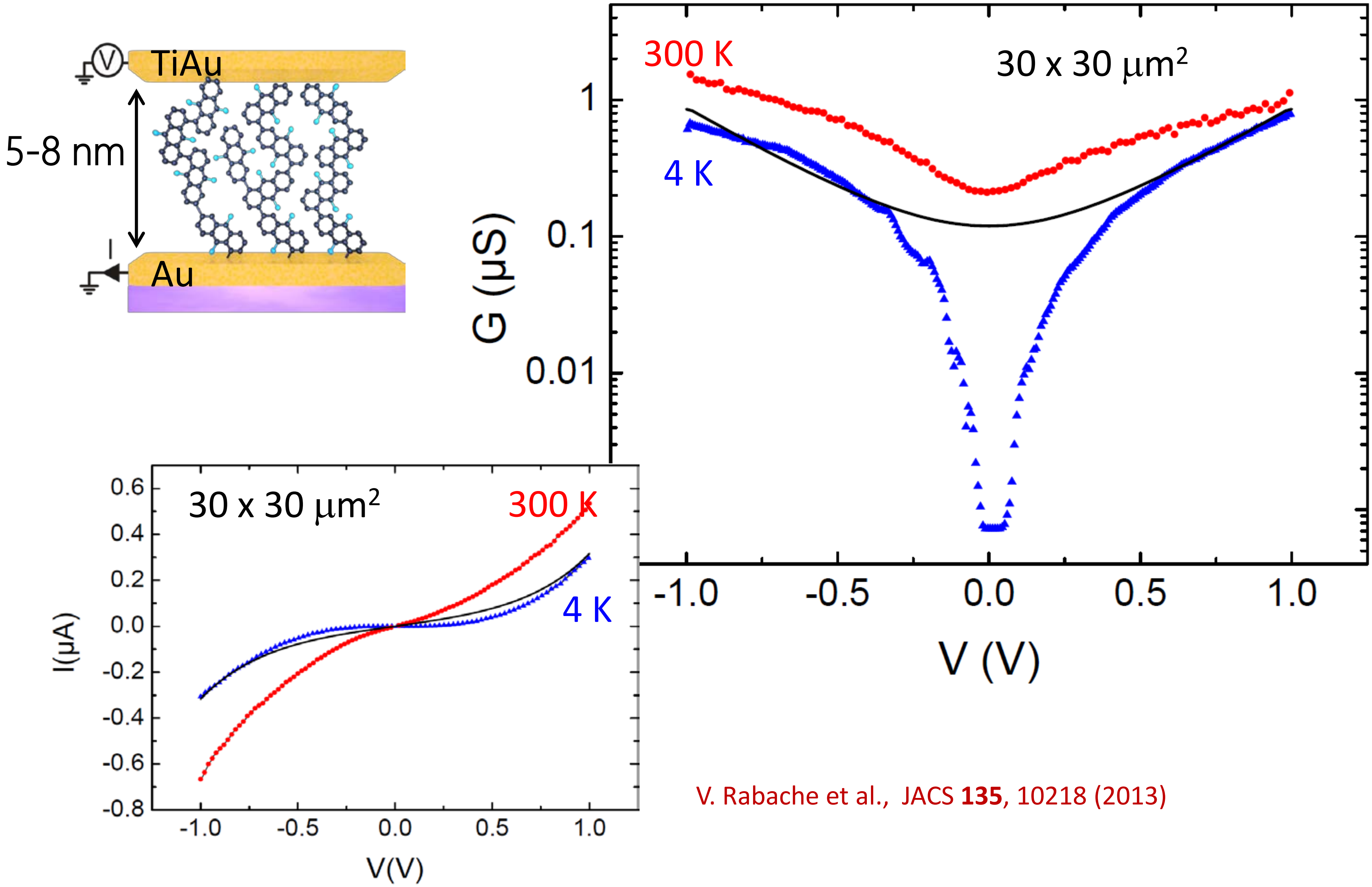

V. Rabache et al., JACS **135**, 10218 (2013)

Conductance of AQ based junctions

strong suppression at low voltage

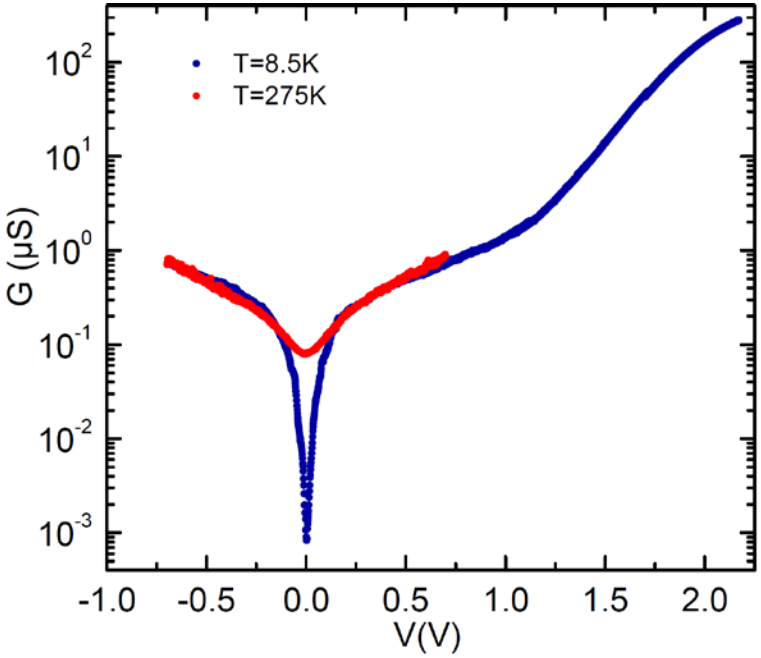

temperature dependence

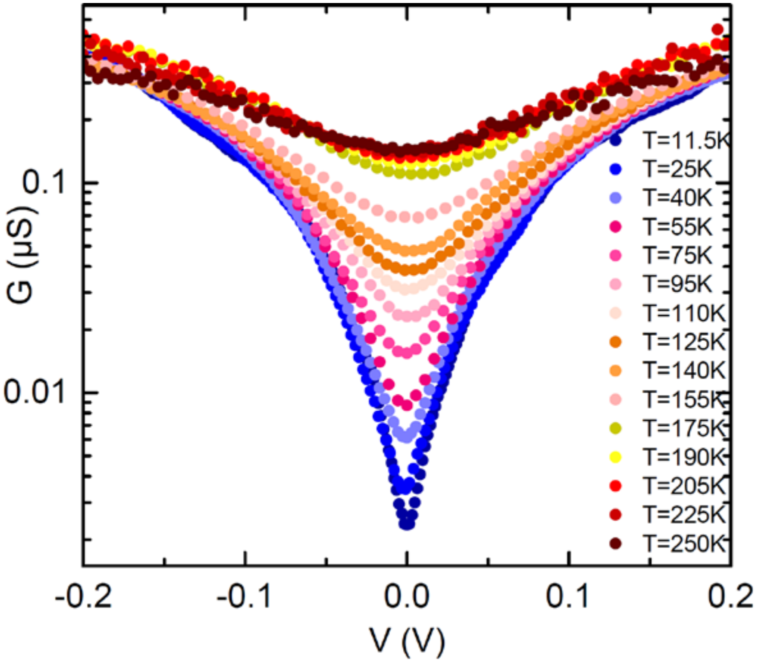

structures in the G(V)
at low temperature

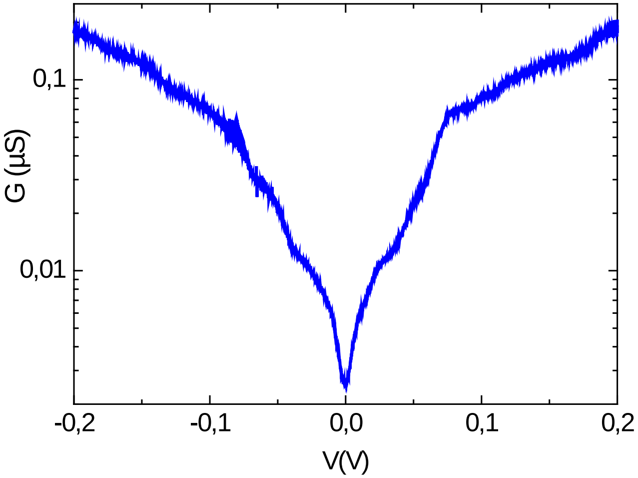

Molecular vs tunnel junctions

➡ Metallic tunnel junctions Al/Al_2O_3/TiAu

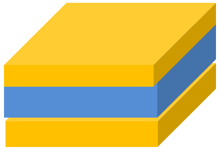

TiAu (2/50nm)

Al_2O_3

Al (50nm)

Same fabrication process via shadow mask

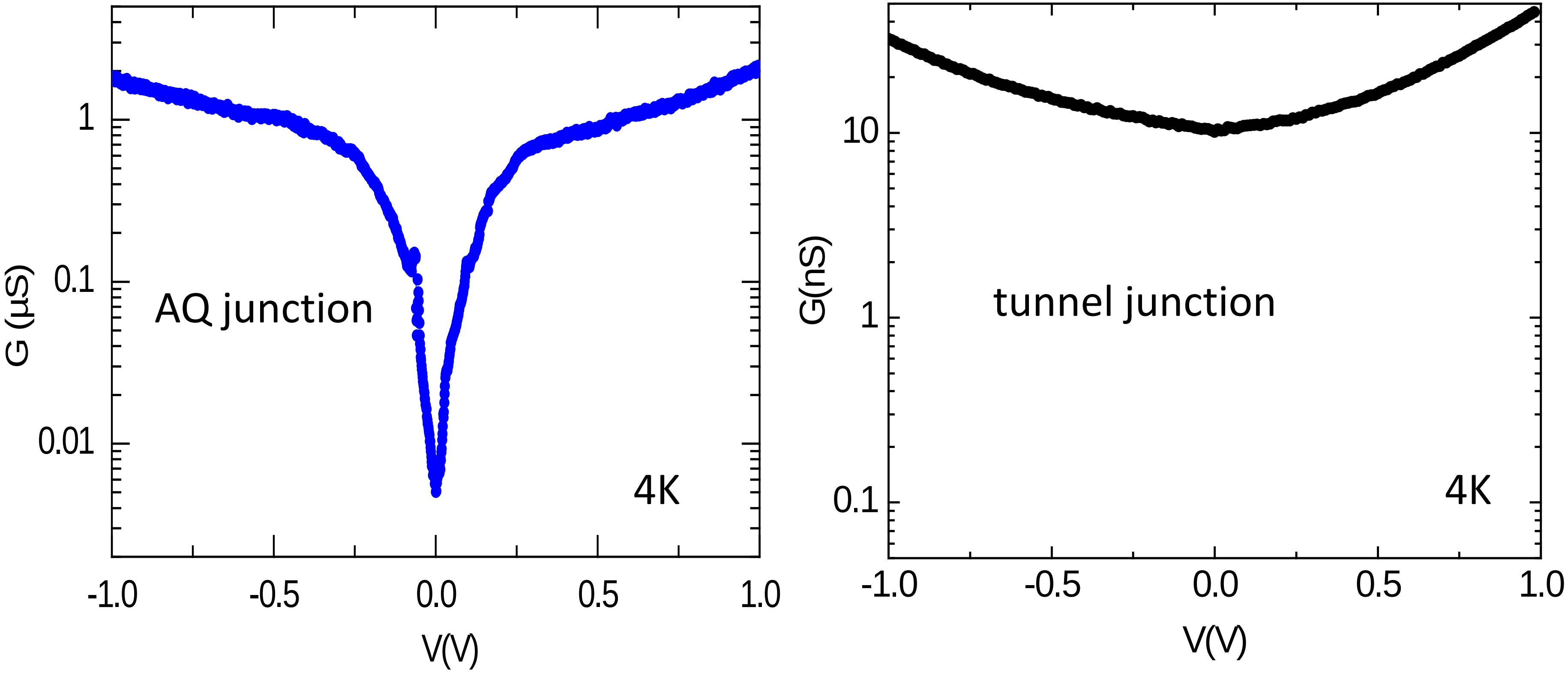

Anthraquinone vs BTB junctions

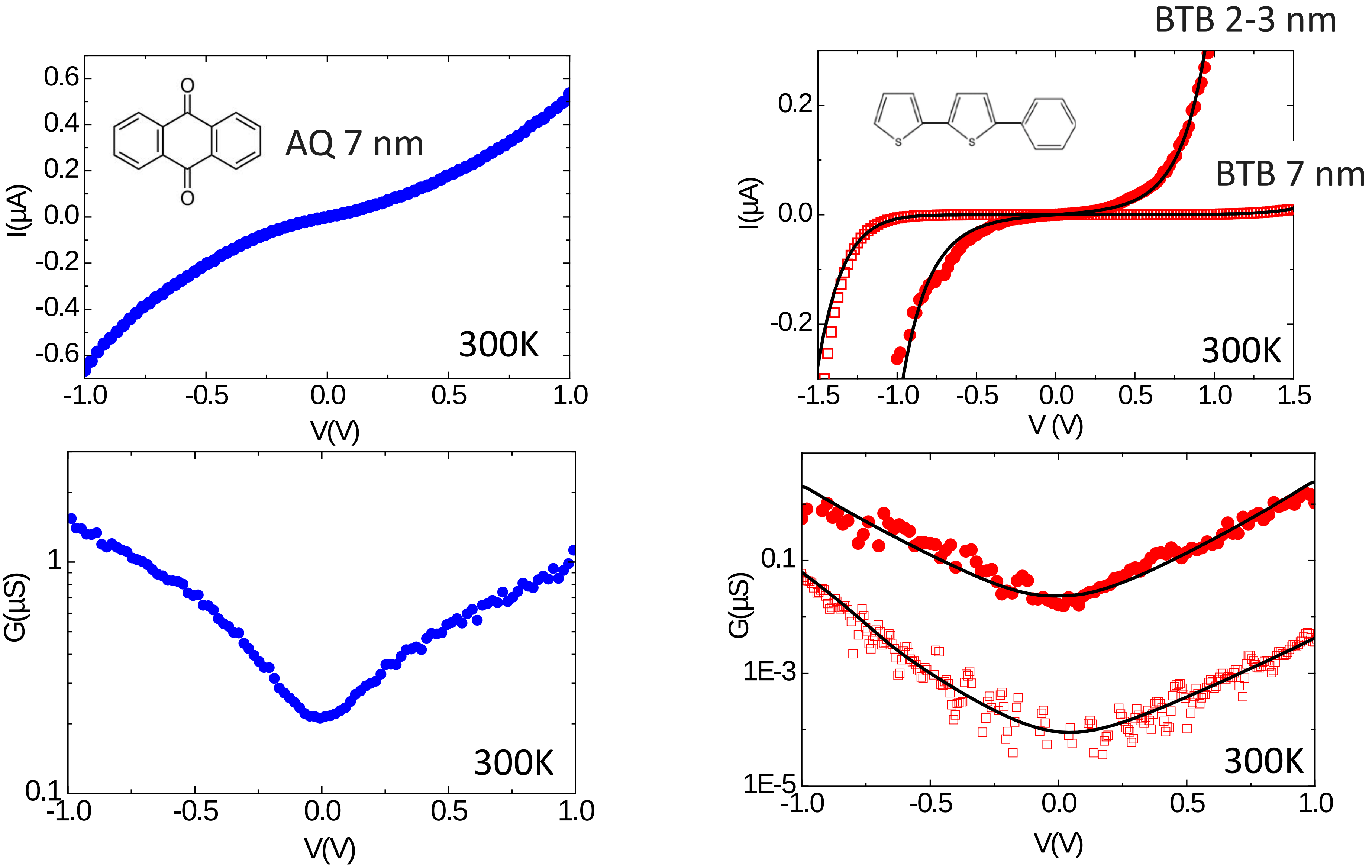

Other possible mechanisms for zero bias anomaly

DOS reduction due to e^--e^- Coulomb interaction in barely insulating disordered solids

Variable range hopping in Mott insulator for non interacting electrons in the 3D limit

N. F. Mott, J. Non-Cryst. Solids **1**, 1 (1968)

$$\sigma(T) \propto exp\left(-\frac{T_0}{T}\right)^{\nu} \quad \text{with} \quad \nu = \frac{1}{4}$$

… by including Coulomb interaction a Coulomb gap opens at low E and $\nu = \frac{1}{2}$

A.L. Efros and B.I. Shklovskii, J. Phys. C **8**, L49 (1975)

Expected linear behavior of $ln(\rho)$ vs $\frac{1}{T^{\frac{1}{2}}}$

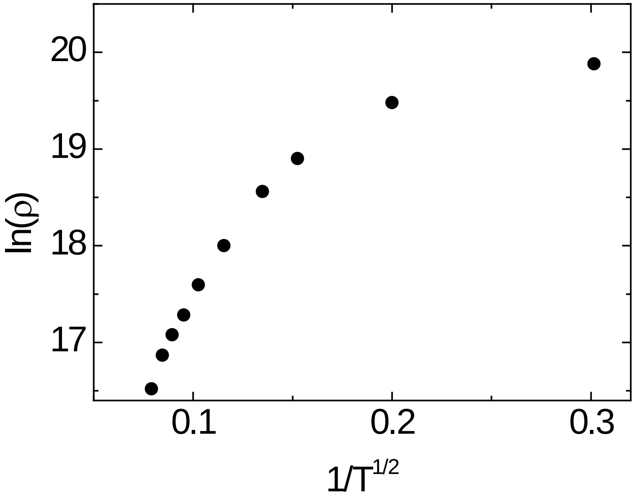

Other possible mechanisms for zero bias anomaly

DOS reduction due to e^--e^- Coulomb interaction in diffusive metallic leads of the junction

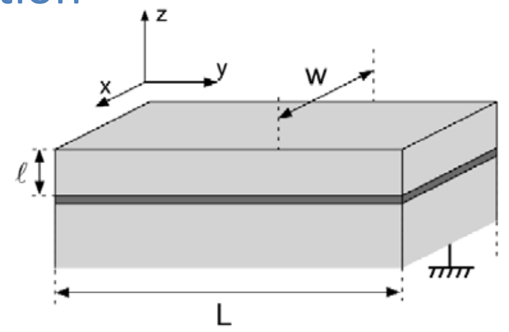

$$\frac{\delta G}{G_\infty} \propto \sqrt{eV}$$ 3D limit

$$\frac{\delta G}{G_\infty} \propto log(eV)$$ 2D limit

$$\frac{\delta G}{G_\infty} \propto -\sqrt{\frac{E^*_{Th}(w)}{eV}}$$ 1D limit

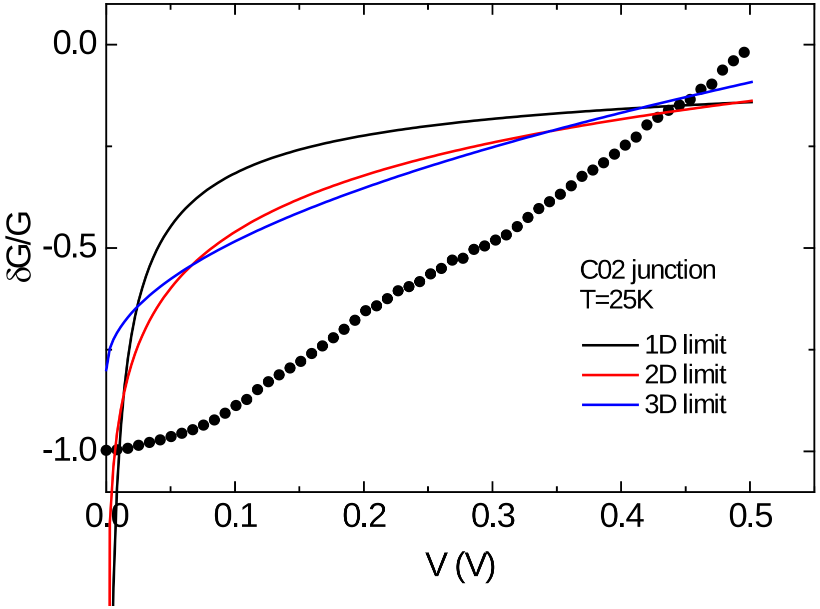

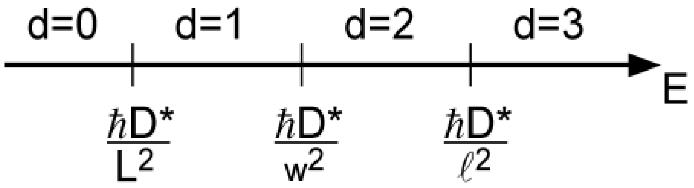

F. Pierre *et al.*, PRL **86**, 1590 (2001)
B.L. Altshuler *et al.*, Sov. Phys. JETP **59**, 415 (1999)
E.V. Sukhorukov *et al.*, PRB **56**, 1456 (1997)

Other possible mechanisms for zero bias anomaly

Dynamical Coulomb blockade: inelastic electron tunneling with energy dissipation in the electromagnetic environnement

P. Joyez and D. Esteve, Phys. Rev. B **56**, 1848 (1997)

Best fit with resistive environment:
T=25K
Z_{ext}= R = 0.8R_k~20kΩ
C = 1.5 10^{-19} F
E_c = 0.53 eV

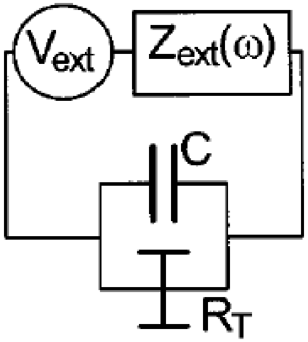

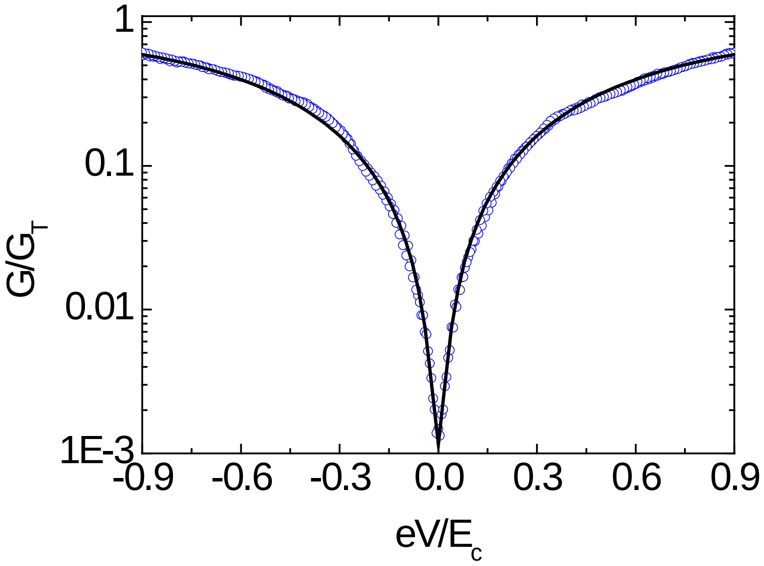

Necessary conditions:
R_T>>R_k (resistance quantum)
only relevant impedance Z_{ext}//C

DFT calculated transmission of AQ chains

Calculations by T. Markussen (Quantum Wise)

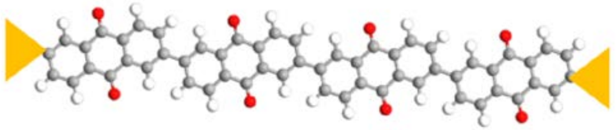

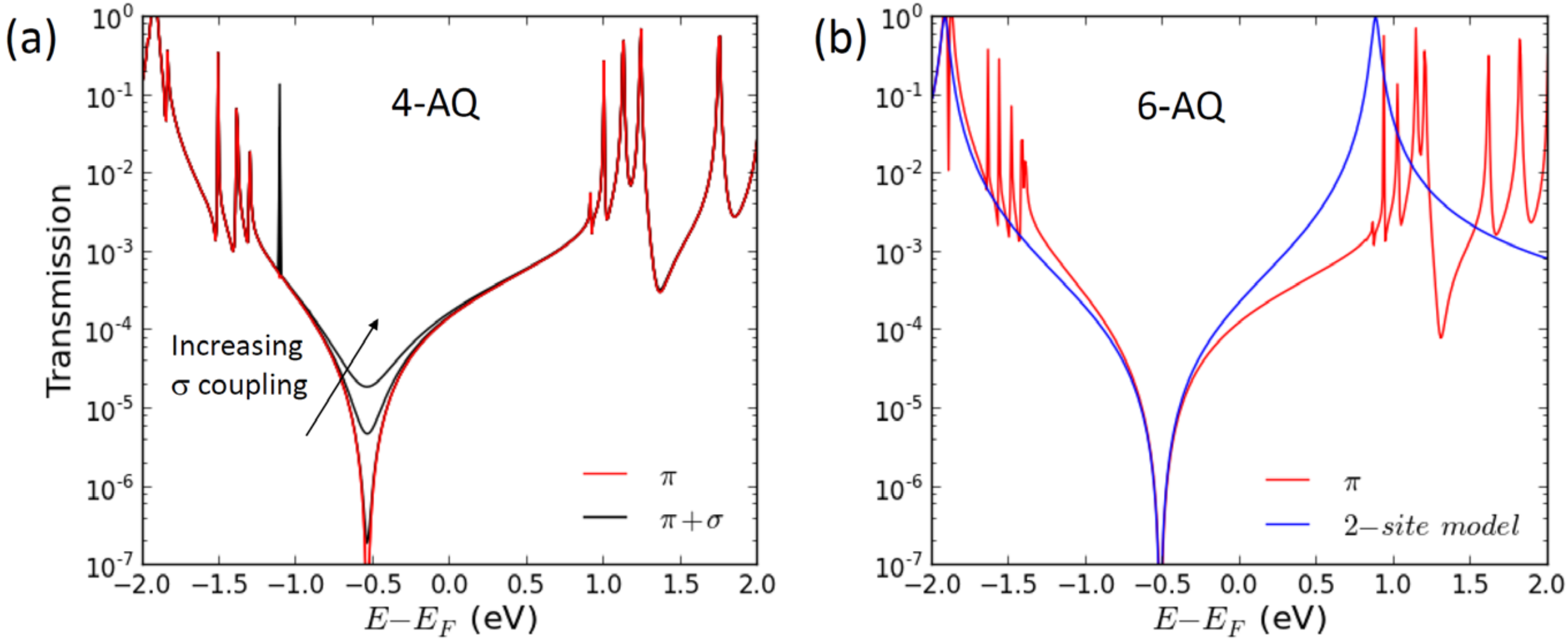

π + σ contributions

DFT vs two-site model

two-site model used to fit DFT calculations

$\varepsilon_1 = -0.52\ eV$

$\varepsilon_2 = -0.52\ eV$

γ= 0.025 eV

t=-1.4 eV

Two-site model for quantum interference

Simplest model capturing the quantum interference effect

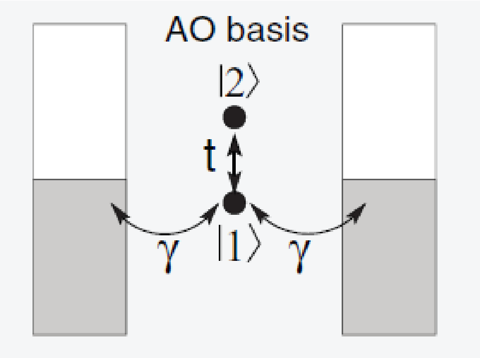

T. Markussen et al., PRB **89**, 085420 (2014)

one site coupled to the leads

Transmission function $T(E) = \mathrm{Tr}[\boldsymbol{\Gamma}_L \boldsymbol{G}^r \boldsymbol{\Gamma}_R \boldsymbol{G}^a]$

- $\boldsymbol{\Gamma}_{L/R}$ coupling matrices to leads L/R
- $\boldsymbol{G}^{r/a}$ Green functions of the molecule

⇨ $$T(E) = \frac{\gamma^2}{\left[(E-\varepsilon_1) - \dfrac{t^2}{E-\varepsilon_2}\right]^2 + \gamma^2}$$

Transmission node at $E = \varepsilon_2$

$\varepsilon_1 = \varepsilon_2 = 0$, γ=0.4 eV, t=-2.6 eV

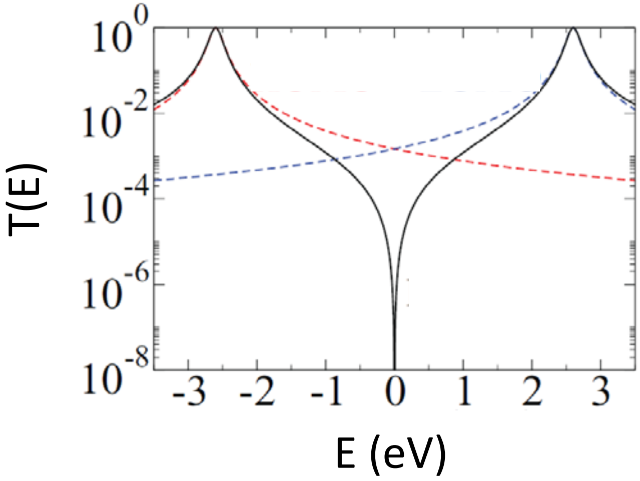

Influence of electron-phonon interaction

Conductance of a single AQ molecule junction with el-ph interaction

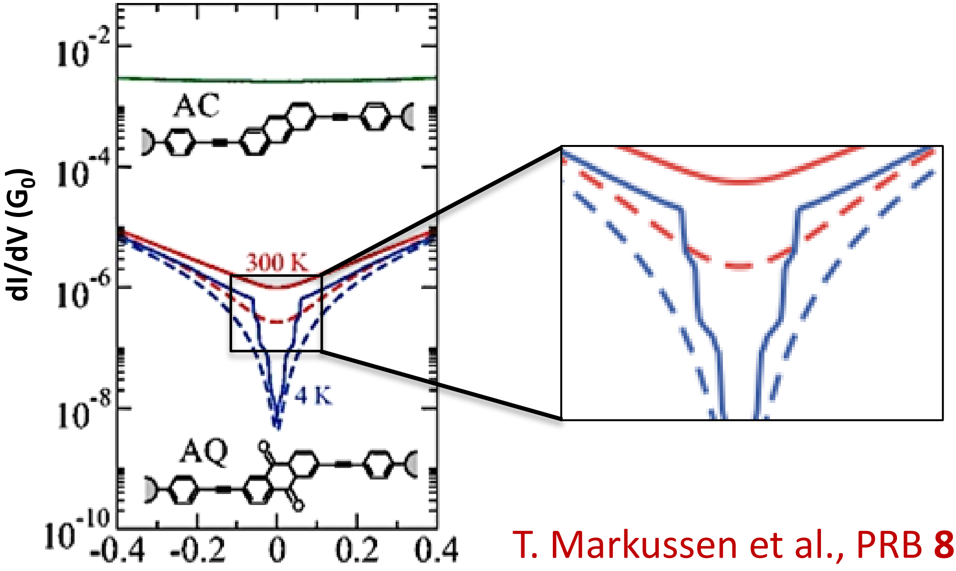

Steps in conductance due to opening of inelastic transport channels

T. Markussen et al., PRB **89**, 085420 (2014)

Current calculated with DFT within the lowest order expansion

Influence of el-ph in transport measurements

simultaneous fitting of G(V) and G(T)

C. Bessis et al., Sci. Rep. **6**, 20899 (2016)

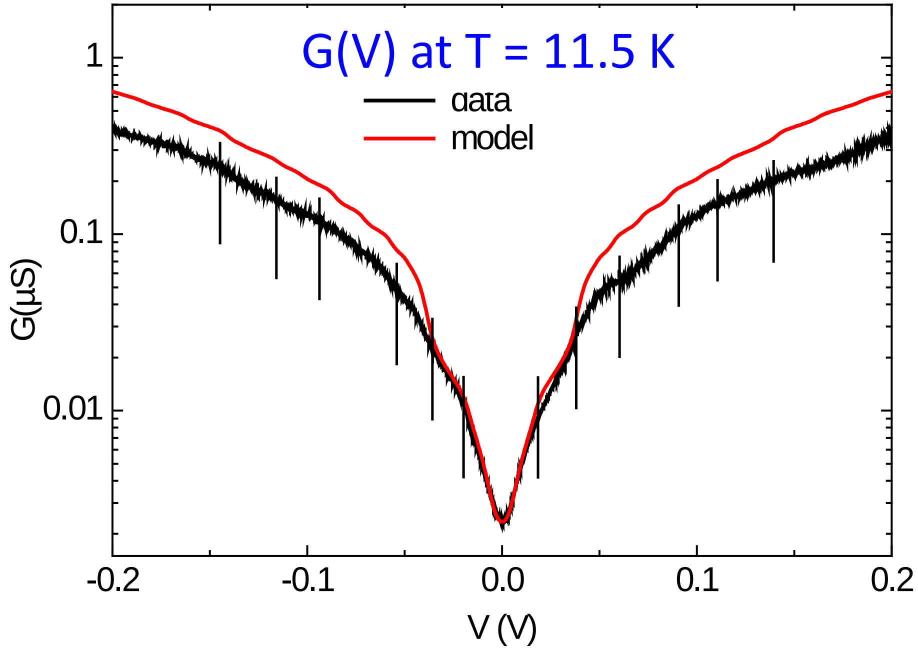

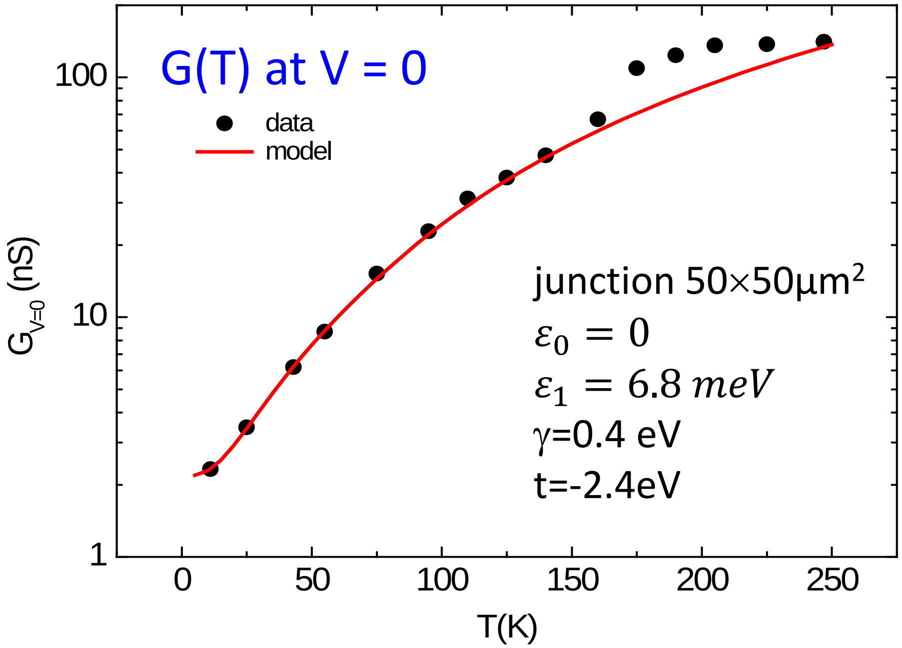

model: lowest order expansion and two-site model

$$I(V,T) = I_{el}(V,T) + \sum_{\lambda} I_{in}(V,\lambda,T\,)$$

sum over each phonon mode $\hbar\omega_\lambda$

T. Markussen, K.S. Thygesen, Phys. Rev. B **89**, 085420 (2014)

Calculated d^2I/dV^2

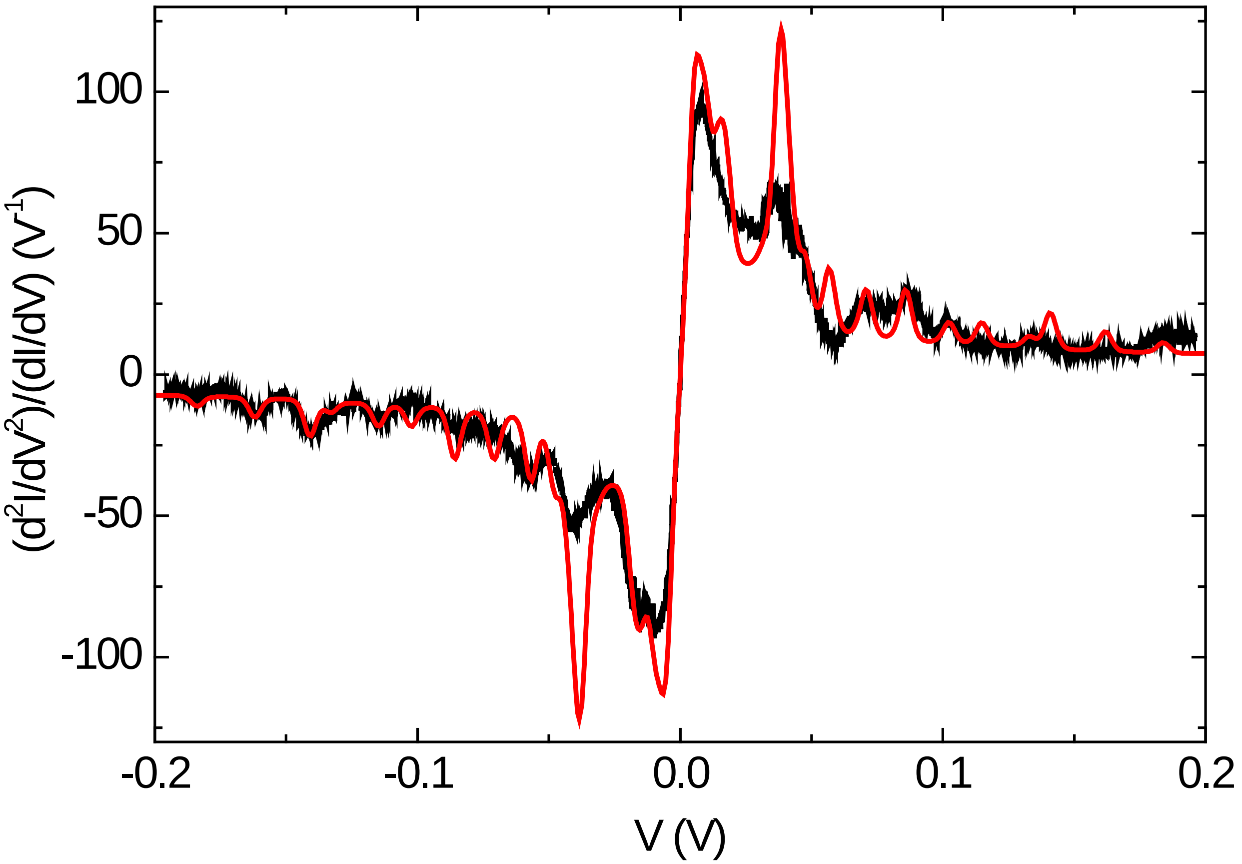

14 ph energies (5 – 160 meV), few dominant modes at low energy

Conductance and el-ph interaction

G(V) and G(T) curves fitted to a two site model with el-ph interaction

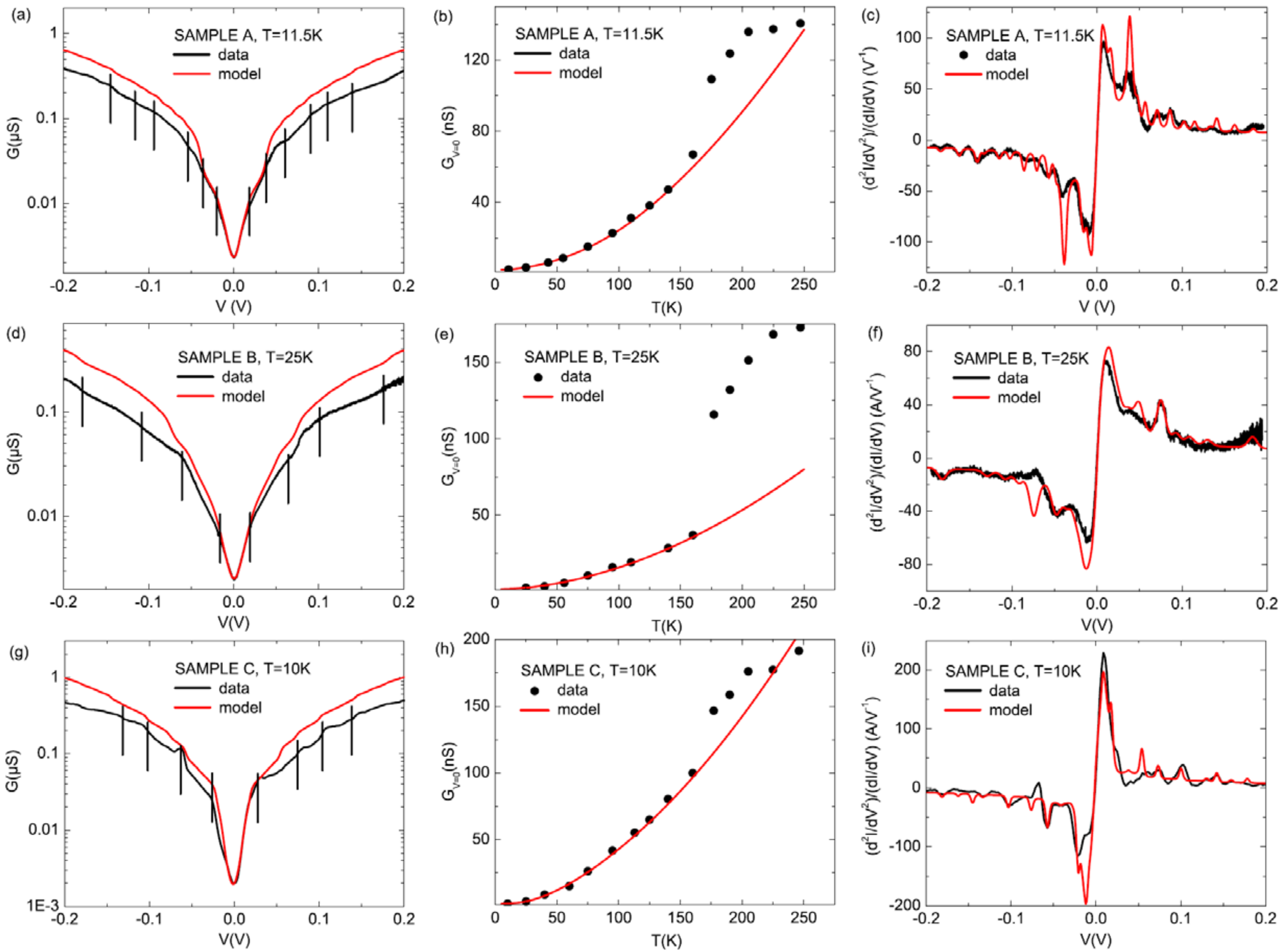

High temperature behaviour

Two sites model with el-ph interaction also described conductance at higher temperature

Solid curves calculated with parameters extracted at the lowest temperature

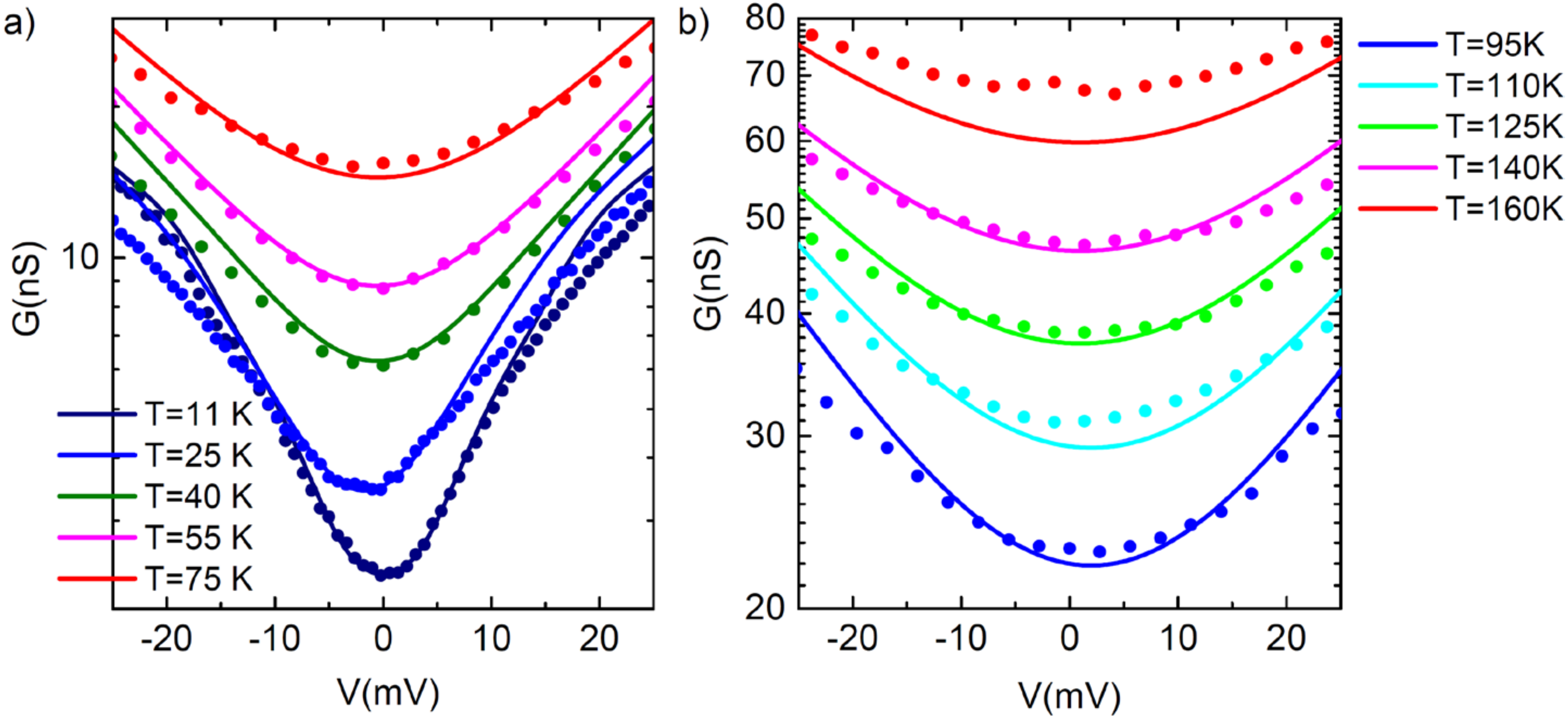

Inelastic electron tunneling spectroscopy

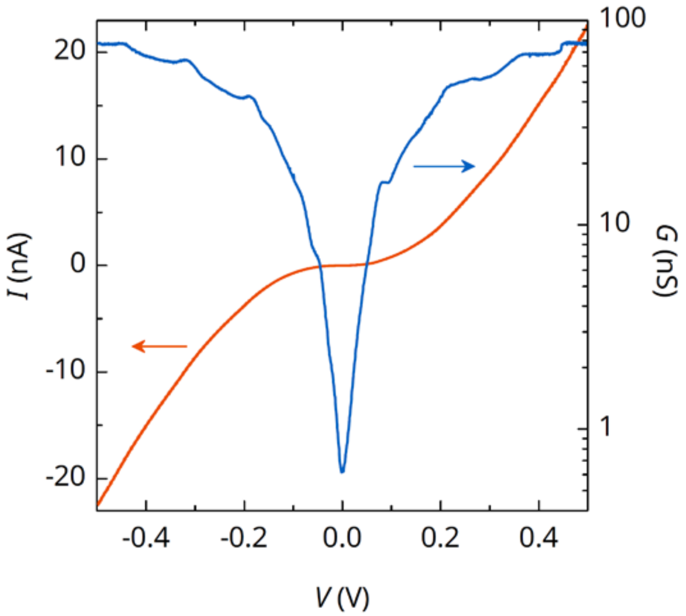

IETS powerfull tool for molecular transport:

M. A. Karimi et al., Nano Lett. **16**, 1803 (2016)

- Detect change in configuration

R. Frisenda et al., Beilstein J. Nanotechnol. **6**, 2477 (2015)

- Predicted improved sensitivity in cross-conjugated molecules

J. Lykkebo et al., ACS Nano **7**, 9183 (2013)

measured d^2I/dV^2 (raw and symmetrized)

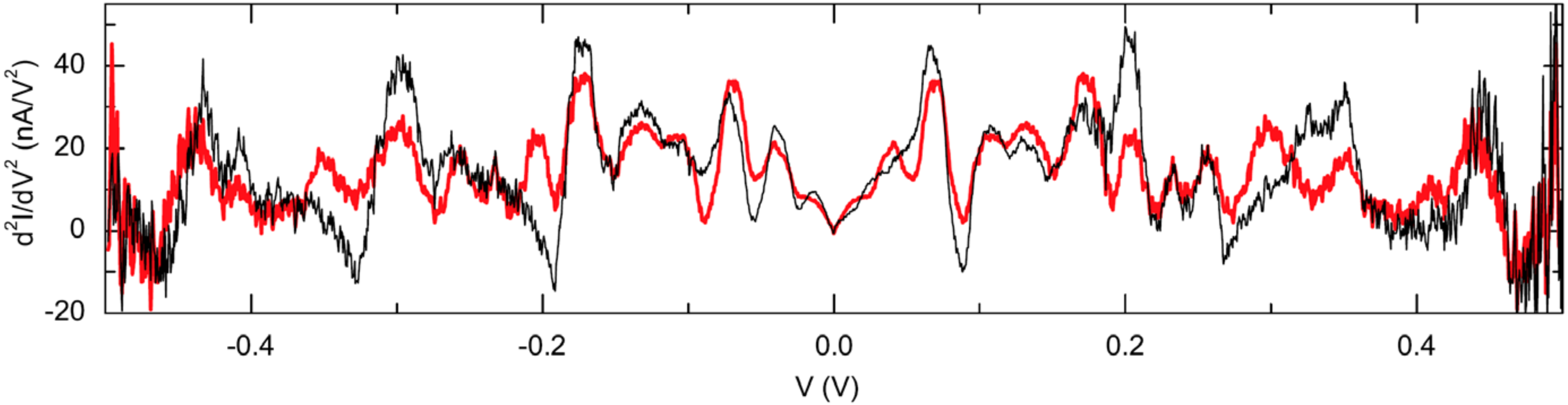

FWHM analysis

$$FWHM \approx \sqrt{W_{intrinsic}^2 + \frac{5.44 k_B T}{e} + 1.7 V_{rms}^2}$$

Peak at – 35 mV, T = 5 K

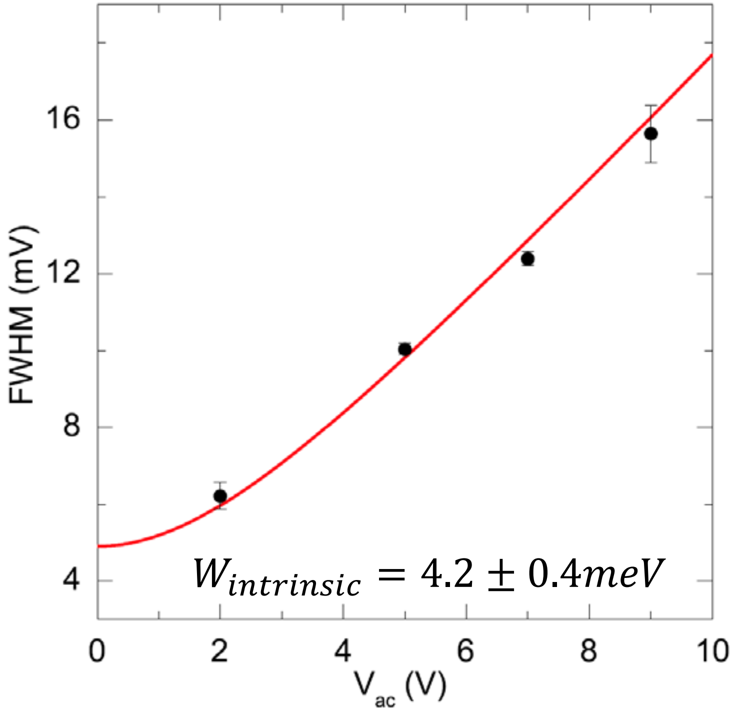

$W_{intrinsic} = 4.2 \pm 0.4 meV$

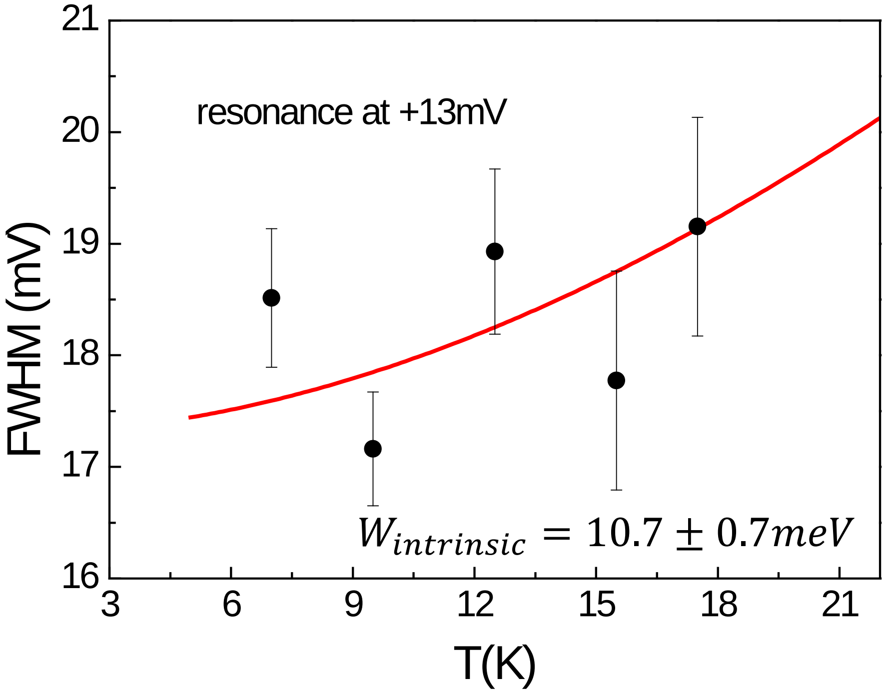

$W_{intrinsic} = 10.7 \pm 0.7 meV$

IETS signal

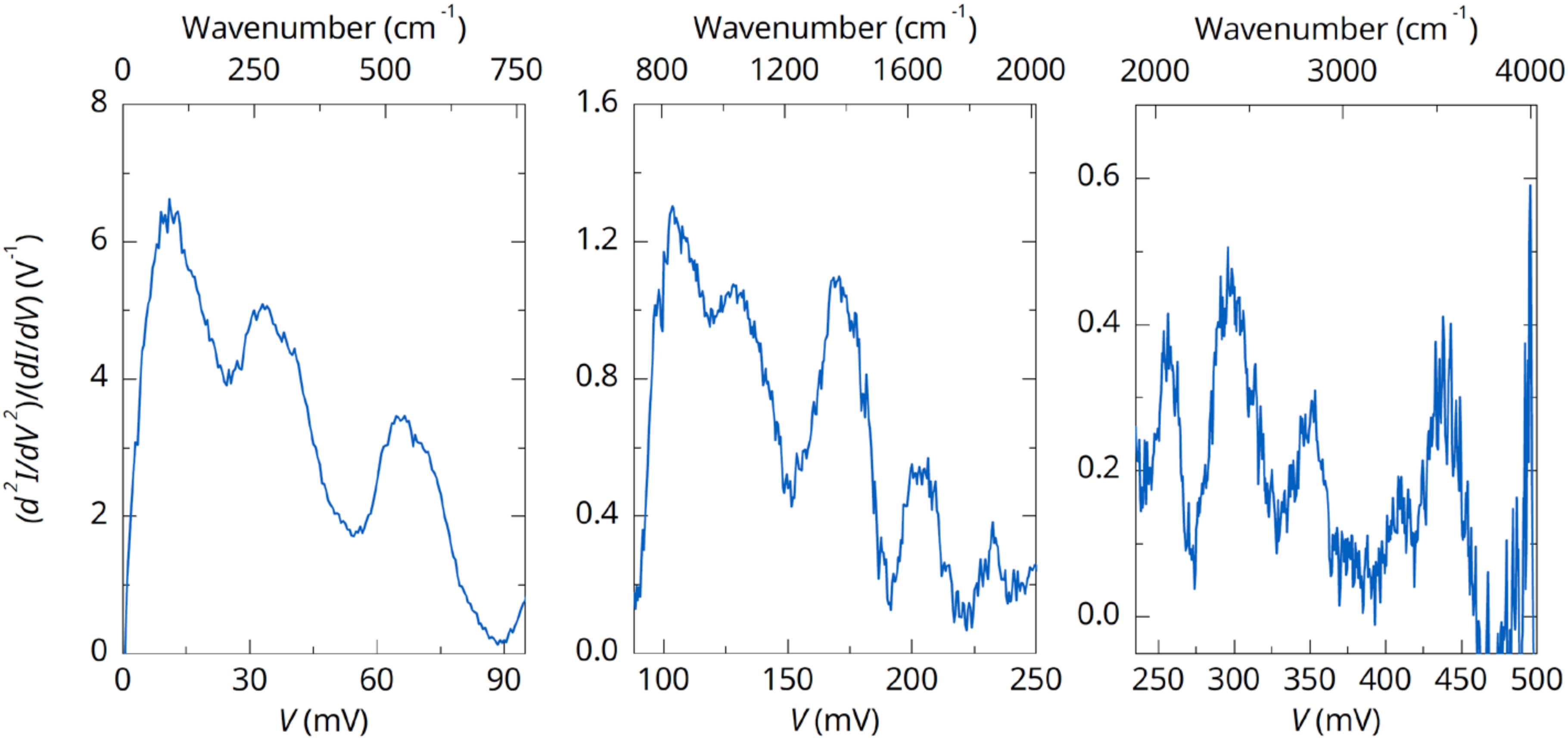

Wavenumber (cm^{-1})
0
250
500
750
800
1200
1600
2000
2000
3000
4000
8
6
4
2
0
1.6
1.2
0.8
0.4
0.0
0.6
0.4
0.2
0.0
$(d^2I/dV^2)/(dI/dV)$ (V^{-1})
0
30
60
90
100
150
200
250
250
300
350
400
450
500
V (mV)

Vibrational modes

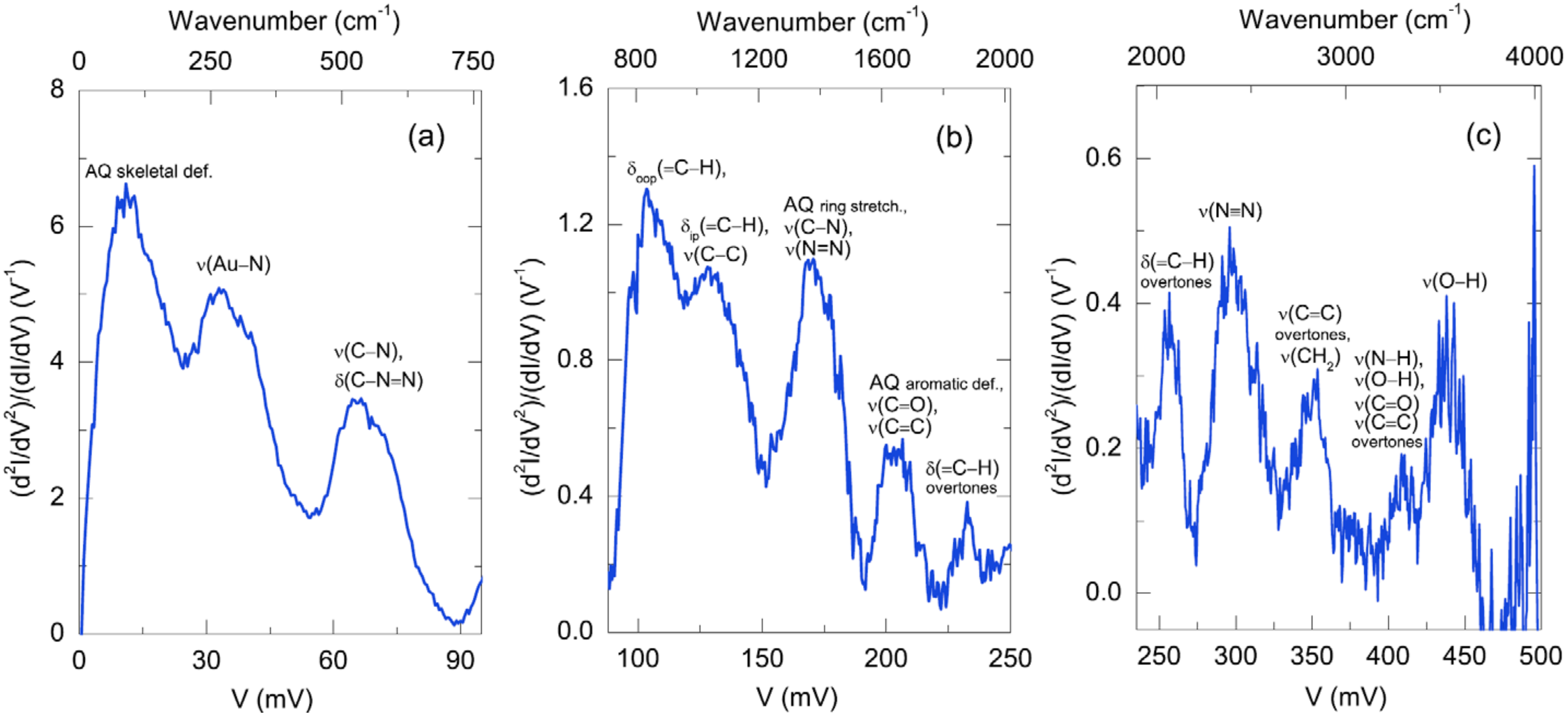

C. Salhani et al., Phys. Rev. B **95**, 165431 (2017)

Poster n°8 by Chloe Salhani

no signature of Au-C bond, signatures of azo-bonds and AQ

Comparaison with IR spectra

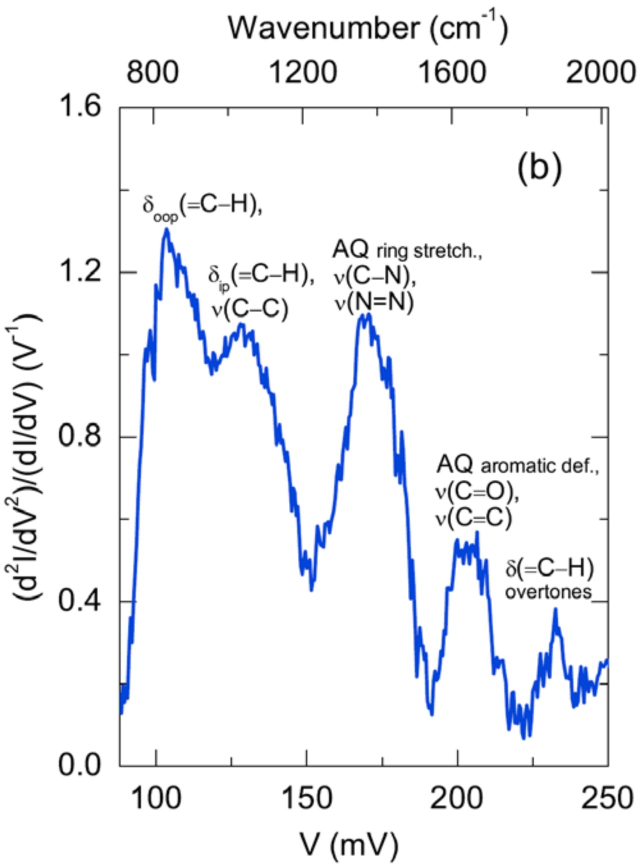

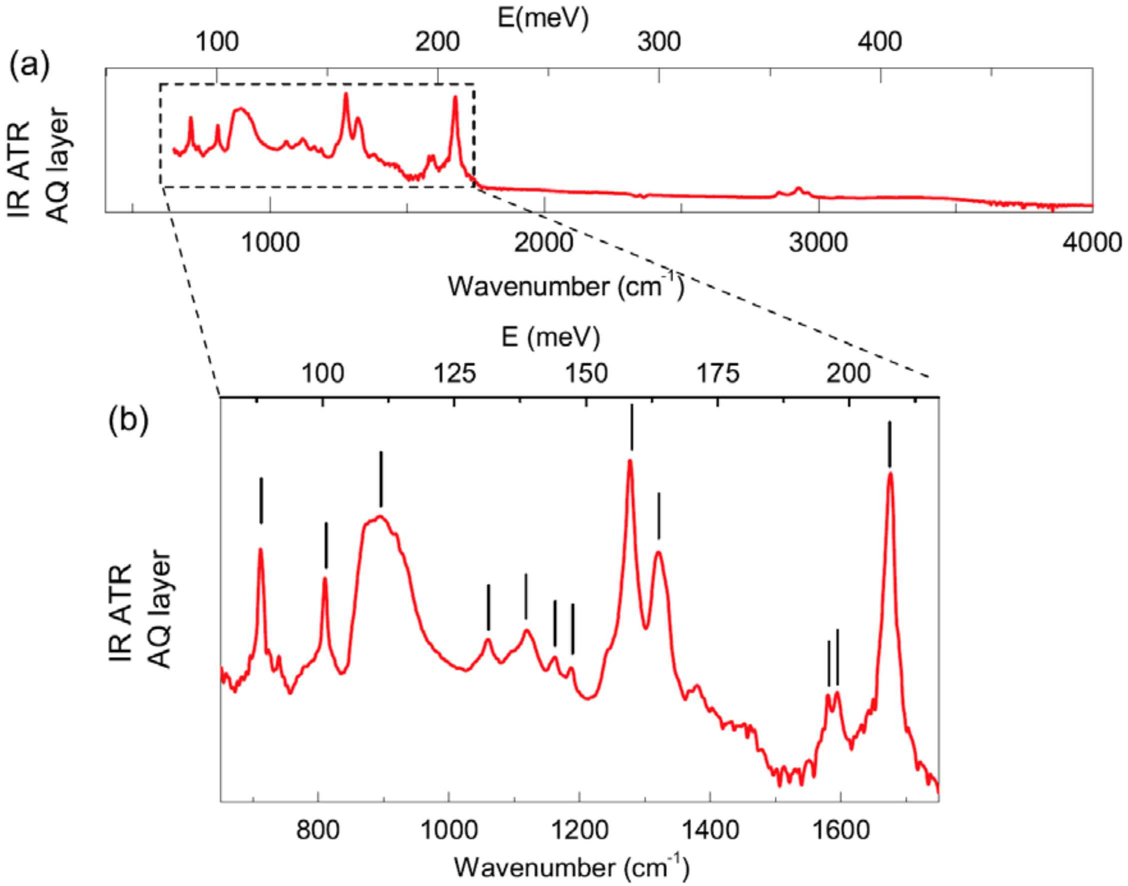

common modes at 100-130 meV and 160-200 meV

Conclusions

- Conductance of large area anthraquinone based junctions based on anthraquinone described by a QI model including e-ph interaction
- IETS reveals vibrational modes and metal/molecule covalent bonds

Perspectives

- Change in the design of the junctions to include a gate electrode

- Thermoelectrics measurements

Charge transport in molecular junctions: Vibrational effects, interference and decoherence

Michael Thoss
University of Erlangen-Nürnberg

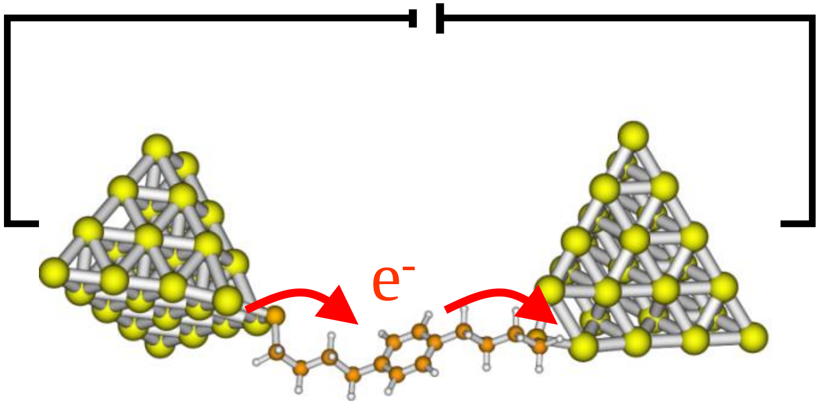

Rainer Härtle (Göttingen), Uri Peskin (Haifa), Heiko Weber (Erlangen)

Quantum transport in molecular junctions

Mechanisms and theoretical aspects

- Molecular resonance states at metal surfaces
- Electron correlation, charging effects, Coulomb blockade, Kondo effect
- Coupling to vibrational degrees of freedom
- Heat transport
- Coupling to external fields, spin-dependent transport, …

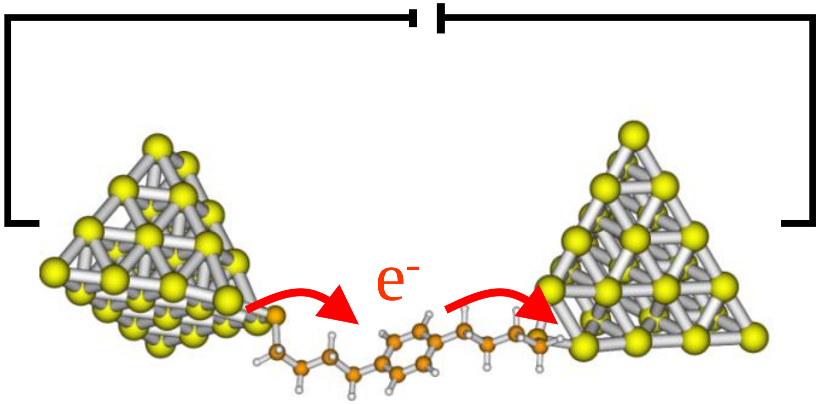

Vibrational effects in molecular junctions

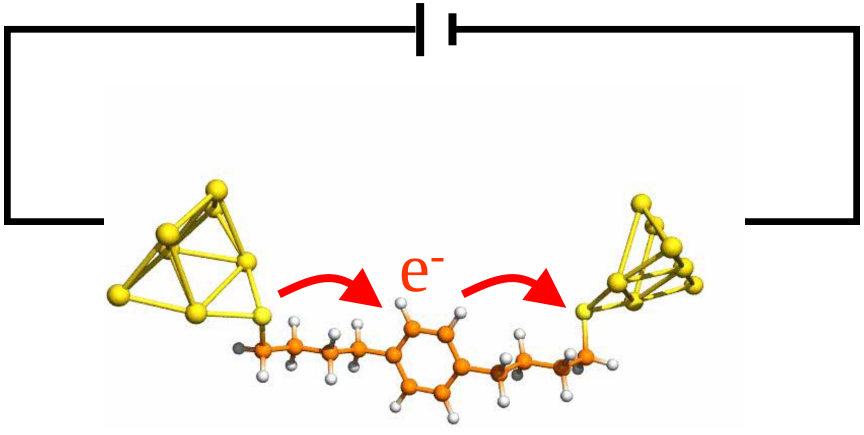

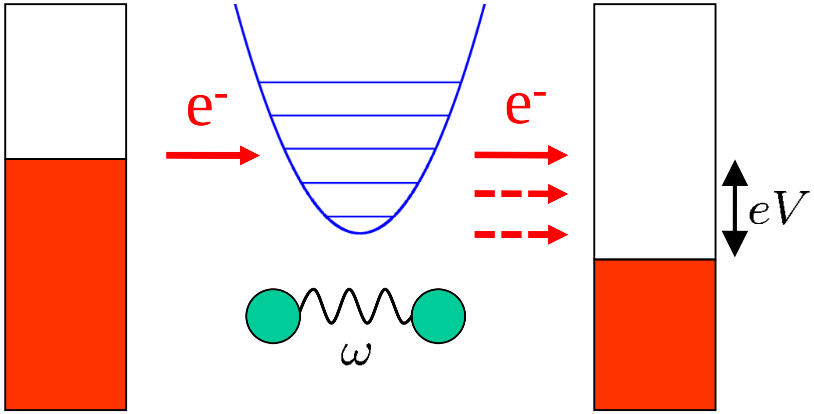

- current-induced excitation of vibrational modes
- vibrational structures in current-voltage characteristics

Vibrational effects in molecular junctions

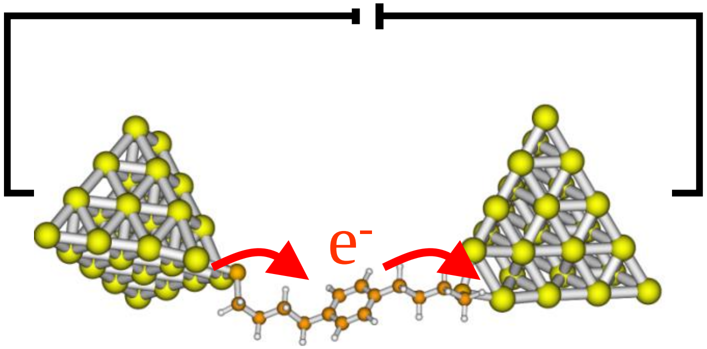

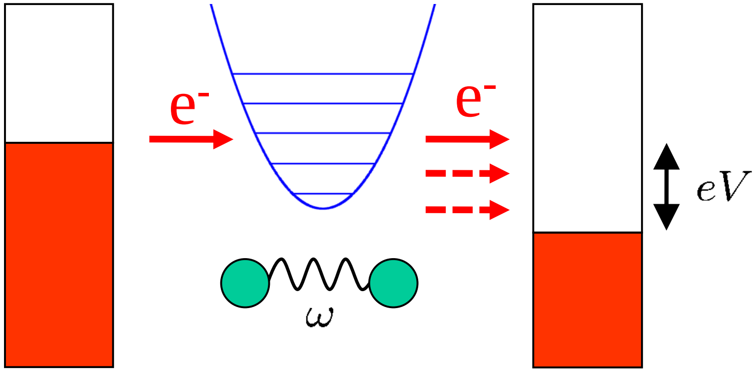

- current-induced excitation of vibrational modes
- vibrational structures in current-voltage characteristics

IETS

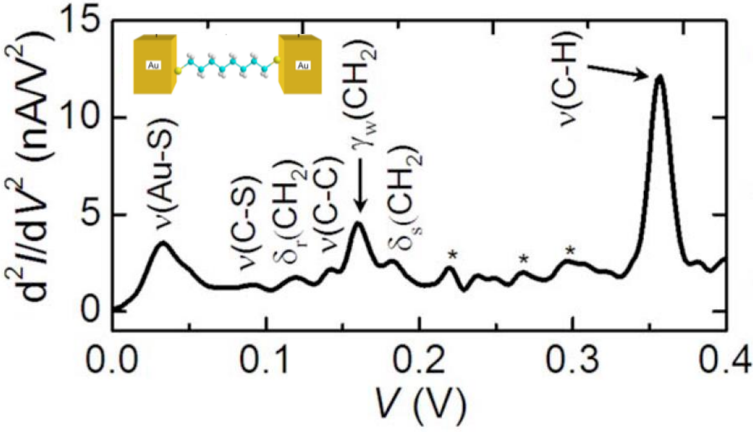

Song et al., Appl. Phys. Lett. **94**, 103110 (2009)

resonant transport

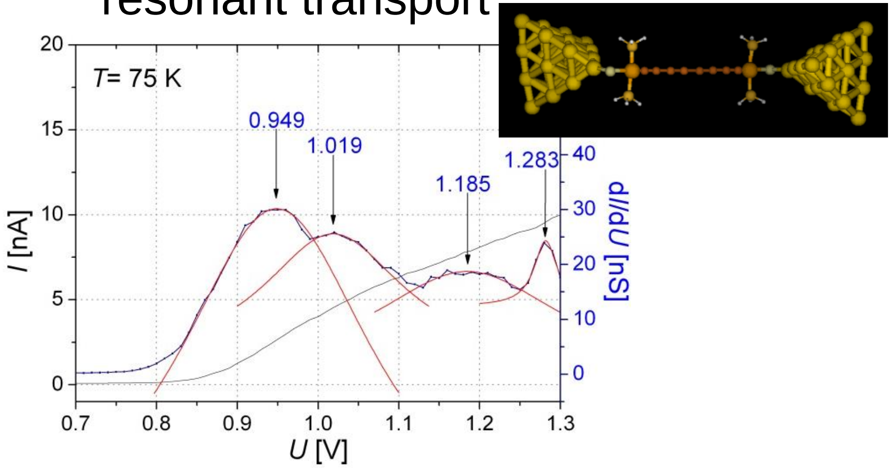

Weber et al., ChemPhysChem **11**, 2256 (2010);
Phys. Stat. Sol. B **250**, 2452 (2013)

Vibrational effects in molecular junctions

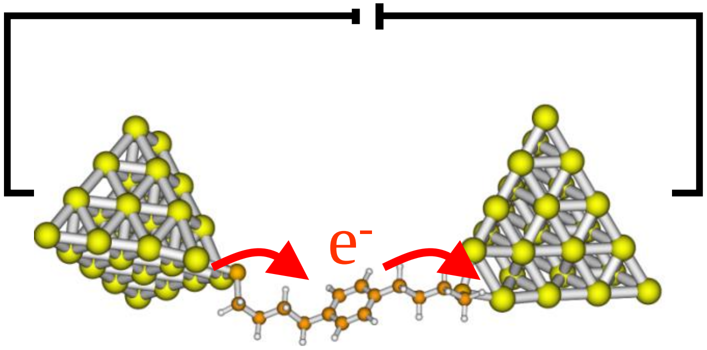

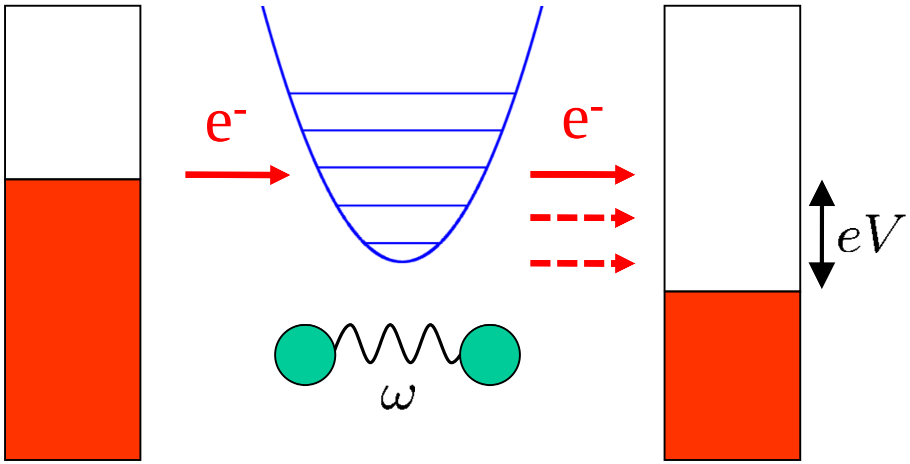

- current-induced excitation of vibrational modes
- vibrational structures in current-voltage characteristics
- vibrational nonequilibrium effects: current-induced heating, cooling, decoherence, rectification, conformational changes, switching, negative differential resistance, noise

Charge transport in molecular junctions

Model

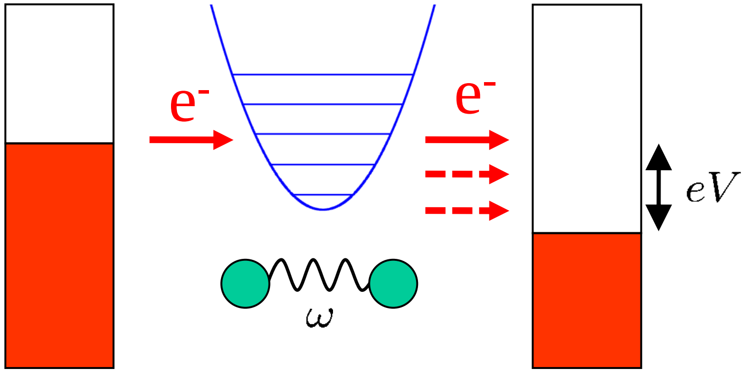

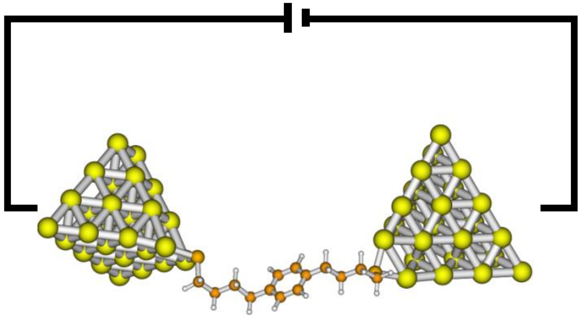

$H = \sum_{k_L} \epsilon_{k_L} c^\dagger_{k_L} c_{k_L} + \sum_j \epsilon_j d^\dagger_j d_j + \sum_{k_R} \epsilon_{k_R} c^\dagger_{k_R} c_{k_R}$	metal – molecule – metal
$+ \sum_k (V_{jk} d^\dagger_j c_k + V_{kj} c^\dagger_k d_j)$	molecule-metal interaction
$+ \sum_l \omega_l a^\dagger_l a_l$	vibrations
$+ \sum_{l,i,j} \lambda^{(l)}_{ij} (a_l + a^\dagger_l) d^\dagger_i d_j$	electronic-vibrational coupling
$+ \sum_{i,j} U_{ij} d^\dagger_i d_i d^\dagger_j d_j$	electron-electron interaction

Charge transport in molecular junctions

Transport methods

- **Approximate methods**

Scattering theory

$$I = \frac{e}{h}\int \mathrm{d}\epsilon_i \int \mathrm{d}\epsilon_f \left\{\mathcal{T}_{R\leftarrow L}(\epsilon_f,\epsilon_i) f_L(\epsilon_i)[1-f_R(\epsilon_f)] - \mathcal{T}_{L\leftarrow R}(\epsilon_f,\epsilon_i) f_R(\epsilon_i)[1-f_L(\epsilon_f)]\right\}$$

Nonequilbrium Green’s functions (NEGF)

$$I = \frac{e}{h}\int \mathrm{d}\epsilon \left(\Sigma_L^{<}(\epsilon)G^{>}(\epsilon) - \Sigma_L^{>}(\epsilon)G^{<}(\epsilon)\right) \qquad G^{<} = G^r\Sigma^{<}G^a$$

Density matrix theory (Redfield)

$$I = \frac{e}{\hbar}\int_0^\infty d\tau\, \mathrm{tr}\{\left[V(\tau),\rho\rho^{\mathrm{eq}}_{\mathrm{leads}}\right]\hat{I}\}$$

$$0 = -i\,[H_0,\rho] - \int_0^\infty d\tau\, \mathrm{tr}_{\mathrm{leads}}\{[V,\left[V(\tau),\rho\,\rho^{\mathrm{eq}}_{\mathrm{leads}}\right]]\}$$

Cizek Thoss, Domcke, PRB **70**, 125406 (2004); Härtle, Benesch, Thoss PRL **102**, 146801 (2009); Volkovich, Härtle, Thoss, Peskin, PCCP **13**, 14333 (2011); Erpenbeck, Härtle, Thoss, PRB **91**, 195418 (2015)

Charge transport in molecular junctions

Transport methods

- **Approximate methods**

  Scattering theory, nonequilbrium Green's functions, density matrix theory (Redfield)

- **Numerically exact methods**

  Time-dependent multiconfiguration methods (ML-MCTDH)

$$I = -e\frac{d}{dt}\left\langle \sum_{k_l} c^\dagger_{k_l} c_{k_l}(t) \right\rangle = -e\sum_{\mathbf{nv}} \rho_{0\mathbf{nv}} \langle \Psi_{\mathbf{nv}} | \, e^{iHt}\, \hat{I}\, e^{-iHt} | \Psi_{\mathbf{nv}} \rangle$$

$$|\Psi(t)\rangle = \sum_{j_1} \cdots \sum_{j_M} A_{j_1 \ldots j_M}(t) \prod_{k=1}^{M} |\phi^k_{j_k}(t)\rangle$$

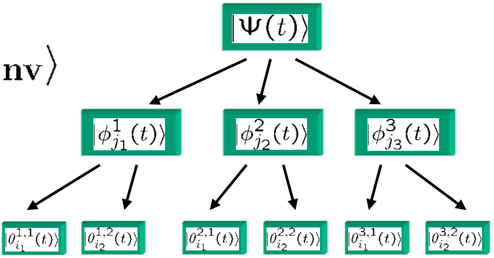

  Density matrix theory (Hierarchical quantum master equation)

$$\frac{\partial}{\partial t}\rho^{(n)}_{\mathbf{j}} = -\left[\mathrm{i}\mathcal{L}_S + \sum_{k=1}^{n} \gamma_{j_k} \right] \rho^{(n)}_{\mathbf{j}} - \mathrm{i}\sum_{k=1}^{n} \mathcal{B}_{j_k} \rho^{(n-1)}_{\mathbf{j}_k^-} - \mathrm{i}\sum_{j} \mathcal{A}^{\bar{\sigma}} \rho^{(n+1)}_{\mathbf{j}j}$$

Wang, Thoss, J. Chem. Phys. **131**, 024114 (2009); **145**, 164105 (2016); Wilner, Wang, Thoss, Rabani, PRB **92**, 195143 (2015); Schinabeck, Erpenbeck, Härtle, Thoss, PRB **94**, 201407(R) (2016)

Vibrational effects in molecular junctions: Basic mechanisms

current-voltage characteristics

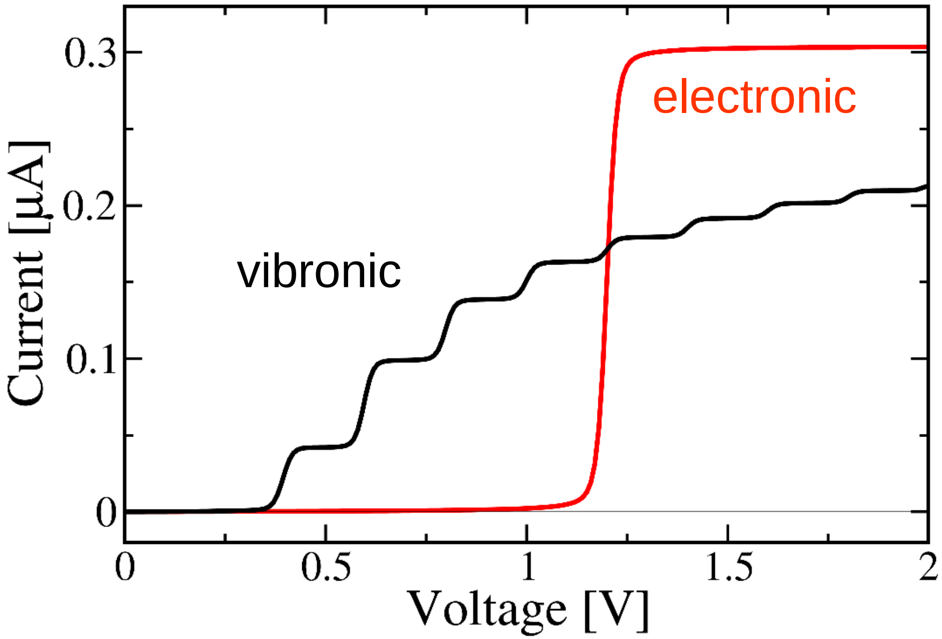

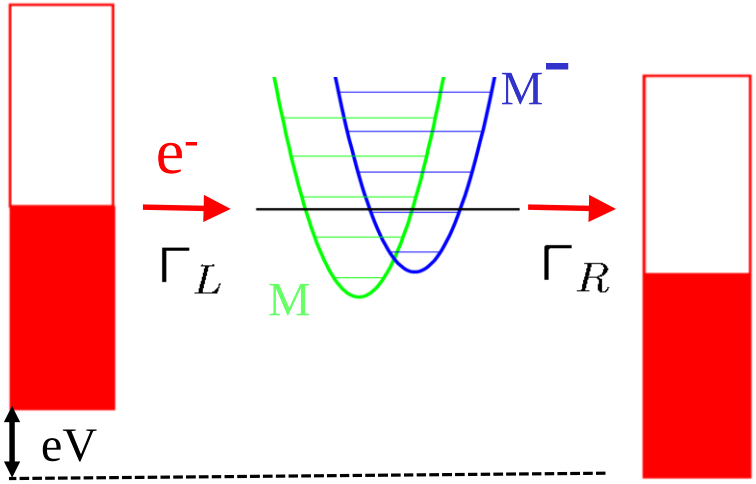

$$H = \epsilon d^\dagger d + \sum_k \epsilon_k c_k^\dagger c_k + \sum_k (V_k d^\dagger c_k + V_k c_k^\dagger d) + \Omega a^\dagger a + \lambda(a + a^\dagger) d^\dagger d$$

$\Omega = 0.1\text{eV}$ $\lambda = 0.2$ eV

$\Gamma_{L/R} = 0.02$ eV T= 50 K

$$\Gamma_L = 2\pi \sum_{k_L} |V_{k_L}|^2 \delta(E - \epsilon_{k_L})$$

Vibrational effects in molecular junctions: Basic mechanisms

Current-induced vibrational excitation

current-voltage characteristics

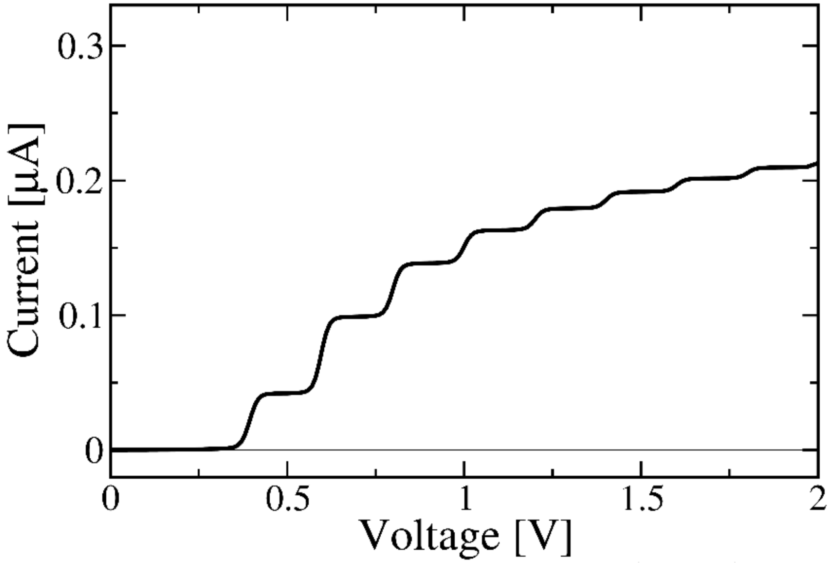

vibrational excitation $\langle a^+ a\rangle$

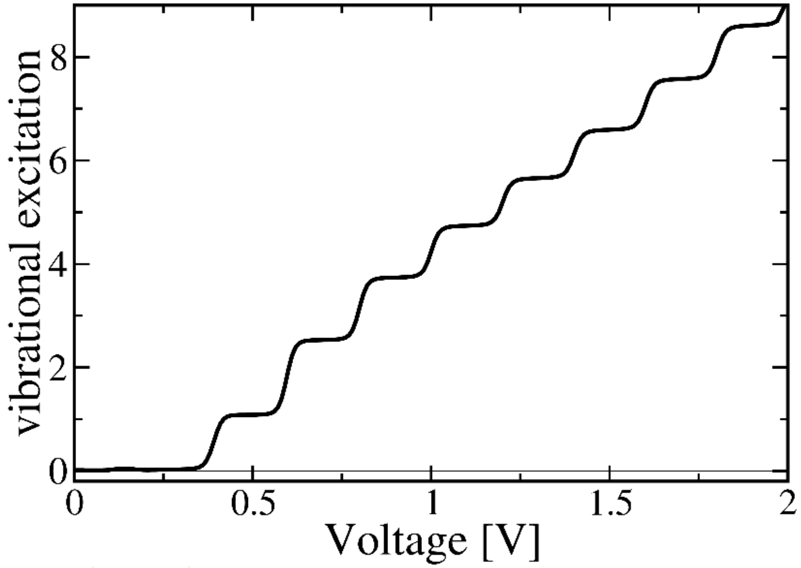

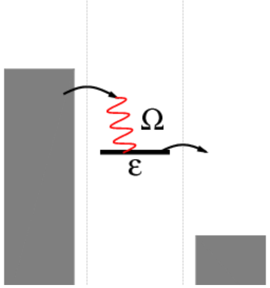

excitation
(heating)

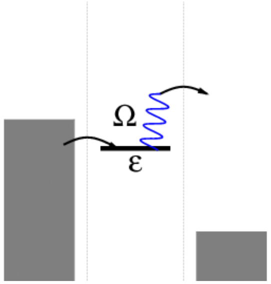

deexcitation
(cooling)

Härtle, Peskin, Thoss, PRB **83**, 115414 (2011); Phys. Stat. Sol. B **250**, 2452 (2013)

Vibrational effects in molecular junctions: Basic mechanisms

Vibrational nonequilibrium effects

current-voltage characteristics

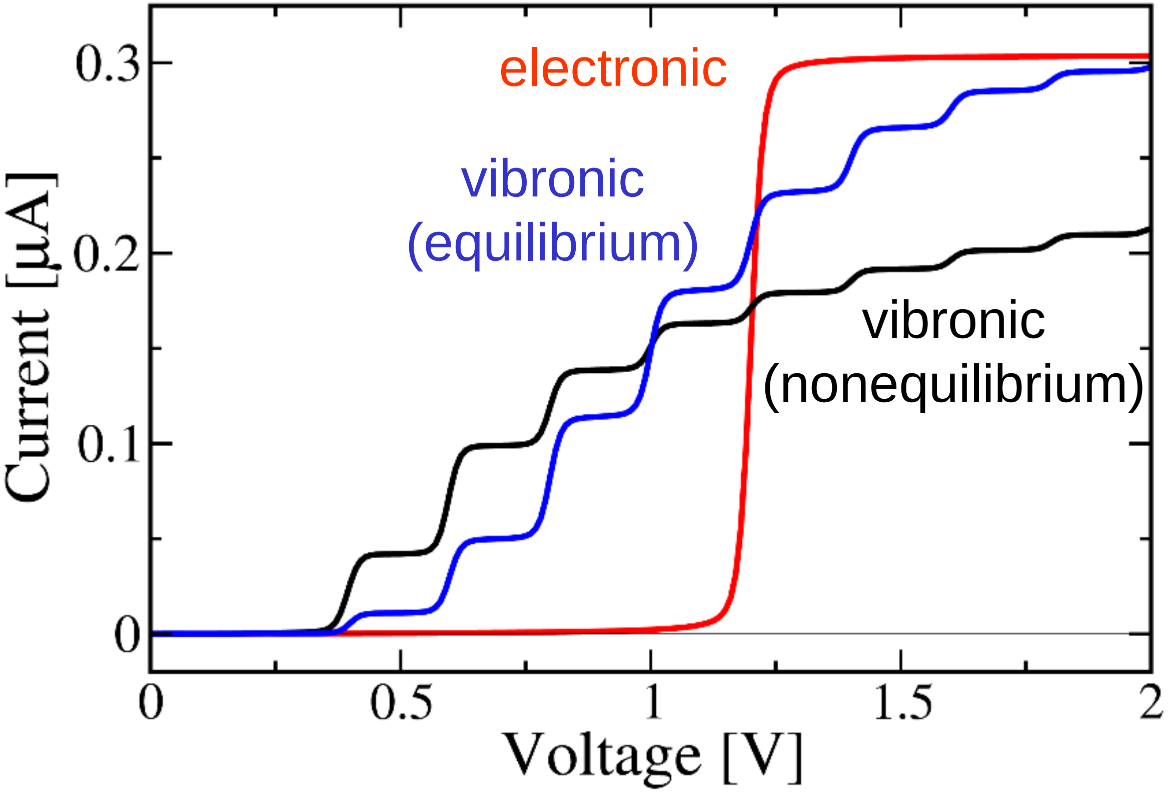

Härtle, Peskin, Thoss, PRB **83**, 115414 (2011); Phys. Stat. Sol. B **250**, 2452 (2013)

Vibrational effects in molecular junctions: Basic mechanisms

current-voltage characteristics

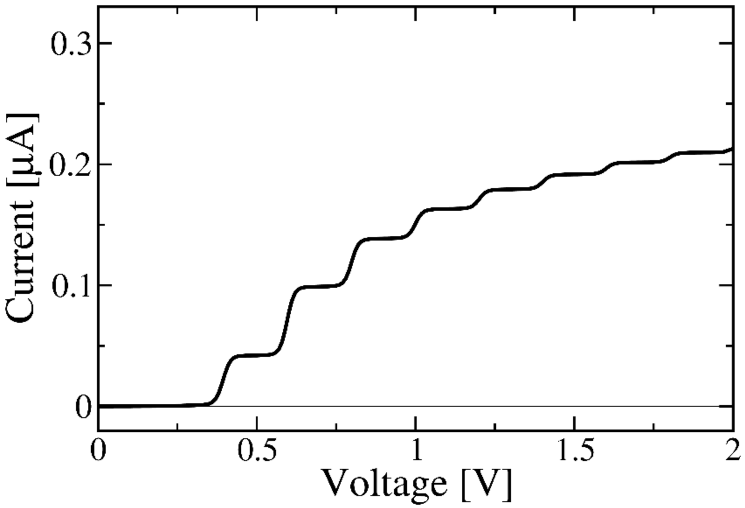

vibrational excitation $\langle a^+ a \rangle$

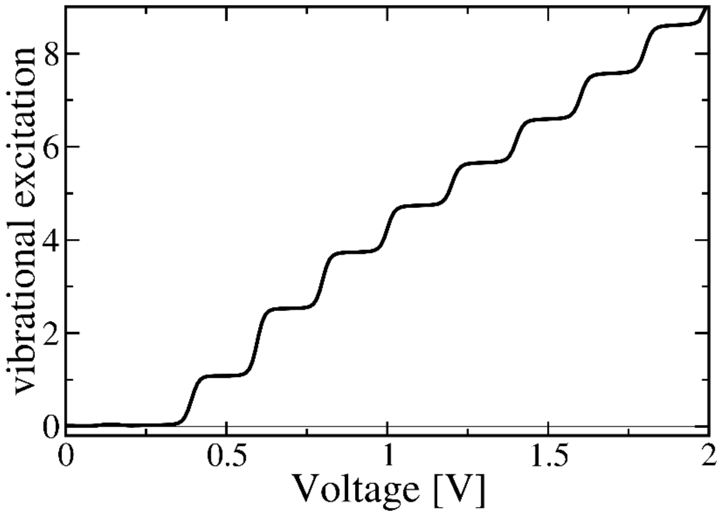

transport-related processes

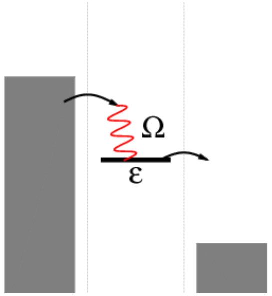

excitation
(heating)

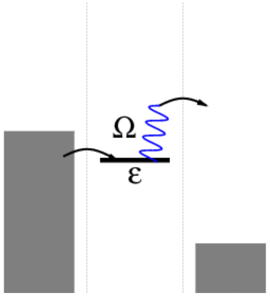

deexcitation
(cooling)

electron-hole pair creation (cooling)

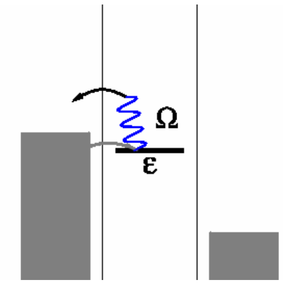

smaller voltage

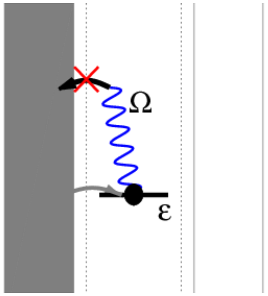

larger voltage

Härtle, Peskin, Thoss, PRB **83**, 115414 (2011); Phys. Stat. Sol. B **250**, 2452 (2013)

Vibrational effects in molecular junctions

Current-induced vibrational excitation

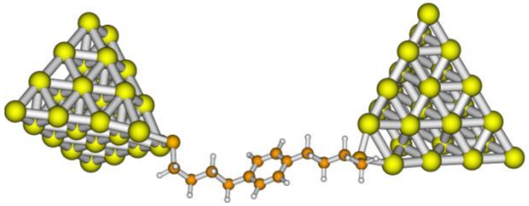

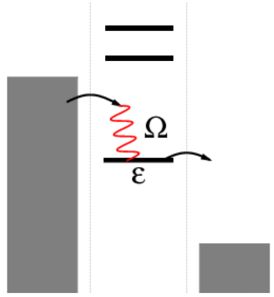

excitation
(heating)

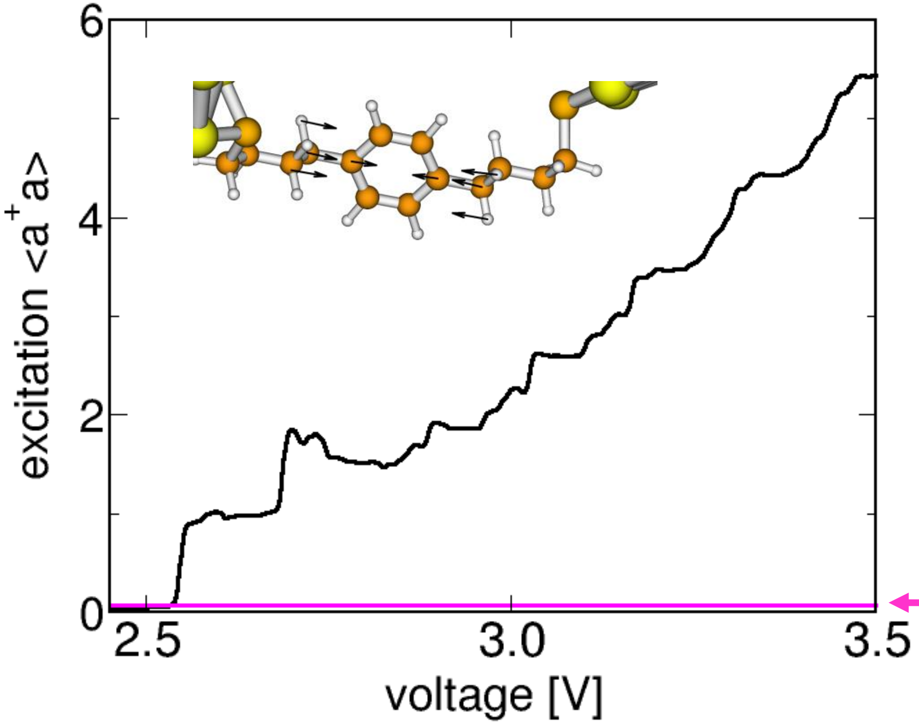

thermal excitation
at T = 300 K

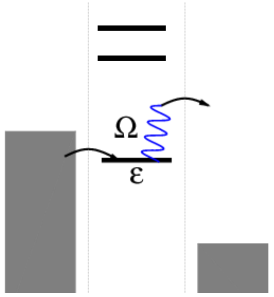

deexcitation
(cooling)

Model: DFT
Transport: NEGF

Härtle, Benesch, Thoss, PRB **77**, 205314 (2008); PRL **102**, 146801 (2009)

Vibrational effects in molecular junctions

Adiabatic vs. nonadiabatic electronic-vibrational coupling

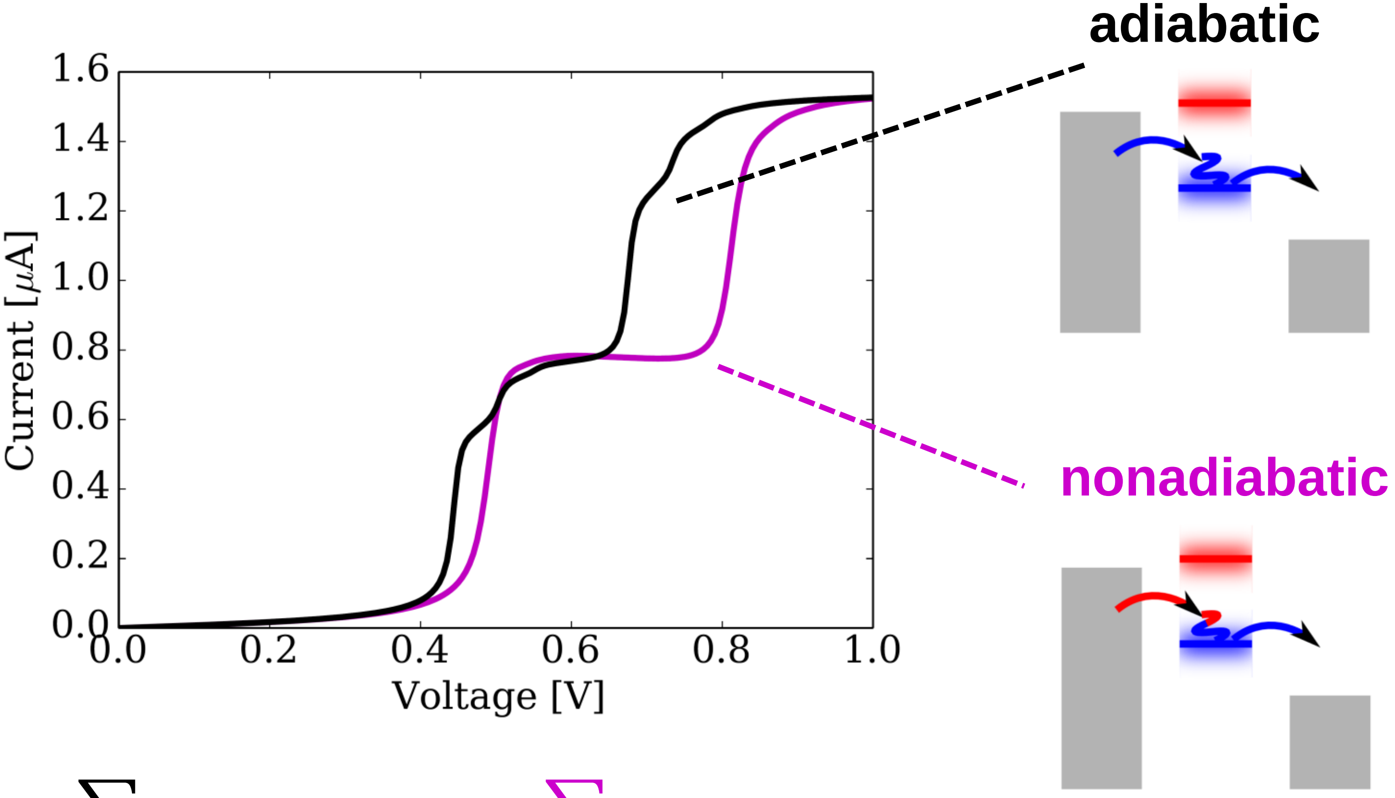

adiabatic

nonadiabatic

$$H = H_0 + \sum_j \lambda_{jj} d_j^+ d_j (a + a^+) + \sum_{i \neq j} \lambda_{ij} d_i^+ d_j (a + a^+)$$

$$\lambda_{12} = 0.03 \text{ eV}$$

$$\lambda_{11} = 0.03 \text{ eV} = \lambda_{22}$$

cf. also:
Repp, Liljeroth, Meyer, Nature Phys. **130**, 975 (2010)
Wegewijs, Schoeller, et al., EPL, **83**, 58001 (2008)

Erpenbeck, Härtle, Thoss, PRB **91**, 195418 (2015)

Vibrational effects in molecular junctions

Adiabatic vs. nonadiabatic electronic-vibrational coupling

adiabatic

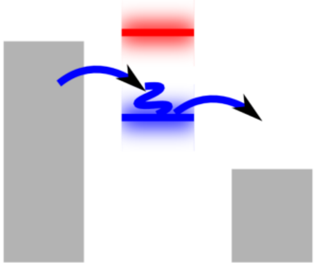

nonadiabatic

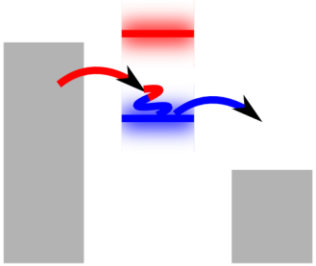

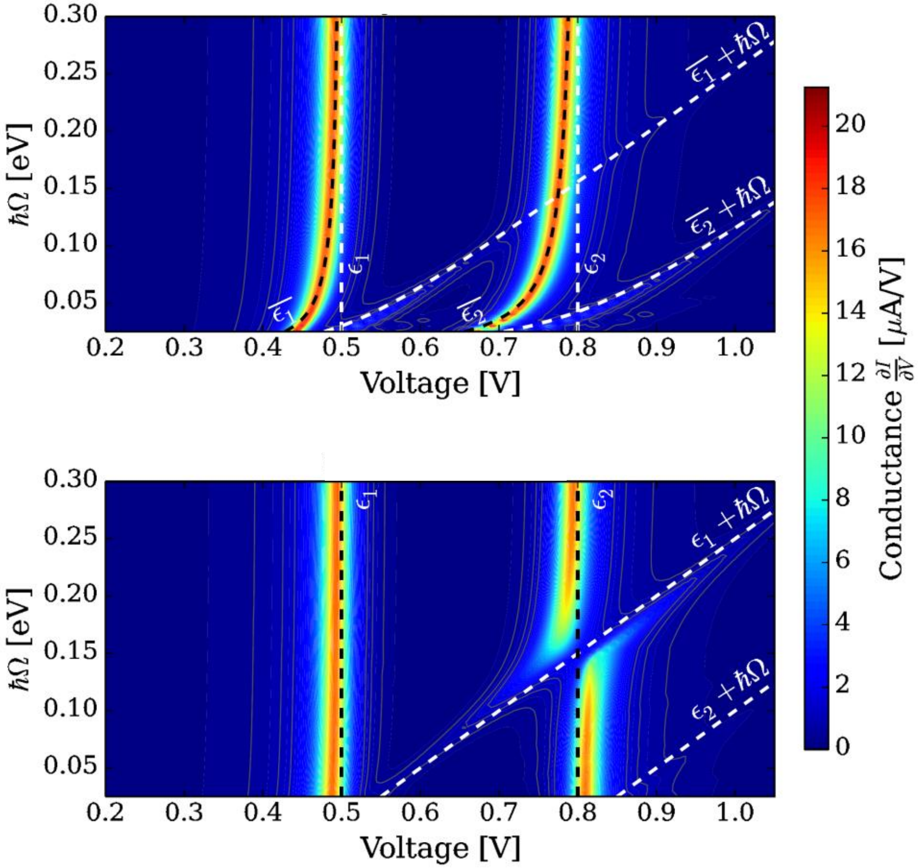

$$H = H_0 + \sum_j \lambda_{jj} d_j^+ d_j (a + a^+) + \sum_{i \neq j} \lambda_{ij} d_i^+ d_j (a + a^+)$$

Poster
Andre Erpenbeck

cf. also:
Repp, Liljeroth, Meyer, Nature Phys. **130**, 975 (2010)
Wegewijs, Schoeller, et al., EPL, **83**, 58001 (2008)

Erpenbeck, Härtle, Thoss, PRB **91**, 195418 (2015)

Vibrational effects in molecular junctions

Transport at low bias voltages:
Inelastic electron tunneling spectroscopy (IETS)

low conductance ($G < G_0/2$)

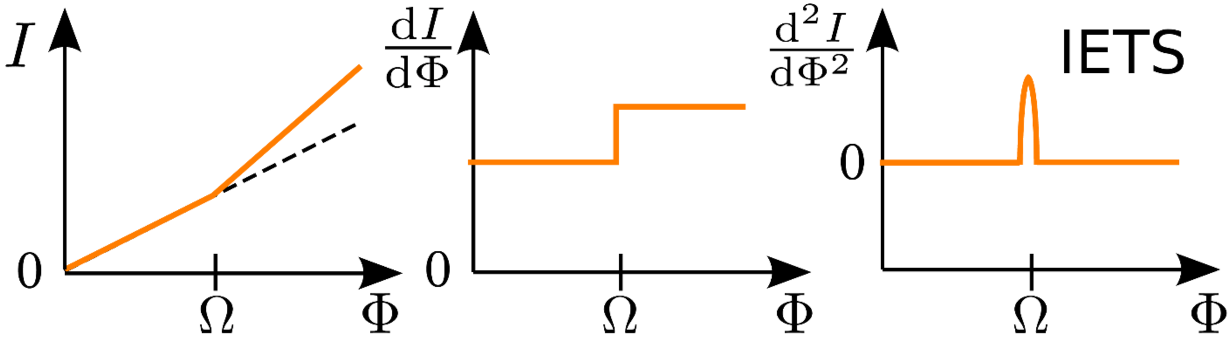

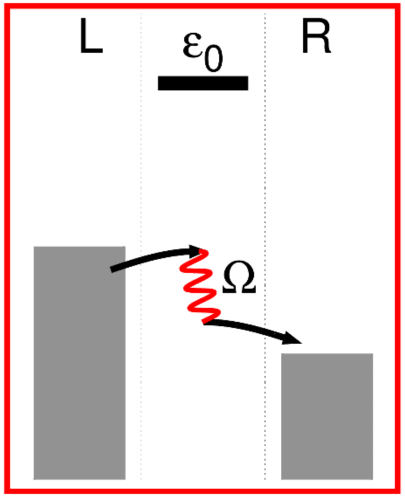

high conductance ($G > G_0/2$)

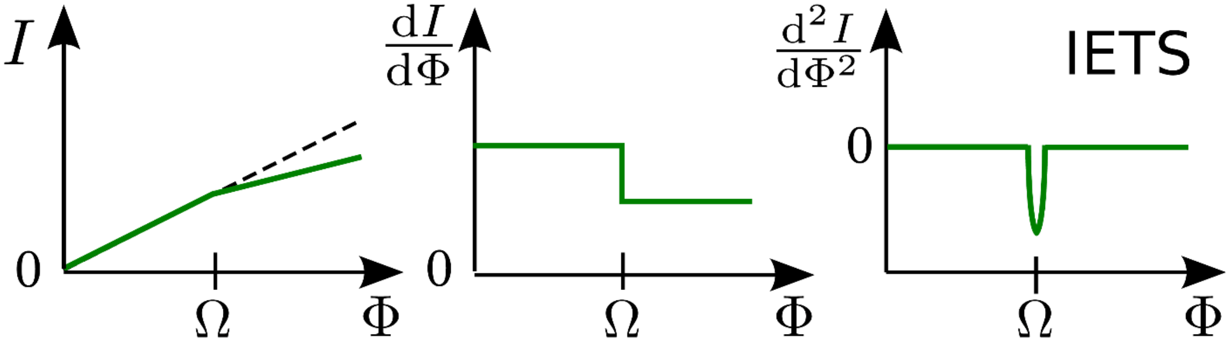

Galperin, Ratner, Nitzan, J. Chem. Phys. **121**, 11965 (2004); Egger, Gogolin, PRB **77**, 113405 (2008); Entin-Wohlman, Imry, Aharony, PRB **80**, 035417 (2009); Avriller, Yeyati, Phys. Rev. B **80**, 041309 (2009); Novotny, Haupt, Belzig, PRB **84**, 113107 (2011); …

Vibrational effects in molecular junctions

IETS for weak molecule-lead coupling in off-resonant regime

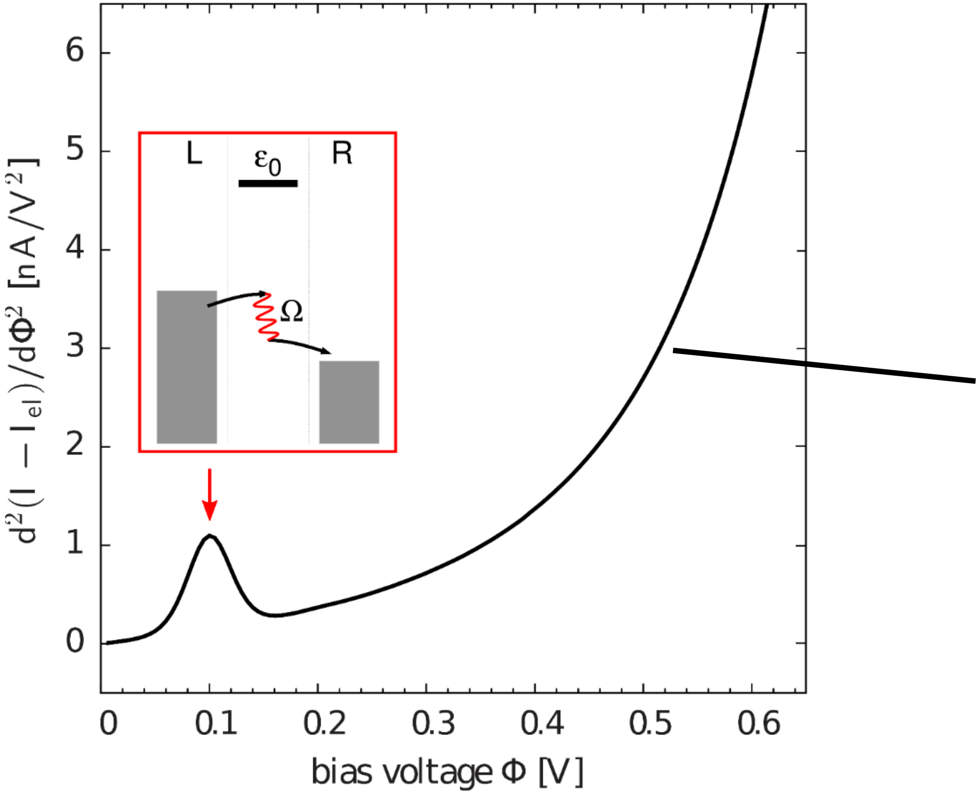

vibrations in **equilibrium**
(NEGF-SCBA)

$\Omega = 0.1\text{eV}$ $\lambda = 0.06$ eV

$\Gamma_{L/R} = 0.007$ eV T= 100 K

$$H = \epsilon_0 d^+ d + \sum_k \epsilon_k c_k^+ c_k + \sum_k V_k (d^+ c_k + c_k^+ d) + \Omega\, a^+ a + \lambda\, d^+ d\, (a + a^+)$$

Schinabeck, Erpenbeck, Härtle, Thoss, PRB **94**, 201407(R) (2016)

Vibrational effects in molecular junctions

IETS for weak molecule-lead coupling

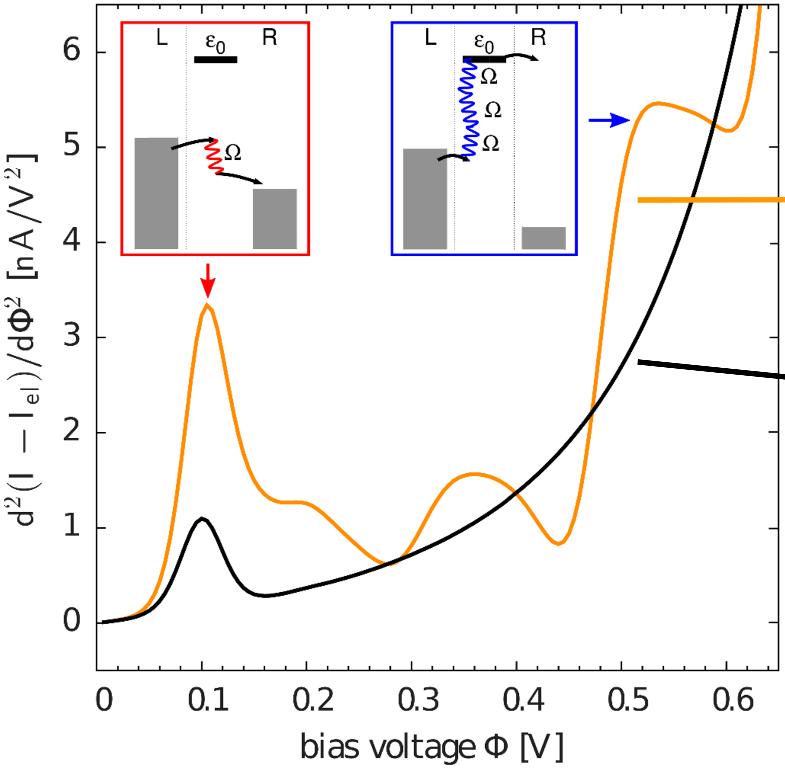

vibrations in **nonequilibrium** (hierarchical quantum master equation)

vibrations in **equilibrium** (NEGF-SCBA)

$\Omega = 0.1\text{eV}$ $\lambda = 0.06$ eV

$\Gamma_{L/R} = 0.007$ eV T= 100 K

$$H = \epsilon_0 d^+ d + \sum_k \epsilon_k c_k^+ c_k + \sum_k V_k (d^+ c_k + c_k^+ d) + \Omega\, a^+ a + \lambda\, d^+ d\, (a + a^+)$$

Schinabeck, Erpenbeck, Härtle, Thoss, PRB **94**, 201407(R) (2016)

Vibrational effects in molecular junctions

IETS: Peak–dip transition

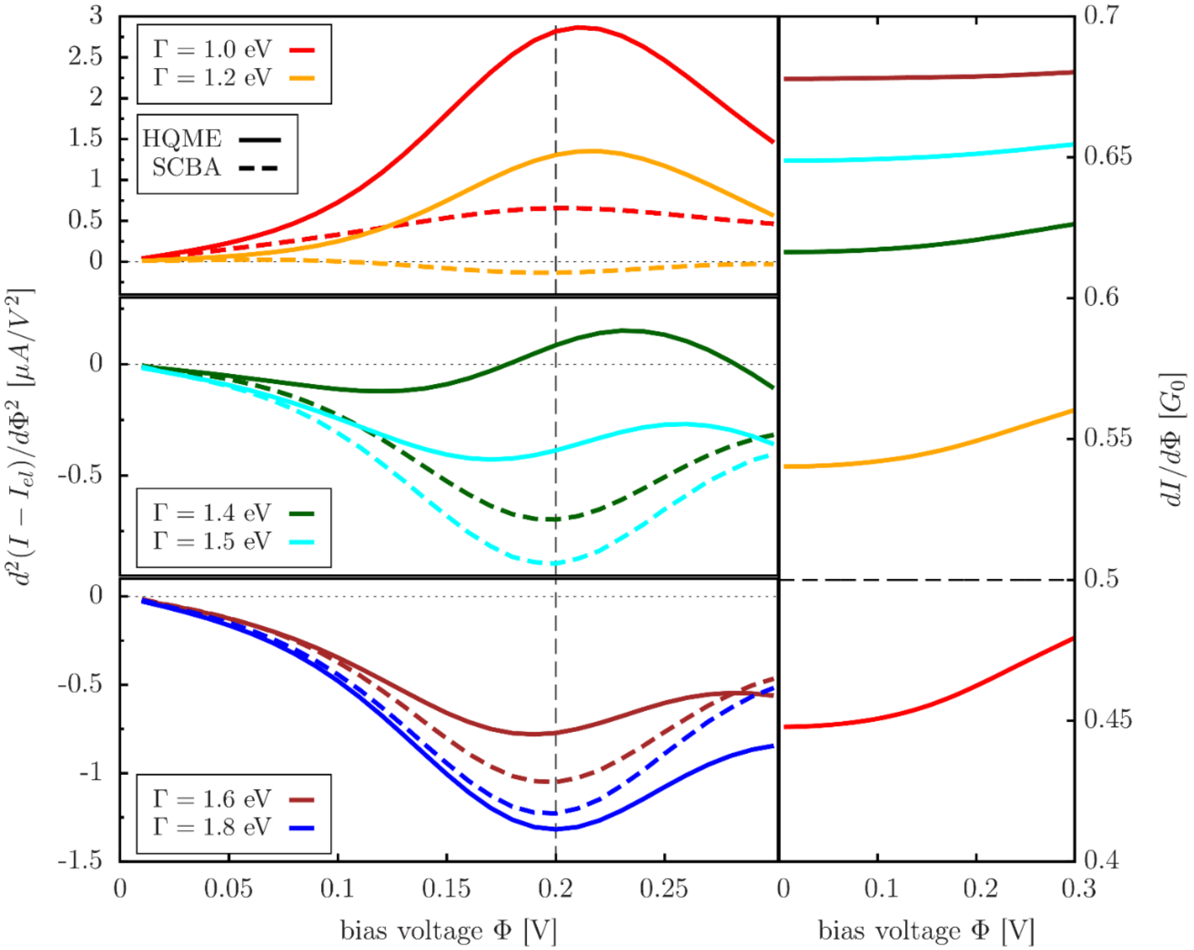

vibrations in **equilibrium**
(NEGF-SCBA):
transition at $G_0/2$

vibrations in **nonequilibrium**
(HQME):
transition at $G \approx 0.63\ G_0$

lowest-order expansion:
transition at $G = 0.625\ G_0$
Novotny et al. PRB **84**, 113107 (2011)
Utsumi et al. PRB **87**, 115407 (2013)

$\Omega = 0.2\text{eV}$ $\lambda = 0.12$ eV T= 300 K

Schinabeck, Erpenbeck, Härtle, Thoss,
PRB **94**, 201407(R) (2016)

Vibrational effects in molecular junctions

Current noise: Sign change of vibrational contribution

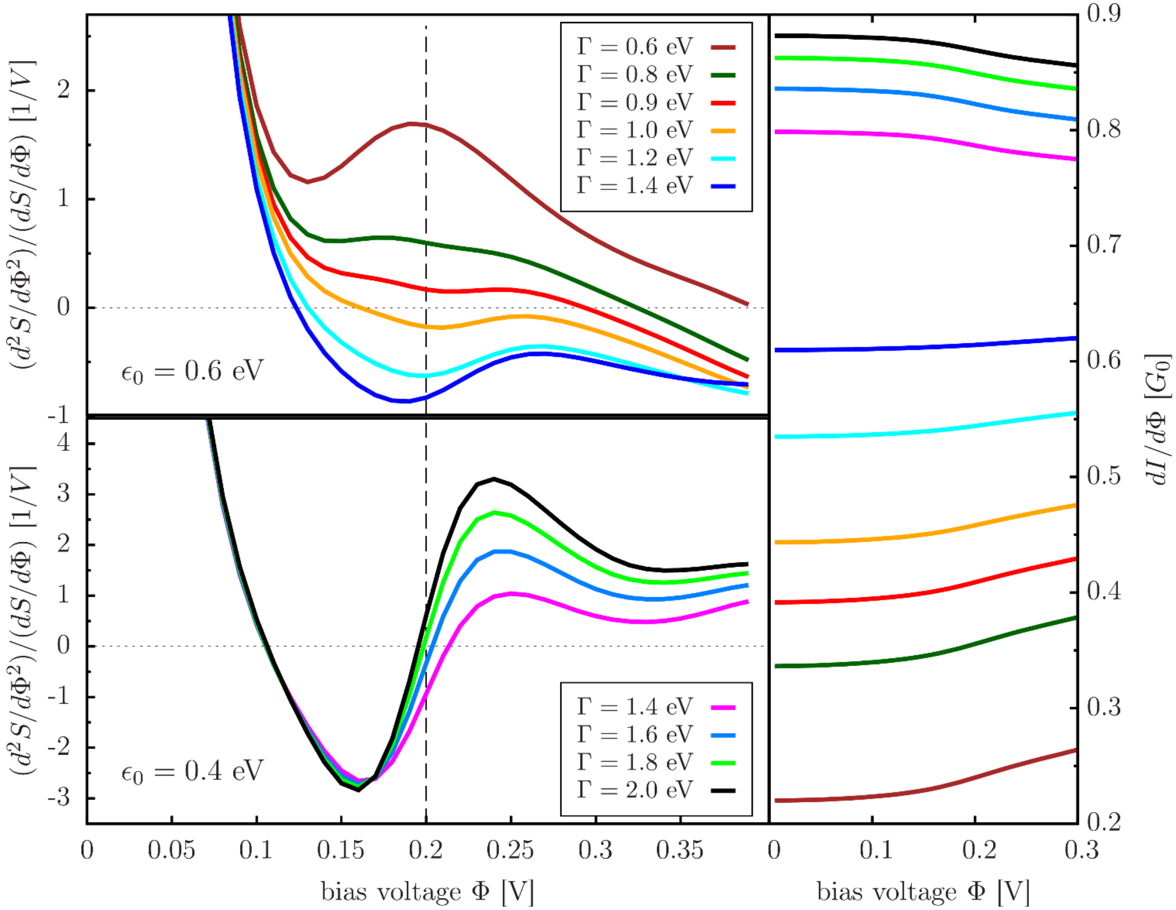

vibrations in **equilibrium** (NEGF-SCBA):

$0.15\ G_0, 0.85\ G_0$

Avriller et al. PRB **80**, 041309 (2009)

vibrations in **nonequilibrium:**

HQME: $\approx 0.43\ G_0, 0.85\ G_0$

perturbative expansion:

$0.43\ G_0, 0.82\ G_0$

Novotny et al. PRB **84**, 113107 (2011)
Utsumi et al. PRB **87**, 115407 (2013)

$\Omega = 0.2$eV $\quad \lambda = 0.12$ eV $\quad$ T= 300 K

Quantum interference in molecular junctions

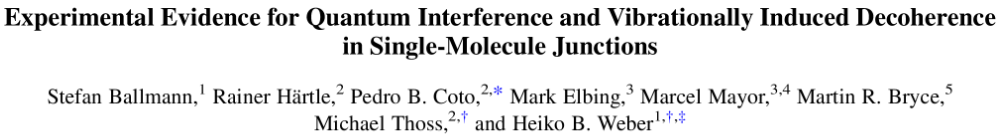

Experimental Evidence for Quantum Interference and Vibrationally Induced Decoherence in Single-Molecule Junctions

Stefan Ballmann,[1] Rainer Härtle,[2] Pedro B. Coto,[2,*] Mark Elbing,[3] Marcel Mayor,[3,4] Martin R. Bryce,[5]
Michael Thoss,[2,†] and Heiko B. Weber[1,†,‡]

Probing the conductance superposition law in single-molecule circuits with parallel paths

H. Vazquez[1‡], R. Skouta[2‡], S. Schneebeli[2], M. Kamenetska[1†], R. Breslow[2*], L. Venkataraman[1*]
and M.S. Hybertsen[3*]

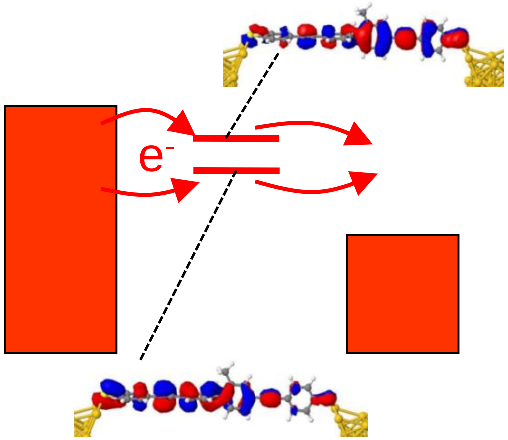

Phys. Rev. Lett. **109**, 056801 (2012)

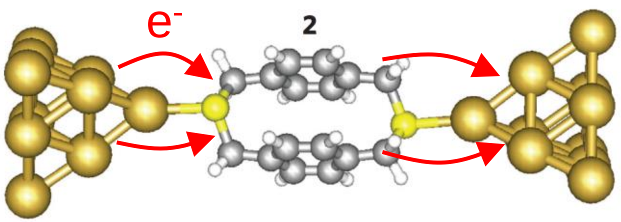

Nature Nanotech. **7**, 663 (2013)

…; Solomon, Ratner et al., JACS **130**, 7788 (2008); Donarini, Grifoni et al., PRB **77**, 201406 (2008); Bergfield, Ratner et al., Nano Lett. **11**, 2759 (2011); van der Molen et al., Nature Nano. **7**, 305 (2012); Venkataraman, Hybertsen et al., Nature Nano. **7**, 663 (2012); Grozema, van der Zant et al., Angew. Chem. **52**, 3152 (2013); Markussen, Thygesen, PRB **89**, 085420 (2014); …

Quantum interference and vibrationally induced decoherence

current-voltage characteristics

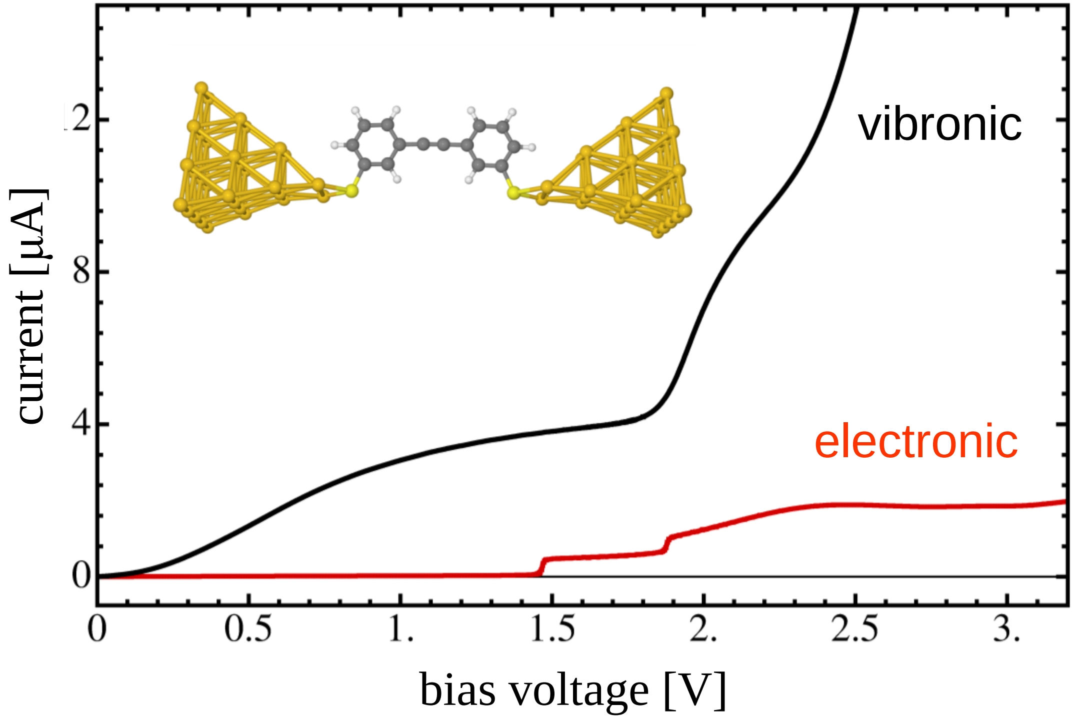

Strongly enhanced current due to coupling to vibrational modes

Härtle, Butzin, Rubio-Pons, Thoss,
Phys. Rev. Lett. **107**, 046802 (2011)

Method: DFT-based model,
NEGF transport calculations

Quantum interference and vibrationally induced decoherence

Quantum interference in junctions with quasi-degenerate electronic states

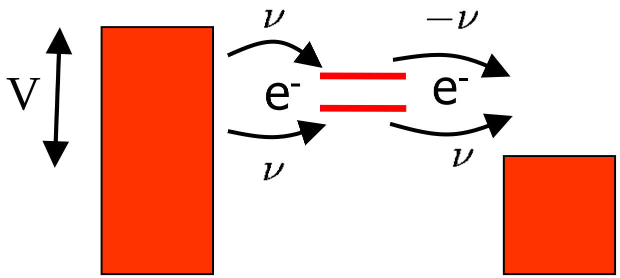

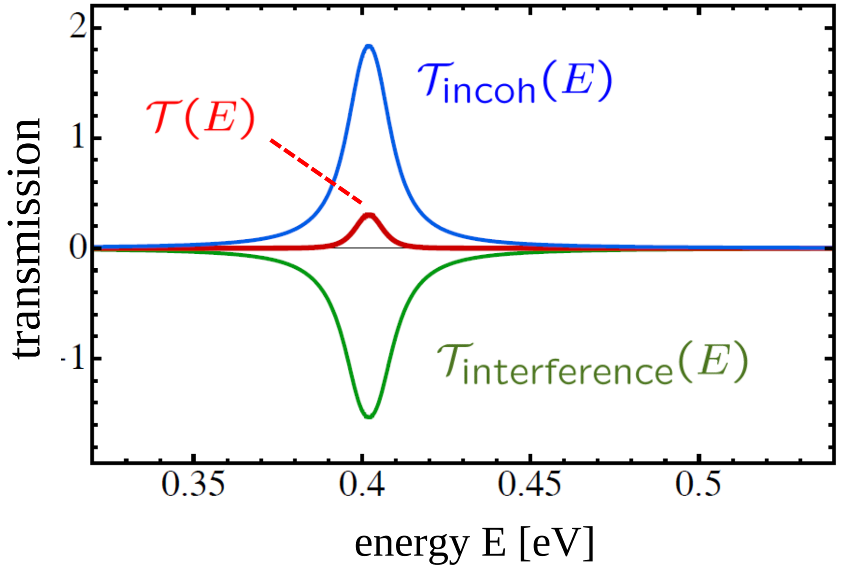

Transmission:

$$\begin{aligned}\mathcal{T}(E) &= \left|\frac{\Gamma}{E-\epsilon_1+i\Gamma} - \frac{\Gamma}{E-\epsilon_2+i\Gamma}\right|^2 \\ &= \mathcal{T}_{\mathsf{incoh}}(E)+\mathcal{T}_{\mathsf{interference}}(E)\end{aligned}$$

$$|\epsilon_1-\epsilon_2| \ll \Gamma \qquad \Gamma = 2\nu^2/\nu_L$$

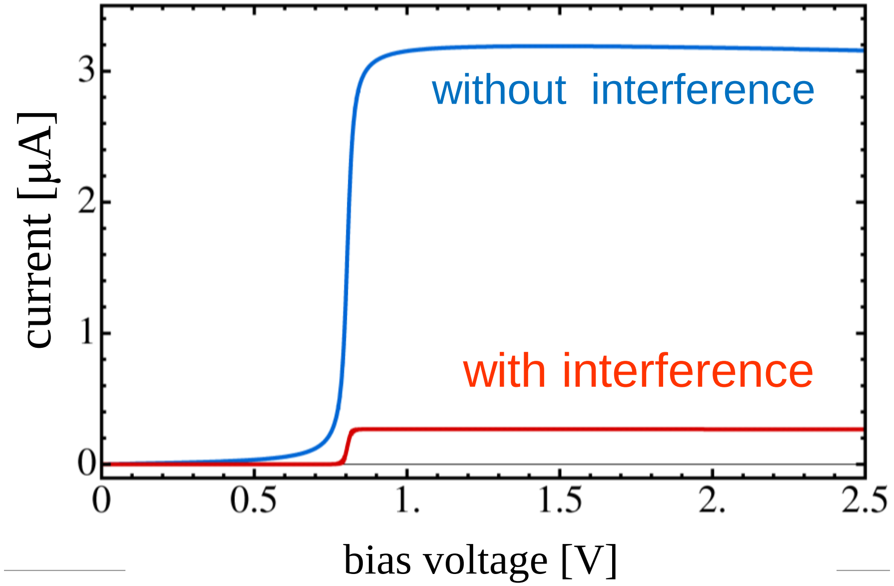

Quantum interference and vibrationally induced decoherence

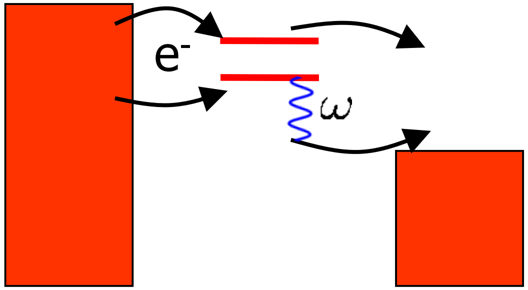

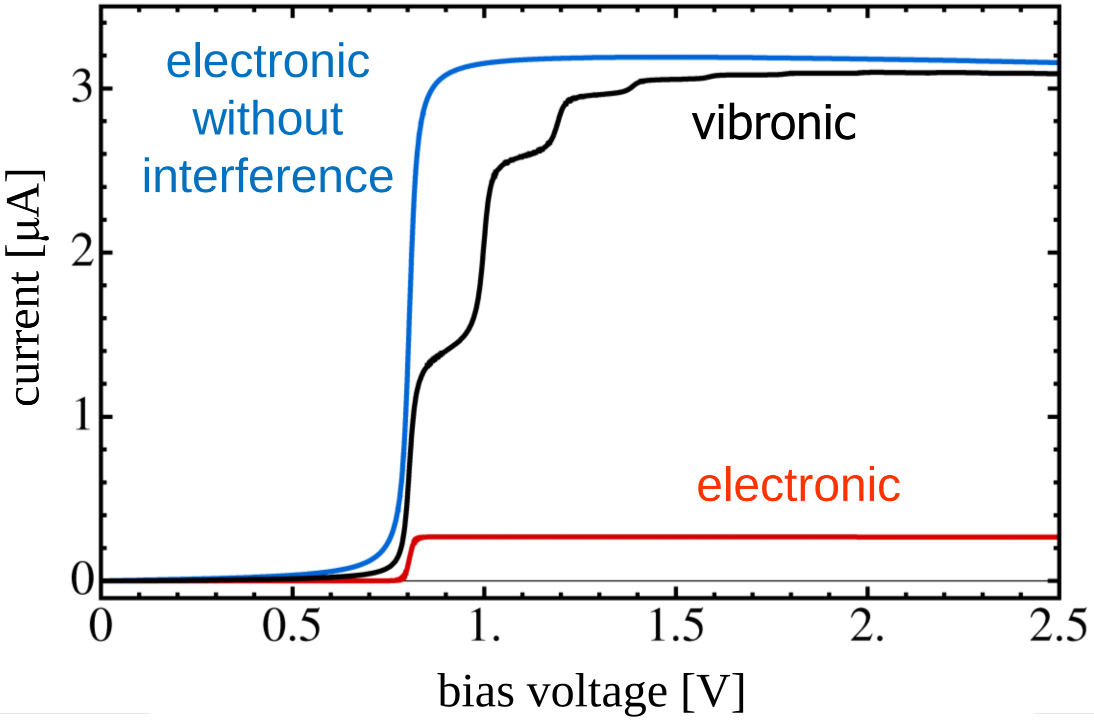

$$H = \epsilon_1 d_1^\dagger d_1 + \epsilon_2 d_2^\dagger d_2 + \sum_k \epsilon_k c_k^\dagger c_k + \sum_{kj} (V_k d_j^\dagger c_k + V_k c_k^\dagger d_j) + \Omega a^\dagger a + \lambda d_1^\dagger d_1 (a + a^\dagger)$$

Transport method: NEGF $\Gamma_{L/R} = 0.02\text{eV}$ $\lambda = 0.06\text{eV}$ $\Omega = 0.1\text{eV}$

Decoherence due to electronic-vibrational coupling results in quenching of electronic interference effects

Quantum interference and vibrationally induced decoherence

Quenching of destructive interference: Equilibrium vs. nonequilibrium

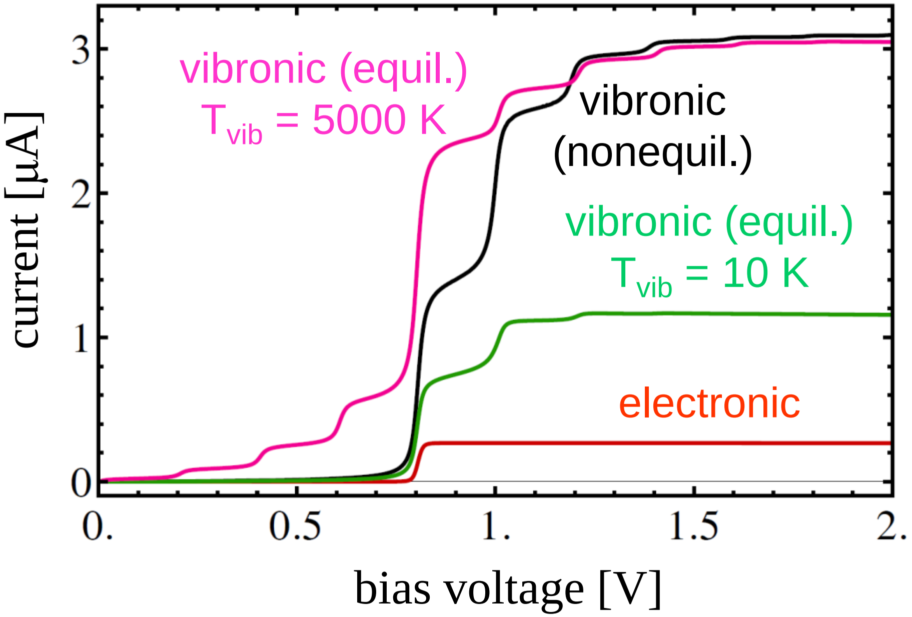

current induced vibrational excitation

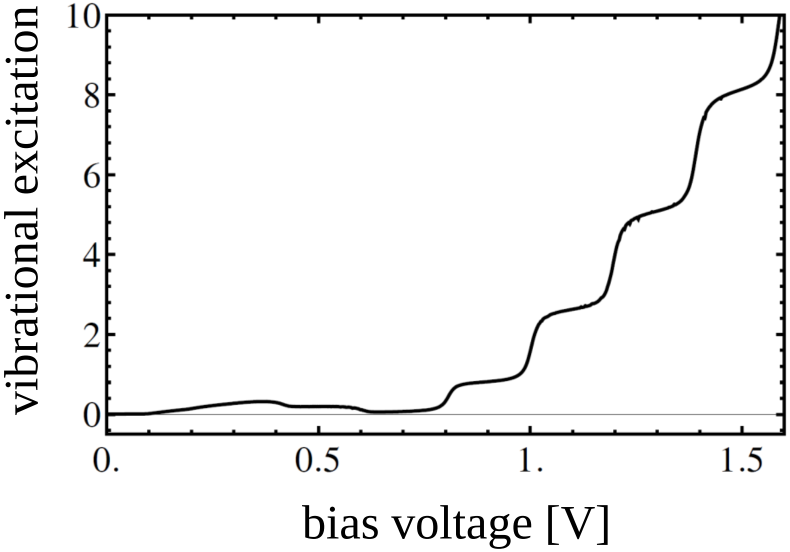

Quantum interference and vibrationally induced decoherence

Analysis of interference/decoherence in terms of transmission function

without electronic-vibrational coupling (λ=0)

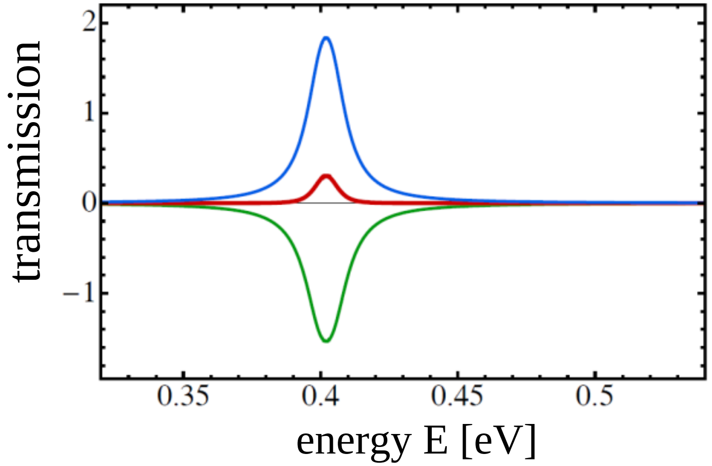

$$I = \frac{2e}{h}\int \mathrm{d}E\,\mathcal{T}(E) \qquad \mathcal{T}(E) = i\mathrm{tr}\{\Gamma_L G^<\}$$

$$\mathcal{T}(E) = \mathcal{T}_{\text{incoh}}(E) + \mathcal{T}_{\text{interference}}(E)$$

Ratio for main peak ($E = (\epsilon_1 + \epsilon_2)/2$):

$$\left|\frac{\mathcal{T}_{\text{interference}}}{\mathcal{T}_{\text{incoh}}}\right| \approx 2\left(1 + e^{\frac{\lambda^2}{\Omega^2}(2N_{\text{vib}}+1)}\right)^{-1}$$

$$N_{\text{vib}} = \left(e^{\Omega/(k_B T_{\text{vib}})} - 1\right)^{-1}$$

with electronic-vibrational coupling (λ=0.06 eV)

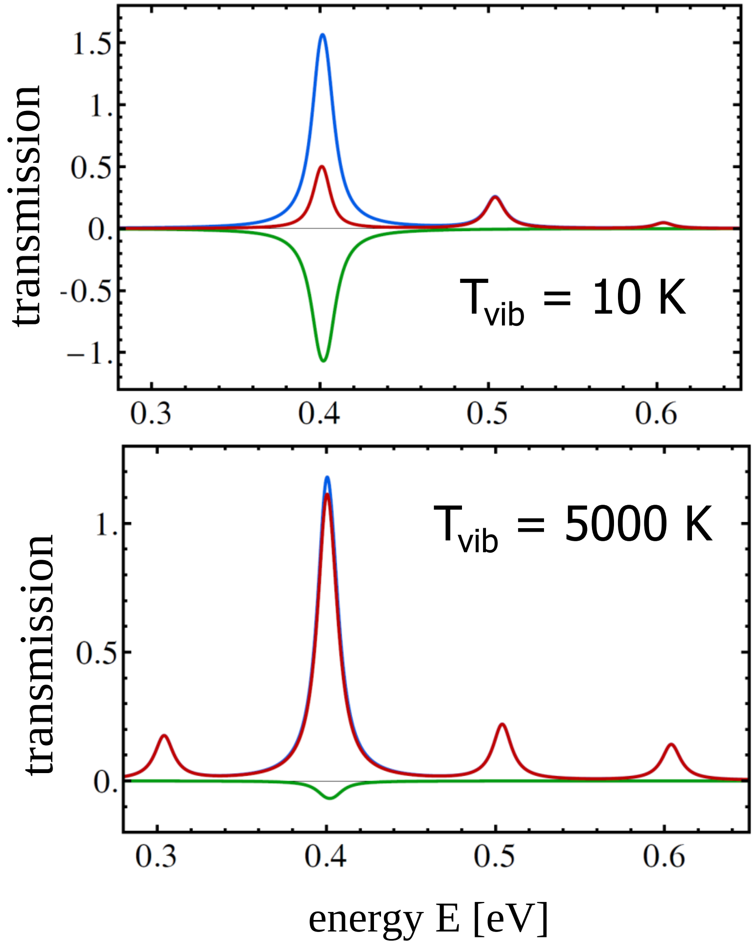

Härtle, Butzin, Thoss, Phys. Rev. B **87**, 085422 (2013)

Quantum interference and vibrationally induced decoherence

Adiabatic vs. nonadiabatic electronic-vibrational coupling

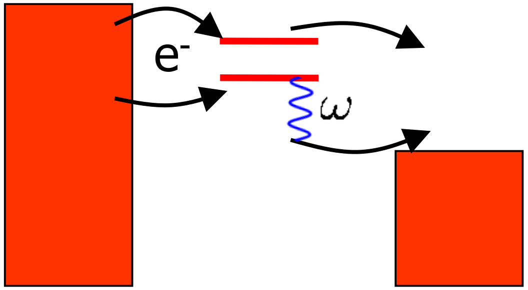

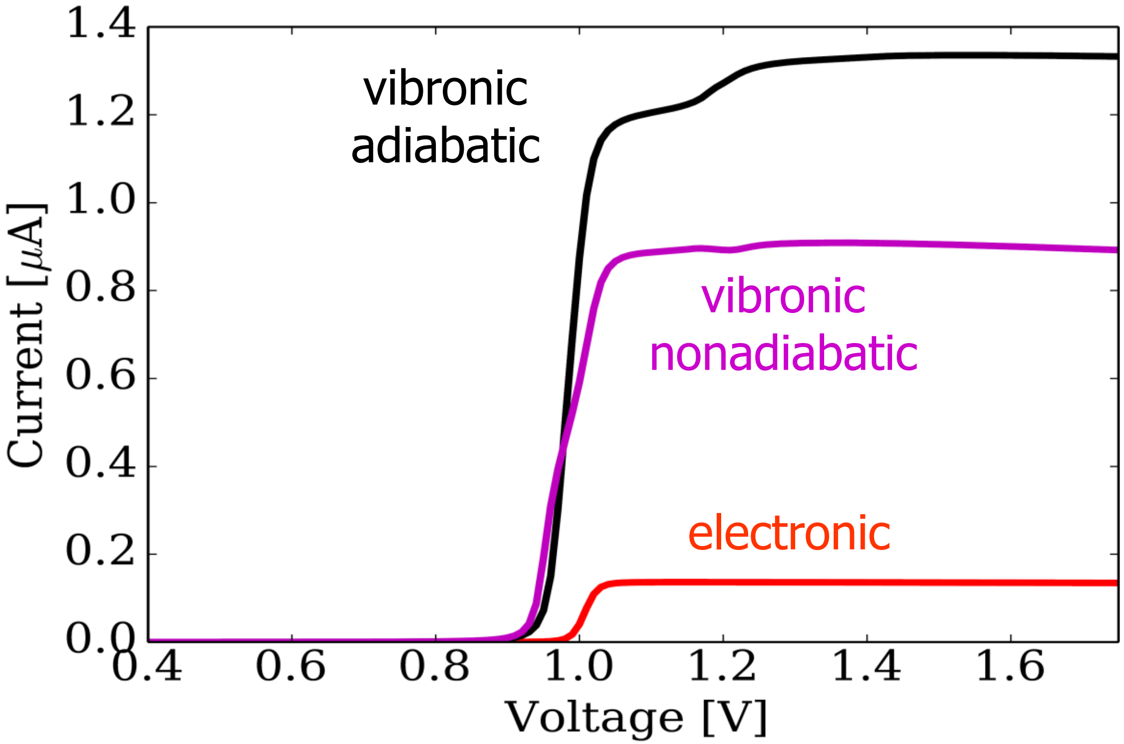

$$H = H_0 + \sum_j \lambda_{jj} d_j^+ d_j (a + a^+) + \sum_{i \neq j} \lambda_{ij} d_i^+ d_j (a + a^+)$$

Poster: Andre Erpenbeck

Erpenbeck, Härtle, Thoss, PRB **91**, 195418 (2015)

Quantum interference and vibrationally induced decoherence

Temperature dependence of current

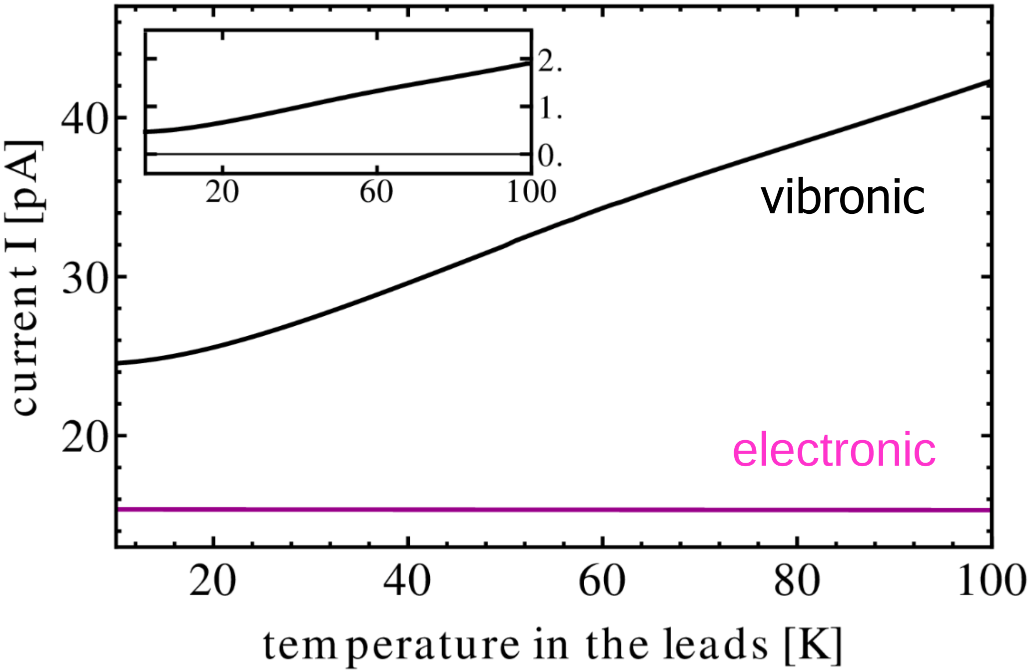

$$H = \epsilon_1 d_1^\dagger d_1 + \epsilon_2 d_2^\dagger d_2 + \sum_k \epsilon_k c_k^\dagger c_k + \sum_{kj} (V_k d_j^\dagger c_k + V_k c_k^\dagger d_j)$$

$$+\Omega a^\dagger a + (\lambda_1 d_1^\dagger d_1 + \lambda_2 d_2^\dagger d_2)(a + a^\dagger) \qquad \lambda_1 \approx \lambda_2 \neq \lambda_1$$

inelastic transport

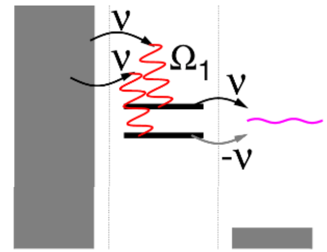

electron-hole pair creation

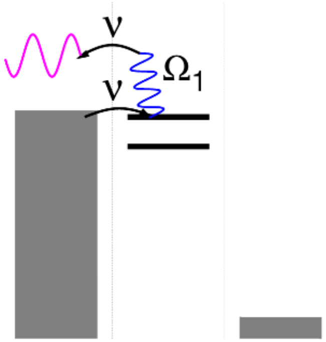

In junctions with quasi-degenerate states and similar vibronic coupling, cooling due to electron-hole pair creation processes dominates heating, resulting in thermalization.

Härtle, Butzin, Thoss, Phys. Rev. B **87**, 085422 (2013)

Quantum interference and vibrationally induced decoherence

Symmetric coupling interference scenario

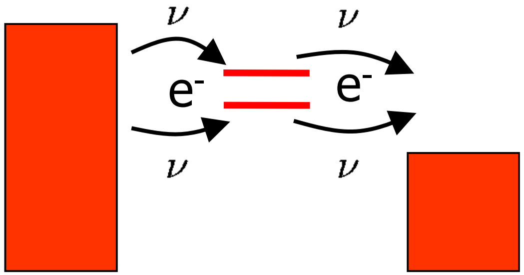

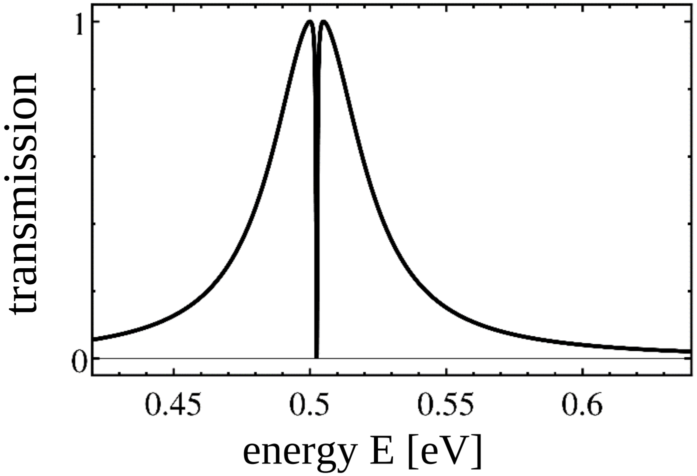

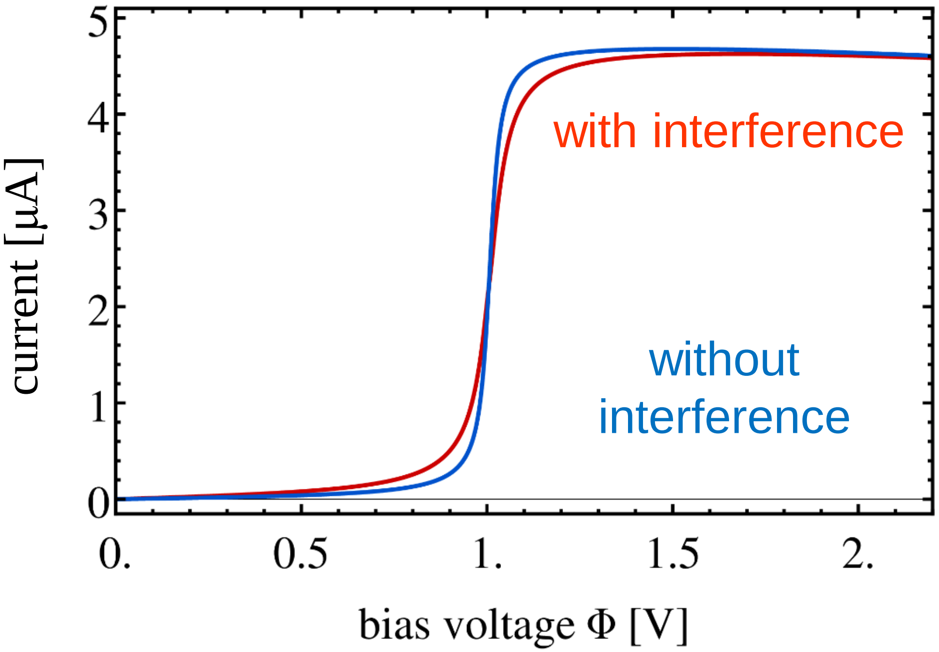

Quantum interference and vibrationally induced decoherence

Symmetric coupling interference scenario

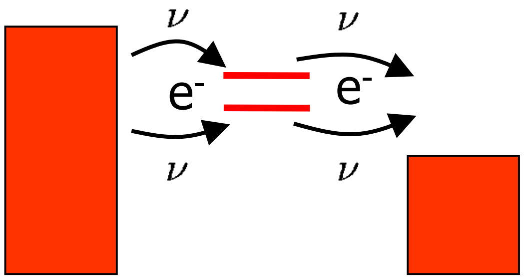

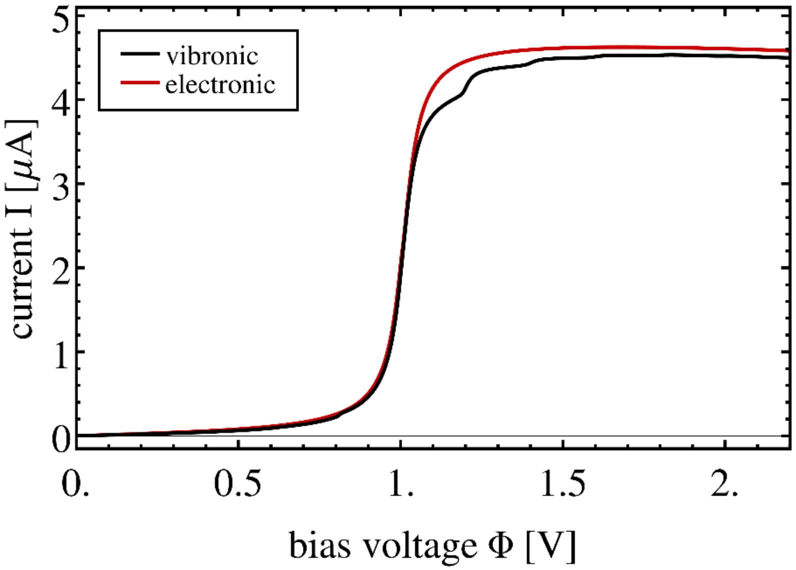

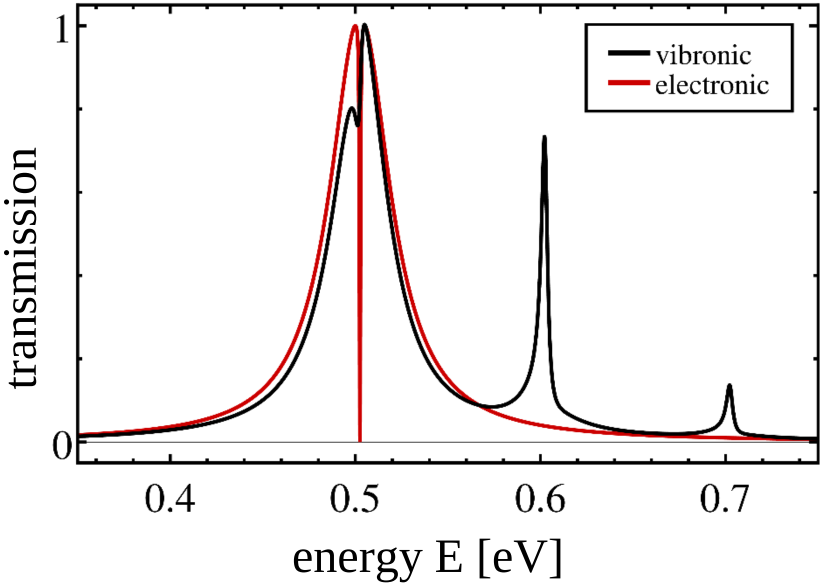

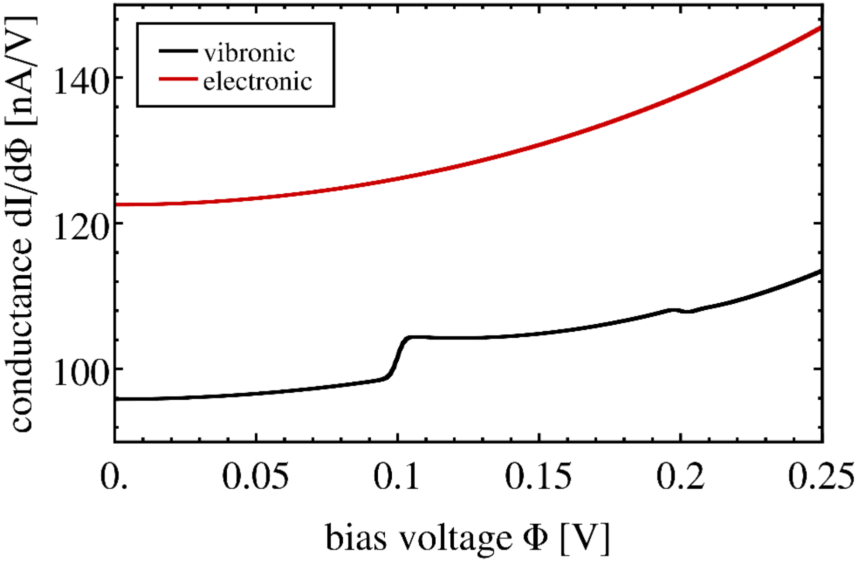

Härtle, Butzin, Thoss, Phys. Rev. B **87**, 085422 (2013)

Quantum interference and vibrationally induced decoherence

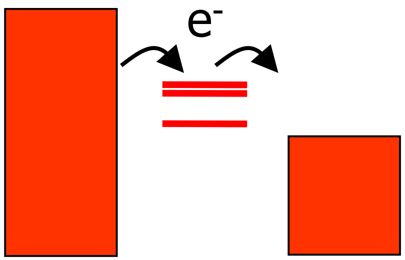

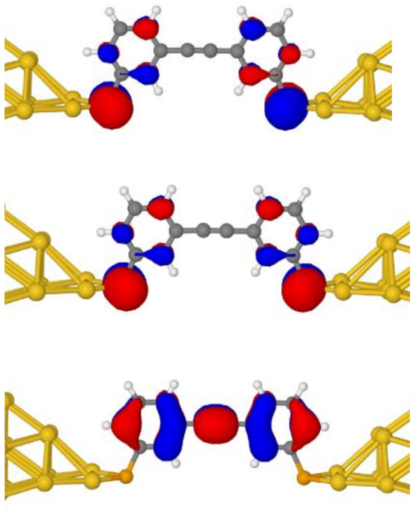

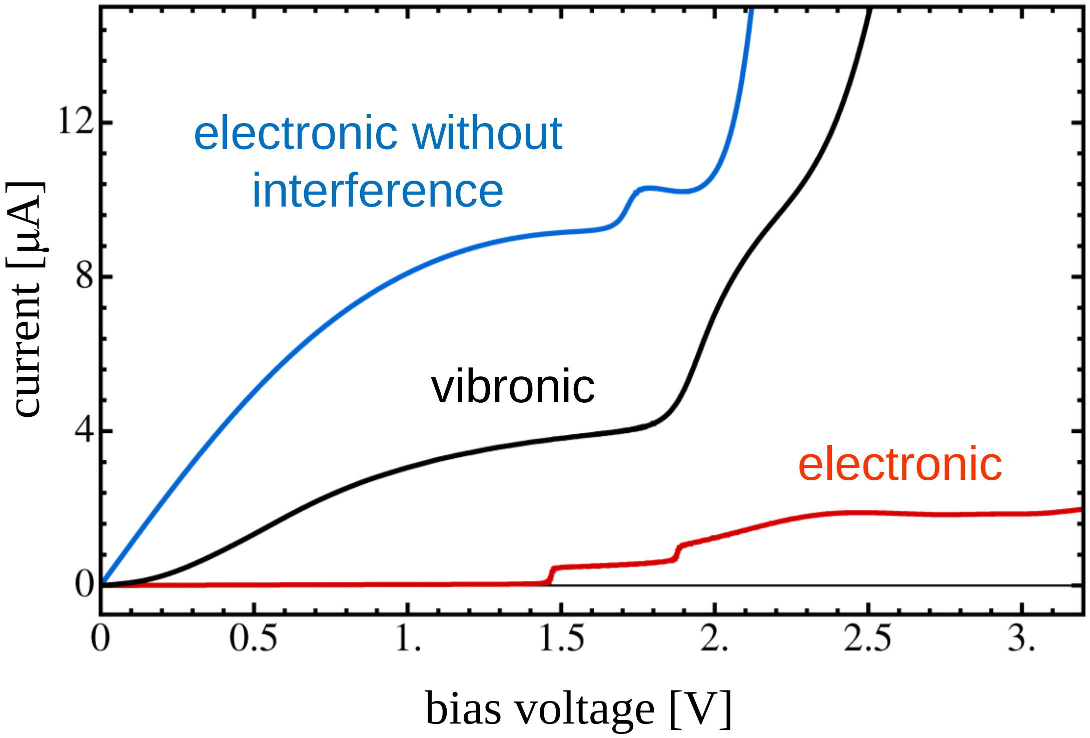

Decoherence due to electronic-vibrational coupling results in partial quenching of electronic interference effects

cf. experiment: S.J. van der Molen et al. Nature Nano. **7**, 305 (2012)

Härtle, Butzin, Rubio-Pons, Thoss, Phys. Rev. Lett. **107**, 046802 (2011)

Quantum interference and vibrationally induced decoherence

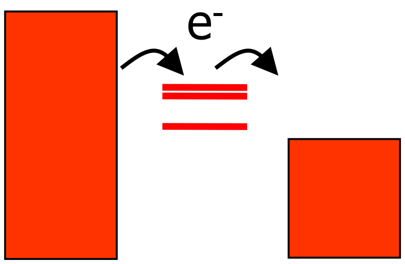

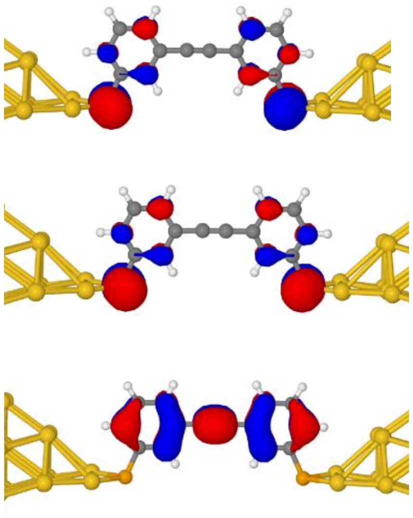

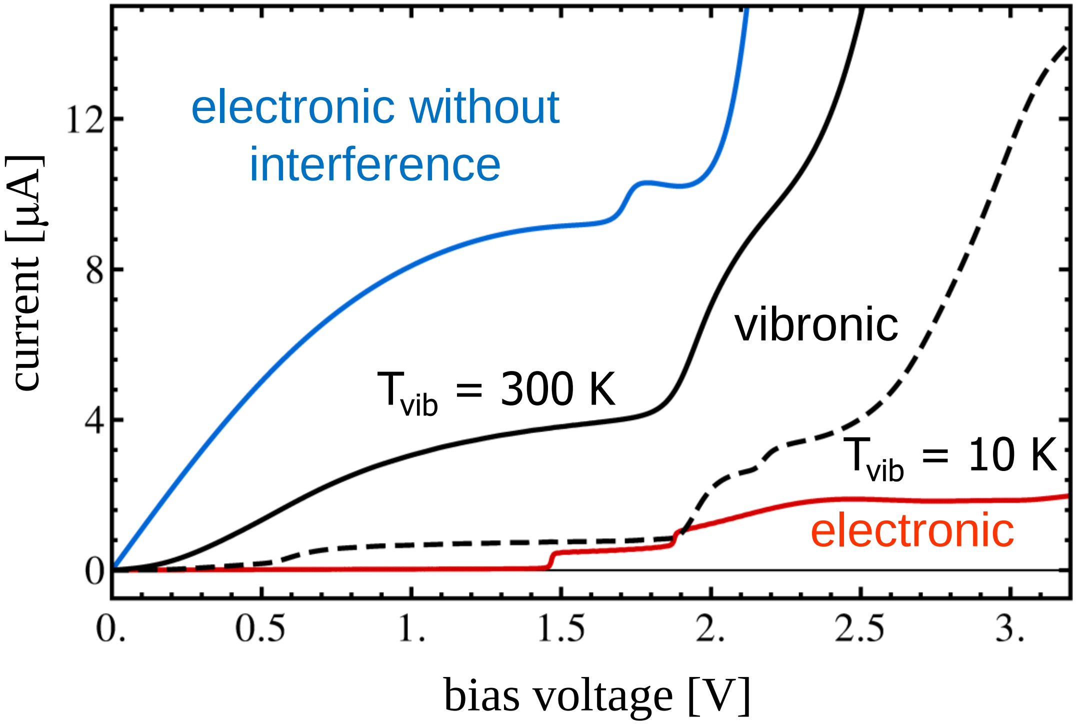

Decoherence due to electronic-vibrational coupling results in partial quenching of electronic interference effects

Quantum interference and vibrationally induced decoherence

Experimental signature: Temperature dependence of electrical current

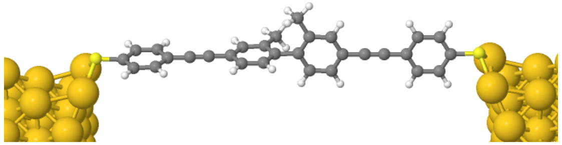

I – T characteristics (experiment)

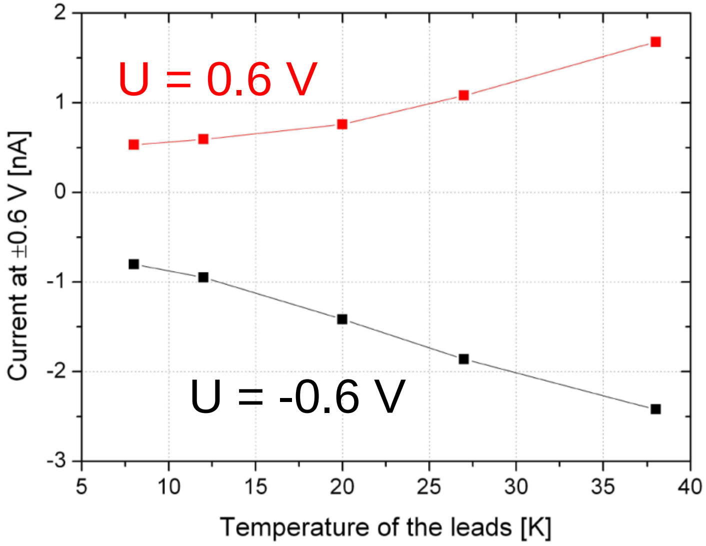

destructive interference due to quasi-degenerate orbitals

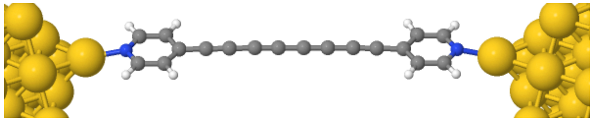

I – T characteristics (experiment)

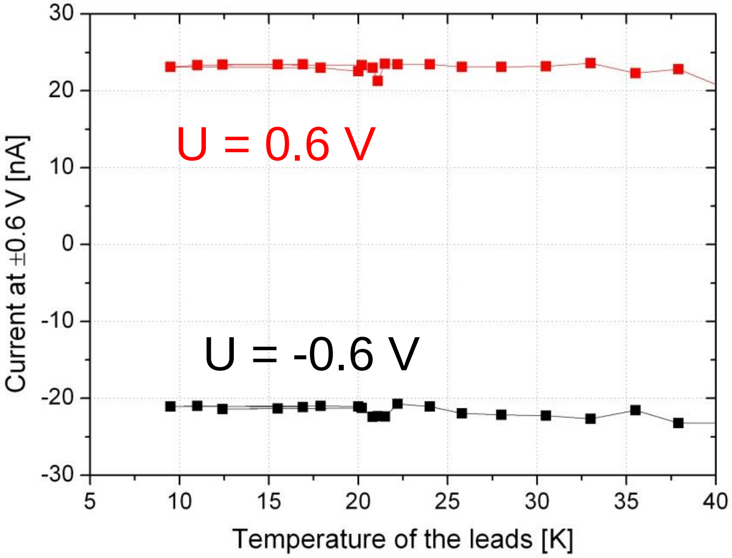

no interference effects

Ballmann, Härtle, MT, Weber, et al.
PRL **109**, 056801 (2012)

Quantum interference and vibrationally induced decoherence

Experimental signature: Temperature dependence of electrical current

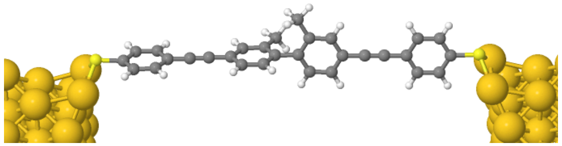

I – T characteristics (experiment)

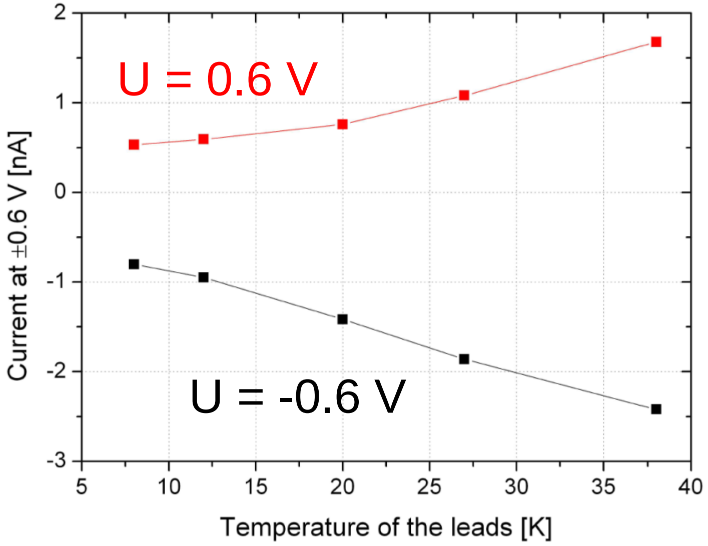

destructive interference due
to quasi-degenerate orbitals

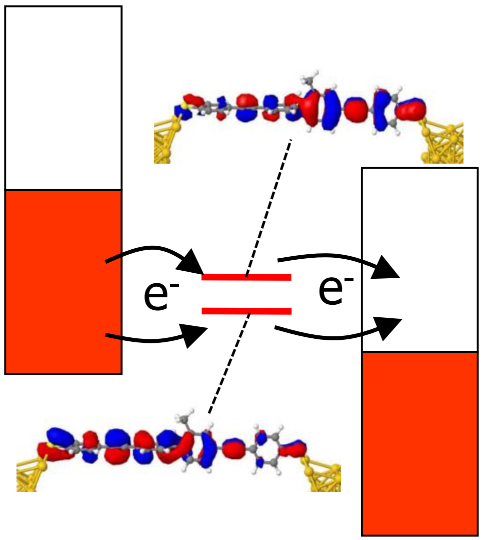

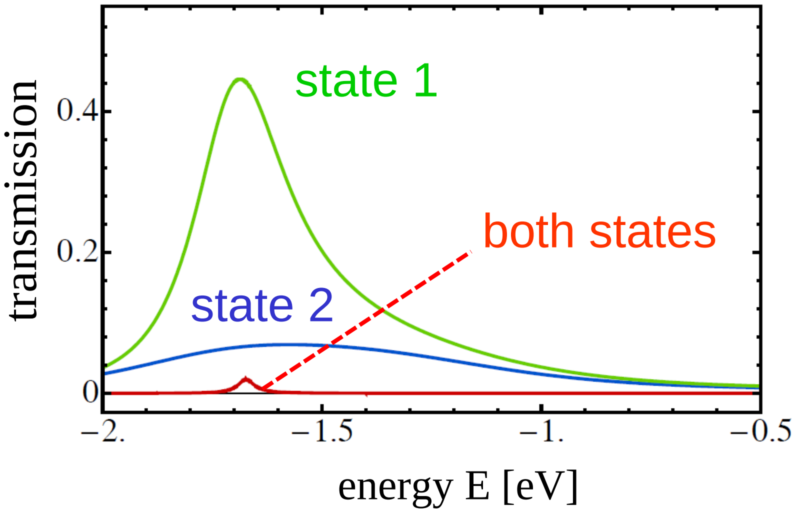

Charge transport in molecular junctions

Summary

- Molecular junctions are interesting architectures to investigate nonequilibrium transport processes at the nanoscale
- Electronic-vibrational coupling influences transport significantly and can cause pronounced vibrational nonequilibrium effects
- Transport in molecular junctions with closely lying electronic states may be strongly influenced by quantum interference effects
- Electronic-vibrational coupling provides decoherence mechanism that is particularly pronounced for larger voltage (resonant transport regime) and higher vibrational excitation

Acknowledgements

Michael Butzin

Pedo Brana Coto

Andre Erpenbeck

Chriszandro Hofmeister

Ivan Pshenichnyuk

Oscar Robio-Pons

Christian Schinabeck

Dominik Weckbecker

Rainer Härtle (Göttingen)

Susanne Leitherer (Kopenhagen)

Uri Peskin (Haifa)

Eran Rabani (Berkeley/Tel Aviv)

Haobin Wang (Denver)

Eli Wilner (Tel Aviv)

Stefan Ballmann (Erlangen)

Konrad Ullmann (Erlangen)

Heiko Weber (Erlangen)

Deutsche Forschungsgemeinschaft DFG

GIF

EAM

ICMM

SCA Synthetic Carbon Allotropes SFB953

Quantum-interference-enhanced thermoelectricity in single-molecule junctions.

Colin Lambert,
Physics, Lancaster University

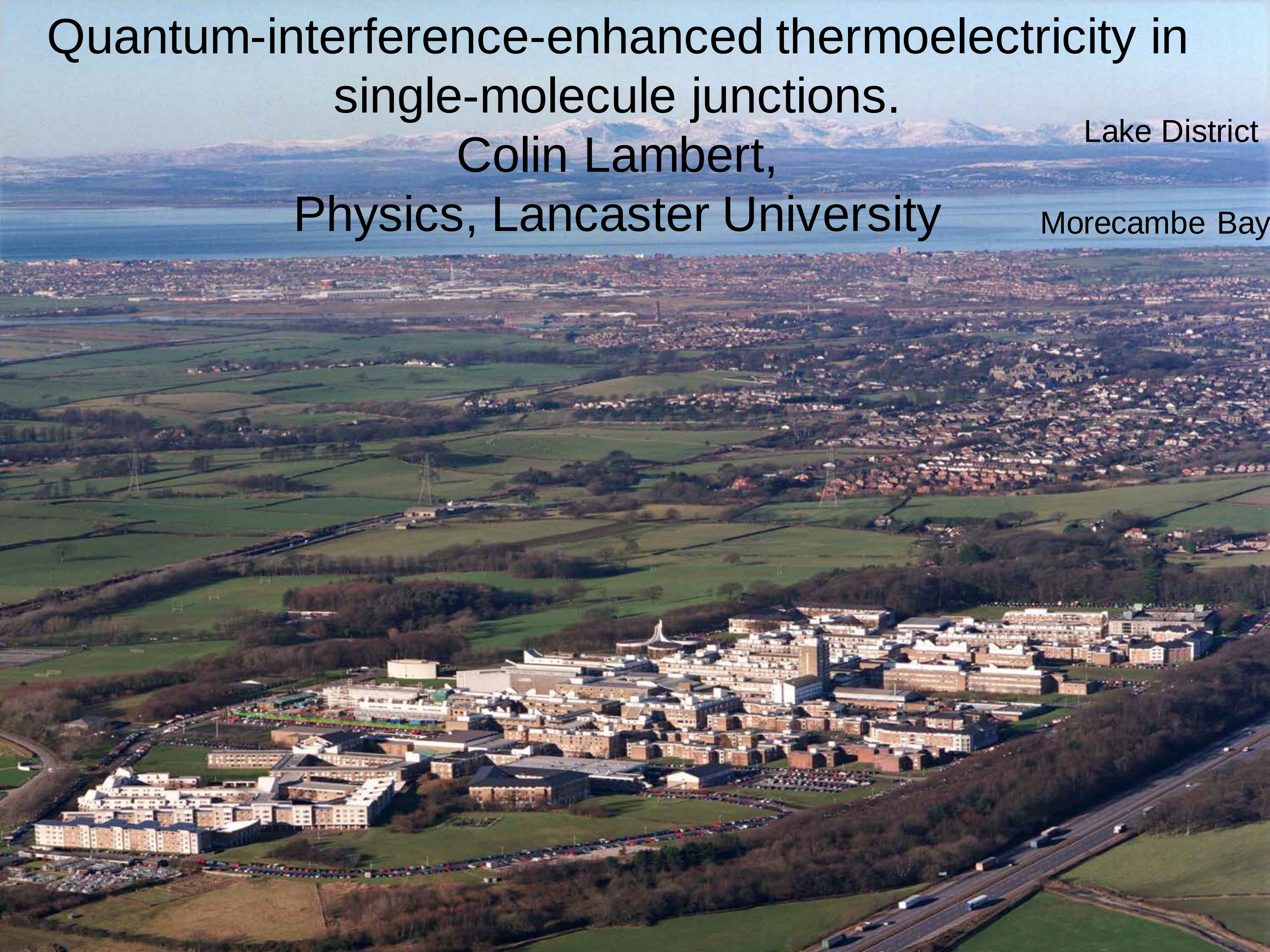

Can interference effects be exploited to enhance thermoelectric properties of single molecule devices and molecular films?

- Can room-temperature electronic quantum interference be used to enhance the Seebeck coefficient of single molecules?
- Can room-temperature phonon interference be exploited to reduce the thermal conductance of single molecules?
- Can these effects be translated into self-assembled arrays of molecules to create high-performance thin-film thermoelectric materials?

Lancaster University

Acknowledgements

R. Tykwinski,
Alberta

R. Nichols
S. Higgins,
E. Leary
Liverpool

H. Anderson,
A. Briggs, J. Mol,
L. Bogani,
P. Gehring,
K. Porphyrakis,
Oxford

T. Albrecht, N. Long,
L. Cohen, Imperial

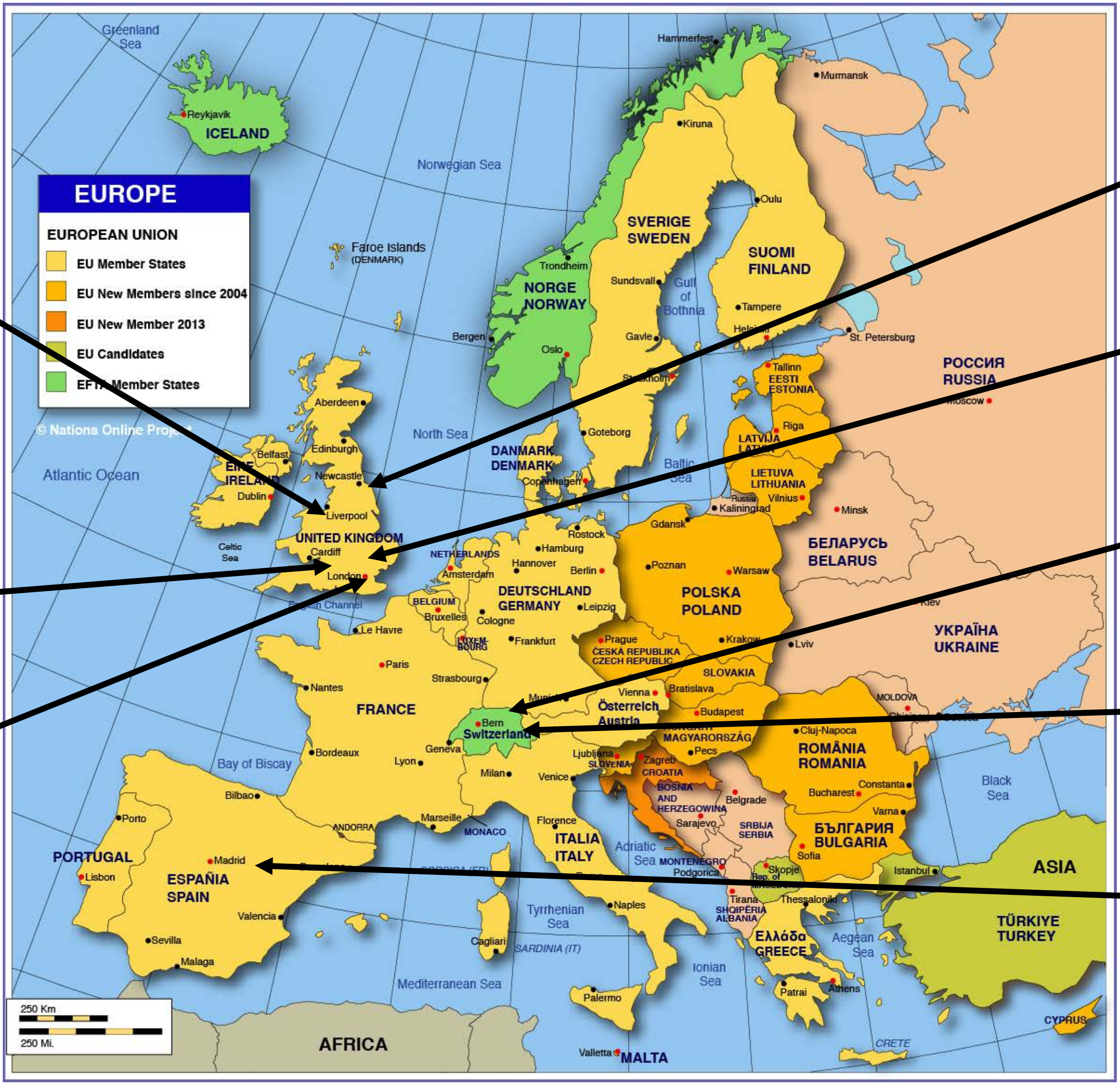

M. Bryce,
Durham

W. Hong,
Xiamen

C. Ford,
Cambridge

T. Wandlowski,
S. Decurtins,
X. Liu, Bern

B. Gottsman,
IBM Zurich

N. Agrait,
Madrid

P. Low,
Perth

Preliminaries

The Seebeck coefficient S:

$(V_2 - V_1) = - S(T_2 - T_1)$

The thermoelectric figure of merit ZT:

$ZT = S^2GT/(\kappa_p + \kappa_e)$

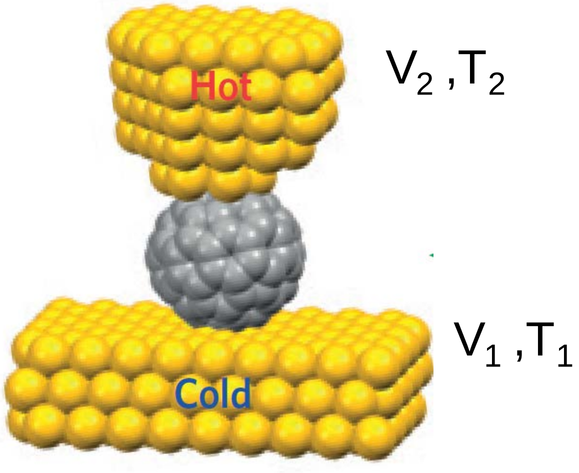

G = electrical conductance, T = mean temperature

κ_p = phonon thermal conductance,

κ_e = electronic thermal conductance

Note regarding a target value for S and κ_p

Wiedemann-Franz: $\kappa_e = \alpha TG$, so if $\kappa_p \ll \kappa_e$, $ZT = S^2GT/\kappa_e = S^2/\alpha$

So to achieve ZT > 1 requires $S^2 > \alpha$ ie $S > 150\mu V/K$

More preliminaries:

Why is quantum interference expected to be helpful?

Mott formula:

$$S \sim -\, d[\log T_e(E_F)]/dE_F$$

$T_e(E)$ = transmission probability for electrons of energy E travelling from the source to the drain via the molecule.

High slope = large S, provided the high slope coincides with the Fermi energy of the electrodes

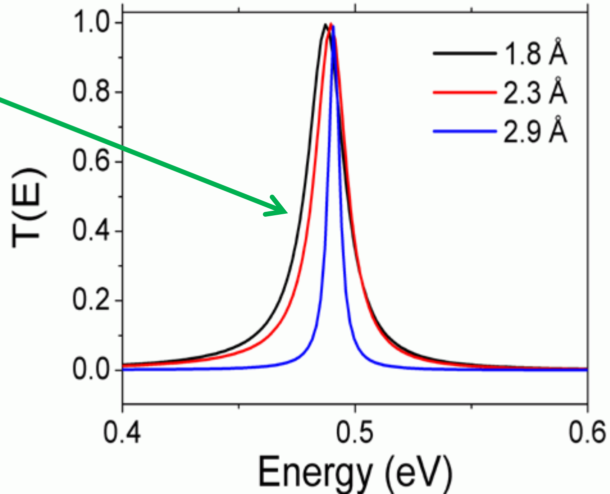

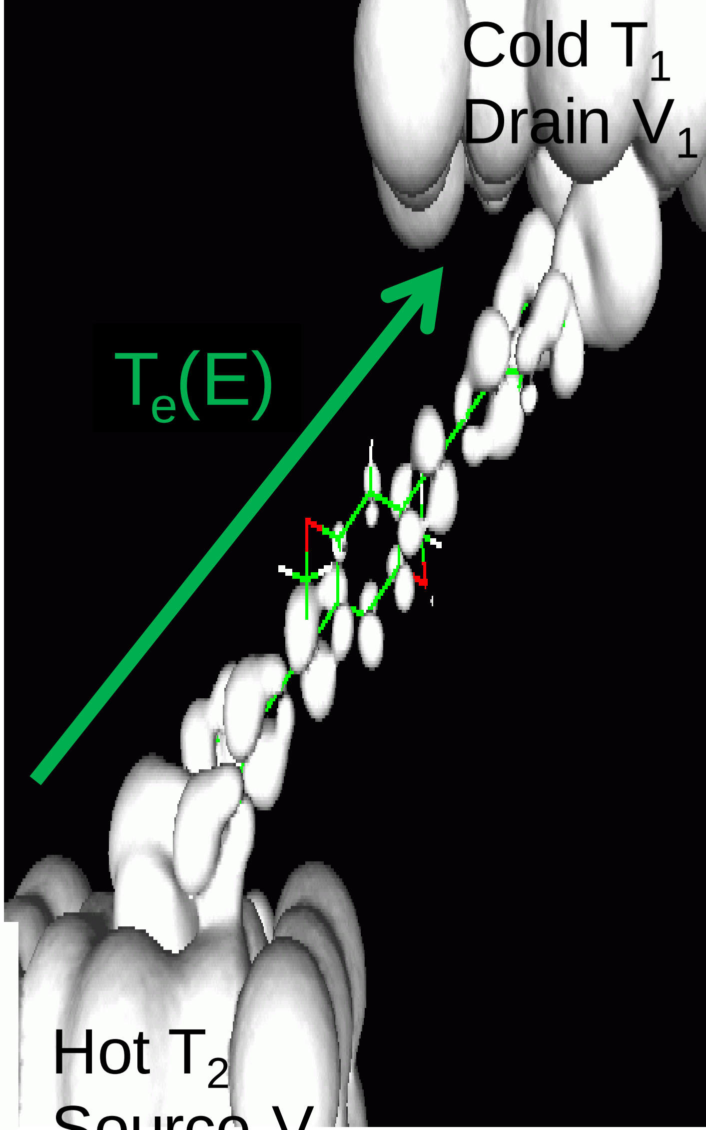

Outline

- Evidence of room-temperature electronic quantum interference
- Strategies for enhancing the Seebeck coefficient of single molecules
- Strategies for reducing phonon thermal conductance

Evidence of QI in electroburnt junctions

Sadeghi et al., PNAS **2015**, *9*, 2658-2663

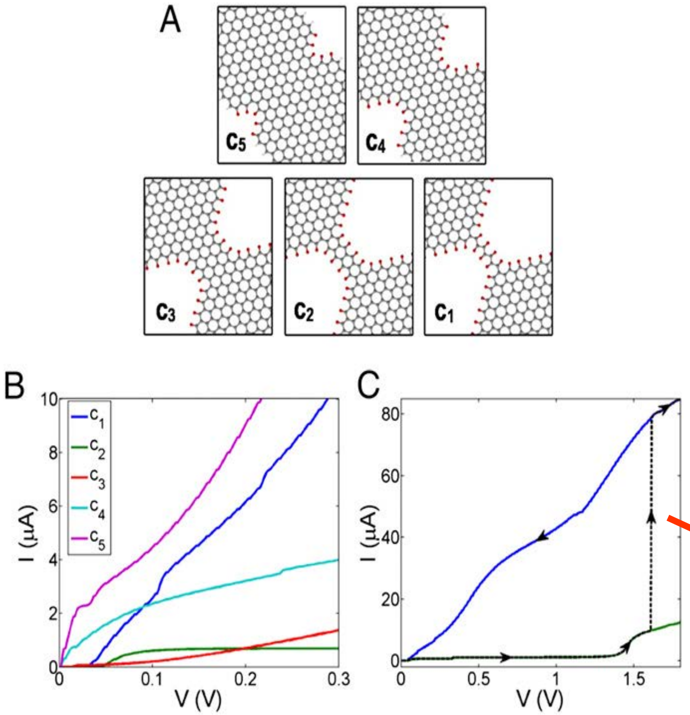

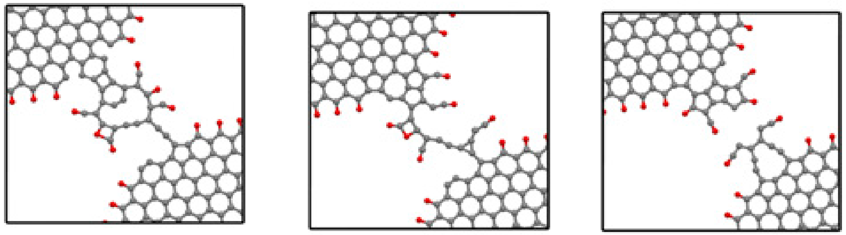

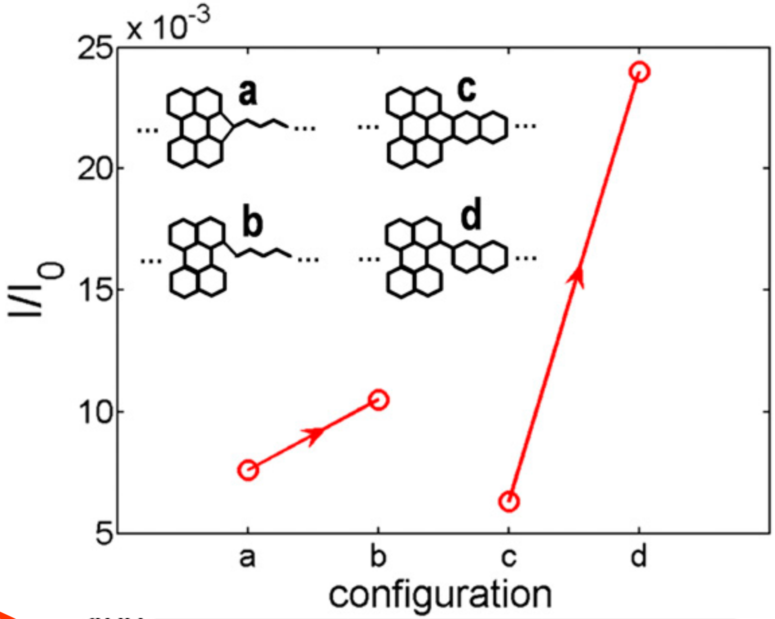

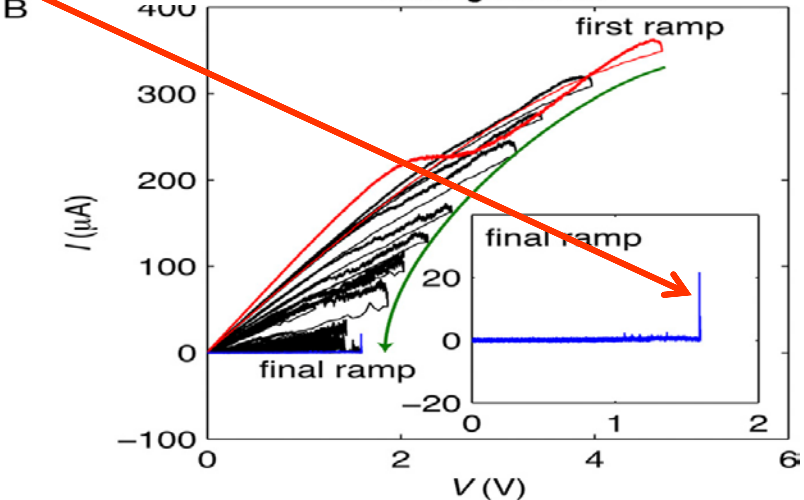

Molecules vs. Quantum dots

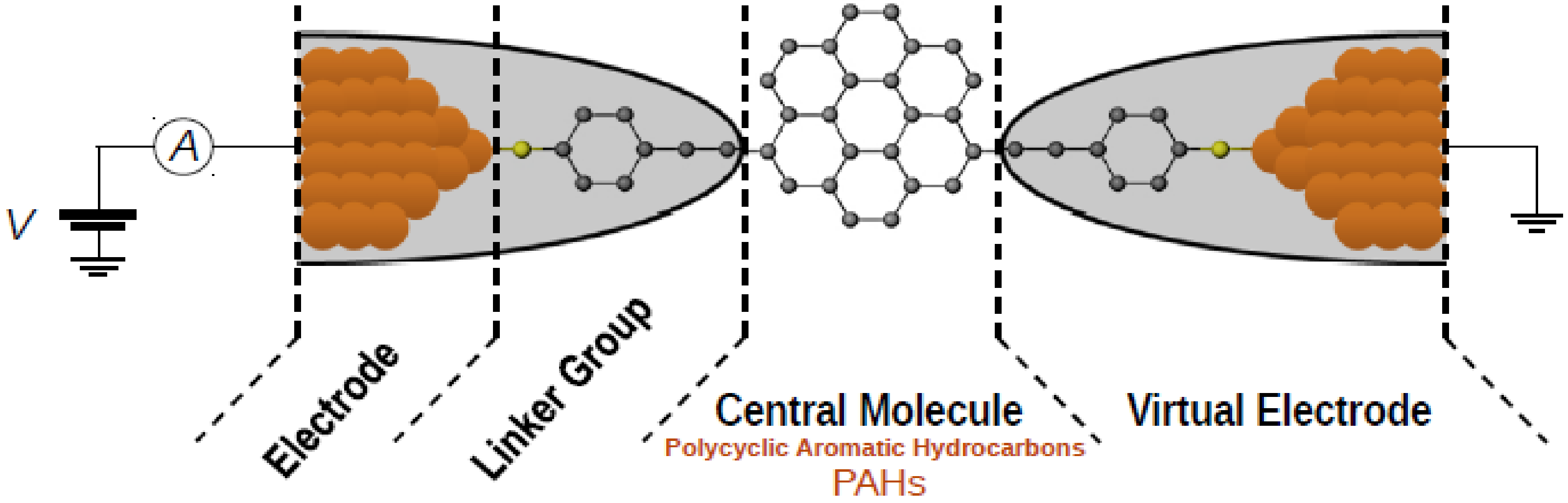

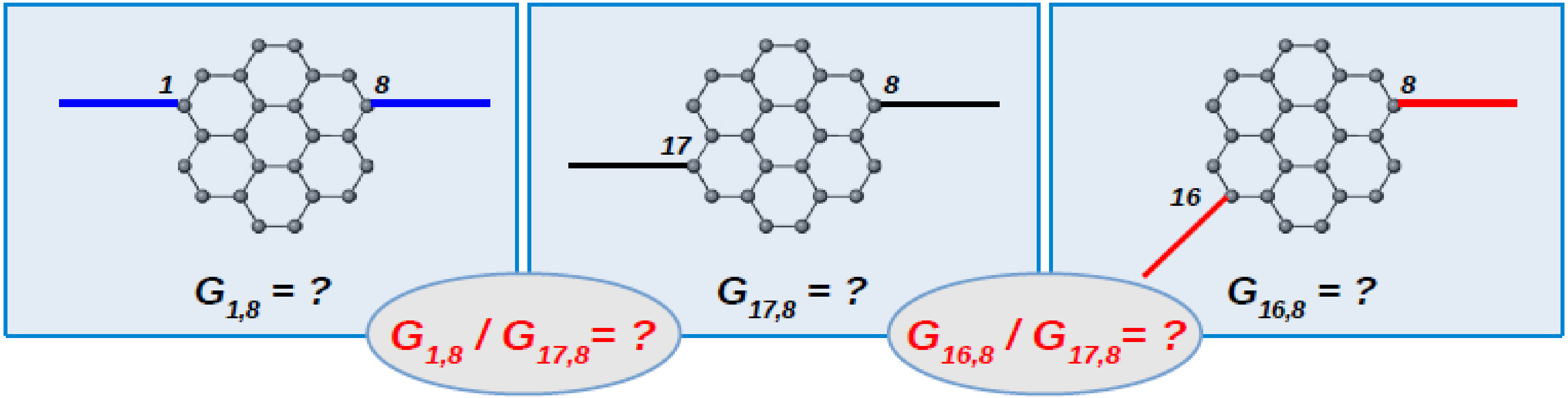

Answer provided by a magic number table.

Magic Ratio Rule (MRR) $G_{1,8}/G_{17,8}$ = ratio of the squares of their magic numbers

An example of constructing M-table

Benzene (Bipartite Lattice)

$G_{11'}/G_{12'} = 1^2/(-1)^2 = 1$

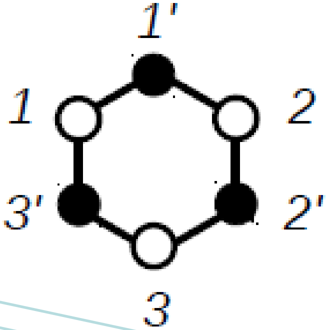

$M = dC^{-1}$

$d \sim \det C$

C =

	1	2	3	1'	2'	3'
1	0	0	0	1	0	1
2	0	0	0	1	1	0
3	0	0	0	0	1	1
1'	1	1	0	0	0	0
2'	0	1	1	0	0	0
3'	1	0	1	0	0	0

$\bar{C}$

$\bar{C}^t$

***M* =**

	1	2	3	1'	2'	3'
1	0	0	0	1	-1	1
2	0	0	0	1	1	-1
3	0	0	0	-1	1	1
1'	1	1	-1	0	0	0
2'	-1	1	1	0	0	0
3'	1	-1	1	0	0	0

$\bar{M}^t$

$\bar{M}$

Sangtarash, et. al, JACS, 2015, 137(35), 11425

Fun with magic numbers:the pyrene M-table

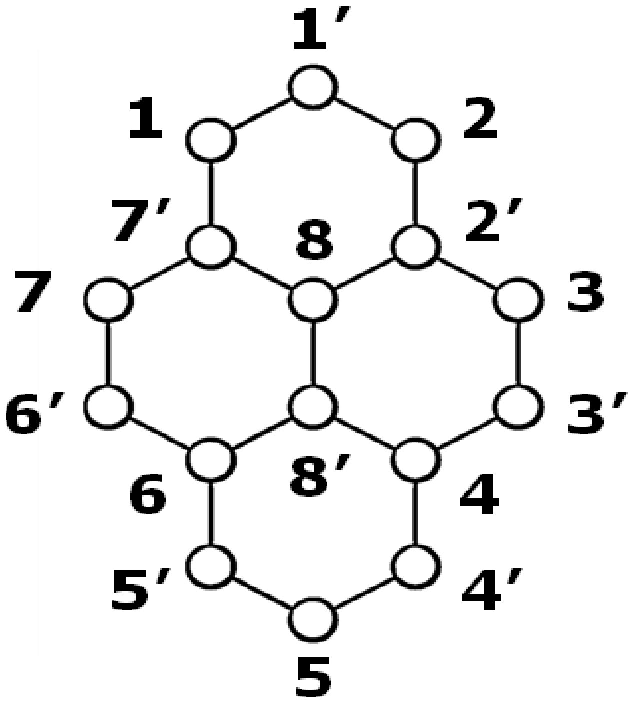

$M \sim C^{-1}$

C=

	1	2	3	4	5	6	7	8
1’	1	1	0	0	0	0	0	0
2’	0	1	1	0	0	0	0	1
3’	0	0	1	1	0	0	0	0
4’	0	0	0	1	1	0	0	0
5’	0	0	0	0	1	1	0	0
6’	0	0	0	0	0	1	1	0
7’	1	0	0	0	0	0	1	1
8’	0	0	0	1	0	1	0	1

M =

	1’	2’	3’	4’	5’	6’	7’	8’
1	3	-3	3	-3	3	-3	3	0
2	3	3	-3	3	-3	3	-3	0
3	-1	1	5	-3	3	-1	1	-2
4	1	-1	1	3	-3	1	-1	2
5	-1	1	-1	3	3	-1	1	-2
6	1	-1	1	-3	3	1	-1	2
7	-1	1	-1	3	-3	5	1	-2
8	-2	2	-2	0	0	-2	2	2

Comparison with experiment

JACS 137, 11425 (2015), JACS 137, 4469 (2015)

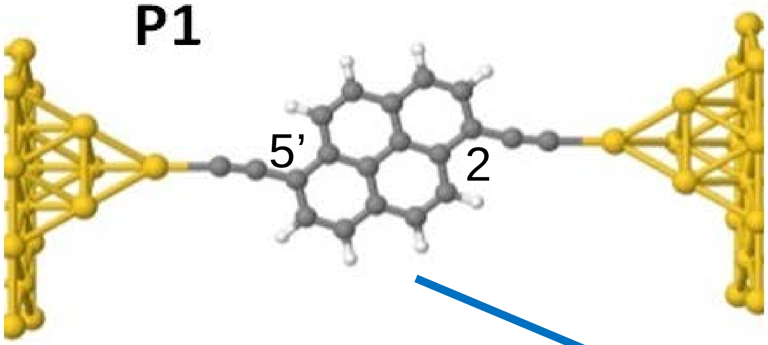

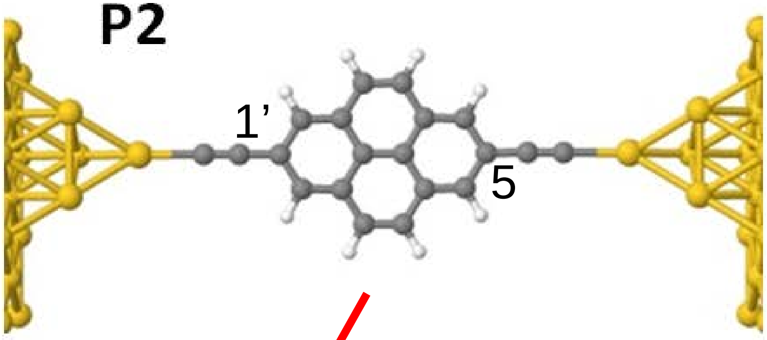

Experiment

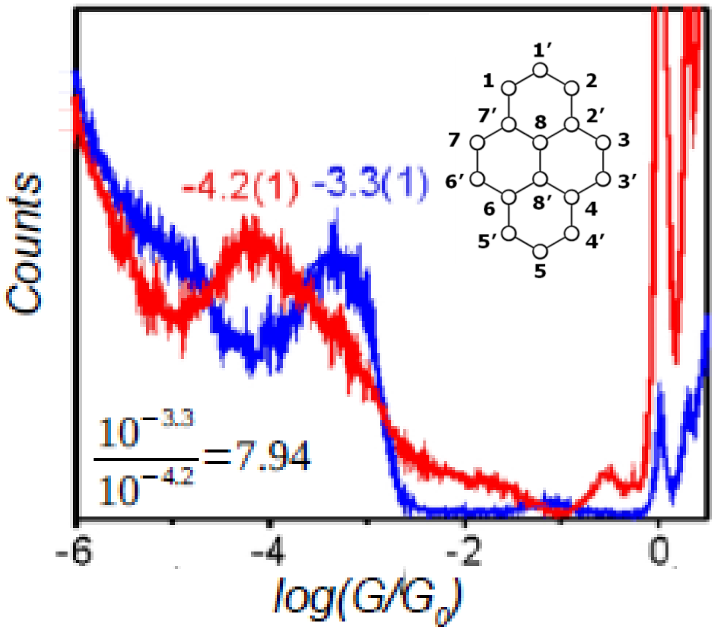

$$M = \begin{array}{c|cccccccc} & 1' & 2' & 3' & 4' & 5' & 6' & 7' & 8' \\ \hline 1 & 3 & -3 & 3 & -3 & 3 & -3 & 3 & 0 \\ 2 & 3 & 3 & -3 & 3 & -3 & 3 & -3 & 0 \\ 3 & -1 & 1 & 5 & -3 & 3 & -1 & 1 & -2 \\ 4 & 1 & -1 & 1 & 3 & -3 & 1 & -1 & 2 \\ 5 & -1 & 1 & -1 & 3 & 3 & -1 & 1 & -2 \\ 6 & 1 & -1 & 1 & -3 & 3 & 1 & -1 & 2 \\ 7 & -1 & 1 & -1 & 3 & -3 & 5 & 1 & -2 \\ 8 & -2 & 2 & -2 & 0 & 0 & -2 & 2 & 2 \end{array}$$

MRR: $G_{25'}/G_{51'} = (-3)^2/(-1)^2 = 9/1 = 9$

Anthanthrene - Bipartite Lattice

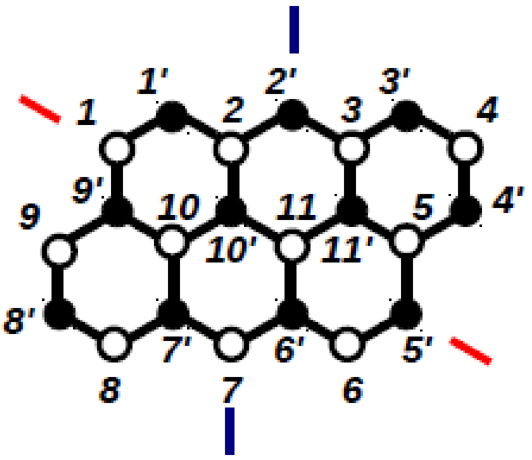

$M =$

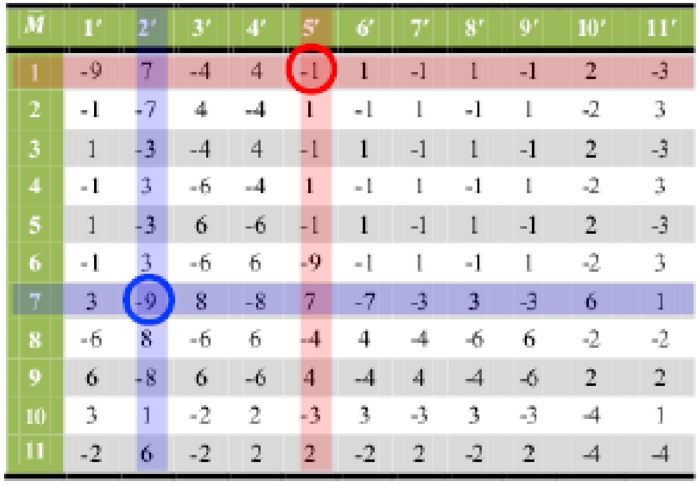

$\bar{M}$	1′	2′	3′	4′	5′	6′	7′	8′	9′	10′	11′
1	-9	7	-4	4	-1	1	-1	1	-1	2	-3
2	-1	-7	4	-4	1	-1	1	-1	1	-2	3
3	1	-3	-4	4	-1	1	-1	1	-1	2	-3
4	-1	3	-6	-4	1	-1	1	-1	1	-2	3
5	1	-3	6	-6	-1	1	-1	1	-1	2	-3
6	-1	3	-6	6	-9	-1	1	-1	1	-2	3
7	3	-9	8	-8	7	-7	-3	3	-3	6	1
8	-6	8	-6	6	-4	4	-4	-6	6	-2	-2
9	6	-8	6	-6	4	-4	4	-4	-6	2	2
10	3	1	-2	2	-3	3	-3	3	-3	-4	1
11	-2	6	-2	2	2	-2	2	-2	2	-4	-4

All numbers are integer

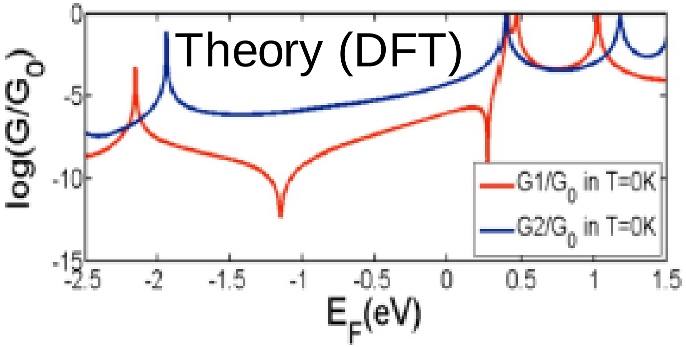

Experiment

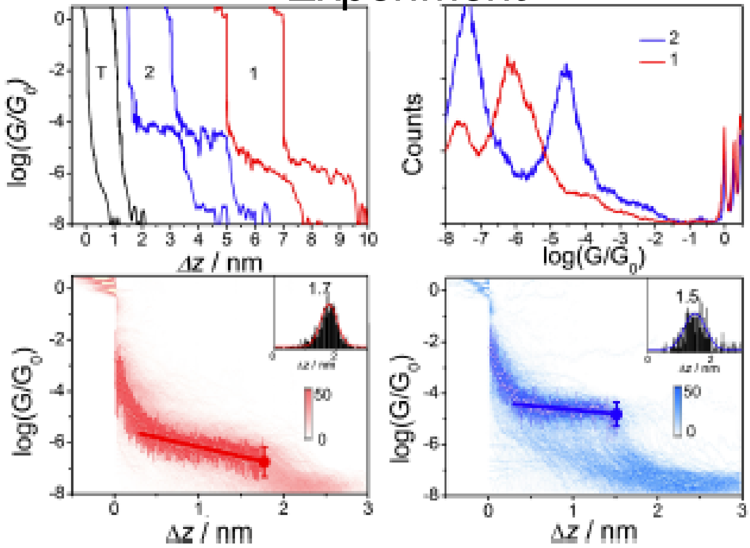

$10^{-6.7}\ G_0$ $10^{-4.8}\ G_0$

MRR: $G_{72'}/G_{15'} = (-9)^2/(-1)^2 = 81/1 = 81$ Experiment: $10^{-4.8}/10^{-6.7} = 79$

Mid-gap Ratio Rule MRR – A new rule

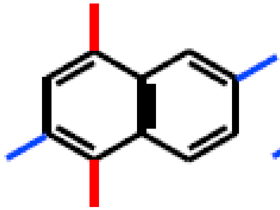
Naphthalene

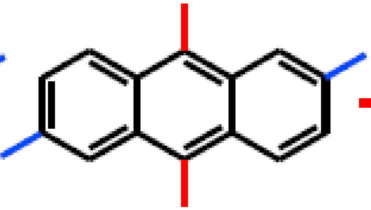
Anthracene

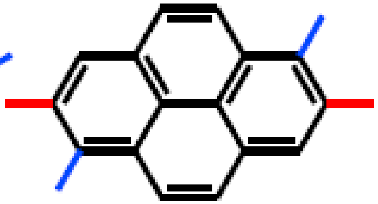
Pyrene

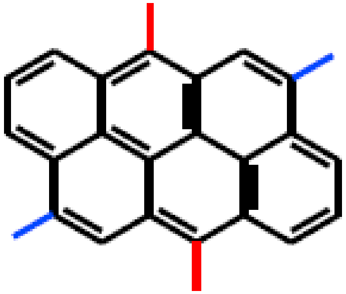
Anthanthrene

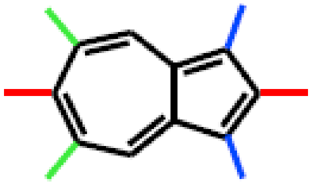
Azulene

Molecular heart	Anchor group	Literature notation "Conductance Ratio of connectivity"	Mid-gap MRR	Experimental ratios	GW prediction	DFT Prediction
Naphthalene	thiol	Red / Blue (JACS, 2012)	4	5.1	NA	2
Anthracene	thiol	Red / Blue (JACS, 2012)	16	10.2	NA	13
Pyrene	carbon	Red / Blue (JACS, 2015)	9	8	NA	9
Anthanthrene	pyridyl	Red / Blue (JACS, 2015)	81	79	NA	81
Azulene	thiochroman	Red / Blue (Nano Lett., 2014)	0.72	1	0.32	0.93
Azulene	thiochroman	Green / Blue (Nano Lett., 2014)	0.003	0.06	0.1	0.05

Sangtarash, et. al, JACS, 2015, 137(35), 11425; Xia, et. Al, Nano Lett., 2014, 14 (5), 2941; Kaliginedi, et. al, JACS, 2012, 134 (11), 5262

Phase coherent interferometers

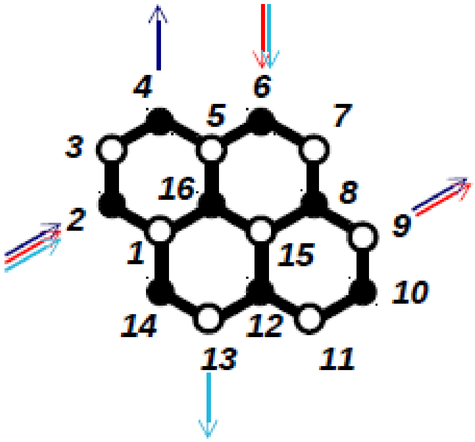

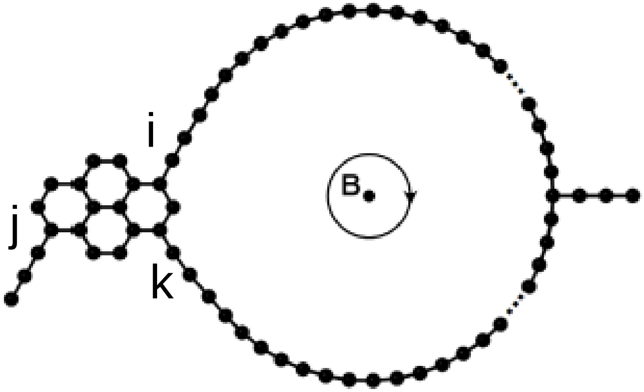

$\overline{M}=$

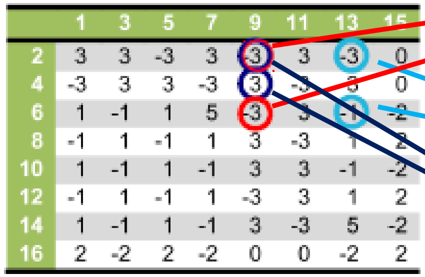

	1	3	5	7	9	11	13	15
2	3	3	-3	3	-3	3	-3	0
4	-3	3	3	-3	3	-3	3	0
6	1	-1	1	5	-3	3	-1	-2
8	-1	1	-1	1	3	-3	1	2
10	1	-1	1	-1	3	3	-1	-2
12	-1	1	-1	1	-3	3	1	2
14	1	-1	1	-1	3	-3	5	-2
16	2	-2	2	-2	0	0	-2	2

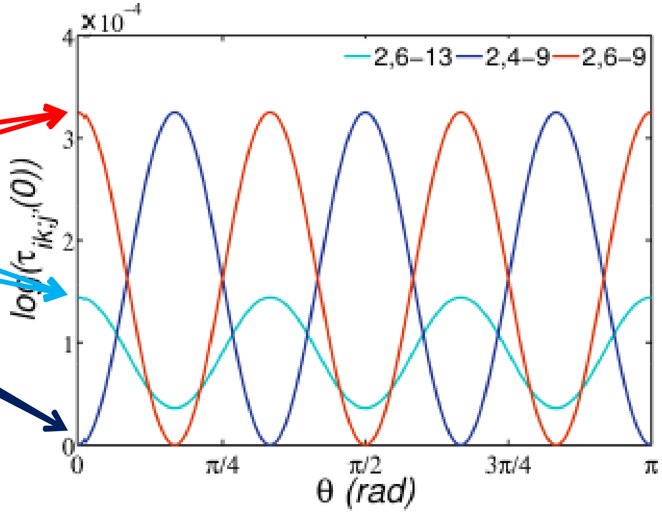

conductance $_{i,k\text{-}j} \sim |\, M_{ij} + M_{kj}\, e^{i\theta}\, |^2$

Sangtarash, et. al, JACS, 2015, 137(35), 11425

Three terminal logic gate

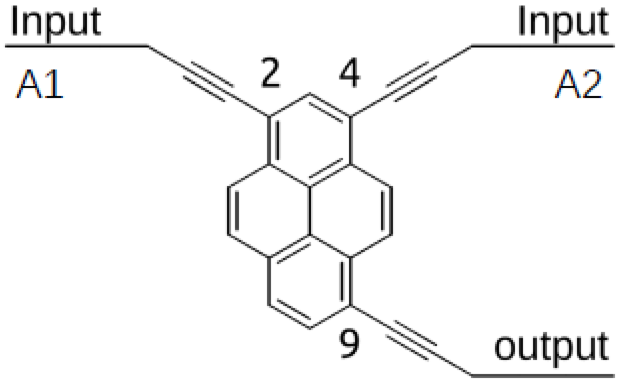

$$\sigma_{i,j,j'} \propto |M_{i,j} + M_{j,j'}|^2$$

Input		Output
A1	A2	$\lvert A1+A2\rvert^2$
0	0	0
1	0	1
0	1	1
1	1	0

$$\bar{M} = \begin{array}{c|cccccccc} & 1 & 3 & 5 & 7 & 9 & 11 & 13 & 15 \\ \hline 2 & 3 & 3 & -3 & 3 & -3 & 3 & -3 & 0 \\ 4 & -3 & 3 & 3 & -3 & 3 & -3 & 3 & 0 \\ 6 & 1 & -1 & 1 & 5 & -3 & 3 & -1 & -2 \\ 8 & -1 & 1 & -1 & 1 & 3 & -3 & 1 & 2 \\ 10 & 1 & -1 & 1 & -1 & 3 & 3 & -1 & -2 \\ 12 & -1 & 1 & -1 & 1 & -3 & 3 & 1 & 2 \\ 14 & 1 & -1 & 1 & -1 & 3 & -3 & 5 & -2 \\ 16 & 2 & -2 & 2 & -2 & 0 & 0 & -2 & 2 \end{array}$$

$$\sigma_{2,9} = \sigma_{4,9} \propto |\pm 3|^2$$

$$\sigma_{2,4;9} \propto |M_{2,9} + M_{4,9}|^2$$

$$\sigma_{2,4;9} \propto |-3+3|^2 = 0$$

Sangtarash, et. al, JACS, 2015, 137(35), 11425

Why does the MRR work?

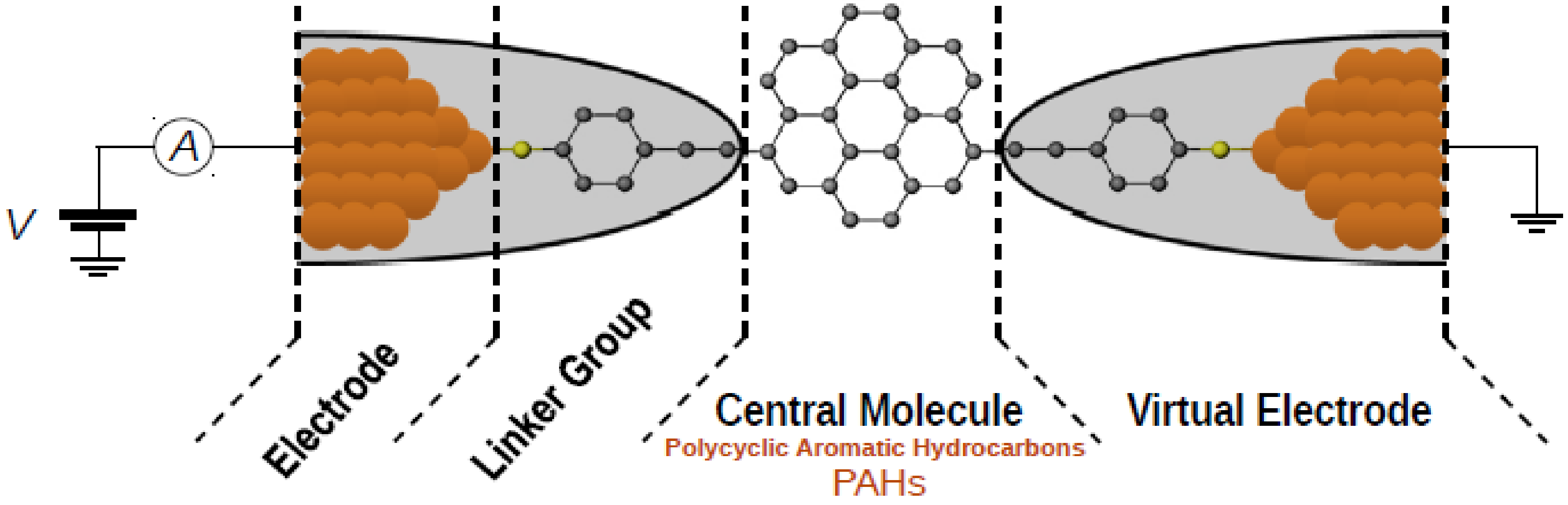

1. Provided E_F lies within the HOMO-LUMO gap:
   $G = G_{left}\, G_{core}\, G_{right} = G_{core}\, R$, where R = random number.

2. Provided the distribution of R is connectivity independent,
   [most probable G_1]/[most probable G_2]= G_{core1} / G_{core2}

3. Provided E_F lies near the centre HOMO-LUMO gap,
   G_{core}= (magic number)^2

Why does the MRR work? Effect of Coulomb interactions – PPP model

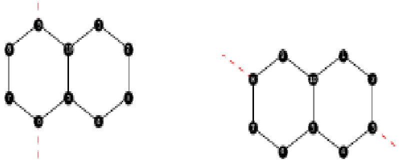

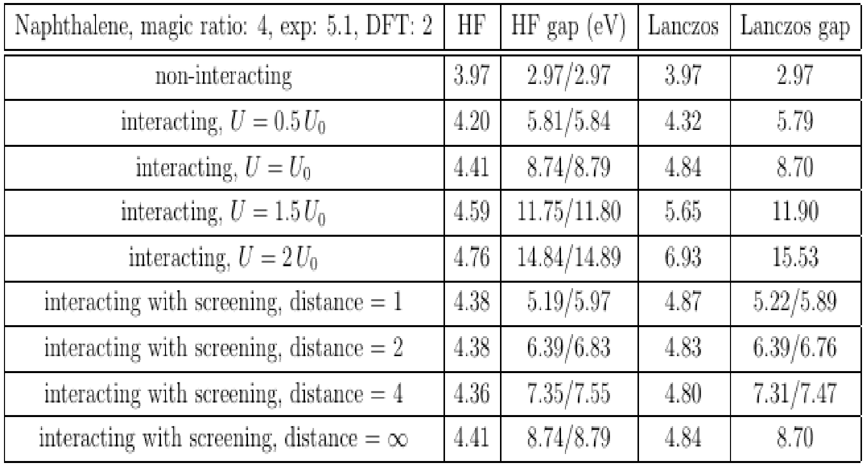

Naphthalene, magic ratio: 4, exp: 5.1, DFT: 2	HF	HF gap (eV)	Lanczos	Lanczos gap
non-interacting	3.97	2.97/2.97	3.97	2.97
interacting, $U = 0.5U_0$	4.20	5.81/5.84	4.32	5.79
interacting, $U = U_0$	4.41	8.74/8.79	4.84	8.70
interacting, $U = 1.5U_0$	4.59	11.75/11.80	5.65	11.90
interacting, $U = 2U_0$	4.76	14.84/14.89	6.93	15.53
interacting with screening, distance = 1	4.38	5.19/5.97	4.87	5.22/5.89
interacting with screening, distance = 2	4.38	6.39/6.83	4.83	6.39/6.76
interacting with screening, distance = 4	4.36	7.35/7.55	4.80	7.31/7.47
interacting with screening, distance = ∞	4.41	8.74/8.79	4.84	8.70

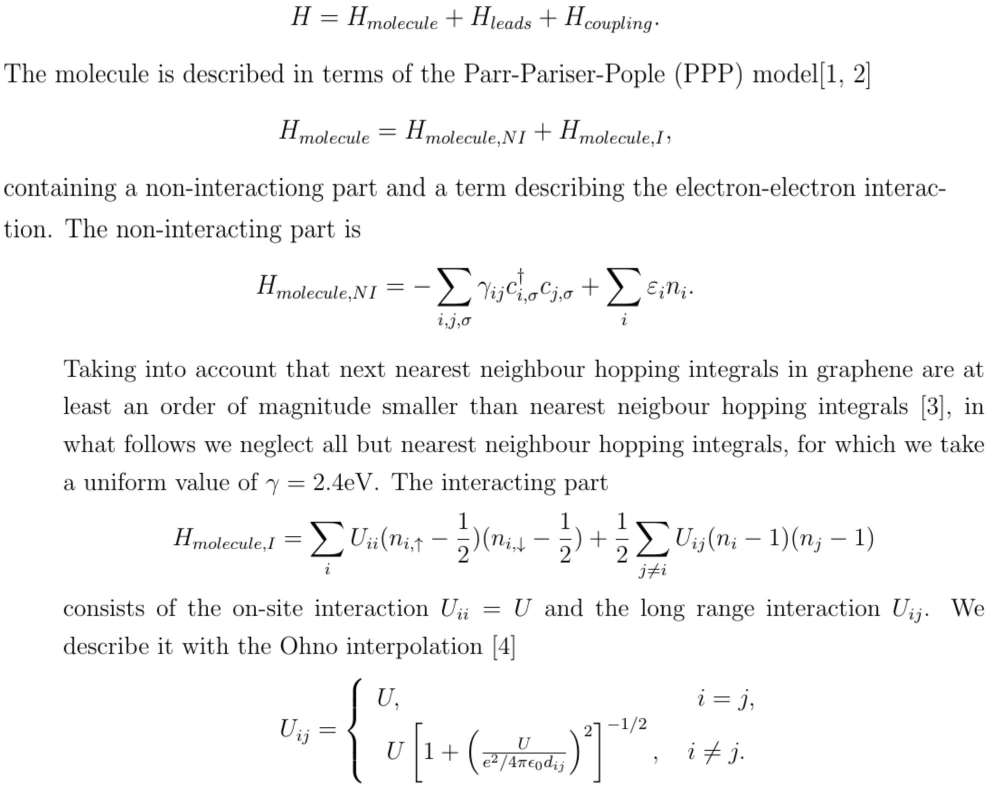

$$H = H_{molecule} + H_{leads} + H_{coupling}.$$

The molecule is described in terms of the Parr-Pariser-Pople (PPP) model[1, 2]

$$H_{molecule} = H_{molecule,NI} + H_{molecule,I},$$

containing a non-interactiong part and a term describing the electron-electron interaction. The non-interacting part is

$$H_{molecule,NI} = -\sum_{i,j,\sigma} \gamma_{ij} c^\dagger_{i,\sigma} c_{j,\sigma} + \sum_i \varepsilon_i n_i.$$

Taking into account that next nearest neighbour hopping integrals in graphene are at least an order of magnitude smaller than nearest neigbour hopping integrals [3], in what follows we neglect all but nearest neighbour hopping integrals, for which we take a uniform value of $\gamma = 2.4$eV. The interacting part

$$H_{molecule,I} = \sum_i U_{ii}(n_{i,\uparrow} - \frac{1}{2})(n_{i,\downarrow} - \frac{1}{2}) + \frac{1}{2}\sum_{j\neq i} U_{ij}(n_i - 1)(n_j - 1)$$

consists of the on-site interaction $U_{ii} = U$ and the long range interaction U_{ij}. We describe it with the Ohno interpolation [4]

$$U_{ij} = \begin{cases} U, & i = j, \\ U\left[1 + \left(\frac{U}{e^2/4\pi\epsilon_0 d_{ij}}\right)^2\right]^{-1/2}, & i \neq j. \end{cases}$$

Ulcakar, Rejec, Ramsak, Jefferson et al. (2017)

More evidence of QI: A quantum circuit rule for room temperature conductance

Nat Comm **2015,** *6*, 6389

$$G_{ppp}G_{mmm}= G_{mpm}G_{pmp}$$

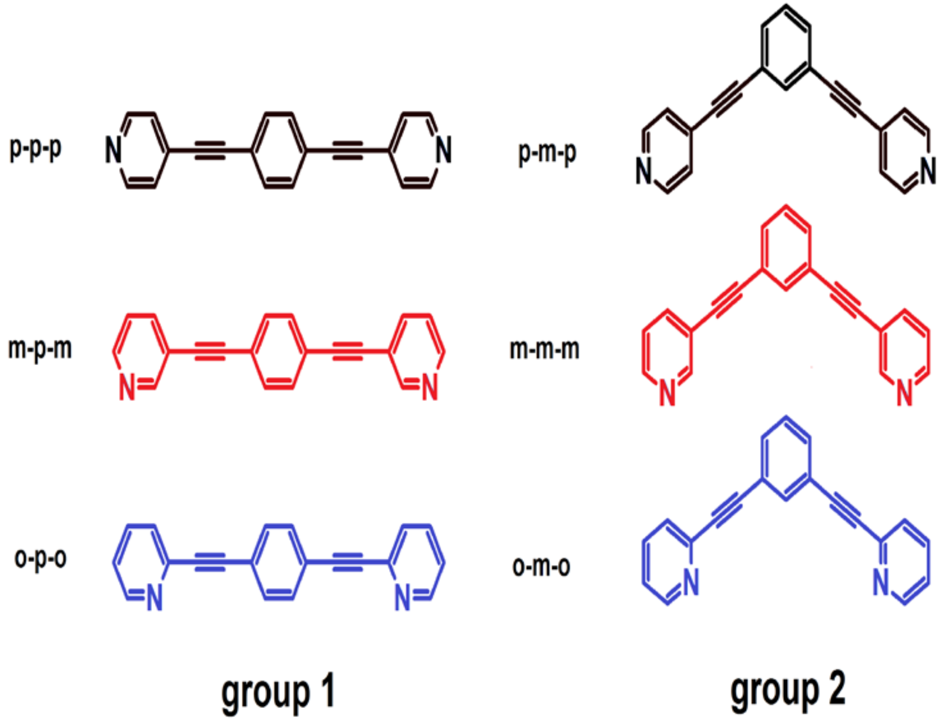

Experiment

Molecule	Log G/G_0
p-p-p	-4.5±0.4
m-p-m	-5.5±0.4
p-m-p	-6.0±0.5
m-m-m	-6.9±0.5

Experiment

$\log(G_{ppp}/G_0) + \log(G_{mmm}/G_0) = -4.5 - 6.9 = -11.4$

$\log(G_{pmp}/G_0) + \log(G_{mpm}/G_0) = -5.5 - 6.0 = -11.5$

A quantum circuit rule for materials discovery

Nano Lett. 2016, 16, 1308

$$S_{ppp} + S_{mmm} = S_{mpm} + S_{pmp}$$

$$G_{ppp}G_{mmm} = G_{mpm}G_{pmp}$$

More generally

$$S_{XBY} = (S_{XBX} + S_{YBY})/2$$

$$(G_{XBY})^2 = G_{XBX}G_{YBY}$$

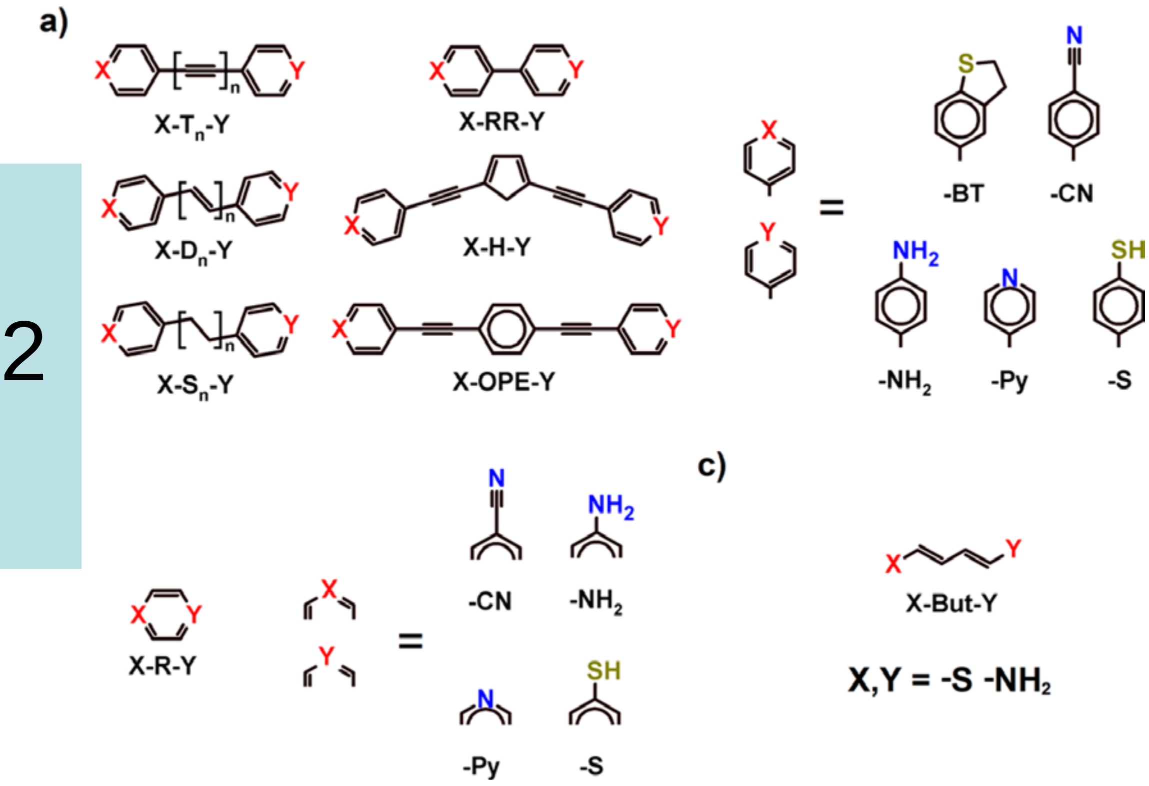

A quantum circuit rule for room temperature conductance and thermopower:

$$S_{XBY} = (S_{XBX} + S_{YBY})/2$$

$$(G_{XBY})^2 = G_{XBX} G_{YBY}$$

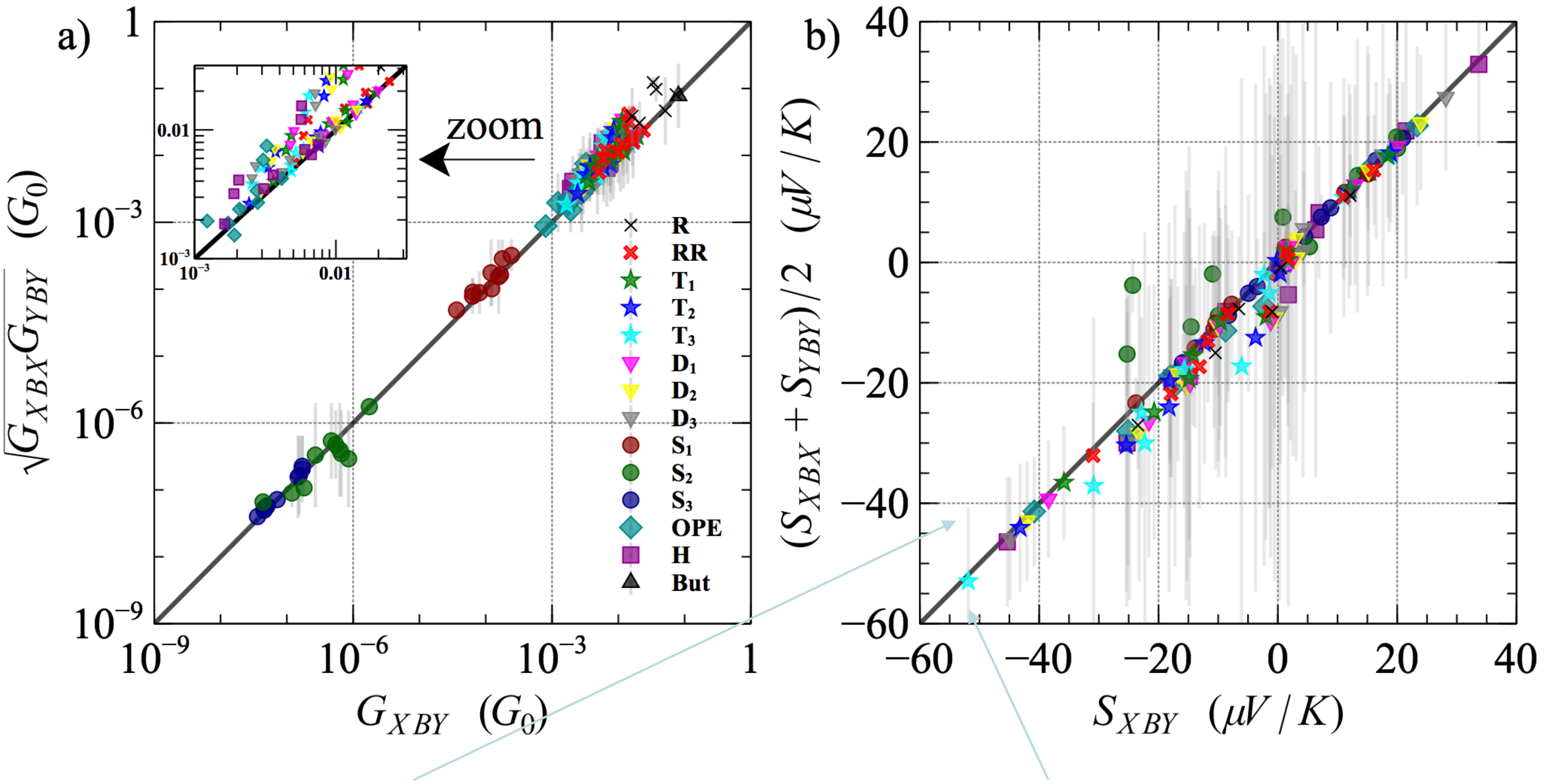

Top of each grey line shows S_{XBX}. Bottom of grey line shows S_{YBY}.

Strategies for controlling thermoelectric properties of single molecules

1. Creating quantum scatterers in series
2. Control of thermopower by mechanical gating
3. Electrostatic gating via charge transfer complexation
4. Suppression of phonon transport in ‘edge-over-edge’ porphyrins and molecular Christmas trees

Strategy 1. Quantum scatterers in series

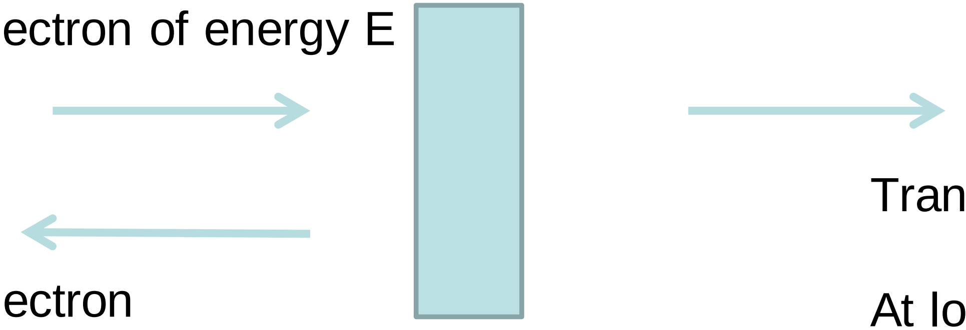

Incident electron of energy E

transmitted electron

reflected electron

Scattering region

Transmission probability $T_e(E)$

At low temperature or for not-too-narrow resonances:

$S=-(\Pi^2 k_B^2 T/2e)\, d\ln T_e(E_F)/dE_F$

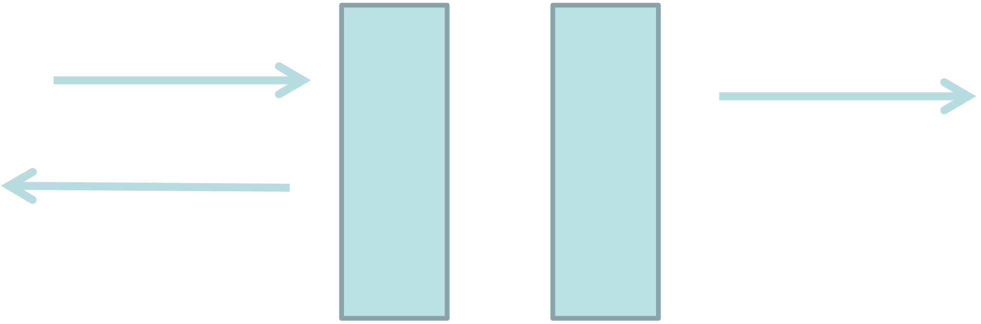

Transmission probability T_e^2

$\ln T^2_e = 2\ln T_e$

So Seebeck coefficient should double!

Two scatterers in series

Does it work?
Application to C_{60} molecular junctions

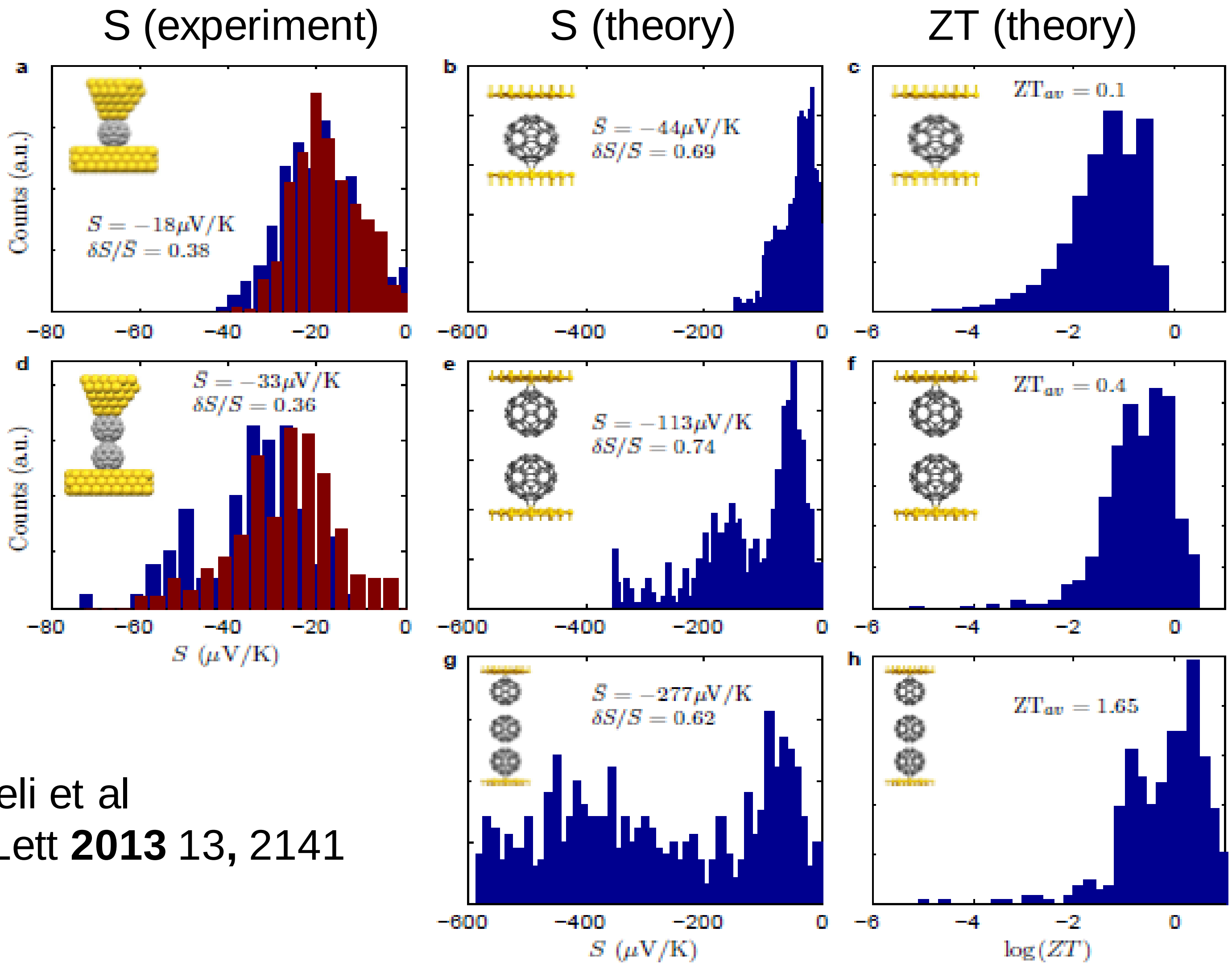

Evangeli et al
Nano Lett **2013** 13, 2141

Strategy 2: Control of thermopower by mechanical gating

L. Rincón-García, A. Ismael, et al. *Nature Materials*, **15**, 289–293 (2016)

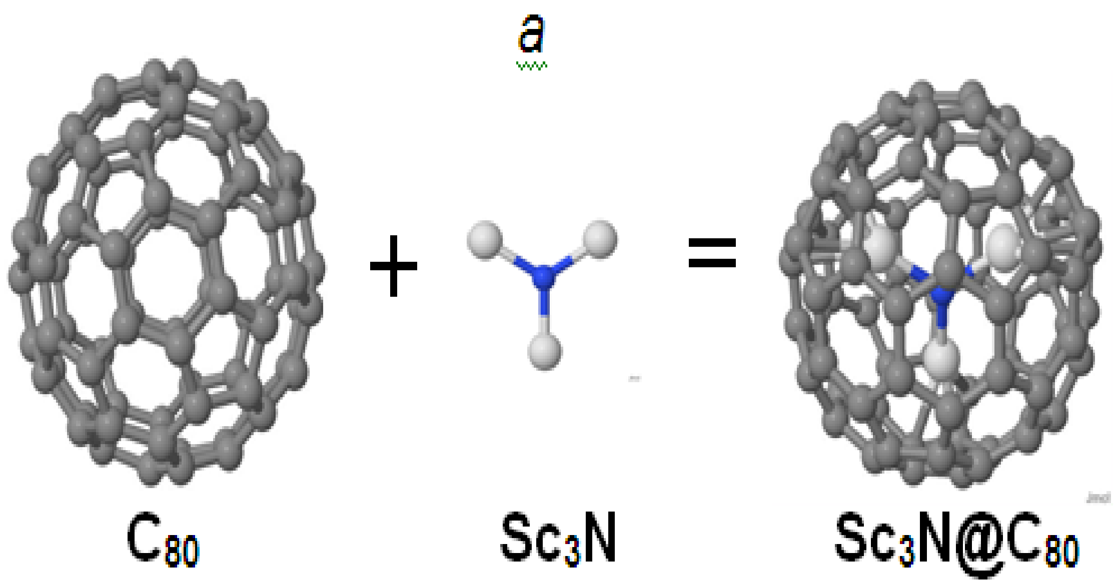

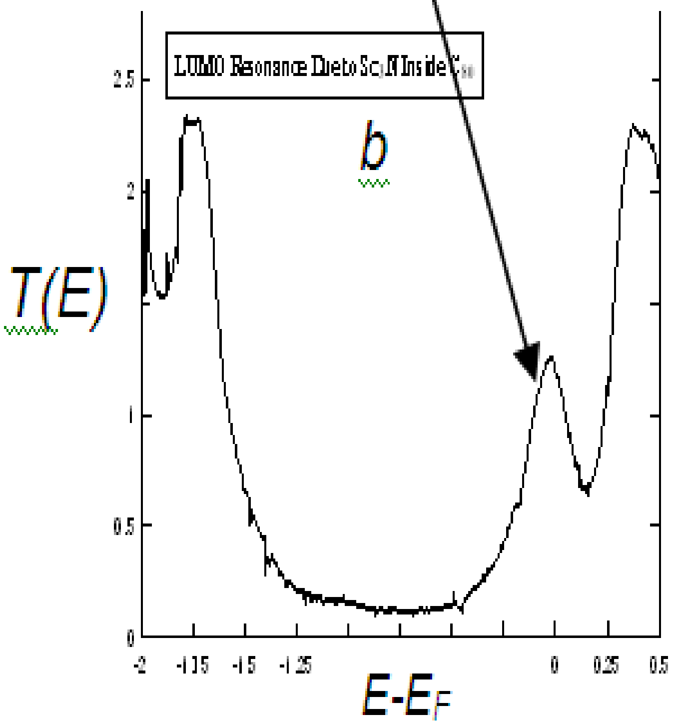

Breit Wigner resonance due to the presence of Sc_3N inside the C_{80}

Control of thermoelectricity via tip pressure

Nature Materials, **15**, 289–293 (2016)

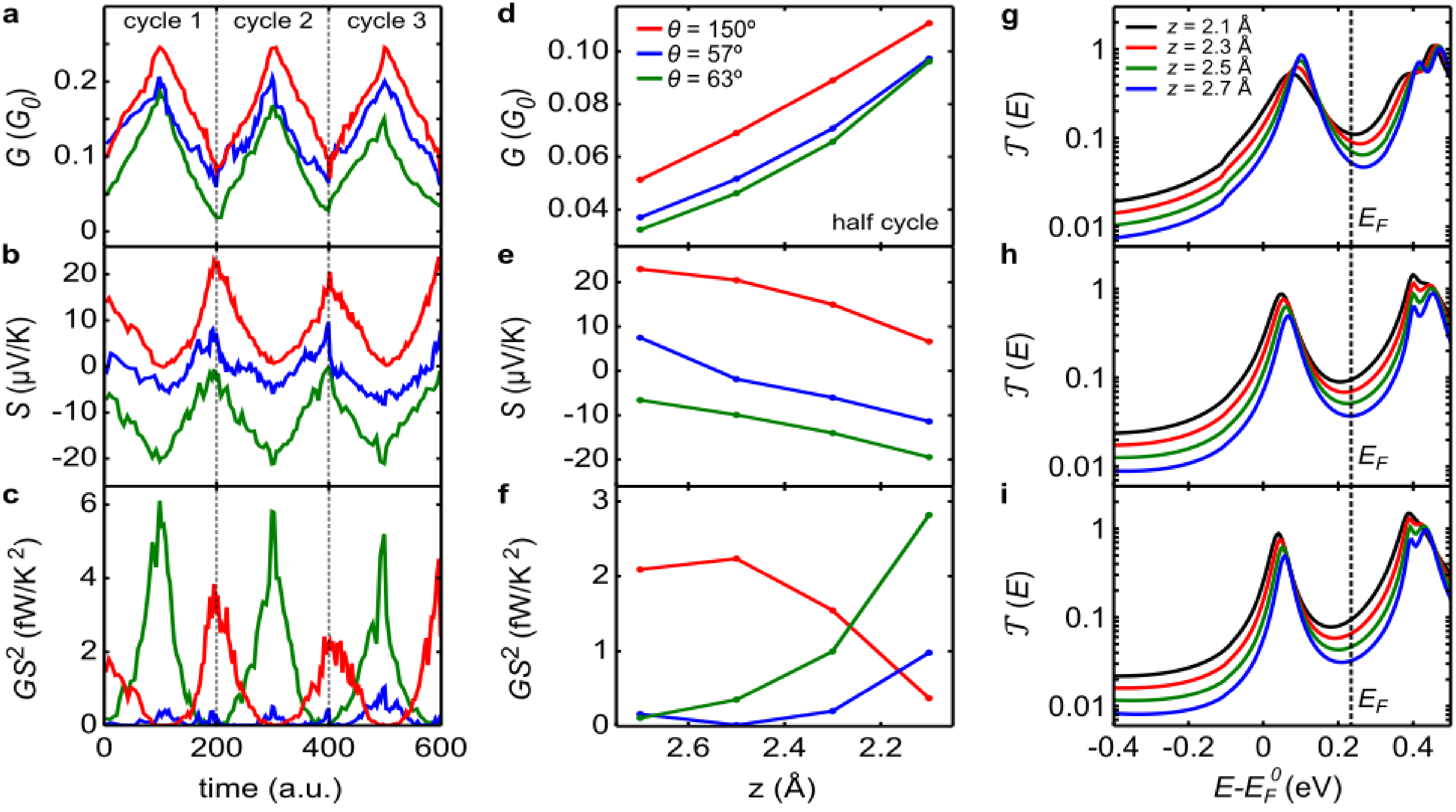

Strategy 3: Electrostatic gating via charge transfer complexation in “crown-ether anthraquinones”

AK Ismael, I Grace, CJL, *Nanoscale* 7 (41), 17338-17342 (2015)

Na^+, K^+, ...

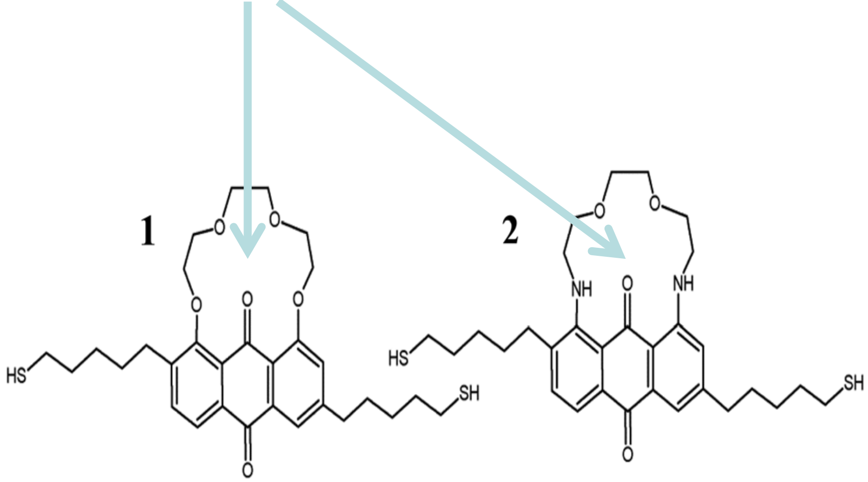

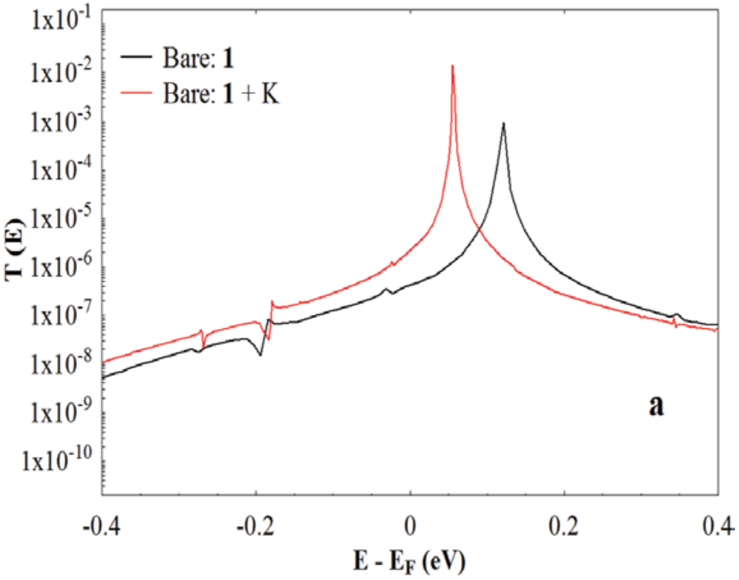

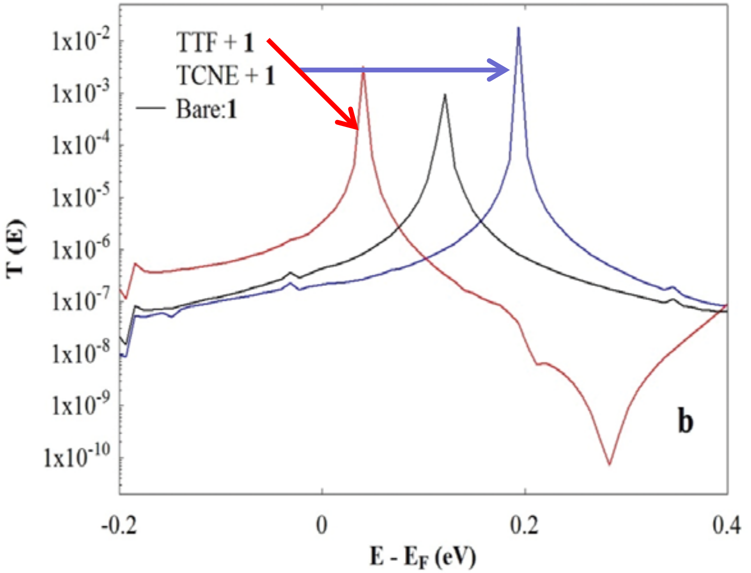

Seebeck coefficient S and power factor P

1

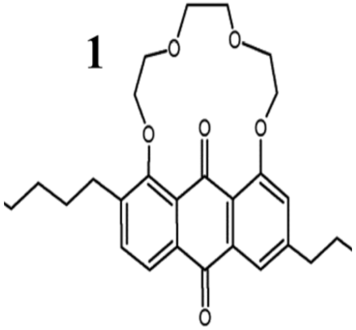

2

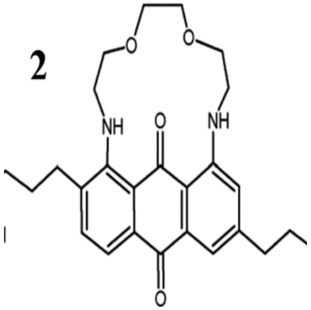

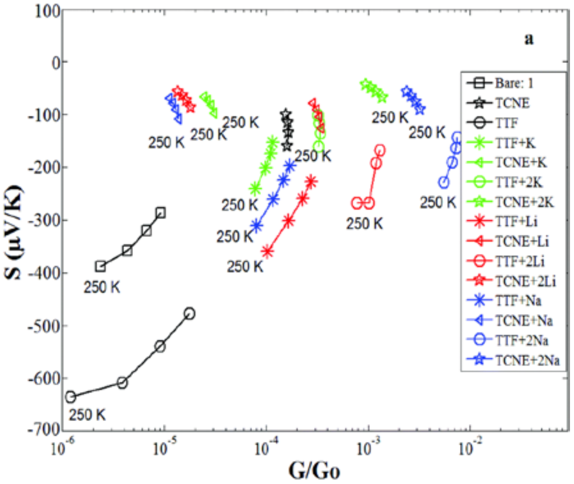

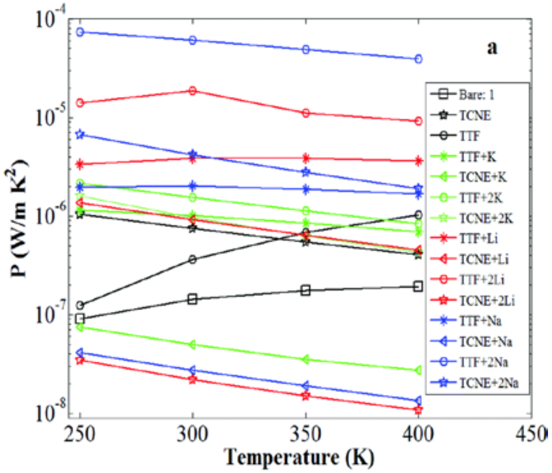

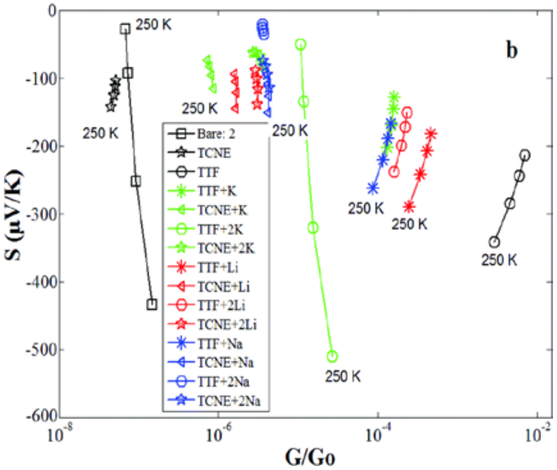

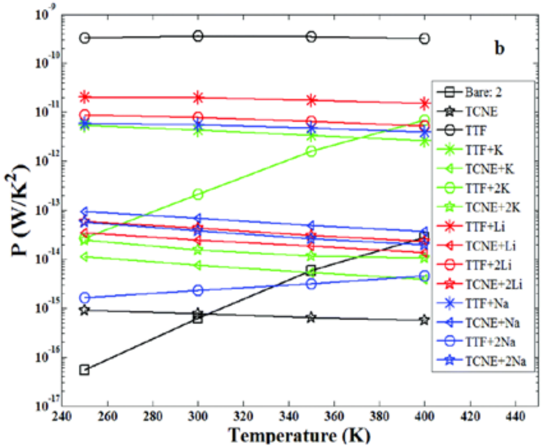

1 doped with TTF possesses S=−640 µV/K, which is higher than any single-molecule thermopower measured to date. At room temp. P= 73 µW m^{-1}K^{-2} for **1** + TTF + 2Na and 90 µW m^{-1}K^{-2} for **2** + TTF. These compare favourably with other organic materials. eg P = 0.016, 0.045 µW m^{-1}K^{-2} and 12 µW m^{-1}K^{-2} for Polyaniline , Polypyrole and PEDOT:PSS.

Thermoelectric properties of metallo-porphyrins

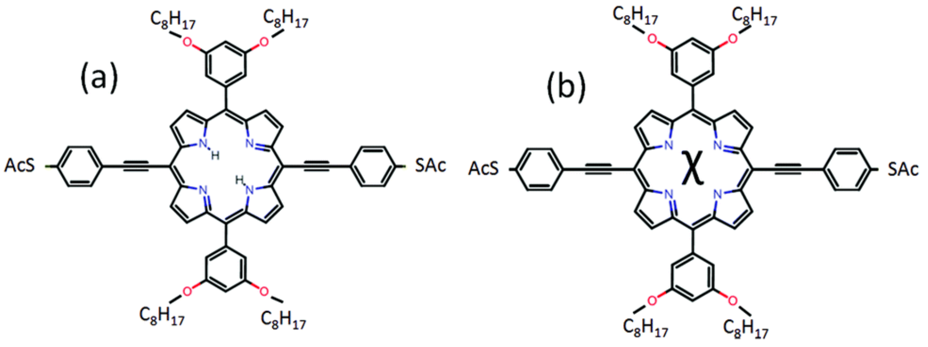

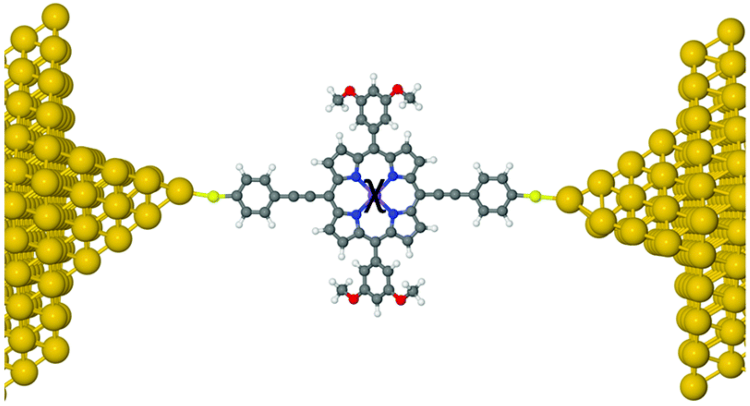

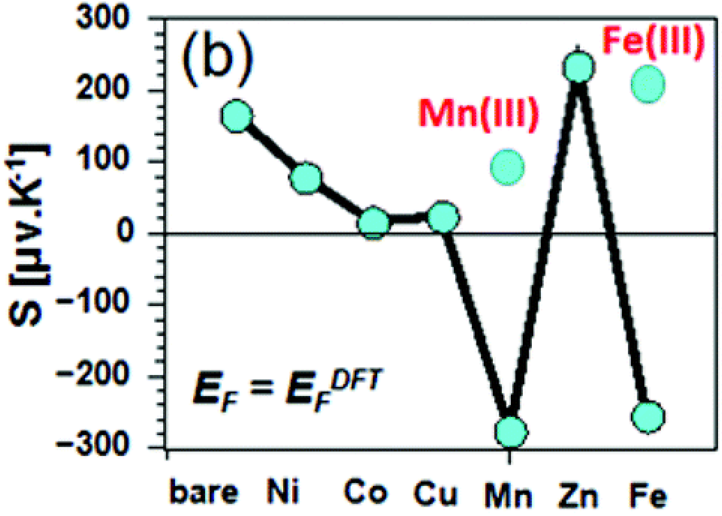

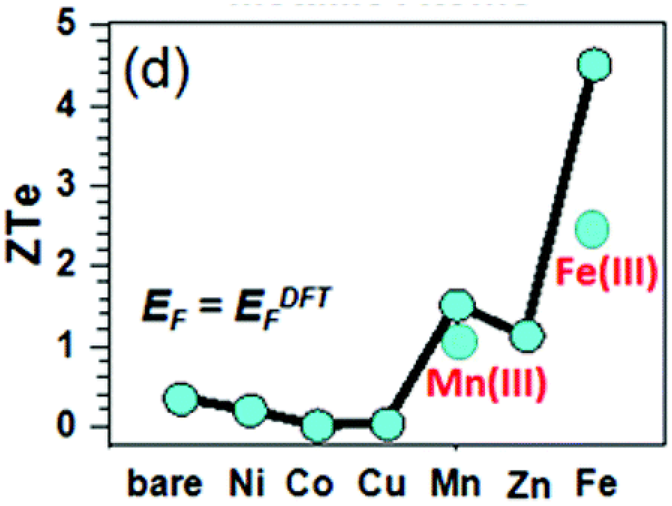

Al-Galiby et al., Nanoscale, 2016, 8, 2428

Reduction of thermal conductance by phonon engineering.

Length dependence of the thermal conductance of alkanes

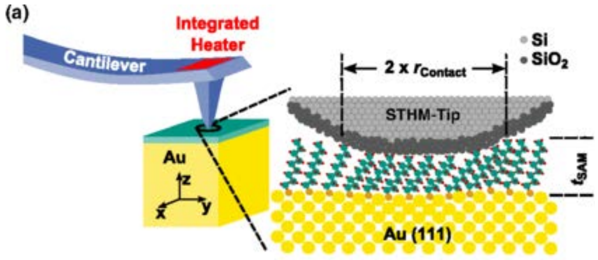

Surprise: κ_{ph} initially increases with length

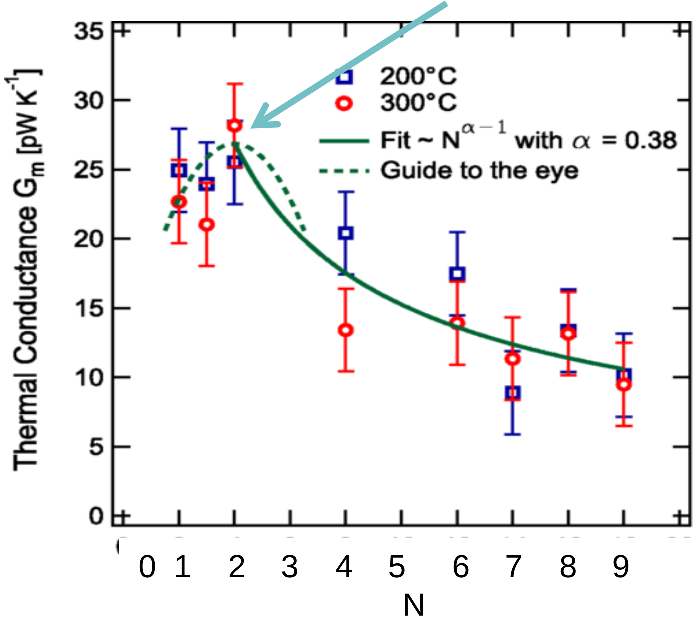

Experiment: Meier et al., Phys. Rev. Lett. (2014) 113, 060801

Theory reveals the origin of this effect

The effect is predicted to be absent for oligoynes

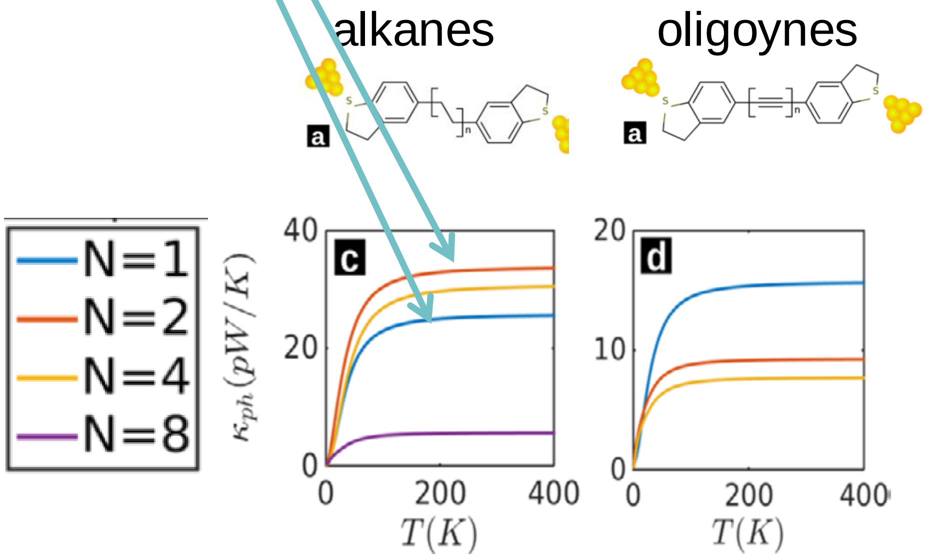

Theory: Sadeghi et al., Nano Lett. (2015) 15, 7467

High-performance thermoelectricity in edge-over-edge zinc-porphyrin molecular wires.

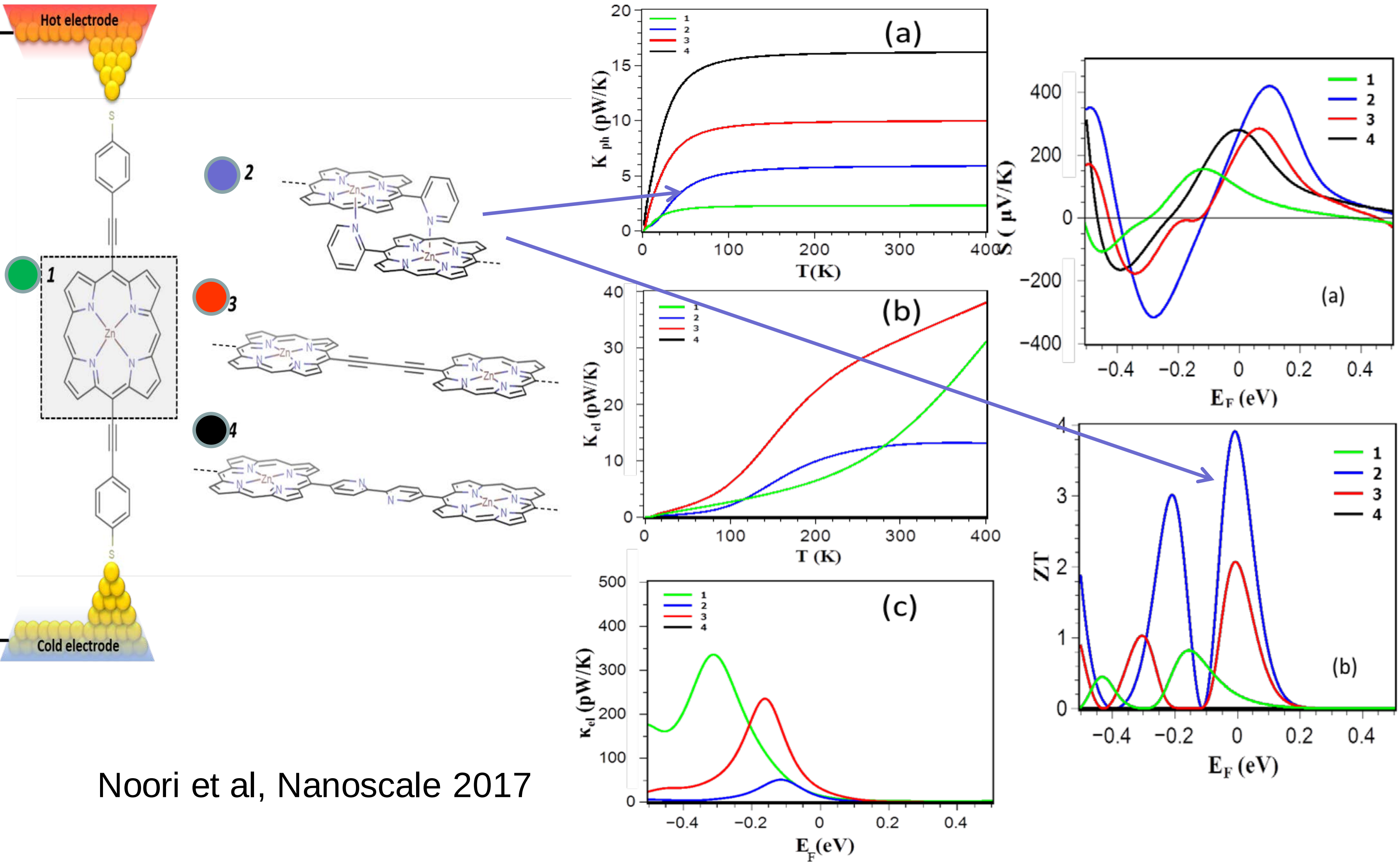

Noori et al, Nanoscale 2017

Can phonon interference effects be exploited to reduce thermal conductance?

Suppression of thermal conductance through molecular christmas trees

$T(\omega)=1/[1+x]$

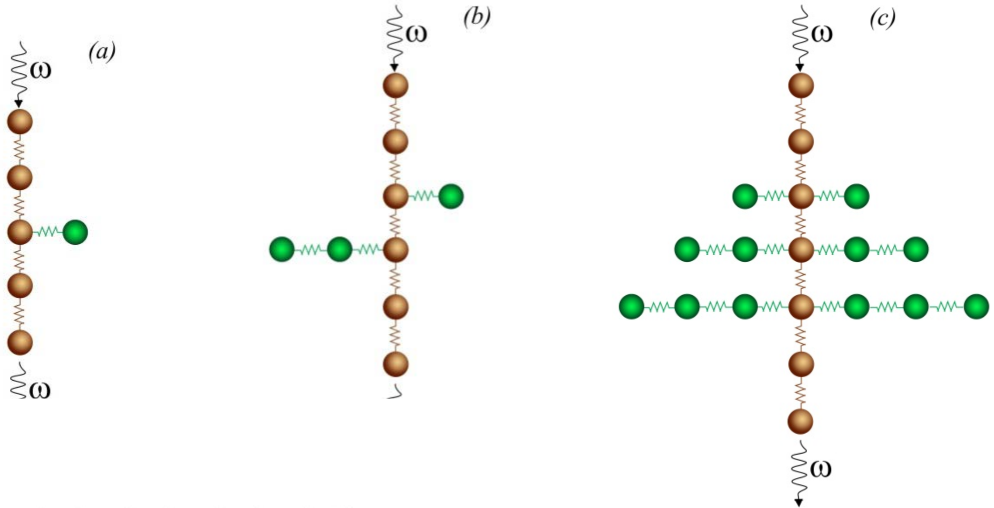

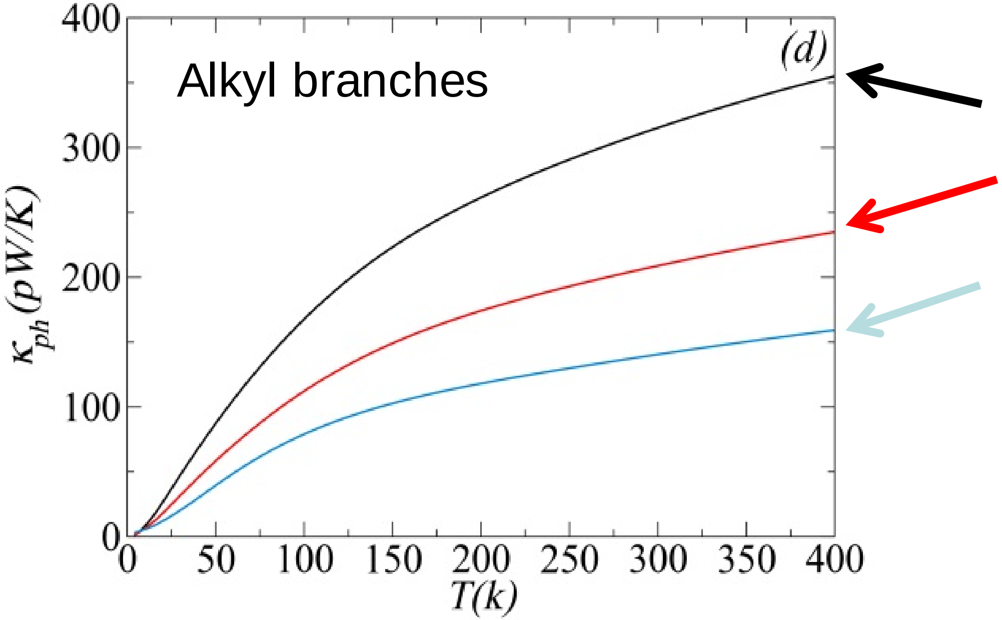

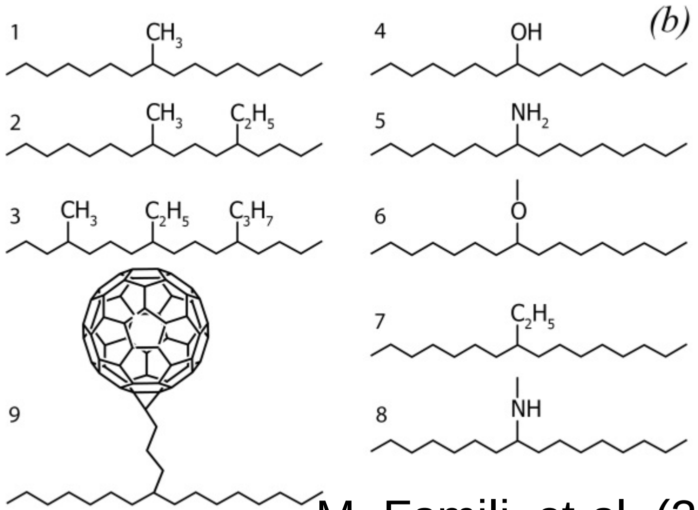

M. Famili, et al, (2017)

Can QI effects be translated into thin films?

Note: QI effects disappear when a molecule is too long.

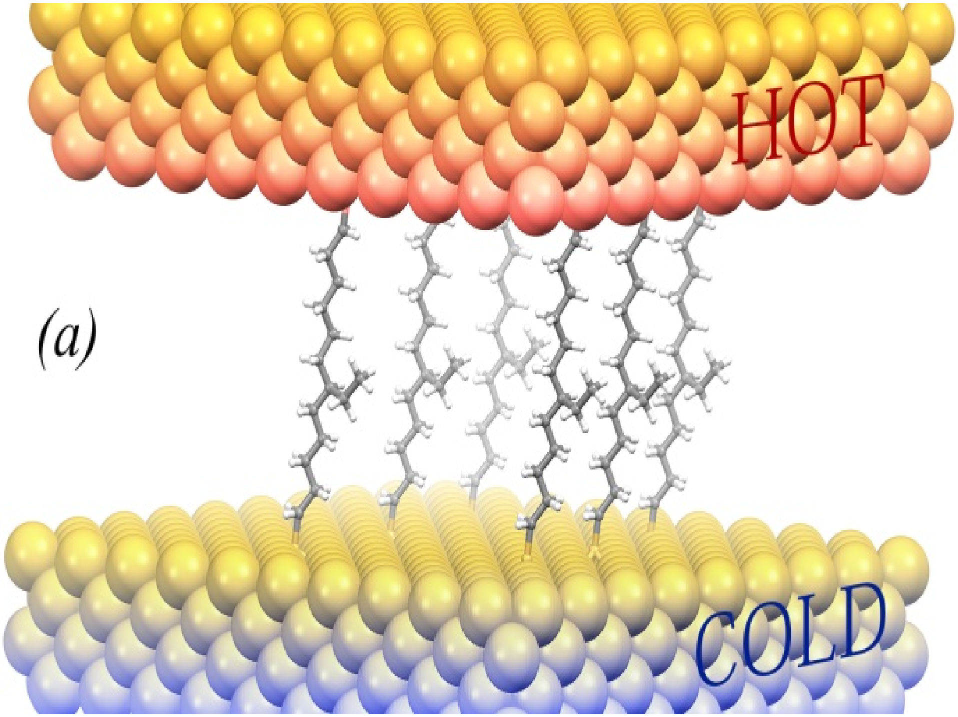

Phase-coherent tunneling for short molecules
G ~ exp –(βL)

Incoherent hopping for long molecules
G ~ 1/L

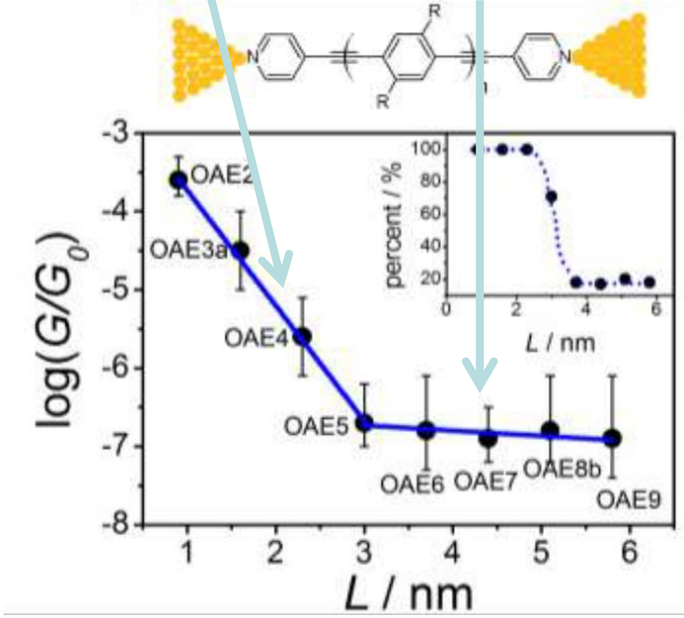

Zhao et al, Chem. of Mat., 25 21 4340 (2013)

Results for two C_{60}s in parallel

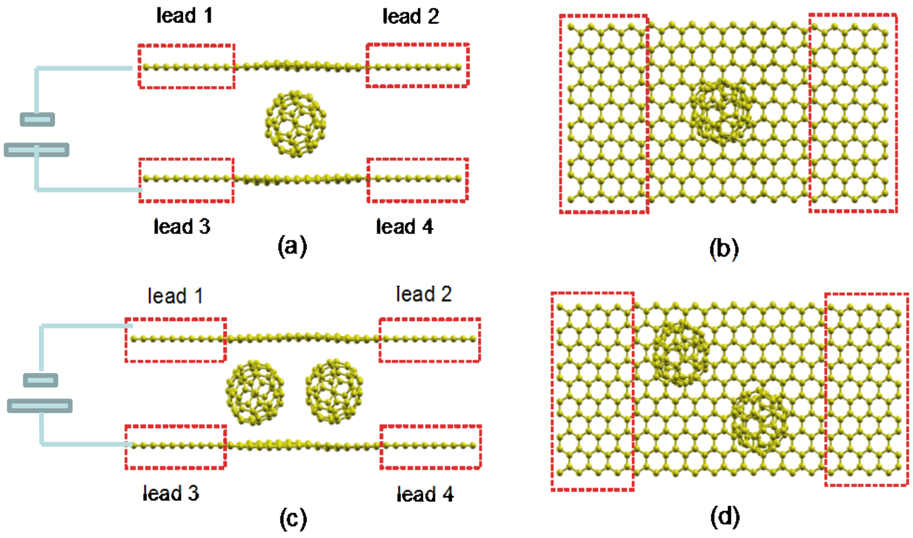

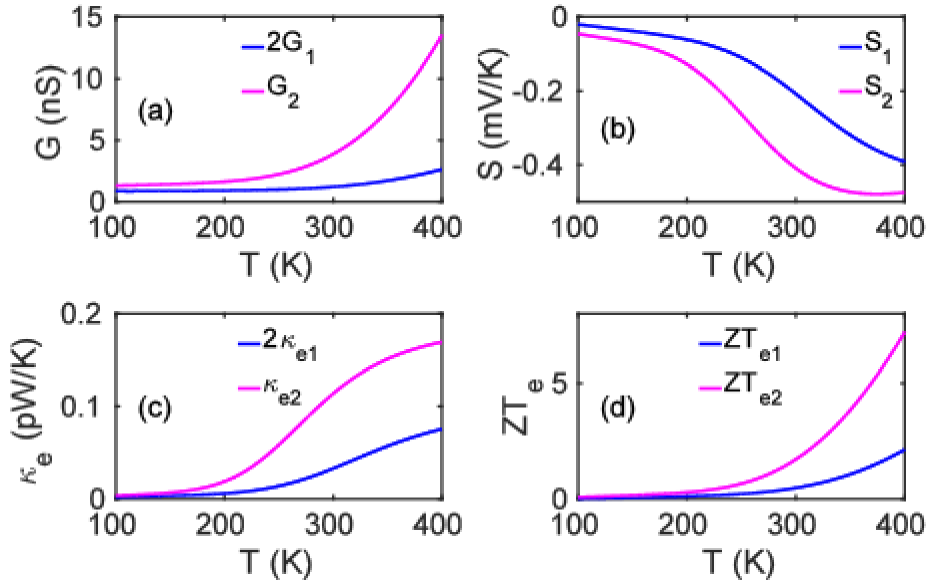

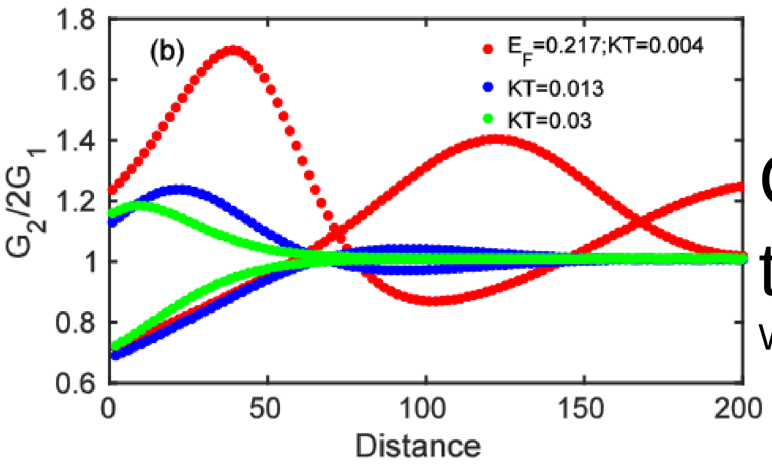

Conductance ratio oscillates with the spacing between the C_{60}s.

Wu et al. 2017

Summary

- QI in electroburnt graphene junctions
- Connectivity-driven electron transport
- Quantum circuit rules for single-molecule electrical junctions
- Fullerene-based thermoelectricity
- Thermoelectricity in crown-ether anthraquinones and metallo-porphyrins
- Suppression of phonon transport in molecular Christmas trees

Calculations were carried out by the following members of the Lancaster theory group: **Q. Wu, M. Famili**, H. Sadeghi, S. Bailey, I. Grace, S. Sangtarash, Q. Al-Galiby, D. Manrique, A. Ismael, M. Noori

Interference-induced thermoelectrics with quantum Hall edge states

Rafael Sánchez

Universidad Carlos III de Madrid

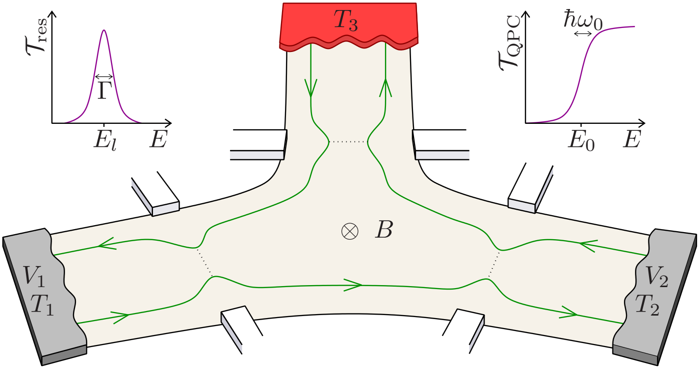

In collaboration with: Björn Sothmann (Genève → Duisburg)
Andrew N. Jordan (Rochester)

Dresden, 19 April, 2017

(Classical) Hall effect

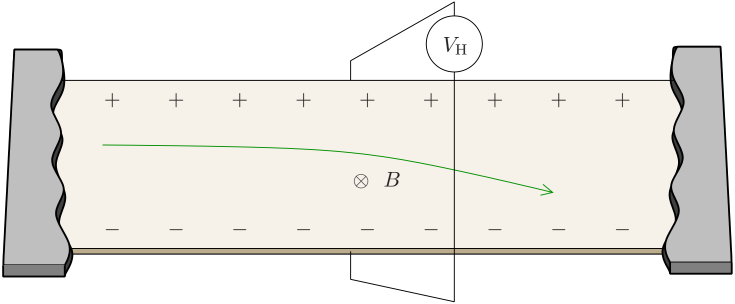

$$F = e(\overrightarrow{E} + \overrightarrow{v} \times \overrightarrow{B})$$

$$V_{\mathrm{H}} = -\alpha B I$$

Transverse resistance increases linearly with the magnetic field

Quantum Hall effect.

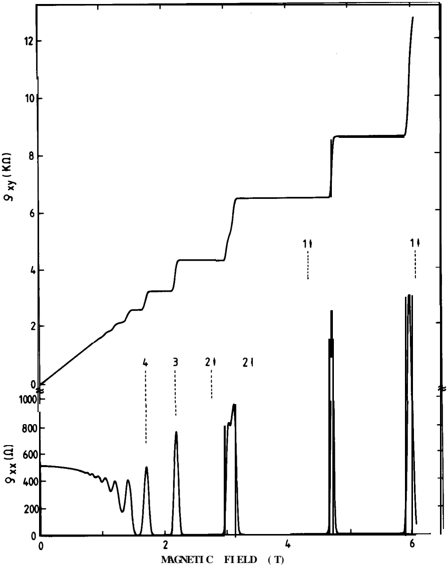

$$R_{\mathrm{H}} = \frac{h}{Ne^2}$$

K. von Klitzing, G. Dorda, M. Pepper, Phys. Rev. Lett. **45**, 494 (1980)
K. von Klitzing, Nobel lecture (1985)

Quantum Hall effect

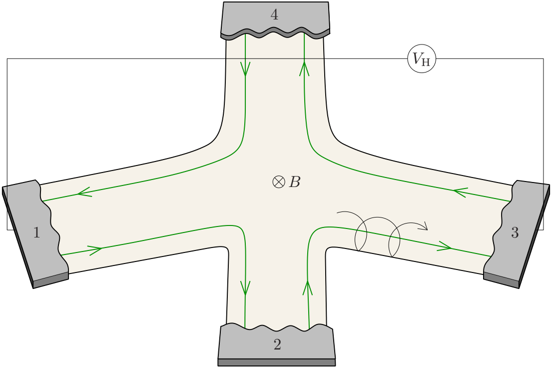

$$I_l^{\mathrm{e}} = \frac{e^2}{h}(V_l - V_{l-1})$$

1,3 are voltage probes

$$V_1 = V_4$$

$$V_3 = V_2$$

Charge conservation:

$$I_2 + I_4 = 0$$

$$I_4 = \frac{e^2}{h}(V_1 - V_3)$$

$$V_{\mathrm{H}} = V_1 - V_3 = \frac{h}{e^2} I$$

Propagation without backscattering along edge states

B. I. Halperin, Phys. Rev. B **25**, 2185 (1982)
M. Büttiker, Phys. Rev. B **38**, 9375 (1988)

Two terminal thermoelectrics

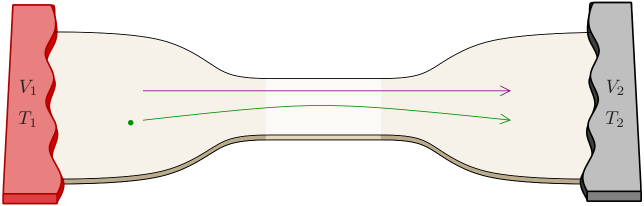

Charge current:

$$I_l^{\mathrm{e}} = \frac{e}{h}\int dE\,\mathcal{T}(E)[f_l(E) - f_{\bar{l}}(E)]$$

Heat current:

$$I_l^{\mathrm{h}} = \frac{1}{h}\int dE(E - E_{\mathrm{F}})\mathcal{T}(E)[f_l(E) - f_{\bar{l}}(E)]$$

$$f_l(E) = \left[1 + e^{(E-eV_l)/k_{\mathrm{B}}T_l}\right]^{-1}$$

U. Sivan and Y. Imry, Phys. Rev. B **33**, 551 (1986)

Seebeck effect

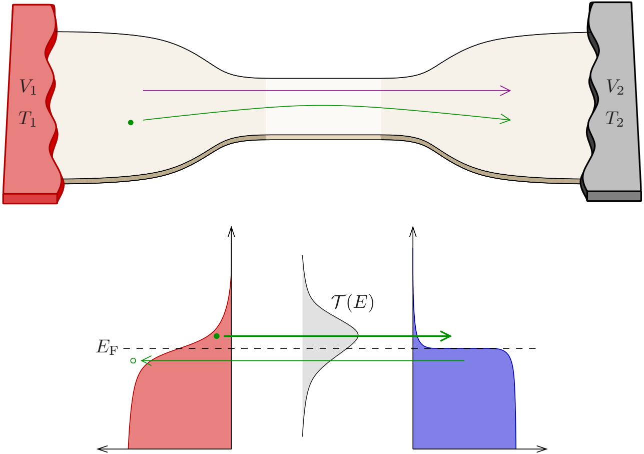

$$I^{\rm e}_l = \frac{e}{h}\int dE \mathcal{T}(E)(-\partial_E f(E))\left[eV_l + E\frac{T_l - T}{T}\right]$$

Useful for thermoelectric power generation

Onsager reciprocity relations

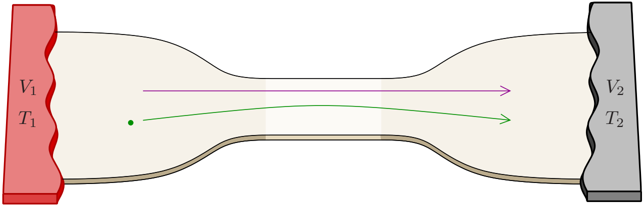

$$I_l^{\mathrm{e}} = G_{lj}\,\frac{eV_j}{k_{\mathsf{B}}T} + L_{lj}\,\frac{k_{\mathsf{B}}\Delta T_j}{(k_{\mathsf{B}}T)^2}$$

$$I_l^{\mathrm{h}} = M_{lj}\,\frac{eV_j}{k_{\mathsf{B}}T} + K_{lj}\,\frac{k_{\mathsf{B}}\Delta T_j}{(k_{\mathsf{B}}T)^2}$$

$$\frac{1}{e}L_{lj} = \frac{1}{T}M_{jl}$$ Seebeck ∼ Peltier

$$K_{lj} = K_{jl}$$ No thermal rectification

Three terminal thermoelectrics

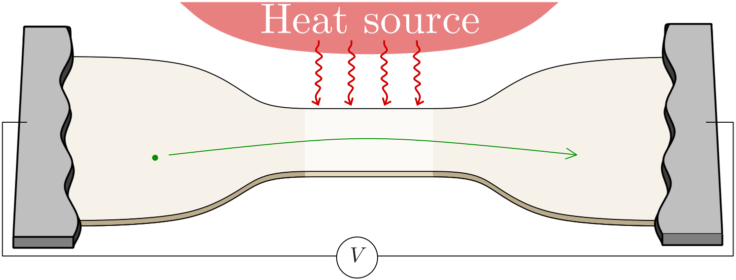

Energy harvesting demands **three terminal** devices

Separation of heat and charge currents

Three terminals. Mesoscopic thermocouple

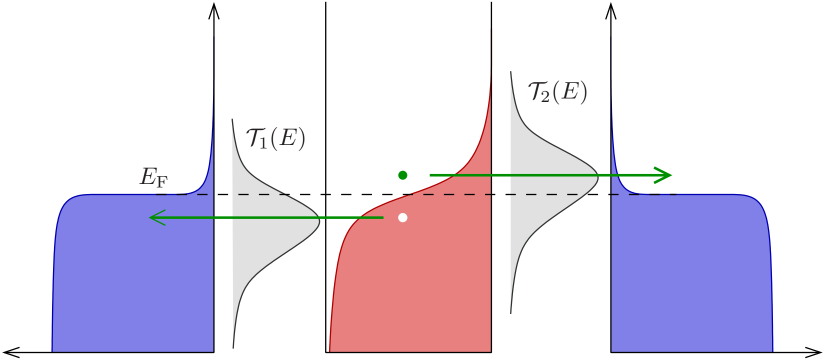

Separate electrons and holes with energy-dependent scattering

Mesoscopic Thermocouple:

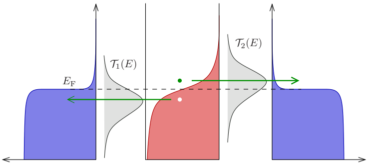

Resonant tunneling:

T. E. Humphrey, R. Newbury, R. P. Taylor, H. Linke, Phys. Rev. Lett. **89**, 116801 (2002)
A. N. Jordan, B. Sothmann, R. Sánchez, M. Büttiker, Phys. Rev. B **87**, 075312 (2013)
B. Sothmann, R. Sánchez, A. N. Jordan, M. Büttiker, New J. Phys. **15**, 095021 (2013)
Y. Choi, A. N. Jordan, Physica E **74**, 465 (2015)

Edge states:

R. Sánchez, B. Sothmann, A. N. Jordan, Phys. Rev. Lett. **114**, 146801 (2015)
New J. Phys. Rev. Lett. **17**, 075006 (2015)
Physica E **75**, 86 (2016)

Interaction based coupling to the heat source:

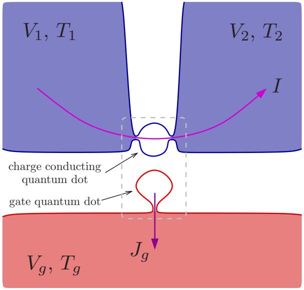

Coupled conductors:

R. Sánchez, and M. Büttiker, Phys. Rev. B **83**, 085428 (2011)
B. Sothmann, R. Sánchez, A. N. Jordan, M. Büttiker, Phys. Rev. B **85**, 205301 (2012)

Experiments:

H. Thierschmann *et al.*, Nature Nanotech. **10**, 854 (2015)
J. V. Koski *et al.*, Phys. Rev. Lett. **115**, 260602 (2015)
F. Hartmann *et al.*, Phys. Rev. Lett. **114**, 146805 (2015)
B. Roche *et al.*, Nature Comm. **6**, 6738 (2015)

Phonons:

O. Entin-Wohlman, Y. Imry, and A. Aharony, Phys. Rev. B **82**, 115314 (2010)

Photons:

T. Ruokola, T. Ojanen, Phys. Rev. B **86**, 035454 (2012)

Spins:

B. Sothmann, M. Büttiker, EPL **99**, 27001 (2012)

Review: B. Sothmann, R. Sánchez, A. N. Jordan, Nanotechnology **26**, 032001 (2015)

Scattering theory. Linear regime. No magnetic field

Terminal 3 is a probe: $I_3^e = 0$.
Assume $\mathcal{T}_3(E) = 1$.

$$G_l = \frac{e^2}{h} \int dE\ \mathcal{T}_l(E)\,(-\partial_E f)$$

$$S_l = \frac{e}{hTG_l} \int dE E\ \mathcal{T}_l(E)\,(-\partial_E f)$$

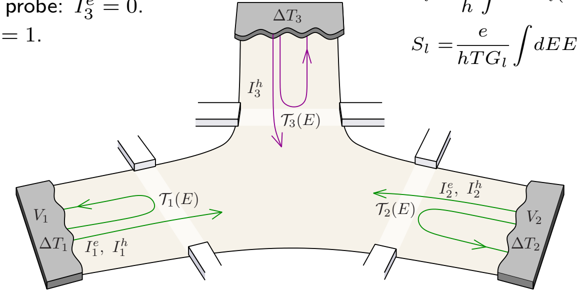

$$\begin{pmatrix} I^e \\ I_j^h \end{pmatrix} = \frac{1}{k_\mathrm{B}T} \begin{pmatrix} k_\mathrm{B}TG & L_{1i} \\ M_{j1} & K_{ji} \end{pmatrix} \begin{pmatrix} e(V_1 - V_2) \\ \Delta T_i/T \end{pmatrix}$$

$$G = \left(\frac{1}{G_1} + \frac{1}{G_2}\right)^{-1}$$

Onsager relates Seebeck and Peltier coefficients:

$$L_{ij} = eM_{ji}$$

Scattering theory. Linear regime. No magnetic field

Terminal 3 is a probe: $I_3^e = 0$.
Assume $\mathcal{T}_3(E) = 1$.

$$G_l = \frac{e^2}{h}\int dE\ \mathcal{T}_l(E)\,(-\partial_E f)$$

$$S_l = \frac{e}{hTG_l}\int dE E\ \mathcal{T}_l(E)\,(-\partial_E f)$$

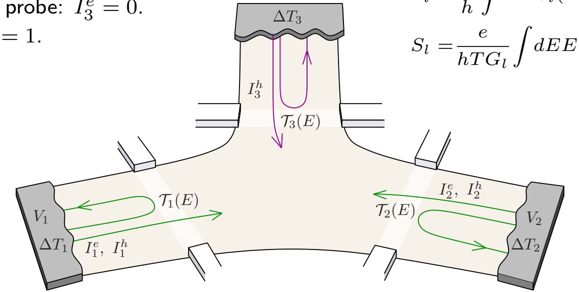

$$\begin{pmatrix} I^e \\ I_j^h \end{pmatrix} = \frac{1}{k_\mathrm{B}T}\begin{pmatrix} k_\mathrm{B}TG & L_{1i} \\ M_{j1} & K_{ji} \end{pmatrix}\begin{pmatrix} e(V_1 - V_2) \\ \Delta T_i/T \end{pmatrix}$$

$$G = \left(\frac{1}{G_1} + \frac{1}{G_2}\right)^{-1}$$

Energy harvesting:

$$L_{13} = k_\mathrm{B}T^2G(S_2 - S_1)$$

Energy harvesting if we break:

- **Left-right** symmetry
- **Particle-hole** symmetry

Scattering theory. Linear regime. No magnetic field

Terminal 3 is a probe: $I_3^e = 0$.
Assume $\mathcal{T}_3(E) = 1$.

$$G_l = \frac{e^2}{h}\int dE\ \mathcal{T}_l(E)\,(-\partial_E f)$$

$$S_l = \frac{e}{hTG_l}\int dE E\ \mathcal{T}_l(E)\,(-\partial_E f)$$

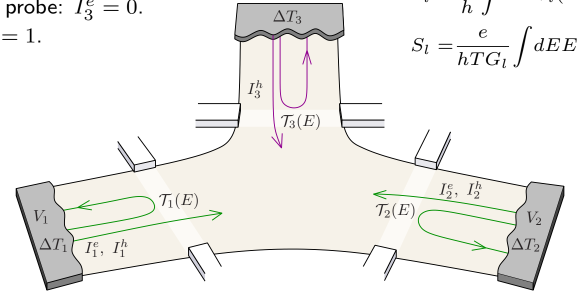

$$\begin{pmatrix} I^e \\ I_j^h \end{pmatrix} = \frac{1}{k_B T}\begin{pmatrix} k_B T G & L_{1i} \\ M_{j1} & K_{ji} \end{pmatrix}\begin{pmatrix} e(V_1 - V_2) \\ \Delta T_i / T \end{pmatrix}$$

$$G = \left(\frac{1}{G_1} + \frac{1}{G_2}\right)^{-1}$$

Energy harvesting:

$$L_{13} = k_B T^2 G(S_2 - S_1)$$

No thermal rectification:

$$K_{ij} = K_{ji}$$

(Onsager, again)

Edge states in the Quantum Hall regime

Terminal 3 is a probe: $I_3^e = 0$.
Assume $\mathcal{T}_3(E) = 1$.

$$G_l = \frac{e^2}{h}\int dE\ \mathcal{T}_l(E)\,(-\partial_E f)$$

$$S_l = \frac{e}{hTG_l}\int dE E\ \mathcal{T}_l(E)\,(-\partial_E f)$$

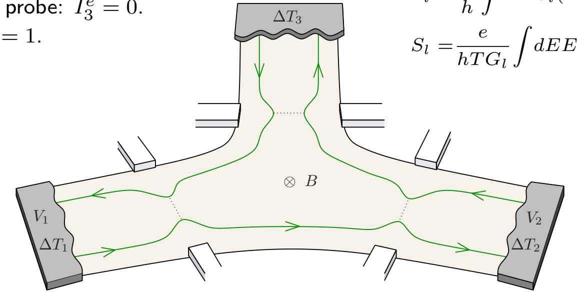

$$G = \frac{1}{\Lambda}\left(\frac{1}{G_1}+\frac{1}{G_2}\right)^{-1}$$

$$\Lambda = 1 - J_1/(G_1+G_2)$$

$$J_n = \frac{e^2}{hk_{\mathsf{B}}T}\int dE E^{n-1}\mathcal{T}_1(E)\mathcal{T}_2(E)\,(-\partial_E f)\,,$$

Energy harvesting:

$$L_{13} = k_{\mathsf{B}}T^2G(S_2 - S_1) + e\mathcal{X}_1$$

$$\mathcal{X}_l = \frac{k_{\mathsf{B}}T}{e^2}\frac{GG_l}{G_1G_2}\,(eTS_lJ_1 - J_2)$$

Current in symmetric configurations!

Chiral (crossed) thermopower

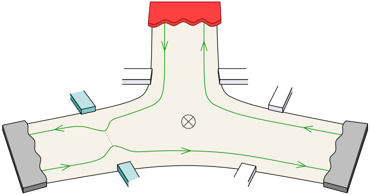

$$\left.\begin{array}{l} S_2 = 0 \\ \mathcal{X}_1 = 0 \end{array}\right\} \Rightarrow L_{13}(B) = ek_{\mathsf{B}}T^2 G_1 S_1$$

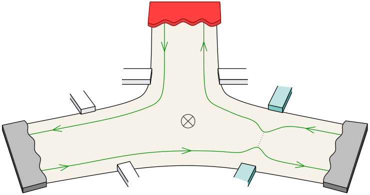

$$\left.\begin{array}{l} S_1 = 0 \\ \mathcal{X}_1 = -ek_{\mathsf{B}}T^2 G_2 S_2 \end{array}\right\} \Rightarrow L_{13}(B) = 0$$

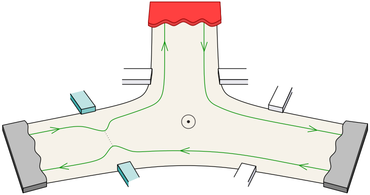

$$\left.\begin{array}{l} S_2 = 0 \\ \mathcal{X}_2 = -ek_{\mathsf{B}}T^2 G_1 S_1 \end{array}\right\} \Rightarrow L_{13}(-B) = 0$$

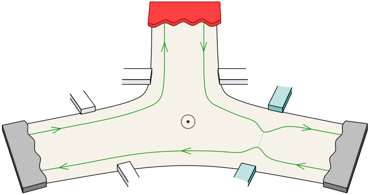

$$\left.\begin{array}{l} S_1 = 0 \\ \mathcal{X}_2 = 0 \end{array}\right\} \Rightarrow L_{13}(-B) = ek_{\mathsf{B}}T^2 G_2 S_2$$

Thermoelectric spin polarization of topological insutators

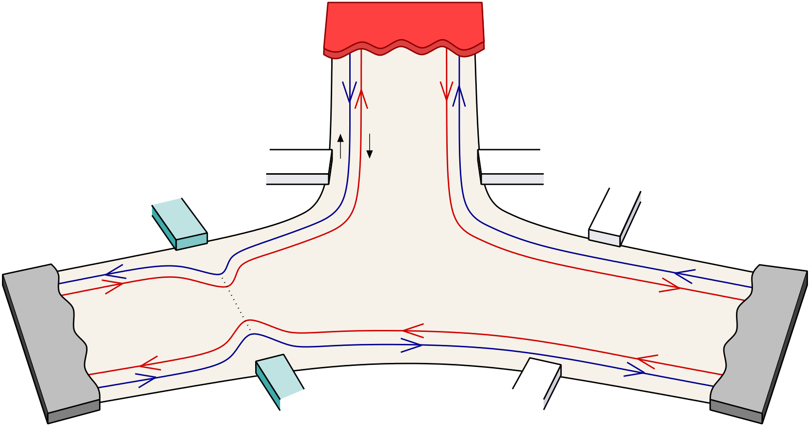

Spin polarization controlled by the QPCs

R. Sánchez, B. Sothmann, A.N. Jordan, Phys. Rev. Lett. **114**, 146801 (2015)

Crossed (non-local) thermoelectrics.

Two QPCs modeled as step transmission:

$$\mathcal{T}_l(E) = \left[1 + e^{-2\pi(E-E_l)/\hbar\omega_l}\right]^{-1}$$

position of the step: E_l

broadening: $\hbar\omega$

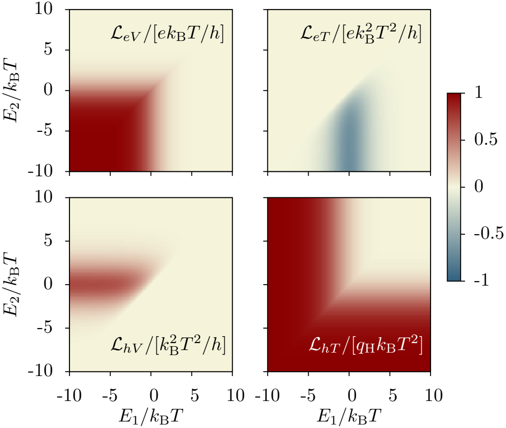

- Oscillation of Seebeck or Peltier coefficients with a noisy QPC. . .

  P. Streda, J. Phys.: Condens. Matt. **1**, 1025 (1989)

  L. W. Molenkamp *et al.*, Phys. Rev. Lett. **68**, 3765 (1992)

  . . . but only one!
- Extreme Seebeck to Peltier asymmetry

Thermoelectric performance:

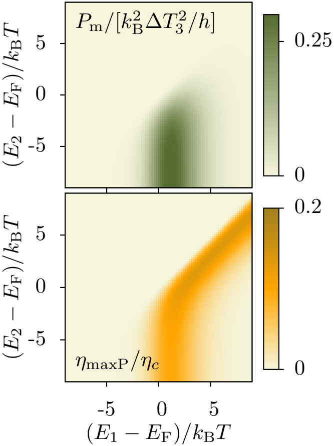

Maximum power: $P_\mathrm{m} = I_l^\mathrm{e}(V_\mathrm{m})V_\mathrm{m}$

Efficiency at maximum power: $\eta_\mathrm{maxP} = \dfrac{P_\mathrm{m}}{I_l^h(V_\mathrm{m})}$

Carnot efficiency: $\eta_C = 1 - \dfrac{T}{T_3}$

(With resonances: $\eta_\mathrm{maxP} \approx 0.5\eta_C$)

R. Sánchez, B. Sothmann, A.N. Jordan, New J. Phys. **17**, 075006 (2015)

Thermal rectification. Turning heat around the bend

$$\mathcal{R}_{12} = \frac{K_{12}}{K_{21}}$$

$\mathcal{R}_{12} = 1$: No thermal rectification

$|\ln \mathcal{R}_{12}| \gg 1$: Thermal diode

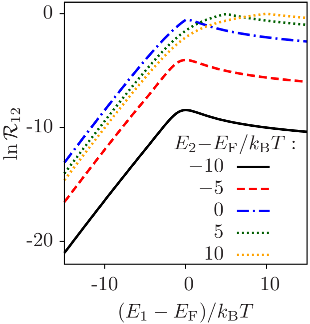

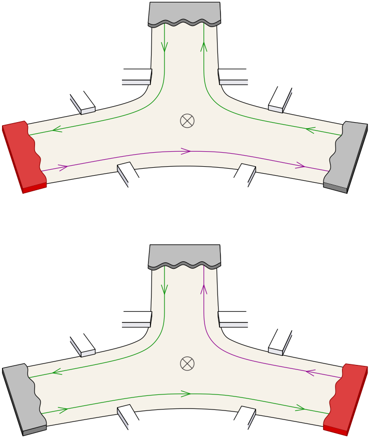

Thermal rectification. Turning heat around the bend

$$\mathcal{R}_{12} = \frac{K_{12}}{K_{21}}$$

$\mathcal{R}_{12} = 1$: No thermal rectification

$|\ln \mathcal{R}_{12}| \gg 1$: Thermal diode

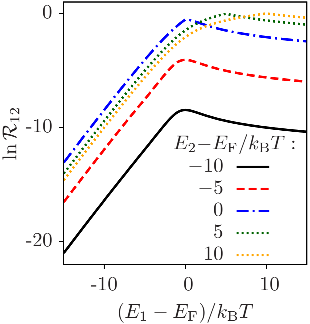

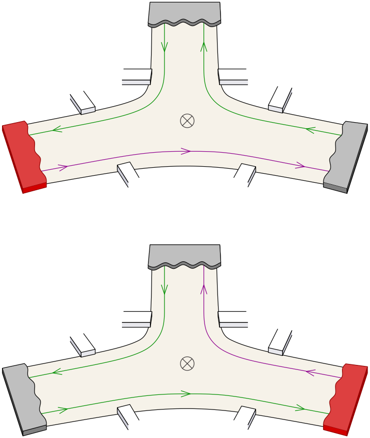

An ideal thermal diode!

R. Sánchez, B. Sothmann, A. N. Jordan, New J. Phys. **17**, 075006 (2015)

Two-path thermoelectric interferometers

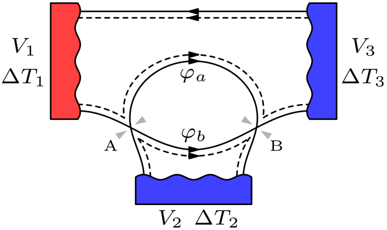

$$\varphi = \phi_{\mathrm{A-B}} + \frac{L_a - L_b}{v_D \hbar} E$$

P. P. Hofer, B. Sothmann, Phys. Rev. B **91**, 195406 (2015)

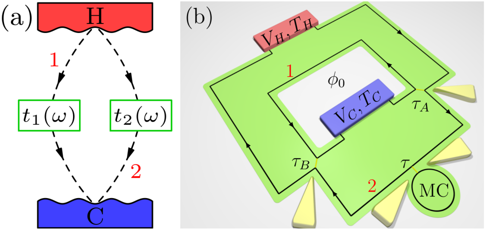

P. Samuelsson, S. Kheradsoud, B. Sothmann, arXiv:1611.02997 (2015)

(Three terminal) Fabry-Pérot thermoelectric interferometers

B. J. van Wees *et al.*, Phys. Rev. Lett. **62**, 2523 (1989)
Y. Zhang *et al.*, Phys. Rev. B **79**, 241304 (2009)
A. Kou *et al.*, Phys. Rev. Lett. **108**, 256803 (2012)
N. Pascher *et al.*, Phys. Rev. B **89**, 245408 (2014)

Breit-Wigner resonance: $\mathcal{A}_{ij} = \dfrac{\Gamma_i\Gamma_j}{(E-E_\mathrm{r})^2+\Gamma^2/4}$

M. Büttiker, Phys. Rev. B **38**, 12724 (1988)

$$g_{ij} = \frac{e^2}{hk_\mathsf{B}T}\int dE\mathcal{A}_{ij}\xi(E) \qquad s_{ij} = \frac{e^2}{hg_{ij}k_\mathsf{B}T^2}\int dE\mathcal{A}_{ij}E\xi(E)$$

Assume energy-independent Γ_i

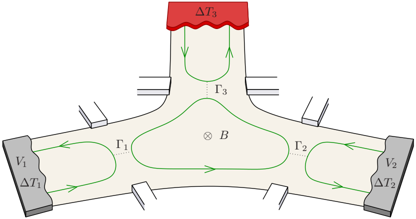

$$L_{13} = 0$$

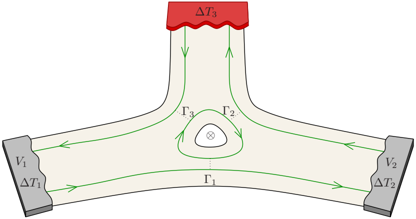

$$L_{13} = k_\mathsf{B}T^2\frac{g_0g_{13}}{g_0-g_{23}}s_{13} \neq 0$$

R. Sánchez, B. Sothmann, A. N. Jordan, New J. Phys. **17**, 075006 (2015)

Conclusions

- Chirality detected by thermoelectric measurements
- Three terminal junctions separate heat and charge flows
- Edge states permit the manipulation of heat currents in micrometer distances
- Extreme asymmetries of Onsager matrix

- Powerful and efficient **energy harvesting** in the crossed response
- Ideal **thermal diodes** in the longitudinal terms

- Manipulation of spin polarized currents in topological insulators

- Interference induced thermoelectrics

- Very few experiments:

  G. Granger, J. P. Eisenstein, J. L. Reno, Phys. Rev. Lett. **102**, 086803 (2009)

  S.-G. Nam, E. H. Hwang, and H.-J. Lee, Phys. Rev. Lett. **110**, 226801 (2013)

R. Sánchez, B. Sothmann, A.N. Jordan, Phys. Rev. Lett. **114**, 146801 (2015)
R. Sánchez, B. Sothmann, A.N. Jordan, New J. Phys. **17**, 075006 (2015)
R. Sánchez, B. Sothmann, A.N. Jordan, Physica E **75**, 86 (2016)

B. Sothmann, R. Sánchez, A.N. Jordan, Europhys. Lett. **107**, 47003 (2014)

Peltier effect

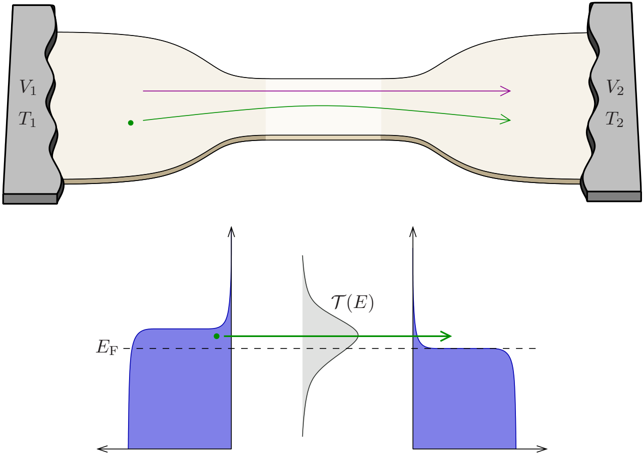

$$I_l^h = \frac{1}{2h}\int dE E \mathcal{T}(E)(-\partial_E f(E))\left[eV_l + E\frac{T_l - T}{T}\right]$$

Useful for refrigeration

Thermoelectrics with edge states

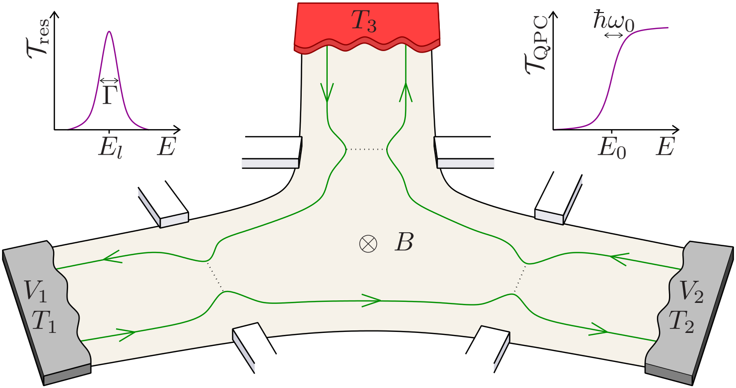

Separate left and right moving electrons

$$\mathcal{O}_{ij}(B) = \mathcal{O}_{ji}(-B)$$

Extreme Seebeck to Peltier asymmetry

Seebeck:

$$L_{13}(B) = ek_{\mathsf{B}}T^2G_1S_1$$

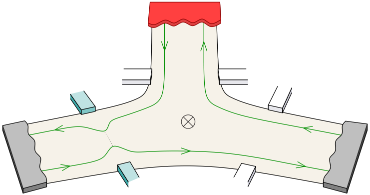

Peltier:

$$M_{31}(B) = L_{13}(-B) = 0$$

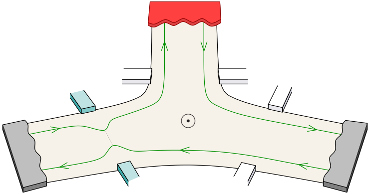

Onsager:

$$M_{ij}(B) = L_{ji}(-B)$$

$$\frac{L_{13}(B)}{M_{31}(B)} = \infty$$

R. Sánchez, B. Sothmann, A.N. Jordan, Phys. Rev. Lett. **114**, 146801 (2015)

Quantum Nernst engines

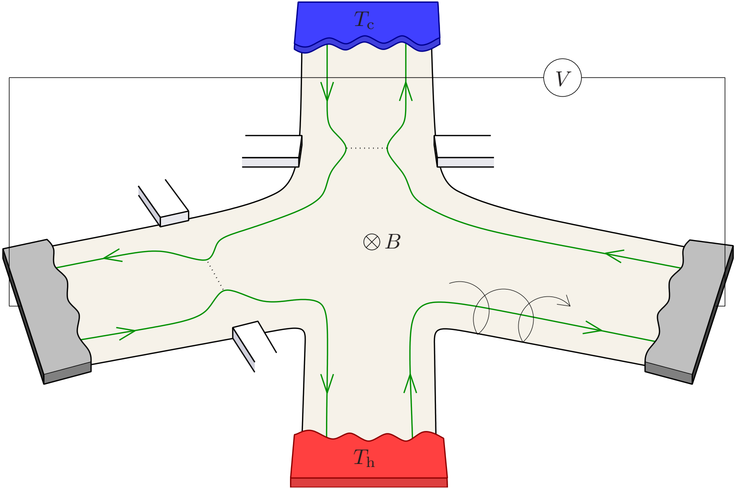

Inject only heat. Measure only charge.

Quantum Nernst engines

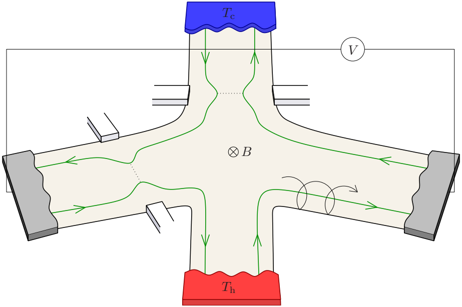

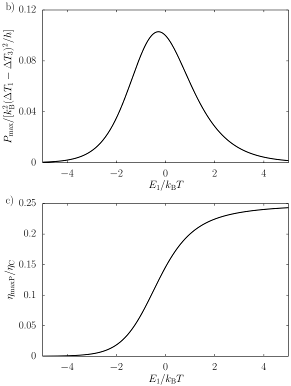

Boundary conditions:

$I_1^h = I_3^h = 0$

$I_2^e = I_4^e = 0$

$$L \neq 0$$

$$M = 0$$

Classical Nernst engine: $\eta_{\mathrm{maxP}} \leq \eta_c/6$

J. Stark, K. Brander, U. Seifert, Phys. Rev. Lett. **112**, 140601 (2014)

Quantum Nernst engine: $\eta_{\mathrm{maxP}} \leq \eta_c/4$

B. Sothmann, R. Sánchez, A.N. Jordan, Europhys. Lett. **107**, 47003 (2014)

Effect of inelastic scattering

Add a voltage probe:

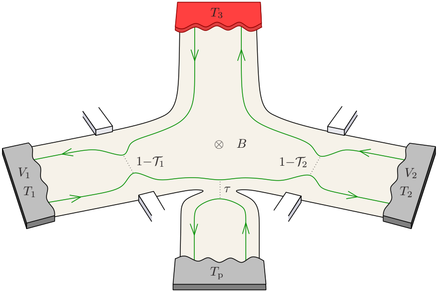

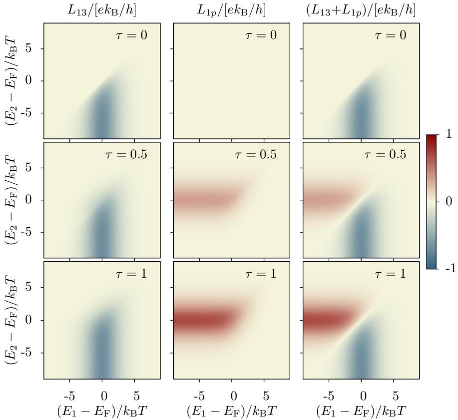

$$L_{13} = k_\mathsf{B} T^2 G(S_2 - S_1) - L_{1p} + (1-\tau)e\mathcal{X}_1$$

$$L_{1p} = \tau G S_2$$

R. Sánchez, B. Sothmann, A.N. Jordan, Physica E **75**, 86 (2016)

Effect of inelastic scattering

Add a voltage probe:

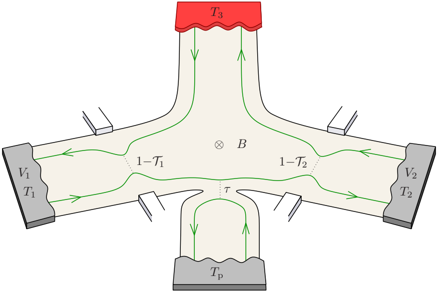

Thermal rectification:

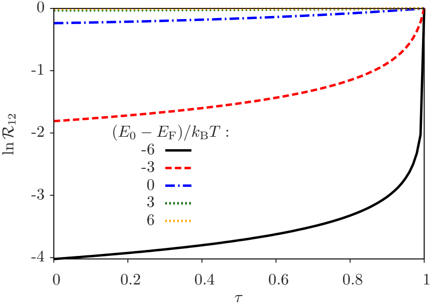

Heat diode effect up to $\tau \sim 99\%$

R. Sánchez, B. Sothmann, A.N. Jordan, Physica E **75**, 86 (2016)

Crossed thermoelectrics

Extreme Seebeck to Peltier asymmetry!

$$\mathcal{L}_{13}^{eT}(B) = ek_{\mathsf{B}}T^2G_1S_1 \qquad \mathcal{L}_{31}^{hV}(B) = \mathcal{L}_{13}^{eT}(-B) = 0$$

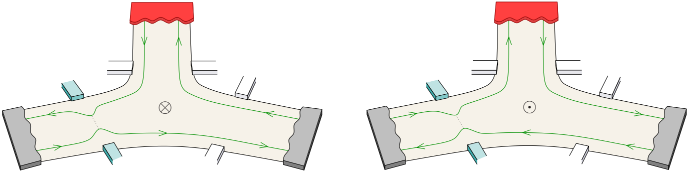

$$\frac{\mathcal{L}_{13}^{eT}(B)}{\mathcal{L}_{31}^{hV}(B)} = \infty$$

Crossed response for symmetric configurations: $\mathcal{L}_{13}^{eT} = e\mathcal{X}_1$

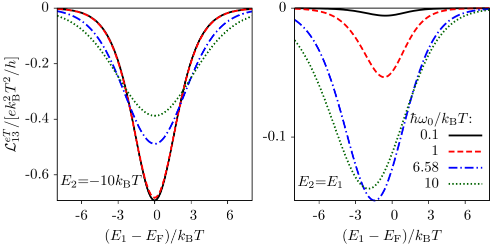

R. Sánchez, B. Sothmann, A.N. Jordan, Phys. Rev. Lett. **114**, 146801 (2015)

Thermoelectric motor

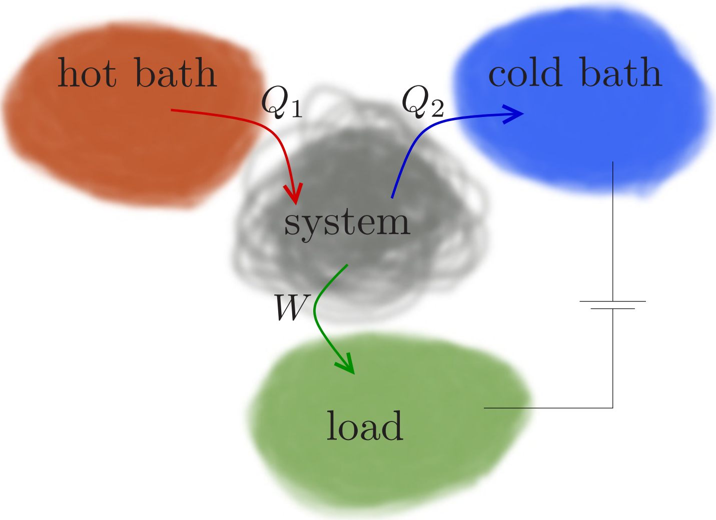

Energy harvesting demands **three terminal** devices

Quantum Hall effect

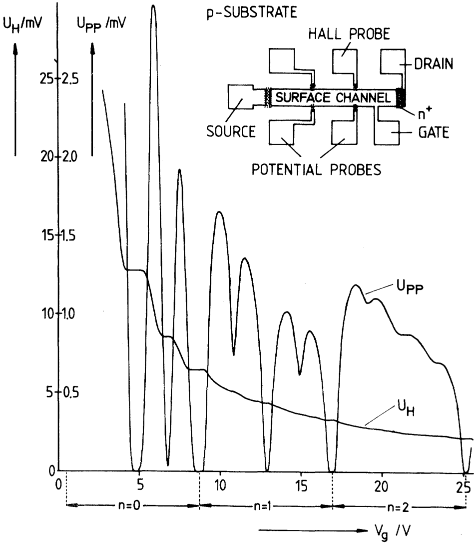

K. von Klitzing, G. Dorda, M. Pepper, Phys. Rev. Lett. **45**, 494 (1980)

Thermal rectification.

$$\mathcal{R}_{ij} = \frac{\mathcal{L}_{ij}^{hT}}{\mathcal{L}_{ji}^{hT}}$$

$\mathcal{R}_{ij} = 1$: No thermal rectification

$|\ln \mathcal{R}_{ij}| \gg 1$: Thermal diode

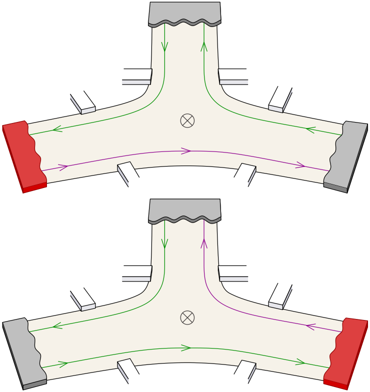

$$\mathcal{R}_{12} = \frac{1}{1 - A_{12}(J_2, J_3)}$$

$$\mathcal{R}_{13} = [1 - B_{13}(J_2, J_3)]^{-1}$$

$$\mathcal{R}_{23} = 1 - B_{23}(J_2, J_3)$$

Heat diode

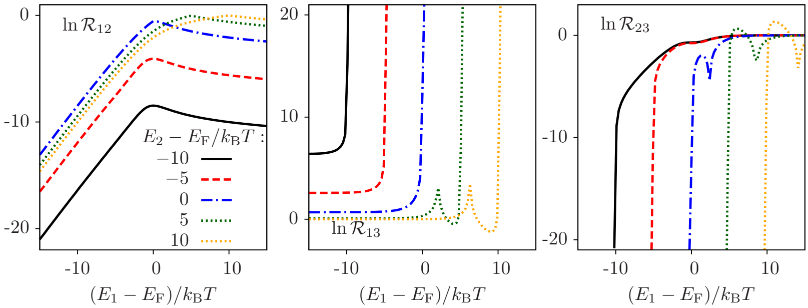

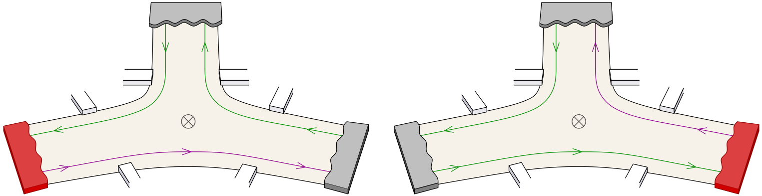

R. Sánchez, B. Sothmann, A.N. Jordan, arXiv:1503:02926

Back to three terminals

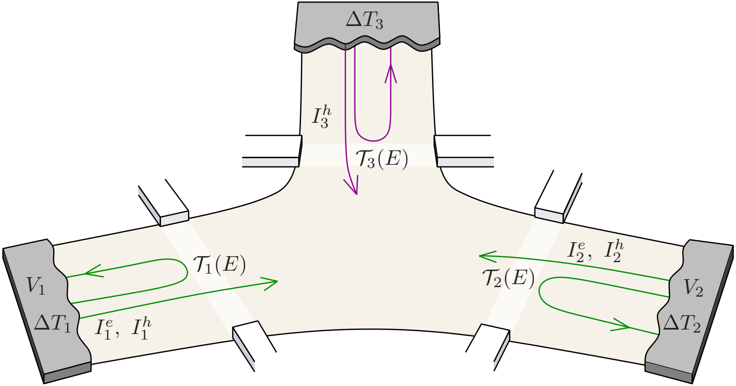

Quantum point contacts. Onsager matrix

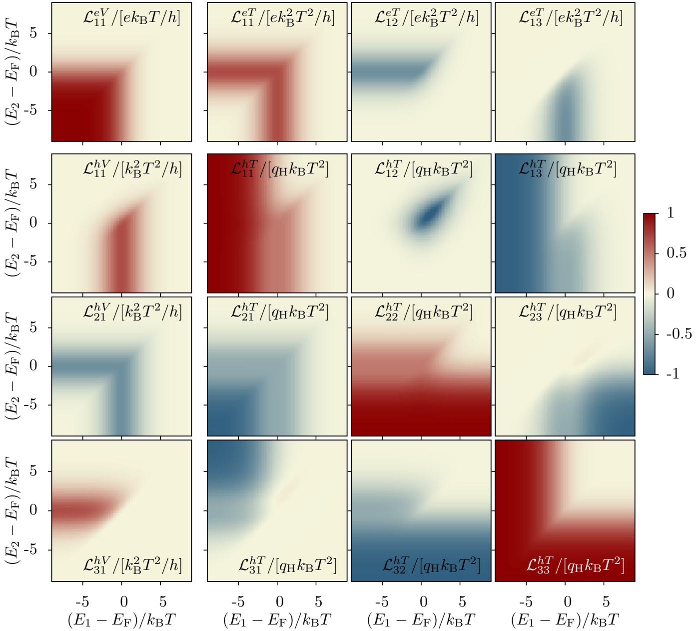

Quantum transport with dephasing: coherent to incoherent crossover

Dmitry A. Ryndyk
with Patrick Karasch and Thomas Frauenheim
Bremen Center for Computational Materials Science (BCCMS)
Department of Physics
University of Bremen

Workshop "Many paths to interference"
Dresden, 18 April 2017

When quantum transport *with dephasing* is important?

2DEG (GaAs,Si) at low temperatures

$\lambda \approx 0.05\ \mu m = 50\ nm$
$l_p \approx 0.5\ \mu m$
$l_\varphi \approx 1\ \mu m$
$l_\varepsilon \approx 3\ \mu m$

Au at $T = 1$ K

$l_\varphi \approx 1\ \mu m$

CNT(10,0) at room temperature

$m^* \approx 0.1 - 0.5\ m_e$
$l_\varphi \approx 100\ nm$
$l_\varepsilon \approx 1\ \mu m$

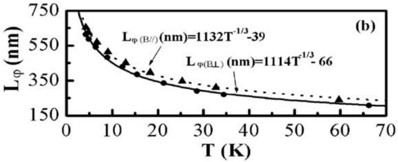

P. Avouris *Chem. Phys.* **281**, 429 (2002)

- Interference
- Coherent to incoherent crossover and Ohmic limit
- Material parameters from first principles

Atomistic quantum transport beyond DFT/Landauer

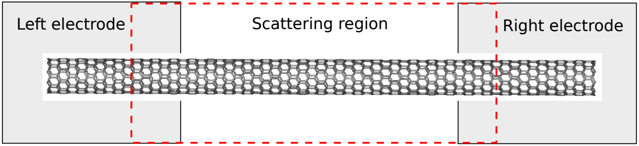

$$I(V)=\frac{e}{h}\int_{-\infty}^{\infty}T(E,V)\left[f_0(E+eV)-f_0(E)\right]dE$$

Atomistic quantum transport beyond DFT/Landauer

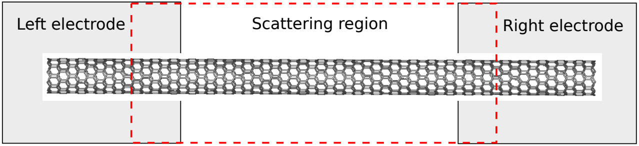

$$I(V) = \frac{e}{h}\int_{-\infty}^{\infty} T(E,V)\left[f_0(E+eV) - f_0(E)\right]dE$$

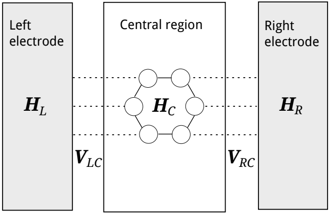

$$\boldsymbol{H} = \begin{pmatrix} \boldsymbol{H}_L & \boldsymbol{V}_{LC} & 0 \\ \boldsymbol{V}_{CL} & \boldsymbol{H}_C & \boldsymbol{V}_{CR} \\ 0 & \boldsymbol{V}_{RC} & \boldsymbol{H}_R \end{pmatrix}$$

$$\boldsymbol{G}_C^R(E) = \left[(E+i\eta)\boldsymbol{I} - \boldsymbol{H}_C - \boldsymbol{\Sigma}_L(E) - \boldsymbol{\Sigma}_R(E)\right]^{-1}$$

$$T(E) = \mathrm{Tr}\left[\boldsymbol{\Gamma}_L(E)\boldsymbol{G}_C^R(E)\boldsymbol{\Gamma}_R(E)\boldsymbol{G}_C^A(E)\right]$$

Elastic dephasing (self-energy models)

$$\boldsymbol{G}_C^R(\varepsilon) = \left[(\varepsilon + i\eta)\boldsymbol{I} - \boldsymbol{H}_C - \boldsymbol{\Sigma}_L^R(\varepsilon) - \boldsymbol{\Sigma}_R^R(\varepsilon) - \boldsymbol{\Sigma}_{deph}^R(\varepsilon)\right]^{-1},$$

$$\boldsymbol{\Sigma}_{deph}^R(\varepsilon) \sim i\gamma(\varepsilon) \text{ or } \gamma^2(\varepsilon)\boldsymbol{G}_C^R(\varepsilon)$$

Elastic dephasing (self-energy models)

$$\boldsymbol{G}_C^R(\varepsilon) = \left[(\varepsilon + i\eta)\boldsymbol{I} - \boldsymbol{H}_C - \boldsymbol{\Sigma}_L^R(\varepsilon) - \boldsymbol{\Sigma}_R^R(\varepsilon) - \boldsymbol{\Sigma}_{deph}^R(\varepsilon)\right]^{-1},$$

$$\boldsymbol{\Sigma}_{deph}^R(\varepsilon) \sim i\gamma(\varepsilon) \text{ or } \gamma^2(\varepsilon)\boldsymbol{G}_C^R(\varepsilon)$$

Current through a nanosystem (Meir-Wingreen formula)

$$I_{s=L(R)} = \frac{ie}{\hbar}\int \frac{d\varepsilon}{2\pi}\mathrm{Tr}\left\{\tilde{\boldsymbol{\Gamma}}_s(\varepsilon - e\varphi_s)\left(\boldsymbol{G}_C^<(\varepsilon) + f_s^0(\varepsilon - e\varphi_s)\left[\boldsymbol{G}_C^R(\varepsilon) - \boldsymbol{G}_C^A(\varepsilon)\right]\right)\right\}.$$

Elastic dephasing (self-energy models)

$$\boldsymbol{G}_C^R(\varepsilon) = \left[(\varepsilon + i\eta)\boldsymbol{I} - \boldsymbol{H}_C - \boldsymbol{\Sigma}_L^R(\varepsilon) - \boldsymbol{\Sigma}_R^R(\varepsilon) - \boldsymbol{\Sigma}_{deph}^R(\varepsilon)\right]^{-1},$$

$$\boldsymbol{\Sigma}_{deph}^R(\varepsilon) \sim i\gamma(\varepsilon) \text{ or } \gamma^2(\varepsilon)\boldsymbol{G}_C^R(\varepsilon)$$

Current through a nanosystem (Meir-Wingreen formula)

$$I_{s=L(R)} = \frac{ie}{\hbar}\int\frac{d\varepsilon}{2\pi}\mathrm{Tr}\left\{\tilde{\boldsymbol{\Gamma}}_s(\varepsilon - e\varphi_s)\left(\boldsymbol{G}_C^<(\varepsilon) + f_s^0(\varepsilon - e\varphi_s)\left[\boldsymbol{G}_C^R(\varepsilon) - \boldsymbol{G}_C^A(\varepsilon)\right]\right)\right\}.$$

Nonequilibrium Green Functions (Kadanoff, Baym, Keldysh)

$$\check{\boldsymbol{G}} = \begin{pmatrix} \boldsymbol{G}^R & \boldsymbol{G}^< \\ 0 & \boldsymbol{G}^A \end{pmatrix}$$

$\boldsymbol{A} = i\left(\boldsymbol{G}^R - \boldsymbol{G}^A\right)$ – spectral function, the density of states

$\boldsymbol{G}^< \Rightarrow iA(\varepsilon)f(\varepsilon)$ – the distribution function of quasiparticles

$$\check{\boldsymbol{G}} = \check{\boldsymbol{G}}_0 + \{\check{\boldsymbol{G}}_0\check{\boldsymbol{\Sigma}}\check{\boldsymbol{G}}\} \quad \Rightarrow \quad \boldsymbol{G}^<(\varepsilon) = \boldsymbol{G}^R(\varepsilon)\boldsymbol{\Sigma}^<(\varepsilon)\boldsymbol{G}^A(\varepsilon)$$

Büttiker probe method for dephasing

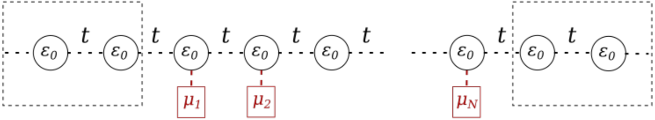

Büttiker Probe (BP) Model

$$\left(\Sigma^R_{deph}(\varepsilon)\right)_{\alpha\beta} = -i\frac{\gamma_{BP}(\varepsilon)}{2}\delta_{\alpha\beta}$$

with zero-current condition

$$I_\alpha = 0 \quad \mu_\alpha \neq 0$$

Büttiker probe method for dephasing

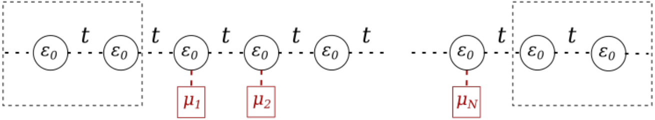

Büttiker Probe (BP) Model

$$\left(\Sigma^R_{deph}(\varepsilon)\right)_{\alpha\beta} = -i\frac{\gamma_{BP}(\varepsilon)}{2}\delta_{\alpha\beta}$$

with zero-current condition

$$I_\alpha = 0 \quad \mu_\alpha \neq 0$$

At small voltage and low temperatures

$$T_{eff}(E) = T_{LR}(E) + \sum_{ij}^{N} T_{Li} W^{-1}_{ij}\left(\{T_{ij}\}\right) T_{jR}$$

J. L. D'Amato and H. M. Pastawski, Phys. Rev. B **41**, 7411 (1990)

Conducting environment $(\mu_\alpha = 0 \quad I_\alpha \neq 0)$

Conducting environment $(\mu_\alpha = 0 \quad I_\alpha \neq 0)$

Molecular wires on metal surfaces

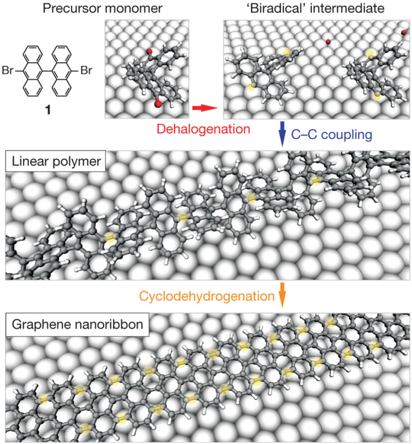

J. Cai, X. Feng, et al., Nature **466**, 470 (2010)

Conducting environment ($\mu_\alpha = 0 \quad I_\alpha \neq 0$)

Molecular wires on metal surfaces

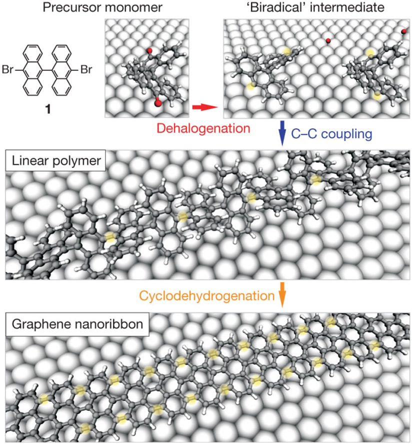

J. Cai, X. Feng, et al., Nature **466**, 470 (2010)

Molecules in conducting liquids

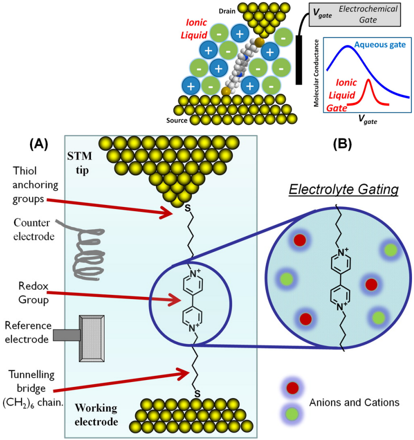

H. M. Osorio, et al., JACS **137**, 14319 (2015)

Vibronic dephasing

Vibronic Dephasing (VD) Model

$$\left(\Sigma^{R}_{deph}(\varepsilon)\right)_{\alpha\beta} = \gamma^{2}_{VD}(\varepsilon)\left(G^{R}_{C}(\varepsilon)\right)_{\alpha\alpha}\delta_{\alpha\beta}$$

can be obtained from the electron-vibron interaction

$$\hat{H}_V = \sum_q \omega_q a^\dagger_q a_q + \sum_{\alpha\beta}\sum_q \lambda^q_{\alpha\beta}(a_q + a^\dagger_q)d^\dagger_\alpha d_\beta$$

Vibronic dephasing

Vibronic Dephasing (VD) Model

$$\left(\Sigma^R_{deph}(\varepsilon)\right)_{\alpha\beta} = \gamma^2_{VD}(\varepsilon)\left(G^R_C(\varepsilon)\right)_{\alpha\alpha}\delta_{\alpha\beta}$$

can be obtained from the electron-vibron interaction

$$\hat{H}_V = \sum_q \omega_q a^\dagger_q a_q + \sum_{\alpha\beta}\sum_q \lambda^q_{\alpha\beta}(a_q + a^\dagger_q) d^\dagger_\alpha d_\beta$$

In the self-consistent Born approximation (SCBA)

$$\Sigma^{R(V)}(\varepsilon) = \frac{i}{2}\sum_q \int \frac{d\omega}{2\pi}\left(M^q G^R_{\varepsilon-\omega} M^q D^K_{q\omega} + M^q G^K_{\varepsilon-\omega} M^q D^R_{q\omega}\right.$$
$$\left. -2D^R_{q\omega=0} M^q \mathrm{Tr}\left[G^<_\omega M^q\right]\right),$$

$$\Sigma^{<(V)}(\varepsilon) = i\sum_q \int \frac{d\omega}{2\pi} M^q G^<_{\varepsilon-\omega} M^q D^<_{q\omega},$$

$G^K = 2G^< + G^R - G^A$, $M^q \equiv \lambda^q_{\alpha\beta}$.

(Equilibrium) vibronic bath

$$D^{<}(q,\omega) = -2\pi i\left[(N_q+1)\delta(\omega+\omega_q) + N_q\delta(\omega-\omega_q)\right]$$

$$\boldsymbol{\Sigma}^{<}(\varepsilon) = \sum_q \left[(1+N_q)\boldsymbol{M}^q\boldsymbol{G}^{<}(\varepsilon+\omega_q)\boldsymbol{M}^q + N_q\boldsymbol{M}^q\boldsymbol{G}^{<}(\varepsilon-\omega_q)\boldsymbol{M}^q\right]$$

(Equilibrium) vibronic bath

$$D^<(q,\omega) = -2\pi i\left[(N_q+1)\delta(\omega+\omega_q) + N_q\delta(\omega-\omega_q)\right]$$

$$\boldsymbol{\Sigma}^<(\varepsilon) = \sum_q \left[(1+N_q)\boldsymbol{M}^q\boldsymbol{G}^<(\varepsilon+\omega_q)\boldsymbol{M}^q + N_q\boldsymbol{M}^q\boldsymbol{G}^<(\varepsilon-\omega_q)\boldsymbol{M}^q\right]$$

In the elastic approximation ($\omega_q \ll \bar{\varepsilon}$)

$$\boldsymbol{\Sigma}^<(\varepsilon) = \int d\omega \sum_q \left[(1+N_{-\omega})\delta(\omega+\omega_q) + N_\omega\delta(\omega-\omega_q)\right]\boldsymbol{M}^q\boldsymbol{G}^<(\varepsilon)\boldsymbol{M}^q$$

(Equilibrium) vibronic bath

$$D^{<}(q,\omega) = -2\pi i\left[(N_q+1)\delta(\omega+\omega_q) + N_q\delta(\omega-\omega_q)\right]$$

$$\boldsymbol{\Sigma}^{<}(\varepsilon) = \sum_q \left[(1+N_q)\boldsymbol{M}^q\boldsymbol{G}^{<}(\varepsilon+\omega_q)\boldsymbol{M}^q + N_q\boldsymbol{M}^q\boldsymbol{G}^{<}(\varepsilon-\omega_q)\boldsymbol{M}^q\right]$$

In the elastic approximation $(\omega_q \ll \bar{\varepsilon})$

$$\boldsymbol{\Sigma}^{<}(\varepsilon) = \int d\omega \sum_q \left[(1+N_{-\omega})\delta(\omega+\omega_q) + N_\omega\delta(\omega-\omega_q)\right]\boldsymbol{M}^q\boldsymbol{G}^{<}(\varepsilon)\boldsymbol{M}^q$$

In the local model $(\boldsymbol{M}^q \equiv \lambda^q_{\alpha\beta} = \lambda_q\delta_{\alpha\beta})$

$$J(\omega) = \sum_q \lambda_q^2\delta(\omega-\omega_q)$$

$$\Sigma^{<}_{\alpha\alpha}(\varepsilon) = \gamma^2 G^{<}_{\alpha\alpha}(\varepsilon), \quad \gamma^2 = \int\left[(1+N_{-\omega})J(-\omega) + N_\omega J(\omega)\right]d\omega \sim TV_{ev}$$

Linear molecules

DNA charge transport

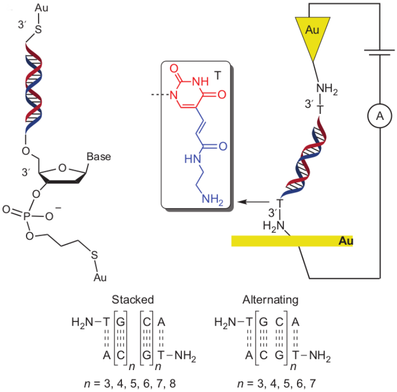

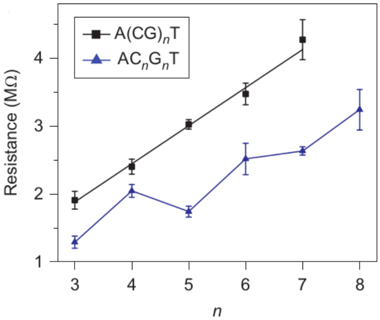

L. Xiang et al., Nature Chem. **7**, 221 (2015)

Semi-infinite 1D electrodes

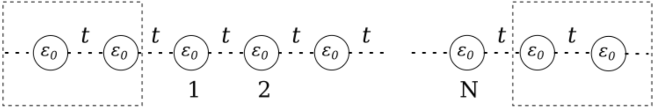

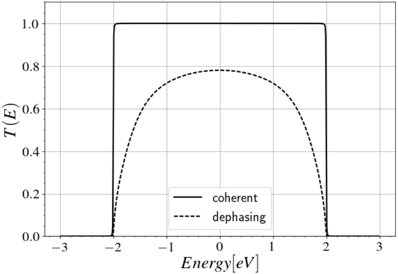

Semi-infinite 1D electrodes

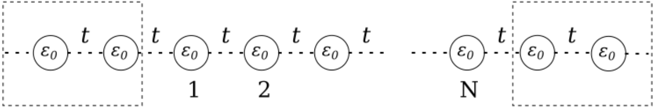

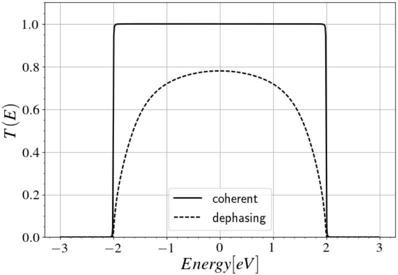

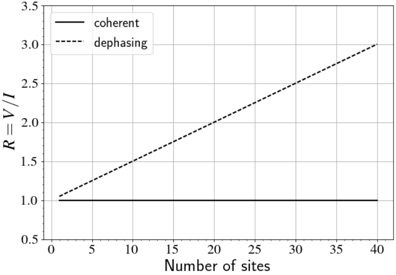

Wide-band limit

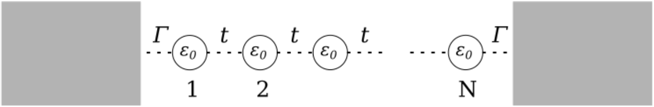

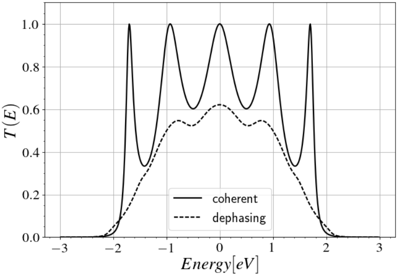

Wide-band limit

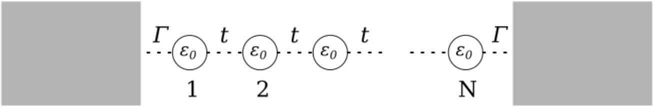

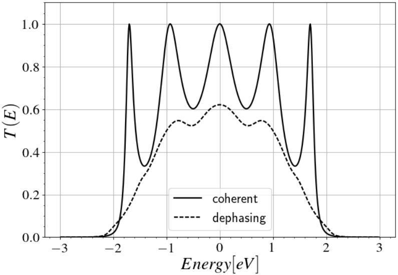

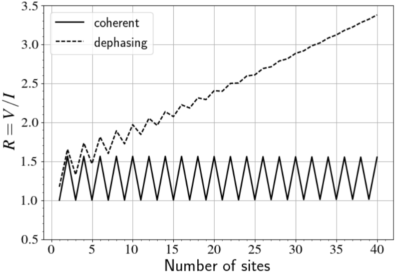

Transmission ($I(E)$) for different dephasing models

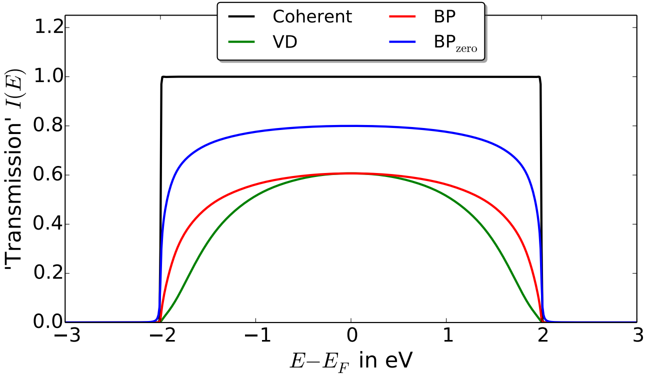

Resistance length dependence - the Ohmic limit

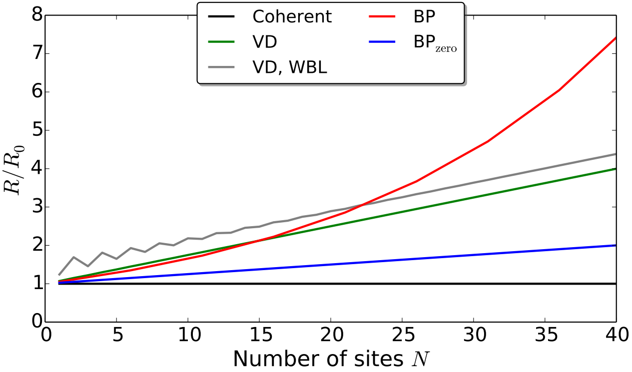

Towards coherent/incoherent transport in DNA

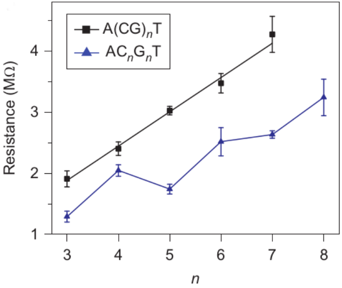

L. Xiang et al., Nature Chem. **7**, 221 (2015)

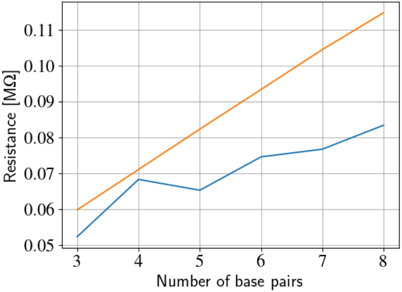

Destructive interference

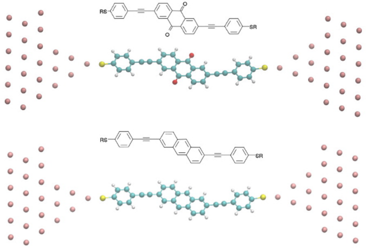

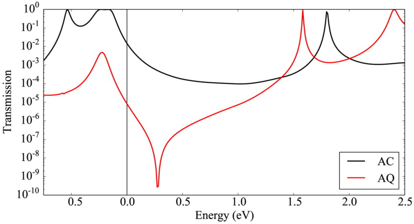

G. Penazzi, et al., *J. Phys. Chem. C* **120**, 16383 (2016)

Anthraquinone vs. anthracene

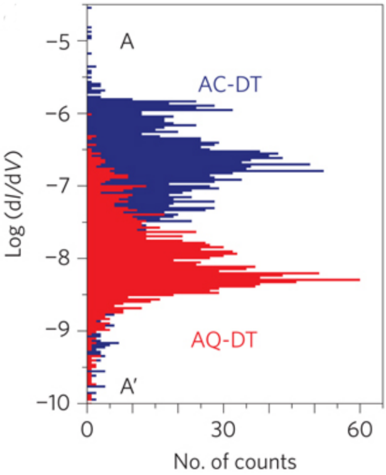

C. M. Guédon,, et al., *Nature Nanotech.* **7**, 305 (2012)

Interference with dephasing

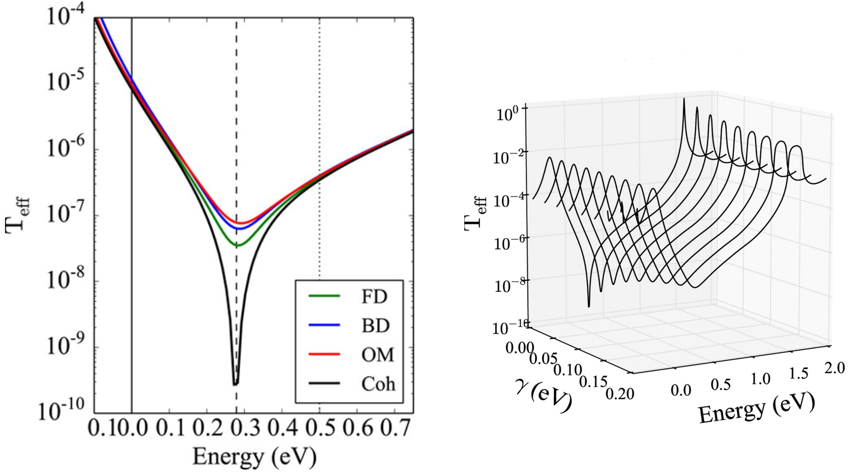

G. Penazzi, et al., *J. Phys. Chem. C* **120**, 16383 (2016)

Mechanically controlled interference

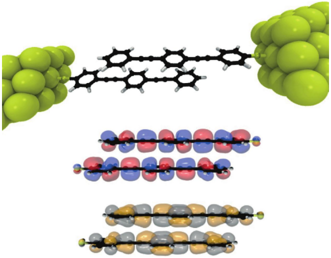

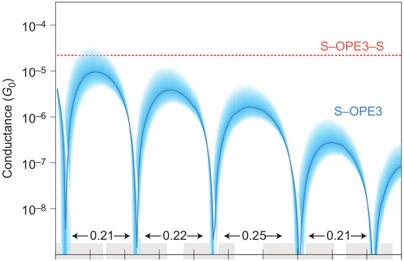

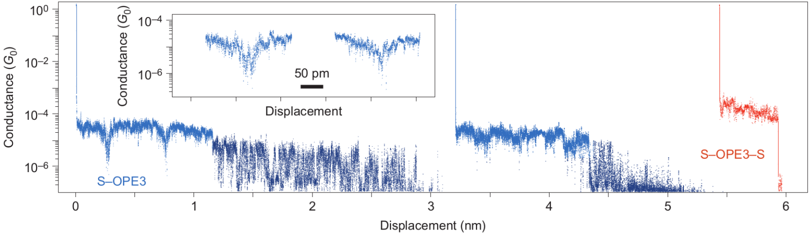

R. Frisenda, et al., *Natur Chem.* **8**, 1099 (2016)

Mechanically controlled interference

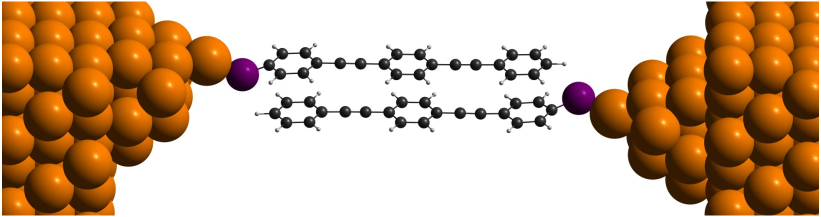

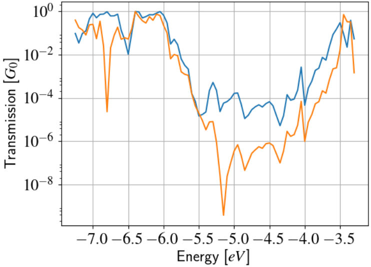

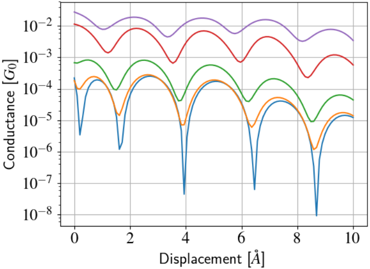

Computational methods: DFTB+ package

http://www.dftb-plus.info/

Computational methods: DFTB+ package

http://www.dftb-plus.info/

The DFTB method

$|\alpha\rangle$ – the basis of atomic orbitals, $\langle\alpha|\beta\rangle = S_{\alpha\beta}$

$$H_{\alpha\beta} = H^0_{\alpha\beta} + \frac{1}{2} S_{\alpha\beta} \sum_k \left(\gamma_{\alpha k} + \gamma_{\beta k}\right) \Delta q_k$$

$$\Delta q_k = \sum_{\alpha\beta\in k} \mathrm{Re}\left(\rho_{\alpha\beta} S_{\beta\alpha}\right) - q^0_k$$

Computational methods: DFTB+ package

http://www.dftb-plus.info/

The DFTB method

$|\alpha\rangle$ – the basis of atomic orbitals, $\langle\alpha|\beta\rangle = S_{\alpha\beta}$

$$H_{\alpha\beta} = H^0_{\alpha\beta} + \frac{1}{2} S_{\alpha\beta} \sum_k \left(\gamma_{\alpha k} + \gamma_{\beta k}\right) \Delta q_k$$

$$\Delta q_k = \sum_{\alpha\beta\in k} \mathrm{Re}\left(\rho_{\alpha\beta} S_{\beta\alpha}\right) - q^0_k$$

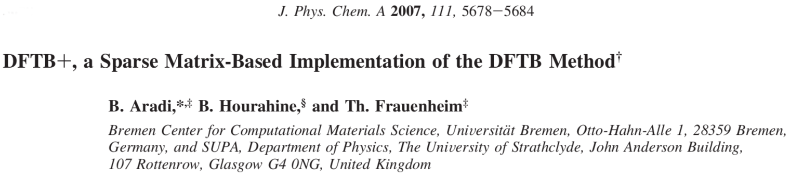

J. Phys. Chem. A **2007,** *111,* 5678−5684

DFTB+, a Sparse Matrix-Based Implementation of the DFTB Method[†]

B. Aradi,[*,‡] **B. Hourahine,**[§] **and Th. Frauenheim**[‡]

Bremen Center for Computational Materials Science, Universität Bremen, Otto-Hahn-Alle 1, 28359 Bremen, Germany, and SUPA, Department of Physics, The University of Strathclyde, John Anderson Building, 107 Rottenrow, Glasgow G4 0NG, United Kingdom

The DFTB+NEGF method (DFT/Landauer)

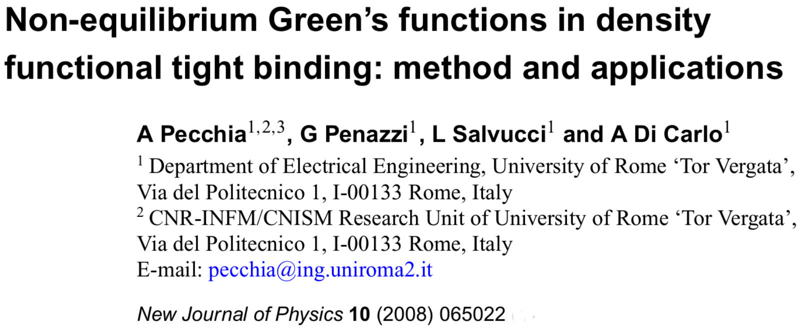

Non-equilibrium Green's functions in density functional tight binding: method and applications

A Pecchia[1,2,3], **G Penazzi**[1], **L Salvucci**[1] **and A Di Carlo**[1]
[1] Department of Electrical Engineering, University of Rome 'Tor Vergata', Via del Politecnico 1, I-00133 Rome, Italy
[2] CNR-INFM/CNISM Research Unit of University of Rome 'Tor Vergata', Via del Politecnico 1, I-00133 Rome, Italy
E-mail: pecchia@ing.uniroma2.it

New Journal of Physics **10** (2008) 065022

The DFTB+NEGF method (DFT/Landauer)

Non-equilibrium Green's functions in density functional tight binding: method and applications

A Pecchia[1,2,3], **G Penazzi**[1], **L Salvucci**[1] **and A Di Carlo**[1]

[1] Department of Electrical Engineering, University of Rome 'Tor Vergata', Via del Politecnico 1, I-00133 Rome, Italy

[2] CNR-INFM/CNISM Research Unit of University of Rome 'Tor Vergata',
, Italy

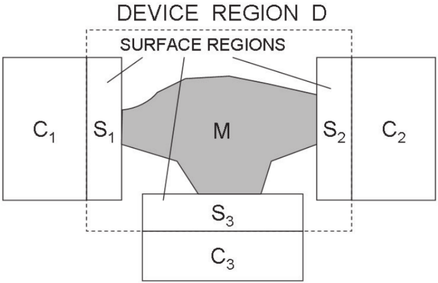

5022

The DFTB+NEGF method (DFT/Landauer)

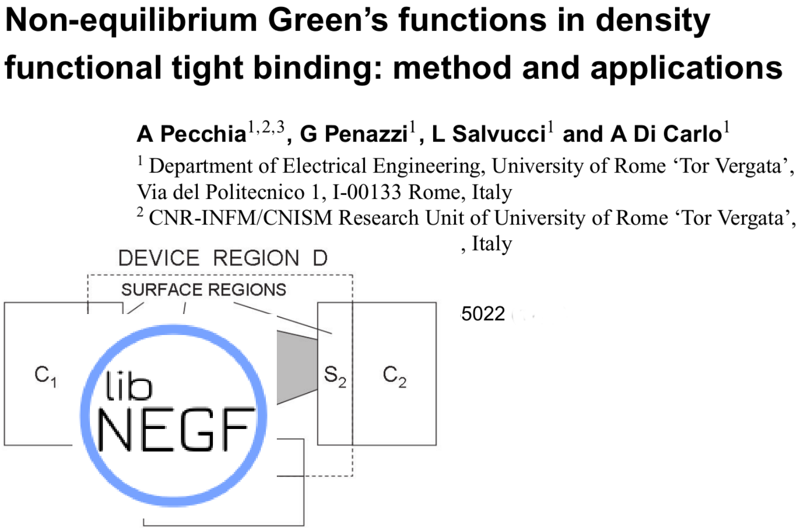

Non-equilibrium Green's functions in density functional tight binding: method and applications

A Pecchia[1,2,3]**, G Penazzi**[1]**, L Salvucci**[1] **and A Di Carlo**[1]

[1] Department of Electrical Engineering, University of Rome 'Tor Vergata', Via del Politecnico 1, I-00133 Rome, Italy

[2] CNR-INFM/CNISM Research Unit of University of Rome 'Tor Vergata', , Italy

5022

The DFTB+NEGF method (DFT/Landauer)

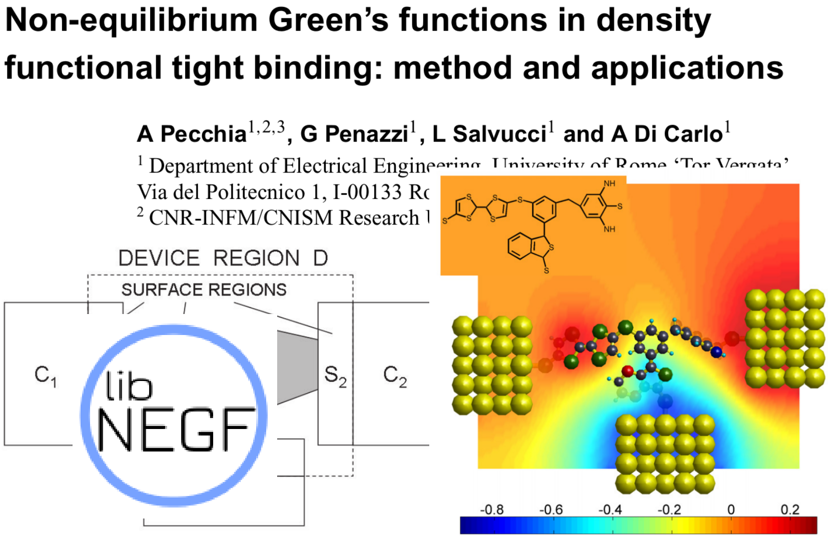

Non-equilibrium Green's functions in density functional tight binding: method and applications

A Pecchia[1,2,3], **G Penazzi**[1], **L Salvucci**[1] **and A Di Carlo**[1]

[1] Department of Electrical Engineering, University of Rome 'Tor Vergata'
Via del Politecnico 1, I-00133 Ro
[2] CNR-INFM/CNISM Research

DFT/Landauer (TRANSIESTA, SMEAGOL, DFTB+ ...)

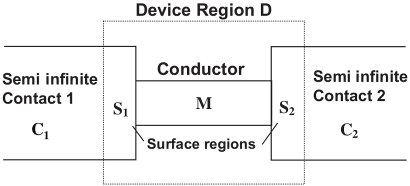

$$\left[-\frac{\hbar^2}{2m}\nabla^2+V_H(\mathbf{r})+V_{XC}\left(\{\rho(\mathbf{r})\}\right)\right]\psi_n(\mathbf{r})=E\psi_n(\mathbf{r})$$

$$\nabla^2 V_H(\mathbf{r})=-4\pi e\left[\rho_0(\mathbf{r})+\rho(\mathbf{r})\right]$$

$$\left[E+i\eta-\hat{H}(\mathbf{r})\right]G^R(\mathbf{r},\mathbf{r}',E)=\delta(\mathbf{r}-\mathbf{r}').$$

$$\hat{H}(\mathbf{r})=-\frac{\hbar^2}{2m}\nabla^2+V_H(\mathbf{r})+V_{XC}\left(\{\rho(\mathbf{r})\}\right)$$

$$\rho(\mathbf{r})=\frac{1}{2\pi i}\int G^<(E,\mathbf{r})dE$$

Pictures from A. Pecchia, A. Di Carlo, Rep. Prog. Phys. **67**, 1497 (2004)

DFT/Landauer (TRANSIESTA, SMEAGOL, DFTB+ ...)

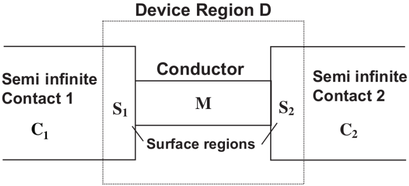

$$\left[-\frac{\hbar^2}{2m}\nabla^2 + V_H(\mathbf{r}) + V_{XC}(\{\rho(\mathbf{r})\})\right]\psi_n(\mathbf{r}) = E\psi_n(\mathbf{r})$$

$$\nabla^2 V_H(\mathbf{r}) = -4\pi e\left[\rho_0(\mathbf{r}) + \rho(\mathbf{r})\right]$$

$$\left[E + i\eta - \hat{H}(\mathbf{r})\right] G^R(\mathbf{r},\mathbf{r}',E) = \delta(\mathbf{r}-\mathbf{r}').$$

$$\hat{H}(\mathbf{r}) = -\frac{\hbar^2}{2m}\nabla^2 + V_H(\mathbf{r}) + V_{XC}(\{\rho(\mathbf{r})\})$$

$$\rho(\mathbf{r}) = \frac{1}{2\pi i}\int G^<(E,\mathbf{r})dE$$

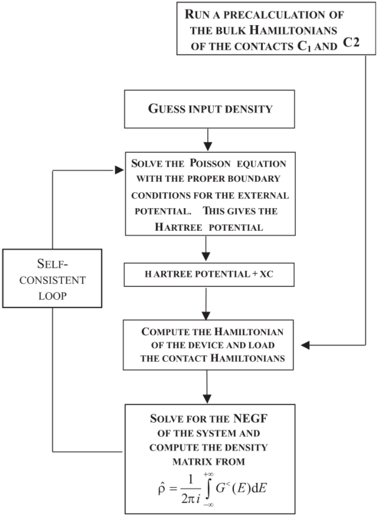

RUN A PRECALCULATION OF THE BULK HAMILTONIANS OF THE CONTACTS C_1 AND C2

GUESS INPUT DENSITY

SOLVE THE POISSON EQUATION WITH THE PROPER BOUNDARY CONDITIONS FOR THE EXTERNAL POTENTIAL. THIS GIVES THE HARTREE POTENTIAL

HARTREE POTENTIAL + XC

COMPUTE THE HAMILTONIAN OF THE DEVICE AND LOAD THE CONTACT HAMILTONIANS

SOLVE FOR THE NEGF OF THE SYSTEM AND COMPUTE THE DENSITY MATRIX FROM

$$\hat{\rho} = \frac{1}{2\pi i}\int_{-\infty}^{+\infty} G^<(E)\mathrm{d}E$$

SELF-CONSISTENT LOOP

Pictures from A. Pecchia, A. Di Carlo, Rep. Prog. Phys. **67**, 1497 (2004)

The many-body DFTB+ transport

$$\begin{aligned} H_{\alpha\beta} =& H^0_{\alpha\beta} + \frac{1}{2} S_{\alpha\beta} \sum_k \left(\gamma_{\alpha k} + \gamma_{\beta k}\right) \overline{\Delta q_k} + e\varphi_\alpha \delta_{\alpha\beta} \\ & + \frac{1}{2} \sum_{\alpha\neq\beta} U_{\alpha\beta} \hat{n}_\alpha \hat{n}_\beta + \sum_q \hbar\omega_q a^\dagger_q a_q + \sum_{\alpha\beta} \sum_q \lambda^q_{\alpha\beta} (a_q + a^\dagger_q) d^\dagger_\alpha d_\beta \end{aligned}$$

$$I_{s=L(R)} = \frac{ie}{\hbar} \int \frac{d\varepsilon}{2\pi} \mathrm{Tr}\left\{ \tilde{\boldsymbol{\Gamma}}_s(\varepsilon - e\varphi_s) \left(\boldsymbol{G}^<_C(\varepsilon) + f^0_s(\varepsilon - e\varphi_s) \left[\boldsymbol{G}^R_C(\varepsilon) - \boldsymbol{G}^A_C(\varepsilon) \right] \right) \right\}.$$

The many-body DFTB+ transport

$$
\begin{aligned}
H_{\alpha\beta} =& H^0_{\alpha\beta} + \frac{1}{2} S_{\alpha\beta} \sum_k \left(\gamma_{\alpha k} + \gamma_{\beta k}\right) \overline{\Delta q_k} + e\varphi_\alpha \delta_{\alpha\beta} \\
& + \frac{1}{2} \sum_{\alpha\neq\beta} U_{\alpha\beta} \hat{n}_\alpha \hat{n}_\beta + \sum_q \hbar\omega_q a_q^\dagger a_q + \sum_{\alpha\beta} \sum_q \lambda^q_{\alpha\beta} (a_q + a_q^\dagger) d_\alpha^\dagger d_\beta
\end{aligned}
$$

$$
I_{s=L(R)} = \frac{ie}{\hbar} \int \frac{d\varepsilon}{2\pi} \mathrm{Tr} \left\{ \tilde{\boldsymbol{\Gamma}}_s(\varepsilon - e\varphi_s) \left(\boldsymbol{G}_C^<(\varepsilon) + f_s^0(\varepsilon - e\varphi_s) \left[\boldsymbol{G}_C^R(\varepsilon) - \boldsymbol{G}_C^A(\varepsilon) \right] \right) \right\} .
$$

The many-body DFTB+ transport

$$H_{\alpha\beta} = H^0_{\alpha\beta} + \frac{1}{2} S_{\alpha\beta} \sum_k \left(\gamma_{\alpha k} + \gamma_{\beta k}\right) \overline{\Delta q_k} + e\varphi_\alpha \delta_{\alpha\beta}$$

$$+ \frac{1}{2} \sum_{\alpha \neq \beta} U_{\alpha\beta} \hat{n}_\alpha \hat{n}_\beta + \sum_q \hbar\omega_q a^\dagger_q a_q + \sum_{\alpha\beta} \sum_q \lambda^q_{\alpha\beta} (a_q + a^\dagger_q) d^\dagger_\alpha d_\beta$$

$$I_{s=L(R)} = \frac{ie}{\hbar} \int \frac{d\varepsilon}{2\pi} \mathrm{Tr} \left\{ \tilde{\boldsymbol{\Gamma}}_s(\varepsilon - e\varphi_s) \left(\mathbf{G}^<_C(\varepsilon) + f^0_s(\varepsilon - e\varphi_s) \left[\mathbf{G}^R_C(\varepsilon) - \mathbf{G}^A_C(\varepsilon) \right] \right) \right\}.$$

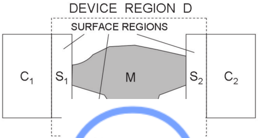

The many-body DFTB+ transport

$$H_{\alpha\beta} = H^0_{\alpha\beta} + \frac{1}{2} S_{\alpha\beta} \sum_k \left(\gamma_{\alpha k} + \gamma_{\beta k}\right) \overline{\Delta q_k} + e\varphi_\alpha \delta_{\alpha\beta}$$

$$+ \frac{1}{2} \sum_{\alpha\neq\beta} U_{\alpha\beta} \hat{n}_\alpha \hat{n}_\beta + \sum_q \hbar\omega_q a_q^\dagger a_q + \sum_{\alpha\beta} \sum_q \lambda^q_{\alpha\beta} (a_q + a_q^\dagger) d_\alpha^\dagger d_\beta$$

$$I_{s=L(R)} = \frac{ie}{\hbar} \int \frac{d\varepsilon}{2\pi} \mathrm{Tr} \left\{ \tilde{\Gamma}_s(\varepsilon - e\varphi_s) \left(G_C^<(\varepsilon) + f_s^0(\varepsilon - e\varphi_s) \left[G_C^R(\varepsilon) - G_C^A(\varepsilon) \right] \right) \right\}.$$

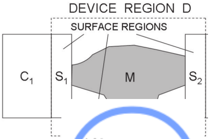

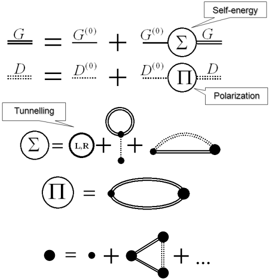

The many-body DFTB+ transport

$$H_{\alpha\beta} = H^0_{\alpha\beta} + \frac{1}{2} S_{\alpha\beta} \sum_k \left(\gamma_{\alpha k} + \gamma_{\beta k}\right) \overline{\Delta q_k} + e\varphi_\alpha \delta_{\alpha\beta}$$
$$+ \frac{1}{2} \sum_{\alpha \neq \beta} U_{\alpha\beta} \hat{n}_\alpha \hat{n}_\beta + \sum_q \hbar\omega_q a_q^\dagger a_q + \sum_{\alpha\beta} \sum_q \lambda^q_{\alpha\beta} (a_q + a_q^\dagger) d_\alpha^\dagger d_\beta$$

$$I_{s=L(R)} = \frac{ie}{\hbar} \int \frac{d\varepsilon}{2\pi} \mathrm{Tr} \left\{ \tilde{\Gamma}_s(\varepsilon - e\varphi_s) \left(G_C^<(\varepsilon) + f_s^0(\varepsilon - e\varphi_s) \left[G_C^R(\varepsilon) - G_C^A(\varepsilon) \right] \right) \right\}.$$

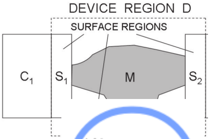

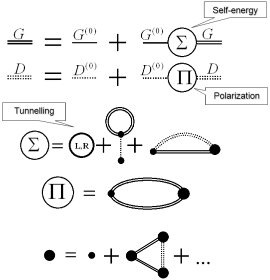

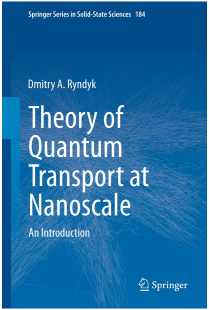
Springer Series in Solid-State Sciences 184

Dmitry A. Ryndyk

Theory of Quantum Transport at Nanoscale

An Introduction

Springer

Destructive quantum interference in electron transport: A reconciliation of the molecular orbital and the atomic orbital perspective

Robert Stadler
Institute for Theoretical Physics
TU Wien

Xin Zhao
TU Wien
Victor Geskin
Universite de Mons

DQI for devices

Bottom Up Nanomachines
IST-FET

BUN
Bottom-Up
Nanomachines

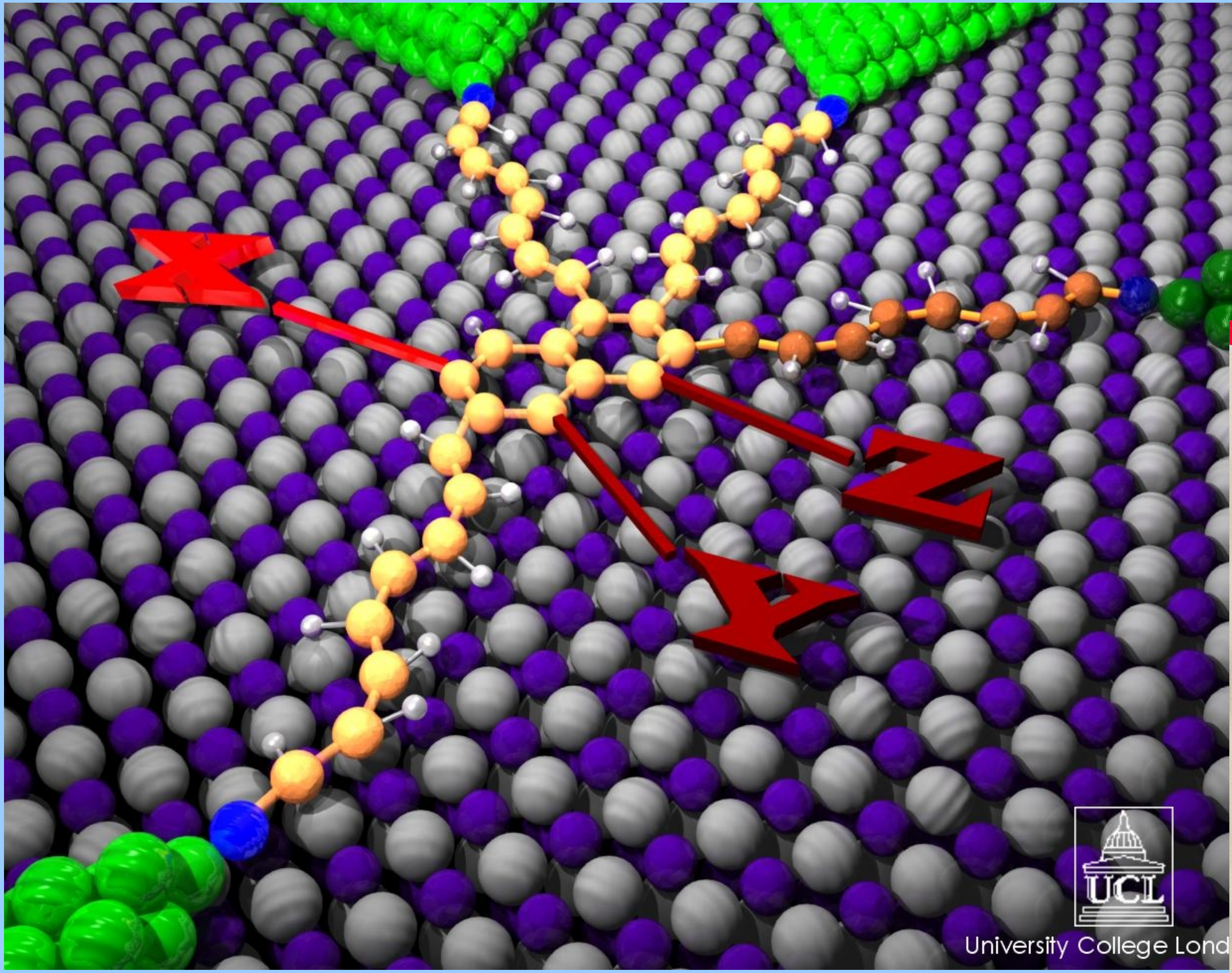

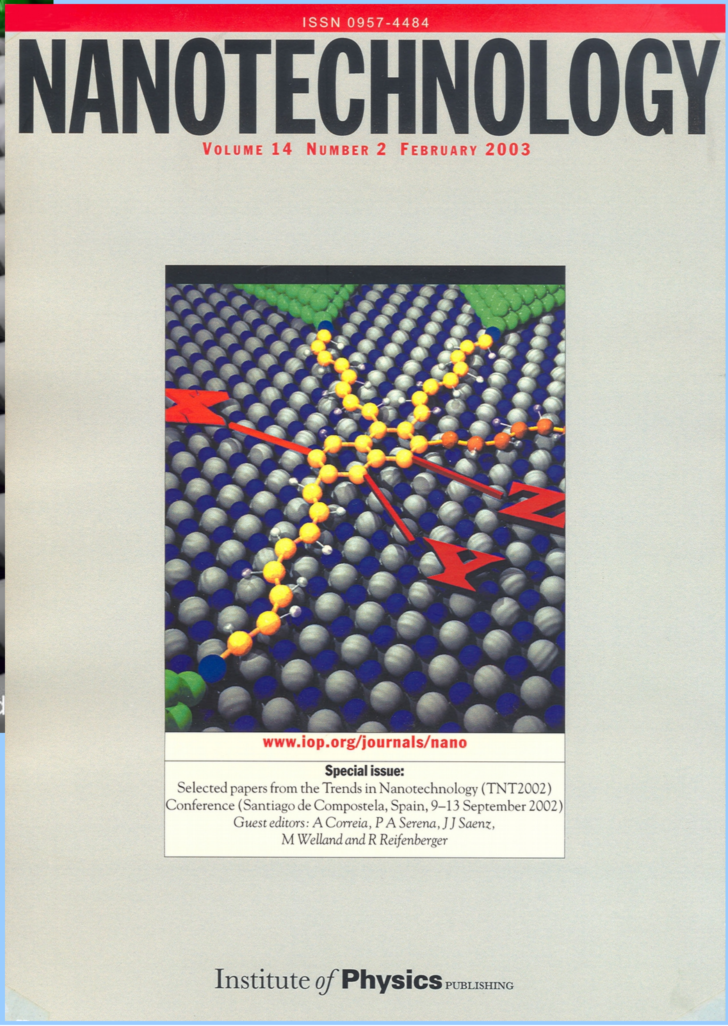
ISSN 0957-4484

NANOTECHNOLOGY

Volume 14 Number 2 February 2003

www.iop.org/journals/nano

Special issue:
Selected papers from the Trends in Nanotechnology (TNT2002) Conference (Santiago de Compostela, Spain, 9–13 September 2002)
Guest editors: A Correia, P A Serena, J J Saenz, M Welland and R Reifenberger

Institute *of* **Physics** PUBLISHING

R. Stadler, M. Forshaw and C. Joachim
Nanotechnology **14** (2003) 138

Graphical rules – Device design

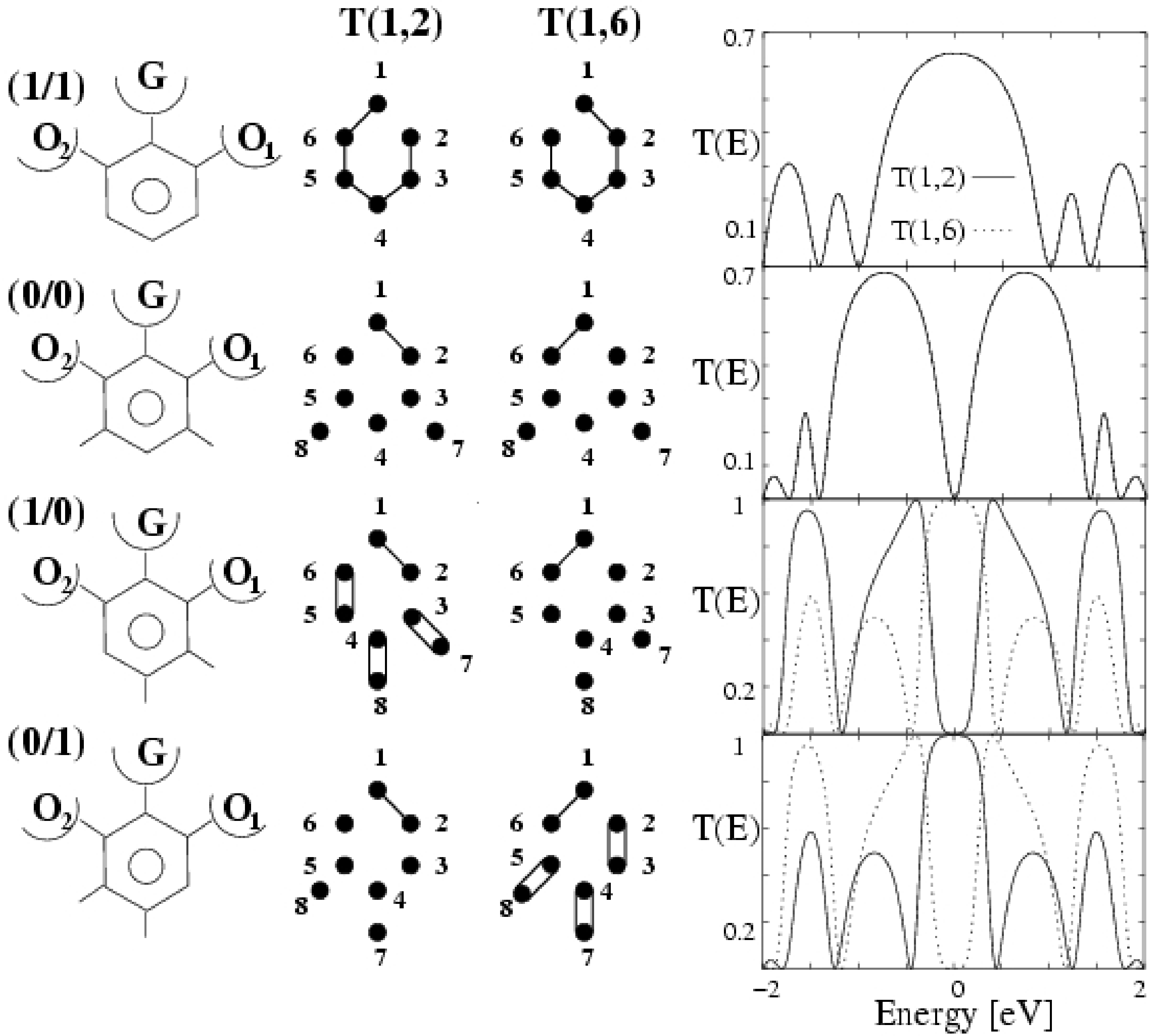

R. Stadler, S. Ami, M. Forshaw and C. Joachim, Nanotechnology **15** (2004) S115

IST-1999-11565

In a first evaluation of the vision on a tight binding-scattering theory level a **proof of concept** was achieved.

BUN
Bottom-Up Nanomachines

Derivation of a graphical design scheme to predict the occurrence or absence of interference effects from the NEGF formalism and tight binding Hamiltonians

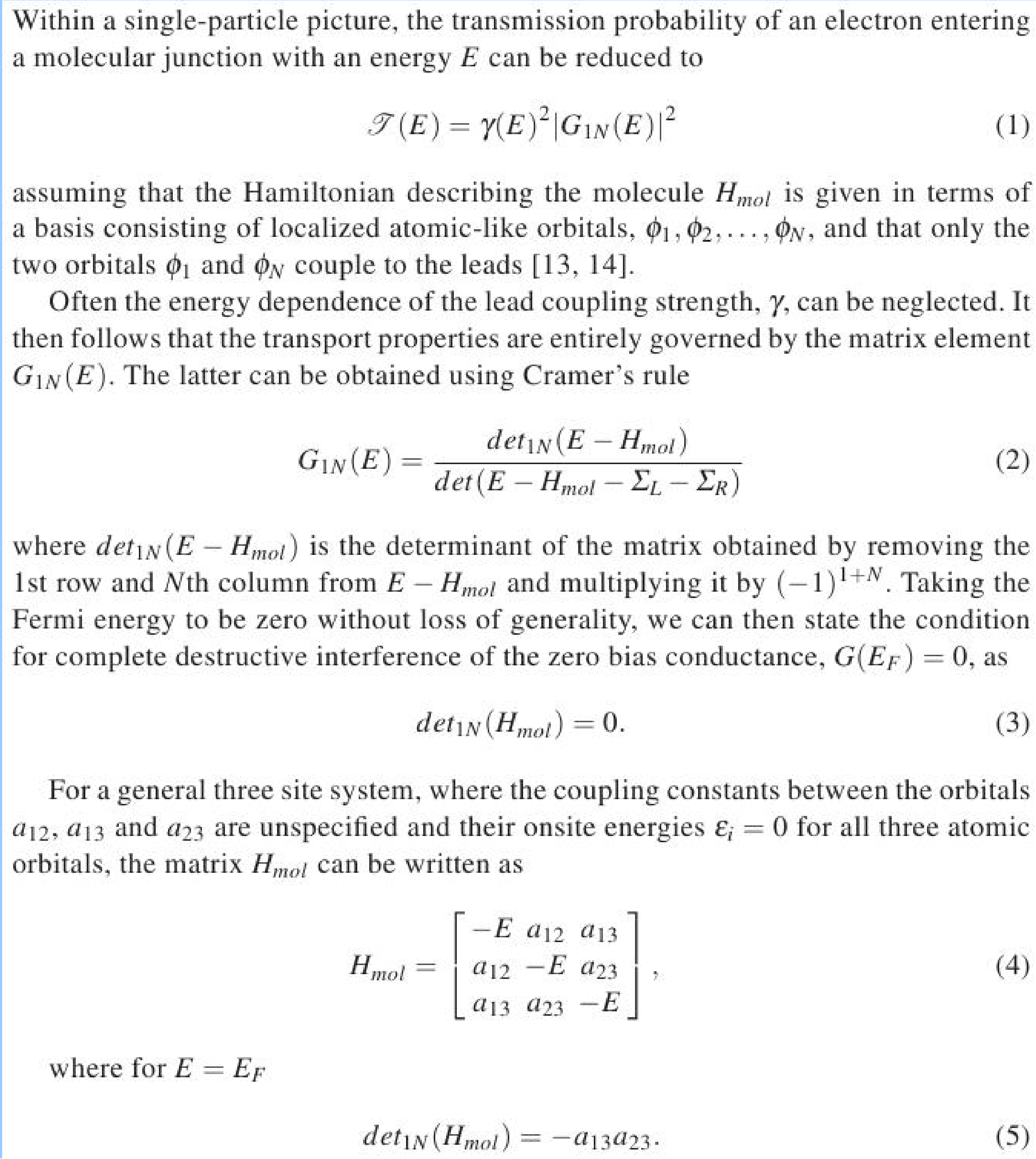

Within a single-particle picture, the transmission probability of an electron entering a molecular junction with an energy E can be reduced to

$$\mathscr{T}(E) = \gamma(E)^2 |G_{1N}(E)|^2 \tag{1}$$

assuming that the Hamiltonian describing the molecule H_{mol} is given in terms of a basis consisting of localized atomic-like orbitals, $\phi_1, \phi_2, \ldots, \phi_N$, and that only the two orbitals ϕ_1 and ϕ_N couple to the leads [13, 14].

Often the energy dependence of the lead coupling strength, γ, can be neglected. It then follows that the transport properties are entirely governed by the matrix element $G_{1N}(E)$. The latter can be obtained using Cramer's rule

$$G_{1N}(E) = \frac{det_{1N}(E - H_{mol})}{det(E - H_{mol} - \Sigma_L - \Sigma_R)} \tag{2}$$

where $det_{1N}(E - H_{mol})$ is the determinant of the matrix obtained by removing the 1st row and Nth column from $E - H_{mol}$ and multiplying it by $(-1)^{1+N}$. Taking the Fermi energy to be zero without loss of generality, we can then state the condition for complete destructive interference of the zero bias conductance, $G(E_F) = 0$, as

$$det_{1N}(H_{mol}) = 0. \tag{3}$$

For a general three site system, where the coupling constants between the orbitals a_{12}, a_{13} and a_{23} are unspecified and their onsite energies $\varepsilon_i = 0$ for all three atomic orbitals, the matrix H_{mol} can be written as

$$H_{mol} = \begin{bmatrix} -E & a_{12} & a_{13} \\ a_{12} & -E & a_{23} \\ a_{13} & a_{23} & -E \end{bmatrix}, \tag{4}$$

where for $E = E_F$

$$det_{1N}(H_{mol}) = -a_{13}a_{23}. \tag{5}$$

Tight binding matrices and their relation to paths through adjacent graphs

3 orbitals

$$M = \begin{bmatrix} -E & a_{12} & a_{13} \\ a_{12} & -E & a_{23} \\ a_{13} & a_{23} & -E \end{bmatrix}, \quad M_{12} \begin{bmatrix} a_{12} & a_{23} \\ a_{13} & -E \end{bmatrix}, \quad c_0 = -a_{13}\, a_{23} \quad -$$

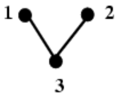

4 orbitals

$$M = \begin{bmatrix} -E & a_{12} & a_{13} & a_{14} \\ a_{12} & -E & a_{23} & a_{24} \\ a_{13} & a_{23} & -E & a_{34} \\ a_{14} & a_{24} & a_{34} & -E \end{bmatrix}, \quad M_{12} \begin{bmatrix} a_{12} & a_{23} & a_{24} \\ a_{13} & -E & a_{34} \\ a_{14} & a_{34} & -E \end{bmatrix},$$

$$c_0 = a_{13}\, a_{23}\, a_{34} + a_{14}\, a_{23}\, a_{34} - a_{12}\, a_{34}^2$$

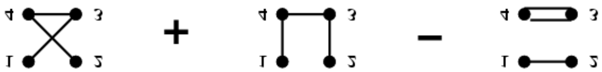

5 orbitals

$$M = \begin{bmatrix} -E & a_{12} & a_{13} & a_{14} & a_{15} \\ a_{12} & -E & a_{23} & a_{24} & a_{25} \\ a_{13} & a_{23} & -E & a_{34} & a_{35} \\ a_{14} & a_{24} & a_{34} & -E & a_{45} \\ a_{15} & a_{25} & a_{35} & a_{45} & -E \end{bmatrix}, \quad M_{12} \begin{bmatrix} a_{12} & a_{23} & a_{24} & a_{25} \\ a_{13} & -E & a_{34} & a_{35} \\ a_{13} & a_{34} & -E & a_{45} \\ a_{15} & a_{35} & a_{45} & -E \end{bmatrix},$$

$$\begin{aligned} c_0 = {} & a_{34}^2\, a_{15}\, a_{25} + a_{35}^2\, a_{14}\, a_{24} + a_{45}^2\, a_{13}\, a_{23} + 2\, a_{12}\, a_{34}\, a_{35}\, a_{45} \\ & -a_{13}\, a_{24}\, a_{35}\, a_{45} - a_{14}\, a_{23}\, a_{35}\, a_{45} - a_{13}\, a_{25}\, a_{34}\, a_{45} \\ & -a_{15}\, a_{23}\, a_{34}\, a_{45} - a_{14}\, a_{25}\, a_{34}\, a_{35} - a_{15}\, a_{24}\, a_{34}\, a_{35} \end{aligned}$$

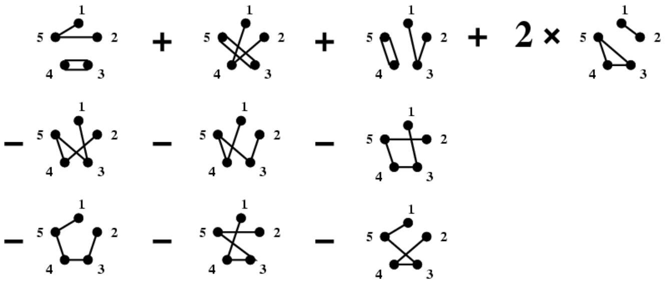

A larger number of orbitals leads also to an increase in the number of possible paths. But the individual terms contain more couplings as well and if only one bond is missing, the path does not exist. Additionally, paths with opposite signs can cancel each other out. For 6 orbitals, there are 46 possible paths, but for e. g. benzene there are only 2:

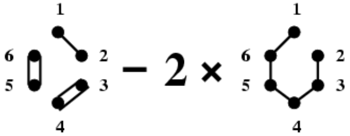

IST-1999-11565

BUN
Bottom-Up
Nanomachines

Graphical rules - anthraquinone configurations

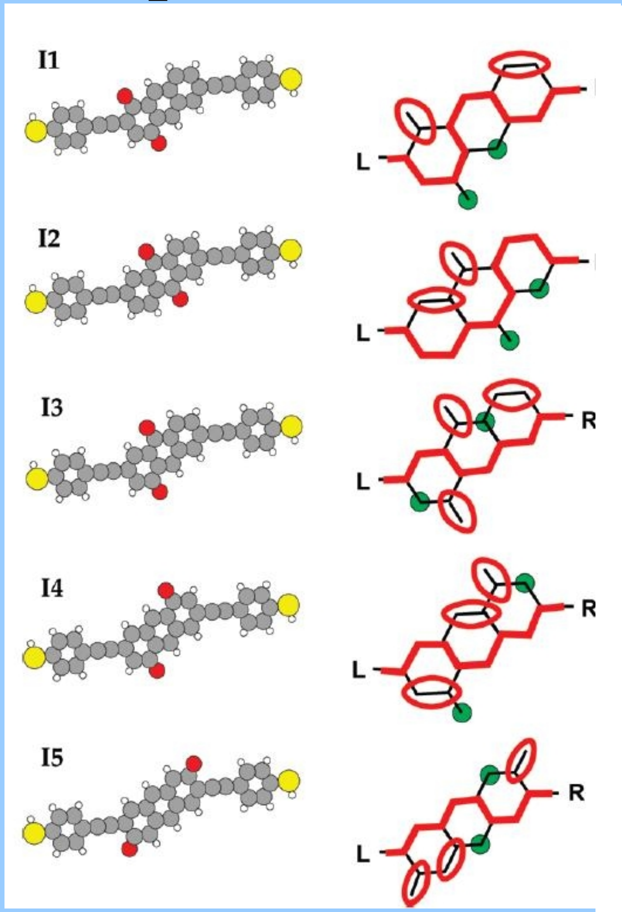

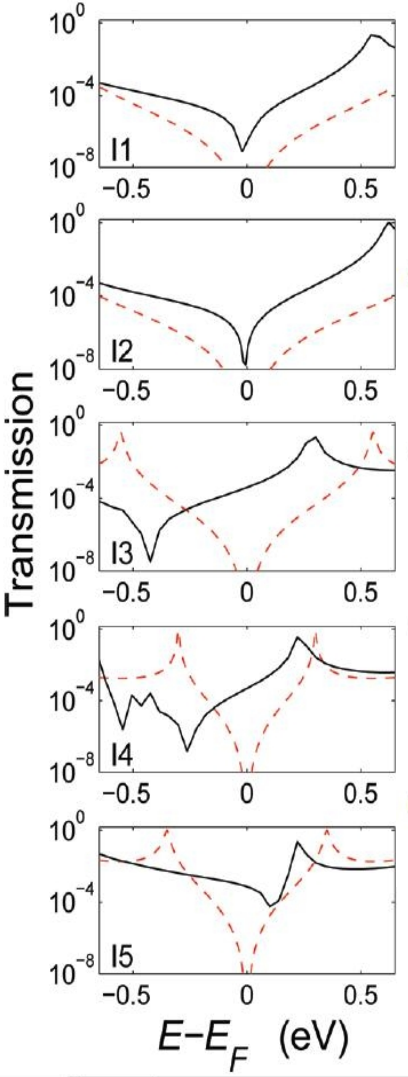

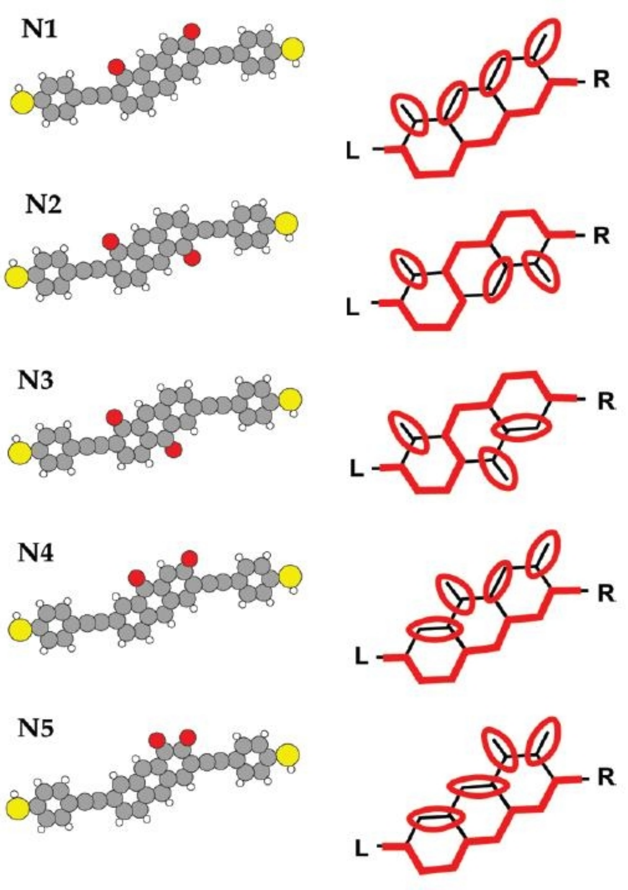

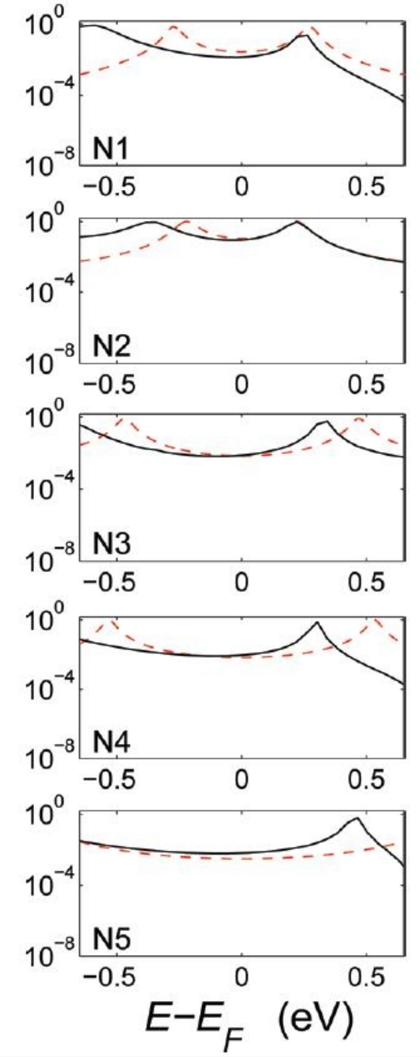

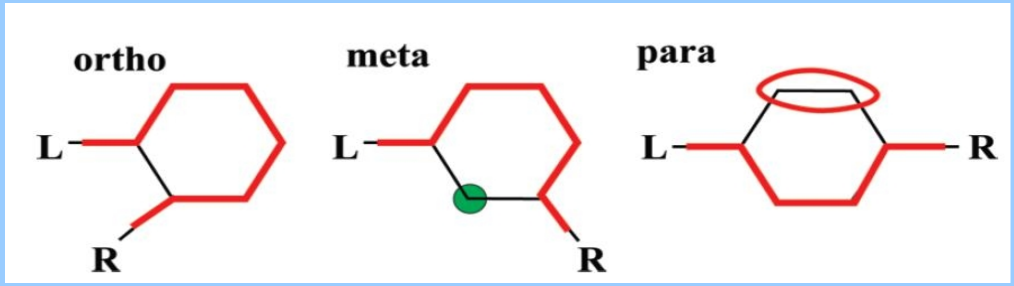

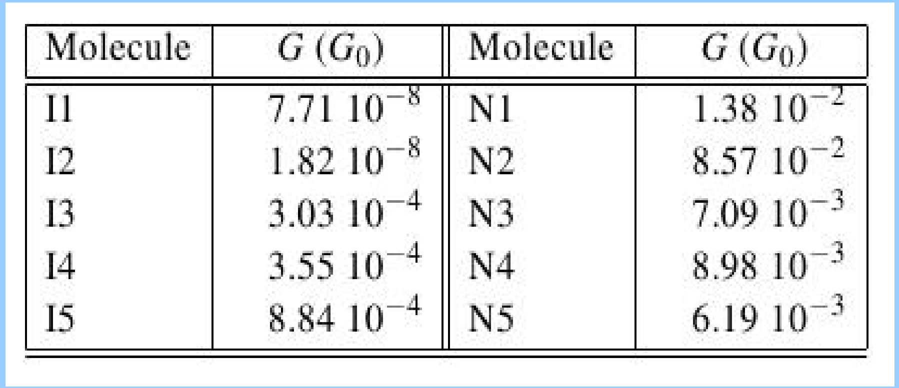

Molecule	G (G_0)	Molecule	G (G_0)
I1	$7.71\ 10^{-8}$	N1	$1.38\ 10^{-2}$
I2	$1.82\ 10^{-8}$	N2	$8.57\ 10^{-2}$
I3	$3.03\ 10^{-4}$	N3	$7.09\ 10^{-3}$
I4	$3.55\ 10^{-4}$	N4	$8.98\ 10^{-3}$
I5	$8.84\ 10^{-4}$	N5	$6.19\ 10^{-3}$

T. Markussen, R. Stadler and K. S. Thygesen, Nano Letters 10 (2010) 4260

Markussen et al., Phys. Chem. Chem. Phys. **13**, 14311 (2011)

Where is the minimum?

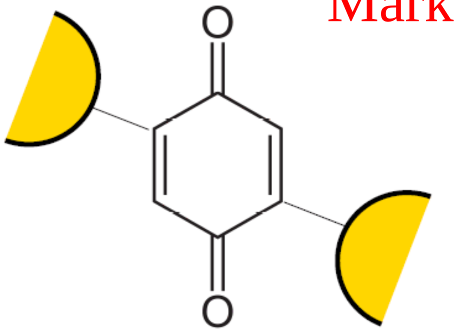

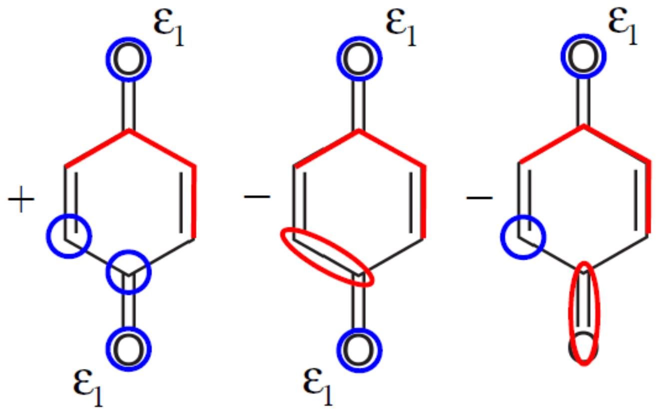

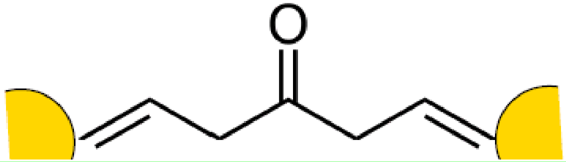

$$\boxed{-(\varepsilon_1 - E)t^6 = 0 \Rightarrow E = \varepsilon_1.}$$

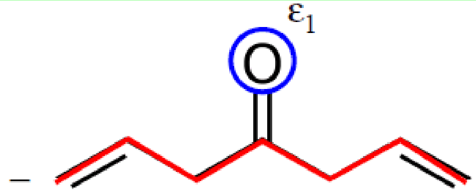

Figure 1: Junction setup for a C7 chain with an oxygen side group (top). The generalized diagram is shown in the bottom.

$$\boxed{(\varepsilon_1 - E)t^3\left[(-E)^2(\varepsilon_1 - E) - t^2(\varepsilon_1 - E) - t^2(-E)\right] = 0}$$

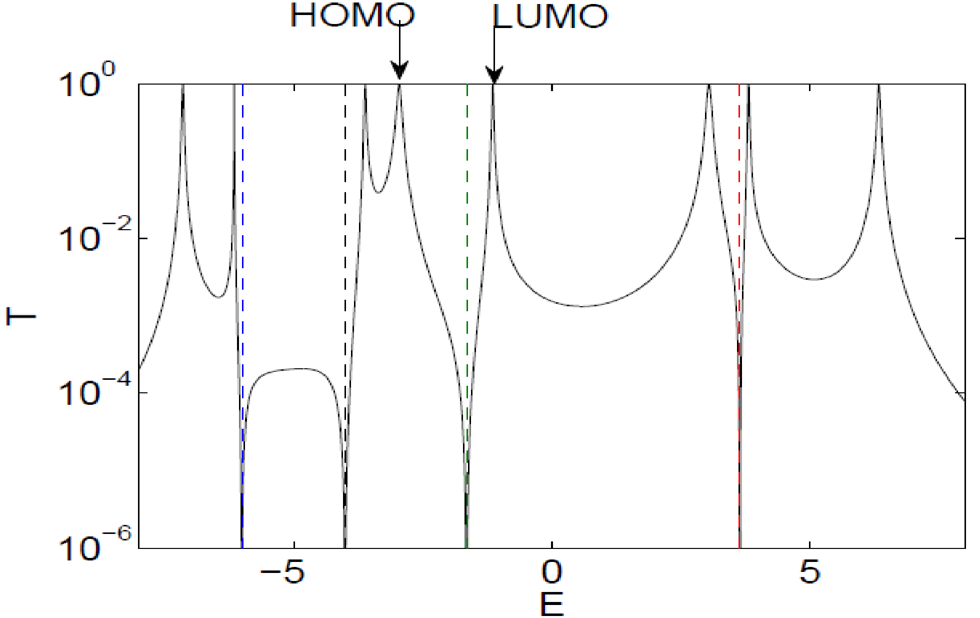

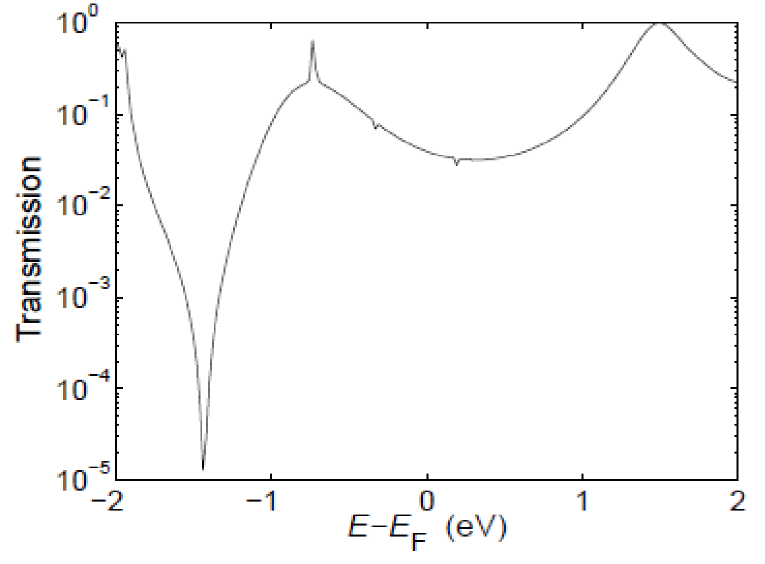

NANO LETTERS
Letter
pubs.acs.org/NanoLett

Breakdown of Interference Rules in Azulene, a Nonalternant Hydrocarbon

Jianlong Xia,[†,¶] Brian Capozzi,[‡,¶] Sujun Wei,[†] Mikkel Strange,[§] Arunabh Batra,[‡] Jose R. Moreno,[†] Roey J. Amir,[∥] Elizabeth Amir,[⊥] Gemma C. Solomon,[§] Latha Venkataraman,*[,‡] and Luis M. Campos*[,†]

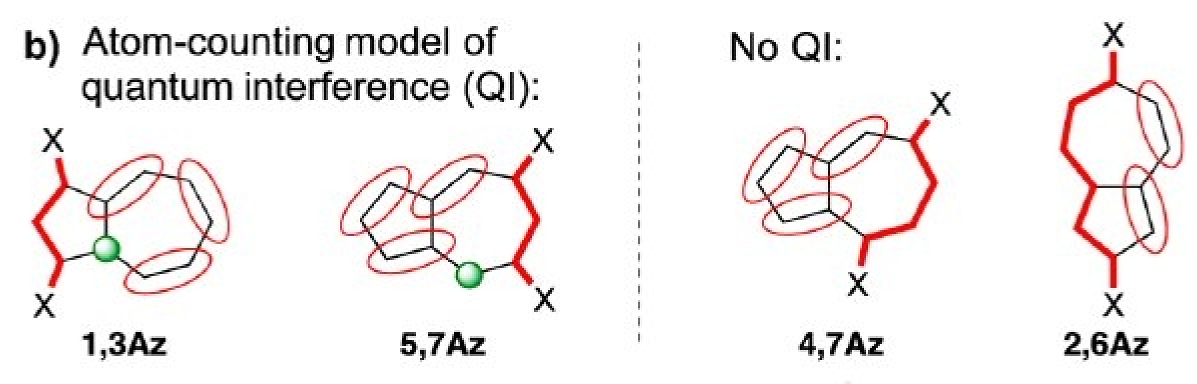

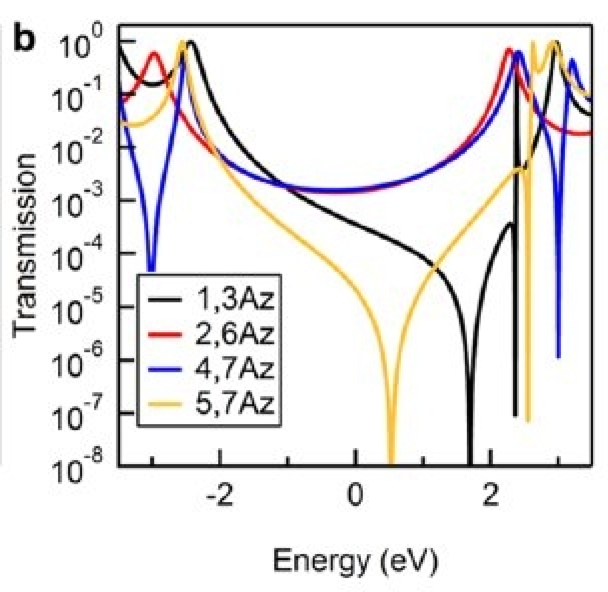

NANO LETTERS
Letter
pubs.acs.org/NanoLett

Comment on "Breakdown of Interference Rules in Azulene, a Nonalternant Hydrocarbon"

Robert Stadler*

Institute for Theoretical Physics, TU Wien - Vienna University of Technology, Wiedner Hauptstrasse 8-10, A-1040 Vienna, Austria

Nano Lett., **2014**, *14* (5), 2941–2945. DOI: 10.1021/nl5010702.
Nano Lett., **2015**, *15*. DOI: 10.1021/acs.nanolett.5b04154

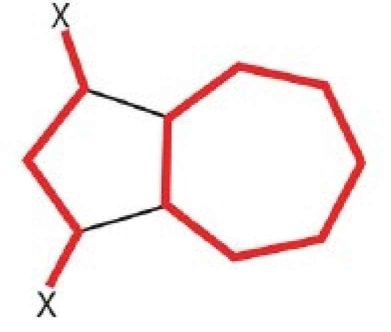

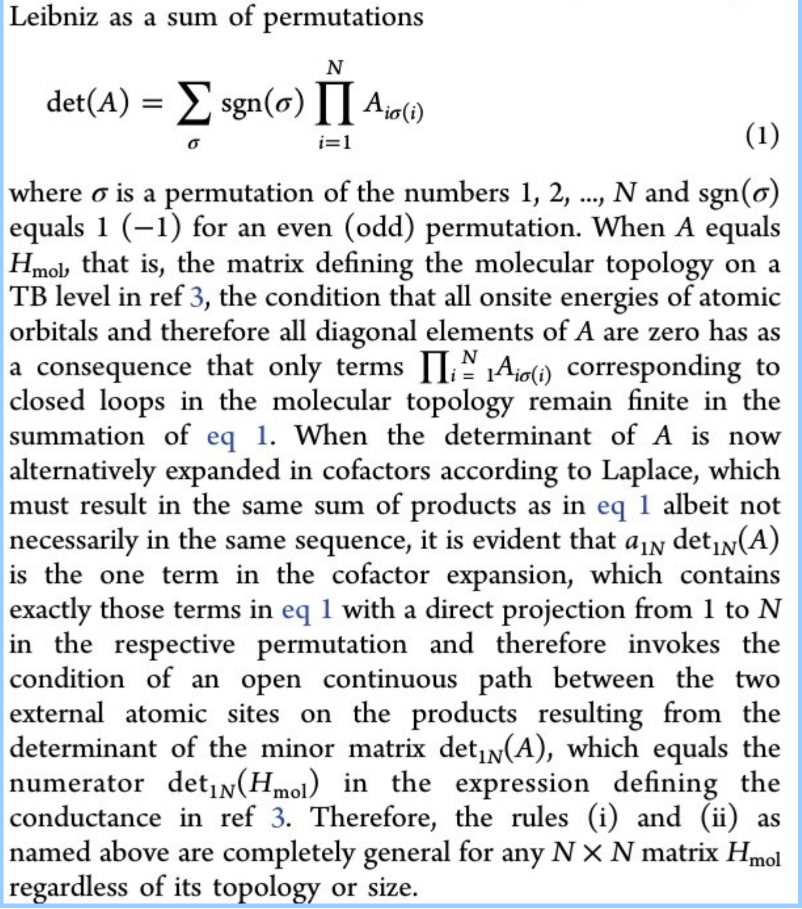

Formally, any $N \times N$ matrix can be developed according to Leibniz as a sum of permutations

$$\det(A) = \sum_{\sigma} \operatorname{sgn}(\sigma) \prod_{i=1}^{N} A_{i\sigma(i)} \tag{1}$$

where σ is a permutation of the numbers 1, 2, ..., N and $\operatorname{sgn}(\sigma)$ equals 1 (−1) for an even (odd) permutation. When A equals H_{mol}, that is, the matrix defining the molecular topology on a TB level in ref 3, the condition that all onsite energies of atomic orbitals and therefore all diagonal elements of A are zero has as a consequence that only terms $\prod_{i=1}^{N} A_{i\sigma(i)}$ corresponding to closed loops in the molecular topology remain finite in the summation of eq 1. When the determinant of A is now alternatively expanded in cofactors according to Laplace, which must result in the same sum of products as in eq 1 albeit not necessarily in the same sequence, it is evident that $a_{1N} \det_{1N}(A)$ is the one term in the cofactor expansion, which contains exactly those terms in eq 1 with a direct projection from 1 to N in the respective permutation and therefore invokes the condition of an open continuous path between the two external atomic sites on the products resulting from the determinant of the minor matrix $\det_{1N}(A)$, which equals the numerator $\det_{1N}(H_{\mathrm{mol}})$ in the expression defining the conductance in ref 3. Therefore, the rules (i) and (ii) as named above are completely general for any $N \times N$ matrix H_{mol} regardless of its topology or size.

Illusory Connection between Cross-Conjugation and Quantum Interference

Kim G. L. Pedersen,[†,‡,¶] Anders Borges,[†,‡] Per Hedegård,[†,¶] Gemma C. Solomon,[†,‡] and Mikkel Strange*[,†,‡]

[†]Nano-Science Center, [‡]Department of Chemistry, and [¶]Niels Bohr Institute, University of Copenhagen, 2100 Copenhagen, Denmark

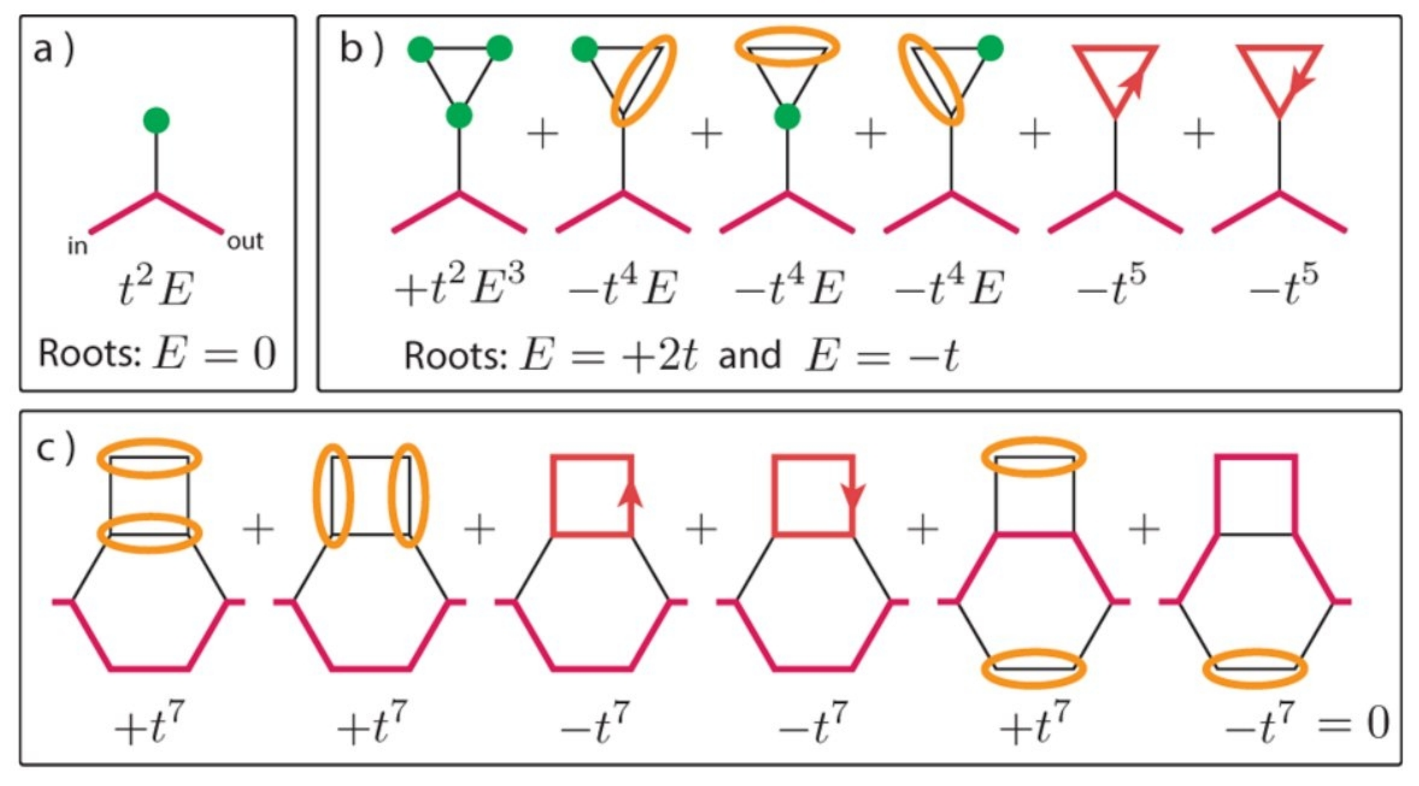

J. Phys. Chem. C 2015, 119, 26919−26924

Frontier MO rules

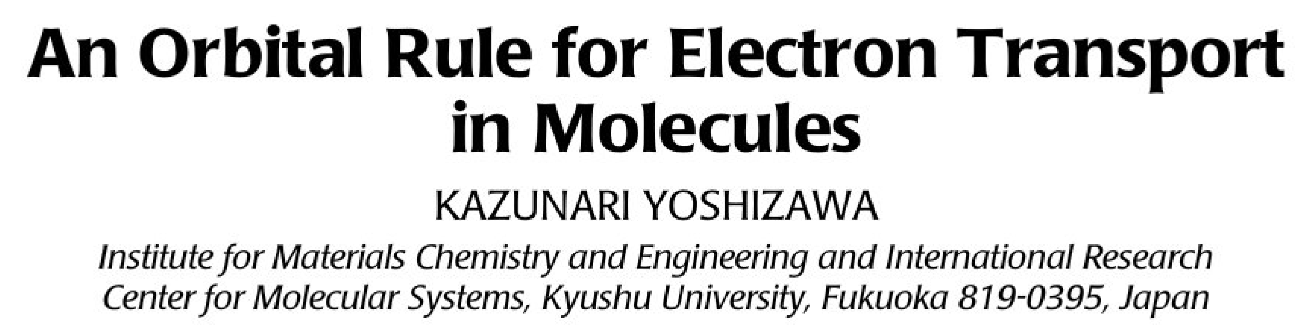

An Orbital Rule for Electron Transport in Molecules

KAZUNARI YOSHIZAWA

Institute for Materials Chemistry and Engineering and International Research Center for Molecular Systems, Kyushu University, Fukuoka 819-0395, Japan

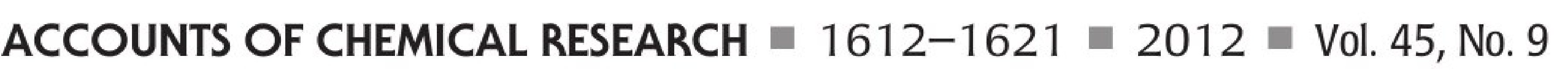

ACCOUNTS OF CHEMICAL RESEARCH ■ 1612–1621 ■ 2012 ■ Vol. 45, No. 9

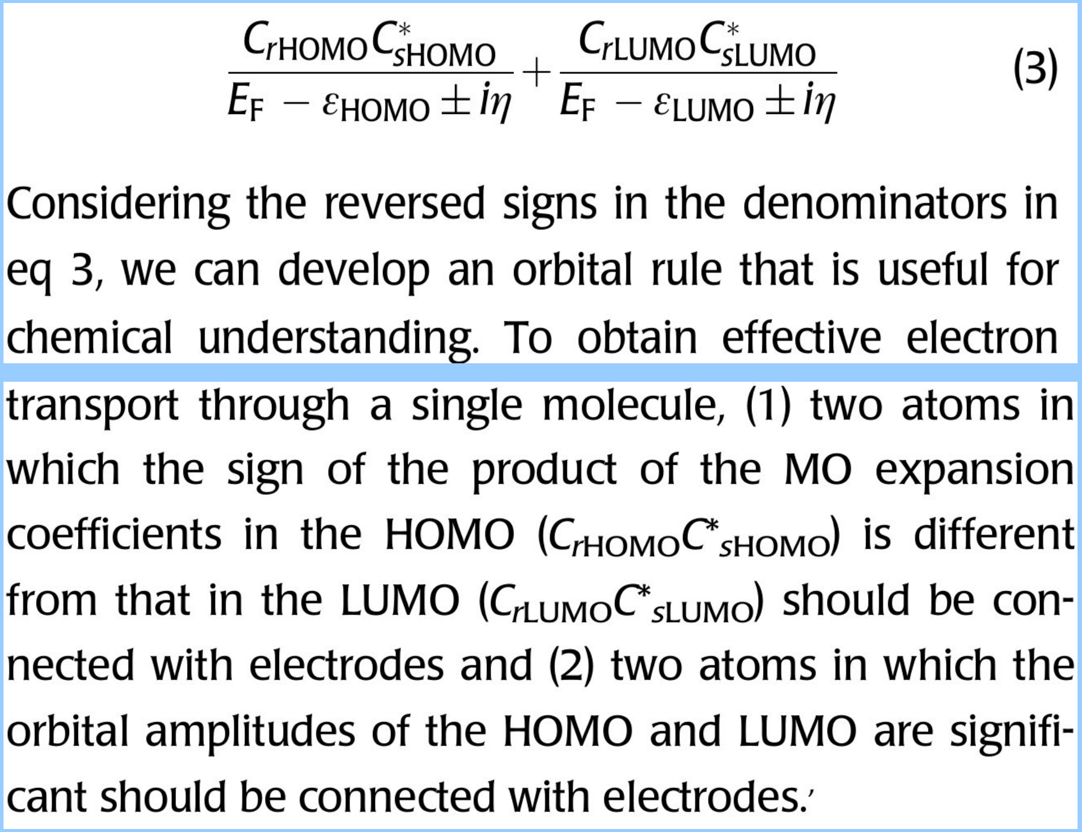

$$\frac{C_{r\mathrm{HOMO}}C^*_{s\mathrm{HOMO}}}{E_{\mathrm{F}} - \varepsilon_{\mathrm{HOMO}} \pm i\eta} + \frac{C_{r\mathrm{LUMO}}C^*_{s\mathrm{LUMO}}}{E_{\mathrm{F}} - \varepsilon_{\mathrm{LUMO}} \pm i\eta} \qquad (3)$$

Considering the reversed signs in the denominators in eq 3, we can develop an orbital rule that is useful for chemical understanding. To obtain effective electron transport through a single molecule, (1) two atoms in which the sign of the product of the MO expansion coefficients in the HOMO ($C_{r\mathrm{HOMO}}C^*_{s\mathrm{HOMO}}$) is different from that in the LUMO ($C_{r\mathrm{LUMO}}C^*_{s\mathrm{LUMO}}$) should be connected with electrodes and (2) two atoms in which the orbital amplitudes of the HOMO and LUMO are significant should be connected with electrodes.

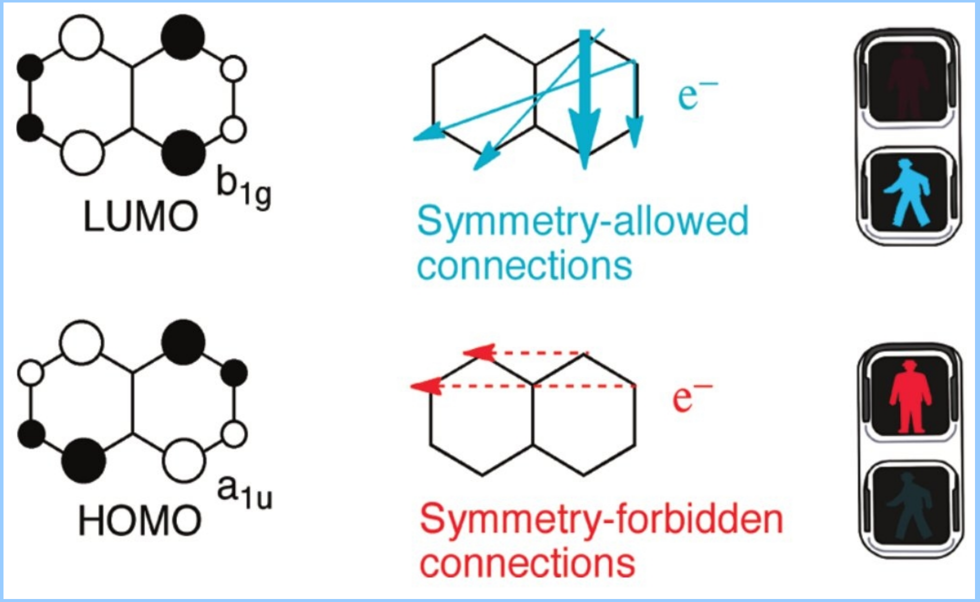

Bending the rules (1)

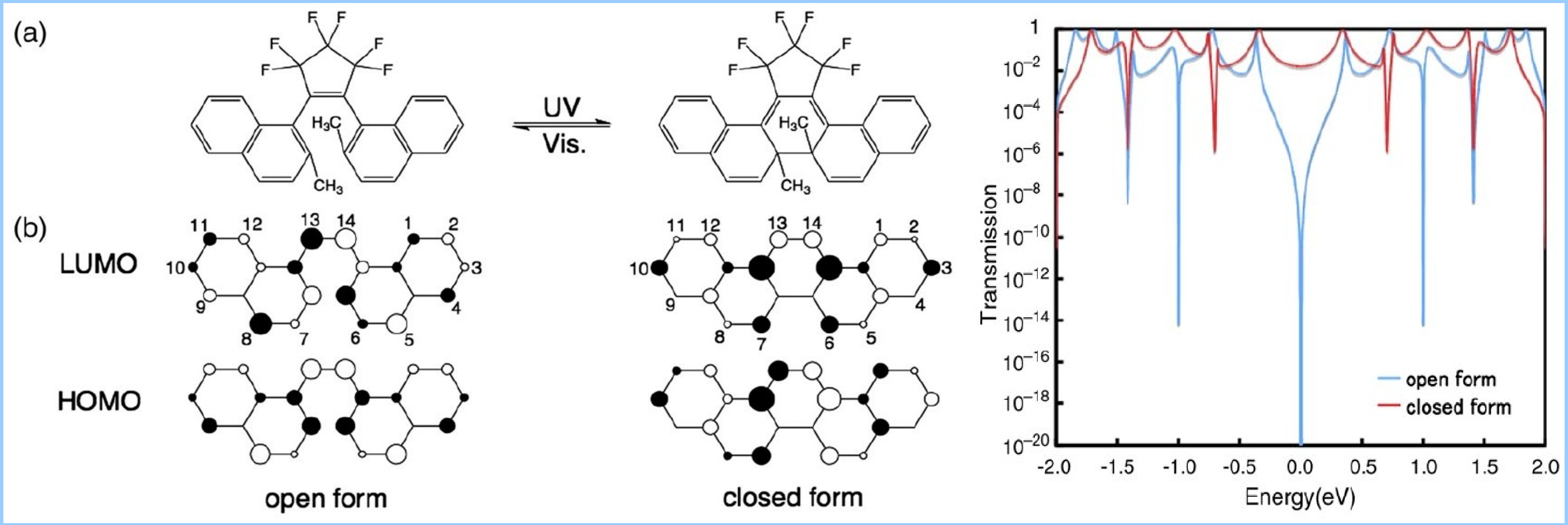

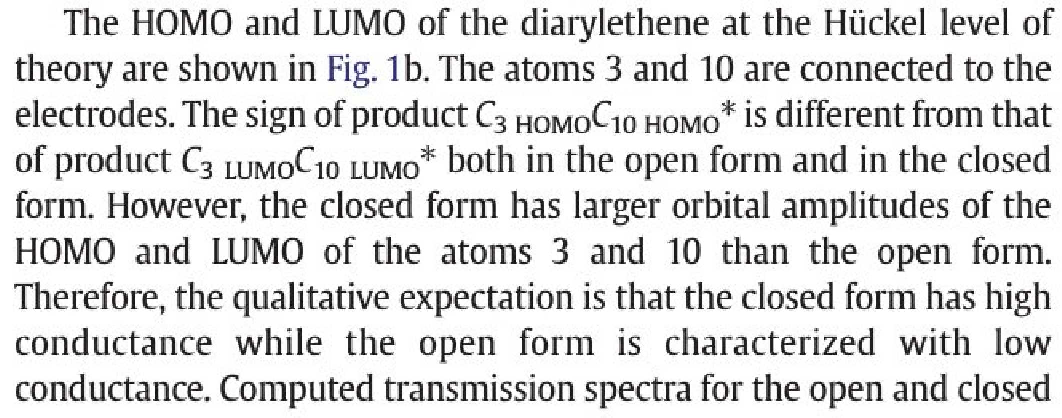
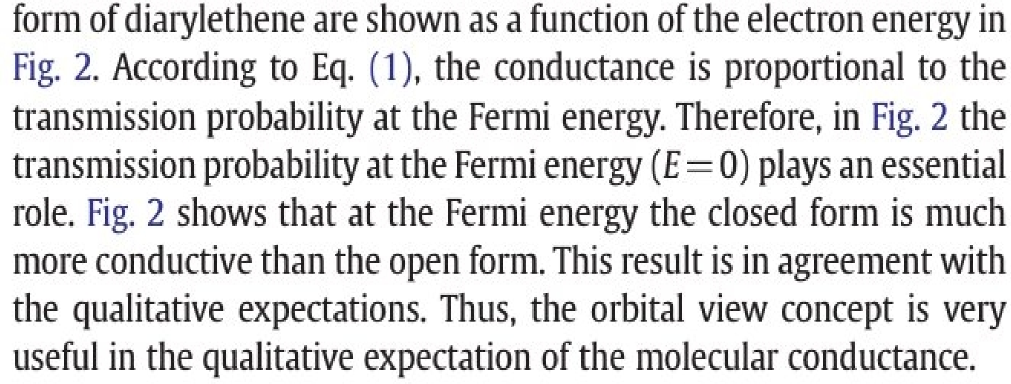

The HOMO and LUMO of the diarylethene at the Hückel level of theory are shown in Fig. 1b. The atoms 3 and 10 are connected to the electrodes. The sign of product $C_{3\ \mathrm{HOMO}}C_{10\ \mathrm{HOMO}}^{*}$ is different from that of product $C_{3\ \mathrm{LUMO}}C_{10\ \mathrm{LUMO}}^{*}$ both in the open form and in the closed form. However, the closed form has larger orbital amplitudes of the HOMO and LUMO of the atoms 3 and 10 than the open form. Therefore, the qualitative expectation is that the closed form has high conductance while the open form is characterized with low conductance. Computed transmission spectra for the open and closed form of diarylethene are shown as a function of the electron energy in Fig. 2. According to Eq. (1), the conductance is proportional to the transmission probability at the Fermi energy. Therefore, in Fig. 2 the transmission probability at the Fermi energy ($E=0$) plays an essential role. Fig. 2 shows that at the Fermi energy the closed form is much more conductive than the open form. This result is in agreement with the qualitative expectations. Thus, the orbital view concept is very useful in the qualitative expectation of the molecular conductance.

Y. Tsuji, A. Staykov and K. Yoshizawa, Thin Solid Films 518, 444 (2009)

Bending the rules (2)

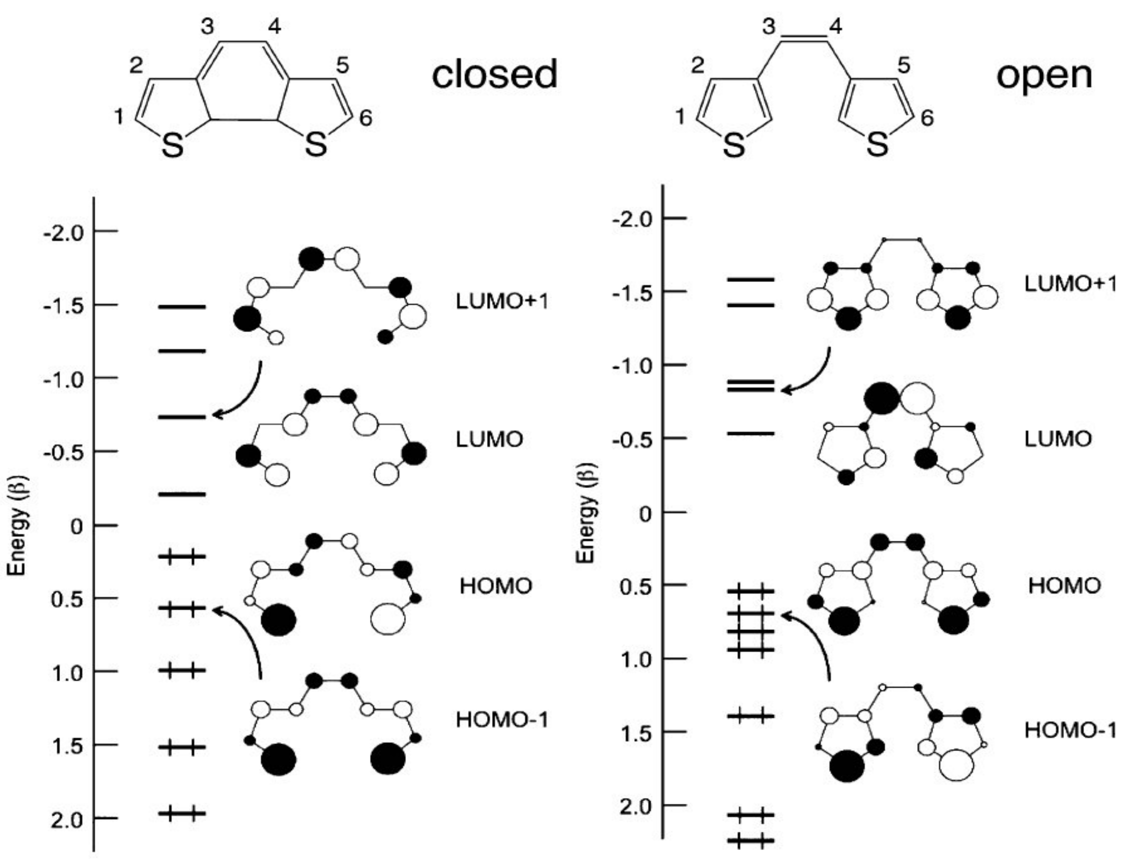

Figure 6. The Hückel MOs of the closed-ring form (left) and open-ring form (right) of dithienylethene. The shape of the FMOs is indicated qualitatively; the black and white circles indicate orbital phases; the circle areas are proportional to the respective coefficient sizes.

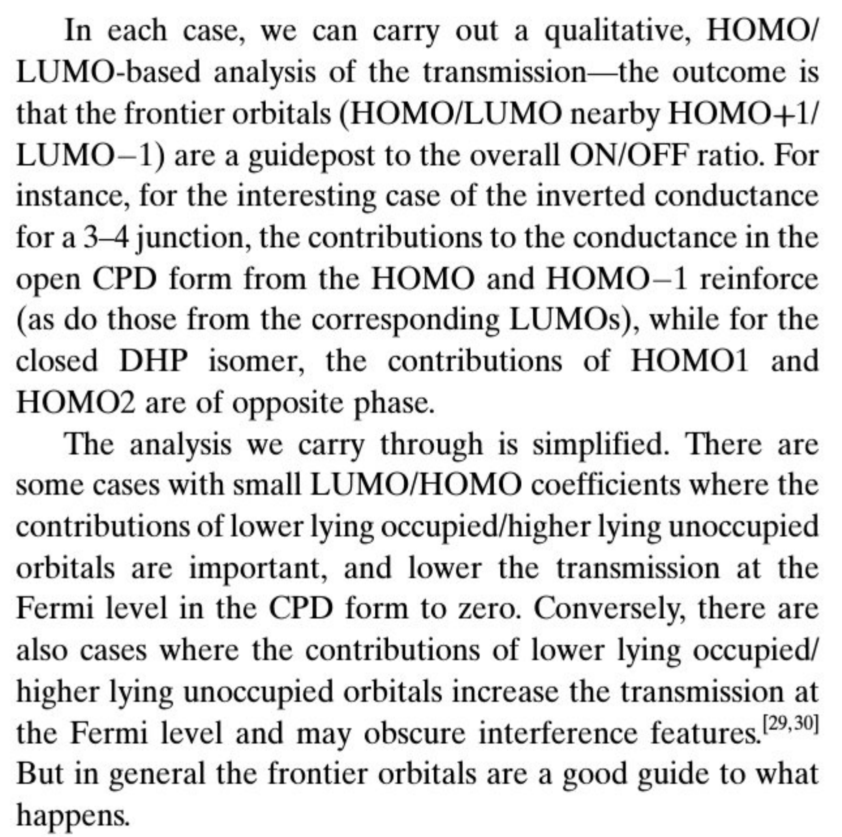

In each case, we can carry out a qualitative, HOMO/LUMO-based analysis of the transmission—the outcome is that the frontier orbitals (HOMO/LUMO nearby HOMO+1/LUMO−1) are a guidepost to the overall ON/OFF ratio. For instance, for the interesting case of the inverted conductance for a 3–4 junction, the contributions to the conductance in the open CPD form from the HOMO and HOMO−1 reinforce (as do those from the corresponding LUMOs), while for the closed DHP isomer, the contributions of HOMO1 and HOMO2 are of opposite phase.

The analysis we carry through is simplified. There are some cases with small LUMO/HOMO coefficients where the contributions of lower lying occupied/higher lying unoccupied orbitals are important, and lower the transmission at the Fermi level in the CPD form to zero. Conversely, there are also cases where the contributions of lower lying occupied/higher lying unoccupied orbitals increase the transmission at the Fermi level and may obscure interference features.[29,30] But in general the frontier orbitals are a good guide to what happens.

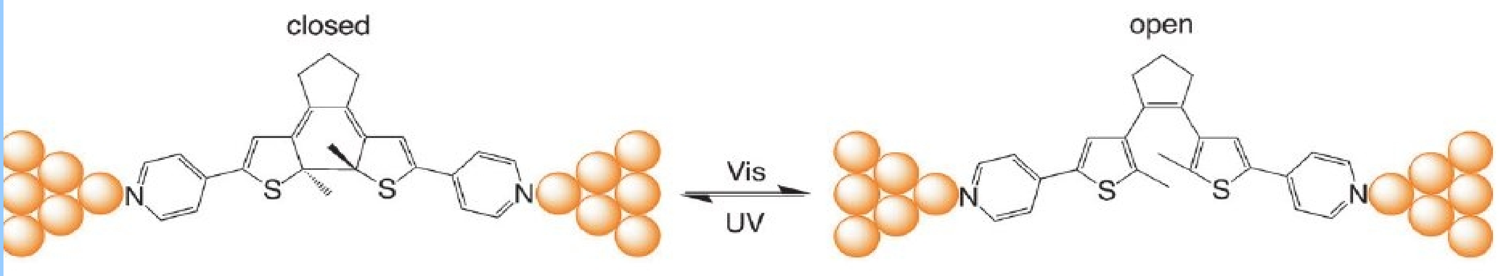

Y. Tsuji and R. Hoffmann, Angew. Chem., Int. Ed. 53, 4093 (2014)

The Coulson-Rushbrooke pairing theorem

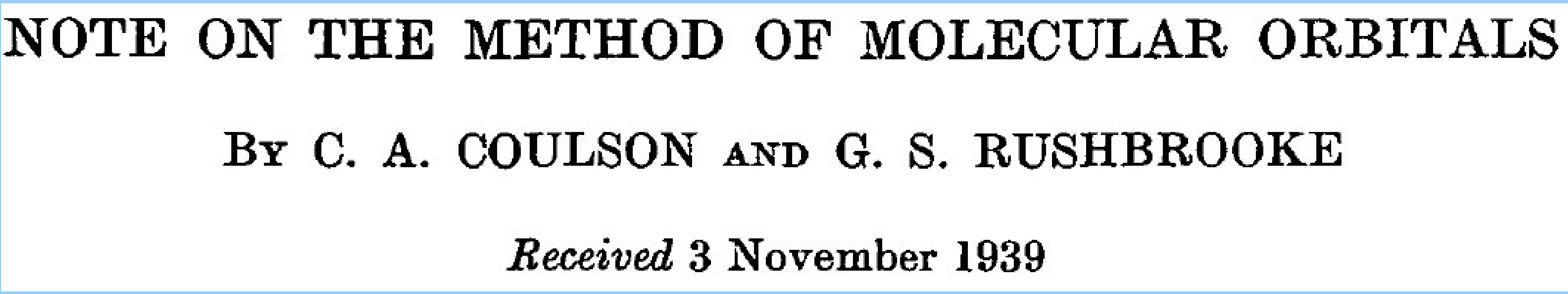

NOTE ON THE METHOD OF MOLECULAR ORBITALS

By C. A. COULSON and G. S. RUSHBROOKE

Received 3 November 1939

For every MO energy $\alpha + x\beta$ in an alternant hydrocarbon, there exists another energy $\alpha - x\beta$; that is, the roots of the MO secular determinants occur in pairs, which are equal in magnitude and opposite in sign. Furthermore, the coefficients of paired MOs are the same except that the Algebraic sign at every second atom is opposite.

C. A. Coulson and G. S. Rushbrooke, Math. Proc. Cambridge Philos. Soc. 36, 193 (1940)

THE JOURNAL OF CHEMICAL PHYSICS **146**, 092308 (2017)

Destructive quantum interference in electron transport: A reconciliation of the molecular orbital and the atomic orbital perspective

Xin Zhao,[a)] Victor Geskin,[a),b)] and Robert Stadler[a)]
Institute for Theoretical Physics, TU Wien - Vienna University of Technology, Wiedner Hauptstrasse 8-10, A-1040 Vienna, Austria

$$T(E) = Tr[G^r(E)\mathbf{\Gamma}_L(E)G^a(E)\mathbf{\Gamma}_R(E)], \qquad (1)$$

$$T(E) = |G^{mol}_{lr}(E)|^2\Gamma_{ll}(E)\Gamma_{rr}(E). \qquad (2)$$

$$G^{mol}_{lr}(E) = [(E \pm i\eta)\mathbf{I} - \mathbf{H}_{mol}]^{-1}, \qquad (3)$$

$$G^{mol}_{lr}(E) = \sum_{m=1}^{N} \frac{C_{lm}C^*_{rm}}{E - \epsilon_m \pm i\eta}, \qquad (4)$$

$$G^{mol}_{lr}(E_F) = \sum_{k=0}^{N/2-1} \frac{C_{l,(H-k)}C^*_{r,(H-k)} - C_{l,(L+k)}C^*_{r,(L+k)}}{\epsilon_k}. \qquad (5)$$

$$\Gamma(E) = \sum_{m=1}^{N} \frac{\alpha_m\beta_m}{E - \epsilon_m}. \qquad (6)$$

The pairing theorem now predicts for AOs l and r on the carbon atoms of the same subset that $C_{l,(H-k)}C^*_{r,(H-k)} = C_{l,(L+k)}C^*_{r,(L+k)}$ because either $C_{l,(H-k)} = -C_{l,(L+k)}$ and simultaneously $C^*_{r,(H-k)} = -C^*_{r,(L+k)}$ or $C_{l,(H-k)} = C_{l,(L+k)}$ and simultaneously $C^*_{r,(H-k)} = C^*_{r,(L+k)}$, as all the coefficients in only one subset change their sign when comparing an occupied with its mirrored unoccupied level. Therefore, the terms in every CR pair of Eq. (5) cancel exactly at E_F for this case and DQI occurs as a result as has also been observed in Refs. 51 and 52.

If on the other hand, the contact AOs l and r belong to the carbon atoms from different subsets, then $C_{l,(H-k)}C^*_{r,(H-k)} = -C_{l,(L+k)}C^*_{r,(L+k)}$ because either $C_{l,(H-k)} = -C_{l,(L+k)}$ and $C^*_{r,(H-k)} = C^*_{r,(L+k)}$ or $C_{l,(H-k)} = C_{l,(L+k)}$ and $C^*_{r,(H-k)} = -C^*_{r,(L+k)}$. For this case, the contributions coming from the two individual parts of each CR pair of MOs (H − k, L + k) including the HOMO and the LUMO always add up constructively at E_F in Eq. (5).

Although any individual CR pair contribution is therefore nonvanishing, it is important to stress that destructive interference is still possible between CR pairs, as each of them can contribute either a positive or a negative term to G^{mol}_{lr}. The pairing theorem, however, does not provide the means for an assessment of prediction of such inter-pair interference.

Relation between frontier MO rules and the pairing theorem

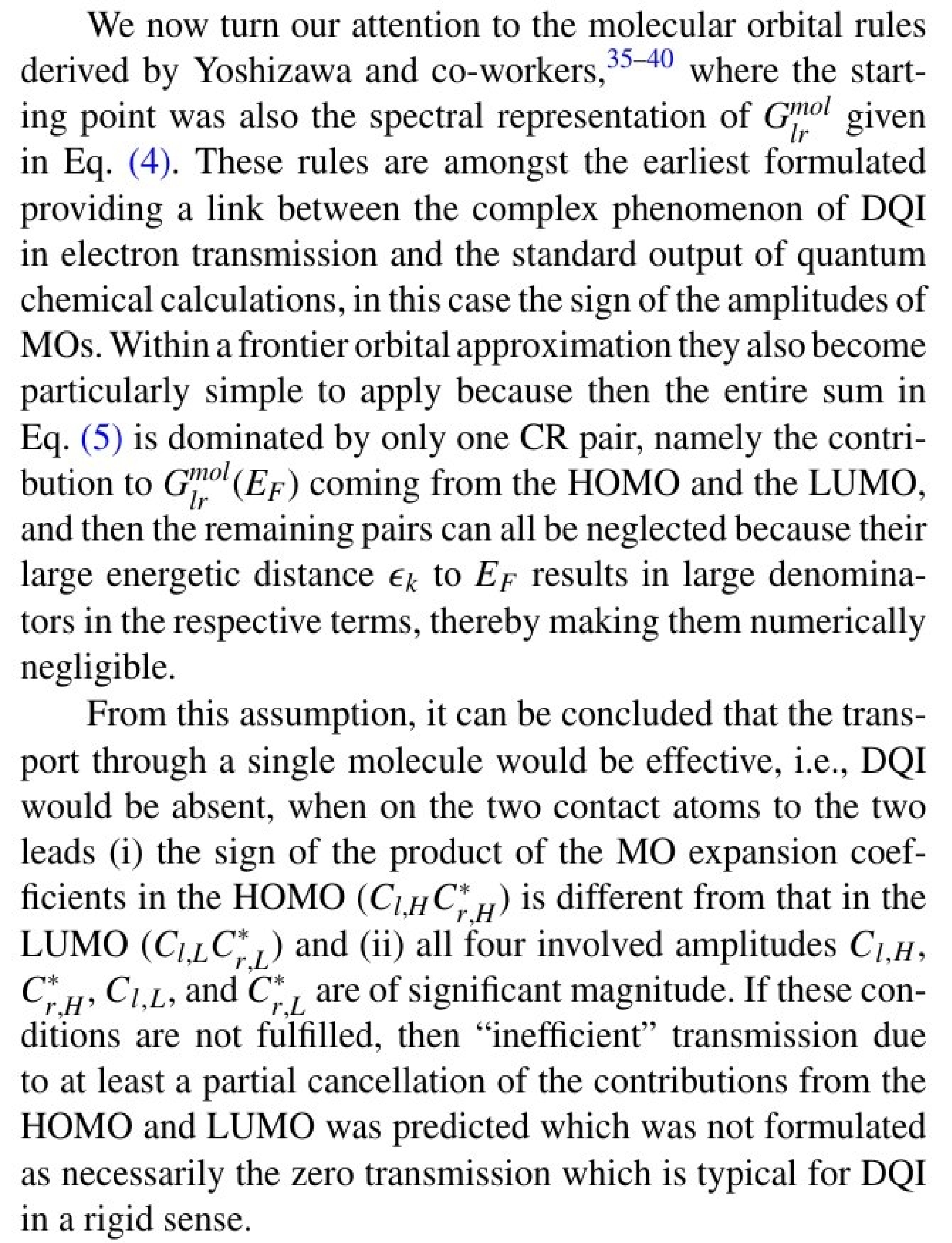

We now turn our attention to the molecular orbital rules derived by Yoshizawa and co-workers,[35–40] where the starting point was also the spectral representation of G_{lr}^{mol} given in Eq. (4). These rules are amongst the earliest formulated providing a link between the complex phenomenon of DQI in electron transmission and the standard output of quantum chemical calculations, in this case the sign of the amplitudes of MOs. Within a frontier orbital approximation they also become particularly simple to apply because then the entire sum in Eq. (5) is dominated by only one CR pair, namely the contribution to $G_{lr}^{mol}(E_F)$ coming from the HOMO and the LUMO, and then the remaining pairs can all be neglected because their large energetic distance ϵ_k to E_F results in large denominators in the respective terms, thereby making them numerically negligible.

From this assumption, it can be concluded that the transport through a single molecule would be effective, i.e., DQI would be absent, when on the two contact atoms to the two leads (i) the sign of the product of the MO expansion coefficients in the HOMO ($C_{l,H}C_{r,H}^*$) is different from that in the LUMO ($C_{l,L}C_{r,L}^*$) and (ii) all four involved amplitudes $C_{l,H}$, $C_{r,H}^*$, $C_{l,L}$, and $C_{r,L}^*$ are of significant magnitude. If these conditions are not fulfilled, then "inefficient" transmission due to at least a partial cancellation of the contributions from the HOMO and LUMO was predicted which was not formulated as necessarily the zero transmission which is typical for DQI in a rigid sense.

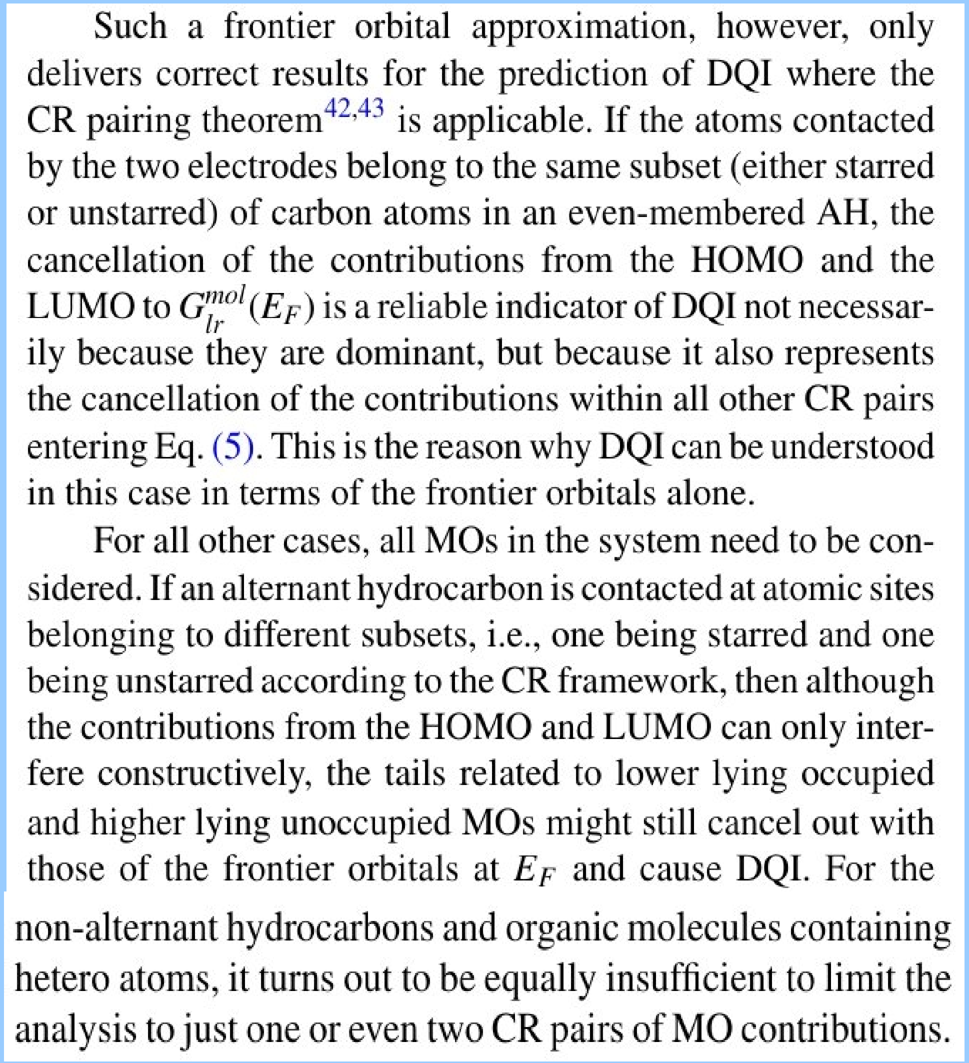

Such a frontier orbital approximation, however, only delivers correct results for the prediction of DQI where the CR pairing theorem[42,43] is applicable. If the atoms contacted by the two electrodes belong to the same subset (either starred or unstarred) of carbon atoms in an even-membered AH, the cancellation of the contributions from the HOMO and the LUMO to $G_{lr}^{mol}(E_F)$ is a reliable indicator of DQI not necessarily because they are dominant, but because it also represents the cancellation of the contributions within all other CR pairs entering Eq. (5). This is the reason why DQI can be understood in this case in terms of the frontier orbitals alone.

For all other cases, all MOs in the system need to be considered. If an alternant hydrocarbon is contacted at atomic sites belonging to different subsets, i.e., one being starred and one being unstarred according to the CR framework, then although the contributions from the HOMO and LUMO can only interfere constructively, the tails related to lower lying occupied and higher lying unoccupied MOs might still cancel out with those of the frontier orbitals at E_F and cause DQI. For the non-alternant hydrocarbons and organic molecules containing hetero atoms, it turns out to be equally insufficient to limit the analysis to just one or even two CR pairs of MO contributions.

X. Zhao, V. Geskin and R. Stadler, Journal of Chemical Physics 146, 092308 (2017)

Benzene works for everybody

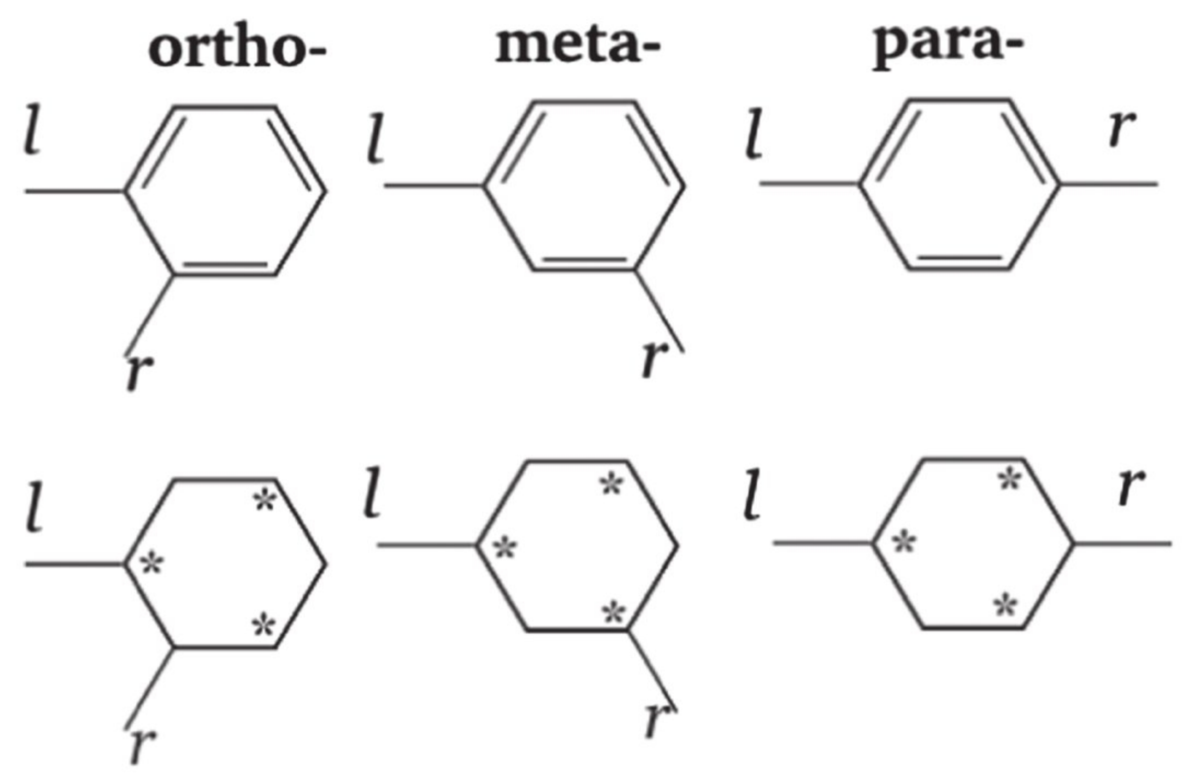

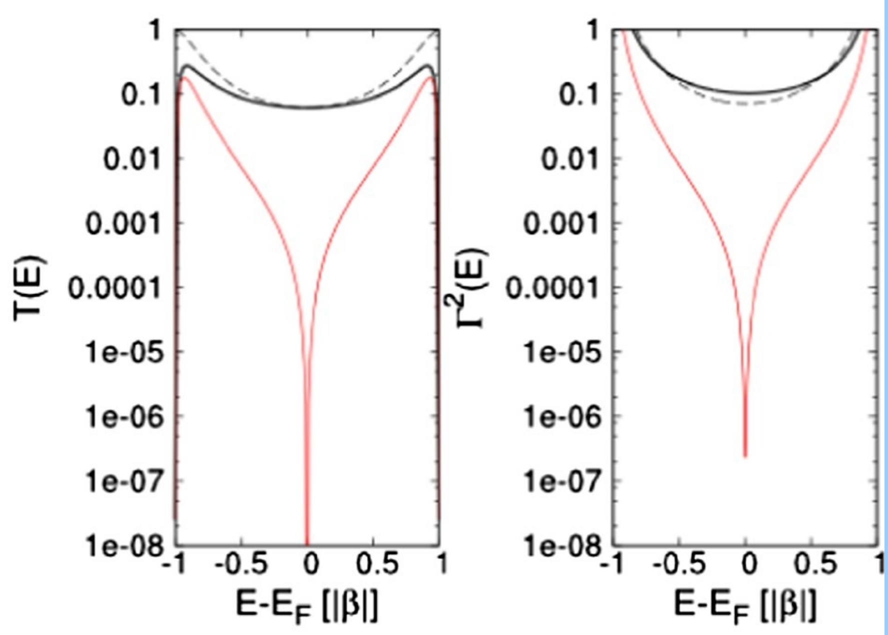

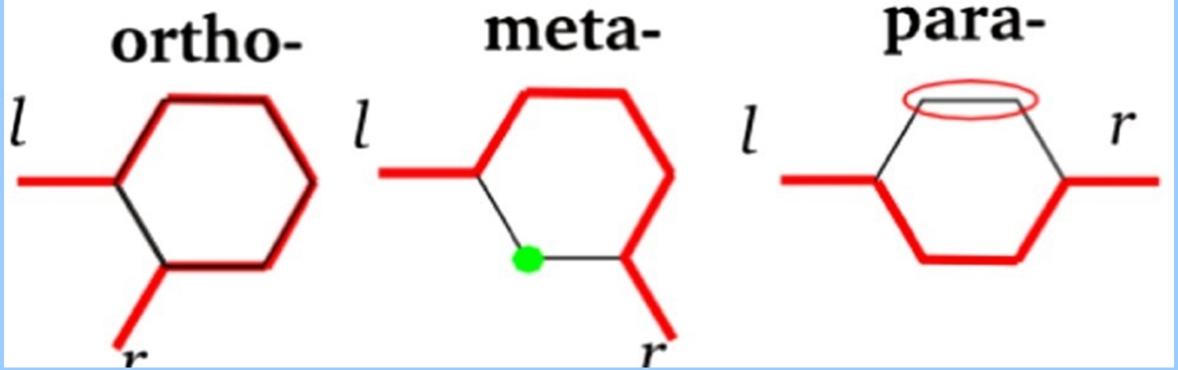

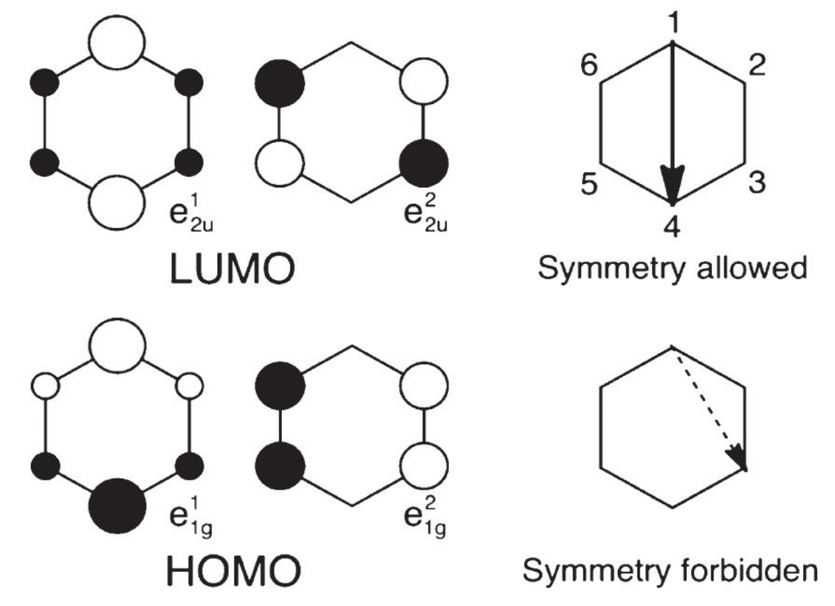

X. Zhao, V. Geskin and R. Stadler, Journal of Chemical Physics 146, 092308 (2017)

Butadiene as the simplest illustrative example

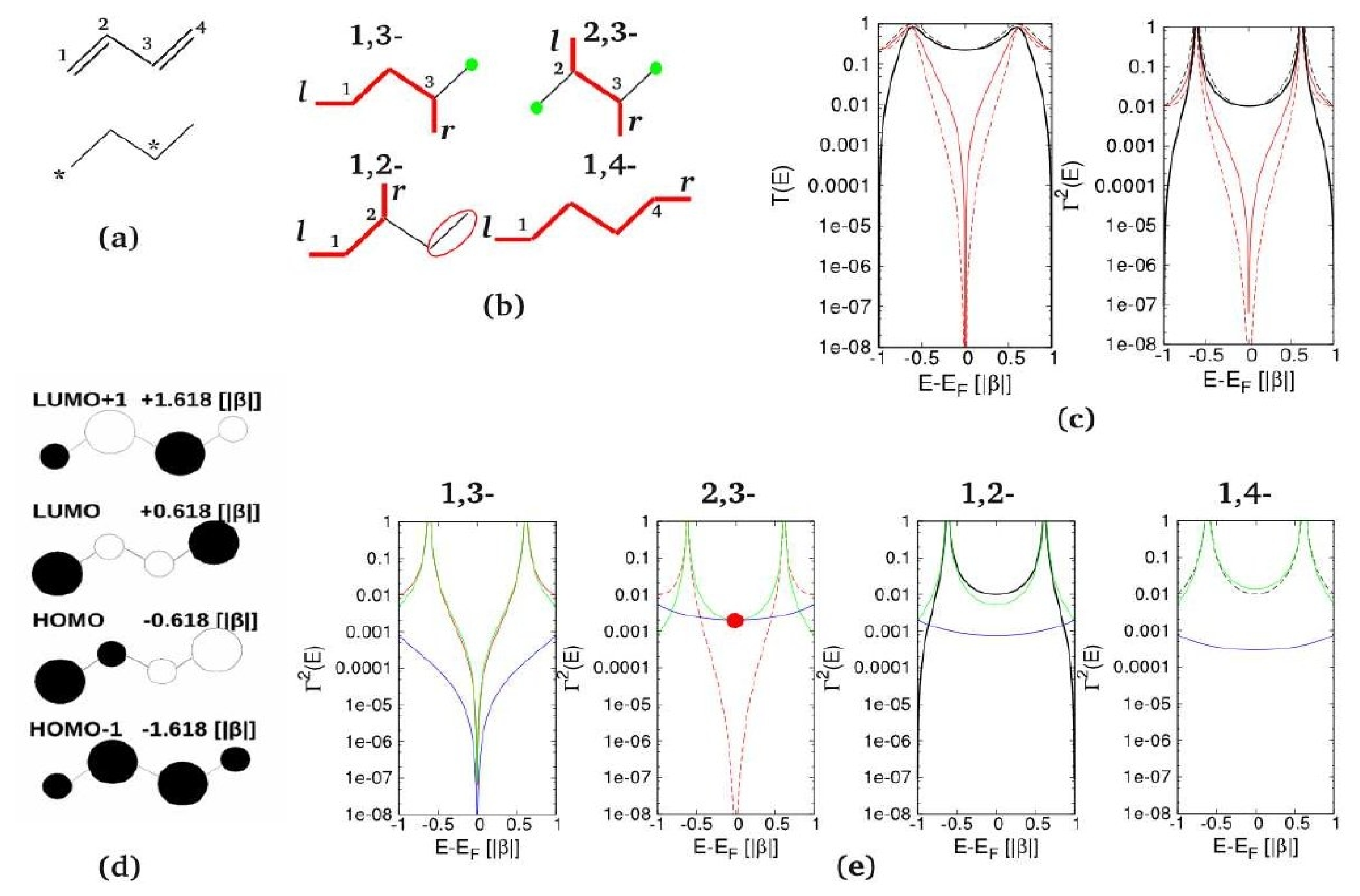

X. Zhao, V. Geskin and R. Stadler, Journal of Chemical Physics 146, 092308 (2017)

The two systems for which the frontier MO rules had to be ad hoc adapted

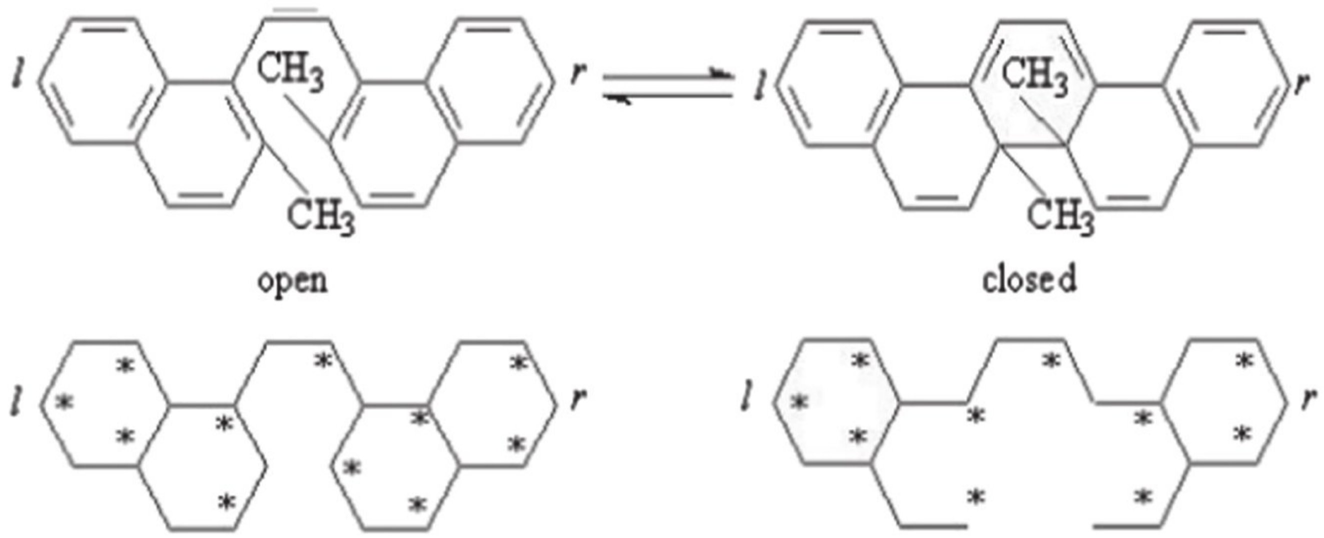

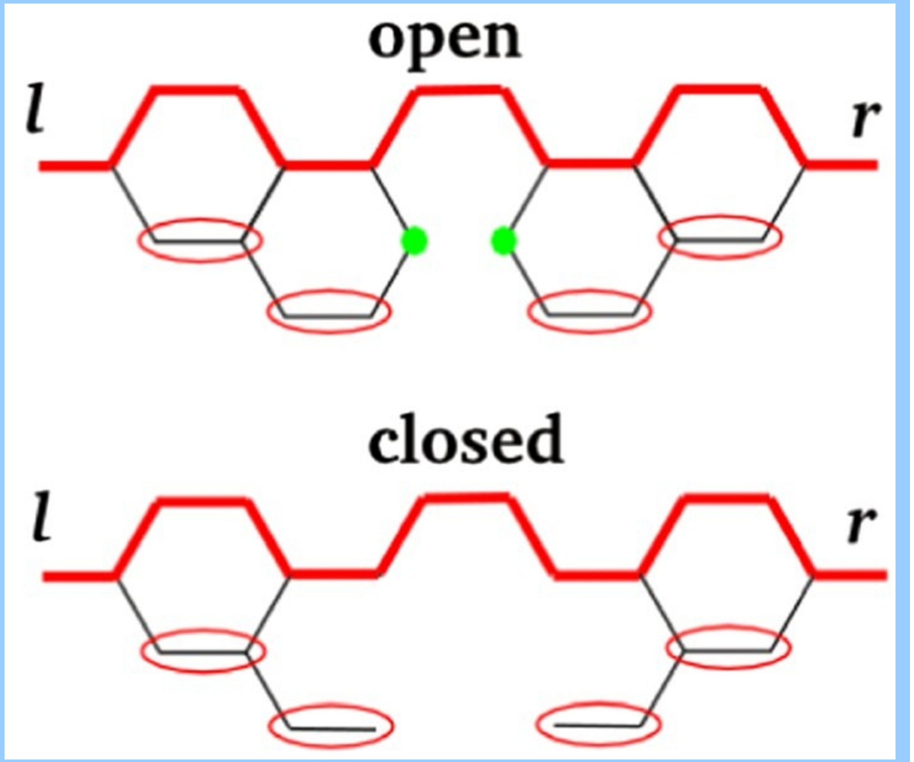

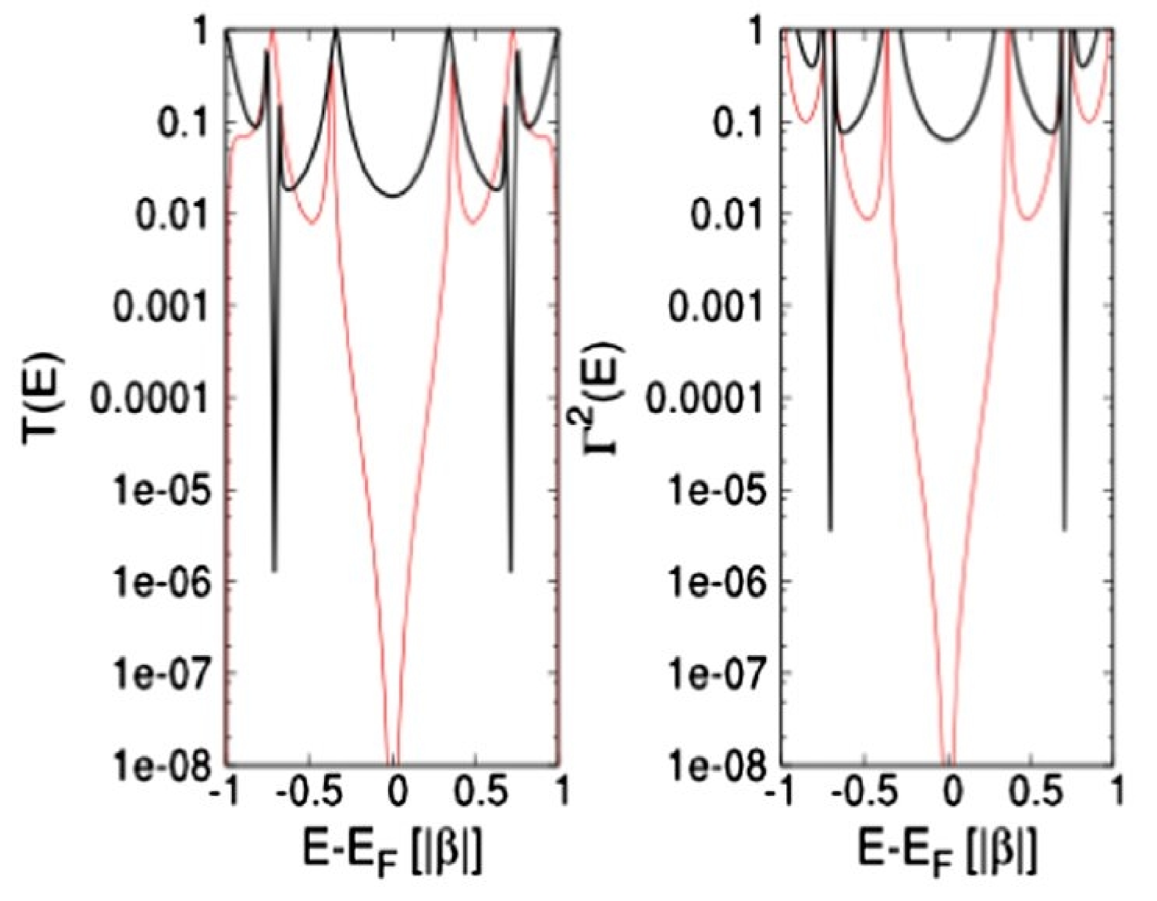

X. Zhao, V. Geskin and R. Stadler, Journal of Chemical Physics 146, 092308 (2017)

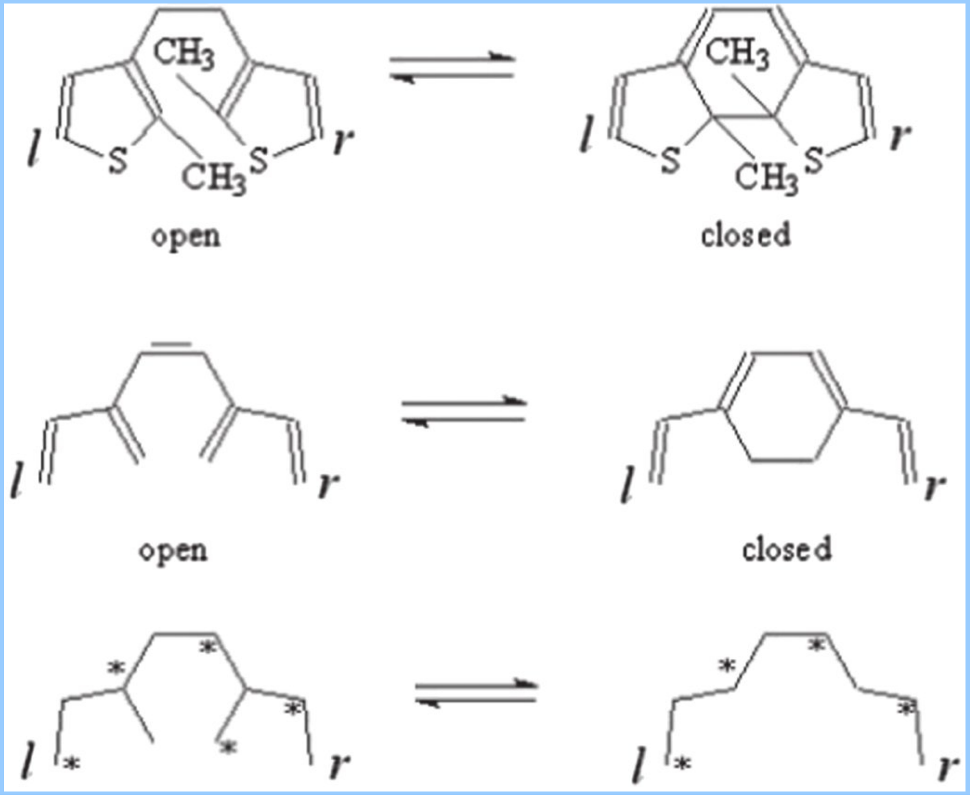

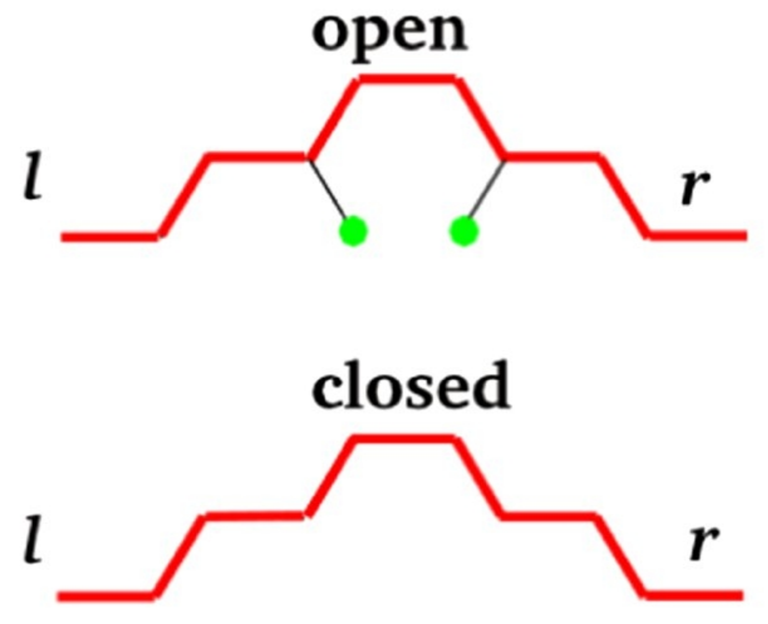

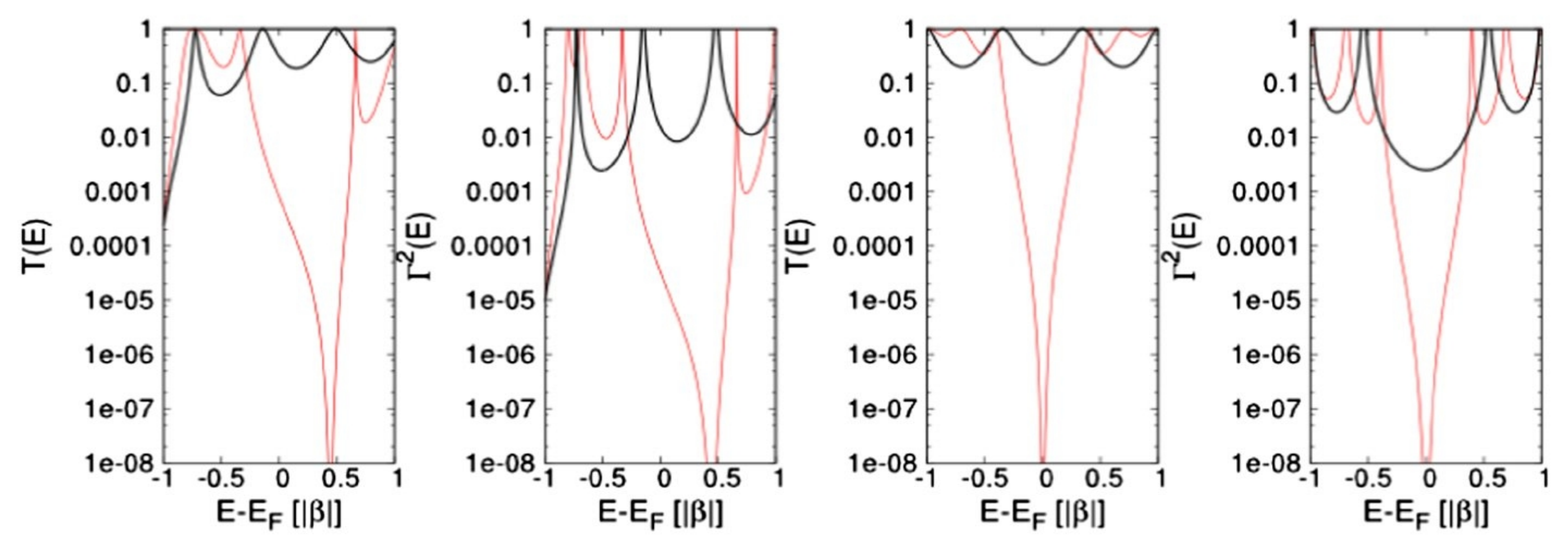

X. Zhao, V. Geskin and R. Stadler, Journal of Chemical Physics 146, 092308 (2017)

Cases where the pairing theorem is not applicable

- nonalternant hydrocarbons

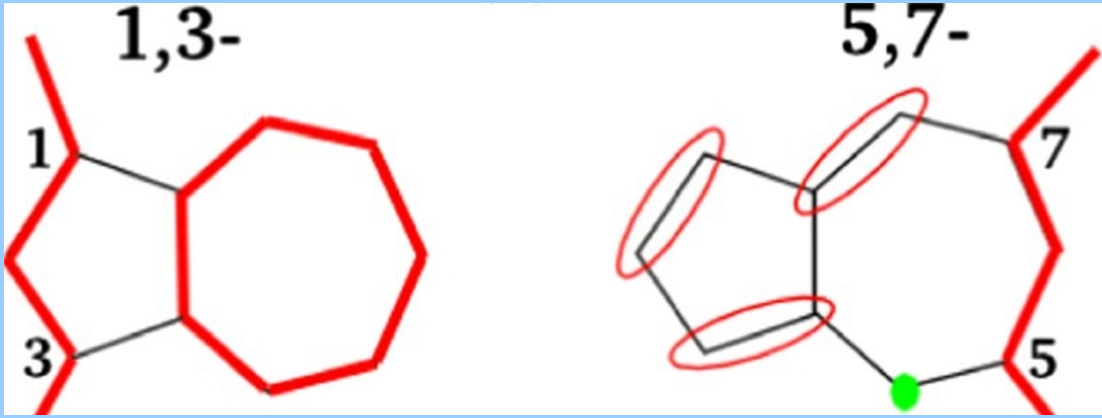

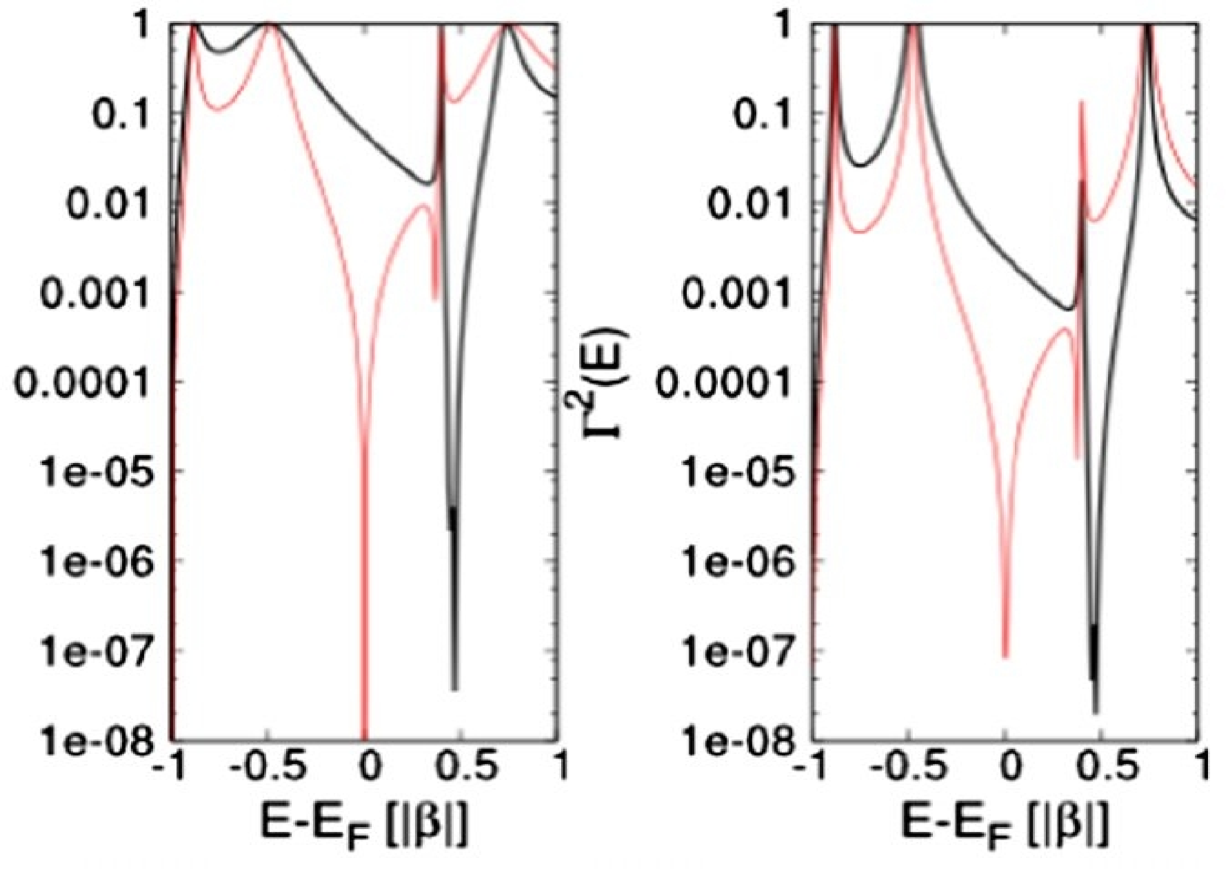

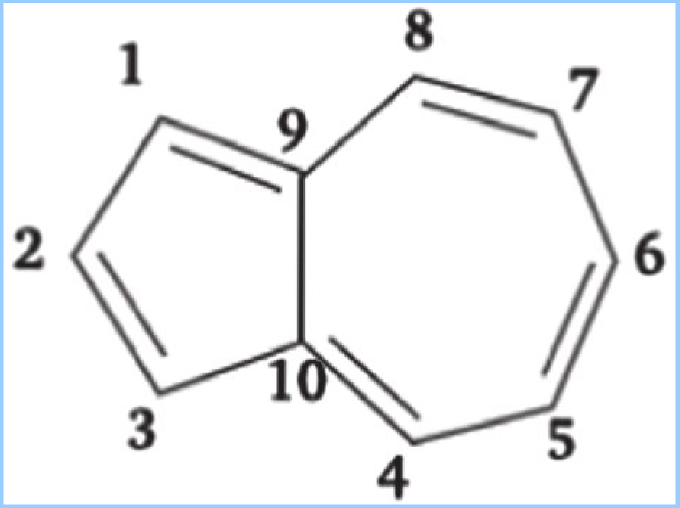

X. Zhao, V. Geskin and R. Stadler, Journal of Chemical Physics 146, 092308 (2017)

Convergence with respect to number of CR pairs (1)

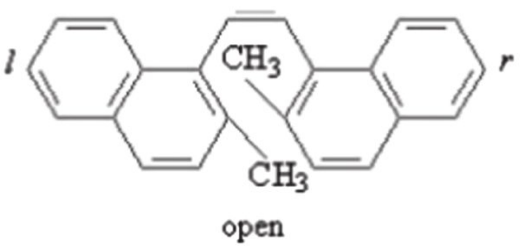

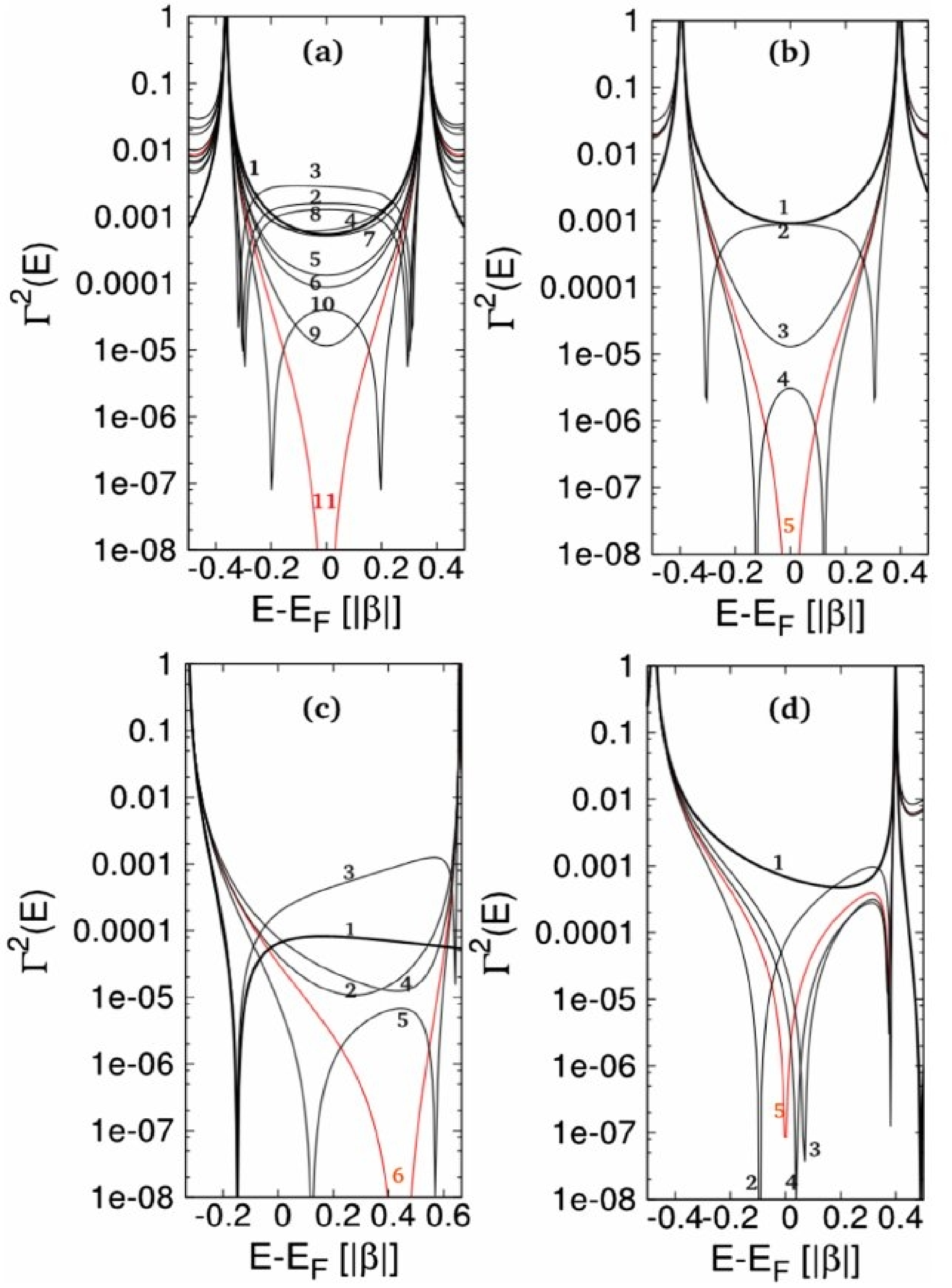

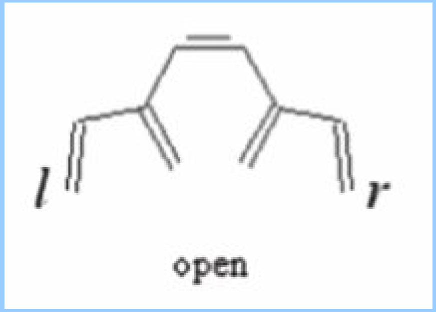

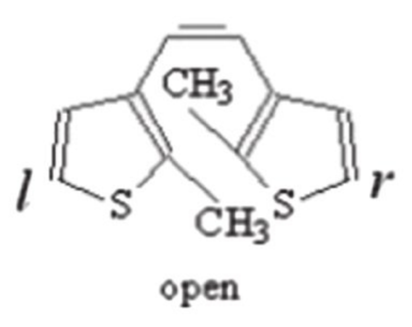

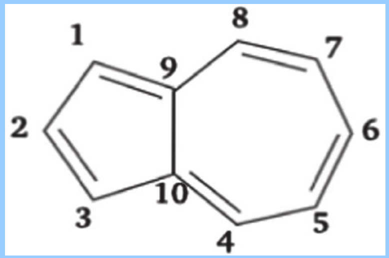

X. Zhao, V. Geskin and R. Stadler, Journal of Chemical Physics 146, 092308 (2017)

Convergence with respect to number of CR pairs (2)

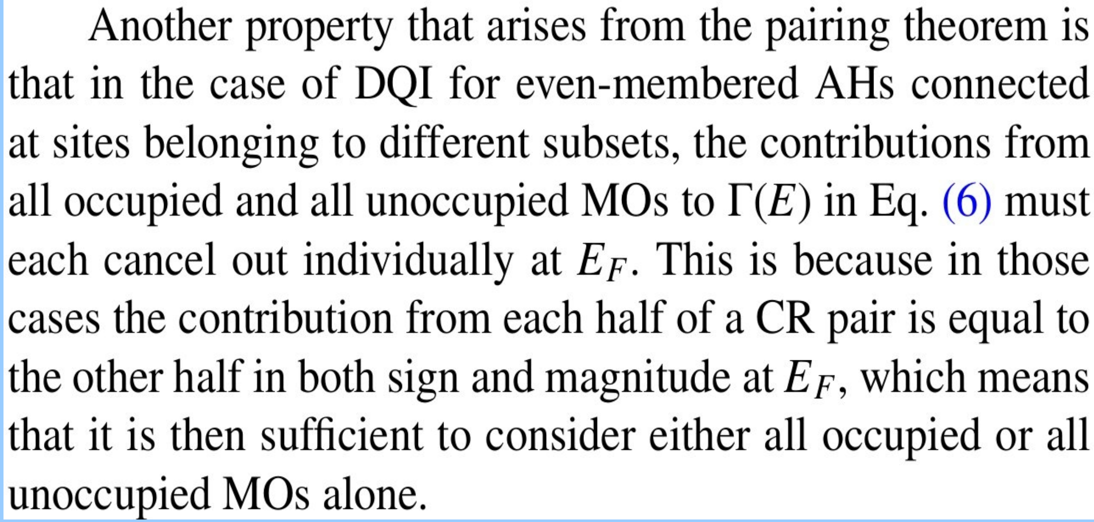

Another property that arises from the pairing theorem is that in the case of DQI for even-membered AHs connected at sites belonging to different subsets, the contributions from all occupied and all unoccupied MOs to $\Gamma(E)$ in Eq. (6) must each cancel out individually at E_F. This is because in those cases the contribution from each half of a CR pair is equal to the other half in both sign and magnitude at E_F, which means that it is then sufficient to consider either all occupied or all unoccupied MOs alone.

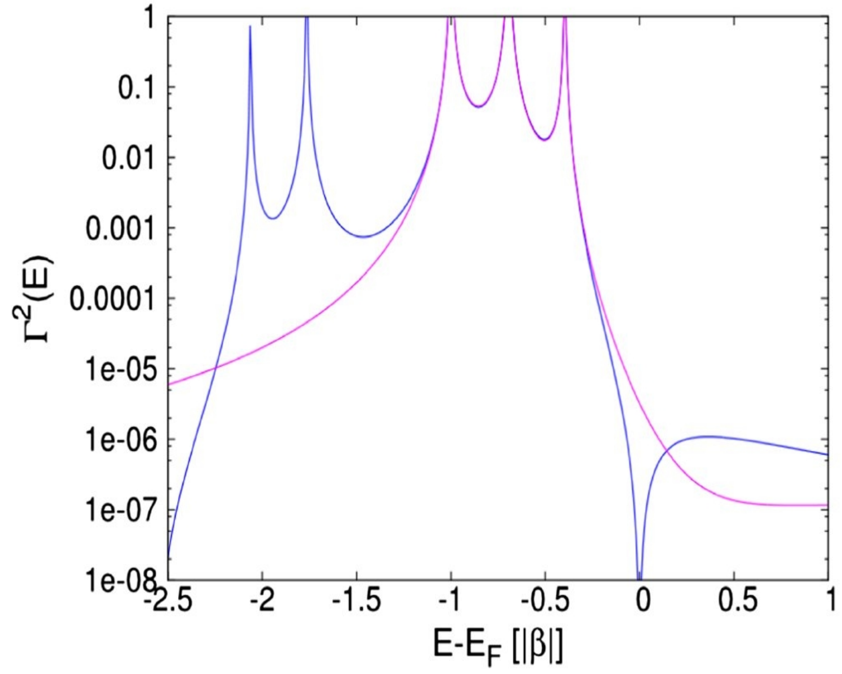

FIG. 6. $\Gamma^2(E)$, where $\Gamma(E)$ is taken as the sum over all the five occupied (blue curve) or only the three occupied MOs closest to E_F (magenta curve) in Eq. (6) for the open form of the AH analog of DTE with the S atoms removed.

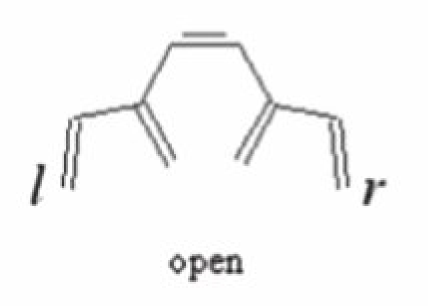

Even MOs around 2 eV above or below the Fermi level can determine qualitatively whether DQI effects are observed in the conductance if their amplitudes at the contact atoms are high enough.

X. Zhao, V. Geskin and R. Stadler, Journal of Chemical Physics 146, 092308 (2017)

Conclusions – DQI in planar hydrocarbons

1) The dependency of the occurrence of destructive quantum interference effects (DQI) on the molecular structure (configuration) can be already studied and understood on the level of topological tight binding models, where simple AO based graphical rules as well as frontier MO rules can be derived.

2) The graphical AO rules have been verified by NEGF-DFT calculations for a set of 10 anthraquinone configurations, where half of them showed QI and the Other half did not, which was correctly predicted by the model for each case. The most significant approximation in the model, namely that all onsite energies are equal to the Fermi energy has been lifted. A further generalisation has been introduced by G. Solomon and her co-workers. It is now beyond doubt that the graphical rules also predict DQI correctly for non-alternant hydrocarbons such as Azulene.

3) The frontier MO rules by Yoshizawa and co-workers have been related to the Coulson-Rushbrook pairing theorem where it could be shown that the rules only give correct predictions where these can be already seen from the CR theorem.

4) Where DQI cannot be predicted directly from the CR pairing theorem, the contributions from all MOs resulting related to the π electrons need to be considered explicitly for planar hydrocarbons.

Branched molecules containing metal centers

P27272

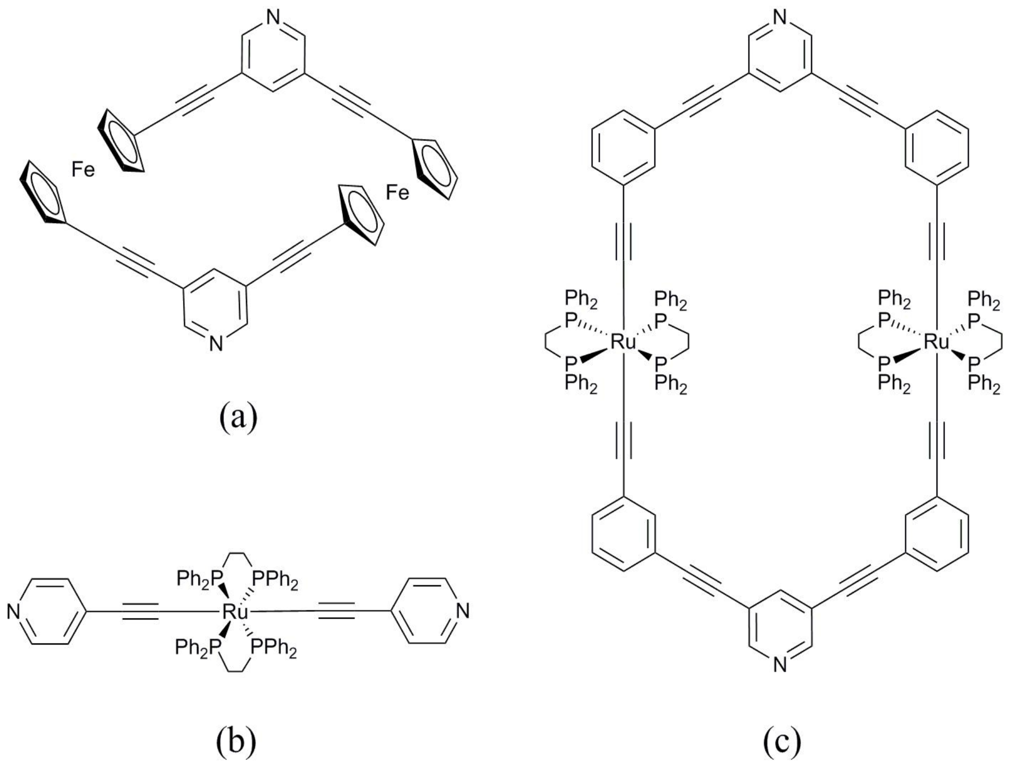

(a)

(b)

(c)

1) Coherent tunnelling vs. hopping electron transport?
2) Can phase-coherent QI be induced by asymmetry in oxidation states?
3) How is charge transport “distributed” over the two branches of the molecule?
4) How does the presence of a temporarily reduced metal centre M1 affect the redox properties of the other centre M2?

This is a collaboration with the group of Tim Albrecht at Imperial College London as experimental partner.

Ferrocene (1)

P27272

Design ideas

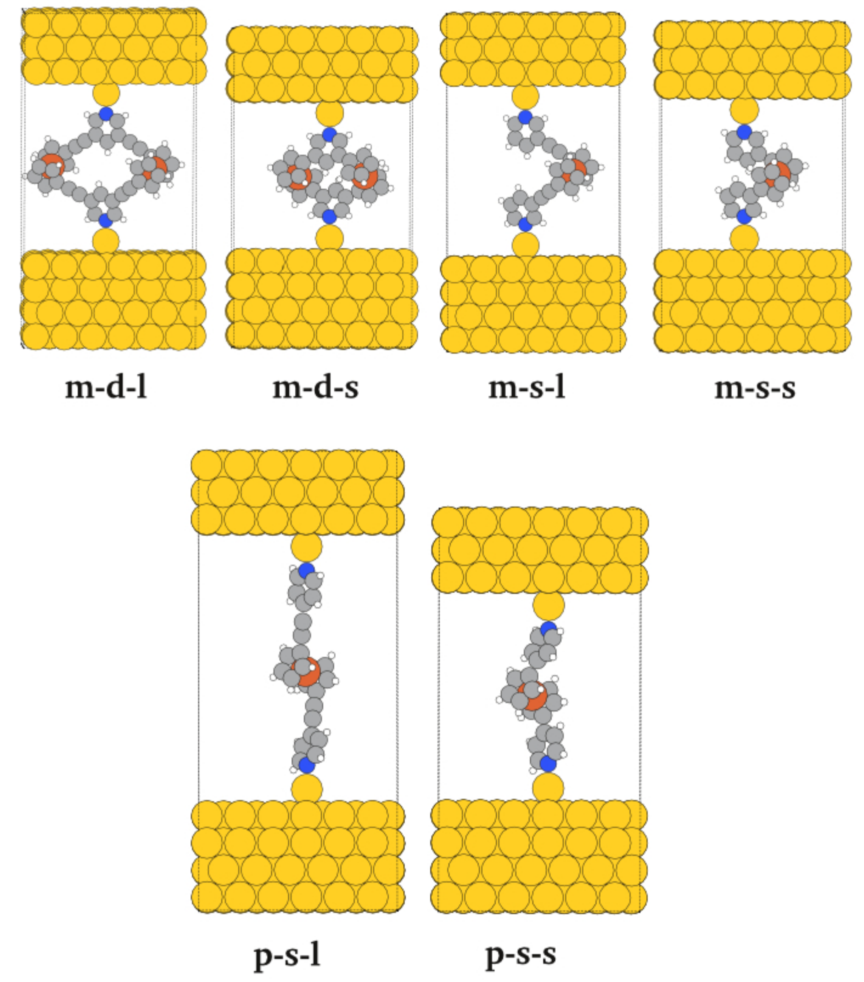

Junction geometries for the six neutral compounds we investigated.

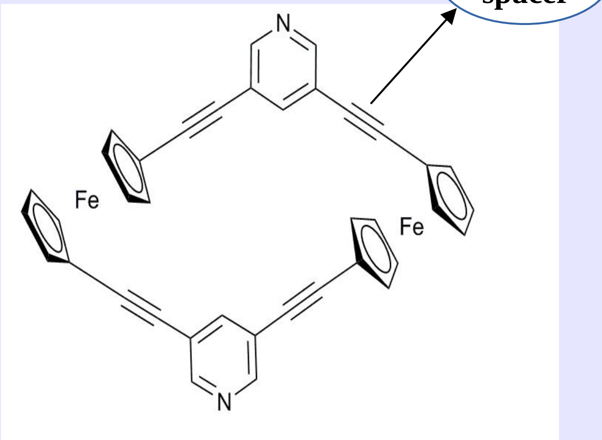

acetylene spacer

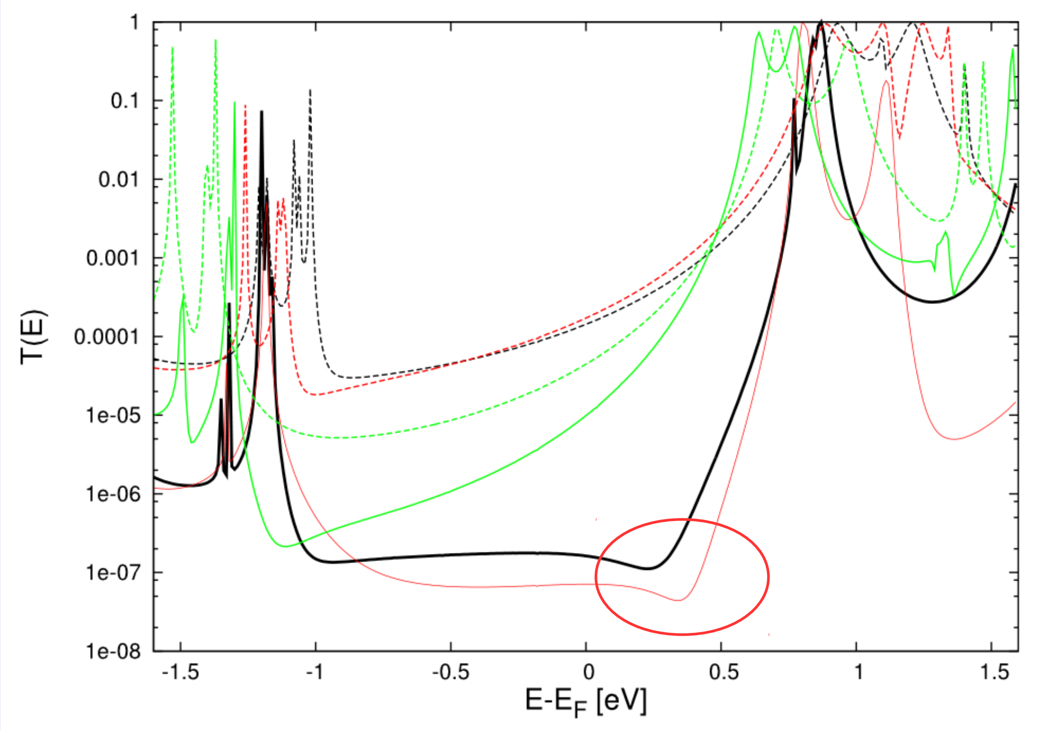

Transmission functions for the six charge neutral ferrocene junctions, which we calculated from NEGF-DFT.

Ferrocene (2)

TB models – direct coupling

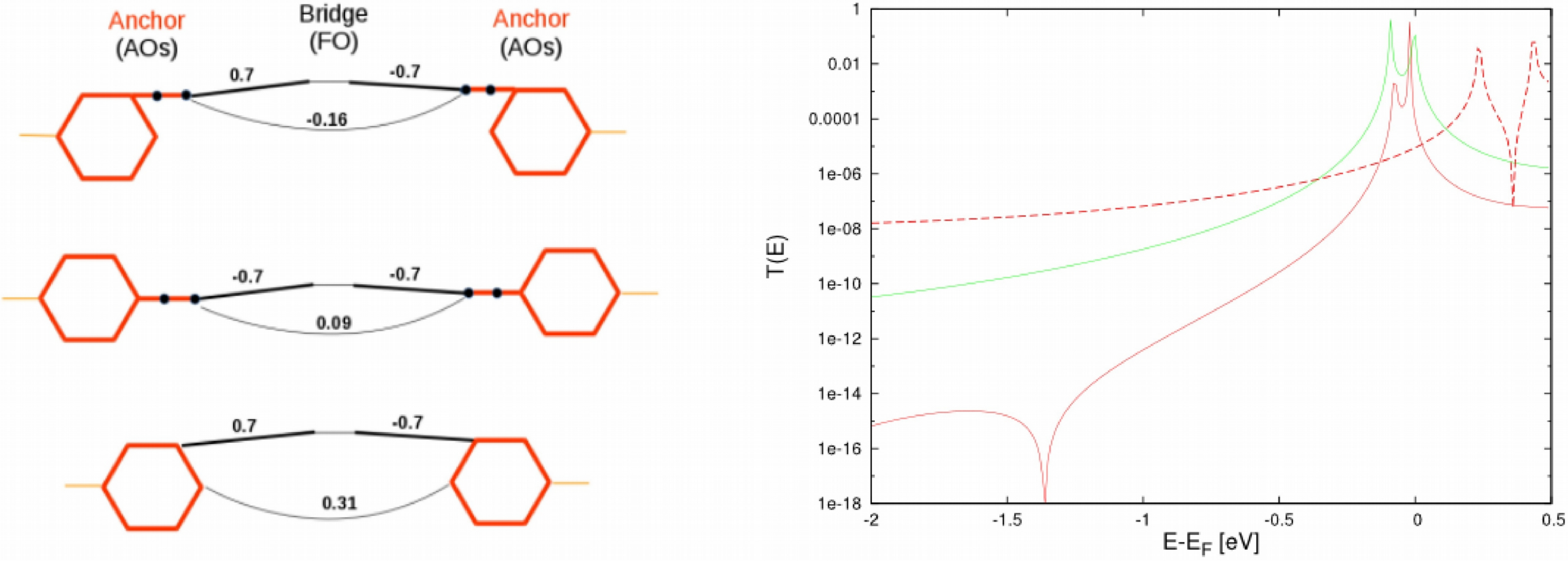

(a) (b)

Ferrocene (3)

Charging of one redox center

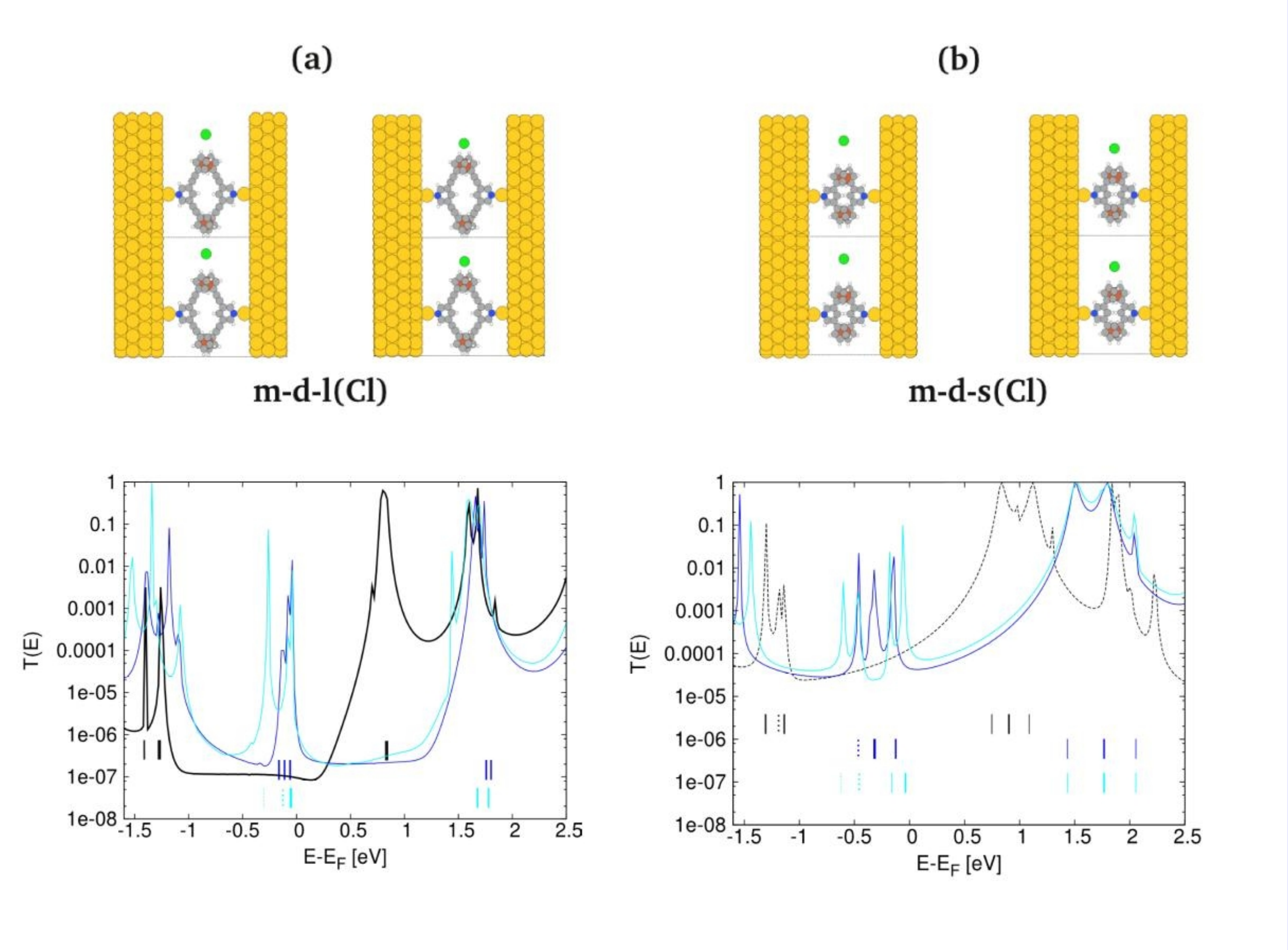

Outlook

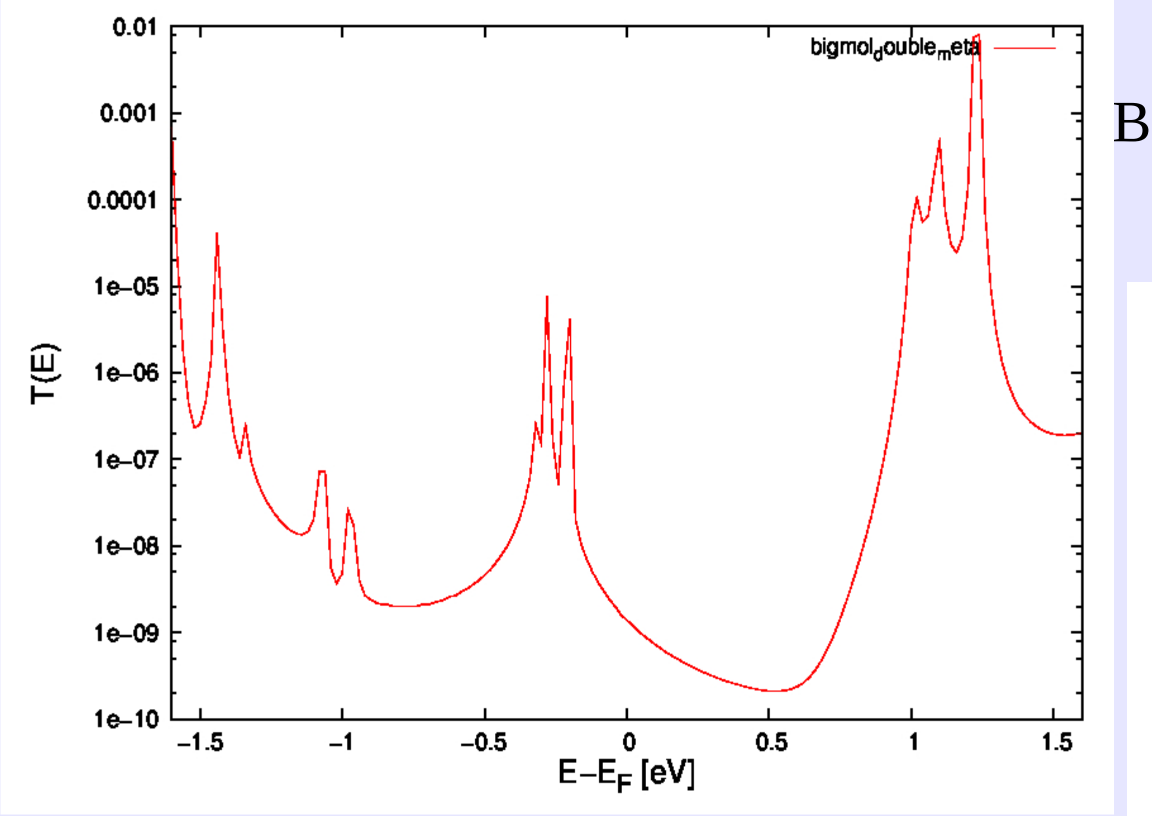

Branched molecule containing Ru and/or Os

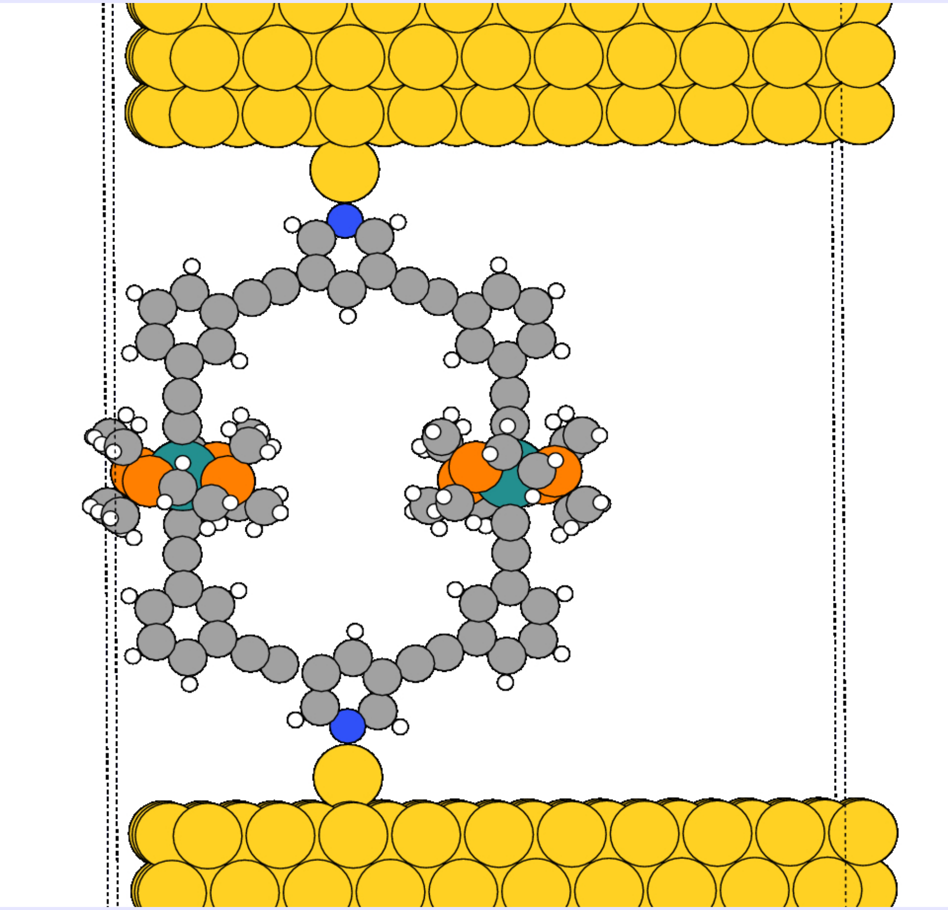

1) Coherent tunnelling or hopping for molecule with Ru/Ru, Os/Os and Ru/Os with in-built asymmetry for comparison.

2) Electron hopping as alternative electron transport mechanism for this larger molecule.

3) Direct comparison with measurements using electrochemical STM in London where some of these molecules have been synthesized and the synthesis of the other ones is in progress.

Thank you for your attention!

Technical Details

- ***Program packages:*** ASE/GPAW
- ***Theoretical framework:*** Density Functional Theory with a PBE (GGA) XC functional
- ***Basis set:*** LCAO (dzp)
- ***Gridspacing for all potentials:*** 0.18 Å
- ***Metal surface:*** fcc Au(111) with 2.88 Å Au-Au, 6x6 atoms in xy-plane, 3 or 4 layers in z-direction, periodical boundary conditions
- ***Relaxations:*** Geometries were relaxed with a convergence criterion of 0.05 eV/Å per atom
- ***Electrode-Molecule distance:*** Equilibrium value determined by means of energy minimization
- ***Atomic charges:*** Bader analysis, Mulliken charges
- ***Solvent description:*** Generalized Born Approximation (GBA) with vdW-radii from OPLS force field

ASE: S. . Bahn and K. W. Jacobsen, An object-oriented scripting interface to a legacy electronic structure code, Comput. Sci. Eng., Vol. 4, 56-66, 2002
GPAW: J. J. Mortensen, L. B. Hansen , and K. W. Jacobsen Real-space grid implementation of the projector augmented wave method Physical Review B, Vol. 71, 035109, 2005